EARLY AGE STRENGTH DEVELOPMENT OF GGBS CONCRETE CURED UNDER DIFFERENT TEMPERATURES

Thesis submitted in accordance with the requirements of the University of Liverpool for degree of Doctor in Philosophy

By

GIDION TURU'ALLO

June 2013

ACKNOWLEDGMENTS

I would like to thank my supervisors Dr. I. A. Kougioumtzoglou and Dr. S.W. Jones for their advice, moral support and guidance, especially during the writing period of this thesis. I would also to express my deepest appreciation to Prof. Dr. M.N. Soutsos for his encouragement, patience, advice and guidance throughout the research. My gratitude is given to Dr. S.J. Barnett for her valuable discussion, advice and recommendations, especially at the early stages of my experimental work. Also for her data provided that was used in this thesis.

I would also to thank to both my examiners: Prof. Mike Forde (external examiner) and Dr. Jonathan Bridge (internal examiner), as this thesis would not have taken shape without encouragement and constructive feedback from them.

I would like to grateful to my friend Dr. Mohammed A. Elsageer for his help and valuable discussions for experimental works. My thanks also to Mr. Marc Bratley, Mr. David Hunter and Mr. Terry Hodge for their assistance during my laboratory work.

Special thanks are given to all my brothers and sisters in All Saints Church Liverpool for their support in praying. My deepest thank is given to Mr Chris Turner for his support, help and contribution for this thesis.

I would like to acknowledge the financial support of the Indonesia Government, in this case the Higher Education Directorate General, Ministry of Education and Culture, Republic of Indonesia.

Finally, I would like to express my deepest thanks to all my families and friends for their support in praying, love, and understanding during my studies.

I dedicate this thesis to both my beloved parents

ABSTRACT

Concrete mixes incorporating ground granulated blast furnace slag (GGBS) has not gained popularity in fast track construction. It is believed to be due to its slower strength development at early age cured under standard curing temperature. The benefits that are obtained when using GGBS in concrete such as economic, sustainability and durability are discussed.

Two grades of mortars/concretes i.e. C45 and C75 containing GGBS at levels of 0, 20, 35, 50 and 70% have been investigated to give guidance for their use in fast track construction. The effect of curing temperature on the strength development of mortars/concretes containing different levels of GGBS at early and later age have been investigated by testing strength of the mortars/concretes. The mortars were cured at 10, 20, 30, 40 and 50^0C and adiabatically cured conditions; while the concrete specimens were cured at 20 and 50^0C, as well under adiabatic curing conditions. The mortars/concretes were tested at age of 0.25, 0.5, 1, 2, 4, 8, 16, 32, 64, 128, 256 and 365 days.

There were also five mixes for lightweight concrete and three mixes for self compacting concrete that cast and cured under different temperatures of 20, 30, 40 and 50^0C, as well as under adiabatic curing conditions. This aims to evaluate the strength development of this kinds of concrete cured at different curing temperatures. The cubes were tested at the age of 0.125, 0.25, 0.5, 1, 2, 4, 7, 14 and 28-days.

The heat outputs using of equivalent mortar mixes are measured using isothermal calorimeter. This is used to assess the temperature sensitivity of the strength development of GGBS concrete. It is also used to investigate the contribution of GGBS on the heat output produced in the hydration of binder.

The accuracy of the existing maturity methods, which were developed based on concrete with Portland cement only, is evaluated to predict the strength of GGBS

concrete investigated in this study. A new method, which is called Modified Nurse-Saul (MNS) method, is recently developed to predict strength development of concrete in this study. This method is used to predict the strength development of both Portland cement and GGBS concretes, as well as to predict the heat output development of equivalent mixes mortar.

Finite element modelling was used to predict the temperature rise in concrete. Both the predicted heat output obtained from adiabatic test and isothermal calorimeter were used as heat sources. The predicted temperature is used to predict the strength development of concrete.

CONTENTS

CHAPTER 1 – INTRODUCTION

1.1. Background

In recent years, engineers have recognised the considerable economic benefits that can be achieved from fast track construction. Typical applications of fast track construction include a number of critical construction activities such as early opening of a busy road pavements to traffic, the termination of concrete curing in cold weather, the removal of formwork and props, the application of post tensioning, etc. These require adequate concrete strength at early ages, if structural elements are to withstand the applied loads.

Nowadays, cement replacement materials such as ground granulated blast furnace slag (GGBS), which is a by-product of iron manufacturing, are commonly used with Portland cement in concrete construction. The use of the two materials in concrete gives many technical benefits, such as improving workability, durability and the long-term strength of the concrete. There are also economic benefits, as GGBS is a waste material and much cheaper than Portland cement. Another benefit of the use of GGBS in concrete is its major reduction of CO_2 emissions compared to Portland cement.

The disadvantage of using GGBS is that the strength development at early age under the standard curing temperature (20^0C) is noticeably slower than that of Portland cement only concrete. Therefore, GGBS is not used for fast track construction, where high early age strength is needed.

However, there are indications that curing the GGBS concrete at elevated temperatures will significantly enhanced the early age strength. The concrete strength is achieved quicker than when it is cured at lower temperatures. Even the higher temperature resulting from the hydration reaction of cement causes the pozzolanic reaction of the GGBS to start earlier. This could lead to considerable enhancement in the early age strength development of GGBS concrete[1-5].

Fast track construction needs concrete with high early age strength, therefore, the factors that affect strength at early ages should be considered such as: mix proportions, cement types, pozzolanic or cementitious additions, the use of admixtures and curing temperature. The amount of GGBS that can be used as the cement replacement material in the concrete is dependent on the required strength at early ages and the curing temperature on site. The contribution of GGBS to the hydration of the total binder content in concrete is needed to be investigated. This can help engineers to determine the levels of GBBS that can be used in the mix design of concrete.

The accuracy of the method of predicting the strength development of concrete on site is needed for designing the mix proportions of concrete to achieve the strength required for fast track construction. Furthermore, it is very important for engineers to optimise the construction schedules. The maturity method is a technique that accounts for the combined effects of time and temperature on the strength development of concrete. This method was developed based on the data of Portland cement concretes. Therefore, is not suitable to predict the strength development of GGBS concretes. This is because GGBS is much more sensitive than Portland cement to the effects of temperature. The method, therefore, needs to be adjusted for GGBS concrete. The activation energy is needed to predict the strength development of concrete using the maturity method. This can be determined according to ASTM C-1074 standard[6].

The heat output obtained from the isothermal calorimeter needs to be assessed for its suitability to be used in modelling the temperature rise history in the concrete. An accurate prediction of the temperature history of the concrete results in more accurate strength prediction.

The problem due to the delayed strength development of GGBS concrete at early age in fast track construction could also be overcome by using precast structural elements, which is made of GGBS concrete. This can reduce the overall

construction programme, where the total construction costs are dependent on the period of the construction.

The ratios of GGBS concrete strengths cured at elevated temperatures to those cured under the standard curing temperature are higher than that of Portland cement concrete. This proves that GGBS concrete is more dependent on curing temperature than concrete with Portland cement only.

The detrimental effect of higher curing temperatures at early age on the later age strength development of GGBS concrete is less than that of concrete with Portland cement only. It is important to find a suitable temperature for curing the concrete under isothermal conditions. This aims to minimise the detrimental effect on the strength development of the concrete at later ages due to the high curing temperature at early age.

1.2. Research Significance

Generally, the construction period greatly influences the total cost of concrete construction. The construction period is generally governed by the minimum required time to remove formwork. The minimum formwork-striking period for a concrete element will depend on: (i) the construction load, which it is expected to withstand, and (ii) the strength development of the concrete element, especially at early ages.

The strength development of GGBS concrete at early age is complicated as its strength mainly depends on the mix proportion of concrete and the environmental conditions under which it is cured. Unfortunately, most of the available information and methods for predicting the strength of concrete were developed based on the Portland cement data. Therefore, when the methods are used to predict the strength development of GGBS concrete, the results are not accurate enough and sometimes led to wrong results. In addition, an accurate method to predict the strength development of GGBS concrete is needed to help contractors

realise the true early age strength development of GGBS concrete. The effects of curing temperature and GGBS content in mixes also need to be assessed.

1.3. Aims and Objectives

The aim of this study is to investigate the early age strength development of concretes made using GGBS that are cured under different temperatures regimes. This will require an assessment of the existing maturity methods to investigate if they can produce an accurate prediction of the strength development of GGBS concrete and other kinds of concrete such as lightweight and self compacted concretes. Modifications to the existing maturity equations are considered when they predict the early age strength of the concrete inaccuracy.

The detailed objectives of this study are as follows:

1. Develop a modified maturity function, which will predict the strength development of GGBS concrete accurately.
2. Investigate the potential and limitations of using GGBS cement replacement for fast track construction in terms of early age strength development.
3. Investigate factors that affect early age strength development of normal and high strength concrete, such as mix proportions, replacement levels of cement with GGBS and casting temperature.
4. Study suitable curing temperatures for GGBS concrete to obtain high early age strength while not affecting the strength development of the concrete at later ages.
5. Investigate the effect of various curing temperatures on the strength development of mortar.
6. Estimate early age strength of GGBS concrete using maturity methods, and examine the suitability of the existing maturity equations developed for Portland cement (PC) to be applied to GGBS mixes.

7. Determine the datum temperature and activation energy of PC and GGBS mortars/concretes cured under isothermal temperatures to predict adiabatic strength using existing maturity equations.
8. Quantify the contribution of GGBS to composite cement hydration in terms of temperature rise and heat output.
9. Model the temperature rise in GGBS concretes with the heat output obtained from isothermal calorimeter, using the Comsol software to predict the temperature rise in concrete. This can then be used to predict the strength development of GGBS concrete.
10. Investigate the strength development of different kinds of concrete such as lightweight and self compacting concrete cured under different isothermal curing temperatures.
11. Assess the accuracy of the maturity methods to predict the strength development on the other kinds of concrete such as lightweight and self compacting concretes.

CHAPTER 2 – LITERATURE REVIEW: Assessment of Early Age of Strength Development of Concretes

2.1. Introduction

This chapter summarises prior work on assessment of strength development of concrete at early and later ages. This includes the mechanical properties of the normal weight concrete using GGBS, lightweight concrete and self-compacting concrete such as mix proportions and factors affecting the strength development of the concretes, which are needed to predict the strength development of the concretes. The accurate prediction of concrete strength on site is very important; as it enables engineers in taking decisions to accelerate the construction schedules.

Furthermore, the effect of thermal properties of concrete on predicting strength development of concrete is also discussed in conjunction with a finite element formulation.

2.2. Strength Development of Concrete

2.2.1. Strength Development of Concrete at Early Ages

Strength development and mechanical properties of concrete at early age is very important. Carino, N.J., et al.[7], pointed out that there are two factors, which have contributed to this redirection of interest i.e. fast track construction and to introduce concrete to significant structural loads at early ages. The recognition that long-term performance of concrete is seriously affected by its early-ages history is needed such as the effect of excessive loading at early age.

Bergstrom and Byfors[8] stated that there is no exact definition of the concept of early age. However, it is commonly known that the properties of concrete during the first two days after casting are crucial. Furthermore, they explained that time is not the best parameter, when trying to term early age. As different cements, curing temperatures and admixtures result in quite different rates of hydration

consequently result in quite different properties of the concrete at early age, even though the mix proportions are the same.

Furthermore, Carino, N.J., et al.[7] attempted to define the early age as the period during which the properties of concrete change rapidly. This usually happens during the period before the degree of hydration was less than 50%. However, it is difficult to assign a single quantity to this age, as the rate of hydration is highly dependent on the chemical and physical properties of the cement, particle size distribution of cement or binder, water-cement ratio, supplementary cementitious materials, chemical admixtures and curing temperature[9]. It is approximately 50% of the cement (Type I) in Portland cement concrete cured at standard curing temperature (20^0C), will hydrate within three days. On the other hand, concrete with high replacement levels of GGBS will take a longer time to achieve hydration degree of 50%.

Recently, Glisic and Simon[10] considered the early age as the period, which begins at pouring and finishes when the thermal processes in concrete terminate. Furthermore, Reinhardt[11] used the term "young" concrete for early age concrete, which is defined as the period from one to seven days. During this period, the concrete skin is expected to develop, which means the concrete is strong enough to against weathering, erosion and other attacks. The concrete has started exhibiting durability already.

2.2.2. Strength Development of Concrete at Long-Term Ages

The strength of concrete is usually categorized by the strength at the age of 28-days. The strength of concrete however, is continuously developed at the age later on. The strength of concrete at later age is important to know, particularly when a concrete structure is subjected to a certain type of loading at later age[12, 13].

Many researchers[13-25] found that the use of supplementary cementing materials such as FA, GGBS, silica fume, etc. and their combination, as a part of cement replacement in concrete, could improve the performance of both fresh and

hardened state, such as the workability, strength and durability of concrete. It is important that concrete structure should continue to perform its function during the service life of the structure. It means the concrete's required strength and serviceability should be maintained during the time. The performance of concrete against all the attacks is called durability.

In 2006, Gonen and Yazicioglu[14] point out that the performance of concrete mixes is determined by short and long-term age tests, which includes compressive strength, porosity, capillary absorption, carbonation, etc. Furthermore, they concluded that the use of silica fume in concrete could significantly improve the strength of the concrete; it can also improve the performance of the concrete against carbonation, the capillary absorption and other deteriorations due to severe environment, where the concrete was placed. Although FA contributed slightly to the compressive strength in comparison to silica fume, incorporating silica fume can improve both the strength and the performance of the concrete.

In 1992, Wood[26] carried out an experiment to evaluate the long-term properties of concrete with Portland cement only. He investigated the compressive strength, flexural strength and modulus of elasticity of concrete during five and 20-years for air and moist curing conditions respectively. He found that there was a slight difference between the strength of the specimens cured in a moist room and the specimens stored outdoors. The ratio of the strength of specimens stored outdoors to the strength of specimens cured in moist-room is from 0.8 to 1.0[26, 27]. The strength of concrete cured in environments of low relative humidity did not increase considerably after 28-days age.

However, the results of flexural strength test show that it is very dependent on the moist curing, where the strength of specimens cured in the condition are higher than that of those cured in dry conditions (difference 20 to 30%). The dynamic measurements of the modulus of elasticity are also sensitive to the quantity of moisture in the samples. For the moist samples, the modulus of elasticity

increased with time, however, it became almost stable after the drying process was started.

A strength development of concretes over a period of 20 years with water/cement ratios of 0.4, 0.53 and 0.71 made with type I cement in 1948 presented in Figure 2.1. The figure shows that as long as concrete is kept wet, the strength of concrete continues to develop with time.

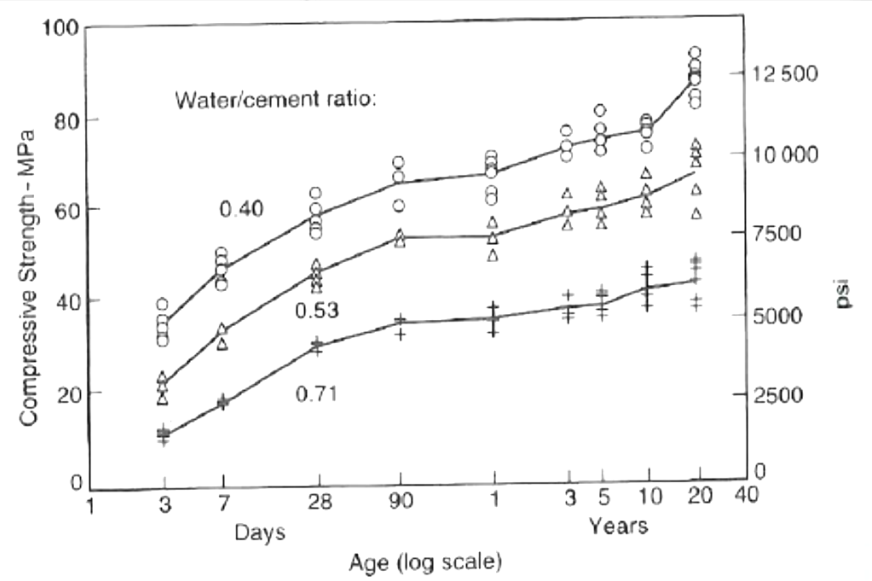

Figure 2.1: Development of strength of concrete (determined on cubes with size of 150 mm) over a period of 20 years under moist conditions[12, 26]

2.2.3. Concrete Compressive Strength

In practice, other properties of concrete such as durability, impermeability and volume stability may in fact be more important. However, the compressive strength, which is the maximum load per unit area that can be carried by concrete, is normally considered as the most valuable property of concrete[28]. It is due to the strength of concrete being directly related to the structure of cement paste; therefore, it usually presents an overall picture of the quality of concrete.

The compressive strength is given by the equation:

$$f_c = \frac{F}{A_c} \qquad \text{Equation 2.1}$$

where: f_c = compressive strength (MPa)

F = maximum load at failure (N)

A_c = cross-sectional area of the specimen on which the compressive force is applied (mm^2).

Factors that can affect the accuracy of measurement of compressive strength are loading rate and end condition[29]. Generally, the lower the rate of loading, results in the lower the measured compressive strength is. It can describe the fact that it requires time to develop the deformation, which was generated by loading. Under slow rates of loading, more subcritical crack growth occurs, which leads to the formation of larger flaws and result in a smaller loading. The slower loading rates result in more creep that will increase the amount of strain. When the maximum value of strain is reached, the cube specimen will fail. Therefore, to obtain a comparable compression results, the ASTM standard[30] controls the loading rate for a cylinder specimen of 0.15 – 0.35 MPa/sec as, while the British European standard[31] requires 0.6 ± 0.2 MPa/sec for a cube specimen as the standard loading rates.

In performing compressive strength testing, it is assumed that both the ends of specimens are in pure uniaxial compression condition. However, this is not really the case, as both the ends of the specimen have contact with the platens of the testing machine. As a result, friction forces occur between the platens of the testing machine and the specimen. Furthermore, the platens restrain the lateral expansion of the ends of the specimens, which allows shear stress to occur. In addition, the effect of the ends restraint can result in an apparently higher reading than the pure compressive strength of the specimen.

2.2.4. Strength Development of GGBS Concrete

The effect of the chemistry of clinker on the early strength development in GGBS concrete was investigated by Gee[32]. He reported that the way in which the clinker liberates calcium and alkalis, influenced the hydration rate at early age of

the composite clinker of cement and GGBS. Siddiq[33] added that the GGBS reacts with water in alkali environment and then reacts with calcium hydroxide released from cement hydration through pozzolanic reaction to form extra C–S–H gel in the paste.

As discussed earlier, the hydration product $Ca(OH)_2$ activates the GGBS hydration of a mixture of low CaO/SiO_2 ratio C-S-H and AFm phases. Pozzolanic reaction can increase the C/S ratio to a value of about 1.7 in GGBS-cement composite due to unstable low calcium C-S-H and $Ca(OH)_2$[33, 34].

Hogan and Meusel[35] reported that the compressive strength of concrete containing 40-60% GGBS was slower than that of Portland cement concrete of the same water-binder ratio for the first three days. However, they further reported that the strength development of GGBS concrete after three days was higher than that of concrete with Portland cement only, especially for concrete with 40% GGBS. Roy and Idorn[5] also reported similar results. They reported, however, that the advantage in strength of concrete comprises 20–60% GGBS has not been obtained yet until 28-days of curing, where similar or higher long-term strength was gained as compared with that of concrete with Portland cement only.

It is similar to that work reported by Barnett et al (2005)[36], Aldea et al. (2000)[37], Hwang and Lin, (1986)[38], and Miura and Iwaki, (2000)[39]. Barnett et al[36] concluded that under standard curing temperature, the strength of GGBS concrete is developed more slowly than PC concrete; however, they achieved similar strength at age 28-days. They further concluded that the level of cement replacement has little effect on the strength at 28-days and it appears that the 28-days strength is most affected by the water-binder ratio.
In 2006, Barnett et al[40] reported that the strength development of mixtures containing GGBS is greatly dependent on temperature. They found that under standard curing conditions, GGBS mortars gain strength much slower than that of mortars with Portland cement only. However, at higher temperatures, strength development of GGBS mortars is much more rapid. The improvement in early age

strength is more significant for mortars with higher levels of GGBS, even when the curing temperature increases by 10^0C only above the standard curing temperature.

Similar with a research, which was conducted by Cakir and Akin[41], they observed the influence of curing conditions on the compressive strength of mortar with and without GGBS. They found that the temperature and humidity curing significantly influenced the strength of concrete, particularly for GGBS mortar, which takes a longer time for hydration.

Soutsos et al[1] reported on the strength development of high strength concrete mixes containing GGBS. They stated that the early age strength of concretes with the same target mean strength at 28-days and cured at 20^0C are adversely affected by the increasing levels of cement replacement with GGBS. However, the strength of GGBS concrete cured at higher temperature, greatly improved at the early age. They reported that the strength development of GGBS concrete cured under adiabatic conditions is comparable to that of concrete with Portland cement only from age 2-days onward.

Rajamane et al[42], reported on the reduction in compressive strength of high performance concrete (HPC) containing GGBS at earlier age, especially when the concretes were cast in winter time. This might be due to two factors, such follows:

a) Increasing in effective water-cement ratio, which is due to reduce cement content with for the same amount of water in the mixture.
b) Delays in the hydration reaction of GGBS, as the Portland cement hydration products that contribute to the starting time of GGBS hydration, are reduced. The GGBS without activator appears to act as filler only at very early age, when only the cement portion contributes to the strength development.

Regourd[43], Roy and Malek[44] and Reeves[45] reported that GGBS hydration is protected by the formation of a protective film on the surface of GGBS particles. The hydration of GGBS will not occur until the pH of pores solution exceeds the

value of 13.2 and the glass fraction of GGBS is broken down either by hydroxyl ions released in the hydration of cement or alkalis from activator agent or admixtures.

Austin et al[46] and Robin et al[47], conducted researches in the hot climate of countries. They found that when concrete are cast under hot climate conditions, the strength of GGBS concrete obtained could be higher than that of their equivalent Portland cement concretes, if they are adequately cured. Furthermore, they suggested the suitable replacement level of GGBS was 50%, which gave strength higher than that of its equivalent Portland cement concrete. The more detail about the properties of ggbs concretes and mix proportion can be found in Appendix A.

2.3. Lightweight and Self Compacting Concretes

This part is included in the literature review, as one chapter of this thesis discusses the kinds of lightweight and self-compacting concretes. Five mixes of the lightweight concretes and three mixes of the lightweight self-compacting concretes were cast. This aims to investigate the strength development of those concretes cured at different temperatures and to predict the strength development of the concretes using the existing maturity methods. This research was performed through a collaboration project between Liverpool University and Queen University Belfast (QUB).

2.3.1. Lightweight Concrete

ACI committee 213[48] defined the structural lightweight aggregate concrete as a concrete made of the lightweight aggregate as defined in ASTM C-330[49]. The concrete should have the minimum compressive strength of 17 MPa (2500 psi) at the age of 28-days; and have a density between 1120 and 1920 kg/m^3 (70 and 120 lb/ft^3), while the British European standard ranges between 800 and 2000 kg/m^3. The aggregate in the concrete consists of all the lightweight aggregate or the combination of lightweight and normal aggregates. Furthermore, the committee

classified the concrete as a high strength lightweight concrete for those having strength of 41.4 MPa (6000 psi) or greater.

Lightweight aggregate concrete has been used for very long time, even before the Christian era[50]. The Port of Cosa was built in about 273 B.C, which used lightweight concrete made from volcanic materials. The Pantheon was completely constructed in 27 B.C., using concrete with varying density from the bottom to the top of the dome. Furthermore, Roman engineers have very successfully constructed a dome with a diameter of 43.3 m (142 ft) using lightweight concrete[48].

The primary advantages of the use of the lightweight concrete is to reduce the dead load of a concrete structure, which enables an engineer to decrease the size of columns, footings and other structural elements[51]. It is necessary to estimate the total cost of a project particularly when considering using lightweight concrete in a project construction. This is due to the cost per cubic meter of the lightweight concrete usually being more expensive than that of normal weight concrete[48]. However, a significant reduction in the size of the structural elements will decrease the overall cost of the construction. The reduction in the dead load of the structure will also decrease the number of steel bars needed for the reinforcement of the concrete structure.

The lightweight concrete has a low apparent specific gravity because of the lightweight aggregate used. Many researchers reported that the properties of lightweight aggregate by means of type, porosity, absorption, etc. greatly affect the properties of lightweight concrete. Ke, Y. et al.[52] found that the compressive strength and the elastic module of the lightweight concrete made from the lightweight aggregate with a density of less than 1000 kg/m^3; are greatly influenced by the volume fraction of aggregate. On the other hand, the increasing of volume fraction of aggregate which has higher density than that used in the lightweight concrete; decreases the elastic module of the concretes but does not affect the compressive strength.

Swamy and Lambert[53] used Lytag aggregate in their research, which is manufactured from sintered pulverised fuel ash. They reported that the porosity of the aggregate that was used to make lightweight concrete has a significant influence on the behaviour of the concrete. Bai et al[54] used FA, furnace bottom ash and Lytag, which they used to replace Portland cement, natural sand and coarse aggregate respectively. They reported that use of the materials could manufacture lightweight concrete with density in the range of 1560-1960 kg/m^3. Even the replacement of Portland cement by 30% with FA could improve the permeability of the lightweight concrete. Similarly, Lo et al.[55] studied the effects of aggregates properties on the lightweight concrete. They concluded that the strength of lightweight concrete highly depends on the strength of the lightweight aggregate used, hardened paste and the bonding of the aggregates and paste in the interfacial zone.

Cui et al.[56] introduced the term *'shape index'* (Is) and underlined that the shape of lightweight aggregate has a significant influence on the mechanical properties of lightweight concrete. The ratio of the maximum to the minimum dimension of the aggregate is defined as the shape index.

Ramamurthy and Harikrishnan[57] reported the influence of binders on the properties of sintered FA aggregate. They concluded that the binders used did not change the chemical composition, but resulted in an improvement in the properties of aggregates as they affected the microstructure of the aggregates. The microstructure properties of the sintered FA (Lytag) aggregate was changed by heat and polymer treatments to obtain aggregates with better quality in strength, absorption and pozzolanic activity[58, 59].

Lo and Cui[60] investigated the effect of the porous surface of lightweight aggregate on the strength of concrete. They reported that the porous surface of the lightweight aggregate could improve the interfacial bond between the aggregates and the paste. Hence, this enhances the strength of the concrete by providing

interlocking sites for the cement paste forming a dense and uniform interfacial zone.

Kockal and Oztura[61] observed the mechanical properties of lightweight concrete in comparison with its equivalent normal weight concrete. They found that the lightweight concrete had a slightly lower compressive strength than that of its equivalent normal weight concrete. It is believed this is due to the higher porosity and lower strength of the aggregate in the lightweight concrete. Similarly, the modulus of elasticity and tensile strength of the lightweight concrete are slightly lower than that of its equivalent normal weight concrete.

Lo et al.[62] investigated the effect of high curing temperature on strength development of lightweight concrete. They concluded that the strength of pulverised FA and silica fume incorporated in mixes cured at higher temperature was higher than that of those cured under standard curing temperature. Conversely, the strength of the lightweight concrete with Portland cement only cured under standard curing temperature was higher than that of cured at higher curing temperature.

Zhang and Gjorv[63] observed the characteristic of lightweight aggregate for high strength lightweight concrete. They reported that the characteristic of aggregate are more important for the lightweight concrete properties of high strength than that of low to medium strength. Various sources of aggregates mean there are different particle shapes, surface texture and pore structure varied within wide limits. They added that the absorption within 30 minutes had reached more than half of the 24 hours water absorption rate.

For further investigation, Zhang and Gjorv[64] studied the mechanical properties of high strength lightweight concrete. They investigated five different types of lightweight aggregates. They found that the strength of lightweight aggregate emerged to be the main factor controlling the strength of lightweight strength concrete. The compressive strength, flexural strength, tensile strength and the

elastic module of the high strength of lightweight concrete were lower than that of the high strength concrete of normal weight aggregate.

Many researchers investigated the effect of pre-wetting on lightweight aggregate to the mechanical properties of lightweight concrete, which improves the properties of the lightweight concrete[65-67]. Ge et al.[65] found that the dry lightweight aggregate highly absorbed water in the plastic stage of concrete, which leads to the least total pore volume after age 28 days, resulted in low permeability concrete. However, the concrete has less improvement in permeability and interfacial transition zone (ITZ) at the age of 28-days and later on, which accounted for the poor hydrating due to lack of water for continuing hydration. Conversely, the water absorption of pre-wetting lightweight aggregate is lower than that of the dry one. As the result, the concrete has more pores and higher permeability. This is believed to be due the lower rate of hydration at earlier age. Nevertheless, after the age of 28-days, the rate of hydration increases resulting in concrete with less porosity, low permeability, stronger interfacial transition zone and a more durable concrete.

Loudon[68] reported that the thermal properties of lightweight concrete can contribute to the better thermal insulation of buildings. He found that the differences between thermal conductivities of different types of lightweight concrete might be due to the different content of glassy materials in the concrete mixes; as glassy materials have a lower thermal conductivity than crystalline materials. Similarly, Demirboga and Gul[69] studied the thermal conductivity of lightweight concrete. They found that the use of cementitious material as part replacement of cement affected the thermal conductivity of lightweight concrete.
Kockal and Ozturan[70] reported that the permeability of water and chloride ions of sintered FA aggregate concrete were comparable and slightly lower than that of normal weight for cold-bonded FA aggregate concrete. The result of accelerated corrosion test of lightweight concrete is also comparable to that of its equivalent normal weight concrete. Chia and Zhang[71] reported that at the medium strength level (30 – 40 MPa), the water permeability of the lightweight concrete was lower

than that of the corresponding normal weight concrete. However, for the high strength level, they were comparable. For resistance to the chloride ion penetration, the results from either lightweight concrete and normal weight concrete were similar in both the normal strength and high strength levels.

2.3.2. Self Compacting Concretes

Self compacting concrete (SCC), which is also known as self consolidating concrete, is a highly flowable concrete with no segregation that can flow through and fill the gaps of reinforcement and corners of moulds, purely by means of its own weight without any need for vibration and compaction during the pouring process[72-76].

Self-compacting concrete was first introduced in Japan by Okamura in 1986. This type of concrete was proposed in order to overcome a problem appearing in Japan at the time where indicated that there was a reduction in the number of skilled workers in Japan's construction industry for several years since 1983. This problem led to a reduction in the quality of concrete construction in Japan such as a decrease in the durability of concrete, which was due to the poor compaction of concrete. Therefore, Okamura proposed this type of concrete to solve the problem, whereby it was hoped to produce (fairly easy) a more durable type of concrete even though using a less skilled workers [75-77].

Some benefits of the use of self-compacting concrete are as follows[73, 74]:

- Saving in placement costs as it can be placed faster and without mechanical vibration.
- Good architectural finishing, with little or no remedial surface work.
- It is easy to fill a restricted section such as corners of moulds and gaps between reinforcement.
- Labour savings and a shortened construction period.
- Improved compaction around reinforcement and the bond between concrete and reinforcement.

Okamura and Ouchi[76] reported that to obtain the adequate performance of self-compacting concrete, the properties of the concrete should satisfy three stages as follows:

- Fresh stage: the concrete should be self-compactable by its own weight without any need for vibration.
- Early age stage: the concrete should enable the avoidance of initial defects.
- Hardening stage: the concrete should be able to with stand external factors, such as bad weather, chemical attack, etc.

They added that in order to achieve self-compacting concrete, what is needed is both a high deformability of paste or mortar and the resistance of segregation between coarse aggregate and mortar when the concrete flows filling the form. In order to achieve these requirements, therefore, it is needed to limit the aggregate content in the mix, a lower water-powder ratio and the use of a superplasticizer.

The use of self-compacting concrete in real structures has gradually increased since Okamura and Ouchi[78] first developed the prototype of this kind of concrete in 1988. In the UK, Rich et al.[79] reported that after 5 or 6 years from applying the self-compaction concrete in construction industry, it is clear that there has been little progress and there remains a lack of general consensus on self-compaction concrete and its role within the construction process. Skarendahl[80] reported great benefits in the use of self-compaction concrete and will change the conventional casting method, where the concrete will be delivered in the formwork. As a result, there is a significant decrease in the need for concrete workers, which is normally provided by a contractor. The business organisation of in-situ concrete seems to be similar to that of precast concrete construction, where one single business unit would handle all the processes of material design, mixing, delivery, casting and curing.

Rilem report 188[81], Khayat[82] and EFNARC[83] report that the workability of self-compacting concrete should satisfy the properties as follows:

- Filling ability – the ability of the self-compacting concrete to fill the form, into which it flows by its own weight.
- Passing ability – the ability of the self-compacting concrete to flow through obstacles, such as narrow sections due to dense reinforcement without blocking as the result of interlocking between coarse aggregates.
- Segregation resistance – ability of the self-compaction concrete to maintain its homogeneity and cohesiveness during mixing, transportation and the placing of the concrete.

To ensure that the self-compacting concrete satisfies the requirements above therefore it is necessary to reduce the content of coarse aggregate, as was suggested by Okura and Ouchi. This aims to reduce the energy needed due to blockages that happen between aggregate particles when the concrete flows. The blockages will increase internal stress and consume much more energy in order to flow smoothly. Therefore, a reduction in aggregate content produces concrete that is more flowable. The blockages that are due to either interlocking between coarse aggregate or dense reinforcement also can be minimised by providing a highly viscous paste.

Jawahar et al.[84] concluded that the blended coarse aggregate and coarse aggregate content affect the unit weight, modulus of elasticity, and tensile strength of self-compaction concrete, but not influences the compressive strength of the concrete. For a given coarse aggregate content and strength, the higher volume of the maximum size of coarse aggregate results in the higher value of the unit weight, modulus of elasticity and tensile strength of the self-compacting concrete mixes. In another report, Jawahar et al.[85] added that when the coarse aggregate content has to be increased, the volume of maximum size aggregate has to be reduced in a given blended coarse aggregate content. Conversely, when the volume of maximum size aggregate has to be increased, the coarse aggregate content has to be reduced. It can be concluded that a change in the blended coarse

aggregate proportion has a significant effect on the fresh properties of self-compaction concrete.

Gesoglu et al.[86] investigated the properties of self-compaction concrete incorporating mineral admixtures such as FA, GGBS and silica fume as a partial replacement of Portland cement; where the mineral admixtures were blended to follow the binary, ternary and quaternary systems. They found that incorporating the mineral admixtures increased the filling and passing ability of the self-compacting concrete.

Ravindrarajah et al.[87] reported that the part replacement of fine and coarse aggregate with FA could improve the flow property and reduce segregation potential in producing high-strength self-compacting concrete without affecting the early age strength. They added that the addition of FA in self-compacting concrete even increases the later age strength.

Bouzoubaa and Lachemi[88] investigated the strength development of self-compaction concrete incorporating a high volume of class F FA. The content of cementitious materials was kept constant (400 kg/m^3), while the water-binder ratio ranged from 0.35 to 0.45. The cement replacement of 40, 50 and 60% by class F FA was applied for self-compaction concrete mixes. They found that the higher the level of cement replacement, the lower the strength gain, however all mixes achieved the targeted mean strength at age 28-days, except for cement replacement of 60% by FA for water-binder ratio of 0.45 and 0.40, where their strengths were lower than that of control mix.
Boukendakdji et al.[89] reported that addition of GGBS as partial replacement of cement in concrete can improve the workability of the concrete. They found that the replacement of cement with GGBS of 15% could improve the workability up to 20% over concrete with Portland cement only.

Ye et al[90] and De Schutter, G.[91] investigated the use of limestone powder as a filler in self-compaction concrete. They found that the presence of limestone

powder in self-compaction concrete influences the heat output of hydration in the concrete. The cumulative heat release in self-compaction concrete containing limestone powder is higher than that of its equivalent concrete mix without limestone powder. The effect of limestone powder on the hydration of cement is primarily to accelerate the hydration process. De Schutter added that in the case of cement used in the mix containing higher C_3A content, a new hydration peak could be occurred in the hydration.

The effect of superplasticizers on the properties of self-compaction concrete has been investigated by many researchers[92-94]. They found that it could improve the workability of the concrete. Boukendakdji et al[95] observed two types of superplasticizers namely: polycarboxylate and naphthalene sulphonate that they used in self-compaction concrete mix. They found that the concrete, which used the polycarboxylate superplasticizer, had more workability than that of concrete using naphthalene sulphonate.

In the work reported by Sahmaran et al.[96]; the effect of superplasticizer and viscosity modifying the admixture on the self-compaction mortars, which is incorporated mineral additives, was investigated. They found that the workability of the mortars using mineral additives highly depended on the type of superplasticizer used. They added that the workability of the mortars could be improved by adding mineral additives into the mortar mixes.

Lightweight aggregates have been used in production self-compaction concrete; where it can give benefits such as reduced dead loads, high insulation capacity, improved durability and improved resistance to fire and chemical attack. It shows clearly the contrast, between the characteristic of the aggregate such as low density (has low dynamic energy of the mixture during flow) and self-compactness (it depends on dynamic features of the mixture); which causes the application of the materials for self-compaction concrete undesirable[97]. However, the experiences gained from previous works that were using the material, verify

that a good design and an appropriate method of production the material, can overcome the challenge of producing high quality concrete.

Kim et al.[98] investigated the characteristic of self-compaction concrete using two different coarse aggregates. They found that the increase of the density of lightweight aggregate used in concrete mix, decreased the flowability and improved the segregation resistance ability of the concrete; nevertheless, the difference in density of both the lightweight coarse aggregates did not influence the filling ability.

Wu et al.[99] studied on the workability of self-compaction concrete using lightweight aggregate by varying the proportion of fine and coarse aggregate and binder. They concluded that the increase of binder result in an increased workability but decreased the segregation resistance ability of the concrete.

Rahman et al.[100] investigated the effect of the mixing time on the properties of self-compaction concrete. They found that the increase of mixing time resulted in the increase in the amount of water added for maintaining the concrete still in the flowable stage. Their experimental results showed that by adding more water, the porosity and permeability of the concrete obtained increased.

2.4. Maturity Method – History and Application

2.4.1. Introduction

The age and temperature history of a given concrete mixture, which has been duly placed, compacted and cured, are two parameters of a function of the strength of the concrete. At early age, curing temperature has a great effect on the strength development of concrete. This temperature dependence creates problems in attempting to predict the in-situ strength of concrete based on strength development data gained under standard laboratory conditions. In around 1950, the combined effects of the two parameters on strength gain were measured by means of a maturity function, which was proposed to estimate the strength development of concrete[101].

2.4.2. History and Development of Maturity Method

2.4.2.1. Nurse-Saul Maturity Function

The development of maturity concept started when some papers dealing with accelerated curing method that carried out in England were published in the late 1940s and early 1950s[101]. In 1949, McIntosh[102] reported the procedures of his proposed method to estimate the strength development of concrete, during electrical curing. He compared the strengths of concrete cured under normal condition to that of concrete cured at elevated temperatures under electrical curing. McIntosh was probably the first to develop a parameter in 1949, which he called *'basic age'*, to combine the influence of temperature and time. He concluded that the combination of time and concrete temperature above a datum temperature of -1.1^0C could be used to measure the effects of curing temperature history.

A few months after, Nurse[103] reported on the effects of steam curing on concrete strength gain. He agreed with McIntosh that the combinations of time and temperature could be used to quantify the effect of different steam-curing cycles on the strength gain. However, he did not use a datum temperature in calculating his predicted strength, as McIntosh did. Nurse also did not take into account the actual concrete temperatures, but used chamber-curing temperatures instead. In order to compare the combination influence of the time and temperature on the compressive strength of different concrete mixtures investigated, Nurse expressed the strength as a percentage of strength after the age of 3-days of concrete cured at normal condition (moist air - 18^0C). The resulting percentages were then plotted

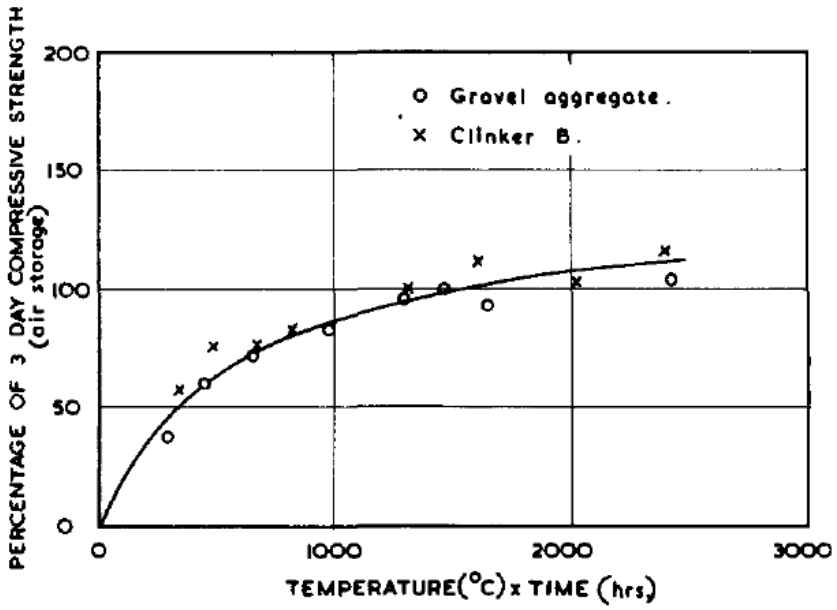

Figure 2.2: Strength development vs. the product of time – temperature (non-reactive aggregate)[103]

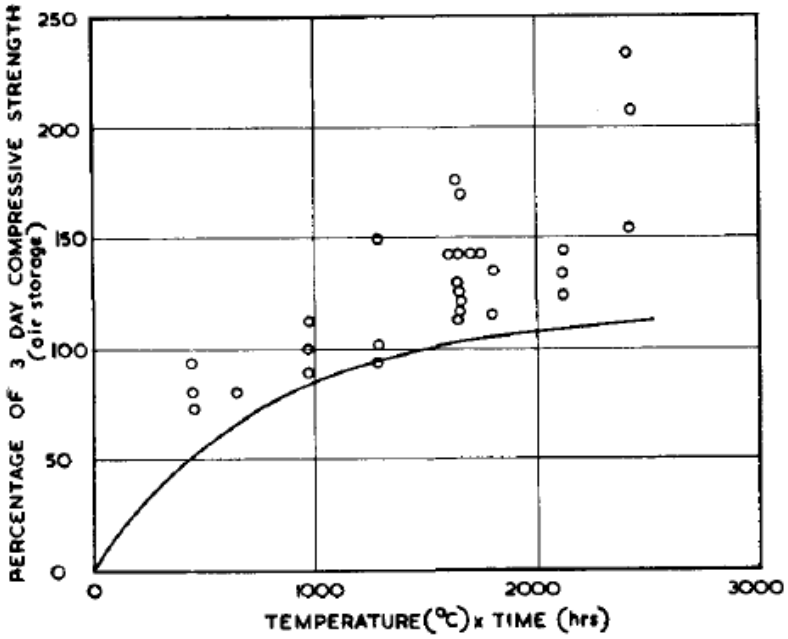

Figure 2.3: Strength development vs. the product of time – temperature (reactive aggregate)[103]

against the product of time and temperature as are presented in Figure 2.2 and Figure 2.3 for the non-reactive and reactive aggregates respectively, which produced a single non-linear curve. He then suggested using the curve to estimate

the strength of concrete cured at other temperatures. This was the first evidence that showed that strength development of concrete could be approximated from the two factors of time and temperature.

In 1951, Saul[104] summarized the conclusion that was obtained from experimental work carried out both at the Cement and Concrete Association Research Station and others regarding the principles of underlying steam curing at atmospheric pressure. He introduced the term of *'maturity'* for the first time and linked it as an indicator of strength gain, dependent on the product of concrete time and temperature. Furthermore, he suggested that the maturity should be determined with respect to a 'datum temperature', which is below the temperature, the hydration process then will cease and no strength be obtained. He recognized that once concrete has set, the strength of concrete would be continuously developed even with temperatures lower than the freezing point, 0^0C (32^0F). Thus, he suggested taking a value of the datum temperature of -10.5^0C (13^0F) to be used in determining the maturity of concrete[101]. In 1956, McIntosh[105] confirmed in his paper that the value of a datum temperature of -10^0C could be better than that of the value he previously proposed.

Saul (1951) then proposed the 'maturity rule' as the following[106]:

> ***"Concrete of the same mix at the same maturity (reckoned in temperature-time) has approximately the same strength whatever combination of temperature and time go to make up that maturity."***

The Nurse-Saul maturity function is defined as follows[6, 101]:

$$M = \sum_0^t (T - T_0)\ \Delta t \qquad \text{Equation 2.2}$$

where:

M = maturity or the temperature-time factor at age t (^{0}C.days or ^{0}C.hours)

t = elapsed time or concrete age, days or hours

Δt = a time interval, days or hours

T = average temperature of the concrete during time interval, Δt, ^{0}C

T_0 = datum temperature

Saul found that the maturity method function would give an accurate result when it was used to estimate the strength of the concrete, which had a temperature that did not reach 50^0C in the first two hours or about 100^0C within the first 6 hours after mixing[101].

The principle of the maturity method can be used to determine the strength development of a given concrete mixture cured at different temperatures. Therefore, when the concrete is cured in either cold or hot conditions, the maturity should be the same and the strength of the concrete can be predicted accurately. Figure 2.4 illustrates the maturity concept for concrete that is cured at different temperatures such as at lower and higher temperatures. When the concrete is cured at lower temperature, it will take a longer time than that of cured at higher temperature to reach the same level of maturity.

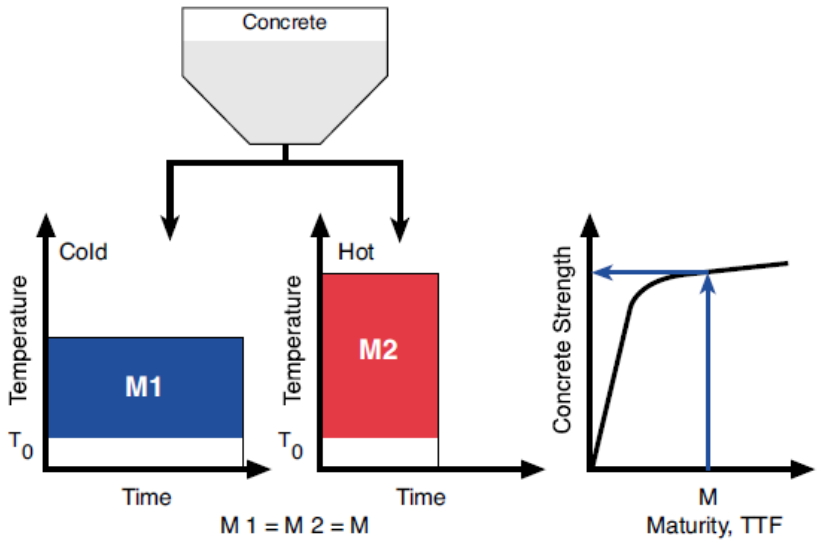

Figure 2.4: Saul's maturity rule using temperature-time factor[107]

Kehl et al.[107] illustrated the maturity rule through the figure above. They found that when the same concrete mixture was cured in both cold and hot conditions, it would reach the same maturity when the temperature-time areas were equal, as shown in the figure M1 = M2 = M. It is clear that the concrete will reach a certain maturity much quicker in hot curing conditions than that of in cold curing

conditions. Therefore, the time needed to reach the maturity of the two curing conditions will be different as well.

2.4.2.2. Weighted Maturity Function

In 1979, De Vree and Tegelaar[108] proposed a maturity method called 'weighted maturity' based on the study carried out by the French researchers Papadakis and Bresson[109]. The Weighted Maturity method can be mathematically expressed as the following equation and is further illustrated in Figure 2.5 [110]:

$$M_w = \sum t_k \,.\, T_k \,.\, C^{n_k} \qquad \text{Equation 2.3}$$

where:

M_w = weighted maturity, (^{0}C.hous)

t_k = hardening time of concrete, corresponding to (Ti – Tj)/2, (hours)

T_k = hardening temperature interval, (Ti – Tj), (^{0}C)

n_k = temperature dependent parameter for T_k

C = cement dependent constant for which the strength-maturity curves for the isothermal strength tests coincide, C – value of cement

For a given temperature history and type of cement that is used in concrete, the area under the temperature-time curve can be subdivided into a small section of area of t_k x T_k. This maturity method appears exactly as the same as that proposed by Nurse-Saul. Similar to Nurse-Saul maturity function, the datum temperature is taken -10 ^{0}C as well. The effect of cement on maturity is taken into account by applying C-value. If the reference temperature is taken as 20^{0}C, therefore, the parameter n is equal to 1.0. The parameter is then taken as positive if the hardening temperature of concrete higher than 20^{0}C, and taken as a negative value if the hardening temperature is lower than 20^{0}C. The weighted maturity can be got by recapitulating the area of each small part t_k x T_k multiplied by C-value.

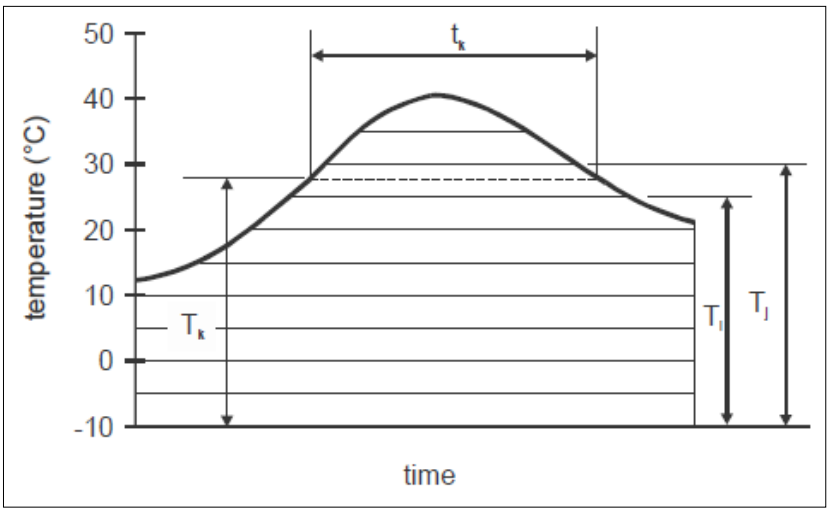

Figure 2.5: Time-temperature product – the Weighted maturity concept[110]

The C-value obtained from experimental work using strength test results from at least 10 cubes of 150 mm. The C-values is provided in the CUR – Recommendation[111]. The *n – value* can be calculated using the equation[110, 112]:

$$n = 0.1\,.T - 1.245 \qquad \text{Equation 2.4}$$

Thus, the Equation 2.3 can be written as follows:

$$M_w = \sum \Delta M_w\,.t \qquad \text{Equation 2.5}$$

where

$$\Delta M_w = \frac{10\,[\,C^{0.1\,T-1.245} - C^{-\,2.245}\,]}{ln\,C}\;\Delta t \qquad \text{Equation 2.6}$$

In practice, usually the time interval Δt is taken as one hour, and the average temperature in this time interval *T* is recorded.

The advantages of this method in comparison to the Nurse-Saul maturity function is that this method takes into account the effect of the type of cement and temperature on the hydration of cement. The effect of the type of cement is considered by means of the C-value, while the effect of temperature on the maturity is considered by using the n_k parameter.

2.4.3. Equivalent Age Concept

In 1954, Rastrup[113] firstly introduced the concept of equivalent age based on Saul's work, where he called it '*temperature-time factor'*. ASTM standard C 1074 – 98[6] defines the equivalent age of a concrete mixture as 'the time that is required to cure the concrete at a reference temperature after casting, in order to attain a maturity index, which is equal to that of obtained from the same concrete, cured at temperature other than the reference temperature during a time interval, '*Δt*.'

2.4.3.1. Nurse-Saul Equivalent Age

Based on Equation 2.2, the equivalent age at the reference temperature according to the Nurse-Saul maturity function can be mathematically expressed as follows:

$$t_e = \frac{\sum(T - T_0)}{(T_r - T_0)}\ x\ \Delta t \qquad \text{Equation 2.7}$$

where

t_e = equivalent age at the reference temperature

T_r = reference temperature, usually is taken as 20 ^{0}C

Equation 2.7 can be written as follows:

$$t_e = \sum \beta\ \Delta t \qquad \text{Equation 2.8}$$

where:

$$\beta = \frac{(T - T_0)}{(T_r - T_0)} = \frac{k}{k_r} \qquad \text{Equation 2.9}$$

β = the age conversion factor.

k = rate constant at temperature T

k_r = rate constant at temperature T_r

The age conversion factor can be used to convert a curing period Δt at curing temperature T, t_e the equivalent curing period at the reference temperature T_r. The age conversion factor is a linear function of the curing temperature. In 1953, Bergstrom[114] applying the Nurse-Saul maturity function to estimate the strength

of a given concrete mix at varying ages and curing temperatures, he found that the maturity method was applicable for concrete cured at normal temperatures. At high curing temperatures, he found that there was an optimum temperature, which corresponded to a maximum final strength. As a result, the age-conversion factor could not be applied in such a case.

2.4.3.2. Rastrup Equivalent Age

Rastrup[113] suggested a method to calculate the equivalent age, using the following equation:

$$t_e = \sum 2^{(T - T_r)/10}\, \Delta t \qquad \text{Equation 2.10}$$

His work based on a concept that was well known as an axiom from physical chemistry, which stated the rate of reaction is double if the temperature at which the reaction is occurring is increased by 10 ^{o}C.

2.4.3.3. Weaver-Sadgrove Equivalent Age

In 1971, Weaver and Sadgrove[115] proposed a method to calculate the equivalent age for Portland cement concrete, which can be expressed as follows:

$$t_e = \sum \left(\frac{T+16}{T_r+16}\right)^2 \Delta t \qquad \text{Equation 2.11}$$

Few years later, Harrison[116] verified the equation by applying it to the assessment of the risk of mechanical damage to concrete due to the early removal of formwork. However, he verified that the concrete cured in the temperature ranging from 7 – 27 ^{0}C. Furthermore, Clear[117] and Wimpenny and Ellis[118] proved that the equation was applicable to estimate the strength of GGBS concrete for a range of GGBS levels. It was reported that the Weaver and Sadgrove method gave a reasonably good result of the strength estimates at low maturity compared to that of the Nurse-Saul function. However, Sadgrove[119] reported that at later maturities, the Nurse-Saul function was more accurate than that of the Sadgrove and Weaver equation.

2.4.3.4. Arrhenius Equivalent Age

In 1960, Copeland et al.[120] proposed that the Arrhenius equation could explain the effect of temperature on the early age rate of hydration. The Arrhenius equation can be written as follows:

$$k_T = Ae^{-\left[\frac{E_a}{R\,(T+273)}\right]} \qquad \text{Equation 2.12}$$

where:

k_T = rate constant, days^{-1} or hours^{-1}

A = constant, days^{-1} or hours^{-1}

E_a = apparent activation energy, J/mol,

R = universal gas constant, 8.314 J/mol K,

T = average temperature of the concrete during interval Δt, ^{0}C

Later, Freiesleben Hansen and Pedersen[121] proposed a method that was developed based on the Arrhenius equation to calculate the equivalent age in the following equation:

$$t_e = \sum_0^t e^{-\frac{E_a}{R}\left[\frac{1}{273+T}-\frac{1}{273+T_r}\right]}\Delta t \qquad \text{Equation 2.13}$$

where:

t_e = the equivalent age at the reference temperature, hours or days

E_a = apparent activation energy, J/mol,

R = universal gas constant, 8.314 J/mol K,

T = average temperature of the concrete during interval Δt, ^{0}C

T_r = reference temperature, ^{0}C

Thus, the age conversion factor can be calculated using the following equation:

$$\beta = e^{-\frac{E_a}{R}\left[\frac{1}{273+T}-\frac{1}{273+T_r}\right]} \qquad \text{Equation 2.14}$$

The age conversion factor is an exponential function and is expressed in terms of the absolute temperature, ^{0}K. The equation above clearly shows that the age

conversion factor with a certain temperature greatly influenced by the value of activation energy, which is used as shown in Figure 2.6.

Byfors[122] and Naik[123] proved that over a wide range of temperature, the maturity-strength relationships obtained from the Arrhenius equation, is more reasonable good than that of the Nurse-Saul function.

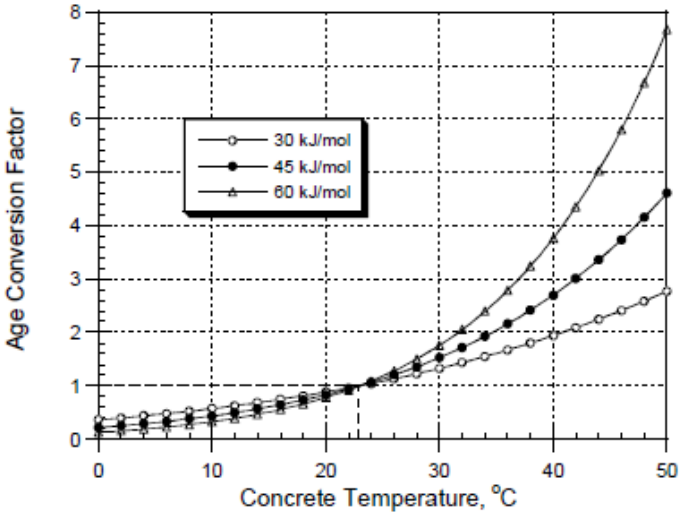

Figure 2.6: The influence of activation energy on the age conversion factor based on the Arrhenius equation (Equation 2.14)[106]

Figure 2.7 shows the effect of temperature on the age conversion factors of different maturity functions. It appears that there is a good agreement among all the maturity methods presented for the curing temperatures between 5 and 25^0C. However, the age conversion factor of all the maturity methods; are considerably different when the concrete is cured at elevated temperatures, i.e. higher than 25^0C. Furthermore, the value of activation energy that is used to calculate the age conversion factor, has a significant effect on the Arrhenius age conversion factor at temperatures that higher than 25^0C.

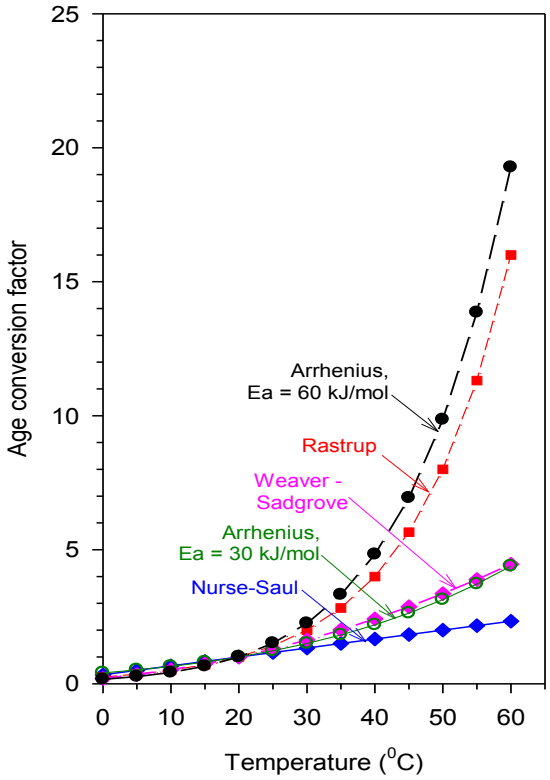

Figure 2.7: Age conversion factors vs. temperature

The age conversion factors (β) that are calculated using both the Weaver-Sadgrove and Arrhenius functions are comparable, when the activation energy of 30 kJ/mol is applied to calculate the age conversion factor using the Arrhenius equation. However, using higher activation energy to determine the age conversion factor gives a huge difference in the value of the age conversion factor and the relationship between the age conversion factor and curing temperature becomes more nonlinear[101].

In 1962, Alexander and Taplin[124] investigated whether the strength gain of concrete followed the maturity rule when the concrete was cured at different temperatures. They found that at low maturities, concretes that were cured at a higher temperature had a higher strength than that of cured at lower temperature. Conversely, at later maturities, concrete cured at a high temperature results in lower strength. This implies that the strength-maturity curve for a specific curing temperature regime at a certain maturity crosses the respective curve for a higher

temperature-curing regime. This is generally called as the *"crossover effect"*, which was introduced by Verbeck and Helmuth[125] in 1968, as is illustrated in Figure 2.8.

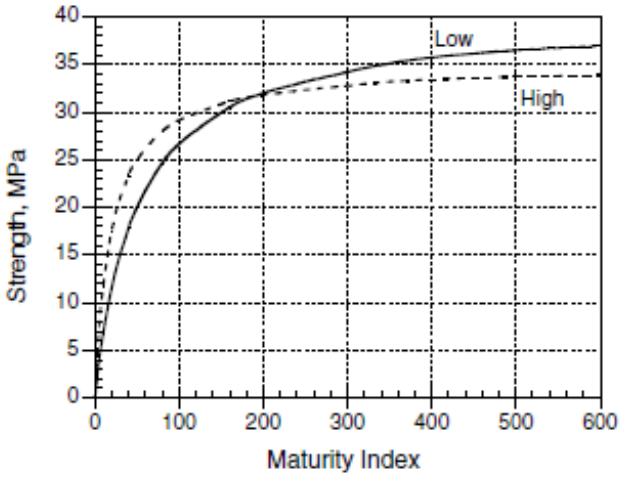

Figure 2.8: The effect of early-age curing temperature on the strength-maturity relationship[101].

Verbeck and Helmuth[125] added that there was a rapid strength development at early age. However, the products of the reactions did not have enough time to be uniformly distributed within the pores of the hardening paste. As a result, 'shells' formed of low permeability surrounded the unhydrated cement grains. Un-uniformly distributed of the hydration products leads to more large pores, which reduces the strength of concrete. The shell obstructs continuous hydration of the unreacted cement at later ages. Therefore, the lower strength at later age of concrete cured at high temperature at early age is believed due to the unreacted cement cannot continue the process of hydration. It is caused water that needed for the hydration of cement cannot reach the unreacted cement as it is hindered by a low permeability shell[40].

The explanation that is given by Verbeck and Helmuth[125] clearly identify the effect of curing temperature at very early ages on the strength development of concrete, especially in the inner structure of concrete. The inner structure of concrete is very important to the strength development at later ages and the durability of the concrete.

A few years later, Hudson and Steele[126, 127] continued investigating the relationships between strength, age and curing temperature. They proposed maturity method to estimate the 28-day strength of concrete based on the results of the tests at early age. Moreover, their results were later included in ASTM standard[128].

2.4.4. Strength-Maturity Relationships

ASTM C-1074[6] provides a procedure to develop the strength-maturity relationship. The mix proportions and constituents of the concrete should be the same to those of the concrete whose strength will be predicted. According to the standard, it is required to prepare at least 15 cylindrical specimens. Two specimens are needed to connect to a temperature sensor embedded in the centre of the specimens for recording the temperature inside the specimens.

The compressive strength should be performed at ages of 1, 3, 7, 14 and 28 days. Once the maturity index or temperature-time factor has been calculated based on the temperature history of the concrete, the next stage then is to develop the relation between the maturity and strength of the concrete by plotting them as presented in Figure 2.9. The curve obtained is the strength-maturity relationship of the concrete that will be used for estimating the strength of the concrete mixture cured under other temperature conditions.

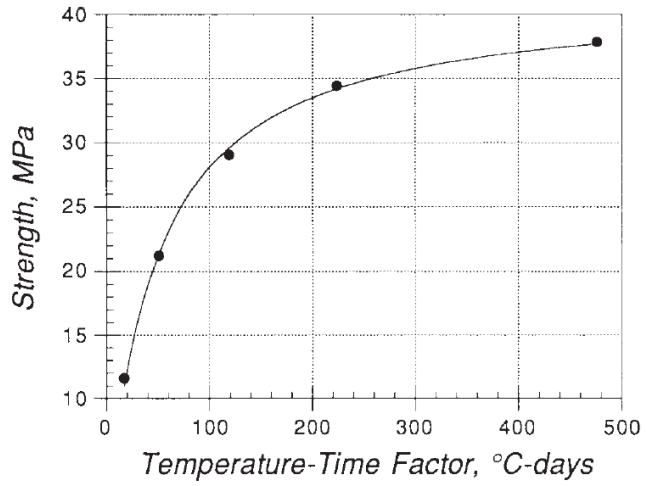

Figure 2.9: Strength-maturity relationship[6]

2.4.4.1. Nykanen method

In 1956, Nykanen[129] proposed the strength-maturity relationship, which can be written as follows:

$$S = S_{\infty}\,(1 - e^{kM}) \qquad \text{Equation 2.15}$$

where:

S = compressive strength (MPa)

S_{∞} = limiting compressive strength (MPa).

M = maturity index or temperature-time factor, (^{0}C.hours or ^{0}C.days)

k = a constant

Nykanen suggested that the value of k is expected to rely on the water-cement ratio and the type of cement, while the limiting compressive strength will be greatly dependent on the water-cement ratio.

2.4.4.2. Plowman Method

Also in 1956, Plowman[130] observed that when plotted the strength data as a function maturity calculated following Nurse-Saul maturity function, the data fell very close to a straight line. Therefore, he proposed the strength-maturity relationship that could be mathematically written as follows:

$$S = a + b\,log\ (M)$$ Equation 2.16

where:

a, b = constants obtained from linear regression

The constants a and b depend on the water-cement ratio of the concrete and the type of cement used in the concrete. This strength-maturity equation led to a controversial discussion regarding its limitations. It is clearly shown from the equation that, as the maturity of concrete continuously increases the strength gain also continues to increase. Another weakness of Plowman's equation is his assumption that there is a linear relationship between the strength and the logarithm of maturity index at very early maturities, which obviously is not true. The linear relationship between the strength and the maturity occurred at approximately intermediate maturity values.

2.4.4.3. Bernhadt Method

In 1956, Bernhardt[131] developed his strength-maturity relationship as a hyperbolic function. Goral[132] proposed the strength-maturity relationship, which is similar to that of Bernhardt, proposed to depict the strength development of concrete with age at a constant temperature. The equation was adopted by the ACI Committee 209[133] to predict the strength at different ages. In 1971, Chin[134] proposed the same relationship and prepared the procedure to predict the strength of concrete using the equation, which can be written as follows:

$$S = \frac{M}{\frac{1}{A} + \frac{M}{S_\infty}}$$ Equation 2.17

where:

A = initial slope of strength-maturity curve.

The equation was developed based on the assumption that the rate of strength development at any age was the function of the strength and temperature at that age, as shown in Figure 2.9.

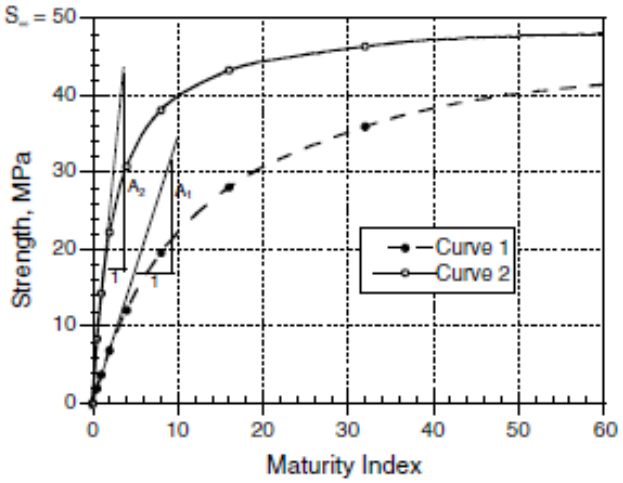

Figure 2.10: Hyperbolic strength-maturity relationship with the same limiting strength, although their initial slopes different[101]

The value of the initial slope controlled the shape of the strength-maturity curve. Figure 2.10 presents two curves that follow Equation 2.17; however, they have a different initial slope. Therefore, Bernhardt converted the hyperbolic equation (Equation 2.17) into a linear equation, which can be written as follows:

$$\frac{1}{S} = \frac{1}{S_\infty} + \frac{1}{A} \, x \, \frac{1}{M} \qquad \text{Equation 2.18}$$

Plotting the inverse of limiting strength vs. the inverse of the maturity index results, the data will lie on a straight line, as shown in Figure 2.11.

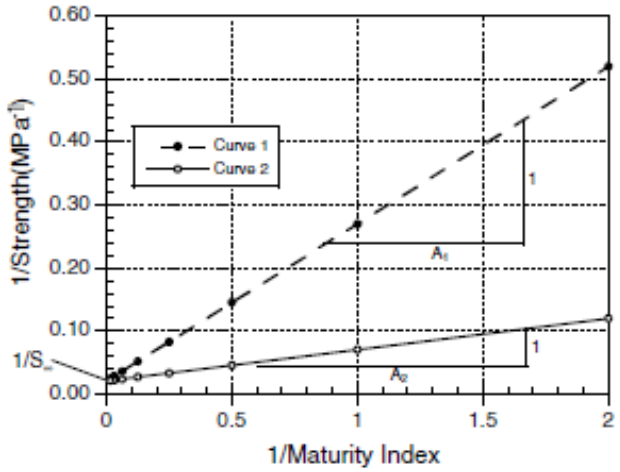

Figure 2.11: Plotting the inverse of strength (1/S) vs. the inverse of the maturity index (1/M)[101]

Because both the hyperbolic curves have the same limiting strength, therefore, both the straight lines curves obtained by converting the hyperbolic equation into linear equation have the same intercept. It is important to note that a steeper straight line corresponds to a lower value of the rate of initial strength gain.

The Bernhardt's equation was confirmed by Chin[135] and researchers working for NBS[136] could give a reasonably good result. However, Carino[137] found that the equation is less accurate when used to predict strength at low values of maturity index. Therefore, he introduced an 'offset' maturity, M_0 to account for the fact that the strength development is not started before the value of M_0 has not been reached, as first suggested by McIntosh[105]. Thus, Carino and Lew[4] modified the Equation 2.18 and it became the following equation:

$$S = \frac{M - M_0}{\frac{1}{A} + \frac{M - M_0}{S_\infty}} \qquad \text{Equation 2.19}$$

where:

M_0 = offset maturity

When the data in Figure 2.9 is plotted again using the Equation 2.19, it results in a curve similar to curve 1 in Figure 2.11 as shown in Figure 2.12. However, the curve in Figure 2.12 has been shifted as far the value of M_0 to the right.

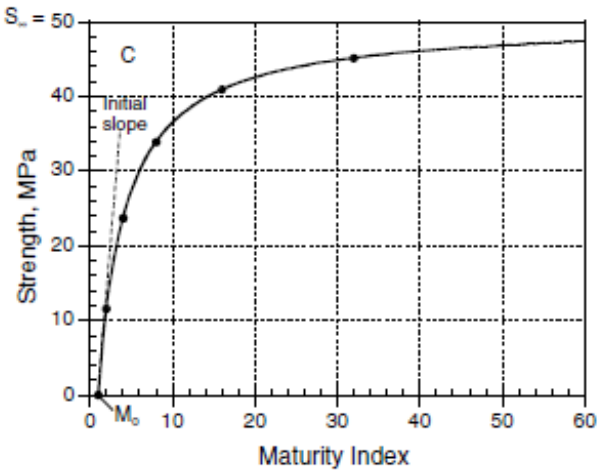

Figure 2.12: Hyperbolic strength-maturity relationship using an offset maturity[101]

2.4.4.4. Lew and Richard Method

Lew and Reichard[138] suggested a different strength-maturity based on their experimental data to improve Plowman's equation. They found that the strength-maturity relationship could be expressed as follows:

$$S = \frac{S_\infty}{1+D\,(M-16.70)^b} \qquad \text{Equation 2.20}$$

where:

S_∞ = limiting strength (MPa)

D, and b = constants

The coefficient of D is related to the rate of strength development, while b is ranged between -1.5 and -4.3, which is dependent on the water-cement ratio and the type of cement. The limiting strength also depends on the water-cement ratio and the type of cement. The maturity index was calculated using the Nurse-Saul; function with a datum temperature T_0 = -12.2^{0}C. The value of an offset maturity is taken as 16.70 as it is seen in Equation 2.20.

2.4.4.5. Freieslaben Hansen and Pedersen Method

Freieslaben Hansen and Pedersen[139] stated that the strength-maturity relationship should be similar to the heat output-maturity relationship. They suggested the strength-maturity relationship as the following equation:

$$S = S_\infty\, e^{-(\frac{\tau}{M})^a} \qquad \text{Equation 2.21}$$

where:

S_∞ = limiting strength (MPa)

M = maturity index (^{0}C.hours or ^{0}C.days)

τ = characteristic time constant (hour or days)

a = shape parameter

Figure 2.13 presents three curves following Equation 2.21 but has taken the time constant (τ) and the shape parameter in different values, to show the effect of the parameters to the strength-maturity relationship. Strength is plotted vs. the

logarithm of maturity index. Curve 2 is plotted using the value of parameter shape, a, the same value as Curve 1, but taken a time constant τ of a higher value than that of Curve 1. Conversely, Curve 3 is plotted by taking the time constant τ, the same as Curve 1, but has a higher value of a than that of Curve 1. The time constant τ, could be described as the value of τ, when the strength = S∞ / e = 0.37 S∞. The changing of the value of τ will result the same general shape of the curve while shifting it to the left or to the right. On the other hand, when changing the shape parameter, a, alters the shape of the curve. The curve obtained is more a pronounced S shape when the value of shape parameter a, increases[101].

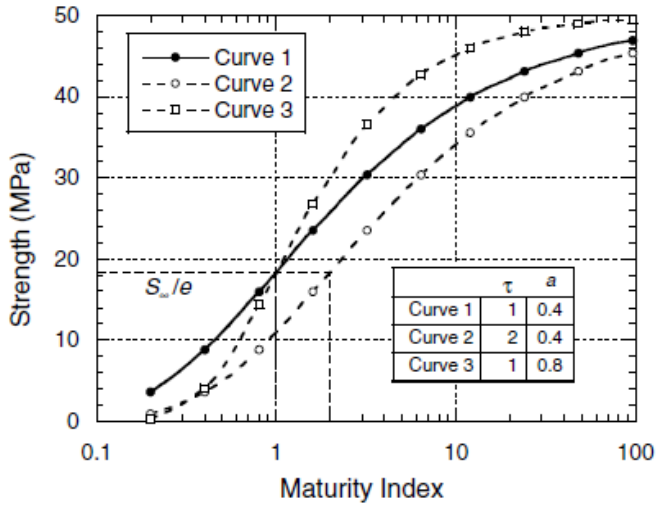

Figure 2.13: The effect of time constant *(τ)* and shape parameter *(a)* on the strength-maturity relationship[101]

2.4.4.6. Carino Method

Based on the work carried out by Bernhardt, Carino[101] performed extensive research on the theoretical basis of the maturity method, which was first introduced in 1956 by Bernhardt. The rate of strength gain (dS/dt) at any age (t) is believed as a function of the current strength (S) and the temperature (T), which can be written as follows:

$$\frac{dS}{dt} = f(S).k(T) \qquad \text{Equation 2. 22}$$

where:

f(S) = a function of strength

k(T) = a function of temperature

Bernhardt simplified it based on empirical evidence into:

$$f(S) = S_\infty \left(1 - \frac{S}{S_\infty}\right) \qquad \text{Equation 2.23}$$

where:

S_∞ = limiting strength a infinite age (MPa)

It is important to note that when strength starts to develop, f(S) = S_∞. As the result, the initial rate of strength development can be expressed as follows:

$$\frac{dS}{dt}|_{S=0} = S_\infty \, k(T) \qquad \text{Equation 2.24}$$

The temperature function, k(T), affects the initial rate of strength development; therefore, it can be taken as the rate constant.

If S_∞ is dependent on curing temperature and Equation 2.22 is combined with Equation 2.23, therefore, it gives the integral equation[101]:

$$\int_0^S \frac{dS}{\left(1-\frac{S}{S_\infty}\right)^2} = S_\infty \int_{t_0}^t k\,(T)dt \qquad \text{Equation 2.25}$$

Introducing the parameter of t_0, that condition, where the strength gain does not start before the time of t_0 after mixing, makes Equation 2.25 different from the original derivation proposed by Bernhardt. The integral on the right side of Equation 2.25 comprises the product of a temperature dependent function and time, which a common form of the maturity function and can be expressed as M(t, T), thus Equation 2.25 can be simplified as follows:

$$M\,(t,T) = \int_{t_0}^t k\,(T)dt \qquad \text{Equation 2.26}$$

where:

t_0 = age at which the strength development is initiated (hours or days)

Integrating the left side of Equation 2.25 and simplifying it to obtain the strength-maturity relationship as follows:

$$S = S_{\infty} \frac{M\,(t,T)}{1+M\,(t,T)} \qquad \text{Equation 2.27}$$

Equation 2.27 has a similar form to that of Equation 2.17, which is the basis for the hyperbolic strength-maturity function proposed by Chin[134]. Carino[101] found that when concrete is cured at a constant temperature or under isothermal condition, the value of the temperature function k(T) is constant and equal to k_T. Therefore, the maturity function can be expressed:

$$M(t,T) = k_T\,(t - t_0) \qquad \text{Equation 2.28}$$

where:

k_T = value of the rate constant at the curing temperature

Tank and Carino[140] suggested that the experimental value of rate constants obtained from the specimens cured under various isothermal conditions could be used to measure the effect of temperature on the strength development of concrete. Even, the value k_T obtained from Equation 2.28 can be used to determine the activation energy and datum temperature of each mixture, as will be discussed later.

Furthermore, they examined the effect of curing temperature, which is not constant during a curing time on the rate constant. This is the most important thing to have a confidence in whether the maturity function can be used to predict the strength development of concrete in-place. Therefore, they suggested the relationship between the rate constant and temperature as follows:

$$k\,(T) = C\,T + D \qquad \text{Equation 2.29}$$

where:

k (T) = rate constant function, hours or days

T = curing temperature, ^{0}C

C, D = regression constant

The datum temperature T_0, is the temperature at which the rate constant is equal to zero. This value is used in Nurse-Saul maturity function (Equation 2.2). Therefore, the datum temperature equals to *–D/C*. By changing *C* by *K*, Equation 2.29 then can be simplified as follows:

$$k\,(T) = K\,(T - T_0) \qquad \text{Equation 2.30}$$

Substituting Equation 2.30 into Equation 2.25, thus, the maturity function becomes:

$$M\,(t,T) = K \int_0^t (\,T - T_0\,)\,dt$$

$$= K \int_0^t (T - T_0)\,dt - K \int_0^{t_0} (T - T_0)\,dt \qquad \text{Equation 2.31}$$

Based on Nurse-Saul function, the two parts on the right-hand side of Equation 2.31 are called temperature-time factor or maturity, which are taken as *M* and *Mo*. Therefore, Equation 2.31 can be simplified as follows:

$$M\,(t,T) = K\,(M - M_0) \qquad \text{Equation 2.32}$$

Substituting Equation 2.58 into Equation 2.53 results:

$$S = S_\infty \frac{K\,(M - M_0)}{1 + K\,(M - M_0)} \qquad \text{Equation 2.33}$$

where:

S_∞ = Limiting strength, N/mm^2

M = maturity, °C-hours or °C-days

K = a rate constant

M_0 = maturity when strength gain begins, ^{0}C-hours or ^{0}C-days

Equation 2.33 is similar to Equation 2.19 proposed by Bernhardt if substitutes *A* by KS_∞.

2.4.5. Strength-Age Relationships

2.4.5.1. Carino Method

Carino and Tank[140] proposed the strength-age relationship by substituting Equation 2.31 into Equation 2.30, which it gives the following equation:

$$S = S_{\infty} \frac{k_T (t - t_0)}{1 + k_T (t - t_0)} \qquad \text{Equation 2.34}$$

where:

S = compressive strength, N/mm^2

S_{∞} = limiting strength, N/mm^2

t = actual curing age at temperature T, hours or days

t_0 = age when strength development is assumed to begin, hours or days

k_T = rate constant that is determined by Arrhenius equation (Equation 2.12), hours^{-1} or days^{-1}

Furthermore, they suggested that the relative strength could be indicated as a function of the equivalent age as shown in the following equation:

$$S = S_{\infty,r} \frac{k_r (t_e - t_{or})}{1 + k_r (t_e - t_{or})} \qquad \text{Equation 2.35}$$

where:

$S_{\infty,r}$ = limiting strength at reference temperature, N/mm^2

t_e = equivalent age at the reference temperature, hours or days

t_{or} = age when strength development is assumed to begin at reference temperature, hours or days

k_r = rate constant at reference temperature, hours^{-1} or days^{-1}

2.4.5.2. Freiesleben Hansen and Pedersen (FHP) Method

Freiesleben Hansen and Pedersen proposed the strength-age relationship using the Three Parameter Equation (TPE) as follows[101, 139, 141]:

$$S = S_{\infty} e^{(-\frac{\tau}{t})^{\alpha}} \qquad \text{Equation 2.36}$$

where:

S = strength at age t, MPa

τ = characteristic time constant, hours^{-1} or days^{-1}

a = shape parameter

It is important to note that all of the strength-maturity and the strength-age relationships above, were developed based on the data obtained from concrete with Portland cement only. Carino and Tank[142] and Brooks et al[141] reported that the type and the amount of supplementary cementitious materials, which was added into a concete mixture as cement replacement, affected the amount of long-term strength reduction due to curing at high temperatures at early ages. The sensitivity of GGBS to a curing temperature is diffrent than that of Portland cement. Therefore, those functions can not be directly applied to GGBS concrete without a modification.

2.4.6. Activation Energy

2.4.6.1. Introduction

The term of 'activation energy' is introduced by the Swedish scientist Svante Arrhenius in 1889. He defined the activation energy as the minimum energy that was required for a chemical reaction to occur[143]. The activation energy is commonly denoted by E_a, and given in the units of kilo joules per mole or joules per mole.

In order to shows clearly the relationship between the activation energy, the constant rate and the curing temperature, the Equation 2.12 (Arrhenius formulation), therefore, can be written as follows:

$$E_a = -R\,(T + 273)\,ln\left(\frac{k_T}{A}\right) \qquad \text{Equation 2.37}$$

where:

E_a = apparent activation energy, J/mol or kJ/mol

k_T = rate constant, days^{-1} or hours^{-1}

A = constant, days^{-1} or hours^{-1}

R = universal gas constant, 8.314 J/mol K or 0.00814 kJ/mol K

T = average temperature of the concrete during interval Δt, ^{0}C

The Arrhenius equation is firstly developed for a simple reaction, which have less complex materials than that of cementitious materials. The cementitious materials commonly consist of four main chemical compounds as discussed in the previous section of this chapter. All single-compounds are expected to follow the Arrhenius equation, which hydrates at a different rate. Therefore, each main compound should have its own activation energy according to Arrhenius principle. The activation energy of concrete is measured and can be used in predicting the strength development of the concrete. The activation energy obtained from the strength data of concrete describes the whole cement hydration rather than a single-compound hydration, it is therefore, always referred as "the apparent activation energy"[101, 144].

Freisleben Hansen and Pedersen(FHP)[121] are known as the first researchers who proposed a formula to calculate the activation energy. Their formulas are as presented in Equation 2.38 and Equation 2.39 for curing temperature of over or equal to 20^0C and less than 20^0C respectively. They also became the first researchers who suggested using the Arrhenius equation to calculate the maturity of concrete. The Freisleben Hansen and Pedersen's formulation is still used for strength prediction applications, irrespective of the concrete composition. Conversely, Malhotra and Carino[101] have reported that the activation energy value depends on concrete mix properties such as the chemistry, type and quantity of the cement and admixtures used in the mix and the cement fineness.

Chanvillard and D'Aloia[145] reported that Arrhenius' theory does not illustrate the temperature sensitivity of the hydration of individual chemical reactions. However, it is probably the best method that is available to account for the influence of temperature on the cumulative rate of hydration of all chemical reactions[146-148].

2.4.6.2. Value of Activation Energy

Freiesleben Hansen and Pedersen[121] proposed a formulation to calculate the value of activation energy as follows[101, 121]:

For $T \geq 20\ ^0C$, $E_a = 33{,}500\ J/mol$ Equation 2.38

For $T < 20\ ^0C$, $E_a = 33{,}500 + 1470\ (20 - T)\ J/mol$ Equation 2.39

Malhotra and Carino[101] summarised the value of activation energy for various types of cement, which were obtained from different tests. This aims to represent the effect of cementitious material and the methods used in determining the value of activation energy. The values of activation energy range from 41 to 67 kJ/mol, as shown in Table 2.1. The values of activation energy presented in Table 2.1 are quite higher than the values that generally obtained from the FHP formulation.

Table 2.1 shows that the mixes incorporating GGBS are likely to have higher activation energy values than that of PC mixes for which the values are obtained from the same test method. Generally, the values of activation energy obtained from the chemical shrinkage method are higher than the other methods, even though they have a similar mix. The values of activation energy listed in Table 2.1 may help to quantify the effect of temperature on the early-age strength development and those values can be used as a comparison to those obtained in this study. However, the authors recommend that they should not be used for calculating the later-age development of mechanical properties[101].

`

Table 2.1: Activation energy values[101]

Cementitious Material	Type of Test	Activation Energy (kJ/mol)	Reference
Type I (mortar)	Compressive Strength	42	Carino N.J (1981)[149]
Type I (mortar)	Compressive Strength	44	Carino N.J (1984)[106]
Type I (concrete)	Compressive Strength	41	Carino N.J (1984)[106]
PC (paste)	Heat of Hydration	42 – 47	Regourd M. et al (1980)[150] and Gauthier, E. et al (1982)[151]
PC + 70% GGBS (paste)	Heat of Hydration	56	Regourd M. (1980) [150] and Gauthier E. et al (1982) [151]
PC (paste)	Chemical Shrinkage	61	Geiker et al (1983)[152]
RHC (paste)	Chemical Shrinkage	57	Geiker et al (1983) [152]
PC (paste)	Chemical Shrinkage	67	Geiker et al (1982)[153]
Type I/II (paste)	Heat of Hydration	44	Roy D. M. et al (1982)[5]
Type I/II + 50% GGBS (paste)	Heat of Hydration	49	Roy D. M. et al (1982)[5]

Tank and Carino[101, 140, 142] carried out another study of the isothermal strength development in concrete and mortar specimens. In the study, they used different cementitious materials and having two different water-cement ratios. They proved the applicability of the hyperbolic strength-age relationship function presented in Equation 2.34 for the strength gain of concrete or mortar cured under constant temperature. They confirmed that the activation energy for a concrete mixture could be gained from the strength data of mortar cubes with the water-cement ratio as the same as concrete. This study led to the use of equivalent mortar in determining the value of activation energy of concrete as recommended in ASTM

standard[6]. They also investigated the effect of admixtures on the activation energy value[101]. Tank and Carino summarised the results from their study in the Table 2.2.

Table 2.2: Activation energy values based on compressive strength tests of concrete cylinders and mortar cubes[101, 140, 142]

Cementitious Material	Activation Energy (kJ/mol)			
	w/c = 0.45		w/c = 0.60	
	Concrete	Mortar	Concrete	Mortar
Type I	63.6	61.1	48	43.6
Type II	51.1	55.4	42.7	41.1
Type III	43.6	40.1	44	42.6
Type I + 20% FA	30	33.1	31.2	36.6
Type I + 50% Slag	44.7	42.7	56	51.3
Type Accelerator	44.6	54.1	50.2	52.1
Type I +Retarders	38.7	41.9	38.7	34.1

The values of activation energy that are listed in Table 2.2 are remarkably higher than that of obtained from FHP formulations. The exception is for the mix incorporating FA and the one incorporating a retarder regardless of the testing method and water-cement ratio.

The mix incorporating GGBS, the lower water-binder ratio results in the lower value of activation energy. The value of activation energy of the GGBS concrete with lower water-binder ratio is lower than that of Portland cement. However, it is conversely for the GGBS concrete with higher water-binder ratio. The addition of admixtures (accelerators and retarders) into a concrete mixture had also a significant effect on the value of activation energy of the concrete. Therefore, Malhotra and Carino[101] recommended to calculate the value of activation energy using the data from experiment, rather than just use the typical values of activation energy available in Table 2.1 and 2.2. Especially, the mix, which added admixtures and/or cement replacement materials such as GGBS, FA and silica

fume. This applies even for Portland cement mixes when it is desired a high level of accuracy of strength prediction.

The effect of water-binder ratio on the value of activation energy was still a discussion topic until now. Malhotra and Carino[101] found that concrete mixes with a lower water-binder ratio usually have higher activation energy values; however, they argued that the results were not clear and required further investigation. Schindler[154] agreed them and reported that the effect of water-cement ratio on activation energy was not consistent. Other authors, such as Jonasson et al[155], however, reported that the activation energy was a function of the water-cement ratio.

The activation energy values, which are presented by Malhotra and Carino[101] and Carino and Tank[142] remain constant and are not dependent on the curing temperature. Therefore, they appear to contradict completely to the Arrhenius law. The RILEM report TC 119-TCE[156] recommends the use of the FHP activation energy formulation in determining the activation energy value, irrespective of the mix proportions, except for concretes incorporating GGBS. For GGBS concrete, it is suggested the use a higher value of 48,804 J/mol. This value is approximately similar to that of proposed by Roy and Idorn[5] for a mix of Type I/II + 50% GGBS i.e. 49,000 J/mol shown in Table 2.1. The value is also quite similar to that reported by Carino and Tank[142] for a mix of Type I + 50% GGBS with a water-cement ratio of 0.45, i.e. 44,700 and 42,700 J/mol for concrete and mortar respectively. The value is also comparable to the value of activation energy that is recommended by ASTM C 1074[6] for predicting strength of concrete with a mix of Type I cement without admixtures or additions, which is ranged from 40,000 to 45,000 J/mol.

In 1993, Kjellsen and Detwiler[157] determined the apparent activation energy as a function of relative strength rather than as a constant in predicting strength at later ages. The relative strength f_{cr} is the strength relative to the 28-day strength at

reference temperature. The apparent activation energy can be expressed as follows:

$$\frac{E\,(T,\ f_{cr})}{R} = \frac{E\,(T)}{R} - \frac{\Delta E\,(T, f_{cr})}{R} \qquad \text{Equation 2.40}$$

where the initial apparent activation energy is determined by the following equation:

$$\frac{E\,(T)}{R} = \left(\frac{1}{273+T_r} - \frac{1}{273+T}\right)^{-1} ln\left(\frac{\tau_e}{t_T}\right) \qquad \text{Equation 2.41}$$

where:

τ_e = the age to reach f_{cr} equals 0.2 at reference temperature T_{ref}, hours or days

t_T = the age to reach f_{cr} equals 0.2 at temperature T, hours or days

For $f_{cr} < 0.2$

$$\frac{\Delta E\,(T, f_{cr})}{R} = 0 \qquad \text{Equation 2.42}$$

For $f_{cr} \geq 0.2$ and T < 20 ^{0}C

$$\frac{\Delta E\,(T, f_{cr})}{R} = 7300\,(f_{cr} - 0.2)^3 + 2200\,(f_{cr} - 0.2) \qquad \text{Equation 2.43}$$

For $f_{cr} \geq 0.2$ and T ≥ 20 ^{0}C

$$\frac{\Delta E\,(T, f_{cr})}{R} = 50000\,(f_{cr} - 0.2)^5 + 3500\,(f_{cr} - 0.2) \qquad \text{Equation 2.44}$$

In 1995, Jonasson et al[155] found that the curing condition significantly affected the values of activation energy. Based on their experiment data that used Standard Swedish cement, they proposed a model to calculate the activation energy as follows:

$$E(T_c) = 44{,}066\ x\ \left(\frac{30}{10+T}\right)^{0.45} \qquad \text{Equation 2.45}$$

where:

T = curing temperature, ^{0}C

It is unlike the equation proposed by Kjellsen and Detwiler[157], the equation above determines the activation energy as a function of the temperature of concrete, which is similar to FHP formulation. It is clearly shown in the equation, the activation energy decreases as the concrete temperature increases. The equation, however, has a weakness as it assumes that the only dominant factor in the cement hydration procedure is temperature. While the age and degrees of hydration have no effect on the sensitivity of concrete to temperature.

In 2001, Kim et al[158] proposed a model, which was a an exponential function to calculate the value of activation energy as follows:

$$E = E_0 \, e^{-\gamma t} \qquad \text{Equation 2.46}$$

where:

E_0 = initial apparent activation energy, J/mol

γ = a constant

t = age of concrete

Concrete with the same mixture proportions will have the same initial apparent activation energy at the initial age after mixing. However, the concrete after mixing and cured at different temperatures will have different properties. The initial rate of relative strength obtained will be a function of temperature as it is affected by the temperature represented by the initial apparent activation energy. The initial apparent activation energy decreases as an increase in temperature. A regression analysis of the variation of initial apparent activation energy with curing conditions result:

$$E_0 = 42830 - 43\,T \qquad \text{Equation 2.47}$$

where:

T = curing temperature, ^{0}C

The apparent activation energy decreases at a faster rate as α increases, where the value of γ is increase with the increase of temperature. The relationship between the value of α and temperature can be expressed as follows:

$$\gamma = 0.00017\,T \qquad \text{Equation 2.48}$$

In 2002, Pane and Hansen[159] proposed a formulation to estimate the activation energy, which is a function of curing temperature and the degree of hydration as the following equation:

$$\ln\left(\frac{d\propto}{dt}\right) = \ln[f(\propto)] - \frac{E(\propto)}{RT} \qquad \text{Equation 2.49}$$

where:

α = degree of hydration

The degree of hydration can be calculated according to FHP formulation[121] as follows:

$$\propto = \propto_{\infty}\ e^{\left(-\frac{\tau}{t}\right)^{a}} \qquad \text{Equation 2.50}$$

where:

α_{∞} = limiting degree of hydration

a = shape parameter

τ = characteristic time constant

By taking a differentiation of the Equation 2.50, it gives the equation as follows:

$$\frac{d\propto}{dt} = \frac{a}{\tau} \propto \left(ln\frac{\propto_{\infty}}{\propto}\right)^{\frac{a+1}{a}} \qquad \text{Equation 2.51}$$

Han et al (2003)[160] proposed a new model, which based on Kim et al's[158] work discussed earlier to determine the apparent activation energy to be used to predict the strength development of fly ash (FA) concrete. Han et al[160] used the same equation to calculate the apparent activation energy as that one proposed by Kim et al[158] i.e. Equation 2.46. However, they determined the initial activation energy using a different equation as follows:

For water-cement ratio ≤ 0.40,

$$E_0 = 39{,}720 + 119\,FA \qquad \text{Equation 2.52}$$

For water-cement ratio > 0.40,

$$E_0 = 42{,}920 - 90\ x\ FA \qquad \text{Equation 2.53}$$

where:

FA = the fly ash replacement ratio (%)

Furthermore, Han et al[160] reported that there was not a strong trend relationship between γ and fly ash replacement or water–binder ratios. Therefore, the following value of γ was proposed:

$$\gamma = 0.000615 \qquad \text{Equation 2.54}$$

In 2004, Schindler[154] developed a new model to calculate the apparent activation energy, which took into account the chemical composition of cement and the fineness of cement. The model for Portland cement mix can be mathematically expressed as follows:

$$E = 22{,}100\ x\ {p_{C_3A}}^{0.30} x\ {p_{C_4AF}}^{0.25} x\ Blaine^{0.35} \qquad \text{Equation 2.55}$$

where:

p_{C3A} = weight ratio of C_3A in terms of total cement content

p_{C4AF} = weight ratio of C_4AF in terms of total cement content

Blaine = Blaine value, specific surface area of cement (m^2/kg)

However, Equation 2.55 above should be multiplied by a modification factor when FA or GGBS are used incorporating Portland cement. The modification factor is expressed as the following equation[154]:

$$f_E = 1 - 1.05\ x\ p_{FA}\ x\ \left(1 - \frac{p_{FACaO}}{0.40}\right) + 0.40\ x\ p_{SLAG} \qquad \text{Equation 2.56}$$

where:

f_E = activation energy modification factor

FA = mass ratio replacement of fly ash

FA_{CaO} = mass ratio of CaO content in FA

p_{SLAG} = mass ratio replacement of GGBS

Furthermore, Schindler[154] assessed the models and he found that the change in the value of apparent activation energy is directly proportional to the amount of mineral admixtures used. He reported that the apparent activation energy decreased as the percentage of FA in concrete mix increased. Conversely, the apparent activation energy increased as the replacement level of cement by GGBS increased.

2.4.6.3. Determination of Activation Energy Based on ASTM-C1704

The ASTM C 1074 standard[6] recommends a method to determine the value of apparent activation energy according to Arrhenius law. The method is based on experimental results from mortar cubes cured isothermally at three or more different temperatures. The mortar cubes are prepared using an equivalent mortar mix of concrete that is to be investigated. The mortar mix should have a similar strength to that of the concrete investigated. The mortar cubes are tested at different ages to specify the strength development of the mortars under different curing temperatures. In order to obtain the rate constant k_T, for each curing temperature, therefore, it is necessary to do a statistical analysis based on the Equation 2.34 by plotting the strength data against age. Rearranging Equation 2.37 results in the following equation:

$$\ln k_T = -\frac{E_a}{R\,(T+273)} + ln\ A \qquad \text{Equation 2.57}$$

The value of activation energy can then be determined by plotting $ln\ (k_T)$ versus the reciprocal of the absolute of curing temperature $(T + 273)$, as shown in Equation 2.57. A regression analysis is carried out in order to obtain a best-fit line, where the slope of the best-fit line will be equal to $-E_a/R$.

2.4.6.4. Determination of Activation Energy Based on FHP Formulation (Three Parameter Equation, TPE).

Freiesleben Hansen and Pedersen[121] proposed a different way of expressing the strength-age relationship as given in Equation 2.36. In relation with equivalent age t_e, therefore, Equation 2.36 can then be written as follows[101, 121]:

$$S(t_e) = S_{r,\infty}\, e^{(-(\frac{\tau_r}{t_e})^a)} \qquad \text{Equation 2.58}$$

where:

$S(t_e)$ = the strength of mortar at equivalent age t_e, MPa

τ_r = characteristic time constant at reference temperature, hour^{-1} or day^{-1}

a = shape parameter

$S_{r,\infty}$ = limiting strength at reference temperature, MPa

It is valuable to examine how this new strength-maturity correlation function influences the estimation of the activation energy and therefore, the temperature sensitivity of the strength development. The equivalent age t_e can be determined by the age conversion factor *f (T)* as follows:

$$t_e = f(T)\ x\ t \qquad \text{Equation 2.59}$$

By combining Equations 2.58 and 2.59, therefore, the age conversion factor is related to the characteristic time constant τ, at temperature *T,* as shown in the following equation[144]:

$$\frac{\tau_r}{f(T)} = \tau \qquad \text{Equation 2.60}$$

Tank and Carino[140] expressed the relationship between the age conversion factor and the rate constant, which can be expressed as follows:

$$f\ (T) = \frac{k(T)}{(k(T_r)} \qquad \text{Equation 2.61}$$

Furthermore, Schindler and Poole et al developed the correlation between the rate constant at temperatures T and reference temperature T_r and the hydration time parameters as follows:

$$\frac{k(T)}{k(T_r)} = \frac{\tau_r}{\tau} \qquad \text{Equation 2.62}$$

where:

k(T) = rate constant at temperature T

$k(T_r)$ = rate constant at the reference temperature T_r

τ = characteristic time constant at temperature T

τ_r = characteristic time constant at reference temperature T_r

The apparent activation energy then can be determined according to the estimated hydration time parameters as follows:

$$-\frac{Ea}{R} = \frac{ln(k(T_r)) - ln(k(T))}{\left(\frac{1}{T_r} - \frac{1}{T}\right)} = \frac{ln(\frac{k(T_r)}{k(T)})}{(\frac{1}{T_r} - \frac{1}{T})} \qquad \text{Equation 2.63}$$

or

$$-\frac{E_a}{R} = \frac{ln\,(^{\tau_T}/_{\tau_{T_r}})}{(\frac{1}{T_r} - \frac{1}{T})} \qquad \text{Equation 2.64}$$

Furthermore, the relationships between *ln (τ)* and *1/T* can be expressed as follows:

$$\ln(\tau) = -\frac{E_a}{R\,T_r} + \frac{E_a}{R\,T} + ln(\tau_r) \qquad \text{Equation 2.65}$$

Furthermore, the value of activation energy can determined by plotting the value *ln (τ)* obtained from regression analysis using Equation 2.36 versus the reciprocal of the absolute of curing temperature *T*, as shown in Equation 2.65. A regression analysis is then carried out in order to obtain a best-fit line, where the slope of the best-fit line will be equal to E_a/R.

2.4.7. Improvement of Maturity Method

Commonly, many countries use maturity concept to predict the in situ strength of concrete. An accurate prediction can be helpful to engineers in scheduling projects. To obtain an accurate prediction of strength, engineers need to understand properly the process of concrete hardening, especially at early ages. Both Nurse-Saul and Arrhenius maturity functions do not take into account the effects of the early age curing temperatures on the ultimate strength, as a result both the methods inaccurately predict the strength of concrete. Many researchers proposed the recent methods to improve the accuracy of the in situ strength development of concrete, some of them are presented here.

2.4.7.1. Kjellsen and Detwiler Method

Kjellsen and Detwiler[157] use the relative strength development and degree of hydration of a concrete in term of the strength at 28-day. As discussed earlier, they suggested using the value of activation energy as a function of temperature shown in Equation 2.40 to Equation 2.44, which argued the Arrhenius formulations. They proposed a model to predict the strength of concrete at age t_i as the following equation[144, 157, 161]:

$$S_i = S_{i-1} + \Delta S_i \qquad \text{Equation 2.66}$$

or

$$S_i = \sum_0^i \Delta S_i \qquad \text{Equation 2.67}$$

$$\Delta S_i = S_{28\,(20^o)}\, x\, \Delta\propto_i \qquad \text{Equation 2.68}$$

where:

ΔS_i = change in strength during the time period t_i

$\Delta\alpha_i$ = change in degree of hydration during t_i

During the time t_i, the degree of hydration is changed, the relation between $\Delta\alpha_i$, and the degree of hydration α_i (relative strength development) at a time t_i can then be express as follows[144, 157, 161]:

$$\Delta\propto_{\boldsymbol{i}} = \propto_{\boldsymbol{i}} - \propto_{\boldsymbol{i-1}} \qquad \text{Equation 2.69}$$

The degree of hydration at age t_i can be written as the following equation:

$$\propto_i = \frac{A\ x\ k\ x\ (\ t_{e_i} - t_0\ )}{1 + k\ x\ (\ t_{e_i} - t_0\ )} \qquad \text{Equation 2.70}$$

where:

A = ratio of ultimate strength to 28-day strength

k = rate constant at a reference temperature, hours^{-1} or days^{-1}

t_{ei} = equivalent age at reference temperature, hours or days

t_0 = age at which the strength development is initiated (hours or days)

The values of the rate constant *k* and t_0 are obtained from the regression analysis for cube specimens cured under standard curing temperature (20^0C). Furthermore, the value of ratio of ultimate strength to 28-day strength *A* is calculated as follows[144, 157, 161]:

$$A = \frac{S_\infty}{S_{28-20^0C}} \qquad \text{Equation 2.71}$$

Where:

$S_{28\text{-}20^0C}$ = 28-day concrete strength for concrete cured at a reference temperature of 20 ^{0}C.

The equivalent age at a time t_i can be calculated as follows:

$$t_{e_i} = \sum_0^i \Delta t_{e_i} \qquad \text{Equation 2.72}$$

By substituting Equation 2.40 into Equation 2.13, the Equation 2.72 can be then re-written as follow:

$$t_{e_i} = (t_i - t_{i-1})\ x\ e^{\left[-\frac{E(T,f_{cr})}{R}\left(\frac{1}{T+273} - \frac{1}{T_r+273}\right)\right]} \qquad \text{Equation 2.73}$$

The value of apparent energy should be determined according to Equation 2.40, as discussed previous. Kjellsen and Detwiler[157] found that the Arrhenius equation was quite accurate at early ages, where the degree of hydration is less than 0.2. However, when the degree of hydration is higher or equal to 0.2, the effect of temperature in the following hydration should be taken into account. The value of apparent activation energy should be rather than takes it constant as Arrhenius

equation. They confirmed that the method they proposed had some limitations because some reasons. First, the accuracy of their model is greatly dependent on the value of apparent activation energy that is used. The other reason, it is needed a further research to quantify the strength loss on concrete cured isothermally at higher temperatures. Finally, they confirmed that their model was developed using mortar specimens cured under isothermal conditions. Therefore, the model might be having a complicated, when applying for concrete that is cured under variable temperature conditions.

2.4.7.2. Chanvillard and Aloia Method

In 1997, Chanvillard and D'Aloia[162] proposed a model to predict the strength development of concrete. The model assumes that the 28-day strength of concrete to decrease by increasing temperature. They suggested a model to define the degree of hydration as follows:

$$\propto = \frac{S}{S_{28}(T_r)} \qquad \text{Equation 2.74}$$

or

$$\propto = \frac{S}{S_{\infty}(T_r)} \qquad \text{Equation 2.75}$$

where:

$S_{28\,(Tr)}$ = Strength of concrete at age 28-day, MPa

$S_{\infty\,(Tr)}$ = Limiting strength of concrete cured at reference temperature, MPa

It is noted that either S_{28} or S_{∞} can be used in practice in the context of early ages.

Chanvillard and D'Aloia[162] found that by taking into account the effect of temperature curing on the strength development of concrete; the assumption that the 28-day strength is a function of the isothermal curing temperature can be confirmed. Therefore, the relation between the 28-day strength at isothermal curing temperature and the strength 28-days at reference temperature is given in the following equation[161, 162]:

$$S_{28,T} = S_{28,T_r}[1 - p(T - T_r)] \quad \text{Equation 2.76}$$

where:

$S_{28,T}$ = the 28-day strength at isothermal temperature T, MPa

$S_{28,Tr}$ = the 28-day strength at reference temperature T_r, MPa

p = constant, which refers to strength loss factor

Determination of the p value corresponds to the average of the p value obtained by fitting the model presented in Equation 2.76 to the compression data. Probably some of the p values are declined because the experimental procedures sometimes getting errors; lead to the values that greatly diverge from the average. Furthermore, they suggested taking the p value of 0.01.

Substituting Equation 2.76 into Equation 2.74 gives an equation as follows:

$$\propto = \frac{S}{S_{28,T_r}\,[\,1 - p\,(T - T_r)]} \quad \text{Equation 2.77}$$

where:

α = degree of hydration at time t

S = the compressive strength at time t cured at temperature T, MPa

The correlation between the degree of hydration and the equivalent age is determined at the reference temperature. While the strength can be computed using the following equation[161, 162]:

$$S = \sum_t S_{28,T_r}\,[1 - p\,(T - T_r\,)]\Delta\propto\,(\Delta t_e) \quad \text{Equation 2.78}$$

where:

$$\Delta t_e = e^{\left[-\frac{E_a}{R}\,(\frac{1}{T+273} - \frac{1}{T_r+273})\right]}\,\Delta t \quad \text{Equation 2.79}$$

Δt = time interval at isothermal curing temperature, T

Δt_e = time interval at the reference temperature, T_r

$\Delta\alpha$ = change in degree of hydration during the time interval

2.4.7.3. Yahia Abdel-Jawad Method

In 2005 and 2006, Jawed[163, 164] proposed two methods to predict the strength development of concrete. He modified the Nurse-Saul and Arrhenius equations. In 2005, Jawed[163] modified the Nurse-Saul maturity function, which is called AJ-05 in this study. In the following year, Jawed[164] proposed the second modification based on Arrhenius formula, which is called AJ-06 in this study.

Jawed[163] proposed a new model to determine equivalent age by modifying the Nurse-Saul equation (Equation 2.7). He took into account the effect of water-cement ratio in determining the equivalent age at reference temperature for concrete cured at other temperatures. The model is expressed in an equation as follows:

$$t_e = \sum \left(\frac{T - T_0}{T_r - T_0}\right)^n \Delta t \qquad \text{Equation 2.80}$$

where:

$$n = \frac{1}{1-(w/c)^2} \qquad \text{Equation 2.81}$$

w/c = water-cement ratio

Based on the data analysis of several sets for concrete and mortar specimens that was cured at different isothermal temperatures; they found that the relationship between the strength of concrete at reference temperature and that of cured at other isothermal temperature is linear. They expressed the relationship mathematically as follows:

$$\left(\frac{S(t,T)}{S(t_e, T_r)}\right) = 1 - k\left(\frac{T - T_r}{T_r}\right) \qquad \text{Equation 2.82}$$

where:

S(t, T) = the strength of concrete at age *t* cured at temperature $T\ (^0C)$, MPa

$S(t_e, T_r)$ = the strength of concrete at equivalent age t_e, cured at reference temperature $T_r\ (^0C)$, MPa

k = the factor depends on the equivalent age at which the strength is estimated.

The value of *k* can be determined using the following equation:

$$k = 0.14\ (\ 1 - \ e^{-0.1t_e}\ ) \qquad \text{Equation 2.83}$$

Jawed[163] proposed the model to predict the strength of concrete cured at temperature *T* at age *t* by combining both the Equation 2.82 and Equation 2.83, which gives:

$$S\ (\ t,T) = \ S\ (t_e\ ,T_r)\ [1 - 0.14\ \left(\frac{T - T_r}{T_r}\right)\ (1 - \ e^{-0.1\ t_e}\ )] \qquad \text{Equation 2.84}$$

The strength development of concrete cured at reference at equivalent age was found described by the Weibul equation as follows:

$$S(t_e\ ,T_r\ ) = a - be^{-c\ (t_e)^d} \qquad \text{Equation 2.85}$$

where a, b, c and d are parameters obtained from regression analysis on the strength data of concrete cured at reference temperature.

Jawed[164] proposed the second modification based on the Arrhenius formula. Jawed and Hansen[165] found that the activation energy was approximately constant at early hydration and tended to decrease rapidly at later ages. They proposed a model to determine the value of apparent activation energy as follows:

$$E = \ \frac{38}{\beta}\ \left(\frac{T_r - T_0}{T - T_0}\right)^{1 - \ w/c} \qquad \text{Equation 2.86}$$

where:

E = the initial activation energy, J/mol or kJ/mol.

β = the ratio of ultimate degree of hydration at temperature *T* to ultimate degree of hydration at reference temperature *Tr*

The parameter of *β* is determined as follows:

$$\beta = \ \left(\frac{\propto_\infty (T)}{\propto_\infty (T_r)}\right) = \ \left(\frac{S_\infty (T)}{S_\infty (T_r)}\right) \qquad \text{Equation 2.87}$$

Jawed and Hansen[165] found that the water-cement ratio and temperature influenced the ultimate degree α_∞, where it decreased as the water-cement ratio decreased and the curing temperature increased. Therefore, the relationship between the β value and the curing temperature T of a given concrete mix that was cured at different temperatures can be determined using the equation:

$$\beta = a - b\,T \qquad \text{Equation 2.88}$$

where: a and b are the parameter obtained from regression analysis.

However, Jawed[164] suggested that for approximation, the β value could be determined as follow:

$$\beta = 1.1 - 0.004\,T \qquad \text{Equation 2.89}$$

Jawed[164] determined the equivalent time t_e at reference temperature as FHP formula given in Equation 2.13. Furthermore, he proposed a model to estimate the strength development of concrete as follows:

$$S\,(t,T) = f_c(t_e\,,T_r)\left[1 - 0.01\left(1 - e^{-0.05t_e}\right)(T - T_r)\right] \qquad \text{Equation 2.90}$$

It was found that both the models that were proposed by Abdel-Jawed underestimated the strength development of concrete cured under non-isothermal conditions at later ages. It was occurred especially when the temperatures rise in concrete were high such as over than three times higher than the reference temperature. It is found that a modification of this method is needed to improve the accuracy of this model. This case will be discussed more detail in Chapter 6.

2.4.7.4. Modification of Nurse-Saul Method Based on Time Temperature Efficiency Factor, Rate of Strength and Maturity Development

The crossover effect has been discussed in many researches, which is the detrimental effect of a high curing temperature at early ages on strength development of mortars or concretes at later ages. Many works have been carried

out to quantify the side effect of high curing temperature at early ages on the strength development of mortar or concrete at later ages. Most of the recent methods considered it by taking into account the value of apparent activation energy used in determining equivalent age[157, 162, 164]. However, it is still complicated about the right method to determine the value of apparent activation energy. It is difficult to determine the amount of the activation energy that has to be reduced when concrete cured at high curing temperature. Moreover, each cementitious material has different sensitive to the high curing temperature when used in concrete.

A new method for estimating the strength development of concrete cured under isothermal and non-isothermal conditions was developed by Soutsos[166]. This model was developed based on both the formulations proposed by Nurse-Saul and Freiesleben Hansen and Pedersen.

Soutsos[166] found that the higher curing temperatures accelerate the hydration of cement much more than that of predicted using the age conversion factor. The age conversion factor was introduced in the Nurse-Saul maturity function (Equation 2.9). In other word, the age conversion factor obtained from Nurse-Saul equation was not enough to bring the interval time Δt, which is needed to achieve a certain maturity at curing temperature T, to the equivalent age t_e at reference temperature T_r, to have the same maturity at curing temperature T.

Soutsos[166] added that an additional 'acceleration' factor was needed to compress a certain part of hydration into a shorter time interval, which results in an increase of the rate of cement hydration. The acceleration factor should be equal to the compression factor when the reaction at higher curing temperature was as efficient as at the lower temperatures. Furthermore, he reported that the reaction at higher temperature was not as efficient as that at lower temperature; therefore, a 'temperature efficiency' factor was needed. A more detail discussion of the method proposed by Soutsos[166] is presented in Chapter 6.

2.4.8. Applications of the Maturity Method

A technique, which takes into account the combined effects of time and temperature on the strength development, is called maturity method. This method can be used to predict in-place strength of concrete to make sure that critical construction schedule, such as formwork removal, applied post-tensioning, can be implemented safely[101, 106].

There were fourteen workers killed and 34 injured in an accident of the collapse of a multi story building, under construction in Fairfax County, Va., in March 1973. The National Bureau of Standards (NBS) reported that the most probable cause of the collapse was premature removal of formwork[4]. In April 1972, another building collapsed, which is being constructed in Willow Island, WV. The accident resulted in 51 workers death. The NBS reported that the most likely cause of the accident was insufficient concrete strength to support the applied construction load[106]. Since the accidents, the NBS researchers started an in-depth study of the maturity method. As a result they laid the foundation for the advance of the first standard in the world for the maturity method i.e. ASTM C-1074.

Maturity method has been used for more than 3-decades on many constructions for prediction the strength of concrete[144]. An accurate predicted strength, enable engineer to reschedule the time of construction. Therefore, it can save a considerable amount of construction time, and it might be used as a tool in scheduling construction activities.

Waller et al[167], reported that in practice, the maturity method involves three phases such as calibration, validation and an on-site application. The calibration phase consist of the measuring of the expected properties of the given concrete mixture, such as the compressive strength, the estimated maximum temperature of concrete, and finding the suitable value of apparent activation energy. This phase leads to the development of the "concrete calibration curve", where the curve was obtained from the expected development of the strength of vs. maturity at 20^0C.

The validating phase occurs during the first week of the project. This phase is to check whether the variations in the characteristics of the concrete do not have significant difference to that of used in calibration phase. If there is no significant differences from those are used in calibration phase, therefore, the "calibration curve" could be used as the 'reference curve' on the project. Finally, the on-site application phase, it continues throughout the project where it is necessary a regular checking of the characteristics of the concrete.

Furthermore, Waller at all reported the use maturity method successfully for over than 20 years in Europe on many different projects in Europe, especially for assessing the early age strength of concrete as shown in Table 2.3.

Table 2.3: Lists some projects used the maturity method successfully to predict the strength of concrete at early ages, in Europe

Project	Year	location
Pylons and deck segments of Normandy bridge	1991	France[167]
"Pas de l'Escalette" tunnels A75	1994	France[167]
Cantilever deck segments of Rhone Viaduct BPNL	1994	France[167]
Cooling towers of Civaux nuclear plant	1994	France[167]
Rochecardon and Duchère tunnels BPNL	1995	France[167]
Montjézieu tunnels A75	1995	France[167]
Mirville viaduct A29	1995	France[167]
Amiens PI4 viaduct	1995	France[167]
Precast segments of "Ile de Ré" bridge	1987	France[167]
TGV viaducts in Avignon	1997	France[167]
Cut and cover in Taverny A115	1997	France[167]
Nièvre viaduct A16	1998	France[167]
Lisieux PI5 viaduct	1998	France[167]
Channel tunnel rail link, Medway bridge	2000	UK[167]

Table 2.4 presents some of the project those used the maturity method to estimate the strength of concrete that used in the projects at early ages.

Table 2.4: Lists some projects used the maturity method successfully to predict the strength of concrete at early ages, in the USA and Canada

Project	Year	location
Scotia plaze 68-story tower	1986	Canada[168]
Creve Coeur Lake Memorial Park Bridge	-	US[169]
Barnes Hospital parking garage	2001	US[169]
Kiefer Creek Overpass	-	US[169]
Residential 30-story tower	2001	US[169]
Interstate 40 bridge reconstruction- Oklahoma	2002	US[169]

Roy et al[170] reported on the use of the maturity method during two projects. They used commercial software, which is called Computer Interactive Maturity System (CMIS) to calculate the heat and strength development. In this software, it is assumed that the relationship between the heat and maturity, and the strength and maturity is an exponential. Two projects were chosen to evaluate the CIMS model. The first project was a central bridge pier, which was placed on a foundation in the middle of Clearfield Creek. The second project was a Highway Slab. The results showed that the predicted temperatures in the concrete were the same trend to that of observed in the field. However, the predicted strengths need further verification in order to obtain an accurate result.

In 1999, Pinto and Hover[171] studied the effect of temperature on the setting times of concrete, using the maturity approach and FHP equation (Equation 2.13). They concluded that the setting time could be used to estimate the apparent activation energy successfully at the early stages of hydration. While the maturity method could be used to estimate the variations I setting times due to different curing temperatures.

In 2004, Schindler[172] observed the effect of temperature on the initial and final setting times of concrete mixtures. It was quite similar to that of Pinto and Hover did. However, Schindler also observed the effect of the use of different cements and supplementary cementitious materials on the initial and final setting times of

concrete. He found that the setting time of concrete with Portland cement only was accurately predicted. However, when GGBS is used in concrete, setting occurs at an earlier degree of hydration. For this reason, he recommended that the interaction between the setting time and the hydration of GGBS needs to be further investigates.

More recent, Han et al[173] investigated the use of maturity method to predict the setting time of concrete incorporating with super retarding agents (SPA). They concluded that the maturity method could be used to predict the setting time of concrete containing SPA, where the results showed a good agreement between the predicted setting time and the measured setting time.

In 2009, Anderson et al[174] used the maturity method on the three case studies on actual construction projects. The three projects were all paving projects in the state of Washington. One of them, was a complete rebuild of a section I-5 in downtown Seattle, while the other two panel replacement, where one on I-5 in Bellingham and the other one on I-205 in Vancouver.

They found that the maturity method is a useful tool for estimating the strength development of the pavement. Proper understanding and use of maturity method results in a reasonable good of strength prediction, thus enables contractors to increase their productivity on projects with accelerate the construction schedule. On all their case studies, there was a lack of compliance with the special provision; such as no verification testing, inadequate recording keeping and in one case a calibration curve was not valid. Furthermore, they also reported the weaknesses of the maturity method, such as when there was a change in brand of cement, the source of type of cement of other cementitious materials, the source of aggregate and water-cement ratio; the strength-maturity relationship, therefore, required a new calibration curve.

2.5. Modelling of Temperature History of Concrete

2.5.1. Introduction

Thermodynamics defines heat as a transfer of energy across the boundary of a system as a result of a temperature difference. The transfer process of energy can occur by three different mechanisms i.e. conduction, convection and radiation. Heat transfer by conduction takes place due to the interactions of molecular scale energy carries within a material. The transfer of energy, which usually occurs in fluids after mixing one part of fluid with another with a temperature difference between one area and the other, or between the temperature of the fluid and the wall licked by the fluid itself, is called convection. The transfer of energy where a warm body emits energy by radiation in all direction is called radiation. The energy or heat in concrete is transferred by conduction mechanism.

Bamforth[175] investigated the early-age thermal crack control in concrete. He concluded that the concrete surface temperature and effect of formwork and curing conditions on it could be modelled by undertaking 1-dimensional heat transfer analysis using a simple spreadsheet. However, the finite element analysis (FEA) appears to be the only reliable method, which takes into account the effect of the size of element to estimate the in-situ temperature development within a structural element.

FEA consists of a computer model of a material, or design that is stressed and analyzed for specific results. It is used to design a new product and to modify an existing product. Modifying an existing product or structure is used to adequate the product or structure for a new service condition. In case of structural failure, FEA may be used to help in determining the design modifications to meet the new condition.

FEA provides solutions to problems that appear to be difficult manually solved. In terms of fracture, FEA most often involves the determination of stress intensity factors. Current days, however, the applications of FEA are in a much broader

range of areas such as fluid flow and heat transfer to solve problems in these areas.

Some thermal properties of concrete are needed before undertaking a modelling of heat transfer in concrete. The most important of the thermal properties are conductivity, specific heat capacity and heat output that is produced from cement hydration. Factors that affect the value of the thermal properties, will also be discussed in this section.

This section aims to review the applications of concrete heat-transfer analysis in relation to prediction and monitoring the in-situ strength development of concrete and control of thermal cracking. Factors that affect the in-situ temperature history and the accuracy of modelling it are discussed.

2.5.2. Heat Transfer in Concrete

The mathematical theory of heat conduction was developed by Joseph Fourier in the early nineteenth century, which is called Fourier's law. The in-situ temperature distribution and heat transfer within the structural element of concrete are determined by solution of the Fourier equation, which is in three-dimensional and transient form for concrete, is written as follows[176-178]:

$$\rho\, C_p\, \frac{\partial T}{\partial t} = k\left(\frac{\partial^2 T}{\partial x^2} + \frac{\partial^2 T}{\partial y^2} + \frac{\partial^2 T}{\partial z^2}\right) + q_t \qquad \text{Equation 2.91}$$

where:

- ρ = density of concrete, kg/m^3
- C_p = specific heat capacity of concrete, J/kg .^{0}C
- T = temperature of concrete, ^{0}C
- t = time
- k = thermal conductivity of concrete, W/m/ ^{0}C
- x, y, z = coordinates at a particular point in the element structure.
- q_t = rate of heat evolution from the hydrating cement, W/m^3

When the thermal conductivity is constant, Equation 2.91 can be then written as follows:

$$\frac{1}{\delta}\frac{\partial T}{\partial t} = \left(\frac{\partial^2 T}{\partial x^2} + \frac{\partial^2 T}{\partial y^2} + \frac{\partial^2 T}{\partial z^2}\right) + \frac{q_t}{k} \qquad \text{Equation 2.92}$$

where:

δ = thermal diffusivity of concrete

In order to solve the Fourier equation, the initial and boundary condition should be given. Ge[179] et al reported there were four major boundary conditions in the heat transfer mechanism that should be considered in the model such as conduction, convection, solar absorption and irradiation as shown in Figure 2.14. The figure illustrates how each of the surroundings affects the heat development in a pavement system.

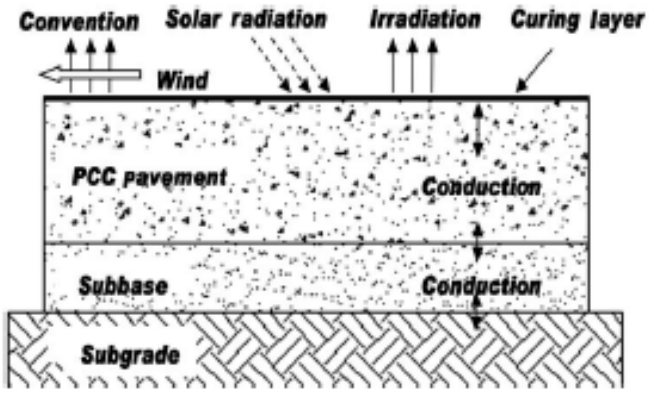

Figure 2.14: Heat transfer mechanism[179]

In the in-situ concrete cured under various temperatures, heat will be transferred to and from the surroundings. The temperature rise in the structural element of concrete is governed by the balance between the heat generation in the concrete and the heat exchange with the environment. When the temperature of surroundings is higher than that of concrete, the surroundings will become an additional source of heat to the concrete. Conversely, when the temperature of surroundings is lower than that of concrete, the heat from concrete will then be transferred to the surroundings[180].

The boundary condition for the case shown in Figure 2.14 that related to environmental effects is generally both the pavement surface and the bottom. The initial and boundary conditions can be expressed as follows[179-181]:

Initial condition:

$$T = T_0 \qquad \text{Equation 2.93}$$

Boundary condition at pavement surface:

$$-k \nabla T n + q_c + q_r - q_s + q_e = 0 \qquad \text{Equation 2.94}$$

Boundary condition at pavement bottom:

$$-k \nabla T n = 0 \qquad \text{Equation 2.95}$$

where:

T_0 = initial temperature, ^{0}C

q_c = heat flux due to convection, W/m^2

q_r = heat flux due to irradiation, W/m^2

q_s = solar radiation absorption, W/m^2

q_e = heat flux due to evaporation, W/m^2

∇ = gradient notation

n = unit direction of heat flow by vector notation.

The boundary conditions are dependent on the time and temperature, which are important for solving Equation 2.91 above. The heat transfer of conduction could be occurred among concrete, sub-base and sub-grade, which follows the equation[179]:

$$q = -k A \frac{dT}{dx} \qquad \text{Equation 2.96}$$

where:

q = heat flow, W

A = area, m^2

dT/dx = thermal gradient, ^{o}C/m.

It is clearly shown in Figure 2.14 that the heat conduction is also occurred between the pavement and the curing layer, beside that flow down to the base layer. According to Holman[176], the heat flow through the installation layer can be determined using the following equation:

$$q_e = \left(\frac{T_s - T_a}{R_{th}}\right) \qquad \text{Equation 2.97}$$

where:

T_s = surface temperature, ^{0}C

T_a = air temperature, ^{0}C

R_{th} = thermal resistance, ^{0}C/W, which is the ratio of thickness to thermal conductivity of curing water

The heat convection due to the air motion should be considered, where all the effects of convection can be expressed using the Newton's law of cooling as follows[176]:

$$q_{conv} = h_c\, A\, (T_s - T_a) \qquad \text{Equation 2.98}$$

where:

h_c = convection heat transfer coefficient, W/m^2 ^{0}C

The h_c coefficient can be determined using the following equation[182]:

$$h_c = 5.7 + 3.8\, V \qquad \text{Equation 2.99}$$

where:

V = wind speed, m/s

The Equation 2.99 above is valid for a slab with a size of 0.5 m^2. When the size of the slab is larger, Nevander and Elmarsson[183] suggested using the following equation:

$$h_c = 6 + 4\, V \qquad \text{for V} \leq 5 \text{ m/s} \qquad \text{Equation 2.100}$$

$$h_c = 7.4\, V^{0.78} \qquad \text{for V} > 5 \text{ m/s} \qquad \text{Equation 2.101}$$

The thermal irradiation, which is the electromagnetic radiation emitted by a body as a result of its temperature, can be expressed as follows[176]:

$$\frac{q_r}{A} = \sigma \varepsilon (T_s^4 - T_{sky}^4) \qquad \text{Equation 2.102}$$

where:

σ = Stefan-Boltzmann constant, 5.669 x 10^{-8} w/m^2 K^4

ε = emissivity, which is taken as 0.94 for a rough concrete surface.

T_{sky} = effective of sky temperature, ^oK, which a function of dew point temperature and cloud cover, it could be obtained from the meteorology stations and not equal to the ambient temperature.

Larsson and Thelandersson[182] suggested using the following equation for determining the T_{sky} can be calculated using the following equation:

$$T_{sky} = \sqrt[4]{\frac{q_{sky}}{\sigma \varepsilon}} \qquad \text{Equation 2.103}$$

where:

q_{sky} = the long wave radiation from the sky, W

Furthermore, the solar absorption, which is the solar radiation absorbed by a pavement surfaces during they receive incoming solar radiation. McCullough and Rasmussen[2] proposed an equation for determining the solar absorption as follows:

$$q_s = \gamma_{abs} I_f q_{solar} \qquad \text{Equation 2.104}$$

where:

q_s = solar absorption of concrete, W/m^2

γ_{abs} = solar absorptivity of concrete, which is 0.1 – 0.35 for the pavement with white curing compound

I_f = intensity factor to account for angle of sun during a 24-h day, which is assumed to be a sinusoidal distribution

q_{solar} = instantaneous solar radiation, W/m^2

Ge et al[179] reported that the initial condition of concrete such as concrete placement temperature and surroundings temperature. The desired initial temperature of concrete placement can be achieved by controlling the temperature of the ingredients. The contribution of the temperature of each ingredient to the initial concrete placement temperature is illustrated in the following equation:

$$T_{con} = \frac{0.22\,(T_a W_a + T_c W_c) + T_a W_{wa} + T_w W_w}{0.22\,(W_a + W_c) + W_{wa} + W_w} \qquad \text{Equation.105}$$

where:

T_{con} = initial concrete placement temperature, ^{0}C

T_a = temperature of aggregate, ^{0}C

T_c = temperature of cement, ^{0}C

T_w = temperature of water, ^{0}C

W_a = weight of dry aggregate, kg

W_w = weight of water, kg

W_c = weight of cement, kg

W_{wa} = weight of aggregate moisture, kg

2.5.3. Thermal Conductivity of Concrete

Incropera and Dewitt[184] define the thermal conductivity of concrete as the quantity of heat that pass through concrete in a unit length (heat transfer rate) for a given temperature gradient. The thermal conductivity affects the temperature gradients and thermal stresses, which are developed inside the concrete. The thermal conductivity is measured in Watts per Kelvin per meter ($W \cdot K^{-1} \cdot m^{-1}$). The values of the thermal conductivity of ordinary concrete generally ranges between about 1.4 and 3.6 W/m K[12, 185].

Factors that affect the thermal conductivity of concrete are as follow:

❖ *Moisture content of concrete*

Kim et al[186] carried out a research to investigate factors, which influence on the thermal conductivity of concrete, mortar and cement paste. They reported that the

aggregate volume fraction and the moisture condition of specimens were declared as the primary factors that affected the thermal conductivity of concrete. Meanwhile, type of admixtures and cementitious materials that were used in mortar or cement paste, strongly influenced the thermal conductivity of mortar and cement paste. Furthermore, Kim et al[186] reported that the thermal conductivity of concrete was also influenced by fine aggregate fraction, water-cement ratio and curing temperature.

Similar to Kim et al[186]'s work, Khan[187] who used the Campell-Allen and Thorne[188]'s model to evaluate the influence of aggregate type with various moisture contents. He found that the type and the moisture content of aggregate influenced the thermal conductivity of concrete.

In 1998, Khan et all[189] reported the effect different water-cement ratios for low, medium and high strength mixes at very early ages on the thermal conductivity of concrete. They found that for the normal strength concrete, the thermal conductivity of the maturing concrete was about 33% higher than that of hardened concrete, while the difference for the high strength concrete was only 2%. It is believed that the thermal conductivity decreases linearly to increased strength gain. They agreed with other researchers that the thermal conductivity of concrete, particularly at early ages was greatly affected by the moisture of the concrete. It is believed due to water has a considerably lower thermal conductivity than that of aggregates, which is estimated 70% of the total volume of concrete. The moisture content of concrete is directly related to the hydration degree of the concrete.

❖ *Mix proportion of concrete*

In 2006, Demirboga[190] observed the effect of cementitious materials, when they were used in concrete, on the thermal conductivity of concrete. He used silica fume, FA, GGBS and combination of them to evaluate their effect on the thermal conductivity of concrete. He found that the maximum thermal conductivity of 1.233 W/m.^{0}K, which was obtained from the concrete mixture with Portland

cement only. The thermal conductivity of concrete decreased with the increase of the percentage of cementitious materials in the concrete. Neville[12] reported that the thermal conductivity of rock aggregate depended on its crystallinity. The increase of the thermal conductivity of the rock aggregate will increase directly the thermal conductivity of concrete.

❖ *Curing temperature of concrete*

Neville[12] found that the effect of temperature on the thermal conductivity of concrete could be neglected when the concrete was cured within the room temperature limits. However, at the higher curing temperatures, the change of values of the thermal conductivity of concrete becomes more considerable and complex. An increase of the temperature up to a maximum at about 50 to 60 ^{0}C increases slowly the thermal conductivity of concrete. The thermal conductivity of concrete decreases sharply when the temperature increased up to 120 ^{0}C as the concrete loss of water/moisture, which was due to the high temperature. The thermal conductivity of concrete then tends to be a constant, at the temperature between 120 and 140 ^{0}C. At the temperature of 800 ^{0}C, the thermal conductivity of concrete is about 50% of that of concrete cured at temperature 20 ^{0}C.

Kim et al[186] demonstrated experimentally that the thermal conductivity of concrete at early age decreases as its temperature increases. It is due to heat released from the cement hydration. Similarly, Morabito[191] also reported that the thermal conductivity of concrete decreased with the increase of the concrete temperature.

❖ *Age of concrete*

Marshall[192] and Brown and Javaid[193] found that the thermal conductivity was affected by the age of concrete, however, it was only for the first few days. Brown and Javaid[193] measured the thermal properties of concrete with the water cement ratio of 0.65 from the first 6-hours to seven days. The results showed that the thermal conductivity of the concrete increased from the first 6-hours up to 1-day

and then decreased at the following days until the age of 7-days. After the age, the thermal conductivity then appeared to remain constant. The thermal conductivity of concrete at 6 hours was measured to be 2176 W/m.^{o}C and at the age of 7-day it had dropped by approximately 30% and was equal to 1.515 W/m.^{o}C. It is appeared that the thermal conductivity decreases linearly to the moisture content and degree of hydration, similar to that was reported by De Schutter and Taerwe[194].

In contrast, Byfors[122] and Rilem Committee No. 42[195] reported that the effect of age on the thermal conductivity of concrete was not notable. Similarly, Kim et al[186] reported that in general, the age of concrete has a very small effect on its thermal conductivity with the exception of the time period 0 to 2 days.

The thermal conductivity of concrete can be determined from the thermal diffusivity relationship as follows:

$$\delta = \frac{k}{\rho \ C_p} \qquad \text{Equation 2.106}$$

The SI units for thermal diffusivity are metres square/hour (m^2/h). Typical values for concrete diffusivity are in the range from 0.002 to 0.006 m^2/h[12]. The thermal diffusivity describes the rate at which a temperature disturbance at one point in a body moves to another point.

The accurate estimation of the value of thermal conductivity is very important in a modelling the temperature of concrete during its hydration period, especially when the formwork of concrete is still used. The heat conduction and the associated temperature gradients within the concrete will generally develop the heat-transfer process within its matrix and greatly influence the development of its temperature profile. The sensitivity of the in-situ temperature of concrete to its thermal conductivity can be verified using heat transfer finite element modelling.

Recently, some methods to measure the thermal conductivity of concrete has been introduced such as the prism method that estimates the thermal properties of concrete with reasonable accuracy[196].

Some values of the thermal conductivity of concrete found in the literatures are presented in Table 2.5 below.

Table 2.5: Thermal conductivity of concrete in relation to ages

Researcher	Thermal conductivity k (W/m.K)	Age (days)
Gibbon and Ballim[197]	0.6 - 2.6	0 - 4
Yoshida[197]	1.5 - 1.8	0 - 2
Rousan and Roy[198]	1 - 1.8	7 - 84
Davey[199]	0.8 - 2.3	not specified
ACI[200]	1.8 - 3.8	14

The typical value of the thermal conductivity of concrete in relation to the type of aggregate used in concrete is shown in the following table.

Table 2.6: Thermal conductivity of concrete in relation to the type of aggregate[186]

Type of aggregate	Wet density of concrete (kg/m^3)	Thermal conductivity K (W/m.K)
Quartzite	2440	3.5
Dolomite	2500	3.3
Limestone	2450	3.2
Sandstone	2400	2.9
Granite	2420	2.6
Basalt	2520	2
Barytes	3040	2
Expanded Shale	1590	0.85

The thermal conductivity of concrete is an input parameter to simulate the temperature of concrete using Finite Element Modelling (FEM). It is difficult to estimate the thermal conductivity of concrete, as the concrete consists of different composite materials (non-homogeneous material). The differences of aggregate types used and moisture conditions of concrete give different values of the thermal conductivity of the concrete, as these are the primary factors influencing the value of the thermal conductivity. However, in respect to temperature variation in a concrete structural element, heat of hydration is the major thermal property of concrete. Therefore, in this study, the values of the thermal conductivity of concrete used are based on literature review values, is discussed further in section 7.3.

2.5.4. Specific Heat of Concrete

The specific heat capacity of concrete is used to measure the amount of heat per unit mass required to increase the temperature of concrete by one degree, and is generally expressed in terms of heat capacity. In the International System of Units (SI), specific heat capacity is expressed in units of joule(s) (J) per kg. Kelvin (K).

Rilem Committee 42[195] and Mindess and Young[201] reported that in general, the specific heat capacity of normal strength concrete varies from 0.8 to 1.2 kJ/kg.^{0}C. Factors affecting the specific heat capacity of concrete are similar to that of affect the thermal conductivity of concrete. The main factors are as follows:

- *Moisture content of concrete*

Kan et al[189] reported that the specific heat capacity of the normal, medium and high-strength of mature concretes, for both saturated and oven-dried aggregates increased by an increase in moisture. However, as expected, the oven-dried aggregate resulted in lower specific heat capacity values than that of concrete used saturated aggregate for the same concrete strength.

It was reported by Whiting et al[202] that the specific heat capacity of normal strength concrete increased with an increase in moisture. The limitations of test procedure they used in their work enabled them to measure the specific heat capacity for saturated concrete samples only. They then proposed a model to calculate the specific heat capacity of concrete for any moisture condition as follow:

$$C_p = \frac{C_{SSD} + \gamma\,(y-1)}{1 + \gamma\,(y-1)} \qquad \text{Equation 2.107}$$

where:

C_p = specific heat capacity of concrete at any moisture content, J/kg.K

C_{SSD} = specific heat capacity of concrete at saturated surface dry, J/kg.K

γ = saturated surface dry (SSD) moisture content (%)

y = moisture content expressed as a function of the SSD moisture content.

They found that when moisture content was low, where γ would be much less than 1, therefore, Equation 2.133 can be rewritten as follows:

$$C_p = C_{SSD} + \gamma\,(y-1) \qquad \text{Equation 2.108}$$

Equation 2.134 shows that the relationship between the specific heat capacity and the moisture content is linear. However, it is different with Equation 2.133, where the increase in moisture content leading the deviation from linearity will also increase.

❖ *Mix proportion of concrete*

Whiting et al[202] found that for normal density concrete the specific heat capacity increased with an increase in concrete density. It was reported by Mindess and Young[201] that the increase in the water content from 4 to 8% caused an increase in the specific heat capacity by 12%. As the aggregate in a concrete mix is the largest portion of constituents, Bamforth[175] reported that the type of aggregate used in concrete is important in determining the specific capacity of concrete. He

found that the values of the specific capacity of rocks were ranged from 0.8 to 1.0 kJ/kg ^{0}C. Bamforth et al[203] suggested the range of values for use in Eurocode 2.

❖ *Curing temperature of concrete*

Khan et al[189] found that the temperature also affected the specific heat capacity of concrete. An increase in temperature resulted in an increase the specific heat capacity. In the temperatures ranged from 30 to 70 ^{0}C, the specific heat capacity resulted were ranged from 0.65 to 2.7 and from 0.65 to 1.1 for the aggregate types of saturated and oven-dried respectively; while they had the same strength of concrete.

❖ *Age of concrete*

Experiment done by Lofqvist[204] on a mortar mix with a water-cement ratio of 0.55 cured from 3-days to 30-days, showed that the influence of age on the specific heat capacity of concrete could be ignored. In other hand, Brown and Javaid[193] reported that the specific heat capacity for normal strength concrete with the water cement ratio of 0.65 at early ages, varied from 1.15 to 0.89 during the age from 6-hours to 7-days. The values of the specific heat capacity tend increasing by the age of concrete.

The relationship between the cumulative heat and the change of temperature can be expressed as follows:

$$Q = C_p \, m \, \Delta T \qquad \text{Equation 2.109}$$

where:

Q = cumulative heat, Joule (J)

C_p = specific heat capacity, J/kg.^{0}C

m = mass, kg

ΔT = change of temperature,^{0}C

Some typical values of the specific heat capacity found in literature presented as follows:

Table 2.7: Typical value of specific heat capacity found in literature

Researcher	Specific heat kJ/kg ^{0}C
Brown and Javaid[193]	0.89 to 1.15
Whiting et al[202]	0.80 to 1.00
Mindess et al[201]	0.80 to 1.20
Mehta and Monteiro[185]	0.90 to 1.00

2.5.5. Heat Hydration of Concrete

2.5.5.1. Factors Affect the Heat Hydration of Concrete

In this section, the process of hydration is not discussed, as it has been discussed in an earlier section. This section discuss the heat output resulted from hydration process. The primary factors affecting the rate of hydration of cementitious materials in related to the heat output rate as follows:

- *Cement type*

The rate of heat output of hydration greatly depends on the chemical composition of cement. The main compound of cement i.e. C_3S and C_3A are the most reactive of compounds, especially at early age[9, 12]. Both the compounds contribute the most of heat output at early age. Cement types that have a low content of C_3S and or C_3A have a low rate of heat hydration and a low cumulative heat output.

- *Water-cement ratio*

Generally, the influence of water-cement ratio to the rate of hydration is not notable. Byfors[122], however, reported that a reduce in the water-binder ratio resulted in a decrease of the rate of heat liberated. This proves that the cement hydration is fully dependent on water. Breugel[205] found that the minimum water-

cement ratio that was required to complete the hydration process is 0.4. Similarly, Mindess and Young[201] found that the hydration process would cease if the availability of water were not enough to support the reaction of cement occurred. They found that the minimum water-cement ratio to complete the hydration process is 0.42. The cement paste will dry quickly when the external source of water is not available due to the hydration process and when the relative humidity is lower than 80%.

❖ *Fineness of cement*

The hydration of cement is significantly affected by the fineness of cement[9, 12, 206]. An increase in cement fineness accelerates the cement hydration even increases the heat liberated. The fineness of modern cement ranges from 3000 to 5000 cm^2/gr. Bentz[206] reported that the hydration of cement occurs on the surface of the cement particles and therefore, finer cements are more reactive due to they provide larger areas for the water to have contact with the cement.

❖ *Sulfate content*

Lerch[207] reported that an increase in the amount of SO3 in cement results in a decrease of heat liberated regardless of the content of C_3A in cement. It is due the reaction of C_3A will be notably retarded.

❖ *Chemical admixtures*

Water reducers are needed to reduce the need of water to achieve a given workability. They may retard or accelerate the hydration process. Generally, the rate of heat generation at early ages increases when a water reducer is added to a mix without changing on the mix proportions. Normally, water reducers are used to decrease the cement content while keeping the target strength, this result in a reduction of the heat output[144].

Ben-Bassat[208] reported that a retarded admixtures is used in concrete mixes to delay the period of setting time of the concrete mixes. Although they reduce the heat output at early ages, the total amount of heat liberated and the associated temperature rise at the age from 3-7 days is not notable. On the other hand, accelerator admixtures are used to accelerate the period of the hardened process of concrete. Nagataki[209] reported that the effect of the accelerators on the heat liberated of cement hydration was dependant on their chemical composition. Currently, the use of hinge-range water reducing agents, in terms superplastiziciers is more increased. Wang et al[9] reported that even though they influenced the rate of heat output at early ages, their effects on the total amount of heat liberated, however, was not notable.

❖ *Casting and curing temperature*

The hydration of cement is highly dependent on the temperature. The increase of curing temperature results in an increase of the maximum of heat output and the rate of heat liberated at early ages. However, the total amount of heat liberated is decreased at later ages, which is called "crossover" effect as has discussed earlier. Wang and Yan[210] reported that an increase in the temperature of casting decreases the cumulative heat output of hydration. However, the increase of casting temperature results in a significant increase of the rate of heat output at early ages, especially for concrete that was cured under adiabatic condition.

❖ *Cement replacement materials*

The type, the amount and the chemical composition of the cementitious materials used in concrete mixes are the primary factors, which determine the amount of heat liberated and the rate of heat output during the cement hydration process. It is also affected by the chemical admixtures, which are used in the mix. Many researchers agree that the use of fly ash generally reduces both the early-age heat output rate and the total heat output and postpones the peak of hydration as well. However, the effect it has still depends on the type of fly ash used[144].

The heat-liberated curve of concrete incorporating GGBS is different with that of concrete with Portland cement only. For GGBS concrete mixes, two peaks of the heat output of hydration may occur. The first peak corresponds to the hydration of Portland cement that is normally not delay, while the second one presents the hydration of the GGBS. Even though the GGBS decreases the rate of heat output at early ages, it however, does not decrease the total amount of heat liberated[211].

Coole[212] reported that in the large construction with a minimum dimension of 3 m, the peak temperature, which can be achieved by concrete incorporating with GGBS, might be higher than that of an equivalent concrete mix with Portland cement only; unless the replacement level of GGBS is higher than 75%. He expected that the replacement of cement with GGBS up to 70% might not effectively reduce the excessive temperature rise in a larger concrete pours. This very high temperature is potential to cause a thermal cracking at early ages. Nevertheless, Bamforth[213] in Ciria report C660 reported that the use of GGBS and slag cements in concrete mixes normally gives a reduction in the peak of temperature; therefore, it can reduce the risk of thermal cracking. Even by using experimental data carried out by Dhir et al[214], he presented Figure 2.15 to show that the use GGBS in concrete could reduce the heat output of hydration at early ages.

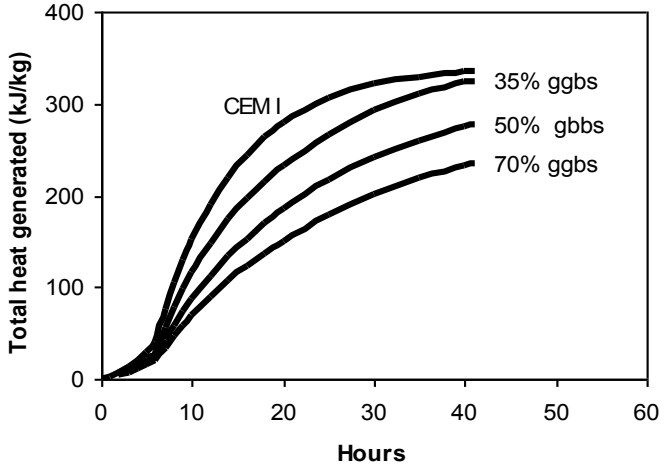

Figure 2.15: Heat output liberated from semi-adiabatic tests on mortar with different levels of GGBS[213, 214]

De Schutter and Taerwe[215] reported that the temperature dependant factors to predict the rates of heat output of the P and S-reaction, where P and S are the reaction of Portland cement and Slag (GGBS) respectively. Both the P and S-reaction heat outputs should be calculated according to the Arrhenius equation. They found that the hydration of the GGBS does not begin immediately when it has contact with water. The heat output of the GGBS remains equal to zero up to the degree of P-reaction achieves a threshold value, which is a temperature dependant. They validated their model by simulating the adiabatic temperature history of the GGBS concrete mixes and the temperature history of massive concrete cured under various temperature conditions.

2.5.5.2. Determination the Total Heat of Hydration of Concrete

Over the years, the rates of heat output haven been used as parameter input in numerical temperature modelling with a number of approaches. As it has been discussed earlier, the four main compounds of cement constituent contribute for the heat output of hydration; where the compounds C_3A and C_3S are the most contribute the heat output. The use of mineral admixtures in concrete mixes may affect the limited or ultimate heat output of hydration. The limited heat output of hydration can be determined when the total cementitious materials content and the heat of hydration per unit weight of each the cementitious material have been known.

The accuracy of the prediction of limited heat hydration depends on the accuracy by which each compound has been determined. Bogue[216]'s calculations are commonly used and recommended by ASTM C 150[217]. Table 2.8 presents the value of heat hydration of each compound proposed by some researchers:

Table 2.8: Heat of hydration of individual compound[217, 218]

Compound	Heat of hydration of individual compound (J/g)			
	Mindess and Young (1981)	SHRP-C-321 (1993)	Bogue (1947)	Kishi and Maekawa (1995)
C_3S	490	500	500	502
C_2S	225	256	260	260
C_3A	1160	721	866	865
C_4AF	375	302	420	419
Free Lime			1165	
MgO			850	
SO_3			624	

Some researchers proposed models to determine the heat output of hydration as follows:

❖ *E. Rastrup*

In 1954, based on his experimental results, Rastrup[113] proposed a model to predict the heat of hydration for concrete cured under variable temperature as follows:

$$Q = A + E \,.\, e^{-\,bt_e^{-\,n}} \qquad \text{Equation 2.110}$$

where:

Q = heat of hydration, J/g or kJ/kg

A, E, b, n = constants depending on the concrete mix proportions and type of cement.

t_e = equivalent age, hour or days

Equivalent age t_e, is calculated using the following equation:

$$t_e = \frac{1}{3600} \sum_0^t 2^{0.10\,(T - T_r)}\, \Delta t \qquad \text{Equation 2.111}$$

where:

T = temperature of concrete during the time interval, Δt, ^{0}C

T_r = reference temperature, ^{0}C

The model proposed by Rastrup can be used after the heat output of concrete under isothermal conditions at reference temperature T_r, has been determined experimentally using isothermal calorimeter. The constants A, E, b and n can then be obtained from linear regression.

❖ *Freiesleben Hansen and Pedersen (FHP)*

Freisleben Hansen and Pederson[121] proposed a model to predict the heat output of hydration of concrete cured at different temperatures than the reference temperature. Similar to the model they proposed for predicting the strength of concrete, rewrite Equation 2.36 gives a model for predicting heat output as follows:

$$Q = Q_{\infty,r}\, e^{-\left(\frac{\tau_r}{t_e}\right)^a} \qquad \text{Equation 2.112}$$

where:

$Q_{\infty,r}$ = Limited heat output at reference temperature, J/g or kJ/kg

t_e = equivalent age, hours or days, Equation 2.13

τ_r = characteristic time constant at reference temperature, hour or days

a = Shape parameter

Parameters $Q_{\infty,r}$, τ_r and a are obtained from a regression linear analysis on the experimental data of concrete cured at reference temperature.

❖ *A. K. Schindler and K. J. Folliard*

Schindler and Folliard[219] suggested a model based on Bogue's formulation[178] to estimate the heat output of hydration for concrete with different mixture proportions, cement types and supplementary cementitious materials (SCMs) as follow:

$$\boldsymbol{Q_{CEM} = 500_{p\,C_3S} + 260_{p\,C_2S} + 866_{p\,C_3A} + 420_{p\,C_4AF}} + 624_{pSO_3} + 1186_{p\,FreeCaO} + 850_{p\,MgO} \qquad \text{Equation 2.113}$$

where:

Q_{CEM} = total heat of hydration of the cement, J/g

p_i = weight ratio of i-th compound in terms total cement content.

Data for the contribution of FA and GGBS on the heat of hydration when they are used in a concrete mixture is limited found in the available literature. Kishi and Maekawa[220] recommended the value of the heat of hydration of 209 and 461 J/g for FA (8% CaO) and GGBS respectively, while Bensted[221] suggested the heat of hydration between 355 and 440 J/g for GGBS.

As the total cementitious material content in a given concrete mix has been known, therefore, the 100% hydration for cement and SCMs can be modelled as follows:

$$Q = C_c \, Q_{CM} \qquad \text{Equation 2.114}$$

where:

Q = total heat of hydration of the concrete, J/m^3

C_c = cementitious material content (g/m^3)

Q_{CM} = total heat hydration of all cementitious materials (included cement) at 100% hydration (J/g), which can be calculated as follow:

$$Q_{CM} = Q_{CEM} \, p_{CEM} + Q_{GGBS} \, p_{GGBS} + Q_{FA} \, p_{FA} \qquad \text{Equation 2.115}$$

where:

p_{CEM} = cement weight ratio in terms of total cementitious content

p_{GGBS} = GGBS weight ratio in terms of total cementitious content

p_{FA} = FA weight ratio in terms of total cementitious content

Q_{GGBS} = heat of hydration of GGBS, J/g

Q_{FA} = heat of hydration of FA, J/g

2.5.5.3. Determination the Degree of Hydration

The degree of hydration *(α)* is a measure to know the amount of the reactions between the cementitious materials and water. It is define as the ratio between the quantity of hydrated cementitious material and the initial quantity of the cementitious materials in a given concrete mix. The degree of hydration is a function of time, where α varying from 0% at the hydration starting to 100%

when it is fully completed. Many researchers reported that in the fact, not all the cementitious materials would hydrate. The degree of hydration can then expressed as follows[219]:

$$\propto (t) = \frac{Q\,(t)}{Q} \qquad \text{Equation 2.116}$$

where:

α (t) = degree of hydration at time *t*

Q(t) = cumulative heat of hydration released at time *t*, J/m^3

Based on the model for predicting the strength development of concrete proposed by Freiesleben Hansen and Pederson, the prediction of degree of hydration at equivalent age t_e can be write as the following equation:

$$\propto (t_e) = \propto_\infty \; e^{-\left(\frac{\tau}{t_e}\right)^a} \qquad \text{Equation 2.117}$$

where:

α (t_e) = the degree of hydration at equivalent age

α_∞ = the limited degree of hydration at reference temperature

τ = hydration time parameter at reference temperature, hours or days

a = hydration shape parameter

Taplin[222] and Mills[223] reported that the limiting degree of hydration is very dependent on the water-cement ratio. Therefore, Mills[223] suggested to calculate it as follows:

$$\propto_\infty = \frac{1.031\,w/c}{0.194+w/c} \qquad \text{Equation 2.118}$$

where w/c is water-cement ratio.

2.5.5.4. Heat of hydration contributed by FA and GGBS

Jonasson[155] et al proposed a model to predict the temperature development adiabatically as follows:

$$\frac{dT}{dt} = \frac{Q_H}{\rho\, C_p} = \frac{dQ}{dt}\left(\frac{1}{\rho\, C_p}\right) \qquad \text{Equation 2.119}$$

where:

T = temperature of concrete, ^{0}C

ρ = concrete density, kg/m^3

C_p = specific heat capacity of concrete, J/kg/^{0}C

Q_H = rate of heat generation, W/m^3

Q = heat of hydration of the concrete, J/m^3

The rate of heat generation Q_H, is greatly influenced by the degree of hydration where the degree of hydration is a function of time and temperature history. This can be indicated by the equivalent age of maturity function. Therefore, the rate of heat generation at time *t*, can then be determined using the following equation:

$$Q_H(t) = Q_{CM}\, C_C \left(\frac{\tau}{t_e}\right)^a \left(\frac{a}{t_e}\right) \propto (t_e)\, \frac{E}{R} \left(\frac{1}{273+T_r} - \frac{1}{273+T}\right) \quad \text{Equation 2.120}$$

where:

Q_H (t) = rate of heat generation at time t, W/m^3

E = activation energy, J/mol

Based on their experiment data, Schindler and Folliard[219] carried out regression analysis on the data to find the best value for both the parameters hydration characteristic time "τ" and hydration shape factor *"a"*. They proposed models to calculate the parameters as follow:

$$\tau = 66.78\, {p_{C_3A}}^{-0.154}\, {p_{C_3S}}^{-0.401}\, Blaine^{-0.804}\, {p_{SO_3}}^{-0.758}\, e^{(2.187 p_{GGBS} + 9.50\, p_{FA-CaO})}$$

Equation 2. 121

$$a = 181.4\, {p_{C_3A}}^{0.146}\, {p_{C_3S}}^{0..227}\, Blaine^{-0.535}\, {p_{SO_3}}^{0.558}\, e^{(-0.647\, p_{GGBS})}$$

Equation 2.122

Equation 2.144 can be re-written by replace w/c with w/cm as follow:

$$\propto_\infty = \frac{1.031\, w/cm}{0.194 + w/cm} + 0.50\, p_{FA} + 0.30\, p_{GGBS} \leq 1.0 \quad \text{Equation 2.123}$$

where:

w/cm = water-cementitious materials ratio

The adiabatic curing condition is a curing system in which the temperature of concrete increases with no heat being exchanged between the concrete and its surroundings. The heat output in the adiabatic test is determined based on the temperature rise. Ballim and Graham[177] proposed a formula to determine the hydration heat output of concrete cured under adiabatic condition as follows:

$$Q(t) = C_p\ (T_t - T_0)\ \frac{\rho_c}{B} \qquad \text{Equation 2.124}$$

where:

Q (t) = heat output of hydration at time t, J/kg

ρ_c = density of concrete sample, kg/m^3

B = binder content, kg/m^3

T_t = temperature of concrete at time t, ^{0}C

T_0 = temperature of concrete at the beginning or casting temperature, ^{0}C

C_p = specific heat capacity of concrete, J/ kg .^{0}C

Currently, it has been recognised that the heat output of hydration obtained experimentally is more reliable; therefore, it is suggested to measure the rate of heat generation using the methods such as adiabatic and semi-adiabatic test, isothermal conduction calorimetry and solution calorimetry[9, 177, 224]. Isothermal calorimetry is the measurement of thermal power (heat production rate) at constant temperature conditions. In this study, the measurement is carried out using an instrument called TAM Air with eight channels manufactured in Sweden.

Wadso[224] carried out isothermal calorimetry tests of 20, 30, 40 and 50 ^{0}C. He also carried out semi-adiabatic tests to simulate the conditions in massive constructions. This aims to simulate the results obtain from the isothermal calorimetry test on the semi adiabatic test. These simulations to check if the heat output resulted from isothermal calorimetry can be used to predict the in-situ heat output development. The results showed that there was a good agreement between the isothermal calorimetry results and the results of semi-adiabatic tests. These prove that it is possible to use the heat output obtained from isothermal calorimetry to estimate the in-situ heat output of hydration. Therefore, it can be

used to predict the in-situ temperature rise in concrete where a good prediction of the in-situ temperature, will result in an accurate prediction of concrete strength.

2.5.6. Predicted Temperature History in Concrete using Finite Element Method

Branco et al[178] used a three-dimensional finite element model to predict the hydration temperatures rise in concrete. They found that the environmental interaction and the concreting phase during the first days after casting should be taken into account as shown in Equation 2.120, in order to obtain an accurate prediction. In order to validate their model, they used a double-box cantilever bridge concrete and a massive concrete block. They concluded that the numerical technique could be used for the non-linear temperature distribution and it was a useful tool, which enables an engineer to redesign the schedule of project.

Bentz[225] developed a computer model to estimate the surface temperature of concrete pavements and bridge decks. The model is based on a one-dimensional finite difference model. The model includes the heat transfer through conduction, convection and radiation and using the available data for environmental conditions such as the weather data. He validated his model by preparing three samples to predict the temperature of concrete surface and in comparison with data from other researchers. The results showed that his model was supported by the validated data. At daytime, the concrete surface temperature rises even above the ambient temperature, which is due to the incoming solar radiation. Conversely, at night, the temperature of concrete surface drops as the result of radiation from the concrete surface to the sky. He added that in a bridge decks, this effect is more notable than that in the concrete for pavement. It is due to no soil sub layer as a thermal insulation mass beneath the concrete decks.

Ruiz et al[226] introduce the HIPERPAV to predict the hydration temperature of various cementitious materials that were used in the Federal Highway Administration (FHWA)'s projects. They validated the HIPERPAV temperature predictions by preparing two Jointed Reinforced Concrete Pavement sections on I-

75 Detroit, Michigan where the projects used blast furnace slag aggregates. Based on the results obtained, they conclude that HIPERVAP could be used to provide an accurate prediction of the temperatures of hydration.

In 2004, Schindler et al[227] proposed a new model added to the HIPERPAV program, in order to account for the effect of evaporation cooling, which may be occurred on the concrete surface. They validated the new model by measuring the temperature in-site and the results then compared to the prediction temperature of the concrete with the new model. They concluded the new model that added to the HIPERPAV program improved the accuracy of the temperature prediction. The comparison of the measured versus predicted pavement temperature in terms of the best-fit line to the 45^0 line was used to evaluate the accuracy of the prediction, where strongly related to the r^2-value as it is determined with two variable. The r^2-values are 0.91 and 0.80 for the new model and the previous model introduced by Ruiz et al respectively. This shows that the new model predict the temperature more accurate than that of previous one.

Ge and Wang[228] developed a model for predicting the temperature development in concrete pavement using a commercial computer program, FEMLAB (Finite Element Modelling Laboratory), which is now known as COMSOL. They took into account the conduction, convection, solar absorption and irradiation as the boundary conditions. They assessed the influences of cementitious materials, concrete mix design, and environmental conditions. The results showed that the new model predicted the temperature of concrete reasonably accurate. They concluded that the model could be used to optimise concrete mix design, evaluate field concrete strength and to select concrete placement temperature, in order to minimising the concrete thermal stress.

The use of COMSOL for modelling the heat output of hydration in concrete is very limited in the literature. This is due to the fact that this program is quite new in comparison to other commercial programs such as Abacus, Ansys, etc. The modelling procedures and results are presented in Chapter 8.

CHAPTER 3 – AIMS, OBJECTIVES AND RESEARCH METHODOLOGY

3.1. Introduction

The use GGBS as cement replacement in concrete gives benefits on both the fresh and hardened concrete. The strength development of GGBS concrete at early age highly depends on the mix proportions and curing temperatures. Under standard curing temperature the strength of GGBS concrete at early age is noticeable slower than that of concrete with Portland cement only. The higher the levels of cement replacement with GGBS the lower the strength of the GGBS concrete at early ages. At elevated curing temperature than the standard curing, however, the strength development of GGBS concrete at early ages improves.

The maturity methods, i.e. Carino – Nurse Saul and FHP methods are the simplest and cheapest method that could be implemented on side to continuously measure of the in-situ strength development of concrete. However, these maturity functions are developed based on the strength data of concrete with Portland cement only, which is similar to the recently improvement maturity methods such as the methods proposed by Chanvillard and D'Loia[162], Kjellsen and Detwiler[157], and Abdel-Jawad[163, 164].

Given the above information, the research questions for this study are:

(i) what is the effect of the curing temperatures, mix proportions and levels of GGBS as cement replacement on the strength development of GGBS concrete at earlier and later ages,

(ii) how is the accuracy of the above existing maturity methods to predict the strength development of GGBS concrete, lightweight and self compacting concretes, and

(iii) is it needed to develop a new method to predict the strength development of GGBS concrete rather than using the existing maturity methods, which were developed based on the data of concrete with Portland cement only.

Isothermal curing temperatures will be varied on different concretes such as Portland cement/GGBS concretes, lightweight and self compacting concrete to simulate the expected in-situ temperature histories. This will be used to investigate the effect of curing temperatures on the strength development of these concretes.

Ten mixes for each mortar and concrete were cast and cured under different isothermal curing temperatures. The mortars were cured at 10, 20, 30, 40 and 50^0C, while the concretes were at 20 and 50^0C. Both the mortar and concrete mixes were cured under adiabatic condition. There were also five mixes for lightweight concrete and three mixes for self compacting concrete, which were cured at the same temperatures and curing conditions as for the mortar, except they were not cured at 10^0C. These were to investigate the strength development of mortar/concrete cured at different curing temperatures, as well as to simulate the possibility of in-situ temperature rise in concrete.

The adiabatic tests were used to develop a model to predict the strength development of concrete in situ. The model was validated against the strength development obtained from experimental work.

An accurate prediction of the strength of concrete at an early age will enable an engineer to accelerate the construction schedule. To do this, it is necessary to develop an accurate method to predict the strength development. Existing maturity functions such as Nurse-Saul and Three Parameter Equation, which were developed based on mortars/concretes made with Portland cement only. These maturity functions seem to be less accurate, when applied to mortars/concretes with GGBS. Heat transfer modelling using the Comsol software can be carried out to predict the temperature rise in concrete. This predicted temperature rise in the concrete can then be used to predict the strength development of the concrete.

3.2. Research Methodology

In order to achieve the above objectives, the following series of research work was undertaken:

3.2.1. Experimental Work to Investigate the Effect of Different Isothermal Curing Temperatures and Adiabatic Condition on the Strength Development of Mortars and Concretes with GGBS.

Two methods were used to calculate the mix proportions of concrete. The BRE method[229] was used for the design of normal strength concretes, where their water-binder ratios were higher than 0.4. However, this resulted in concrete mix proportions with very high cement contents when used to design medium and high strength concretes with the water-binder ratios equal to or lower than 0.4. Therefore, the mix proportions for medium and high strength concretes were calculated based on the modified maximum density theory (MMDT)[230, 231]. Both these methods are discussed in Appendix A.

A polycarboxylate superplasticizer, Structuro 111X supplied by Fosroc Ltd[232], was used in high strength mortar/concrete mixes to maintain their workability. The absorption, density, sieve analysis, and the maximum void content of both coarse and fine aggregates were measured in the laboratory. These were needed in the calculation of mix proportions.

Eight mixes with different water-binder ratios, ranging from 0.25 to 0.69, were used. For each of these water-bender ratios there were five mixes with different replacement levels of GGBS i.e. 0, 20, 35, 50 and 70%. All mixes were expected to have target mean strengths in the range 35 to 100 MPa. Three 100 mm cube samples were made for each mix and testing age and the testing was carried out at ages 3, 7 and 28 days. The compressive strengths achieved were plotted against water-binder ratio.

There were two strength grades investigated for concrete and its equivalent mortar mixes i.e. C45 (normal strength) and C75 (high strength), which had target mean

strengths of 55 and 85 MPa, respectively. Each grade of mortar or concrete/mortar consisted of five different mixes with five different levels of GGBS i.e. 0, 20, 35, 50 and 70%, where 0% GGBS means mortar/concrete with Portland cement only used as the control. The mix proportions for concrete were calculated based on the trial mix results. The equivalent mortar mixes of all investigated concretes were calculated according to the ASTM standard[6].

The equivalent mortar mixes were cast into 50 mm cubes, cured under isothermal temperature, i.e. 10, 20, 30, 40 and 50^0C, as well as under adiabatic curing conditions. This aimed to investigate their strength development under different curing temperatures. They were tested at ages 0.25, 0.5, 1, 2, 4, 8, 16, 32, 64, 128, 256 and 365 days. The concretes were cured under two different isothermal temperatures only, i.e. 20 and 50^0C and under adiabatic conditions. The parameters obtained from regression analysis of the equivalent mortar's data, was used in predicting the adiabatic strength development of the concretes. The parameters are the activation energy, the acceleration and compression factors, the age conversion factor (ACF) and the temperature efficiency factor (TEF).

3.2.2. Experimental Work to Investigate the Effect of Changing Curing Temperature to the Strength Development of GGBS Mixes

One grade of mortar (C45) with replacement levels of 0, 20, 35, 50 and 70% of GGBS was produced for this experimental work to investigate the effect of a sudden change of curing temperature on the strength development of mortar/concrete, as well as its effect on strength development at later ages.

Five different curing methods were applied on the mortars. Two cured the mortars at either 20 or 50^0C until the testing age. The three other methods involved curing the samples at 20^0C and transferring them up to 50^0C after either 1, 2 and 3 days after they were cast.

3.2.3. Experimental Work to Study the Heat Output of Cement or Composite Cement (Cement and GGBS)

Two grades of mortar (C45 and C75) with all the GGBS replacement levels were used to investigate heat output. These mortars had the same mix proportions as the mortars for 50 mm cubes used in Section 3.3.2 above. The mortars were cast into ampoule glasses; they were then put into the channels in the TAM Air isothermal calorimeter. The experimental works were carried out under isothermal temperatures i.e. 20, 30, 40 and 50^0C, to investigate the heat output of cement/binder under these different temperatures.

The effect of the proportion of GGBS on the heat output produced in the hydration process was investigated using the equivalent mortar mixes without GGBS. These were calculated based on the mix proportions of equivalent mortars with GGBS. The mix proportions of mortar mixes without GGBS had the same water-binder ratio and the same paste volume as the equivalent mortar mixes with GGBS.

3.2.4. Finite Element Analysis to Predict Temperature History of GGBS Concretes

The temperature rise in mortars/concretes in-situ is very similar to the temperature rise in mortars/concretes cured under adiabatic conditions in the laboratory. The temperature rises in mortars/concretes cured under both curing conditions are changed by time. Once a model can produce an accurate prediction of temperature rise in mortars/concretes that are cured under adiabatic conditions, it can be applied to predict the temperature rise in mortars/concretes in situ. An accurate prediction of temperature rise in mortars/concrete will result in an accurate prediction of strength gain.

3.2.5. Experimental Work to Investigate the Effect of Different Curing Temperatures on the Strength Development and the Temperature Rise in Lightweight and Self Compacting Concretes

This experimental work was carried out through a research collaboration developed between Queens University Belfast and the University of Liverpool.

Eight mixes were produced; five lightweight concrete mixes and three self compacting concrete mixes. The aim of this work was to investigate the strength development of these concretes cured under different isothermal temperatures, i.e. 20, 30, 40 and 50^0C and under adiabatic conditions. These results were then used to assess the accuracy of existing maturity methods to predict early age concrete strength.

The concretes were cast into 100 mm cubes, wrapped with cling film plastic and then put them into temperature controlled curing tanks to cure the samples under isothermal curing temperatures. The cubes to be cured under adiabatic conditions were also wrapped in cling film before putting them into a temperature controlled chamber beside the adiabatic test box. The cubes were transferred into a constant curing temperature tank, when the adiabatic temperature rise was completed.

CHAPTER 4 – MATERIALS, EXPERIMENTAL PROCEDURES AND MIX DESIGN OF GGBS CONCRETE

4.1 Introduction

This chapter describes the materials used, the mixing, casting, and curing procedures of concrete investigated in this study. The methods of measuring workability, density, compressive strength and heat output, as well as the apparatus used, are also described.

4.2 Materials

All materials used throughout this study were the same. They were in accordance with relevant BS EN standards and were confirmed to be suitable for the scope of this study.

4.2.1 Cement

The type of cement used was Portland cement type CEM I 52.5, except for the lightweight concrete mixes, which used Portland cement type CEM I 42.5. They were supplied by Castle Cement Ltd[233] and complied with the requirements of BS EN 197-1[234]. The chemical composition of the cement type CEM I 52.5 provided by the supplier is presented in Table 4.1.

4.2.2 Ground Granulated Blast Furnace Slag (GGBS)

The GGBS was supplied by Civil + Marine Ltd[235]. The chemical analysis is presented in Table 4.1 alongside the chemical composition of the cement.

4.2.3 Pulverised Fuel Ash (FA)

The FA was supplied by Hargreaves Coal Combustion Products Limited. The FA was used in the mixes for lightweight concretes undertaken as part of the cooperation project between the University of Liverpool and Queen's University

Belfast. The chemical analysis of the FA provided by the supplier is given in Table 4.2.

Table 4.1: Chemical composition of Portland cement type CEM I 52.5 and GGBS[233, 235]

Compound	Oxides: % by weight		Phase (Bogue) Portland cement	
	Portland cement	**GGBS**		
CaO	62.12	41.41	C_3S	49.4
SiO_2	19.88	35.35	C_2S	24.5
Al_2O_3	5.06	14	C_3A	10.8
Fe_2O_3	2.66	0.36	C_4AF	7.5
SO_3	3.19	0.10		
MgO	2.09	7.45		
K_2O	0.59	-		
Na_2O	0.27	-		
IR	0.71	0.21		
LOI	2.93	0.31		
Cl	0.06	0.014		

Table 4.2: Chemical composition of FA[236]

Compound	**Oxides: % by weight**
CaO	1 - 5
SiO_2	45 - 51
Al_2O_3	27 - 32
Fe_2O_3	7 - 11
SO_3	0.3 - 1.3
MgO	1 - 4
K_2O	1 - 5
Na_2O	0.8 - 1.7
CI	0.05 - 0.15
LOI	≤ 7

4.2.4 Coarse Aggregate

The coarse aggregate used was graded aggregate comprising crushed dolerite stone with a nominal size ranging from 5 to 20 mm. Sieve analyses were carried out in accordance with BS 882:1992[237], in order to check whether the size distributions of the aggregate satisfy the limits required in the standard; the results are presented in Figure 4.1. The absorption and density of the aggregate were also measured according to BS EN 1097-6[238]. The absorption was equal to 0.79% and the density in saturated surface dry (SSD) condition was equal to 2790 kg/m^3.

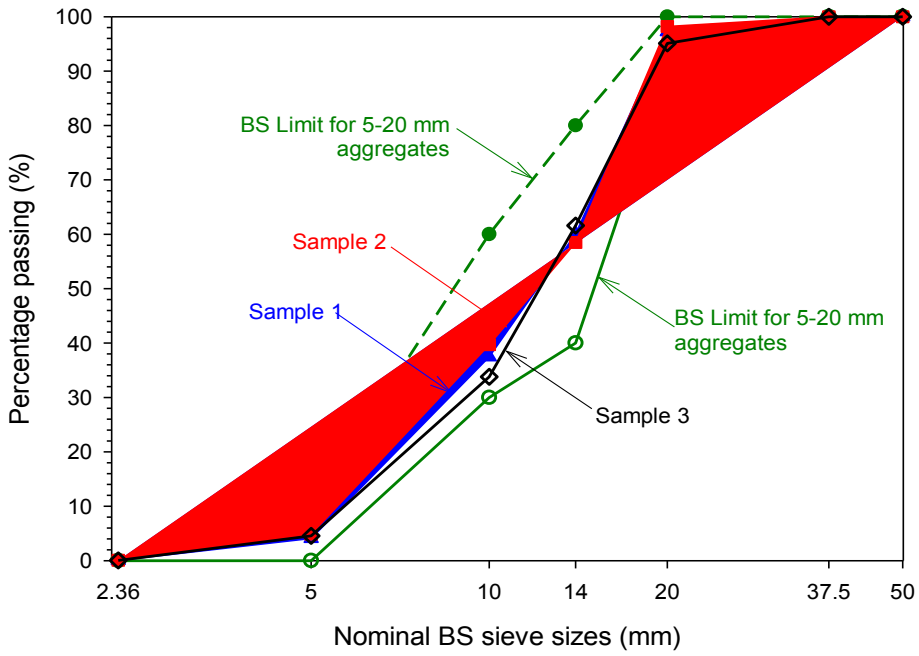

Figure 4.1: Coarse aggregate grading curves

4.2.5 Fine Aggregate

The fine aggregate was well-graded medium (M) sand, which was taken from Boras Quarry in Wrexham. The same tests carried out on the coarse aggregate were also undertaken on the fine aggregate. The sieve analysis results are shown in Figure 4.2.

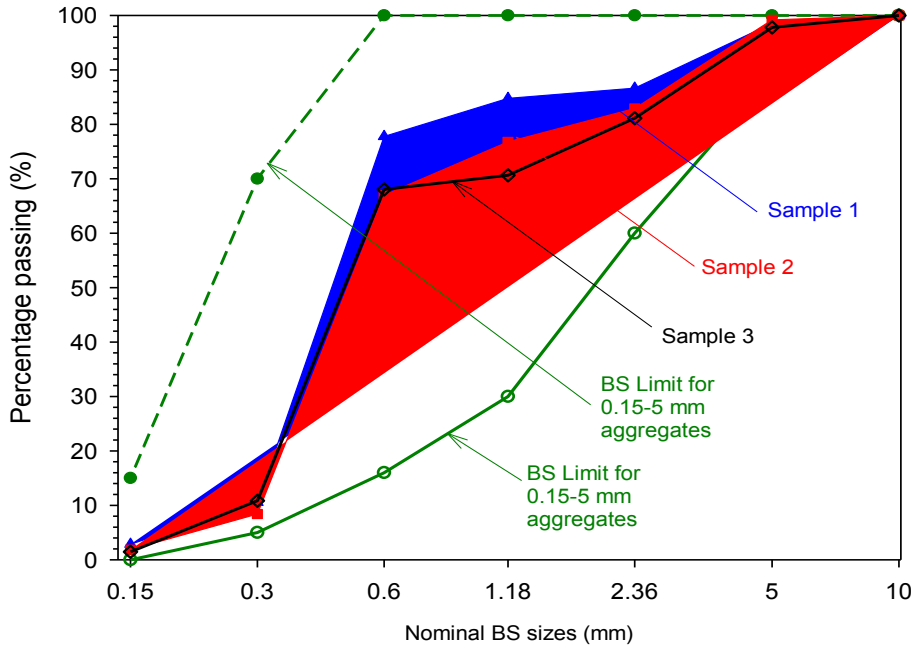

Figure 4.2: Fine aggregate grading curves

The absorption and density of the fine aggregate were equal to 0.63% and 2563 kg/m^3. The percentage of the sand passing through the sieve size of 600 µm was 69.9%. Both fine and coarse aggregates were oven-dried before using them, and allowance was made for water absorption when calculating batch weights for mixing.

4.2.6 Lightweight Aggregate

The lightweight aggregate used to produce lightweight concrete and lightweight self-compacting concrete was Lytag aggregate supplied by Lytag Ltd. This was in accordance with BS EN 13055-1[239]. The aggregate size ranged from 4 to 14 mm and the absorption of the Lytag aggregate was approximately 15% of its own weight in water[240]. Prior to mixing, two samples of the Lytag aggregate were weighed out, dried in an oven and then reweighed to calculate the amount of free moisture in the aggregate to determine the water absorption of the material.

4.2.7 Water

Mixing water for concrete should be good quality; it should not contain undesirable organic substances or inorganic ingredients above allowable amount. In the UK, water used in concrete mix shall conform to BS EN 1008[241]. Therefore, tap water was used throughout the mixing and curing procedures for the concrete in this study.

4.2.8 Chemical Admixtures

The admixture used for all normal weight concrete in this study was Structuro 11180 based Polycarboxylate superplasticiser supplied by FOSROC Ltd UK[232]. The admixtures used for the lightweight self-compacting concretes were SPA-Sika Viscocrete Premier and SPA-Larsen Chemcrete. Trial mixes were needed to find out the optimum dosage of Structuro 11180. The supplier suggested that the starting dosage should be within the range 0.2 to 0.8 litres/100 kg of binder.

4.3 Experimental Procedures

4.3.1 Mixing, Casting and Curing Procedures for Measurement the Strength of Concrete Cubes

4.3.1.1. Mixing

Three pan mixers were used throughout this study with capacities of 0.01 m^3, 0.02 m^3 and 0.1 m^3, which were chosen depending on the volume of the concrete batch needed. The concrete mixes were done in accordance with BS 1881-125:1986[242]. The aggregates were added in the following order: initially about half of the coarse aggregate, then the fine aggregate and the remainder of the coarse aggregate. The mixer was then started for 15 to 30 seconds. The mixing continued after adding about half of the total water for two to three minutes. All the cementitious materials were then added and the mixing was continued. Then the remaining water was added after 30 seconds, continuing mixing until two to three minutes after all the materials were added.

4.3.1.2. Casting

To measure the compressive strength of the concrete, samples were cast into 100mm 3-gang cube moulds placed on a vibrating table. The moulds were half filled as shown in Figure 4.3a, vibrated and then filled up to the top before they were vibrated again to have a sufficient level of compaction as shown in Figure 4.3b. The time for vibrating was dependent on the workability of the concrete mixes.

a). Moulds were half filled b) Moulds filled to top then vibrated

Figure 4.3: Concrete was cast into 100 mm 3-gang moulds and placed on a vibrating table

4.3.1.3. Curing

The concrete moulds were then wrapped with cling film immediately after casting. Some of them were then submerged in water tanks set at 50^0C and the remainder of the wrapped specimens were then placed in a controlled humidity/ temperature environmental chamber called Temperature Applied Science (TAS) for adiabatic curing (the curing procedures are discussed in Section 4.3.6). In addition, concrete cubes cured at 20^0C were covered with a damp hessian and polythene sheeting and left on the vibrating table. After 24 hours, they were demoulded and then transferred to a water tank and placed in another environmental chamber set at 20^0C, as shown in Figure 4.4. Concrete cubes that had been cured at other temperatures (50^0C and adiabatic) were also demoulded

after 24 hours. They were returned back into their curing place immediately after demoulding. They were subsequently tested for compressive strength at 0.25, 0.5, 1, 2, 4, 8, 16, 32, 64, 128, 256 and 365-days.

Figure 4.4: Environmental chamber set at 20^0C for standard curing

4.3.2 Mixing, Casting and Curing Procedures for Measurement the Strength of Mortar Cubes

4.3.2.1. Mixing

Mortar equivalent to the concrete mixtures under investigation were prepared in accordance with ASTM C-1074[6]. A quantity of 0.30 m^3 of each mortar mixture was prepared using a horizontal pan mixer. Materials were added in the order: cement/ggbs, sand and water mixed with the superplasticisers (if they were used). The mortar was mixed for three minutes[40].

4.3.2.2. Casting

To investigate the strength development of mortar cured at different curing temperatures, the mortar was cast into 50 mm 3-gang cube moulds placed on a vibrating table. Similar to the way that was concrete cast, the moulds were filled in two phases and compacted.

4.3.2.3. Curing

The specimens were wrapped in cling film immediately after casting. They were then transferred to water tanks set at 30, 40 and 50^0C (shown in Figure 4.5). Mortars that were cured under adiabatic conditions were placed in a controlled humidity/temperature environmental chamber. While the mortar cured at 10^0C was cured in the Temperature Match Curing (TMC) tank (shown in Figure 4.6), which could be set to the temperature of 10^0C. As with the concrete cubes, all the mortar cubes were demoulded after one day and returned back to their curing temperature. Mortar cubes cured at 20^0C were covered with a damp hessian and polythene sheeting and left on the vibrating table. After 24 hours, they were demoulded and then transferred to a water tank set at 20^0C, in a similar way to the concretes cured at the same temperatures. They were subsequently tested for compressive strength at 0.25, 0.5, 1, 2, 4, 8, 16, 32, 64, 128, 256 and 365-days.

Figure 4.5: Isothermal curing tanks

Figure 4.6: Temperature Matched Curing (TMC) tank for curing

4.3.3. Mixing, Casting and Curing Procedures for Measurement the Strength of Mortars Cured Under Rapid Temperature Rise

Five mortar mixes of grade C45 with different levels of GGBS (0, 20, 35, 50 and 70%) were prepared to investigate the effect of changed curing temperatures on the strength development of the mortars. The mixing and casting procedures were the same as those of mortars cured at different isothermal temperatures. Mortar cubes were cured inside two tanks with different isothermal temperatures i.e. 20 and 50^0C. There were five different curing regimes, as presented in Table 4.3. Three cube specimens of each mix were prepared for each testing age.

Table 4.3: Curing regimes for mortars with changing curing temperatures

No	Curing regime	Testing age (days)
1	Isothermal 20 ^{0}C (Control)	0.5, 1, 2, 3, 4, 5, 7, 14, 28, 56 and 91
2	20^0C 1-day and then 50^0C onwards	2, 3, 4, 5, 7, 14, 28, 56 and 91
3	20^0C 2-days and then 50^0C onwards	3, 4, 5, 7, 14, 28, 56 and 91
4	20^0C 3-days and then 50^0C onwards	4, 5, 7, 14, 28, 56 and 91
5	Isothermal 50^0C	0.5, 1, 2, 3, 4, 5, 7, 14, 28, 56 and 91

All mortar cubes, except for the specimens cured at 50^0C from the beginning, were left for 24 hours on the vibrating table, covered with damp hessian and polythene sheeting. They were demoulded after 24 hours, when 27 cube specimens were transferred into a tank set to 50^0C. The remaining cubes were transferred into a water tank placed in a controlled chamber at 20^0C. After 2-days, another 24 cube specimens were transferred from 20 into 50^0C. Finally, after 3-days, 21 cube specimens were transferred from 20 to 50^0C. They were subsequently tested for compressive strength at the ages shown in Table 4.3.

4.3.4 Mixing, Casting and Curing Procedures for Lightweight and Self Compacting Concretes

There were eight mixes in total, which consisted of five mixes of lightweight concrete, two mixes of lightweight self-compacting concrete and a mix of normal weight self-compacting concrete as a control. The aim was to investigate the effect of temperature on the early-age strength development of lightweight self-compacting concrete, where the mix proportions were prepared by Queens University Belfast.

4.3.4.1. Lightweight Concrete

All aggregates used in these mixes were expected to be in saturated surface dry condition. However, initially the aggregates were not in that condition. Therefore, prior to mixing, a sample of each aggregate was weighed and dried in an oven for 24-hours. They were then reweighed and the free moisture calculated in the aggregates. A recalculation of the mix proportions was needed to take into account the water absorption of the materials.

For mixes, which contained the activator sodium sulphate, the sodium sulphate was dissolved in the mixing water approximately one hour prior to mixing. The materials were then added in the following order: coarse aggregate, sand and half of the mixing water. They were then mixed for 30 seconds; the mixer was then stopped and left to stand for 10 minutes. The cement and other powders along

with the remaining water were added and mixed for two to three minutes. The superplasticisers were then added and mixed again. The superplasticisers could be adjusted if necessary. The slump of the concrete should be between 120 and 140 mm. If the slump was too high, it was left for a while until the slump was within the ranges.

The moulds were filled in two levels with vibration of no less than 30 seconds for each level. After pouring into the moulds, they were then wrapped and transferred into water tanks set to 30, 40 and 50^0C. The concrete specimens cured at 20^0C were left on the vibrating table for 24-hours where they were covered with damp hessian and polythene sheeting. They were then demoulded and transferred into a water tank placed in the TAS chamber set at 20^0C. In addition, cube specimens cured at 30, 40 and 50^0C were demoulded and immediately after demoulding those concrete cubes were placed back into their curing tanks. The concrete specimens cured under adiabatic conditions were placed in a controlled humidity/temperature environmental chamber. They were subsequently tested for compressive strength at 3, 6 and 12 hours, 1, 2, 4, 7, 14 and 28 days.

4.3.4.2. Lightweight Concrete Self Compacting Concrete

The aggregates which were used in calculating the mix proportions obtained from Queen's University Belfast, were assumed to be in the dried-oven condition. Therefore, the water content in the mixes was free water content. In a similar way to the lightweight concretes, the recalculation of the proportions in the obtained mixes from Queen's University Belfast was needed for adjusting for the water absorption of the materials.

The materials were added in the order: coarse aggregate, sand and 2/3 of the total water. It was then mixed for 2 minutes. After that, the limestone powder or GGBS (if was used) was then added and mixed for a minute. The cement was then added and mixed for another one minute. In the next stage, the remaining water and superplasticisers were added and mixed for 2 minutes to allow the

superplasticisers to distribute evenly. It was found to be better to hold back some of the superplasticisers until after the slum flow test. The slump test was carried out on top of a moist (not wet) plastic sheet. The slump value should be between 700 and 750 mm. If the slump value is less than 700 mm, then more superplasticisers should be added to the mix. If the slump value was higher than 750 mm, then mix was discarded and repeated.

The moulds were filled until full without vibration as the concrete compacted itself by its own weight. After casting the moulds, they were then wrapped in cling film and transferred into water tanks set to 30, 40 and 50^0C, as done on the lightweight concrete specimens. For concrete specimens cured at 20^0C and those cured under adiabatic conditions, the procedures were the same as for the lightweight concrete. They were subsequently tested for compressive strength at 3, 6 and 12 hours, 1, 2, 4, 7, 14 and 28 days.

4.3.5 Mixing and Casting Procedures of Mortar Samples for Heat Output Measurement Using Isothermal Calorimeter

4.3.5.1. Mixing and Casting Procedures of Mortar Samples

The mix proportions of the equivalent mortar mixes investigated were prepared to measure the heat output rate of hydration. One litre of each mix was prepared to easily weigh the materials in a small portion of the mix. The mortar was mixed using a small bench-top mixer as shown in Figure 4.7.

Figure 4.7: Bench-top mixer

All the materials, except the mixing water, were added together into mixing bowl; they were then mixed for 30 seconds; then mixing water was added and mixed again for two to three minutes where the time when the water was added was recorded. After mixing, the temperature of the mortar was recorded (i.e. the casting temperature). Two samples from each mortar mix were then filled into 20ml glass ampoules (about 45g), they were sealed with aluminium covers. The ampoules filled with mortar were then weighed, where the weight of the empty ampoule was known before. They were then inserted into the calorimeter carefully through the holes on the lid. Great care was taken to prevent any dust contaminating the calorimeter. The times when the ampoules were put into the calorimeter were recorded.

The temperature of the mortar when it was put into the isothermal calorimeter should be maintained as close as possible to the temperature setting on the isothermal calorimeter. Therefore, before mixing, all the materials including the water were put in an oven overnight. The oven was set to a temperature that was usually taken to be 10 ^{0}C higher than the curing temperature setting on the calorimeter, although it was higher when the ambient temperature was low. This aims to take account of the temperature lost during mixing and casting periods and to ensure that the casting temperature was close to the calorimeter temperature.

The heat output of all the mortars were measured at four curing temperatures i.e. 20, 30, 40 and 50^{0}C.

4.3.5.2. Isothermal Calorimeter Test

The isothermal calorimeter used in this study was the 3314/3236 TAM Air with eight-calorimetric channels that was capable of measuring heat flow in the milliwatt range. It was manufactured by Thermometric AB, Sweden[243]. Each calorimetric channel is constructed in twin configuration with one side for the

sample and the other side for a static reference made out of an inert material shown in Figure 4.8.

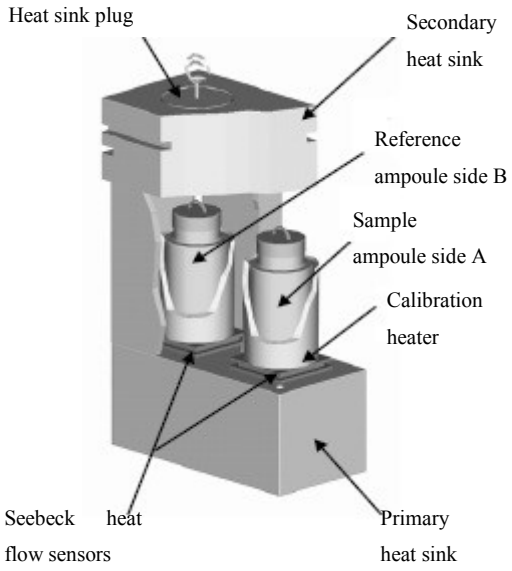

Figure 4.8: One of the 8 calorimetric channels showing the twin configuration[243]

Each calorimeter operates based on the heat flow principle. Heat produced by any physical or chemical reaction in the sample of mortar will flow rapidly to its surroundings. There are two Seebeck heat flow sensors within each calorimetric channel; one beneath the sample and another one beneath the reference as shown in Figure 4.8. The principal route of heat exchange between the sample and its surroundings passes through the Seebeck heat flow sensors. The heat exchange between the heat sensor and the sample, caused by the gradient across the sensor, generates a voltage signal that is proportional to the heat flow[243].

The heat output rate was recorded continuously using a modified version of the Pico TC-08 data logger inside the calorimeter. The data logger is connected to a computer as shown in Figure 4.9 and all the data is stored using the PicoLog Recorder software[244].

Figure 4.9: TAM Air Isothermal calorimeter is connected to a computer to record data

The colorimeter was recalibrated every time it was set to a new temperature. The heat output rate, which is often referred to in literature as thermal power, was recorded using the data acquisition software package for approximately 7 days.

The advantage of using the isothermal calorimeter to measure the heat output of hydration is that the apparatus measures the heat output rate of the mortar directly. In an adiabatic test, it measures the temperature change in the mortar or concrete sample, which can then be converted into heat output using Equation 2.124 in the literature review chapter. The specific heat capacity of the mortar or concrete however, had to be known in order to calculate the heat output based on the temperature rise. The heat output that is obtained from the isothermal calorimeter test can be used to calculate the apparent activation energy. Consequently it can be used to calculate the maturity of the mortars, which reflect their equivalent concretes. In addition, the isothermal calorimeter is generally more sensitive and more accurate than the adiabatic test apparatus.

The isothermal calorimeter test has some limitations when compared to the adiabatic tests. Unlike the adiabatic tests, where the actual concrete mix was used to measure the heat output of the cement in concrete, the isothermal calorimeter can only be used for mortar specimens. Therefore, further study is needed to identify how accurate the heat output of the cement hydration in mortars reflects the heat output of cement hydration in concrete. It is important to note that a concrete mix usually has a lower cement or binder content than its equivalent mortar mix. Another thing is the size of the mortar samples is significantly smaller than the concrete specimens that are used for the adiabatic tests. In addition, the temperature of mortar when it is first put into the isothermal calorimeter should be as close as possible to the temperature of calorimeter. These probably limit the accuracy of the heat output results.

In this study, in all cases heat output recordings for the first 1.5 hours were not used in the analysis. This aims to avoid undesirable mistakes in the data analysis. This means that only heat produced from the main reaction phase was analysed.

4.3.6 Adiabatic Test – TAS Chamber procedures

The adiabatic temperature rise produced by the hydration of cement is the temperature rise that will occur if concrete is cured in a perfectly insulated environment (i.e. no loss of heat). The temperature surrounding the concrete should be the same as the temperature of the concrete[1]. Therefore, a room, which has a controlled temperature/humidity, is needed to carry out the adiabatic test. In this study, the Temperature Applied Science (TAS) controlled temperature/ humidity environmental chamber was used. A stainless steel box mould lined with 100 mm expanded polystyrene for insulation and heavy-duty polythene to prevent moisture loss was prepared for the adiabatic test, as shown in Figure 4.10.

A 200 x 200 x 200 mm concrete specimen was cast into the insulated stainless steel box (adiabatic box). After casting, two thermocouple wires were inserted into the centre of the concrete specimen through a hole in the top of the lid of the

adiabatic box. The adiabatic box then was covered on top with insulation and the stainless steel lid was bolted down.

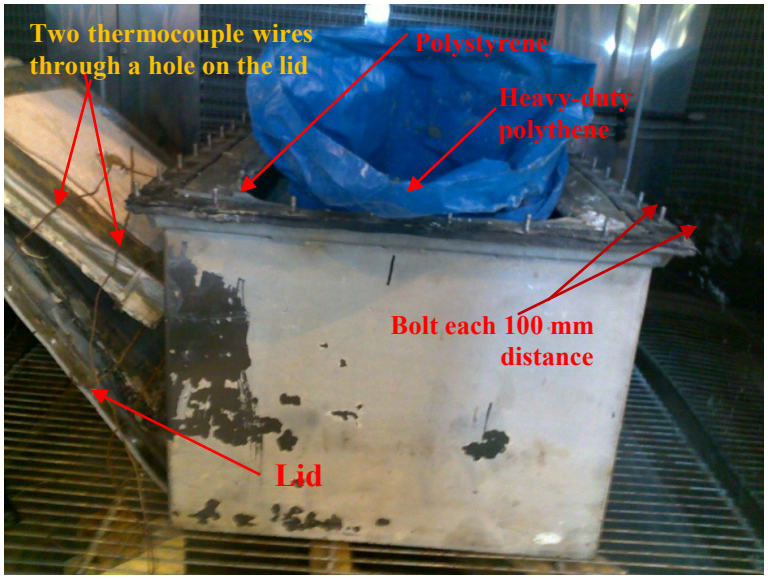

Figure 4.10: Insulated stainless steel box (adiabatic box) for adiabatic test

The concrete cube specimens that were cured under adiabatic conditions were placed alongside of the adiabatic box as shown in Figure 4.11.

Figure 4.11: Concrete specimens placed inside of the controlled temperature/humidity environmental chamber

It is important to check the thermocouple wires before they were inserted into the concrete specimen in order to make sure they work.

After all the concrete specimens for the adiabatic testing were placed in the controlled temperature/humidity environmental chamber, the computer was switched on. The thermocouples were connected to a computer through the Pico TC-08 data logger. A computer program recorded the temperature of the concrete inside the adiabatic box in the environmental chamber. It then controlled the temperature of the environmental chamber to be approximately equal to the recorded temperature of the concrete specimen, within a difference of ± 1 ^{0}C, as shown in Figure 4.12. In fact, after the peak of temperature rise had been reached, there was no temperature drop; and there was only very little heat loss, there was no need to adjust the results.

Figure 4.12: Controlled temperature/humidity environmental chamber

The relative humidity of the air in the environmental chamber was maintained at 90%. Barnet et al[161] found that curing cubes at relative humidity of 90% had no significant difference on strength development of the adiabatically cured cubes compared to those cured under water. Therefore, the standard and the adiabatic cube strengths could be compared directly.

The adiabatic test was normally performed for five days, depending on the time when the temperature rise in the concrete specimen reached its peak. The remaining cube specimens were then transferred into a water tank with constant temperature set at the maximum temperature reached in the adiabatic test.

4.4 Mix Design of Portland Cement and GGBS Concretes, Lightweight and Self Compacting Concretes

In this study, there were two methods selected to determine the mix proportions of concretes as discussed in the literature review chapter in Section 2.5. The Building Research Establishment (BRE)[229] method was used to design the mix proportions of normal strength concrete. While the method that was used to design the mix proportions of high strength concrete was the Modified Maximum Density Theory (MMDT) method[230, 245].

4.4.1 Measurement of Void Content of Aggregates

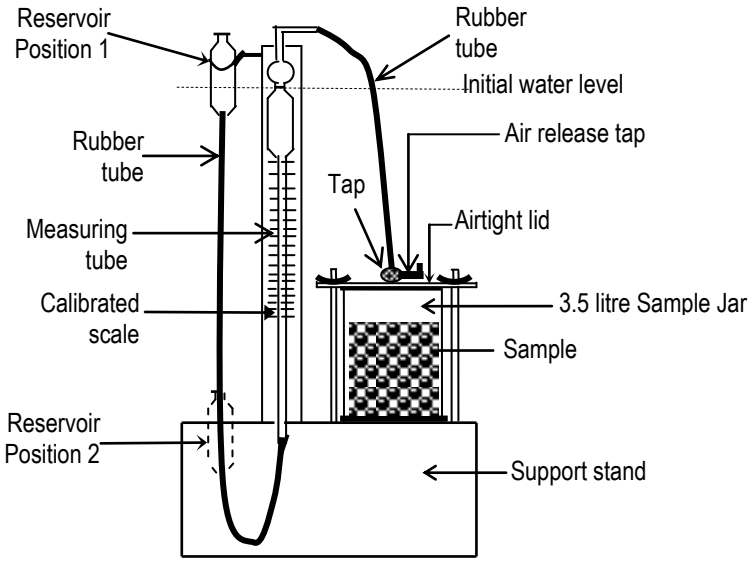

Figure 4.13: Sketch of apparatus for void content measurement[245]

The experiment aimed to measure the maximum void content of mixed aggregates (fine and coarse aggregates), which is required in the Modified Maximum Density Theory (MMDT) to calculate the mix proportion of concrete.

The total volume of the void content of mixed aggregates with overfill (lubricant layer) is the same as that of cement paste needed in concrete. The measurement of the void content of the mixed aggregate was done using the apparatus shown in Figure 4.13 above.

The apparatus for void content measurement consists of a sample jar, which is connected to a glass bulb at the top of a measuring tube through a rubber tube. A reservoir is connected to the lower end of the measuring tube through another rubber tube as shown in Figure 4.13. The sample jar is made of steel, graduated in 0.2 litre divisions up to 3.5 litres, which is fitted between a supported stand and a steel airtight lid with a rubber seal. Four screwed rods with wing nuts are used to make the container airtight, as shown in Figure 4.13. Before any measurements were taken, the scale was calibrated with known quantity of distilled water. The aggregates were then mixed such that the proportion of sand by weight to the total of aggregate was increased in 5% intervals from 0% to 100%. The test was carried out with the procedures as follows:

- The aggregate sample was placed in the 3.5 litre sample jar in 25mm thick layers until it reached the level that was marked when it was calibrated. Each layer was tamped 10 times by dropping a piston through the layer.
- The sample jar with aggregate in it was then placed in the apparatus. The air release tap was left open to the atmosphere, while the lid was screwed. The reservoir was in Position 1.
- The quantity of water in the tubes was adjusted to bring the water level to the required initial level.
- The air release tap was then closed, and then the reservoir was lowered to Position 2. This created a partial vacuum and the water in the measuring tube flowed down until the equilibrium position was reached. This occurred when the pressure of air in the system plus the pressure of air due to the height of the water column was equal to atmospheric pressure. As the volume of air above the sample was constant, the variations in the distance that the water column falls in the measuring tube were directly related to the

void volume in the sample. Therefore, the voids content of the sample could be read from the equilibrium position of the water surface against the calibrated scale reading on the column. To avoid the possibility of a faulty reading, the measuring was repeated three times and the average was taken. The procedure was repeated for other proportions of sand to the total aggregates.

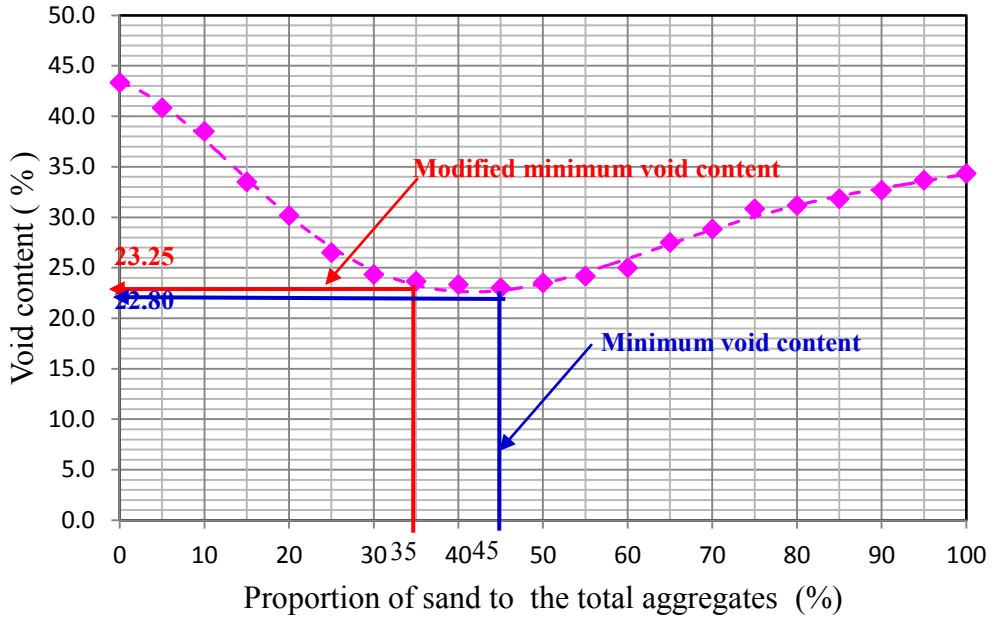

Figure 4.14: Percentage of sand to the total of aggregate at the modified minimum void content

The results of the measurement of minimum void content are shown in Figure 4.14. The minimum void content obtained was 22.8% at the percentage of sand to the total aggregates of 45%. By modifying the proportion of sand to the total aggregate in order to obtain good workability of the concrete, the percentage of sand was taken to be 35%. This gave a minimum void content of 23.25% as shown in Figure 4.14. By taking an overfill (lubricant layer) of 5.45%, the proportion in 1 m^3 concrete consists of 0.272 m^3 of cement paste and the remaining 0.728 m^3 being aggregates (both fine and coarse aggregates).

4.4.2 Trial Mixes

4.4.2.1. Introduction

Trial mixes were carried out to find a suitable mix for the desired target mean strength of concrete at 28-days, workability and other properties of the concrete that were investigated. In this study, there were 40 mixes varying in water-cement ratio and replacement levels of cement with GGBS. The water cement-ratios used in the trial mixes were 0.25, 0.30, 0.35, 0.40, 0.45, 0.56, 0.63 and 0.69. The levels of cement replacement with GGBS were 0, 20, 35, 50 and 70%.

Concrete with water-cement ratios equal to or lower than 0.4 were designed using the MMDT method, while those concrete that had water-cement ratios higher than 0.40 were designed using the BRE method. Superplasticisers were used in concrete that had water-cement ratios lower than or equal to 0.40. The mix proportions and the compressive strength obtained for the trial mixes are attached in Appendix C.

A 0.01 m^3 sample of concrete was prepared for each of the trial mixes. After mixing, the slump of the concrete was measured; it was then cast into a 3-gang mould of 100 mm cubes. The concrete specimens were tested at ages 3, 7 and 28-days, with three cubes used for each test. The concrete was vibrated on the vibrating table, and left there for 24-hours, where they were covered with damp hessian and polythene sheeting. They were demoulded and then transferred into a water tank that was placed in the TAS room set to the standard curing temperature, as shown in Figure 4.4.

4.4.2.2. Strength Development of Trial Mixes

The results of all the trial mixes are presented in Figures 4.15 to 4.17 for the strengths of concrete at ages 3, 7 and 28-days, respectively. The results were used to design concrete mixes with the required target strengths at age 28-days.

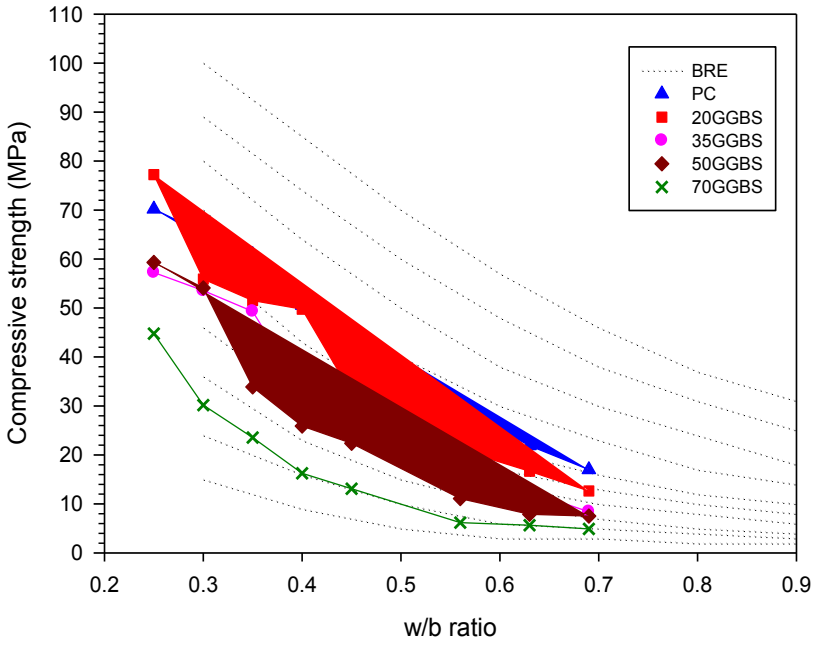

Figure 4.15: Strength of concrete at age 3-days

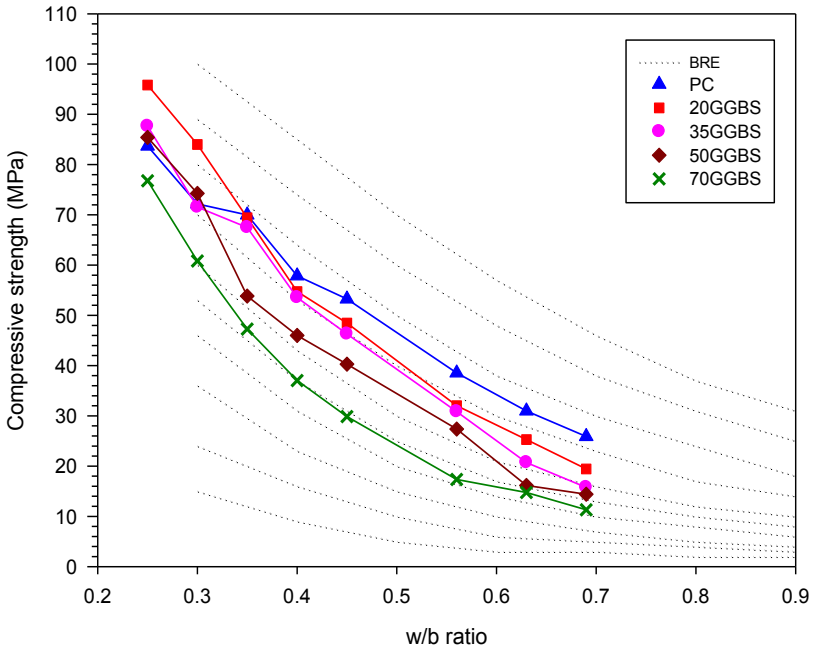

Figure 4.16: Strength of concrete at age 7-days

The figures show that the strengths of GGBS concrete vary depending on the replacement levels of cement with GGBS. Therefore, in order to obtain a good estimation of the mix proportions of GGBS concrete, it is necessary to carry out an individual trial mix of each concrete with different levels of GGBS, rather than

just adjust the trial mix obtained from concrete with Portland cement only, especially when designing a concrete mix with a high level of GGBS that requires certain strength at early age.

However, the strength of GGBS concretes with lower water-binder ratios (high strength concrete) at age 28-days are similar to that of concrete with Portland cement only, as shown in Figure 4.17. Even the strengths of GGBS concrete with a water-binder ratio of 0.25 are higher than that of PC concrete.

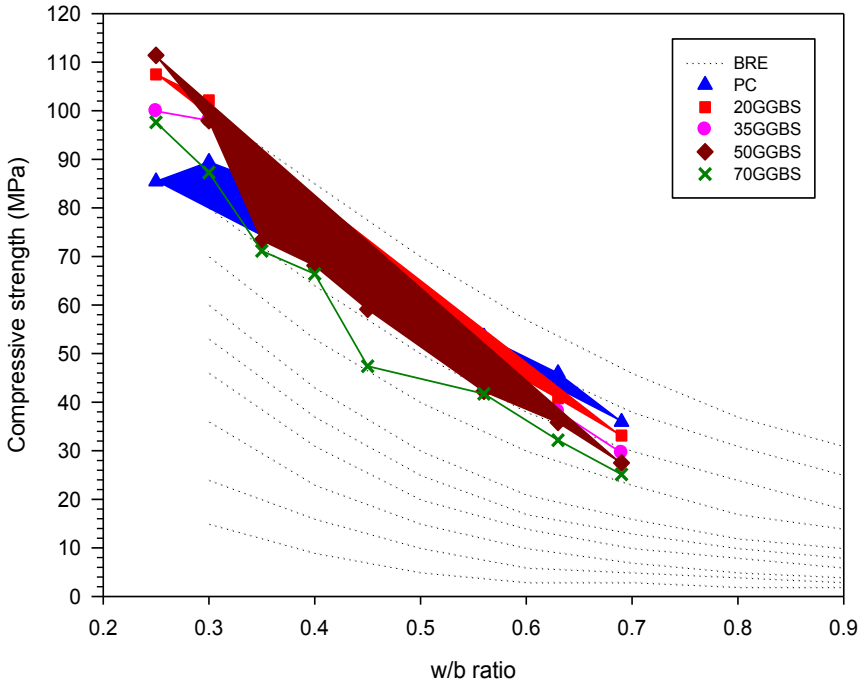

Figure 4.17: Strength of concrete at age 28-days

4.4.3 Mixes Proportion of Investigated Concretes

In this study, there were two grades of concrete investigated, i.e. concrete grades C45 and C75. The target mean strengths at age 28-days for both these grades are 55 and 85 N/mm^2, respectively. Based on the results of the concrete trial mixes, the water-binder ratios of all concrete grades C45 and C75 with different levels of GGBS were then determined by plotting the water-binder ratios to strengths gain at age 28-days. These can be seen in Figures C1 to C5 in Appendix C.

The mix proportions of each concrete mix were then calculated using the BRE method and the MMDT method for concrete grades C45 and C75. The results are shown in Tables 4.4 and 4.5 for concrete grades C45 and C75, respectively.

Table 4.4: Mix proportion for concrete grade C45

Concrete	% GGBS	Quantity per m³ of Concrete (kg)							w/b ratio
		Cement	GGBS	Sand (Oven-dried)	Granite (Oven-dried)	Free water	SPA (liquid)	Added water	
PC45	0	373		612	1241	190	-	204	0.51
20GGBS45	20	317	79	605	1225	190	-	204	0.48
35GGBS45	35	263	141	602	1220	190	-	204	0.47
50GGBS45	50	216	216	593	1201	190	-	204	0.44
70GGBS45	70	136	316	586	1188	190	-	204	0.42

Table 4.5: Mix proportion for concrete grade C75

Concrete	% GGBS	Quantity per m³ of Concrete (kg)							w/b ratio
		Cement	GGBS	Sand (Oven-dried)	Granite (Oven-dried)	Free water	SPA (liquid)	Added water	
PC75	0	417		685	1270	138	3.336	149.808	0.33
20GGBS75	20	336	84	685	1270	134	3.360	145.790	0.32
35GGBS75	35	267	144	685	1270	136	3.124	147.968	0.33
50GGBS75	50	207	207	685	1270	133	3.146	144.951	0.32
70GGBS75	70	127	297	685	1270	127	3.392	138.766	0.30

4.4.4 Equivalent Mortar Mixes of Investigated Concrete

The equivalent mortar mixes of the concrete grades C45 and C75 were calculated in accordance with ASTM C-074[6]. The mortars had a fine aggregate to cement ratio (by mass) that was the same as the coarse aggregate to cement ratio of the concrete investigated. The mortars also have the same water-binder ratio as the concrete. In addition, when a superplasticiser admixture (SPA) was used in the concrete, this also should be used in the equivalent mortar mixes in the same

proportion. The equivalent mortar mixtures for concrete grades C45 and C75 are presented in Tables 4.6 and 4.7, respectively.

Table 4.6: Equivalent mortar mix proportion for **grade C45**

Mortar	Quantity per m^3 of mortar (kg)						w/b ratio
	Cement	GGBS	Sand (Oven-dried)	Free water	SPA	Added water	
PC45	455.00	-	1505.00	232.00	-	242.00	0.51
20GGBS45	385.00	96.00	1476.00	231.00	-	241.00	0.48
35GGBS45	318.50	171.50	1470.00	230.00	-	240.00	0.47
50GGBS45	260.50	260.50	1438.79	229.24	-	238.45	0.44
70GGBS45	163.00	380.00	1418.92	228.00	-	237.08	0.42

Table 4.7: Equivalent mortar mix proportion for **grade C75**

Mortar	Quantity per m^3 of mortar (kg)						w/b ratio
	Cement	GGBS	Sand (Oven-dried)	Free water	SPA (liquid)	Added water	
PC75	502.00	-	1521.00	166.00	4.016	173.00	0.33
20GGBS75	406.00	101.00	1523.00	162.00	4.056	169.00	0.32
35GGBS75	324.00	174.00	1529.00	164.00	3.785	171.00	0.33
50GGBS75	250.50	250.50	1527.00	160.00	3.808	167.00	0.32
70GGBS75	153.60	358.40	1523.00	153.60	3.891	160.43	0.30

4.4.5 Mix Proportions for Lightweight and Self-Compacting Concretes

Eight mixes for lightweight and self-compacting concretes were prepared according to mixtures proportions derived at Queen's University Belfast. The mix proportions were calculated by assuming that all aggregates used in the mixes were in saturated surface dry condition. Therefore, the mix proportions, which were used in producing the concretes, were adjusted as the moisture content of the aggregates changed. The adjusted mix proportions can be found in the Appendix B.

CHAPTER 5 – STRENGTH DEVELOPMENT OF GGBS MORTARS AND GGBS CONCRETES – RESULTS AND ANALYSIS

5.1. Introduction

This chapter presents the strength development results and analysis of the investigated Portland cement and GGBS concretes and their equivalent mortars. The replacement level of cement with GGBS was 0%, 20%, 35%, 50% and 70% with the symbols: PC, 20GGBS, 35GGBS, 50GGBS and 70GGBS, respectively.

Both concretes and mortars for grade C45 and C75 were cast and isothermally cured with a variety of temperatures, as described in sections 4.3.1 and 4.3.2 of Chapter 4, in order to simulate the in-situ temperatures. This was also to provide the basis for development of models to estimate the in-situ temperature histories and strength development. The activation energies were determined using the mortar strength data. The results were used to predict the strength development of the mortars/concretes cured under adiabatic conditions, discussed in Chapter 6. The accuracy of the recent maturity functions, as they apply to GGBS concrete, was evaluated (as they were developed based on only Portland cement concretes) by comparing the predicted strength development to the data obtained from the experimental data in this work. A modification on the existing maturity method is carried out to obtain better prediction of strength development of concrete[166]. Also the contribution of GGBS to the strength development of both concretes and mortars will be investigated.

5.2. Strength Development

5.2.1. Strength Development of Equivalent GGBS Mortars

The equivalent mortar mixes were presented in Table 4.6 and Table 4.7 (Chapter 4) for mortar grades C45 and C75, respectively. The results for the compression strength tests for all mortars cured at 10, 20, 30, 40 and 50^0C are shown Tables D-1 to D-10 in Appendix D.

The target mean 32-day strengths of the mortar specimens were 55 MPa and 85 MPa for grades C45 and C75, respectively, under the standard curing temperature. The results show that the strengths of mortars grade C45 at 32-days cured under the standard curing temperature were as expected. However, the strengths of mortars grade C75 at 32-day cured at the same curing temperature was lower than the expected strength/target mean strength at that age. The obtained strengths of all mortars grade C75 cured under standard curing temperature were lower than the target mean 32-days strength i.e. 85 MPa as mentioned above. They were varied from 72.47% to 81.35% of the target mean 32-day strength. This is believed to be due to the mortars grade C75 containing a little more sand than that of the C45 grade and the casting temperature for all mortars grade C75 were slightly higher (above 20^0C). This caused the mortar specimens to dry quickly, which resulted in the specimens being short of water for further cement hydration.

The effect of curing temperature on the strength development of mortars was investigated by casting and testing the equivalent mortars of investigated concretes. The mortar test results at different curing temperatures were plotted with error bars based on the three replicate samples in Figure 5.1 to Figure 5.2 for mortar grade C45 and C75 respectively.

The strength development of all mortars for both grades C45 and C75 highly depend on the curing temperature. As expected, at an early-age, the strength development of mortar cured at higher curing temperatures was higher than that for lower curing temperatures. It is confirmed that higher curing temperatures result in greater rate of reaction than that of lower curing temperatures at early ages. However, mortars cured at higher curing temperatures have lower strength at later ages; this is the so-called “crossover effect”. This is the result of the formation of dense hydrated phases around the un-hydrated cement particles, hindering further hydration[40]. Higher curing temperatures result in larger pores in the microstructure due to the non-uniform distribution of hydration products as explained in the additional literature review section in Appendix A.3.4.

The crossover effect appeared earlier in PC mortars than in GGBS mortars. The crossover effect was delayed significantly, as the replacement levels of cement by GGBS increased. The later age strength of PC mortars for both grades were much more detrimentally affected by higher curing temperatures, compared to GGBS mortars. The strength development of both grades C45 and C75 GGBS mortar cured at 10^0C, gradually continues to develop. Even their strengths were higher than that of mortars cured at the standard curing temperature at ages after 32-days.

Both Figures 5.1 and 5.2 show that the strength developments of mortars containing high levels of GGBS were more dependent on temperature, with the strengths at early ages having a wider variation with temperature as the GGBS level increased. After 2 days, the Portland cement grade C45 shown in Figure 5.1(a) had strengths varying from 17 to 37 N/mm^2, where the lowest and the highest strength at that age was obtained at curing temperatures 10 and 30^0C, respectively. The mortar grade C45 with 70% GGBS (Figure 5.1(e)) achieved a 2-day compressive strength of 33 N/mm^2 at curing temperature 50 ^{0}C; which is very close to the strength of Portland cement mortar at the same age and curing temperature i.e. 34 N/mm^2. There is no delay in strength development of mortar with GGBS cured at an elevated curing temperature.

However, under standard curing temperature, the strength development of both GGBS mortars of grade C45 and C75 is lower than that of PC only mortars. For mortar grade C45 under the standard curing temperature (20^0C), the strength gained from PC mortar at age 2-day was 27 N/mm^2; it is about four times that of 70% GGBS mortar strength i.e. 6.5 N/mm^2. Compared to mortar grade C75; the ratio is smaller, which is about two times where the strength of PC mortar and 70% GGBS mortar are 43.35 N/mm^2 and 20.35 N/mm^2, respectively. This proves that strength development of GGBS mortar cured under the standard curing temperature is slower than that of PC mortar and it is clear that the higher GGBS level results in slower strength development. However, the strengths development of GGBS mortar cured at higher curing temperatures were comparable to that of PC mortar.

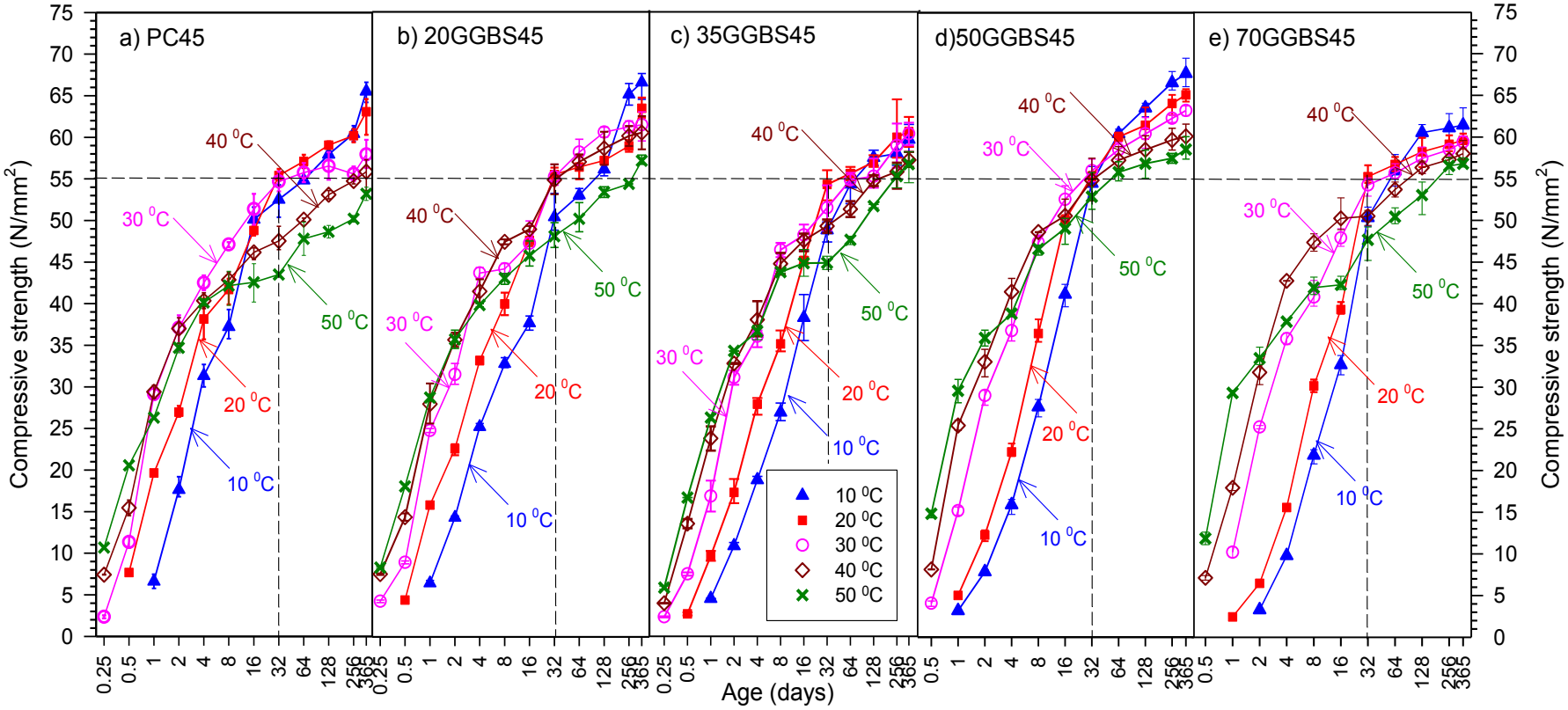

Figure 5.1: Strength development of PC and GGBS mortar under 10, 20, 30, 40 and 50^{0}C curing temperatures **(grade C45)**

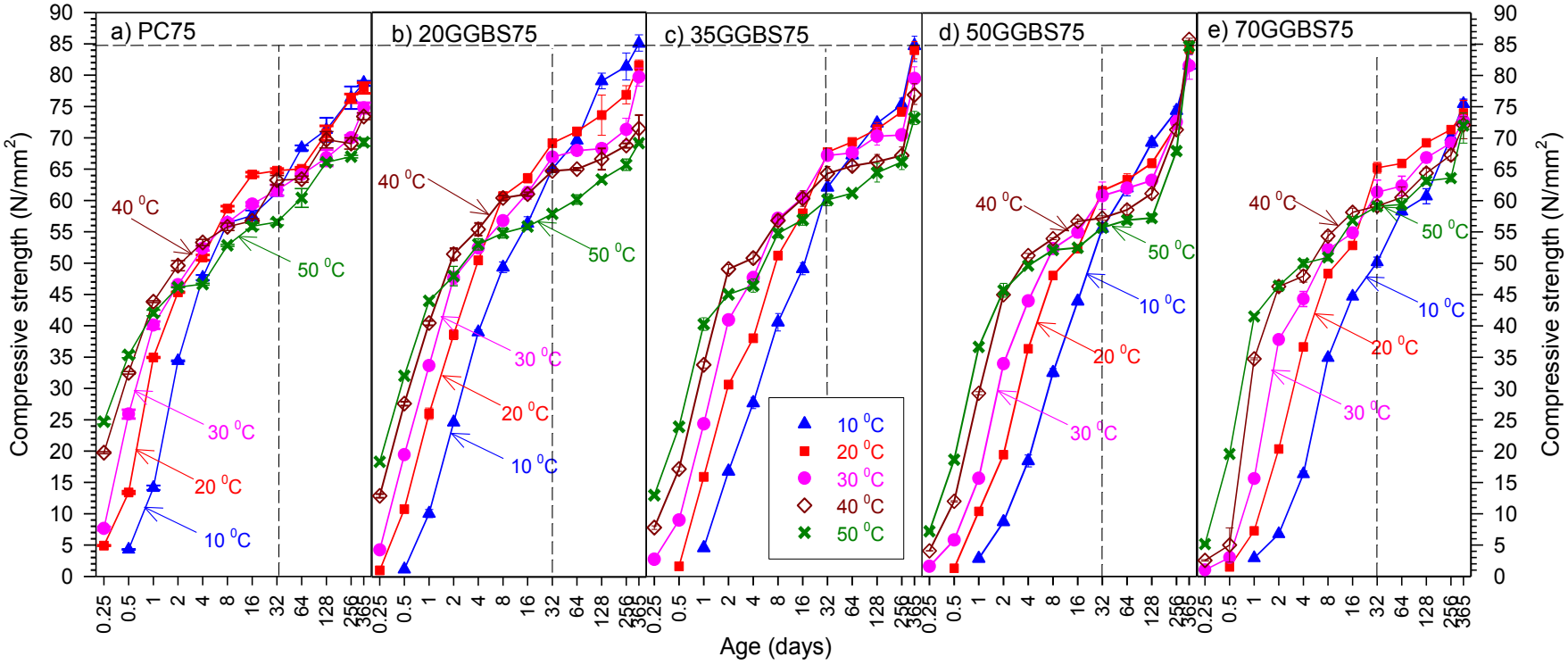

Figure 5.2: Strength development of PC and GGBS mortar under 10, 20, 30, 40 and 50^{0}C curing temperatures **(grade C75)**

The result also shows that water binder ratio also had a significant effect on the strength development on GGBS mortar especially at early age. The mortar with lower water binder ratio contains much more cement/binder than one with the higher water binder ratio; therefore, initially the hydration of mortar with lower water binder ratio produced hydration products like calcium hydroxide, lime, and heat output more than that of mortar with a higher water binder ratio. Those cement hydration products can activate the subsequent hydration of GGBS in the cement composite.

The ratio of strength of the mortar cured at 10, 30, 40 and 50^0C to the strength of mortar cured under the standard curing temperature (20^0C) for mortars grade C45 and C75 are shown in Figures 5.3 and 5.4, respectively. In general, the strength ratios gradually decreased as the ages of mortars increased for mortar that had cured at higher temperatures (30. 40, and 50^0C) than the standard curing temperature (20^0C). On the other hand, the ratio of strength of mortars cured at lower temperature (10^0C) slowly increased and it took a longer time to reach the strength of mortars cured at the standard curing temperature as the GGBS level increased.

At an earlier-age (1-day), the higher curing temperatures (above 20^0C) with the higher GGBS levels, particularly 50% and 70% GGBS, resulted in the higher strength ratios. This confirms that the strength development of GGBS mortars, which were cured at standard curing temperature, is slower than those cured at elevated temperatures. Furthermore, the higher GGBS level for cement replacement, results in slower strength development. The strength ratios of 20 and 35% GGBS level are quite similar to the strength ratios of mortar with PC only.

Both the figures clearly show that the strength development of GGBS mortar depends on curing temperature as mentioned before. At an age of 1-day, the strength of 70% GGBS mortar grade C45 that cured at 50^0C was 12 times than the one cured at the standard curing temperature (20^0C) i.e. 29.3 N/mm^2 and 2.44 N/mm^2, respectively.

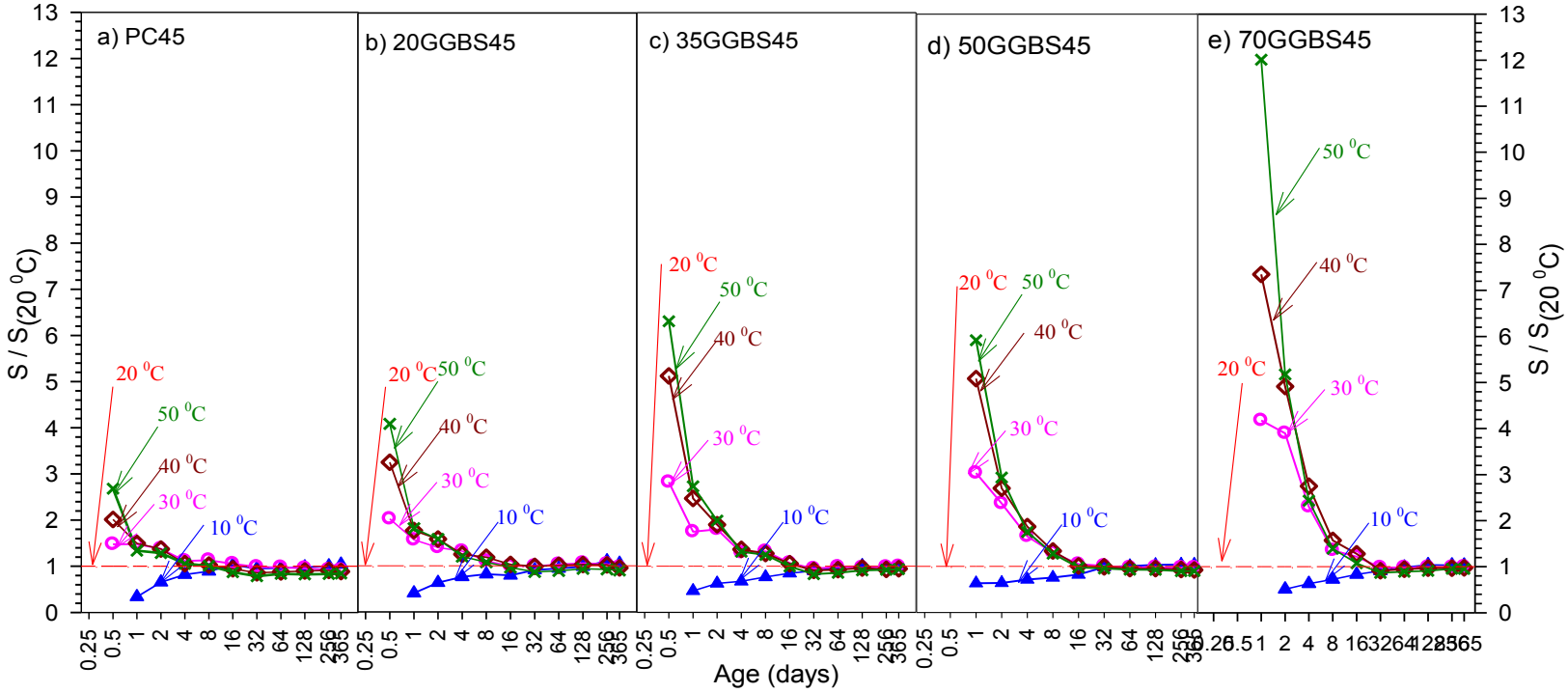

Figure 5.3: Ratio strength $S/S_{(20^{o}C)}$ PC and GGBS mortar **grade C45**

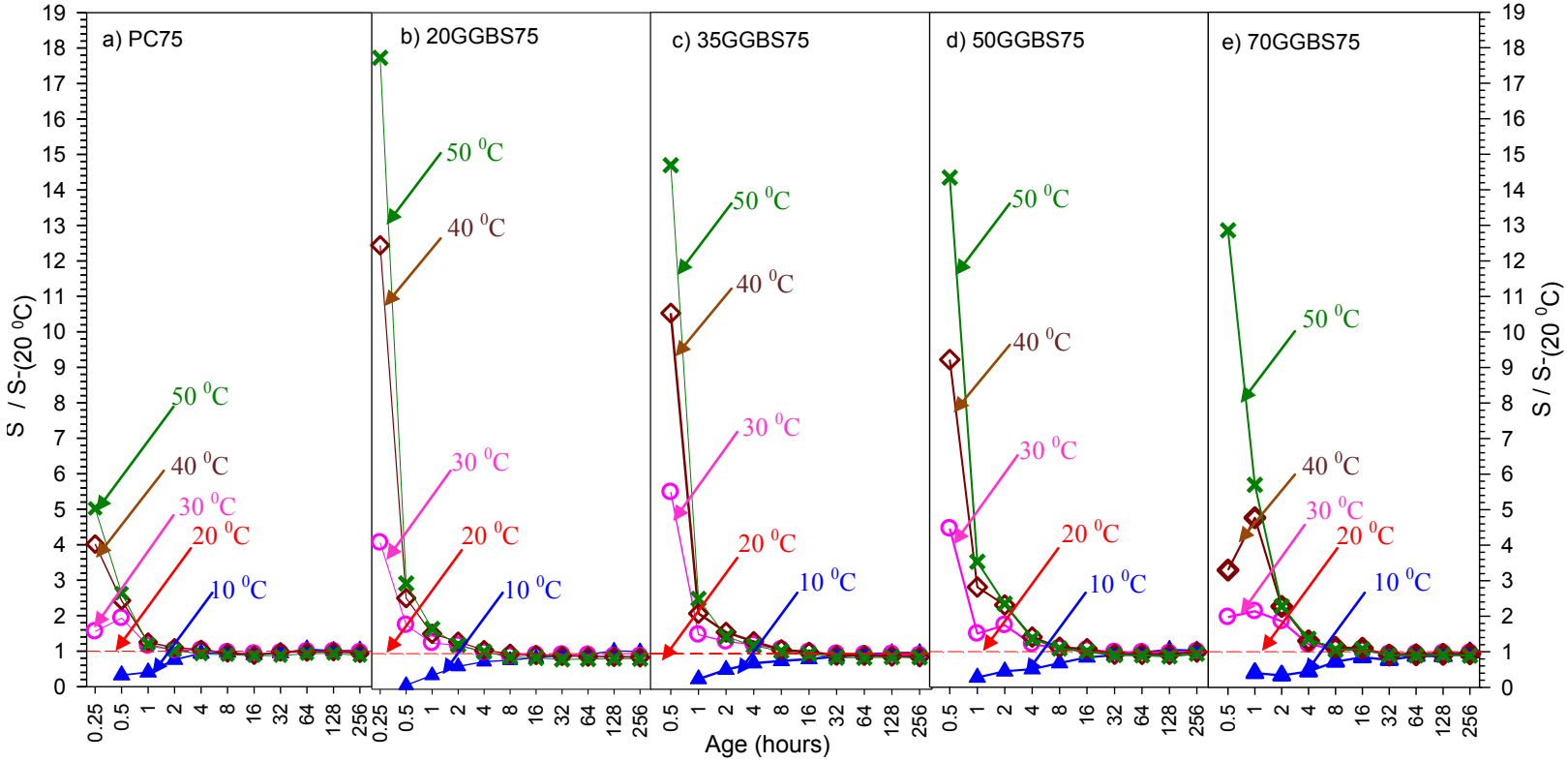

Figure 5.4: Ratio strength $S/S_{(20^{o}C)}$ PC and GGBS mortar **grade C75**

Even the strength of 70% GGBS mortar cured at 50^0C was slightly higher than the strength of PC mortar of the same grade cured at 20^0C, i.e. 27.0 N/mm^2. In comparison with mortars with PC only and a lower GGBS level (20% GGBS), the strength ratio of mortar that cured at 50^0C to those cured at standard curing temperature (20^0C) at age of 1-day were 1.34 and 1.82, respectively. At a later age (after 32-days), the detrimental effect due to higher curing temperatures on GGBS mortars is less than that on mortar with PC only. At age 365 days, the ratio of strength of mortars that cured at 50^0C to those cured at the standard curing temperature for mortar with PC only and 70% GGBS are 0.89 and 0.95, respectively, and it appears that the higher GGBS levels result in higher strength ratios.

The ratios of strength of GGBS mortar to PC mortar strength are shown in the Figures 5.5 and 5.6 for mortar grade C45 and C75 respectively. In general, at early age, the strength ratios of GGBS mortar to PC mortar increased with an increase of age. It is clearly shown in Figure 5.5 (mortar grade C45) that the ratios are highly dependent on GGBS level until the age of 16-days for the mortars cured at standard curing temperature. The higher GGBS levels result in lower strength ratios at early ages.

At later ages (after 32-day), the strength developments of GGBS mortar grade C45 were higher than that of mortar with PC only as the strength ratio was over the value of one. Except for mortars with GGBS levels of 35% and 70%, cured at 10 and 20^0C, which seem slightly lower than of PC mortar at age 365 days. GGBS mortars, particularly mortar with 50% GGBS, that cured at higher curing temperatures i.e. 40 and 50^0C at age 365 days, had strength of about 10% higher than of a PC mortar cured at the same temperatures.

The ratios of strength of GGBS mortars to PC only mortar for grade C75 are unexpected, as the strength of GGBS mortars cured at higher temperatures than 20^0C at early age is lower than that of PC mortar. This is due to the C75 mortars containing much more sand, which made them dry quickly.

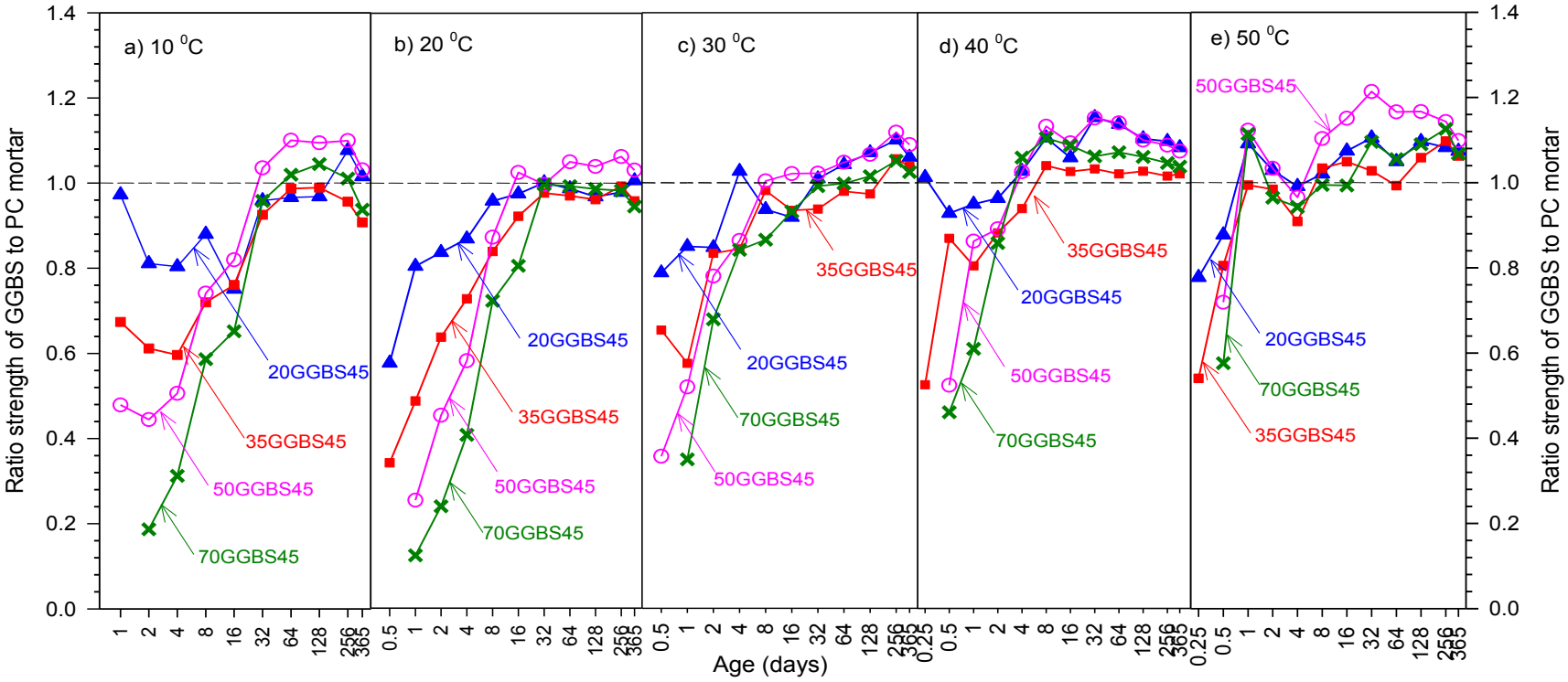

Figure 5.5: Ratio strength of GGBS mortar to strength of PC mortar **grade C45**

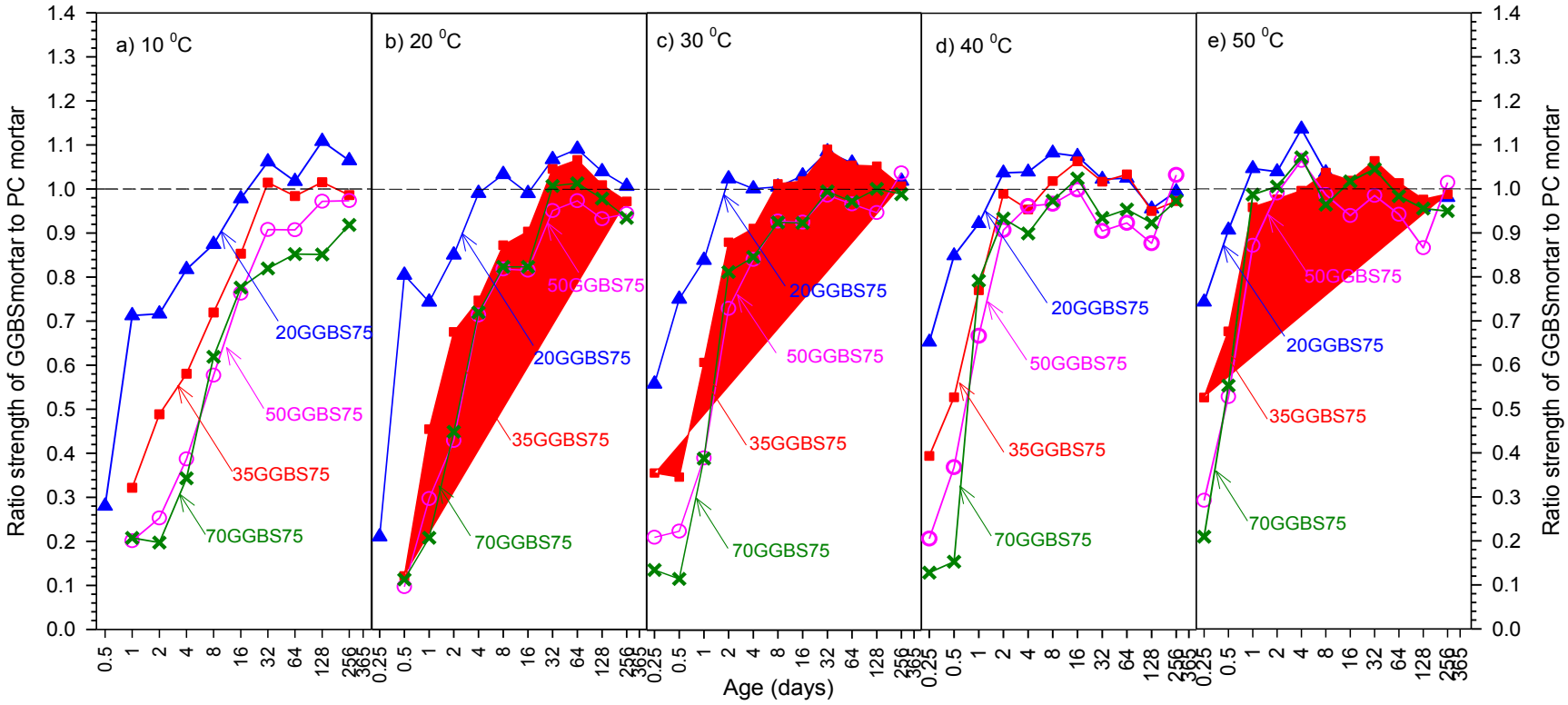

Figure 5.6: Ratio strength of GGBS mortar to strength of PC mortar **grade C75**

Figure 5.7 shows the effect of curing temperature to the time taken (t_{50}) of each mortar reached 50% of its calculated ultimate strength. The t_{50} was calculated using the equation:

$$t_{50} = t_0 + \frac{1}{k} \qquad \text{Equation 5.1}$$

where:

t_0 = time at which strength development is assumed to begin, hours or days

k = rate constant, hours^{-1} or day^{-1}

In general, the t_{50} increased with decreasing curing temperature, increasing water-binder ratio and increasing GGBS level; except for mortar grade C75, where at curing 10^0C, the t_{50} of mortar with 50% GGBS was unexpectedly higher than that of mortar with 70% GGBS. Figure 5.7 shows the benefits of higher curing temperatures on the early age strength development of mortars incorporating GGBS. The time taken for mortars to reach 50% of calculated ultimate strength (t_{50}) for lower water-binder ratio is shorter than that of mortars with higher water-binder ratios. It is due to the hydration rate of mortars with lower water-binder are higher than that of mortars with higher water-binder ratios.

At curing temperature 10^0C, mortar grade C45 with 70% GGBS took a longer time, which is almost three times (2.83) to reach 50% of its ultimate strength than Portland cement mortar. However, at curing temperature 50^0C, the difference is much smaller i.e. one and a half times (1.54), where all mortars reached 50% of their ultimate strength within 2-days and for the mortar grade C75 within 1-day. Increasing curing temperature from 20 to 30^0C for mortars with 50 and 70% GGBS levels (both grades C45 and C75), mortars cured at 30^0C have the value of t_{50} about halved than that of mortars cured at the standard curing (20^0C). This indicates that there is a significant increase in earlier-age strength development using 50 and 70% GGBS in mortar/concrete that can be achieved if the in-situ temperature rises by even a small amount above the standard curing temperature.

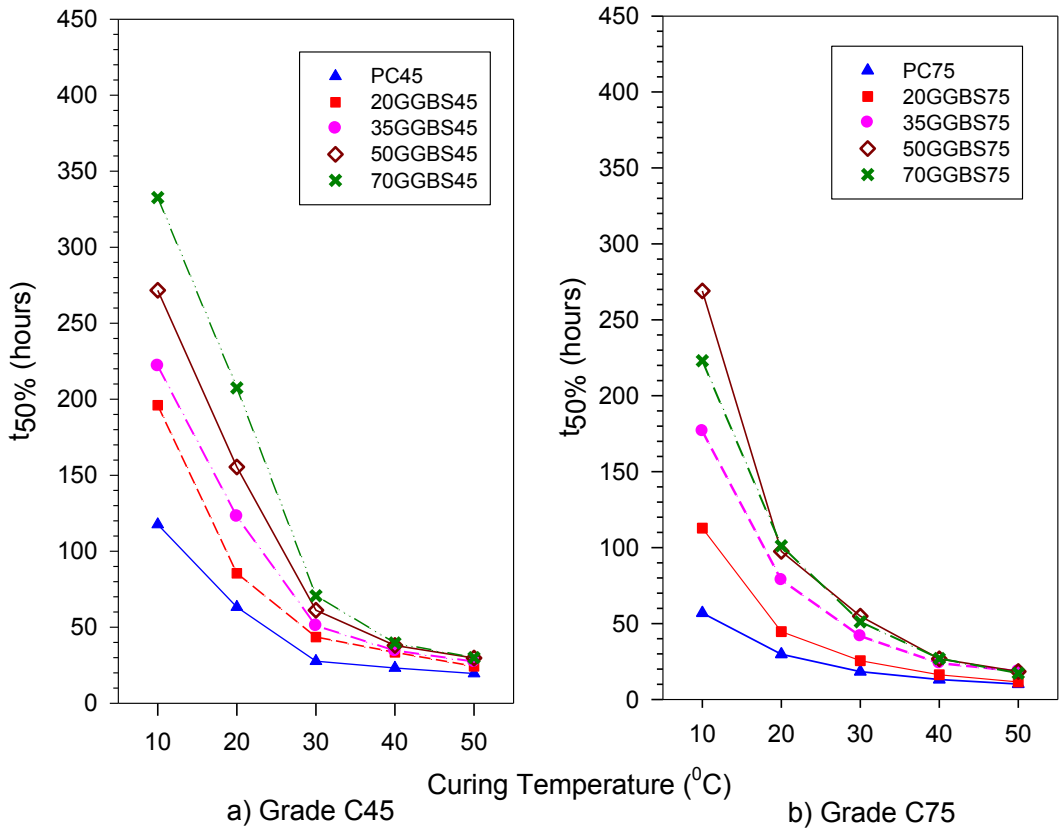

Figure 5.7: Effect of curing temperature on the time taken to reach 50% of ultimate strength

The effect of curing temperature on the age conversion factor is shown in Figure 5.8, where the reference temperature was taken as 20^0C. The rate constant values obtained from the regression were used to calculate the age conversion factors at different curing temperatures for each mortar.

The graph clearly shows that the age conversion factor increases exponentially with temperature. The linear relationship that is expressed by the Nurse-Saul equation is inadequate to illustrate the variation of k with temperature for all the mortars, especially for higher levels of GGBS, the deviation from linear behaviour is greater.

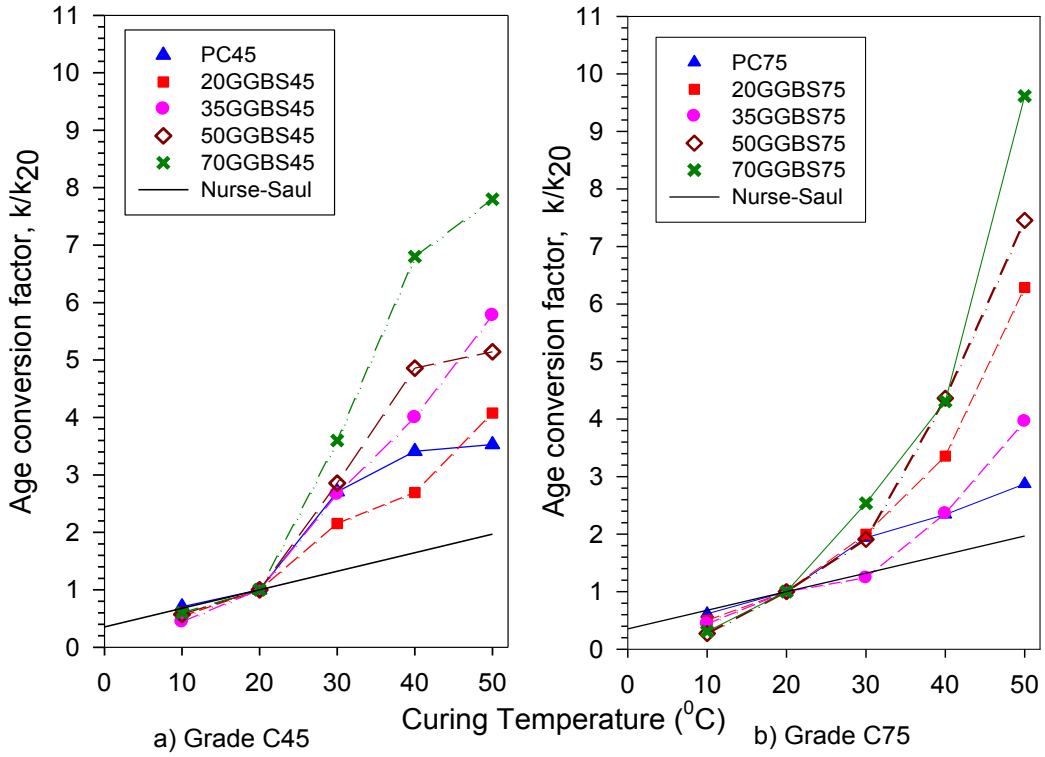

Figure 5.8: Effect of curing temperature on age conversion factor

5.2.2. Strength Development of GGBS Concrete at Curing Temperatures of 20 and 50^{0}C

Five mixes were cast with different GGBS levels for each grade C45 and C75 to investigate the effect of GGBS levels and different curing temperature on the strength development of concrete. The concretes were cured at curing temperatures of 20, 50^{0}C and under adiabatic condition. This aimed to compare the strength development of concrete to that of its equivalent mortar at different curing temperatures.

The results of cube specimens cured at 50^{0}C will also be used to investigate the effect of higher curing temperatures from a very earlier-age on the strength development of concrete at earlier-age and later on. While the results of cube specimens cured at 20^{0}C was needed to predict the adiabatic strength development of concrete.

The compressive strength test results of each concrete mix at different curing temperatures, which was based on the three replicate cube samples with a size of 100 mm, are plotted with error bars in Figures 5.9 to 5.10 for concrete grade C45 and C75, respectively. The concrete mix can be found in the Tables 4.4 and 4.5, while the strength test results can be found in Tables C-11 to C-20 in Appendix C. The target mean strength at 32-day of both concrete grades cured under the standard curing temperature, which was obtained from experimental works as they were expected, i.e. 55 and 85 MPa for concrete grade C45 and C75, respectively, except for concrete grade C75 with 70% GGBS. The strength of the concrete at age 32-day was slightly lower than that target mean strength, where it only reached 92.86% of the target mean strength. However, it developed continuously and eventually reached the target strength after the age of 32-day.

At an earlier-age, the strength development of PC and GGBS concretes at higher curing temperature (50^0C) is greater than that of the standard curing temperature (20^0C) in both concrete grades C45 and C75. This is attributed to an increase in the hydration rate. However, at later ages, strength development of the PC concrete only cured at 50^0C is slightly lower than that of concrete cured at the standard curing temperature.

In both concrete grades C45 and C75, as shown in Figures 5.9 and 5.10, the strength development of the concretes with the cement replacement levels of 0, 20, 35, 50 and 70% continuously increased after age 32-day and subsequently. This shows that the hydration processes continue as the age of concrete increases. Especially for GGBS concrete, the strength development of the concretes takes a longer time than that of PC concrete, where it appears to be continuously increasing after 365- days.

In the grade C45 concretes shown in Figure 5.9, the strength of GGBS concrete at age 4-days, cured under the standard curing temperature varies between 66 and 96% of the strength of PC concrete where the higher cement replacement level with GGBS resulted in the lower percentage of strength to the strength of concrete

with PC only. The strengths of the concretes that cured under the standard temperature at the 4-day age were 38.6, 37.0, and 25.5 N/mm^2 for concretes with PC only, 20 and 70% GGBS, respectively. However, at an elevated curing temperature i.e. 50^{0}C, the strength ratio of GGBS concrete to the PC concrete at the age 4-days were over 100%, except for concretes with 35 and 70% of GGBS. The strength of the concretes reached only 97 and 92% of the strength of concrete with PC only for concretes with 35 and 70% of GGBS respectively cured at the same temperature. The strength of GGBS concrete cured under the standard curing temperature exceeded the strength of concrete with PC only at age 16-day except for 70% GGBS concrete, where it reached only 93% of the strength of concrete with PC only. However, its strength continued to develop and it reached the 32-day target mean strength of 55 N/mm^2 at age 32 days.

At age 32-days, the strength of GGBS concrete grade C45 with GGBS levels of 20, 35 and 50% were higher than that of concrete with PC only. The strength of GGBS concrete with 50% GGBS was 11% higher than the strength of concrete with PC only. After age 32-days, the strength of all concretes grade C45 continuously develop, where the strengths of all GGBS concretes at age 365-day were higher than that of PC concrete. The strength of concrete with 50% GGBS at that age, cured under the standard curing temperature had the highest increase over the strength of concrete with PC only i.e. 25%, than that of other concretes with different GGBS levels.

The strength of GGBS concretes grade C75 at age 4-day, that were cured under the standard curing temperature, varied between 64 and 81% of the strength of concrete with PC only, as shown in Figure 5.10. The higher cement replacement levels resulted in the lower percentage strengths on GGBS concrete to that of PC concrete. At age 32-day, the strength of both concretes with 20 and 35% GGBS achieved 101% of PC strength, while the strength of concrete with 50 and 70% achieved strength slightly lower than that of PC concrete, i.e. 99 and 92% respectively. The strength of PC concrete grade C75 at the age of 32-day was about 86.13 N/mm2. The strength of all concretes grade C75 continued to develop

even after age 32-day, where at the age of 365-day, the strength of all GGBS concretes were higher (varied between 3 and 9%) than the strength of PC concrete. The lower cement replacement with GGBS results in higher increased strength over the strength of PC concrete at the age of 365-day.

There was no significant decrease in the strength of GGBS concrete with cement replacement levels up to 35% for both concrete grades C45 and C75 cured under the standard curing temperature. The strength of GGBS concrete at the age of 4-day reached 96 and 84% of the strength of PC concrete for grade C45, while for the concrete grade C75 were 81% and 79% for replacement cement with GGBS of 20 and 35%, respectively.

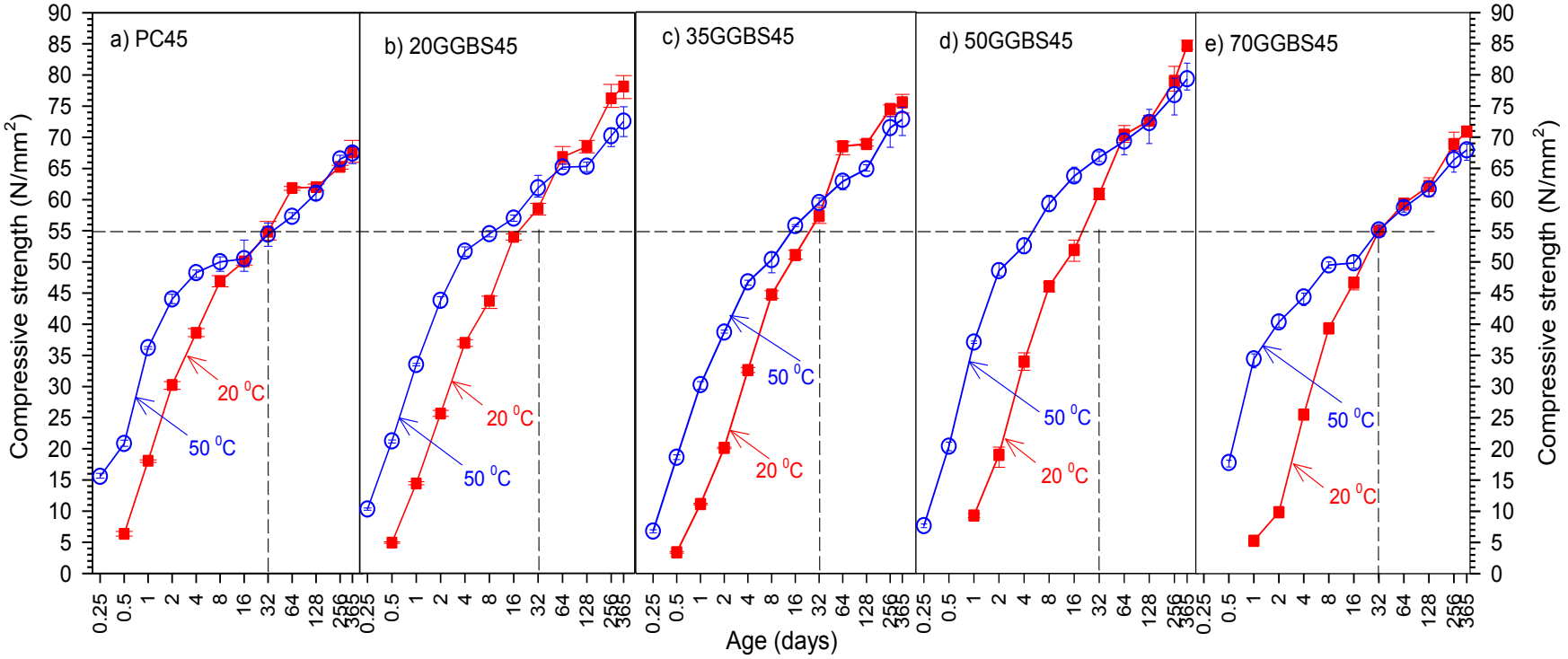

Figure 5.9: Strength developments of PC and GGBS concrete at curing temperatures of 20 and 50^{0}C **(grade C45)**

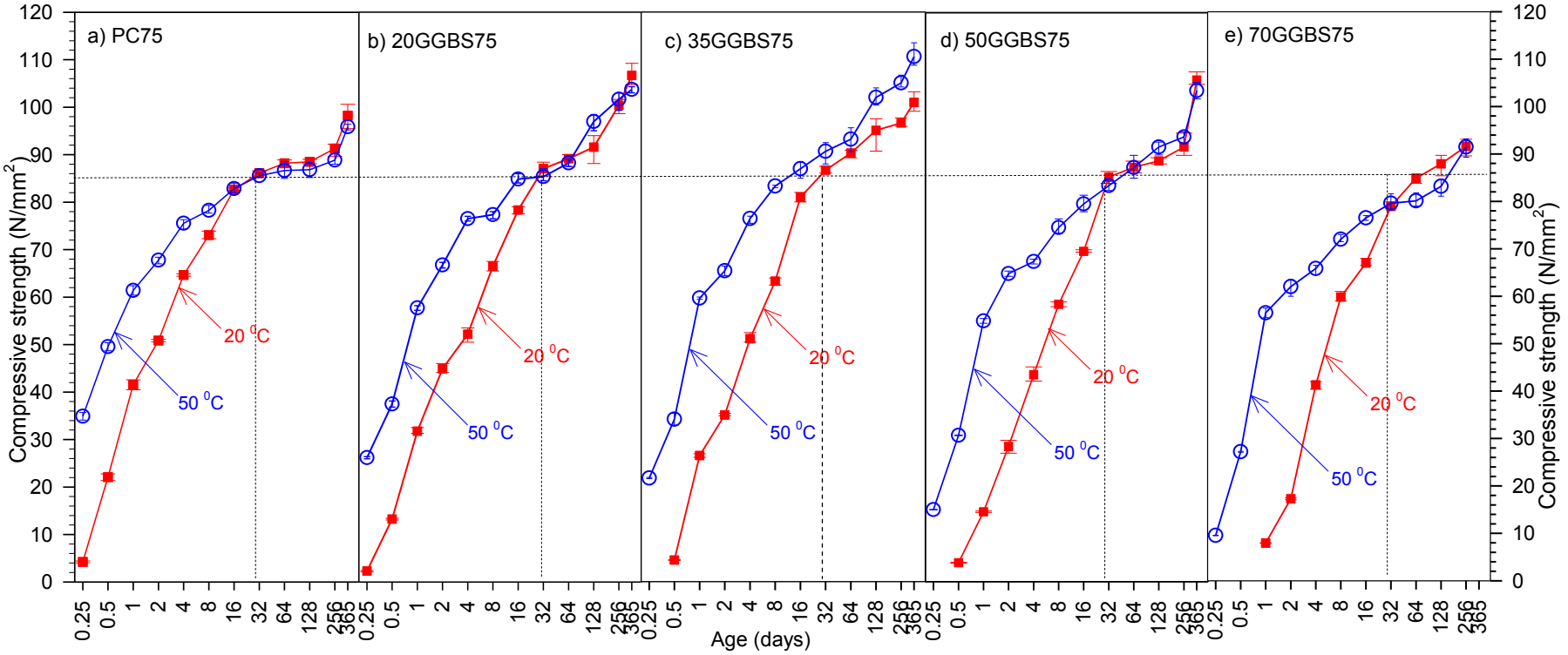

Figure 5.10: Strength developments of PC and GGBS concrete at curing temperatures of 20 and 50^{0}C **(grade C75)**

Figures 5.11 and 5.12 show the ratios of strength of concrete at certain age to its strength at age 32-days that cured at the same curing temperature for grade C45 and C75, respectively. The strength development of PC concrete for both grades C45 and C75 up to age 4-day that cured at 50^0C increased more quickly than those of concretes cured 20^0C. The strength ratios of PC concrete at age 4-day to its strength at age 32-day that cured at 50^0C were 0.89 and 0.88 for grades C45 and C75 respectively. At the same age, the strength ratios for PC concretes, which were cured under the standard curing temperature reached 0.70 and 0.75 only to their 32-day strength for grades C45 and C75, respectively.

At an elevated curing temperature i.e. 50^0C the ratio of strength of GGBS concrete at age 4-day to its strength at age 32-day are similar to that of concrete with PC only cured at the same temperature. The value of ratio varies between 0.80 and 0.90 for both concrete grades C45 and C75. However, the strength ratio for GGBS concrete cured under standard curing temperature are much lower, particularly for concrete with higher replacement level such as 50 and 70% GGBS than that of PC concrete with the same curing temperature. The strength of concrete with 70% GGBS at the age of 4-day, that cured at 50^0C reached 80 and 83% of its strength at age 32-day for concrete grades C45 and C75, respectively; while the strengths of the concretes cured under the standard curing temperature reached only 46 and 52% of its strength at age 32-day for concrete grade C45 and C75 respectively.

From the age of 32-day onwards, the strength of all the concretes were still continuously developed for the both grades C45 and C75, while their strengths at a very later ages, i.e. 365 days, were higher than their strengths at age 32-day, those on average they were higher than 20% stronger. In concrete grade C45, it appeared that cement replacement by 50% GGBS cured under standard curing temperature gave more contribution in enhancement of concrete compressive strength, i.e. 39% higher than its compressive strength at age 32-day. In concrete grade C75, however, the replacement of cement with 70% GGBS resulted in the highest increase (28%) in compressive strength at a much later age of 365 days.

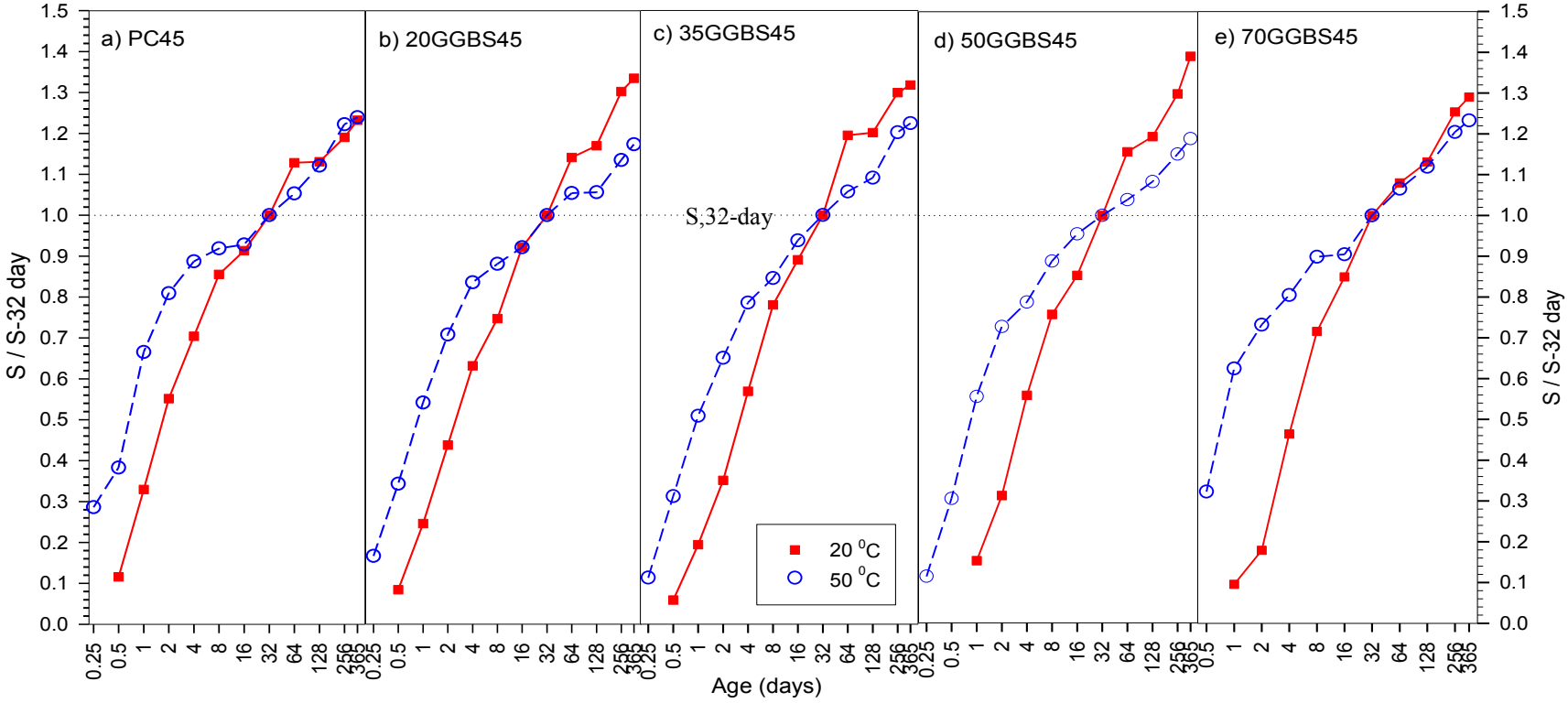

Figure 5.11: Ratio of strength, $S/S_{,32\text{-day}}$ of PC and GGBS concrete cured at 20 and 50^0C (**grade C45**)

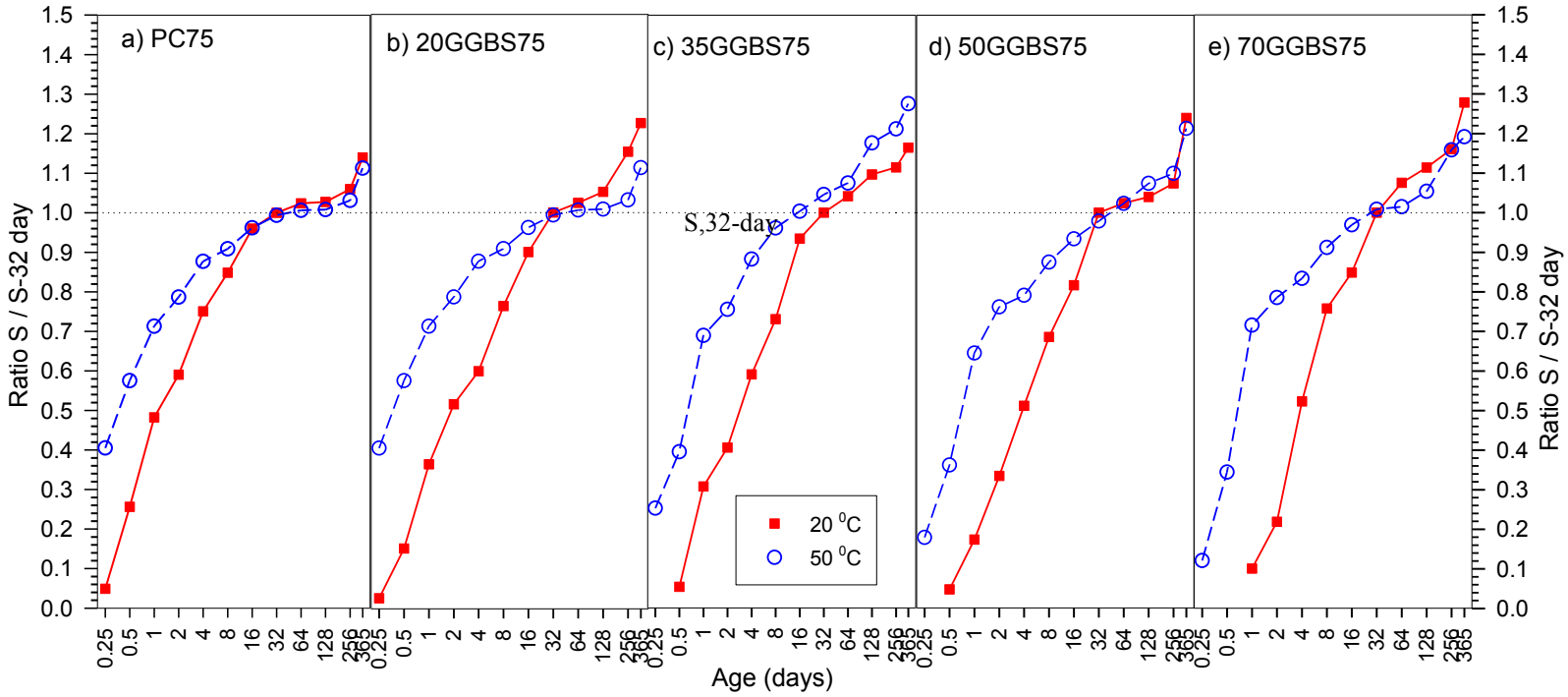

Figure 5.12: Ratio of strength, $S/S_{,32\text{-day}}$ of PC and GGBS concrete cured at 20 and 50^0C (**grade C75**)

The ratio of strength of concrete at a certain age to its strength at age 32-day cured at 20 and 50^0C for concrete grades C45 and C75 are shown in Figures 5.13 and 5.14, respectively. Generally, both these figures show that the higher levels of GGBS in concrete cured under the standard curing condition (20^0C) resulted in a lower strength of the concrete at early ages. However, the strength development of both concrete grades were continuously developed, where at age 32-day, the strength of all the concretes cured at 20^0C reached their target mean strength.

At age 1-day, the strengths of PC concrete grade C45 cured at 20 and 50^0C reached 33% and 66% respectively of the 32-day strength of concrete cured at 20^0C. Concrete with 70% GGBS of the same grade and age had strength 10% and 63% of its strength at 32-days (cured 20^0C) at curing 20 and 50^0C, respectively. Similar to concrete grade C75, the strengths of PC concrete at 1-day at curing temperature 20 and 50^0C were 48% and 71%, respectively of their 32-day strength cured at 20^0C. Concrete with 70% GGBS of the same grade and curing temperature, 20 and 50^0C had the strength 10% and 72% of its strength at 32-day (cured 20^0C).

The strength ratios of all GGBS concretes of both grades C45 and C75 at age 4-day to their strength at age 32-day cured under standard curing condition were lower than those of PC concrete. The ratio for GGBS concrete grade C45 varied between 0.46 (70% GGBS) and 0.63 (20% GGBS), while the ratio for PC concrete was 0.70. The ratio for GGBS concrete grade C75 was slightly higher than that of grade C45, which it varied between 0.52 (70% GGBS) and 0.60 (20% GGBS) with the strength ratio of 0.75 for PC concrete grade C75.

At the curing temperature 50^0C, however, the ratios obtained from PC only and GGBS concretes were similar. The ratios for GGBS concrete grade C45 ranged from 0.81(70% GGBS) to 0.88 (20% GGBS), where the ratio of 0.88 for concrete with PC only. For concrete grade C75, the ratios appeared slightly higher than those of concrete grade C45, which was similar to concrete that had been cured under the standard curing temperature. The ratios were between 0.83 (70% GGBS) and 0.88 (20% GGBS), while the ratio for PC concrete was 0.88.

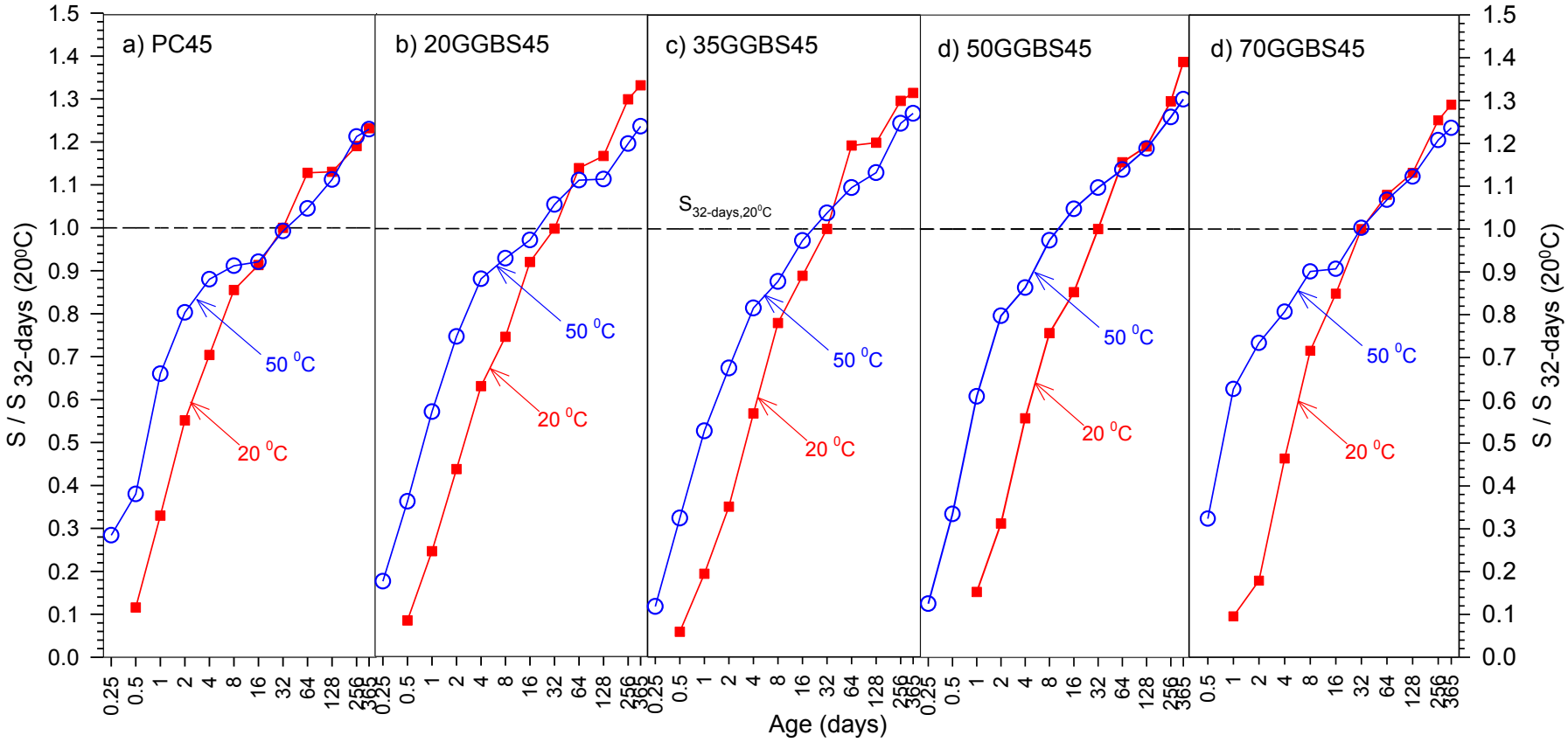

Figure 5.13: Ratio strength S / S-$_{(32\text{-days, }20^{o}C)}$ concretes **grade C45**

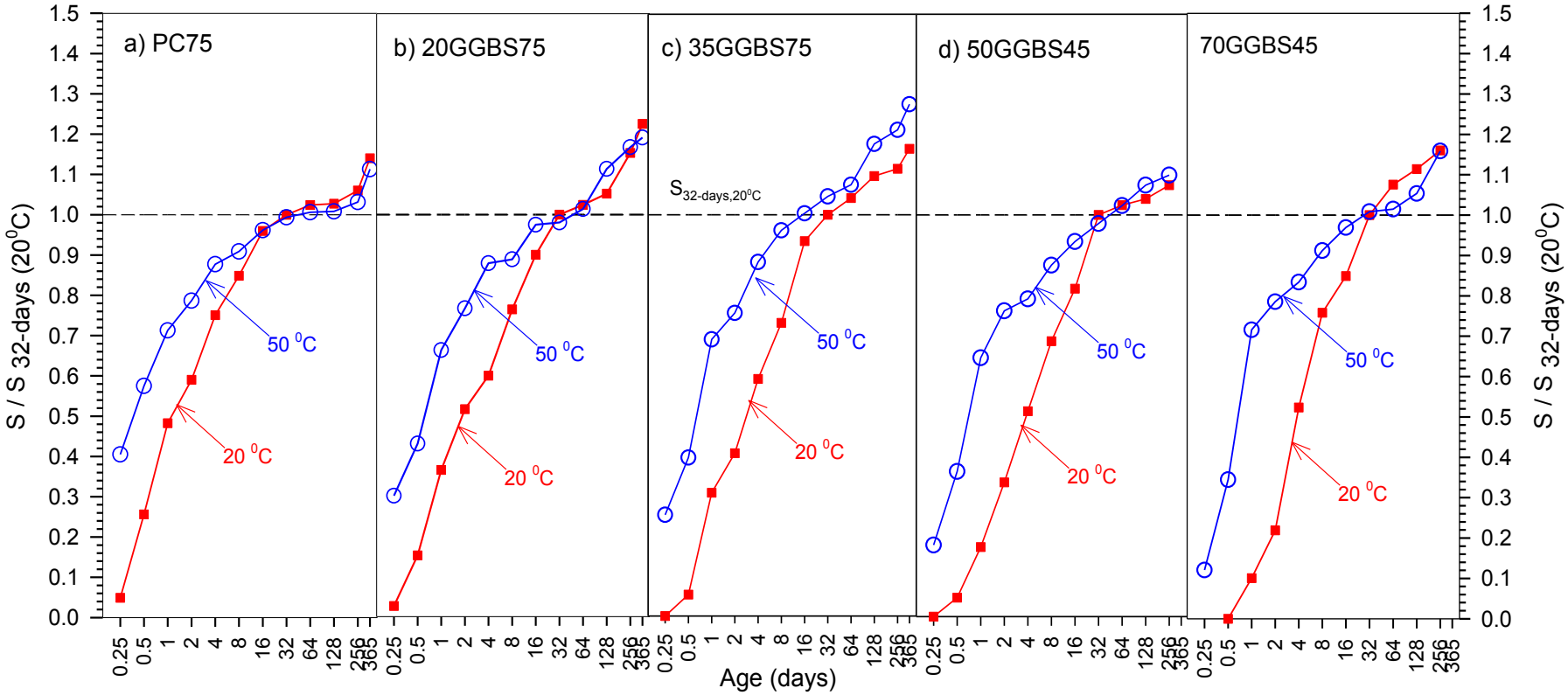

Figure 5.14: Ratio strength S / S-$_{(32\text{-days},\ 20^{o}C)}$ concretes **grade C75**

At very late age, i.e. at 365-days, the strength of all GGBS concretes grade C45 cured at 20^0C were higher than those of PC concrete cured at the same temperature. The ratio of strength of concrete at age 365-day to the strength at age 32-day for GGBS concrete ranged from 1.24 (70% GGBS) to 1.39 (50% GGBS). The value of the ratio for PC concrete was 1.23. At curing 50 ^{0}C, the ratios varied between 1.24 (20% GGBS) and 1.30 (50% GGBS), whereas the value of the ratio of PC concrete was 1.23.

The ratios of strength at age 365-day to the strength at age 32-day for GGBS concrete grade C75 cured under standard curing were slightly lower than those of concrete grade C45. Values of the ratio varied between 1.16 (35% GGBS) and 1.28 (70% GGBS), whereas the value of the ratio for PC concrete was 1.14. The ratios obtained from concrete grade C75 varied between 1.19 (70% GGBS) to 1.28 (35% GGBS) with PC concrete 1.14.

It can be seen from the graph that the strength development of concrete with high levels of GGBS such as 70% cured at the standard curing temperature is much slower than that of PC concrete cured under the same curing condition. However, at an elevated curing temperature, such as 50^0C, the strength of 70% GGBS concrete is quite similar to the strength of PC concrete. This indicates that the use of GGBS levels up to 70% in concrete can be applied in fast track construction if the in situ temperature rises by even a small amount above the standard curing temperature (20^0C).

Figure 5.15 shows the ratios of strength of concretes that were cured at 50^0C to those cured at the standard curing temperature. At early ages, such as up to first 8-day, the higher GGBS levels resulted in the higher strength ratios, however, from this age onwards, the strength ratios were similar.

This result shows that the strength development of GGBS concrete is more dependent on the curing temperature than Portland cement concrete. The effect of higher curing temperatures at earlier-age on the strength development of GGBS

concretes is more significant than on PC concretes. At age 1-day, the strength ratio of concrete cubes for both grades C45 and C75 with 70% GGBS that were cured at 50^0C to that of those cured at 20^0C (standard curing temperature) are 7.11 and 6.56, respectively; compared to PC concretes, the ratios are 2.0 and 1.48 for PC45 and PC75 concretes, respectively.

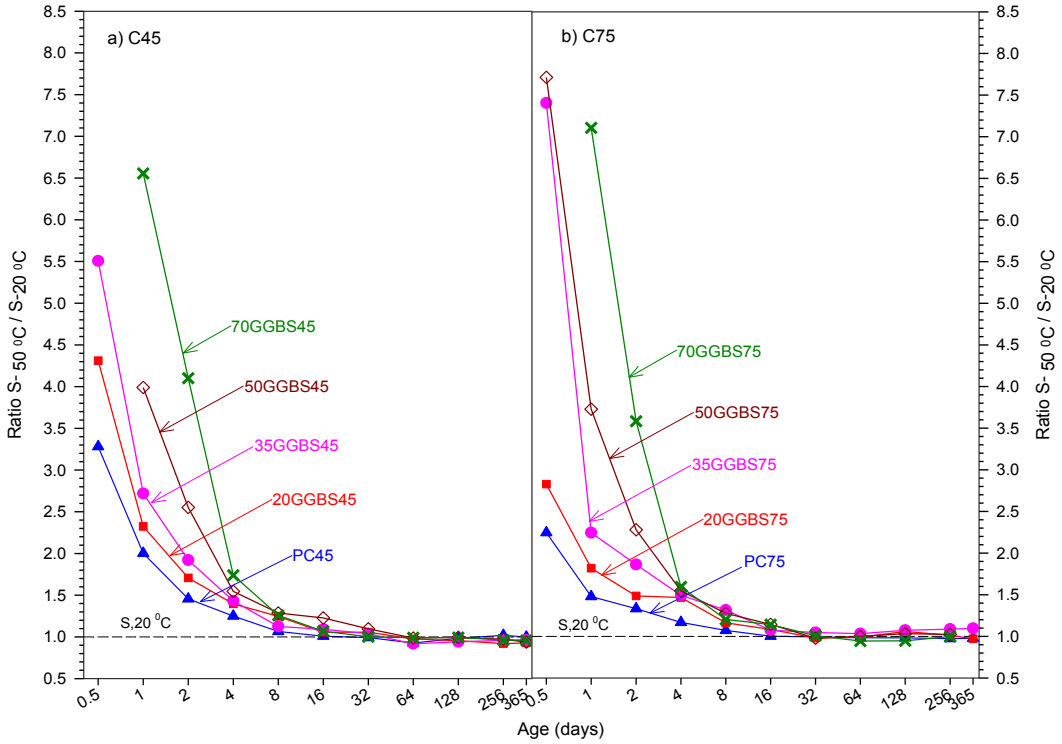

Figure 5.15: Ratio strength S-$_{50^oC}$ / S-$_{(20^oC)}$ PC and GGBS concretes **grades C45** and **C75**

At age 8 days, the strengths of PC concretes that were cured at 50^0C are similar to the strengths of those cured at 20^0C, where the strength ratio for both grades C45 and C75 is the same, i.e. 1.07. In comparison, the strength ratio of 70% GGBS concretes grades C45 and C75 at the same age are 1.26 and 1.20, respectively. This means that the strength development of concretes with high GGBS levels that were cured at 20^0C was slower than that of those cured at 50^0C.

Figures 5.16 and 5.17 show the ratio of strength of GGBS concrete to the strength of PC concrete for both concrete grades C45 and C75, respectively. Under

standard curing temperature, both Figures 5.16a and 5.17a show that at very earlier-ages, the strength development of GGBS concrete was much slower than that of PC concrete. The strength of GGBS concrete at age 1-day varies between 29% (70% GGBS) and 80% (20% GGBS) of the strength of PC concrete for concrete grade C45. For concrete grade C75, the strength of GGBS concrete varies between 19% (70% GGBS) and 76% (20% GGBS) of the PC strength.

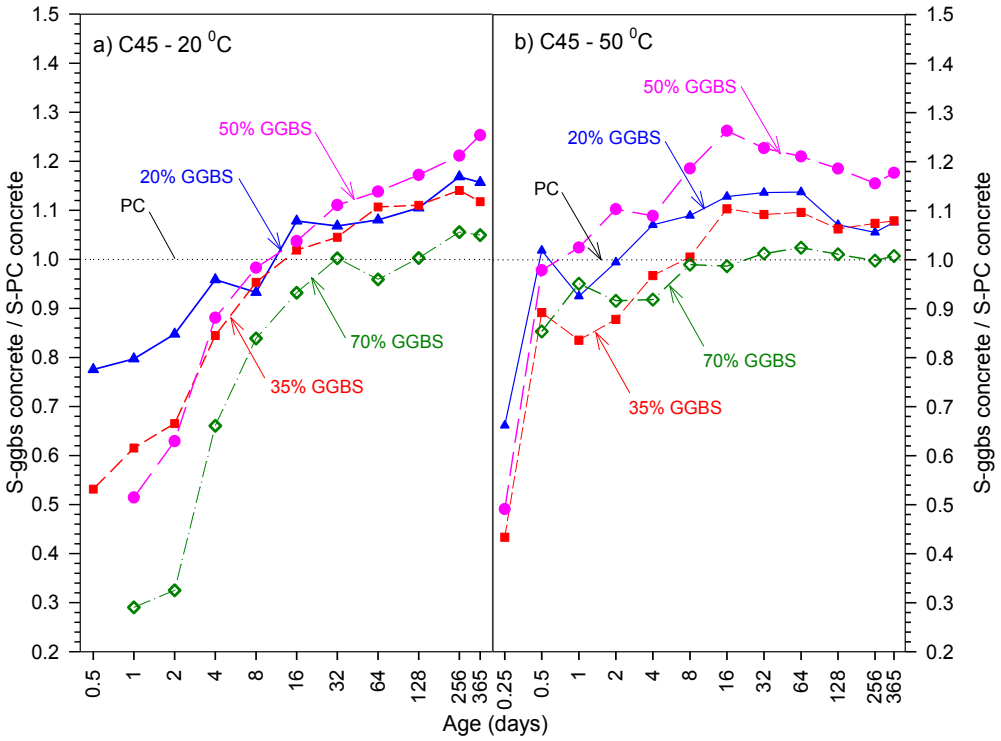

Figure 5.16: Ratio strength of GGBS concrete to PC concrete **grades C45**

At curing 50^{0}C, the strengths development of GGBS concrete at a very earlier age, i.e. age 1-day, to the strength of concrete with PC only are higher than of concrete cured under the standard curing temperature. At the 1-day age, the strength development of GGBS concrete grade C45 varies between 84% (35% GGBS) and 102% (50%GGBS) of the strength of PC concrete.

The ratios of GGBS concrete strength to PC concrete strengths at the same age and curing temperature for grade C75 varies between 0.90 (50% GGBS) and 0.97

(35% GGBS). The variation of strengths in both concrete grades C45 and C75 cured at 50^{0}C is inconsistent to the replacement levels of cement with GGBS.

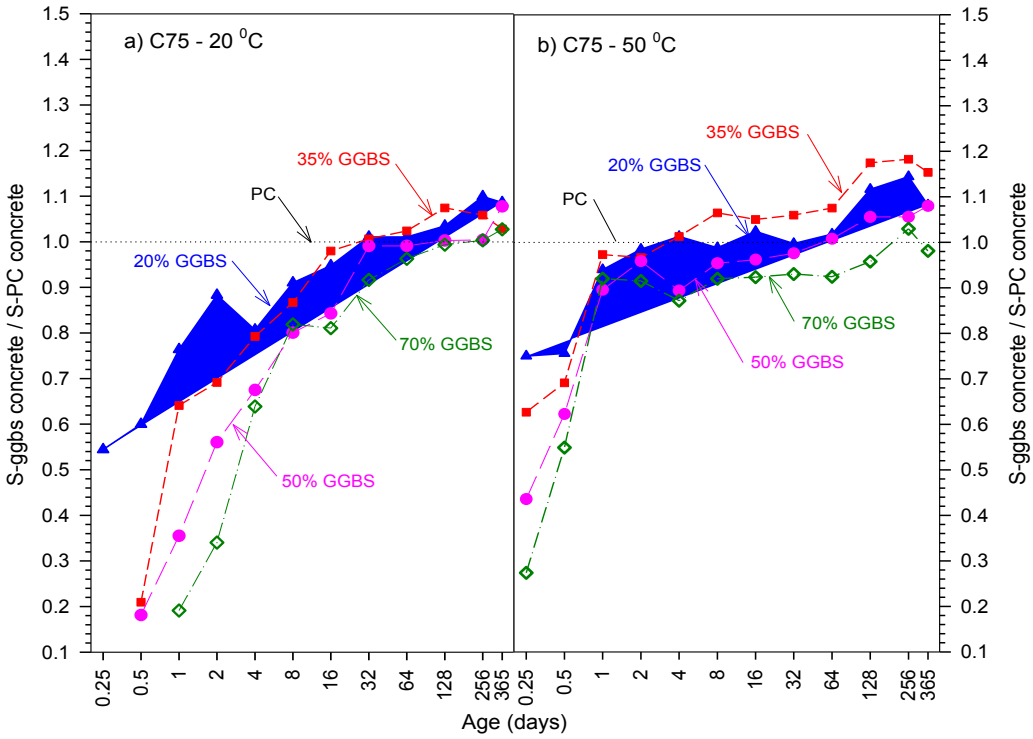

Figure 5.17: Ratio strength of GGBS concrete to PC concrete **grades C75**

The ratios of GGBS concrete strength to the strength of PC concrete at age 4-day cured under standard curing temperature varied between 0.66 (70% GGBS) and 0.96% (20% GGBS) for concrete grade C45 and between 0.64 (70% GGBS) and 0.81 (20% GGBS) for grade C75. The significant increase in the strength ratios from age 1-day to age 4-day occurred in 50 and 70% GGBS concretes; i.e. increased from 0.51 to 0.88 and from 0.29 to 0.66, respectively.

The strength of GGBS concretes cured at 50^{0}C at age 4-day were similar to the PC concrete strengths. The ratios of concrete strength with 20 and 50% of GGBS to the PC concrete strength at age 4-day, which cured at 50^{0}C were 1.07 and 1.09, respectively; while the strength ratios of concrete with 35 and 70% of GGBS were 0.97 and 0.92, respectively. So, the differences of GGBS concrete strength to the PC concrete strength were less than 10%.

At age 32-days, all GGBS concrete strengths for grade C45 cured under standard curing temperature reached and even exceeded the PC concrete strength. The minimum strength of GGBS concrete, which was 54.95 N/mm^2 (70% GGBS), was similar to the strength of concrete with PC only, i.e. 54.83 N/mm^2. The replacement of cement by 50% GGBS resulted in the maximum increase in compressive strength, i.e. 11% and 23% higher than the PC concrete strength cured under the standard curing temperature and 50^{0}C at the same age and curing condition, respectively. On the other hand, at age 32-day, the strengths of GGBS concrete grade C75 cured under standard curing temperature and 50^{0}C were very similar to the PC concrete strength of the same grade, where their differences were less than 10%.

Furthermore, the strengths of GGBS concrete grade C45 (Figure 5.16) at a very later age i.e. 365-day cured under standard curing temperature and 50^{0}C, were higher than the PC concrete strength. The maximum strength difference between GGBS and PC concretes was found at 50% GGBS; i.e. 25% and 18% for concrete cured the under standard curing temperature and 50^{0}C, respectively. In grade C75 (Figure 5.17), the strengths of GGBS concrete at very later age (365-day) were also higher than the PC concrete strength as in grade C45, except concrete with 70% GGBS cured at 50^{0}C, where its strength reached only 98% of the PC only concrete strength. The maximum increase of GGBS concrete strength to PC concrete strength were 9% (20% GGBS) and 15% (35% GGBS) for concrete cured under standard curing temperature and 50^{0}C, respectively.

Figures 5.18 and 5.19 show the strength development of concretes and their equivalent mortars grades C45 and C75 with GGBS levels of 0, 35 and 70% cured under the standard curing temperature and 50^{0}C. Trends for the concretes with 20 and 50% of GGBS are similar, which can be seen in Figures E-1 and E-2 in Appendix E. The graphs show that the strength development of concrete is similar to the equivalent mortar's strength development for concrete grade C45 with PC only. However, the strength development of concrete grade C75 (high strength

concrete) with all levels of GGBS are different from their equivalent mortars' strength throughout the range of testing ages until at the age of 365-day, as the strength developments of mortar grade C75 are lower than that expected/target mean strength, as mentioned above.

The discrepancy between the strength of mortar to concrete strength for grade C45 appeared from the age of 4-day to age 32-day, where their strengths at the age of 32-day is close to the target mean strength i.e. 55 N/mm^2. The strength development of concrete is higher than that of its equivalent mortar. It is believed that it is due to the hydration rate in the concrete specimens are greater than that in the mortars due to the two different size of specimens and materials contained in both specimens.

In comparison to their equivalent mortar mixes, the strength development of concretes cured at a higher curing temperature, i.e. 50^0C has much less detrimental effect at later age as shown in Figures 5.18 and 5.19. The "crossover effect" on strength development of concrete occurred at much later ages than on their equivalent mortars. It is clear from the figures that the "crossover effect" occurred earlier in PC concretes than that in GGBS concretes; although this did not occurred in concrete grade C75 with 35% GGBS until the age of 365-day.

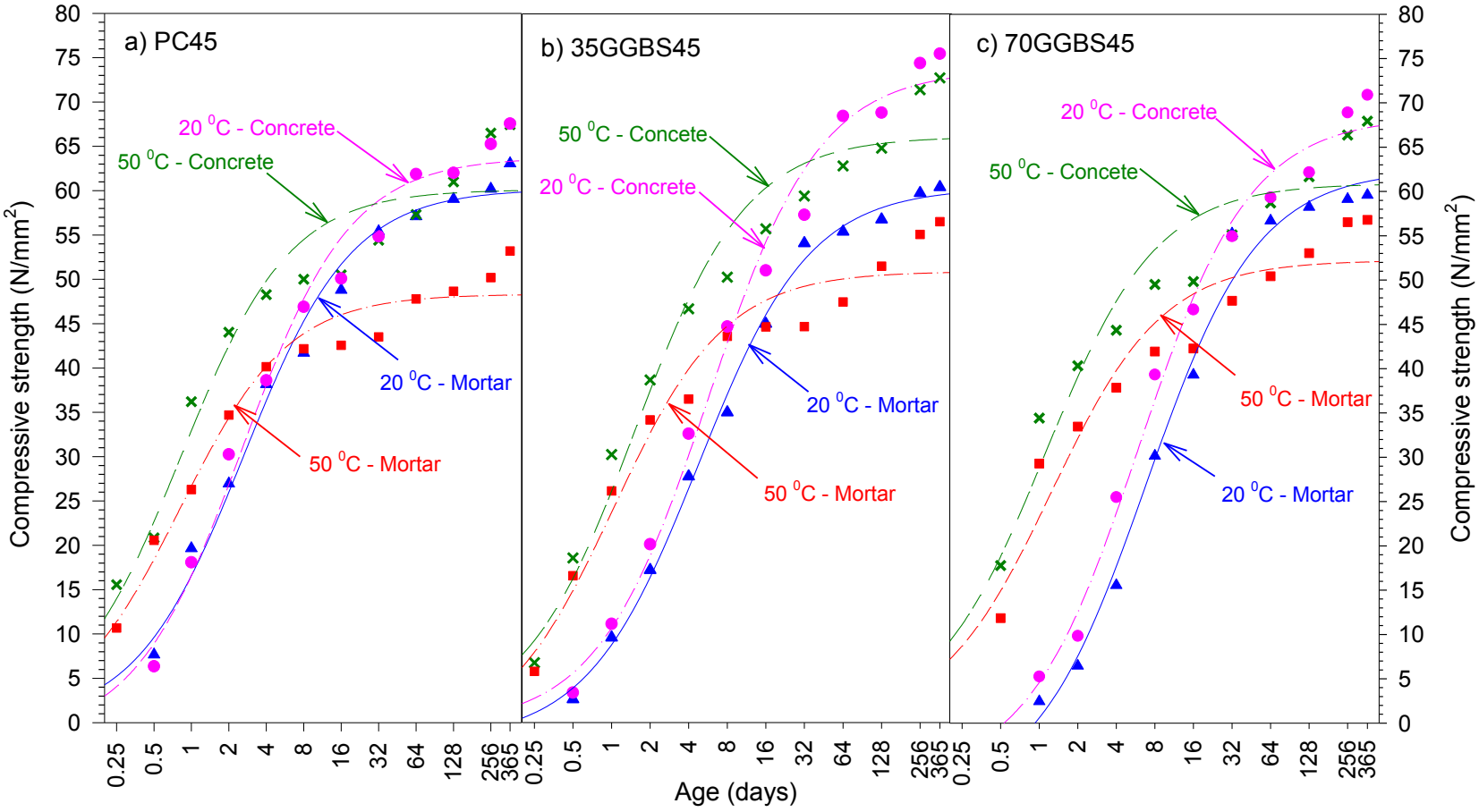

Figure 5.18: Strength developments of mortar and concrete **grade C45** with 0, 35 and 70% of GGBS cured at 20 and 50^{0}C

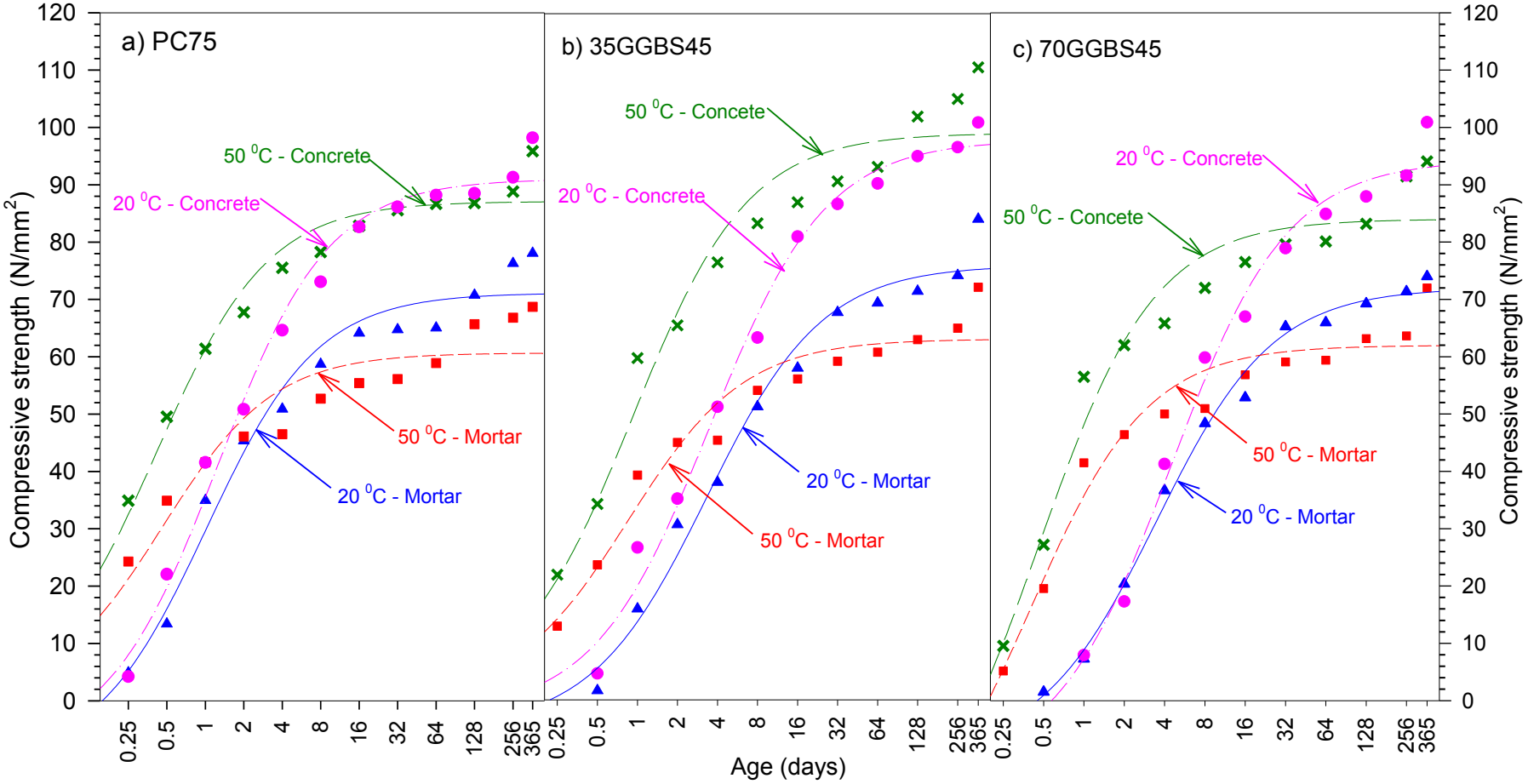

Figure 5.19: Strength developments of mortar and concrete **grade C75** with 0, 35 and 70% of GGBS cured at 20 and 50^{0}C

A research project funded by ESPRC has been carried out at University of Liverpool to investigate the strength development of mortar and concrete with varying levels of GGBS, for concrete and mortar grades C30, C60 and C90[40, 161]. Figures 5.20 and 5.21 present the strength developments of mortar with PC only, 35 and 70% GGBS that were cured under the standard curing temperature and 50^0C, respectively. Mortars with other levels of GGBS can be found in Figures D-3 and D-4 in Appendix D. The graphs present the results from the previous work, which has been combined with the work of this research i.e. mortars grade C45 and C75. Mortar grades C60, C75 and C90 are considered as high strength mortars with water-binder ratios less than or equal to 0.4. The target mean strength of mortar grades C60, C75 and C90 are 70, 85 and 100 N/mm^2, respectively. The aim was to investigate the effect of water-binder ratio and curing temperature on strength development of mortar with varying water-binder ratios.

Under standard curing temperature, the strength developments of mortar grades C60, C75 and C90 were unexpected, where their strength at age 32-days were lower than their target mean strength, except for strength of mortar grade C90 with 35% GGBS; it had a strength of 99.6 N/mm^2, compared to its expected i.e. 100 N/mm^2. The strength development of mortars grades C60, C75 and C90 with PC only (Figure 5.20a) appeared to have a decrease in strength greater than that in mortars with GGBS (Figures 5.20b and c). Moreover, Figure 5.20a shows the strength development of mortar grade C60 with PC only was lower than that of grade C45.

Strength development of mortars grades C30 and C45 with PC and GGBS were reasonably good as their strength at age 32-days reached their target mean strength at the age i.e. 40 and 55 N/mm^2, respectively.

Curing at 50^0C, the strength development of all mortars grades C30, C45, C60, C75 and C90 are higher than that of cured under standard curing temperature at early age, but they have a detrimental effect on the strength development at later ages. It seemed that a reducing in strength in the GGBS mortars at later ages is

less than that in mortar with Portland cement only. It is believed that the use GGBS in concrete as cement replacement can reduce the temperature rise, which can lead to a reduction in strength at later ages.

On the other hand, the strength development of concretes for all the grades with 0, 35 and 70% GGBS as shown in Figure 5.22, appear to be reasonable good as their target mean strength at 32-days under standard curing temperature was as expected, except for concretes with 70% GGBS (Figure 5.22c). The strength obtained was a little bit less than the target mean strength, except for concrete grade C45. However, the strength increased continuously; even at later age it exceeds the target mean strength, like concrete with other GGBS levels. The concrete mixes were equivalent to the mortar mixes. The target mean strength of all GGBS levels concretes grade C30 were lower than their target mean strength at the age of 32-days. In comparison to the strength of GGBS concretes of higher grades, this indicates that the strength development of GGBS concrete of lower strength grade is slower than that of higher strength. The strength development of concretes with 20 and 50% GGBS can be found in Figure E-5 of Appendix E.

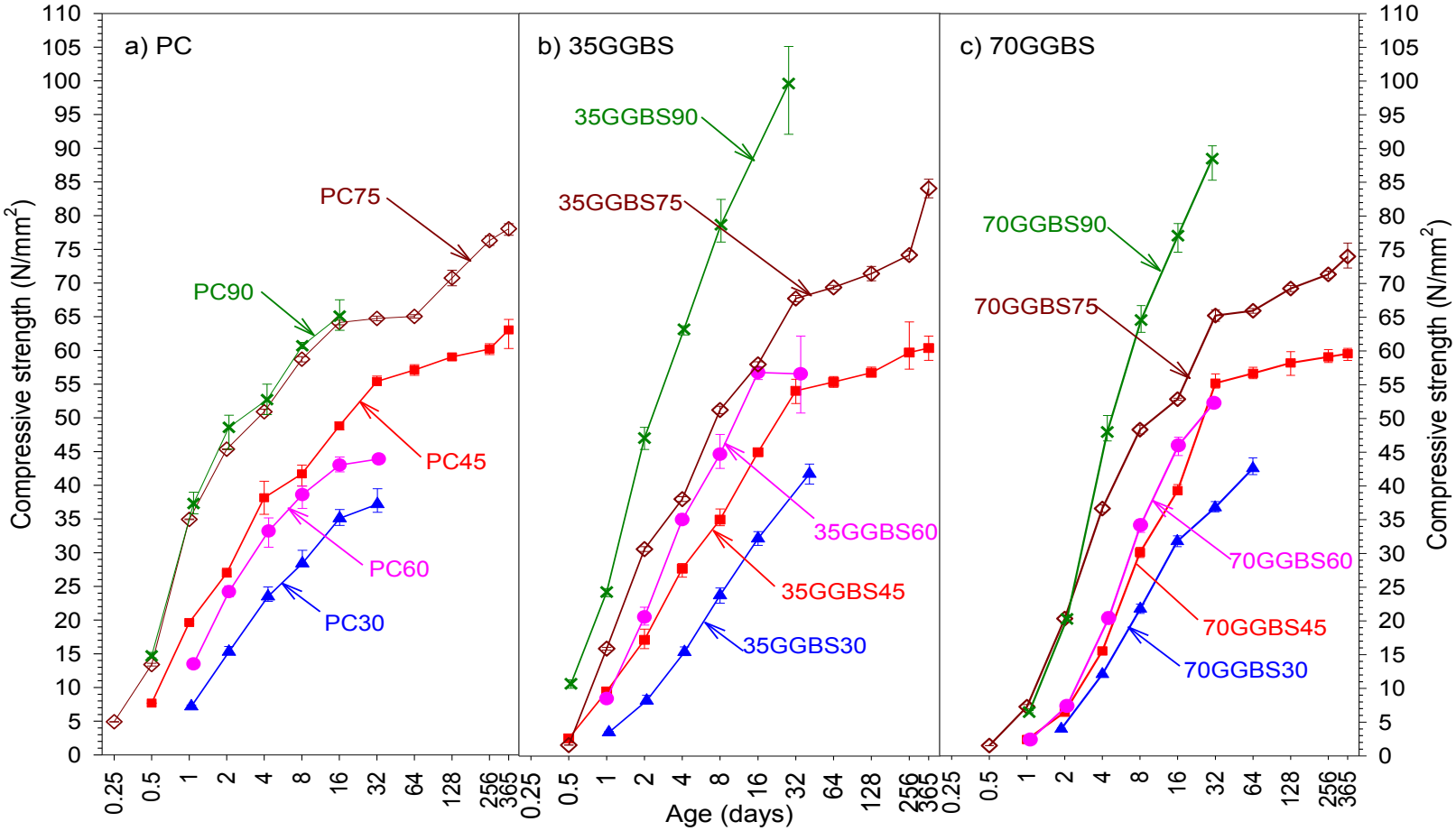

Figure 5.20: Strength developments of mortars with 0, 35 and 70% of GGBS levels cured at 20^0C (**grade C30, C45, C60, C75 and C90**)

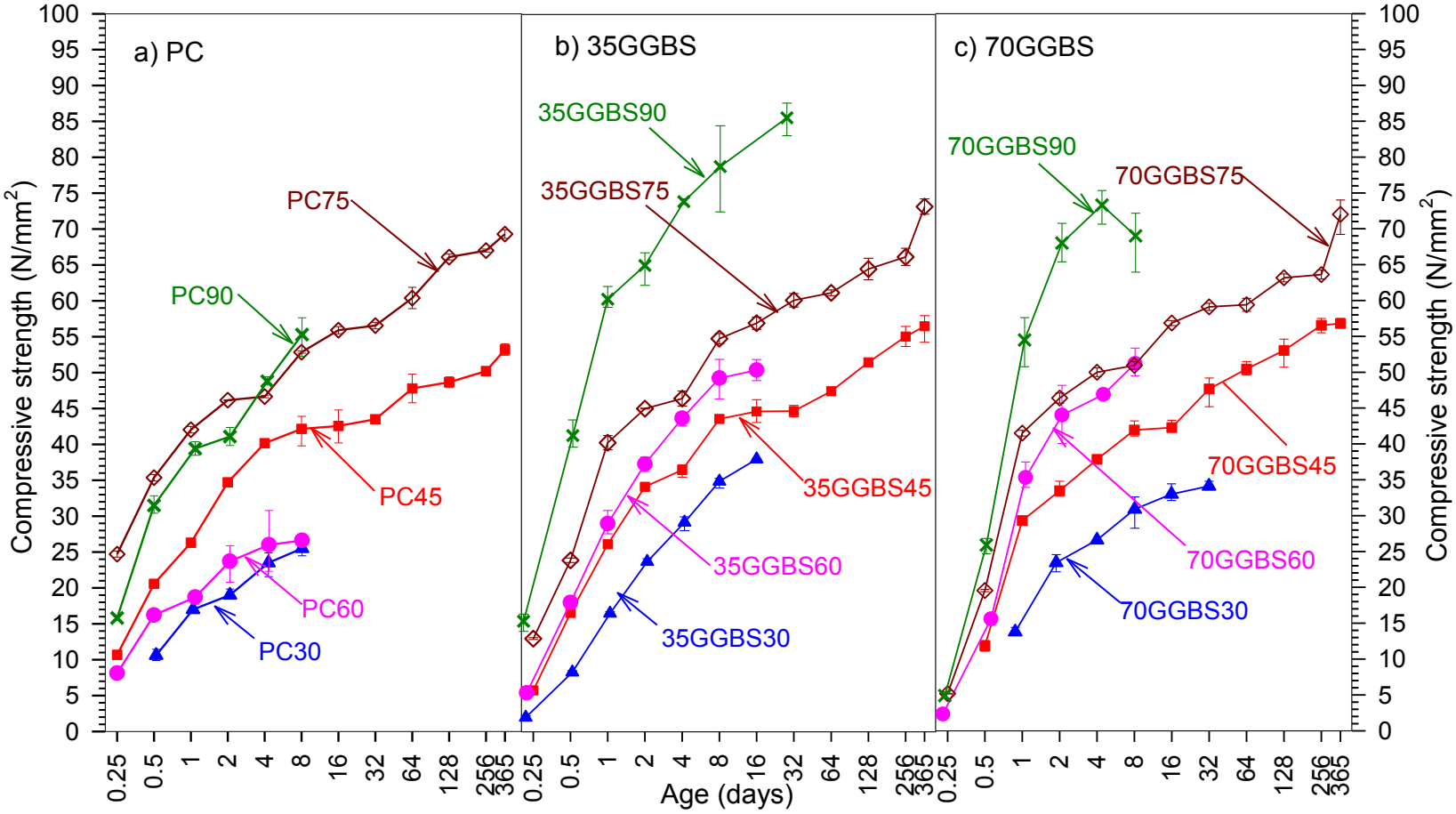

Figure 5.21: Strength developments of mortars with 0, 35 and 70% of GGBS levels cured at 50^0C (**grade C30, C45, C60, C75** and **C90**)

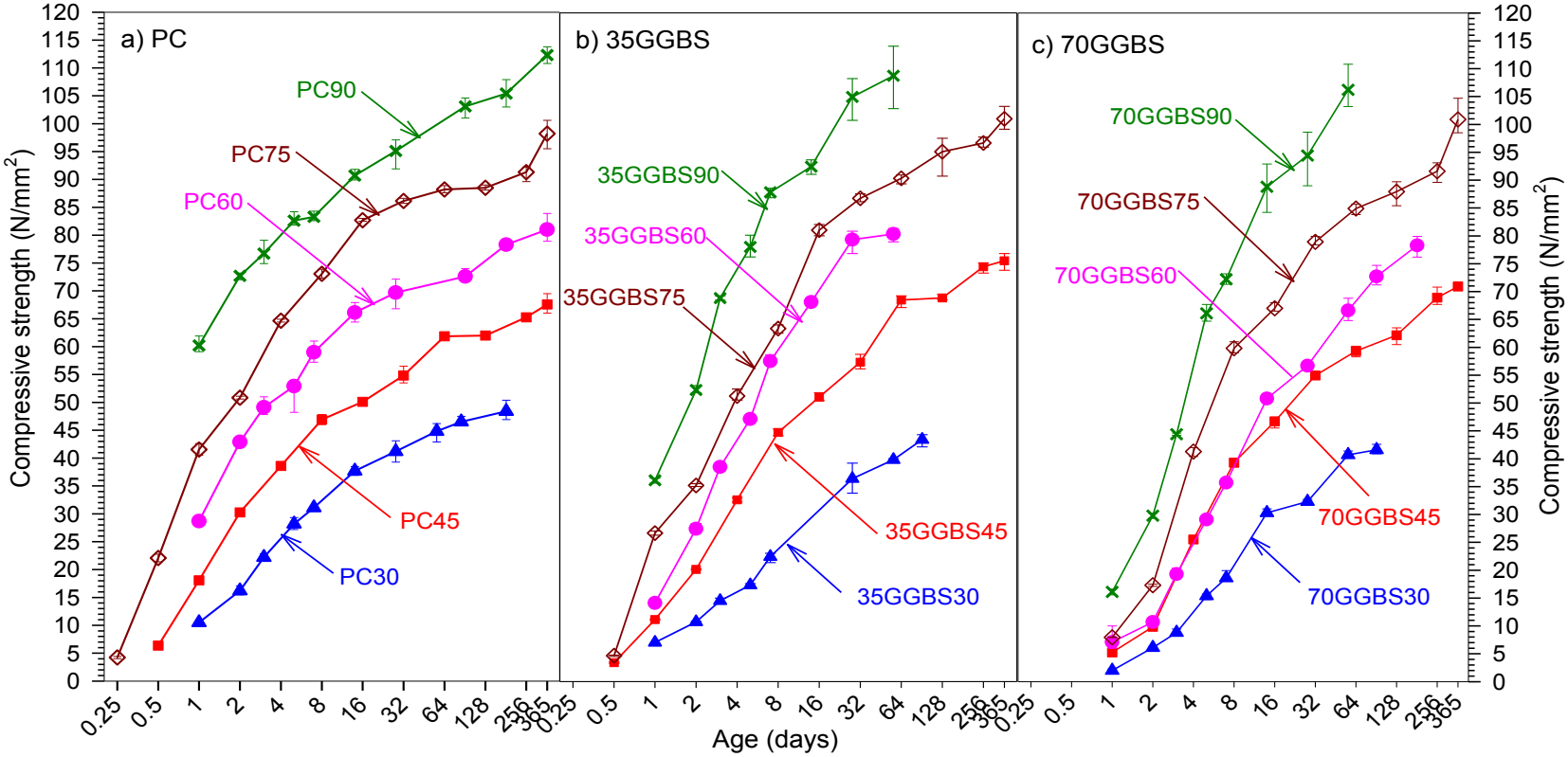

Figure 5.22: Strength developments of concretes with 0, 35 and 70% of GGBS levels cured at 20^0C **(grade C30, C45, C60, C75** and **C90)**

5.3. Adiabatic Temperatures Rise

It is important to consider the recorded adiabatic temperature histories before investigating the strength development of mortar/concrete under adiabatic curing conditions. It is necessary to quantify the strength that may be expected under these curing conditions because they are close to in-situ temperatures and they can also be used to evaluate the accuracy of the maturity method to predict strength development.

There are two stages of development of the adiabatic temperature rise. An initial period of near-constant temperature corresponding to the so-called dormant period. This is then followed by an acceleration of temperature rise, which subsequently asymptotically to a near-maximum value where there is no more significant increase of temperature. In general, the adiabatic temperature and the casting temperature increase as the total binder content and concrete strength increase.

5.3.1. Adiabatic Temperature Rise of Equivalent Mortars

The adiabatic temperature histories for all equivalent mortars grades C45 and C75 are shown in Figure 5.23. The casting temperatures varied from 17.0 to 22.3^{0}C and from 22.5 to 25.0^{0}C for mortar grades C45 and grade C75, respectively. The Portland cement mortars grades C45 and C75 had adiabatic temperature rises of 53.5 and 60.0^{0}C from their casting temperature 22.5 and 23.0^{0}C, respectively.

The adiabatic temperature rises of mortar with 70% GGBS of both grades C45 and C75 were 38.0 and 42.0^{0}C from their casting temperatures of 17.0 and 22.5 ^{0}C, respectively. The replacement cement with lower GGBS levels i.e. 20 and 35% did not appear to enable a reduction in the peak temperature. The higher level of 70% GGBS can reduce the peak temperature by 15^{0}C. In addition, using GGBS in mortar/concrete up to 70% also reduces the rate of temperature rise at early ages.

There are many factors that can affect the adiabatic temperature rise such as: binder content, level of GGBS in mortar/concrete, casting temperature etc. The adiabatic temperature rise in mortar with Portland cement only grades C45 and C75 were 53.8^{0}C and 59.8^{0}C, respectively. The discrepancy of the adiabatic temperature rise in PC mortar grades C45 and C75 is due to the difference in binder content of both the mortars i.e. 455 kg/m^3 and 502 kg/m^3.

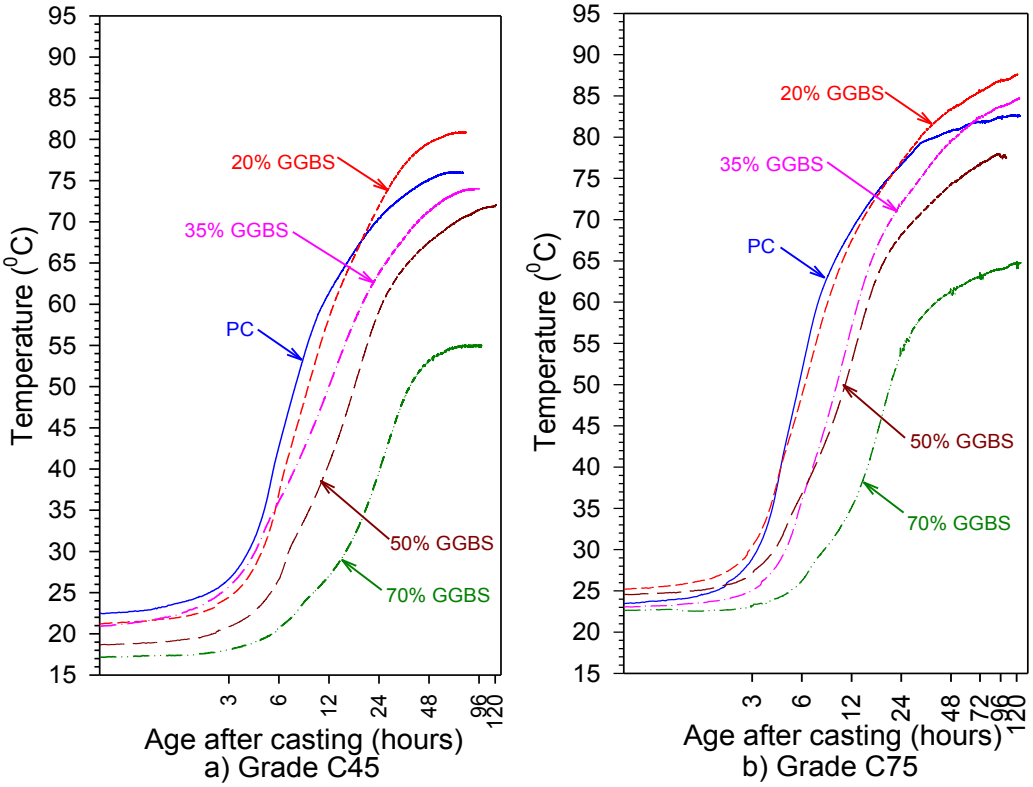

Figure 5.23: Adiabatic temperatures of equivalent mortars

5.3.2. Adiabatic Temperatures Rise of Concretes

Figure 5.24 presents the adiabatic temperature rise of concretes grade C45 and C75. The adiabatic temperature rises in concretes are similar to that in their equivalent mortars. The casting temperatures of concretes grade C75 were slightly higher than that of grade C45, as the ambient temperatures when the concretes grade C75 casted were higher. One of the main compounds of cement i.e. tricalcium aluminate (C_3A), which reacts very quickly with water means that its

contribution to early age of temperature rise is higher due to its greater quantity, however, it only occurs for a short time.

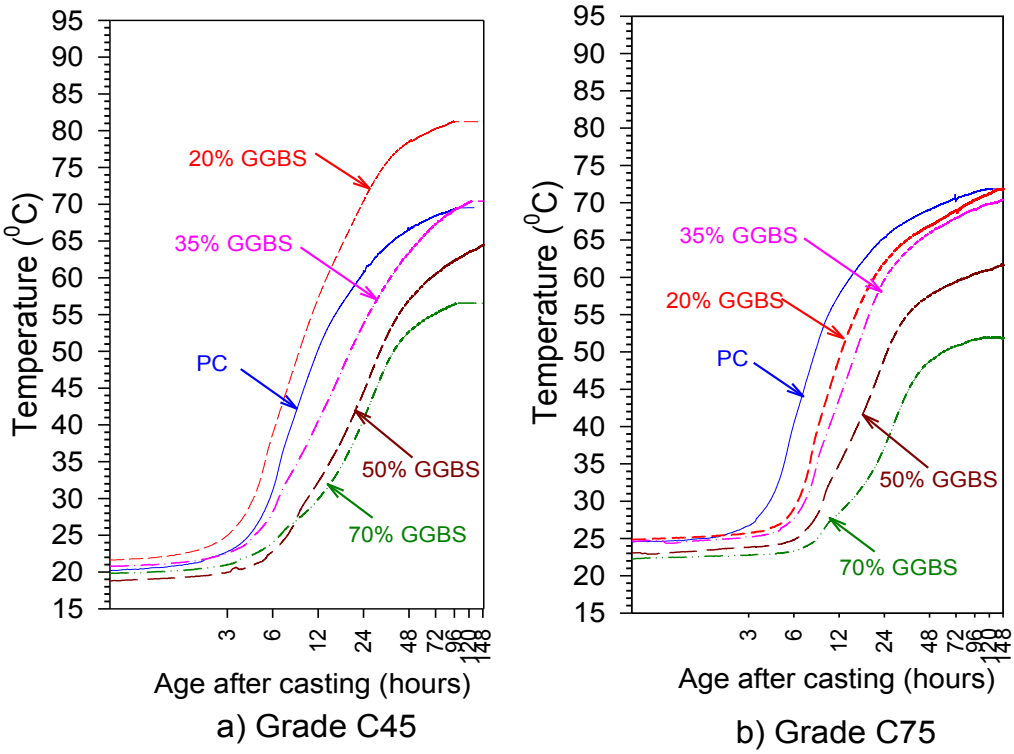

Figure 5.24: Adiabatic temperature rise of concretes **grade C45** and **C75**

The temperature rise of concrete grade C45 with 20% GGBS is higher than that of concrete with Portland cement only, where the difference is about 11.8^{0}C. It is believed that the concrete with 20% GGBS contain more binder than that of PC concrete, i.e. 373 kg/m^3 and 396 kg/m^3 for PC and 20% GGBS concretes, respectively. Compared to the grade C75 concretes that have binder contents of 417 kg/m^3 and 420 kg/m^3 for PC and 20% GGBS concretes, respectively. These have similar temperature rises with the difference of peak temperature of only 0.9^{0}C. However, these are not the true maximum temperatures as some heat will continue to be generated for some time.

There are two important points of adiabatic temperature rise. The first point is called the *"dormant period"* where there is no temperature rise after casting. The second one is when the mortar/concrete reaches its maximum temperature rise.

Figure 5.26 shows these points for both mortar and concrete with all GGBS levels. The figure clearly shows that the dormant periods slightly increase with an increase of GGBS levels for both mortars and concretes, except for concrete grade C75 where concrete with 70% GGBS has the dormant period much longer than that of lower levels of GGBS. The dormant periods of mortar grade C45 range from 4.42 to 12.02 hours for mortar with PC only and 70% GGBS respectively; while the dormant periods for mortar grade C75 range from 3.72 to 10.27 hours.

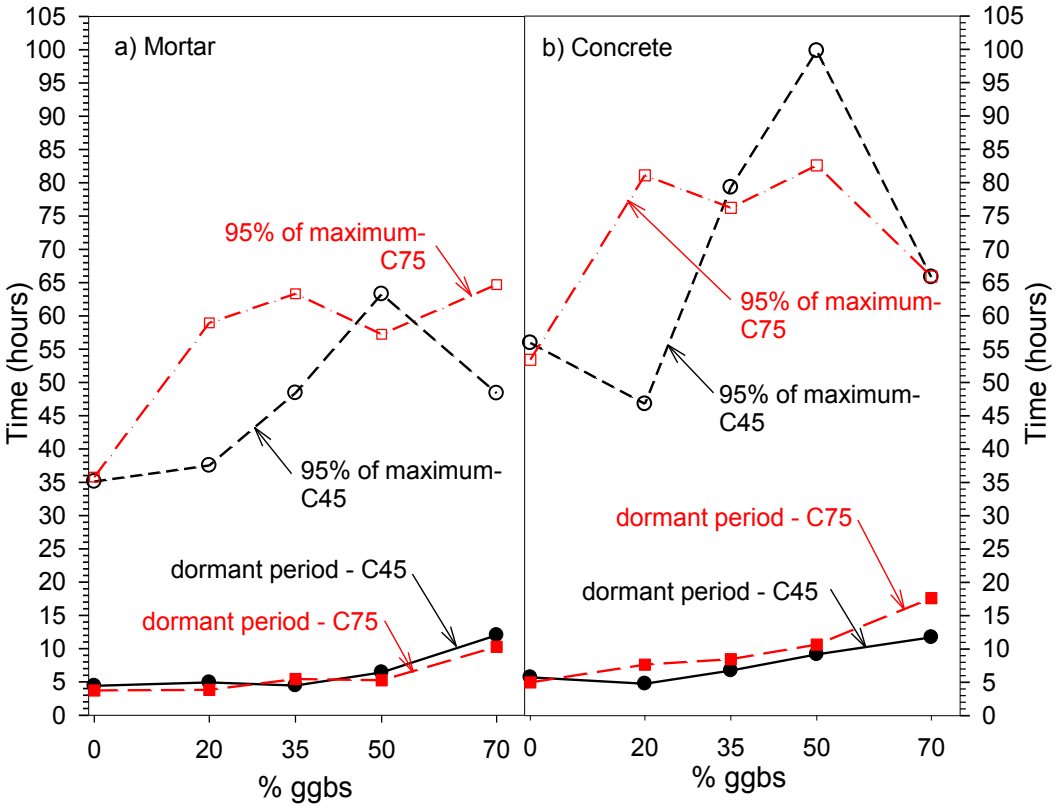

Figure 5.25: Dormant and time to reach 95% of maximum temperature both mortars and concretes **grade C45** and **C75**

The dormant periods of concrete are slightly longer than those of their equivalent mortars. This is as a result of their equivalent mortars contains much more binder than that of the concretes. The dormant period of concrete grade C75 with 70% GGBS is 3.5 times longer than that of concrete with PC only, i.e. 4.99 and 17.64 hours for PC and 70% GGBS concrete, respectively. Compared to the concrete

grade C45, the difference of the dormant period is shorter i.e. 5.75 and 11.75 hours for PC and 70% GGBS concretes, respectively.

It is also important to note that the use of GGBS in mortar/concrete will reduce the maximum temperature rise particularly for high level of GGBS i.e. up to 70%. The incorporation of GGBS with cement resulted in retardation in the time to reach 95% of the maximum temperature.

5.4. Strength Development of mortars and concretes under Standard Curing Temperature and Adiabatic Conditions

This section presents the strength development of concretes/mortars cured under adiabatic conditions. The adiabatic strengths are then compared to the strengths of concretes/mortars cured at standard curing temperature (20^0C).

5.4.1. Strength Development of Equivalent GGBS Mortars under Standard Curing and Adiabatic Conditions

The strength development of mortars cured at 20^0C and under adiabatic conditions for grades C45 and C75 is shown in Figures 5.26 and 5.27, respectively. For mortars grade C45 that cured under adiabatic conditions, the detrimental effect only occurred on mortars with low levels of GGBS and with PC. For mortar with PC only grade C45, the detrimental effect occurred after the age of 8-days, where the strength at the age of 8-days i.e. 51.85 N/mm^2 decreased to 48.97 N/mm^2 and 46.27 N/mm^2 at the ages of 16-days and 32-days, respectively. However, its strength from age of 64 to 365 days increased and again followed the strength development of mortars that had been cured at the standard curing temperature. It is believed that the decrease in strength due to the so called "thermal shock"[246]. This occurred when the cubes were removed from curing tank for testing; the concrete surface is rapidly cooled. Similar to what occurred on mortars with low GGBS levels such as 20 and 35%, the decrease of strength occurred at a much later age and then increased again followed the strength of samples that cured at 20^0C. In mortars with higher GGBS levels such as 50 and 70%, the detrimental

effect on the adiabatic strength development is negligible, as their peak temperatures were lower than that of mortars with low GGBS levels (20 and 35 %) and PC only, even the strength development of 50% GGBS mortar over the strength of samples that cured at 20^0C.

The strength development of all mortars grade C75 cured under adiabatic curing conditions seemed to be a good result compared to that of cured under isothermal curing condition. The detrimental effects due to the higher curing temperature at earlier-age on strength development of grade C75 mortars under adiabatic curing conditions are much less, than that of grade C45 mortars. The effects also occurred at much later ages compared to grade C45 mortars. However, the adiabatic strengths are higher than the strength of mortars cured at 20^0C for throughout the testing ages until 365 days. This is because the strength development of mortars cured under isothermal curing temperatures were unexpected as they were lower than that of their target mean strengths as previously explained.

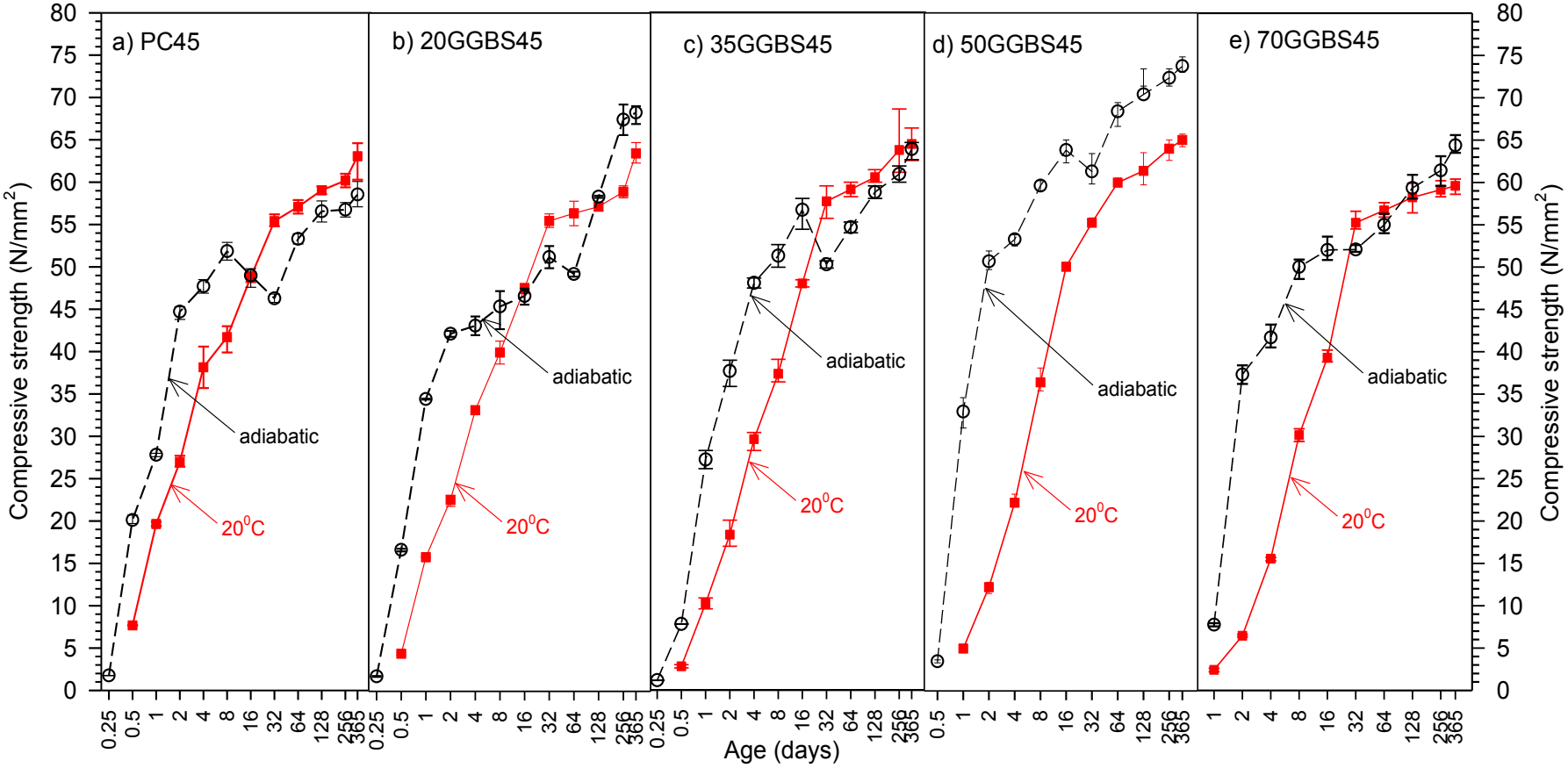

Figure 5.26: Strength developments of mortars cured at 20^0C and under adiabatic curing condition **grade C45**

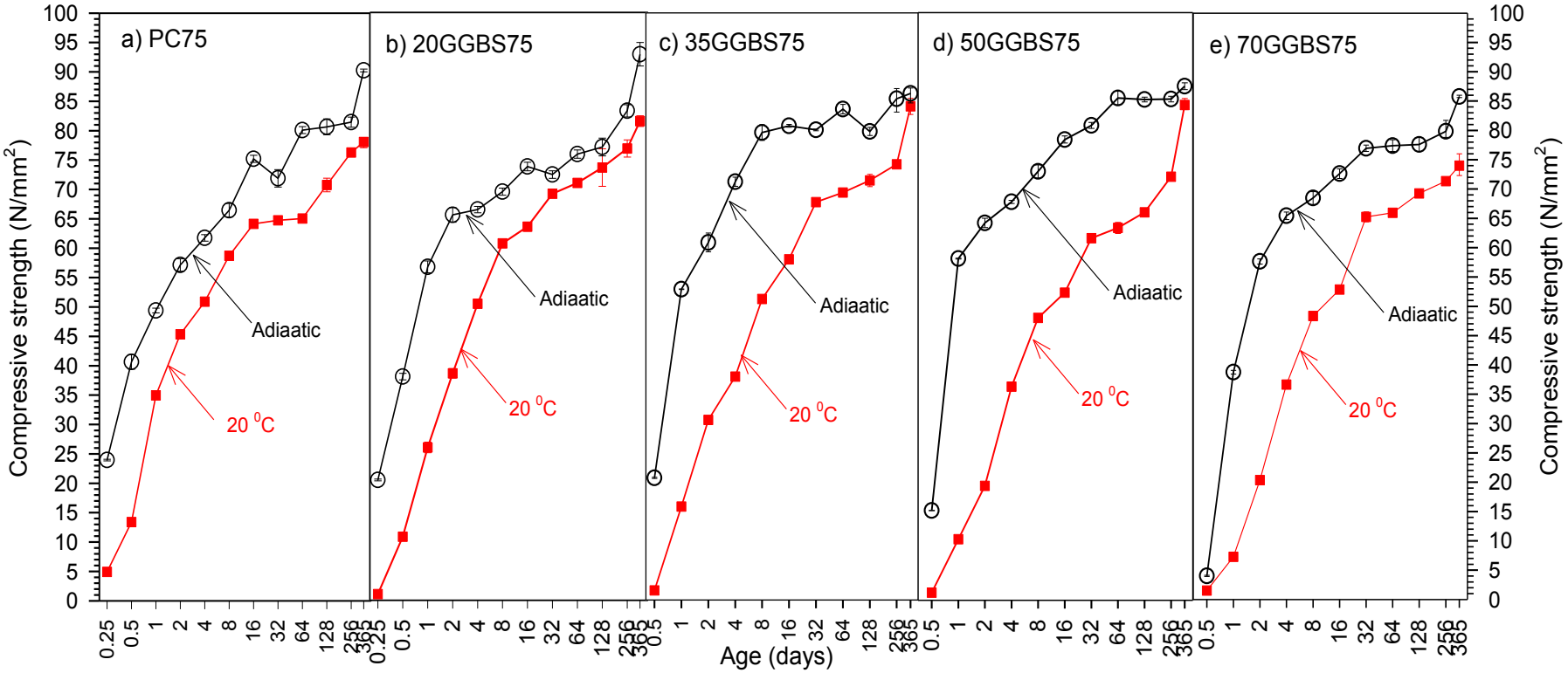

Figure 5.27: Strength developments of mortars cured at 20^0C and under adiabatic curing condition **grade C75**

Figure 5.28 presents ratios of the strength of mortars cured under adiabatic curing temperatures and those of cured at 20^0C. At an early age (1-day), the ratio of mortars with higher replacement levels of GGBS (50 and 70%) was higher than that of mortars with lower levels of GGBS (0, 20 and 35%). However, the strength development of mortars cured at 20^0C appeared to be similar with that of mortars cured under adiabatic conditions after eight and 16-days for mortars grades C75 and C45, respectively. The graph clearly shows that the strength of GGBS concretes with higher levels of GGBS are dependent on curing temperature at earlier-ages.

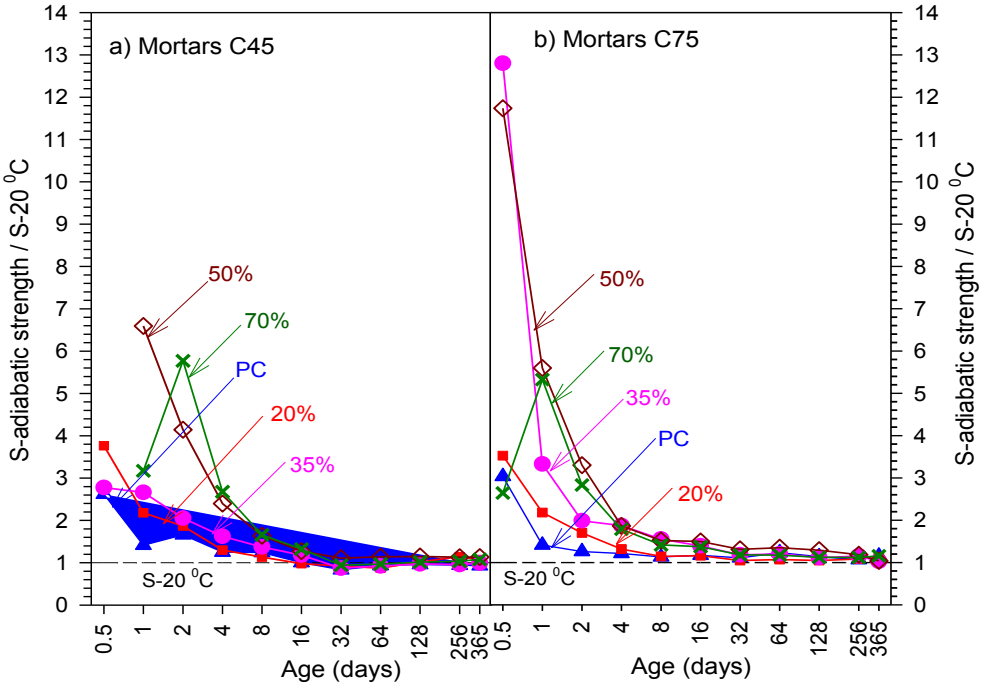

Figure 5.28: Ratio S-adiabatic/S-20^0C mortar **grades C45** and **C75**

Figures 5.29 and 5.30 show the strength ratios between mortars cured under adiabatic conditions and mortars cured at 20^0C at 32-days for mortars grade C45 and C75, respectively. At an age of 1-day, the ratio of strength at the age to that of 32-days for mortar C45 with Portland cement only that had been cured at 20^0C and under adiabatic conditions are 0.35 and 0.50, respectively. In comparison to the mortar with 50% GGBS, the ratios are 0.09 and 0.60 for mortars that cured at 20^0C and under adiabatic conditions, respectively.

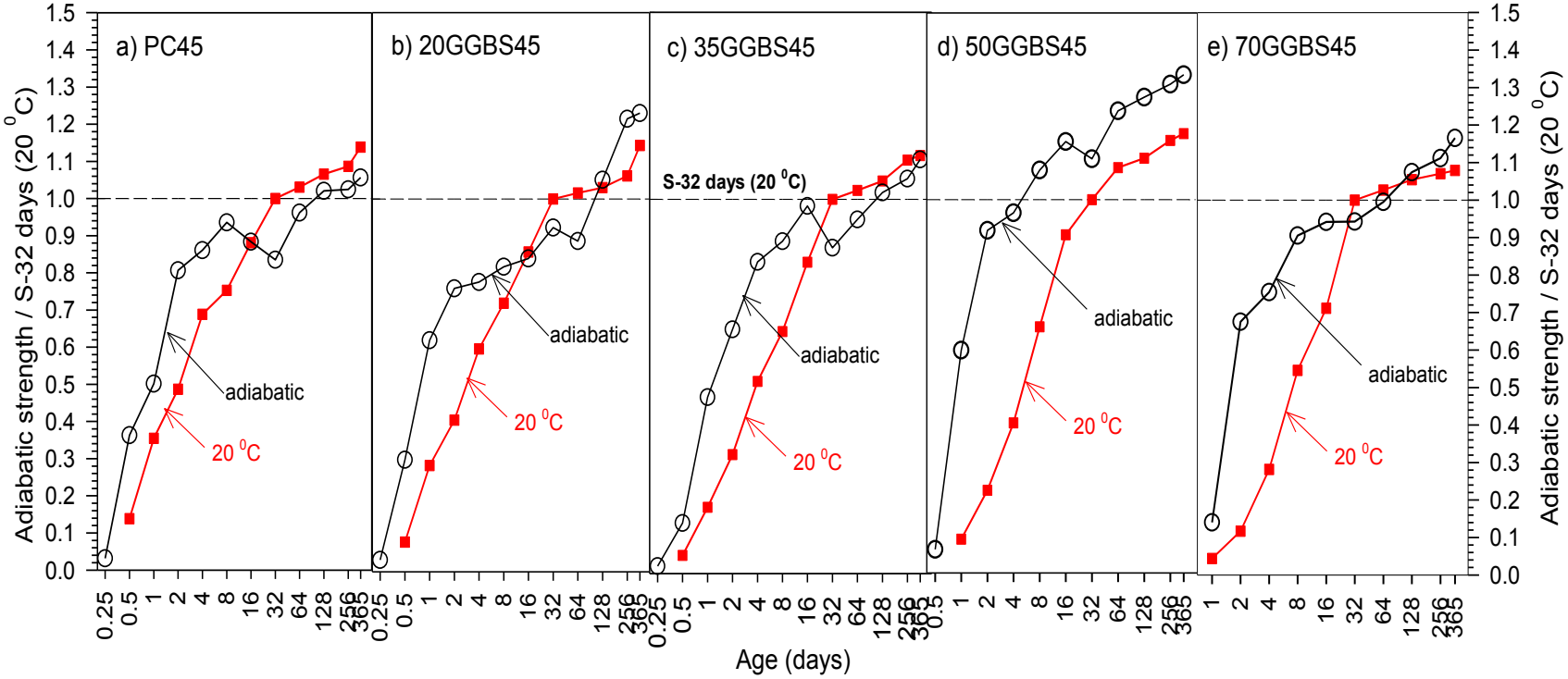

Figure 5.29: Ratio S/S-32-days (20^0C) mortars at curing temperature 20^0C and under adiabatic curing condition **grade C45**

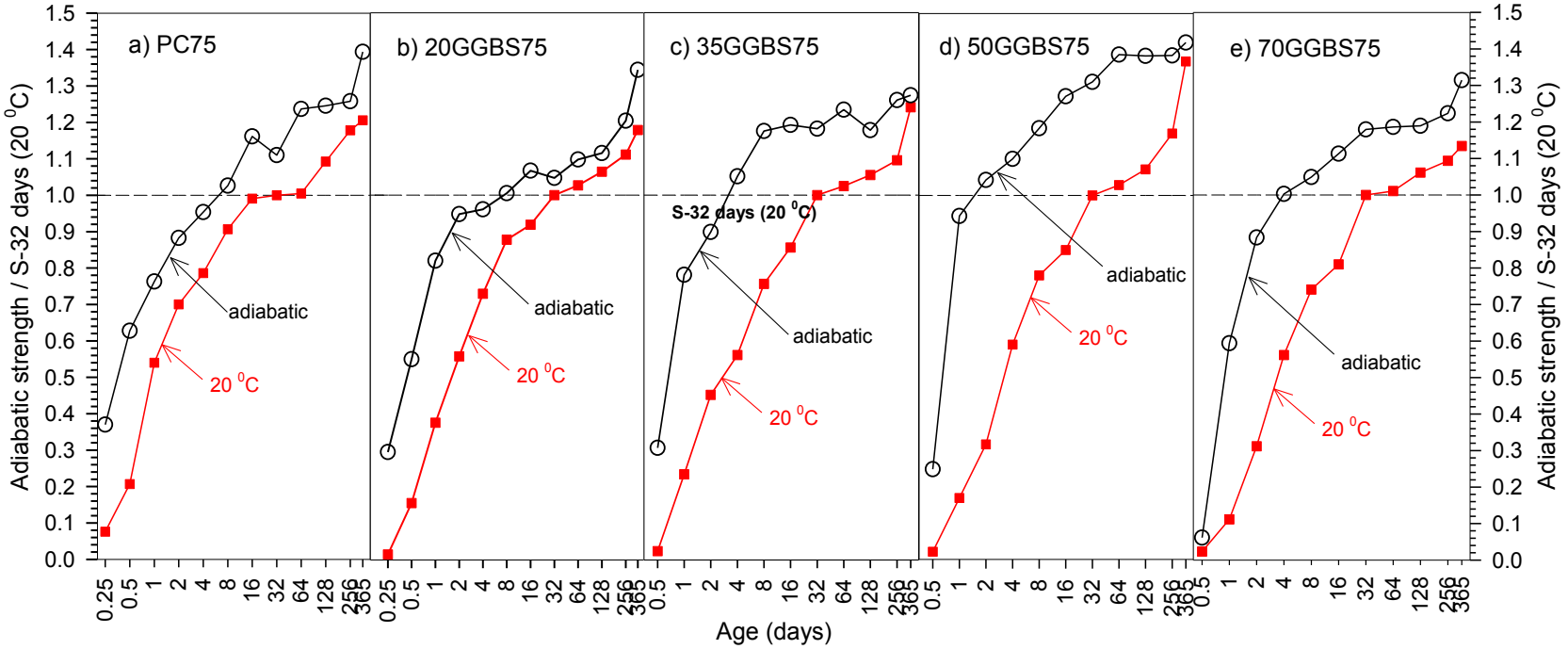

Figure 5.30: Ratio S/S-32-days (20^0C) mortars at curing temperature 20^0C and under adiabatic curing condition **grade C75**

That meant that at the age 1-day, the strength of mortar with 50% GGBS cured at 20^0C was only about a quarter of the strength of mortar with Portland cement only that cured at the same curing temperature. However, the strength of mortar with 50% GGBS cured under adiabatic conditions at the same age, was higher than that of mortar with Portland cement only, where the strengths were 32.93 N/mm^2 and 27.80 N/mm^2 for mortar with 50% GGBS and PC only, respectively. Furthermore, the ratios of strength of mortar grade C45 with 70% GGBS at the same age (1-day) to the strength of the mortar at 32-days were 0.04 and 0.14 for mortar that cured at 20^0C and under adiabatic conditions, respectively.

The strength development of mortar with 70% GGBS under adiabatic conditions at age 1-day was much lower if compared to mortar with 50% GGBS, as the mortar with 70% GGBS took a longer time to set compared to the 50% GGBS mortar. It is important to note that the difference of adiabatic temperature rise of both mortars 50% and 70% GGBS at the age 1-day is significant i.e. 20^0C as shown Figure 5.23.

The ratio of strength development of all mortars grade C75 under adiabatic curing condition to that of cured at 20^0C at early age was higher that of mortar grade C45. It is believed that mortar with lower water-binder ratios have a greater rate of hydration.

The ratio of strength at age 1-day to the strength at 32-days, for PC mortar grade C75 that cured at 20^0C and under adiabatic conditions are 0.54 and 0.76, respectively, as shown in Figure 5.30. In comparison to the mortar with 50% GGBS, the ratios are 0.17 and 0.94 for mortar that cured at 20^0C and under adiabatic conditions, respectively. The strength ratio of mortars cured under adiabatic conditions to the strength of mortar cured at 20^0C at 32-days is higher than the strength ratio of mortar cured at 20^0C during all the testing age until 365 days. It is unlike mortar grade C45, as the strength development of all mortars grade C75 are lower than expected.

5.4.2. Strength Development of Concretes under Standard Curing and Adiabatic Condition

Figures 5.31 and 5.32 present strength development of concretes both grades C45 and C75 that cured at 20^0C and under adiabatic conditions. At early age, the strength development of all concretes for both grades C45 and C75 cured under adiabatic conditions was higher than that of concretes cured at 20^0C. The detrimental effects on strength development of concrete grade C45 is much less than that of their equivalent mortars. The adiabatic temperature rise of mortars are higher than that of its equivalent concrete mix as mortars contain much more binder than their equivalent concrete. Even, the detrimental effects on strength development of GGBS concretes grade C75, which had been cured under adiabatic conditions, do not appear along the period of testing age until age-365 days.

The greatest increase in strength development of concretes cured under adiabatic curing conditions appears to take place within the first 4 days. At this age, the strength of concrete with 0% (Portland cement only), 50%, and 70% GGBS cured under adiabatic conditions were 46.07, 54.07, and 45.33 N/mm^2, respectively, where they reach 84%, 99% and 83% of the strength of concrete grade C45 with Portland cement only cured at 20^0C, at age 32-days (54.83 N/mm^2). For concrete grade C75 (Figure 5.32), the strength of concretes that are cured under adiabatic conditions on average reach 90% of their strength at age 32-days, which cured at 20^0C; i.e. 90, 89, and 92% for GGBS levels of 0, 50, and 70%, respectively.

In comparison with the strength development of concretes cured at the standard curing temperature (20^0C), the strength of concrete grade C45 with Portland cement only at age 4-days reached 70% of the strength at 32-days. The strength of concretes with 50 and 70% GGBS reached 56 and 46%, respectively, of their strength at age 32-days. Furthermore, the strength of concrete grade C75 (Figure 5.32) with Portland cement only, 50 and 70% of GGBS at age 4-days were 75, 51 and 52%, respectively, of their strength at 32-days.

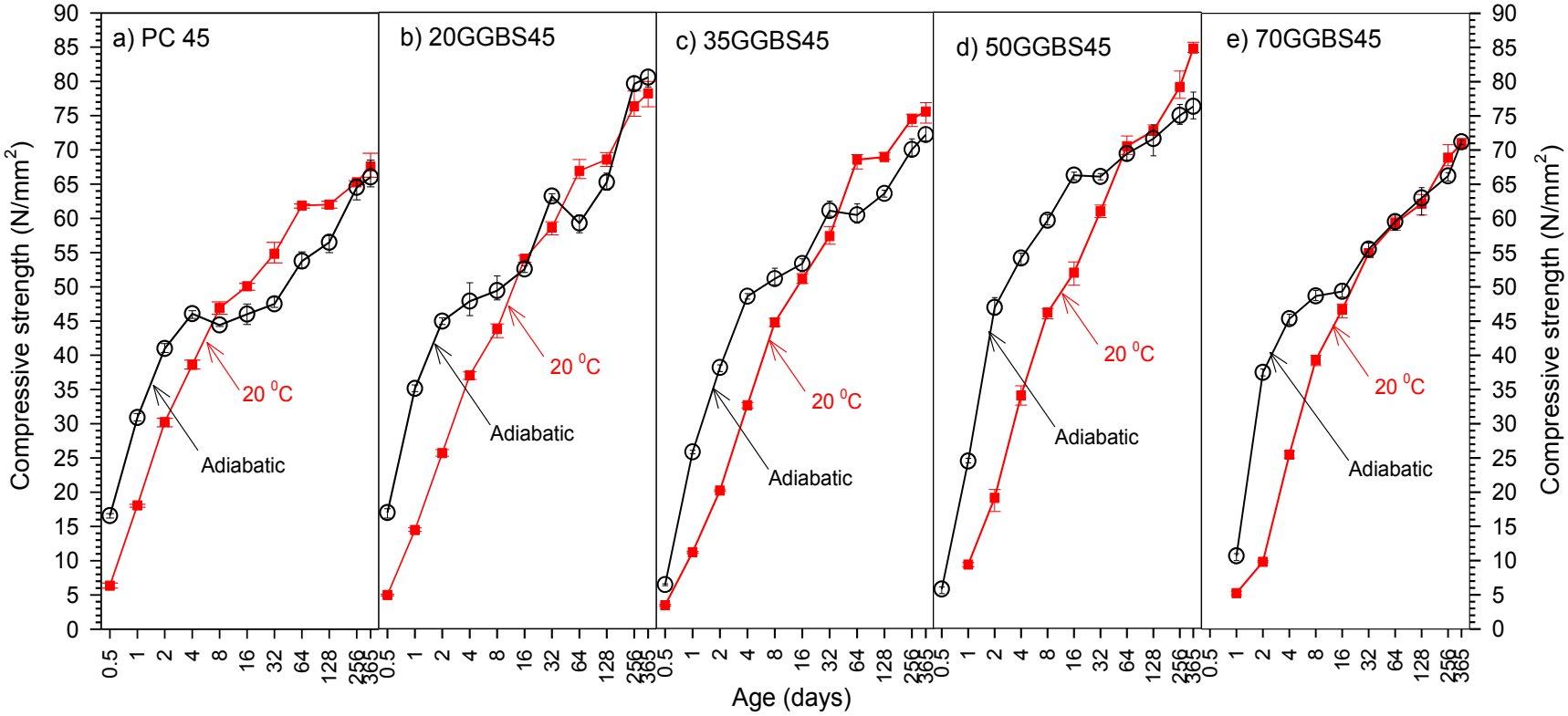

Figure 5.31: Strength developments of concrete at curing temperature 20^0C and under adiabatic curing condition **grade C45**

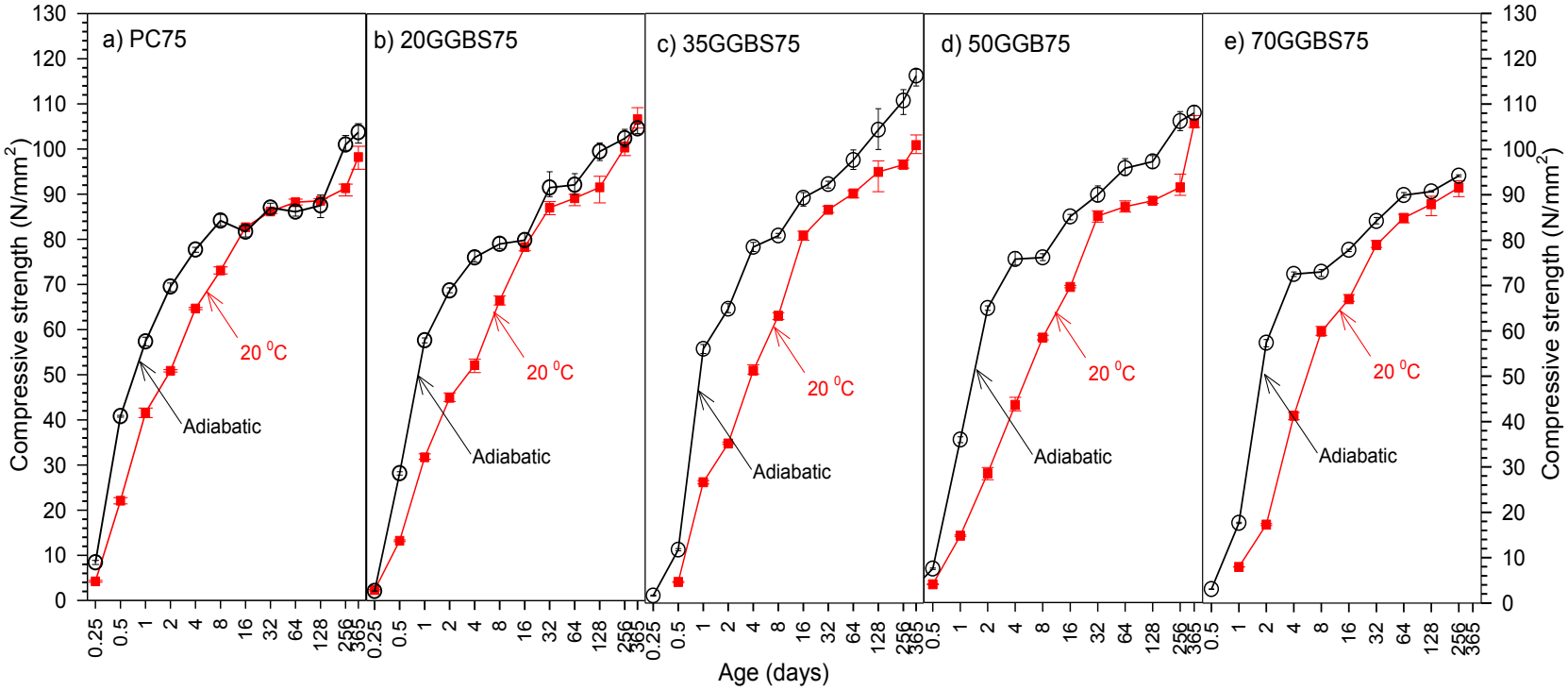

Figure 5.32: Strength developments of concrete at curing temperature 20^0C and under adiabatic curing condition **grade C75**

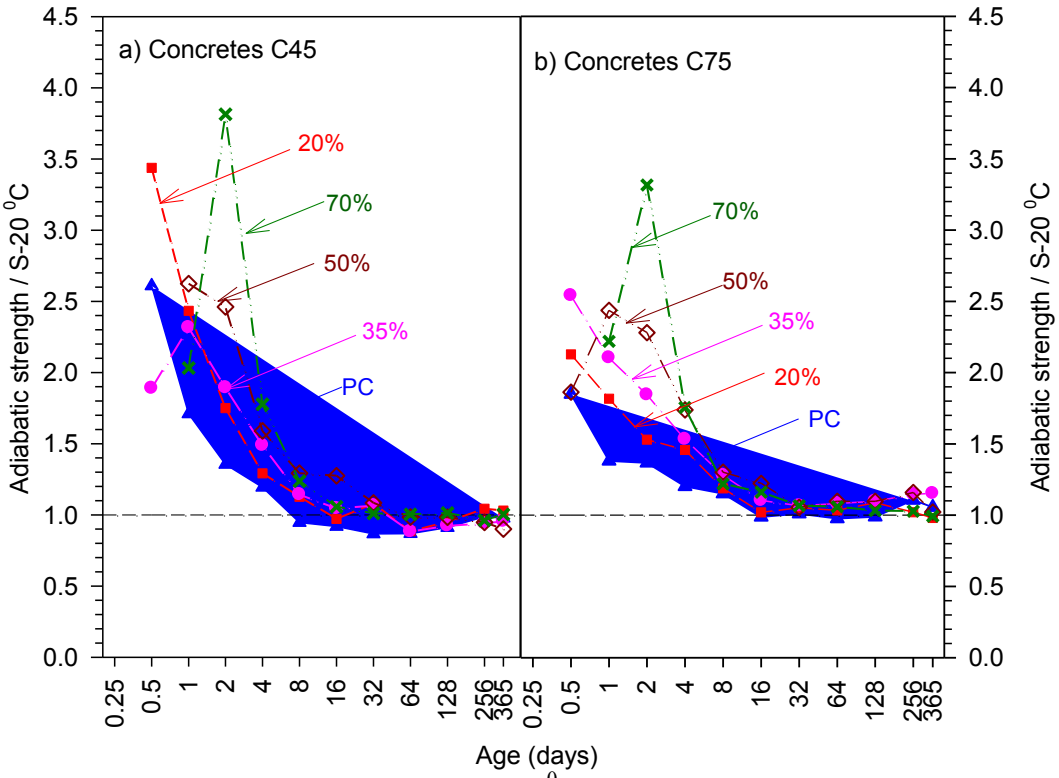

Figure 5.33: Ratio S-adiabatic/S-20^{0}C concrete grades **C45 and C75**

Figure 5.33 shows the strength ratio of concretes cured under adiabatic conditions to that of cured at 20^{0}C for concretes grade C45 and C75. At age 2-days, the higher GGBS levels resulted in higher strength ratios. Also the strength ratio of higher concrete strength (C75) was lower than that of lower strength concrete (C45). This is due to the hydration rate of concrete grade C75 under standard curing temperature being greater than that of concrete grade C45. Therefore, the strength development of concrete grade C75 cured at 20^{0}C is higher that of concrete grade C45.

At age 2-days, the strength ratios for the concrete grade C45 varied between 1.35 and 3.81; and for the concrete grade C75, the strength ratios varied between 1.37 and 3.32 for GGBS level of 0% (Portland cement only) and 70%, respectively. This shows that there is no delay in the strength development of GGBS concrete, even with replacement levels up to 70% at elevated curing temperatures.

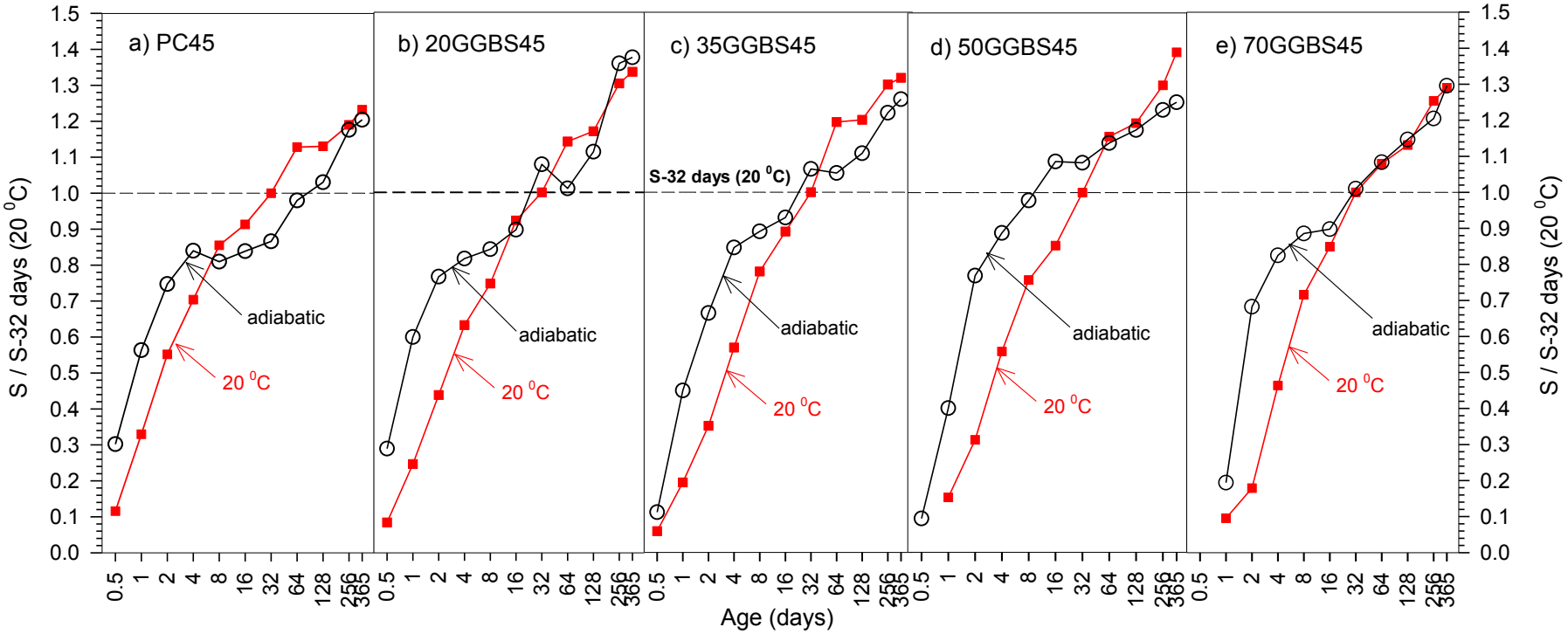

Figure 5.34: Ratio S/S-32-days (20^0C) concretes at curing temperature 20^0C and under adiabatic curing condition **grade C45**

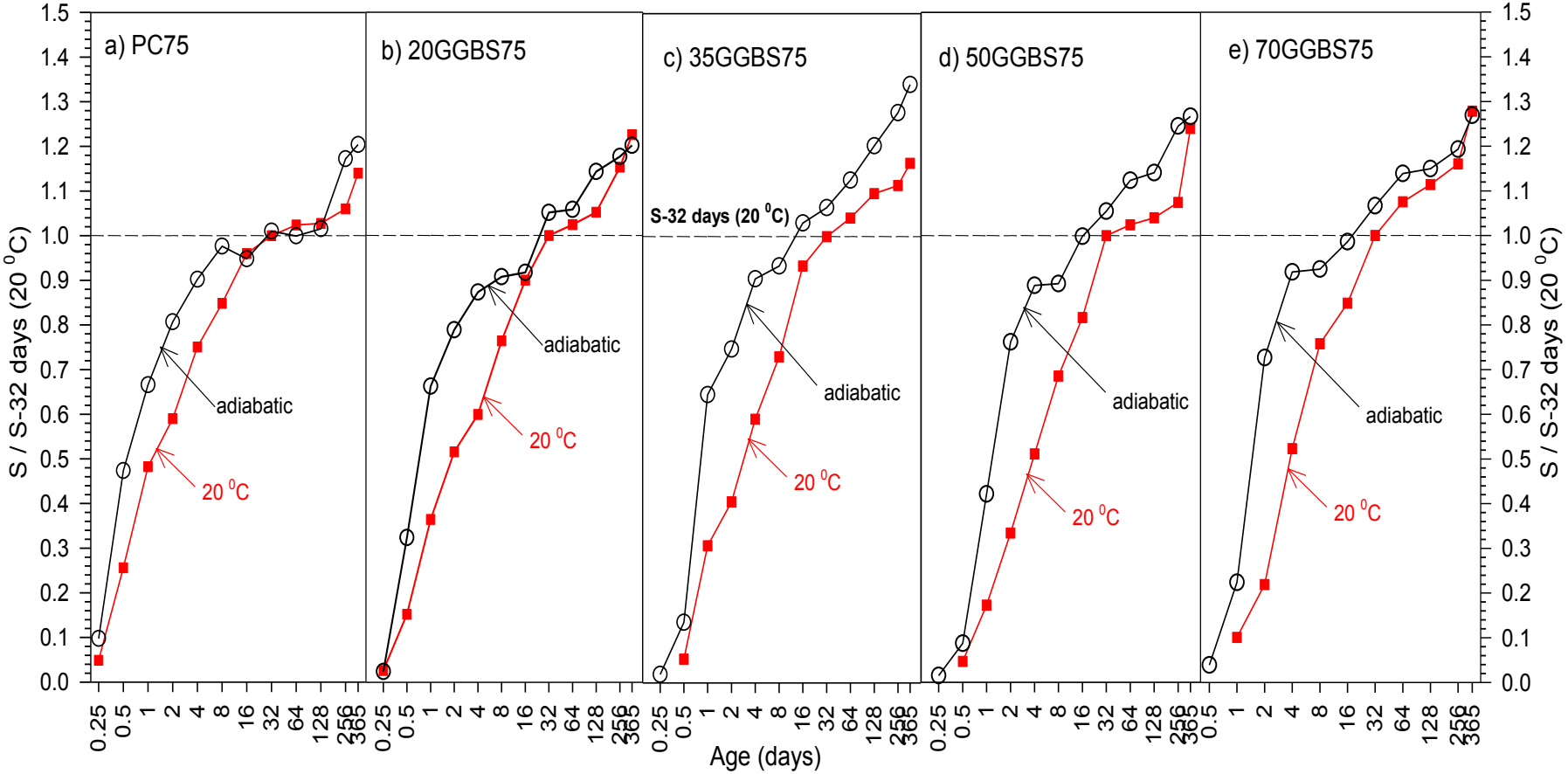

Figure 5.35: Ratio S/S-32-days (20^0C) concretes at curing temperature 20^0C and under adiabatic curing condition **grade C75**

Figures 5.34 and 5.35 present the ratios of strength of concrete cured under adiabatic conditions to strength of the concrete at age 32-days, cured at 20^0C, for both grades C45 and C75. In general, the strength of concrete at later ages are higher than the strength at age 32-days, which meant that the strength development of concrete after 32-days is still developing, although it is not as great an increase as at earlier age.

Concrete grade C45 with Portland cement only cured under adiabatic conditions appeared to display detrimental effects; as its strength at 32-days reached only 87% of strength of the concrete cured at 20^0C. However, the GGBS concrete of the same grade seemed to be less affected by the high curing temperatures at earlier ages except the concrete with 20% GGBS. The strength of this concrete at age 64-days slightly decreased, but it increased again at later ages until age 365-days. The strength at age 365-days, on average were 20% higher than the strength at age 32-days for concrete cured at 20^0C, for both concretes cured at 20^0C and under adiabatic conditions.

The strength development of concrete grade C75 under adiabatic conditions is much less affected by high curing temperatures at earlier ages, particularly concrete with Portland cement only. In comparison to concrete grade C45 with Portland cement only, the detrimental effect on the strength development of concrete grade C75 with Portland cement only is much less. At age 16-days, the strengths of concrete with 35, 50 and 70% GGBS cured under adiabatic conditions reach the strength at 32-days of concrete cured at 20^0C.

5.5. Strength Development of Mortars Cured Under Rapid Temperature Rise

Experimental work was carried out to investigate the effect of high-temperature curing and sudden temperature rise on the strength development of mortar/concrete. There were five mixes of mortar grade C45 with varied replacement levels of 0, 20, 35, 50 and 70% of GGBS. One of the aims was to investigate how the effect of a sudden curing temperature rise increases on the

strength development of mortar/concrete, as well as its effect on strength development at later-ages.

The result of three mixes of mortar grade C45 with 0, 35 and 70% GGBS is presented in Figure 5.36. Other levels of GGBS i.e. 20 and 50% GGBS can be found in Figure E-6 in Appendix E. The figure shows that the sudden change of curing temperature from 20^0C to 50^0C significantly affects the strength development of all mortars, even if the temperature was changed at 3 days after casting. The crossover effect on strength development of PC mortar occurred at earlier ages than that for all GGBS mortars.

In general, there is no negative effect that showed the strength development for all mortar mixes grade C45 at later ages, due to suddenly changing curing temperature after 1, 2 and 3-days casted from the standard curing temperature (20^0C) to 50^0C; unlike the strength development of mortar cured at 50^0C after casting. The strengths of all mortars cured under changing curing temperature at age 28-days are similar even a little bit higher than that of mortars cured under the standard curing temperature. The ratios between the strength of mortars cured under changing curing temperature to that of cured under standard curing temperature varies from 0.99 to 1.07.

The strength development of mortar C45 with PC only that cured under changing curing temperature after 1, 2 and 3-days after casting at 4-days was higher than that of mortar cured under standard curing temperature at the same age. The strength ratios of mortar cured under changing temperature at 1, 2 and 3-days after casting to the strength of mortar cured at 20^0C were 1.28, 1.13 and 1.03, respectively; while the strength ratio of mortar cured at 50^0C from the time after casting to the strength of mortar cured at 20^0C was 1.03. The strength of mortar with PC only at age 4-days that cured at 20^0C was 38.93 N/mm2. Except for mortar with 20% GGBS, the strength of all other GGBS mortars at age 4-days that cured under standard curing temperature were lower than that of mortar with Portland cement only.

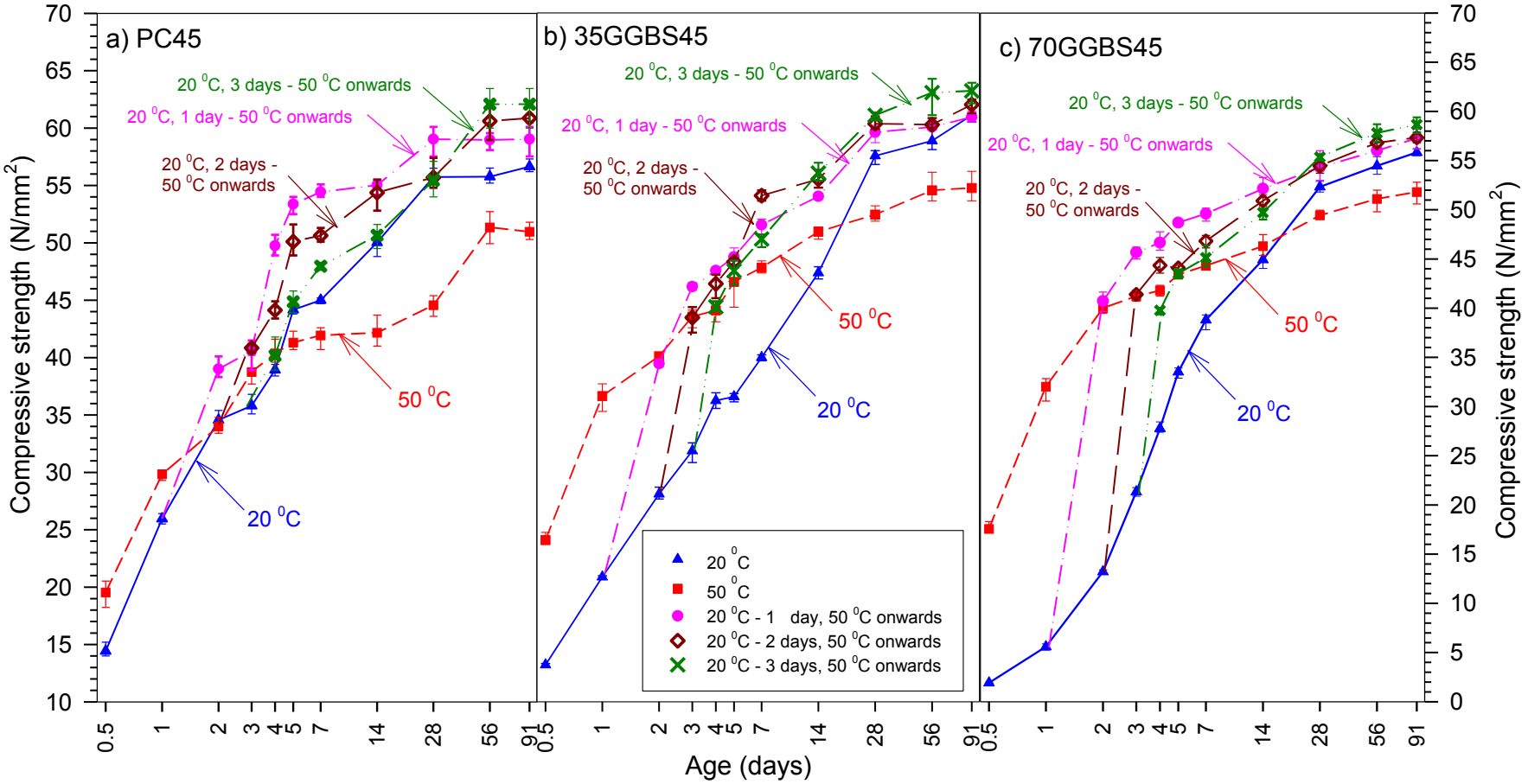

Figure 5.36: Strength development of mortar **grade C45** with 0, 35 and 70% GGBS cured under changing curing temperature

At the age of 28-days, the strength of mortar cured under changing curing temperature for PC mortar was similar to that cured at 20^0C. However, the strength was higher than that of mortar cured at 20^0C at a later age. The strength of PC mortar at age 28-days that cured at 50^0C from the time after casting was about 20% lower than the strength of that cured at 20^0C. The results clearly showed that the high curing temperature at an early-age affected the strength development of mortar at later ages, unlike the strength development of mortars with the sudden rise in the curing temperature from 20 to 50^0C, after 1, 2 and 3-day casting. Furthermore, the strength of GGBS mortars cured under changing curing temperature was higher than that cured at standard curing temperature (20^0C) from the time their curing temperature was changed to their age later on.

5.6. Summary

The summary of this chapter can be drawn as follows:

- Under standard curing temperature (20^0C), the strength development of GGBS concrete is lower than that of concrete with Portland cement only. The higher levels of GGBS replace cement in concrete results in the slower strength development of the concrete at early ages.
- The strength development of GGBS concretes cured at higher temperatures (over than standard curing temperature) are similar to the strength of concrete with PC only.
- The strength development of GGBS concrete cured under adiabatic conditions is comparable to the strength development of concrete with Portland cement only from the age 1-days onward depends on the levels of GGBS in concrete as cement replacement.
- The detrimental effect to the strength development of mortar/concrete at later age due to a higher curing temperature at early age can be minimised by transferring the mortar/concrete to higher curing temperature after one day at standard curing temperature.

CHAPTER 6 – ADIABATIC STRENGTH PREDICTION

6.1. Introduction

One of the main objectives of the study is to develop a strength-maturity correlation that could be used to predict adiabatic strength development of GGBS concrete based on its temperature history. The strength development of concrete that cured under adiabatic conditions is similar to the in-situ strength development, which occurs under varying temperature conditions.

The Nurse-Saul and Equivalent Age methods have become the most popular and widely used to predict the strength of concrete. The Equivalent Age equation is based on the Arrhenius formula. This method needs a determination of the activation energy of concrete, which is needed to calculate the equivalent age of concrete that is cured at a certain temperature, compared to when it is cured at reference temperature. There are other methods such as Chanvillard and D'Aloia[162], Kjellsen and Detwiler[157] and Y.A. Abdel-Jawad[163, 164]. Furthermore, a new theory that is a modified version of the Nurse-Saul maturity function[166] was recently developed at The University of Liverpool in order to improve strength predictions of concrete cured under non-isothermal curing regimes.

The adiabatic strength prediction was estimated based on strength data obtained from standard curing. The predicted strength results were then compared to the actual adiabatic strength obtained from compressive strength tests. This aims to compare and evaluate the accuracy of the methods used for GGBS mortar/concrete, the limitations in their use for predicting the strength of concrete and to indentify if scope improvement. The activation energies were determined from the equivalent mortar mixes, were used to predict the strength of concretes in order to examine whether the activation energies were applicable for predicting concrete strength.

6.2. Determination of Activation Energy

The first stage of the concrete strength prediction is determining activation energy. Both ASTM C1074[6] and TPE[6, 101] methods were used to calculate the activation energy, which were discussed in the literature review (Section 2.4.6). All parameters needed in the calculation were obtained from linear regression using each equation from both methods.

6.2.1. Determination of Activation Energy and Datum Temperature based on ASTM C1074 Standard

The ASTM C 1074 standard[6] recommends the use of the rate constant k to determine the activation energy. The rate constant *k* was obtained from regression analysis by using Sigmaplot to find out the best-fit curve, which was carried out on a plot of the strength data of cubes cured under different isothermally curing temperatures of 10, 20, 30, 40 and 50^{0}C against the age of each mix, based on Equation 2.60. The results of regression analysis are parameters such as S_∞, k and t_0 for all mortars can be seen in Tables E-1 and E-2 in Appendix E.

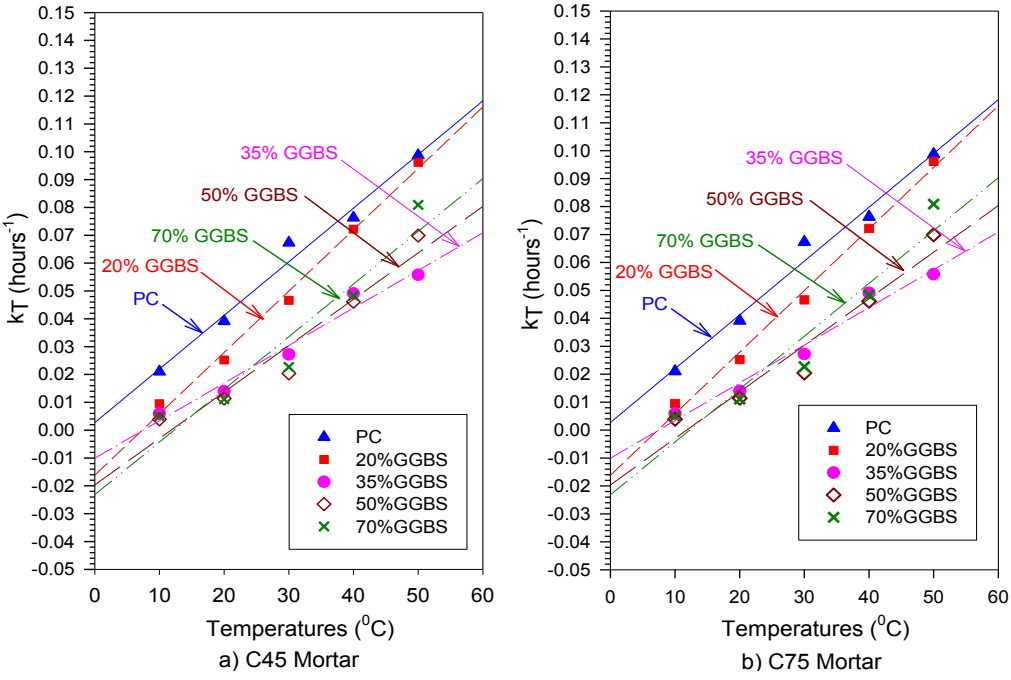

Figure 6.1: Rate constant (k) versus curing temperature for determining the datum temperature

The datum temperature was determined by plotting the rate constant (k) value obtained from regression analysis against curing temperature, as shown in Figure 6.1. A regression analysis was carried out to find out the best-fit curve of the points was fitted for each mix. It is assumed that under the datum temperature there is no strength gain, therefore, the datum temperature can be determined from the point intercept of the best-fit line to the temperature axis. The values of the datum temperatures of all mortars of both grades C45 and C75 are presented in Table 6.1 below.

Table 6.1: Datum temperatures for mortar grade C45 and grade C75

GGBS level (%)	Datum temperature, ^{0}C	
	Grade C45	Grade C75
0	1.42	-1.42
20	5.44	7.36
35	6.89	7.77
50	7.63	11.59
70	8.67	12.21

The results in Table 6.1 clearly show that the datum temperature increases as the GGBS level increase for both grades C45 and C75. GGBS mortar was more dependent on temperature than Portland cement mortar. The table also shows that mortar with the same level of GGBS but have lower water-binder ratios have higher datum temperatures. The exception was the PC mortar, where decrease of the water-binder ratio from 0.51 (grade C45) to 0.33 (grade C75) resulted a decrease in datum temperature by 2.84^{0}C.

In order to calculate the activation energy of the mortars, the rate constants k that are obtained from regression analysis of each mix was plotted against the reciprocal of absolute temperatures (K^{-1}) as shown in Figure 6.2 for both mortars grades C45 and C75. The regressions analyses were carried out to find out the best-fit straight line of each mix.

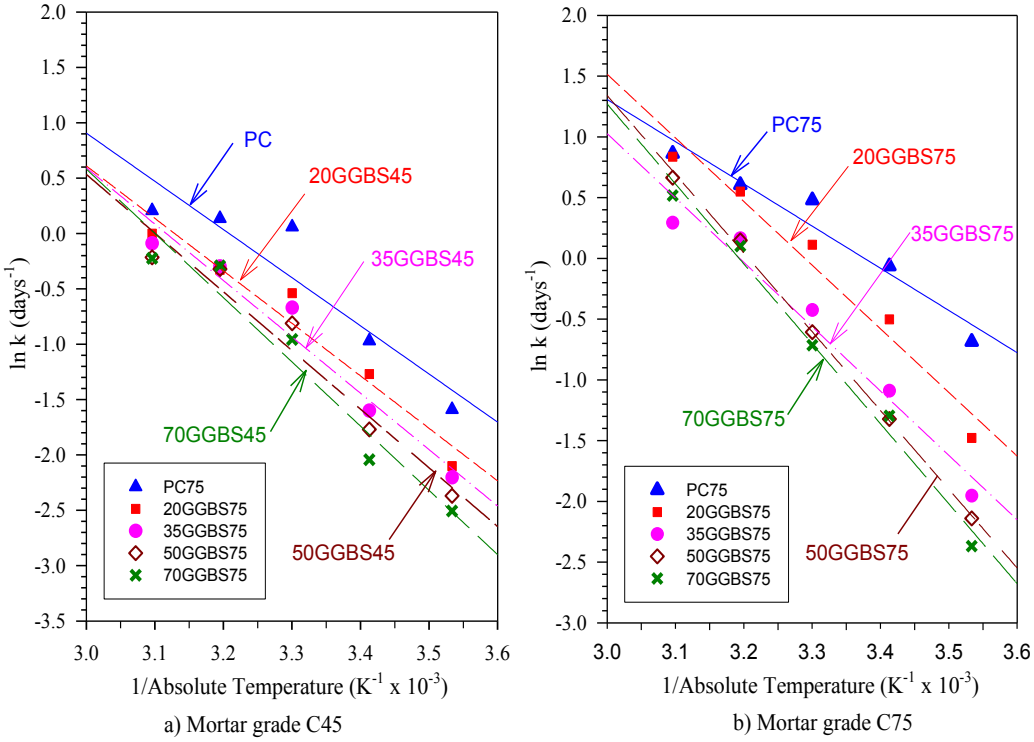

Figure 6.2: Natural logarithms of the rate constant (k) versus the reciprocal of absolute temperature

The slope of the best-fit straight line, therefore, is equal to $-E_a/R$. The activation energy of all mortars then can be calculated as presented in Table 6.2.

6.2.2. Determination of Activation Energy using Three Parameter Equation (TPE) Strength-Age Correlation

The parameters such as S_∞, τ and a were obtained from regression analysis based on Equation 2.62 by plotting strength data against age for each mortar cured at curing temperatures of 10, 20, 30, 40 and 50^{0}C. The results of the regression analysis can be seen in Tables E-3 and E-4 in Appendix E.

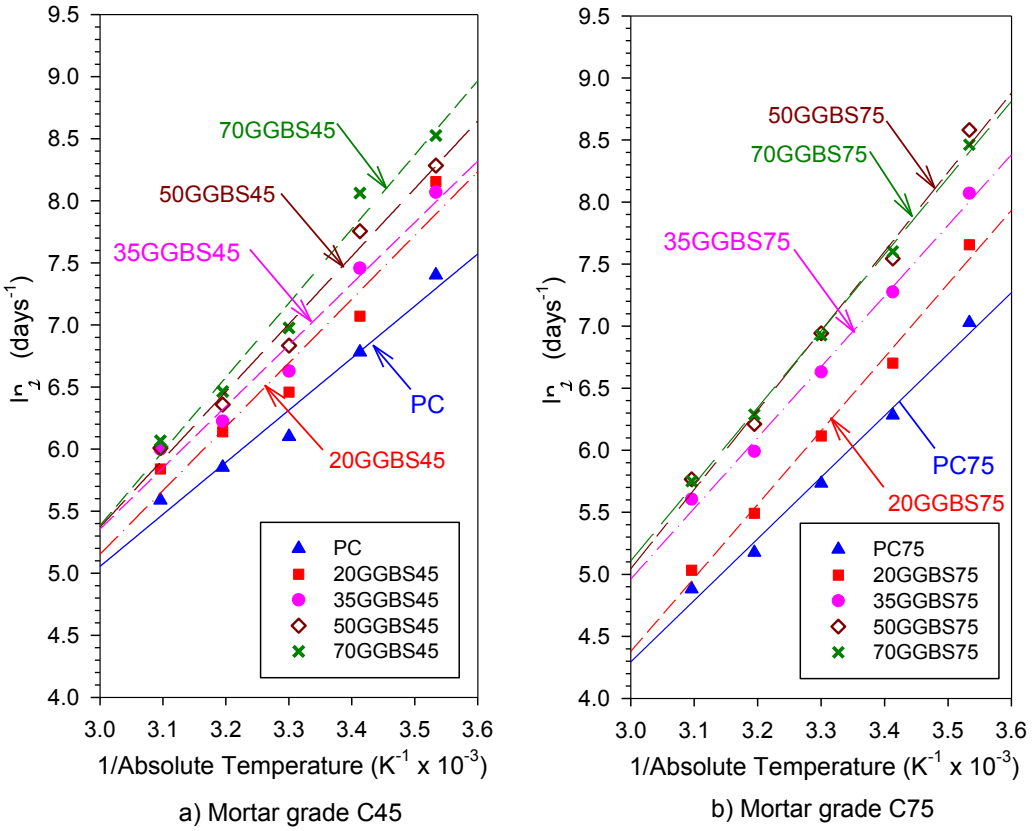

Figure 6.3: Natural logarithms of the characteristic time (τ) versus the reciprocal of absolute temperature.

Figure 6.3 shows graphs *ln (τ)* (obtained from regression analysis based on Equation 2.36) against *1/T* for both mortars grade C45 and grade C75. A linear regression analysis was carried out based on Equation 2.65 to find out the best-fit straight line, where the slope of the line is equal to E_a/R. Accordingly, the value of the apparent activation energies can be calculated for each mortar from the slopes of the best-fit straight lines shown in the Figure 6.3 and presented in Table 6.2. The apparent activation energy values determined from two methods (ASTM standard and TPE) were found to be similar as shown in Table 6.2. The values vary between 28 and 55 kJ/mol. For mortars that have the same grade, the higher levels of GGBS, the higher the activation energy values. Also the higher the activation energy, the higher is the effect on temperature on the strength development of the mortar mixtures.

Table 6.2: Apparent activation energy for mortar **grade C45** and **C75** based on both ASTM C1074 and TPE methods

GGBS level (%)	Activation energy (kJ/mol) based on ASTM method		Activation energy (kJ/mol) based on TPE method	
	Grade C45	Grade C75	Grade C45	Grade C75
0	36.179	28.87	34.88	37.13
20	39.42	43.54	42.71	43.83
35	42.33	44.03	43.58	44.14
50	44.05	53.89	45.34	46.65
70	48.24	54.71	49.65	49.79

For comparison, the apparent activation energies of different grades of mortar obtained from previous work[40] that was carried out at the University of Liverpool, (funded by ESPRC) are presented in Table 6.3. These values were calculated based on the ASTM standard.

Table 6.3: Apparent activation energy for mortars **grade C30**, **C60 and grade C90** based on ASTM C1074 standard[40]

GGBS level (%)	Activation energy (kJ/mol) based on ASTM method		
	Grade C30	Grade C60	Grade C90
0	34.8	35.1	32.9
20	36.6	35.2	36.8
35	47.1	47.0	46.8
50	54.6	48.0	52.6
70	58.8	62.1	57.9

The values of activation energy obtained from this study (grades C45 and C75) and previous work (grades C30, C60 and C90) were plotted in Figure 6.4. The graph shows that the apparent activation energy is relatively independent of water-binder ratio and dependent primarily on the GGBS level in the binder. The higher replacement levels of GGBS in binder leading to the higher apparent activation energies.

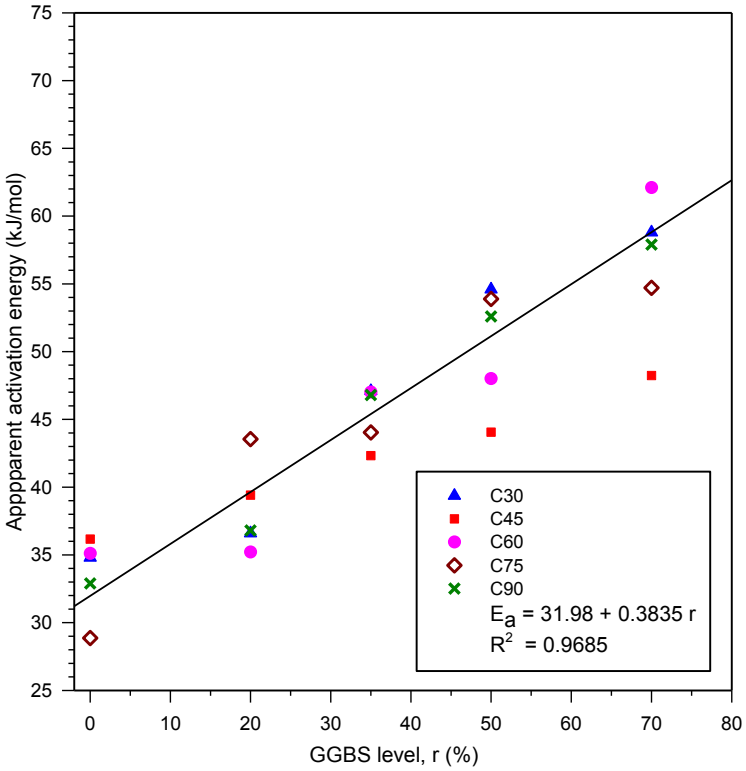

Figure 6.4: Apparent activation of varying mortar grades and GGBS levels

The apparent activation energies increase approximately linearly with increasing GGBS levels, as the correlation factor obtained from regression analysis was 96.85%. A linear regression analysis was carried out to find a model to calculate the apparent activation energy of GGBS mortars as follows:

$$E_a = 31.98 + 0.3835\ r \qquad \text{Equation 6.1}$$

where: E_a = apparent activation energy (kJ/mol)

r = level of GGBS (%)

6.2.3. Activation Energy Values

Some values of apparent activation energy found in literature that has not been presented in the Literature chapter are presented in Table 6.4, as a comparison to that obtained from experimental work of this study.

Table 6.4: Apparent activation energy obtained from literature

Concrete mix	Source	w/b	Activation energy (kJ/mol)
PC30 Type I Cement	Hatzitheodorou[144]	0.66	37.4 and 22.9
PC50 Type I Cement	Hatzitheodorou[144]	0.46	29.7 and 18.1
C37N Type I Cement	Hatzitheodorou[144]	0.45	27.5 and 24.5
C85MS High Strength Mix + Micro silica Type I Cement	Hatzitheodorou[144]	0.25	38.0 and 51.0
FA30 (30% FA) Type I Cement	Hatzitheodorou[144]	0.53	22.5 and 19.4
FA 50 (30% FA) Type I Cement	Hatzitheodorou[144]	0.35	27.3 and 34.5
GGBS 30 (50% FA)	Hatzitheodorou[144]	0.65	53.3 and 59.6
GGBS 50 (50% FA)	Hatzitheodorou[144]	0.46	41.6 and 41.3

The activation energies that found in this reference vary from 18 to 60 kJ/mol, where the apparent activation obtained from this study is within this range. The strength-age relationship based on the TPE method gave reasonably good results which were similar to those obtained from the ASTM standard.

6.3. Strength prediction based on maturity functions

6.3.1. Regression Analysis on Strength Data Obtained from Experimental Work

Regression analysis is needed to obtain the parameters that are needed in the prediction of the adiabatic strength. The results of the regression analysis that based on both Carino and Three Parameter Equation (TPE) suggested by Freiesleben Hansen and Pederson[121] using the Arrhenius equivalent age for all mortar and concrete mixes and grades, are shown in Appendix E (Figures E-7 to E-10).

In mortar grade C45 with all levels of GGBS cured at 10, 20, and30^{0}C, the curves for the strength development obtained from regression analysis that are based on both the Carino and TPE equations are reasonably good, when compare to the actual strength development during a year of testing. However, the regression curves in the mortar cured at higher temperatures i.e. 40 and 50^{0}C, appear to be

accurate to the actual strength up to 8 days, from this age to the age of 64-days, the accuracy drops down in the Carino equation, as the regression analysis curves appears to overestimate the strength. Furthermore, from the age of 64-days onwards the equation appears underestimate the strength. The TPE equation, however, seems to be accurate enough due to the use of the variable shape parameter, *a*.

The limiting strength S_∞ of GGBS mortars grade C45 cured under standard curing temperature that are calculated based on both Carino and TPE equations (strength-age relationship), are higher than that of mortar with Portland cement only. The strength appears to increase as the GGBS level increase, except for mortar with 70% GGBS, where it is a little bit lower than that of mortar with 50% GGBS, but it is still higher than that of other GGBS levels.

The datum temperature obtained based on the ASTM C1074 increased with increasing levels of GGBS. Table 6.5 shows the significant difference in datum temperature between mortar with Portland cement and GGBS mortars. The replacement of cement with 20% GGBS increases the datum temperature of the GGBS mortar by about four times more than that of PC mortar (1.42 to 5.44^0C). This proves that GGBS mortars are more dependent on temperature curing than PC mortar.

In mortars grade 75, the curves obtained from both Carino and TPE equations describe accurately the actual strength development up to the age of 64 days. From this age onwards, the curves end to a level until the age of 365-days, which appear be underestimate the actual strength development of the mortars. The strength developments of mortars grade C75 are unexpected as their strength at age 32-days are lower than their target mean strengths. However, from the age of 128-days the strength increase is significant, where some of them reached the target mean strength at the age 32-days i.e. 85 MPa, such as mortar with 20 and 35% of GGBS. Similarly in the mortar grade C45, the datum temperature in

mortar grade C75 obtained using ASTM C1074, increases by increasing levels of GGBS in the mortar.

The rate constant *k*, in both mortars grade C45 and C75 appear to decrease linearly with increasing GGBS levels. In mortar grade C45, the rate constant *(k)* value of mortar with 70% GGBS only reached 33.8% of the rate constant of the PC mortar. It decreased from 0.3803 $days^{-1}$ (k of mortar with PC only) to 0.1286 $days^{-1}$ (k of 70% GGBS mortar), while in mortar grade C75, the value of the rate constant (k) decrease from 0.9386 $days^{-1}$ (PC mortar) to 0.2657 $days^{-1}$ (mortar with 70% GGBS) as shown in Tables 5.5 and 5.6. This shows that the hydration rate of GGBS at standard curing temperature is lower than of cement, which is directly related to the strength development of mortar/concrete.

On the other hand, the characteristic time *(τ)* for both grades of mortar increase linearly with increasing levels of GGBS in the mortar. In the mortar grade C45, the characteristic time *(τ)* increases 3.6 times when Portland cement is replaced with 70% GGBS i.e. from 1.53 days (τ of PC mortar) to 5.508 (τ of mortar with 70% GGBS). Similarly in mortar grade C75, the time constant *(τ)* increases by 3.3 times by replacing cement with 70% GGBS, i.e. from 0.8113 to 2.6908 days for mortar PC and 70% GGBS, respectively.

The parameters such as S_∞, k and t_0 of Carino and S_∞, τ and a of the Three Parameter Equation were obtained from cube specimens cured under standard curing temperature (20^0C) as the reference temperature should be calculated first. The regression parameters are listed in Tables 6.5 and 6.6.

Table 6.5: Parameters to predict strength based on Carino and TPE equation (strength-age relationships) for mortar **grade C45**

Mixes	PC	20GGBS	35GGBS	50GGBS	70GGBS
Activation energy Ea, kJ/mol (ASTM C1074)	36.169	39.409	42.328	44.054	48.237
Activation energy Ea, kJ/mol (TPE method)	34.879	42.714	43.583	45.339	49.645
T_0 datum temperature (ASTM C1074)	1.42	5.44	6.89	7.63	8.67
T_0 datum temperature (recommended value)	-11	-11	-11	-11	-11
Carino (strength vs. age)					
S_∞ (N/mm^2)	60.181	60.297	60.348	65.611	62.433
k (days^{-1})	0.3803	0.2870	0.2026	0.1700	0.1286
t_0 (days)	2.86E-10	0.0388	0.1595	0.6067	0.9273
R^2	0.9852	0.9892	0.9963	0.9972	0.9902
TPE (strength vs. age)					
S_∞ (N/mm^2)	64.334	63.924	63.617	66.653	61.932
τ (days)	1.5300	2.0440	3.004	4.0510	5.5080
a	0.5770	0.6060	0.6360	0.7960	0.9150
R^2	0.9940	0.9930	0.9960	0.9970	0.9920

Table 6.6: Parameters to predict strength based on Carino and TPE equation (strength-age relationships) for mortar **grade C75**

Mixes	PC	20GGBS	35GGBS	50GGBS	70GGBS
Activation energy Ea, kJ/mol (ASTM C1074)	28.867	43.543	44.034	53.888	54.710
Activation energy Ea, kJ/mol (TPE method)	37.125	43.829	44.138	46.645	49.787
T_0 datum temperature (ASTM C1074)	-1.42	7.36	7.77	11.59	12.21
T_0 datum temperature (recommended value)	-11	-11	-11	-11	-11
Carino (strength vs. age)					
S_∞ (N/mm^2)	69.451	73.7092	72.9002	68.903	71.0519
k (days^{-1})	0.9386	0.6036	0.3349	0.2742	0.2657
t_0 (days)	0.1740	0.2078	0.3049	0.4073	0.4626
R^2	0.9778	0.9955	0.9907	0.9923	0.9945
TPE (strength vs. age)					
S_∞ (N/mm^2)	71.436	75.921	76.432	71.553	72.630
τ (days)	0.8113	1.1858	2.0800	2.5968	2.6908
a	0.7595	0.7433	0.6881	0.7320	0.7862
R^2	0.9818	0.9971	0.9931	0.9940	0.9957

Tables 6.7 and 6.8 below include lists of parameters obtained from regression analysis on mortar cured under standard curing temperature such as S_∞, k, and M_0 of the Carino equation, and S_∞, τ and a of the TPE equation, which are based on strength-maturity relationship. The results show that the limiting strengths obtained from the strength-age relationship is similar to that obtained from strength-maturity relationship.

Table 6.7: Parameters to predict strength based on Carino and TPE equation for (strength-maturity relationship) mortar **grade C45**

Mixes	PC	20GGBS	35GGBS	50GGBS	70GGBS
Activation energy Ea, kJ/mol (ASTM C1074)	36.169	39.409	42.328	44.054	48.237
Activation energy Ea, kJ/mol (TPE method)	34.879	42.714	43.583	45.339	49.645
T_0 datum temperature (ASTM C1074)	1.42	5.44	6.89	7.63	8.67
T_0 datum temperature (recommended value)	-11	-11	-11	-11	-11
Carino (strength vs. maturity)					
S_∞ (N/mm^2)	60.181	60.297	60.348	65.611	62.433
k (^0C-days)$^{-1}$	0.0123	0.0093	0.0065	0.0055	0.0041
M_0 (^0C-days)	4.20E-008	1.2037	4.9459	18.8089	28.7459
R^2	0.9852	0.9892	0.9963	0.9972	0.9902
TPE (strength vs. maturity)					
S_∞ (N/mm^2)	64.334	63.924	63.617	66.653	61.9323
τ (^0C-days)	47.4347	63.3683	93.1356	125.5735	170.7454
a	0.5773	0.6058	0.6359	0.7961	0.9151
R^2	0.9941	0.9931	0.9961	0.9965	0.9916

In concrete grades C45 and C75, the regression analysis curves for both the Carino and TPE equations, especially for concrete cured at 20^0C, appear reasonably good to describe the strength development of all mixes of both the concrete grades.

Table 6.8: Parameters to predict strength based on Carino and TPE equation (strength-maturity relationship) for mortar grade C75

Mixes	PC	20GGBS	35GGBS	50GGBS	70GGBS
Activation energy Ea, kJ/mol (ASTM C1074)	28.867	43.543	44.034	53.888	54.710
Activation energy Ea, kJ/mol (TPE method)	37.125	43.829	44.138	46.645	49.787
T_0 datum temperature (ASTM C1074)	-1.42	7.36	7.77	11.59	12.21
T_0 datum temperature (recommended value)	-11	-11	-11	-11	-11
Carino (strength vs. maturity)					
S_∞ (N/mm^2)	71.129	75.400	71.698	73.272	71.998
k (^{0}C-days)$^{-1}$	0.0273	0.0178	0.0188	0.0070	0.0082
M_0 (^{0}C-days)	4.8454	5.9380	5.7997	9.5351	13.8840
R^2	0.9701	0.9894	0.9834	0.9673	0.9937
TPE (strength vs. maturity)					
S_∞ (N/mm^2)	74.044	78.383	74.213	80.280	73.914
τ (^{0}C-days)	26.7274	38.9549	37.1623	101.0903	85.8906
a	0.6883	0.6900	0.7072	0.5821	0.7567
R^2	0.9778	0.9936	0.9880	0.9767	0.9954

However, the regression analysis curves obtained from concrete cured at 50^{0}C appear to accurately describe the strength development of the concretes up to age 128-days only. From this age onwards the accuracy decreases in the Carino equation, where this equation predicts the strength developments of concrete cured at the curing temperature tend to a constant value, while the actual data shows that the strength development increases again at age 256-day onwards. In the TPE equation, however, this appears much less than that in the Carino equation. It is believed this is due to the TPE equation using the varying shape factor (*a*).

Tables 6.9 and 6.10 are lists of the results obtained from regression analyses using the Carino and TPE equations based on the strength-age relationship. The

apparent activation energy and datum temperatures are taken from equivalent mortars of the concrete. The parameters are results from the concrete cured under standard curing temperature, which will be used to predict the adiabatic strength development of the concretes. In general, limiting strength of GGBS concretes are higher than those of concrete with Portland cement only for both grade C45 and C75. The increase of limiting strength is inconsistent with the increase of GGBS levels in concrete.

Table 6.9: Parameters to predict strength based on Carino and TPE equation for (strength-age relationship) concrete **grade C45**

Mixes	PC	20GGBS	35GGBS	50GGBS	70GGBS
Activation energy Ea, kJ/mol (ASTM C1074)	36.169	39.409	42.328	44.054	48.237
Activation energy Ea, kJ/mol (TPE method)	34.879	42.714	43.583	45.339	49.645
T_0 datum temperature (ASTM C1074)	1.42	5.44	6.89	7.63	8.67
T_0 datum temperature (recommended value)	-11	-11	-11	-11	-11
Carino (strength vs. age)					
S_∞ (N/mm^2)	63.766	73.563	73.679	79.491	68.399
k (days^{-1})	0.3768	0.2103	0.1743	0.1498	0.1327
t_0 (days)	0.0694	1.63E-009	0.0287	1.95E-009	0.5310
R^2	0.9799	0.9789	0.9895	0.9788	0.9885
TPE (strength vs. age)					
S_∞ (N/mm^2)	68.267	84.621	81.322	91.098	72.237
τ (days)	1.6494	3.1750	3.5688	4.4802	4.5106
a	0.5888	0.4788	0.5437	0.4981	0.6734
R^2	0.9918	0.9946	0.9964	0.9925	0.9928

Table 6.10: Parameters to predict strength based on Carino and TPE equation (strength-age relationships) for concrete **grade C75**

Mixes	PC	20GGBS	35GGBS	50GGBS	70GGBS
Activation energy Ea, kJ/mol (ASTM C1074)	28.867	43.543	44.034	53.888	54.710
Activation energy Ea, kJ/mol (TPE method)	37.125	43.829	44.138	46.645	49.787
T_0 datum temperature (ASTM C1074)	-1.42	7.36	7.77	11.59	12.21
T_0 datum temperature (recommended value)	-11	-11	-11	-11	-11
Carino (strength vs. age)					
S_∞ (N/mm^2)	91.011	94.398	97.976	92.946	91.230
k (days^{-1})	0.7226	0.3756	0.2776	0.2308	0.2234
t_0 (days)	0.1167	0.0435	0.0831	0.2335	0.6554
R^2	0.9853	0.9835	0.9875	0.9968	0.9936
TPE (strength vs. age)					
S_∞ (N/mm^2)	94.672	108.627	103.639	104.364	98.136
τ (days)	0.9123	1.8655	2.1507	3.1678	3.6243
a	0.6673	0.5060	0.6137	0.5918	0.7201
R^2	0.9912	0.9903	0.9922	0.9891	0.9891

The highest limiting strength for concrete grade C45 was found in concrete with 50% GGBS, while in concrete grade C75, the maximum limiting strength was in concrete with 35% GGBS. Furthermore, the rate constant *(k)* in the both grades, decrease as the levels of GGBS in concrete increase. In contrast, the time constant *(τ)*, increases as the GGBS levels in concrete increase.

The regression analysis results on cubes cured under standard curing temperature using the Carino and TPE equations (strength-maturity relationship) are presented in Tables 6.11 and 6.12.

Table 6.11: Parameters to predict strength based on Carino and TPE equation for (strength-maturity relationship) **concrete grade C45**

Mixes	PC	20GGBS	35GGBS	50GGBS	70GGBS
Activation energy Ea, kJ/mol (ASTM C1074)	36.169	39.409	42.328	44.054	48.237
Activation energy Ea, kJ/mol (TPE method)	34.879	42.714	43.583	45.339	49.645
T_0 datum temperature (ASTM C1074)	1.42	5.44	6.89	7.63	8.67
T_0 datum temperature (recommended value)	-11	-11	-11	-11	-11
Carino (strength vs. maturity)					
S_∞ (N/mm^2)	63.971	73.563	73.679	79.491	68.399
k (^{0}C-days)$^{-1}$	0.0116	0.0068	0.0056	0.0048	0.0049
M_0 (^{0}C-days)	2.27E-008	1.51E-008	0.8890	6.96E-008	16.4622
R^2	0.9797	0.9789	0.9895	0.9788	0.9885
TPE (strength vs. maturity)					
S_∞ (N/mm^2)	68.267	84.6214	81.322	91.098	72.237
τ (^{0}C-days)	51.1302	98.4263	110.6336	138.8872	139.8284
a	0.5888	0.4788	0.5437	0.4981	0.6734
R^2	0.9918	0.9946	0.9964	0.9925	0.9928

The limiting strengths obtained from regression analysis (strength-maturity relationship) tend to fluctuate with increasing levels of GGBS in concrete. However, all limiting strengths of GGBS concrete cured under the standard curing temperature are higher than that of PC concrete. In concrete grade C45, the limiting strength calculated using the TPE equation of concrete with 50% GGBS increase 33% than that of PC concrete, while the limiting strength calculated using the Carino equation in concrete with 50% GGBS increase by 24% only. Similarly in the concrete grade C75, the maximum increase is found in concrete with 20% GGBS, where it increases by 7 and 14.7% for the Carino and TPE equations, respectively.

Table 6.12: Parameters to predict strength based on Carino and TPE equation for (strength-maturity relationship) concrete **grade C75**

Mixes	PC	20GGBS	35GGBS	50GGBS	70GGBS
Activation energy Ea, kJ/mol (ASTM C1074)	28.867	43.543	44.034	53.888	54.710
Activation energy Ea, kJ/mol (TPE method)	37.125	43.829	44.138	46.645	49.787
T_0 datum temperature (ASTM C1074)	-1.42	7.36	7.77	11.59	12.21
T_0 datum temperature (recommended value)	-11	-11	-11	-11	-11
Carino (strength vs. maturity)					
S_∞ (N/mm^2)	91.011	97.601	97.900	97.360	94.316
k (^{0}C-days)$^{-1}$	0.0233	0.0106	0.0090	0.0060	0.0064
M_0 (^{0}C-days)	3.6184	2.36E-008	2.5924	2.08E-008	17.7877
R^2	0.9853	0.9764	0.9890	0.9848	0.9854
TPE (strength vs. maturity)					
S_∞ (N/mm^2)	94.672	108.627	103.640	104.364	98.136
τ (^{0}C-days)	28.2820	57.8317	66.6707	98.2023	112.3523
a	0.6673	0.5060	0.6137	0.5918	0.7201
R^2	0.9912	0.9903	0.9922	0.9891	0.7201

The time constant *(τ)* and rate constant *(k)*, calculated based on the strength-maturity relationships were found to be similar with that one calculated based on the strength-age relationship. The time constant *(τ)* increase as the GGBS levels in concrete increase. However, the increase of GGBS levels in concrete decreases the rate constant *(k)*.

6.3.2. Adiabatic Strength Prediction of Equivalent GGBS Mortars

Figures 6.5 and 6.6 show the predicted adiabatic strengths based on the Carino and TPE equations using a datum temperature T_0 of -11^{0}C as shown in the Tables 6.5 and 6.6, for both mortar grades C45 and C75 with GGBS levels of 0, 35% and 70%. The results for mortar with 20% and 50% of GGBS for both the grades can

be found in Appendix E (Figures E-11 and E-12). There are four models used in predicting the adiabatic strength development, which are the combinations from the existing equations. The models and the abbreviations used in the plotted graph can be explained as follows:

- C-NS means that the predicted strengths are calculated based on the strength-maturity relationships proposed by Carino with maturity calculated according to Nurse-Saul equation.
- C-Arr means that the predicted strengths are calculated based on the strength-maturity relationships proposed by Carino with the equivalent age calculated according to the Arrhenius equation.
- TPE-NS means that the predicted strengths are calculated based on the strength-maturity relationships i.e. the Three Parameter Equation (TPE) that was proposed by Freiesleben Hansen and Pederson, where the maturity is calculated according to the Nurse-Saul equation.
- TPE-Arr means that the predicted strengths are calculated based on the strength-maturity relationships i.e. the Three Parameter Equation (TPE) that was proposed by Freiesleben Hansen and Pederson, with the equivalent age calculated according to the Arrhenius equation.

In general, both the Carino and TPE equations appear to predict the adiabatic strength development of all mortars of both grades inaccurately during the testing. The predicted strength using the C-Arr is similar to that of TPE-Arr, while the C-NS and TPE-NS models are also similar.

In PC mortar grade C45 (Figure 6.5), the C-NS and TPE-NS models appear to predict the strength development of mortar with Portland cement quite well up to age 8 days. Both the models then predict the strength overestimate on age later. In comparison to the C-NS and TPE-NS models, the C-Arr and TPE-Arr models predict the adiabatic strength well at very earlier ages only and they then overestimate the strength at later ages. Similarly in the PC mortar grade C75 (Figure 6.6), the predicted strength using both the C-NS and TPE-NS models

appear better than that of both the C-Arr and TPE-Arr models. However, all the models predict the adiabatic strength to be much lower than the actual strength at later ages. This is believed to be due to the unexpected strength development of mortar grade C75, where the limiting strength of the mortars are lower than the expected strength or target mean strength at age 32-days.

It is similar in GGBS mortar grade C45, both the C-NS and TPE-NS models underestimate the adiabatic strength at early age and overestimate the strength at later ages, as the mortars have a detrimental effect of high earlier-age curing temperature. On the other hand, the TPE-Arr and C-Arr models predict the adiabatic strength reasonable well at early age i.e. up to an age of 4-days; except for mortar with 50% GGBS (as shown in Figure D-11 in Appendix D), where both the models estimate the strength development quite well until the age of 16-days. In general, the TPE-Arr and C-Arr models predict the strength of GGBS mortar better than the TPE-NS and C-NS models, as the models have different way of calculating maturity.

Furthermore, in GGBS mortar grade C75, both the TPE-Arr and C-Arr models again predict the strength reasonably well up to an age of 16-days as shown in Figure 6.6. On the other hand, both the Carino and TPE equations that are based on the Nurse-Saul maturity function (C-NS and TPE-NS models) predict the lower strength than the actual adiabatic strengths during the testing ages. At the later ages, all the models underestimate the strengths development.

It is believed this is due to the limiting strengths obtained from regression analysis are lower than that of the targeted value. The strengths development of mortar grade C75 were unexpected, as all mortars grade C75 do not reached their target mean strength at age 32-days. In addition, both the Carino and TPE equations do not consider the effect of the high earlier-age curing temperatures at earlier and later ages and the significant strength increase of mortar with GGBS at very later ages.

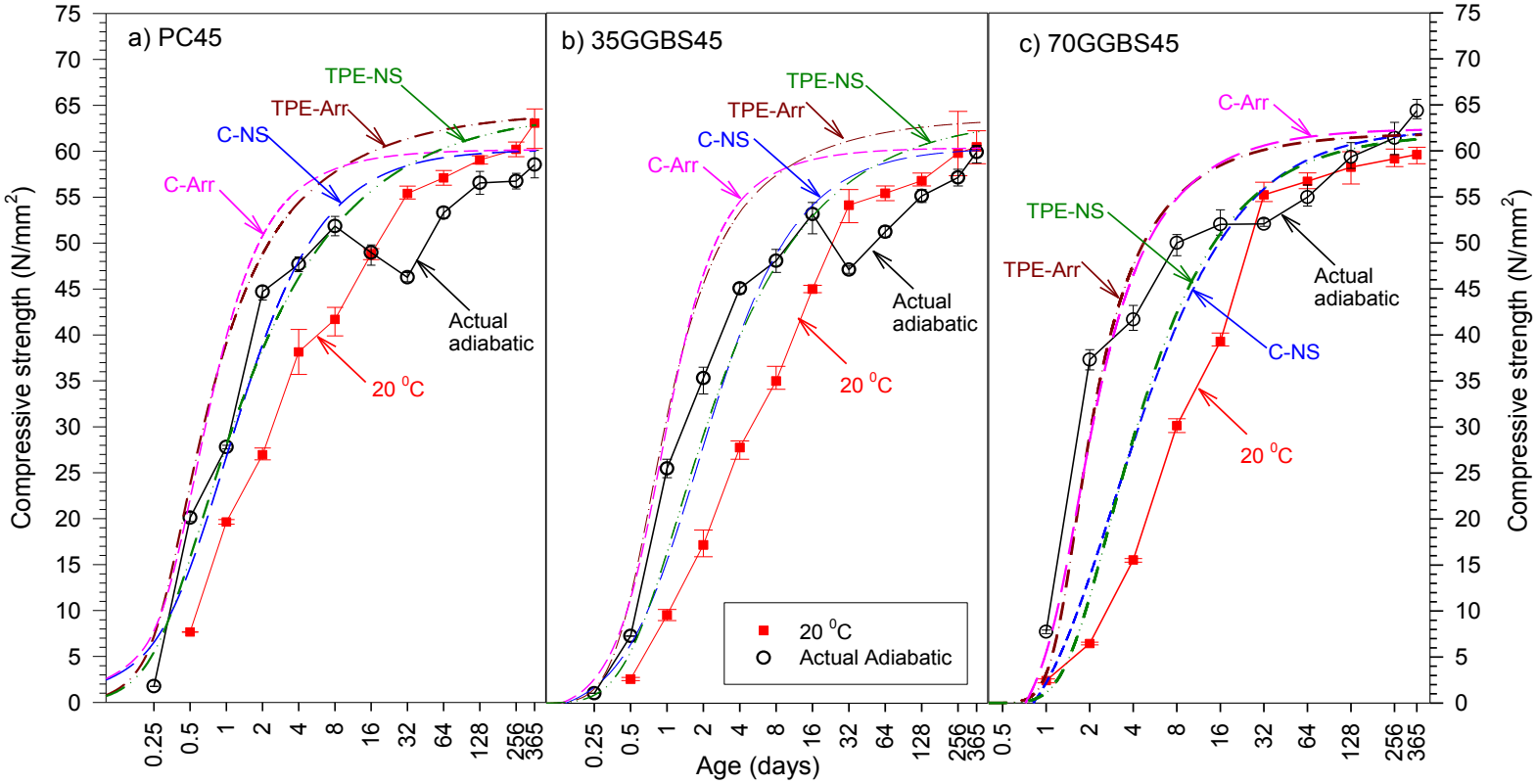

Figure 6.5: Predicted adiabatic strength development based on the Carino and TPE equation using a datum temperature of -11^{0}C mortar with 0, 35 and 70% GGBS **grade C45**

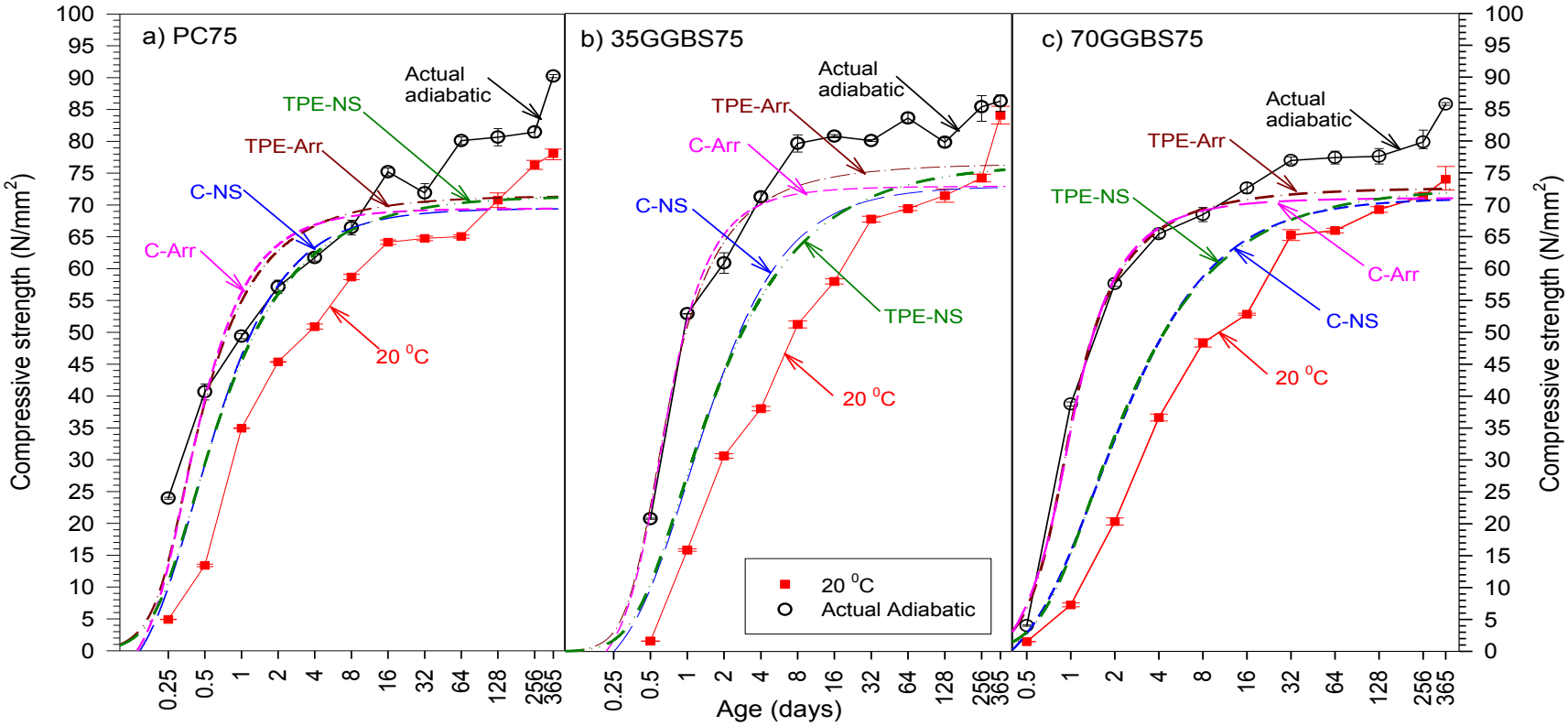

Figure 6.6: Predicted adiabatic strength development based on the Carino and TPE equation using a datum temperature of -11^{0}C mortar with 0, 35 and 70% GGBS **grade C75**

The Figures 6.7 and 6.8 show the predicted strength using both the Carino and TPE equations, which are based on the Nurse-Saul maturity function. The maturity is calculated using the datum temperatures (T_0) determined according to ASTM C-1074 (Table 6.1) and also a method suggested from previous works.

Generally, it appears the C-NS model with a datum temperature based on ASTM standard is similar to the TPE- NS model with a datum temperature of -11^0C. On the other hand, the C-NS model with the datum temperature of -11^0C is similar to the TPE-NS with the datum temperature that was calculated based on the ASTM standard.

In mortar with PC only, for both grades C45 and C75, the predicted strength using both the Carino and TPE equations with different values of datum temperature are similar, where both the equations predict the strength reasonably well up to age 8-days. Both the models then overestimate the adiabatic strength of PC mortar grade C45 from the age 8-days to later ages. This is believed to be due to the mortars experiencing a detrimental effect due to high early-age curing temperature. However, in PC mortar grade C75, both the models underestimate the adiabatic strength development. This is believed to be due to the unexpected values of parameters that limited the strength of the mortars cured under standard curing temperature, which is used to predict the adiabatic strength.

The TPE-NS (To = -11^0C) and C-NS (To-ASTM) models predict the strength of GGBS mortars grade C45 at early age better than the other two models (Figure 6.7), TPE-NS (To-ASTM) and C-NS (To =-11^0C) except mortar with 50% GGBS. The last two models predict much lower strength at early age than the actual strength; they then overestimate the strength at later ages. All the models overestimate the strength of mortar with 50% GGBS during the testing ages.

Furthermore, in GGBS mortars grade C75, all the models underestimate the strength during the testing ages, except the mortar with 50% GGBS (Figure E-14b in Appendix E). The adiabatic strength of the mortar is well predicted using both the Carino and TPE equations, where the maturity is calculated from the datum temperature based on the ASTM standard.

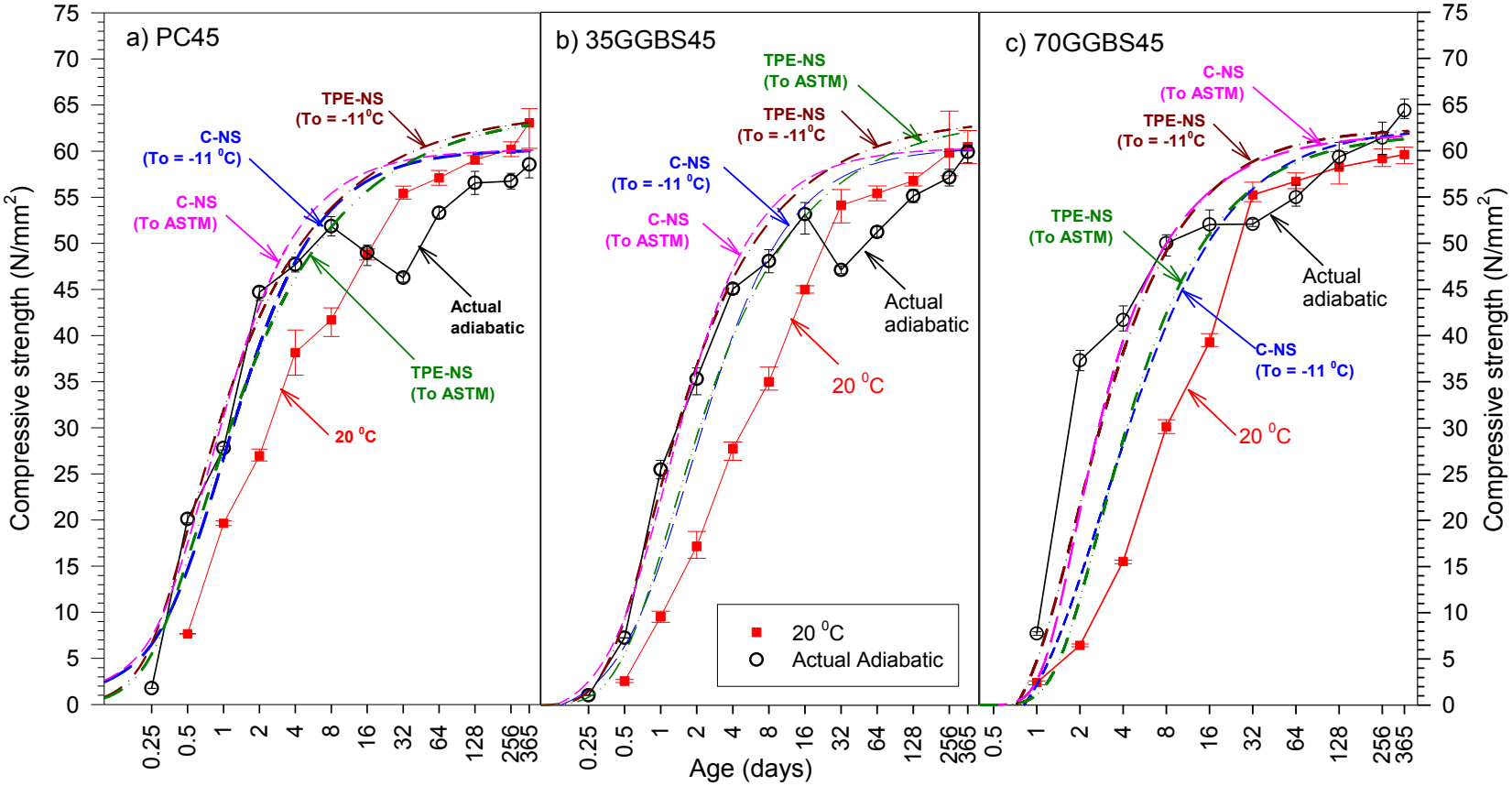

Figure 6.7: Predicted adiabatic strength development using the Carino and TPE equations with a datum temperature based on ASTM C 1074 mortar with 0, 35 and 70% GGBS **grade C45**

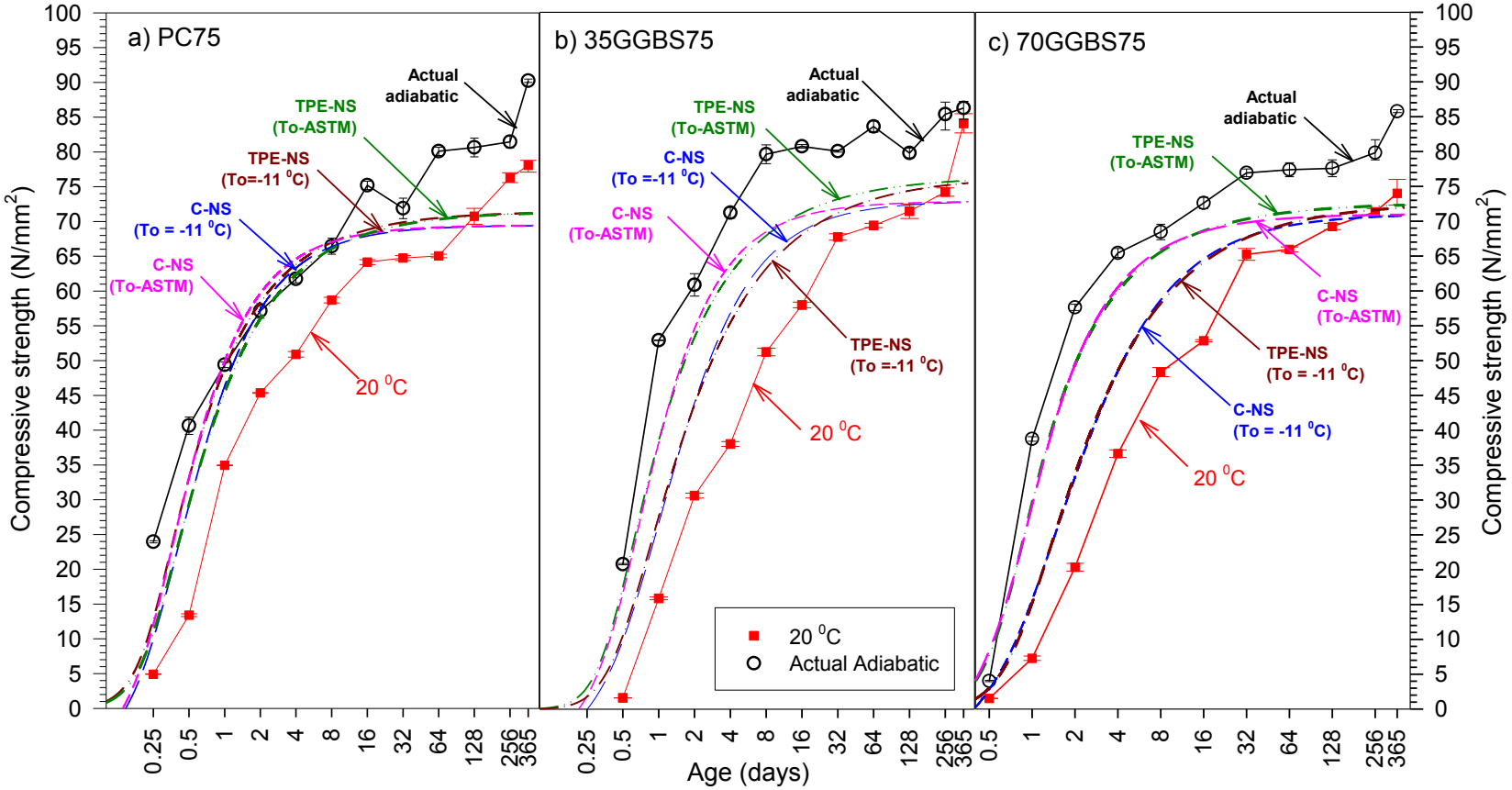

Figure 6.8: Predicted adiabatic strength development using the Carino and TPE equations with a datum temperature based on ASTM C 1074 mortar with 0, 35 and 70% GGBS **grade C75**

6.3.3. Adiabatic Strength Prediction of GGBS Concretes

The adiabatic strength prediction for concrete with 0, 35% and 70% GGBS grades C45 and C75 are shown in Figures 6.9 and 6.10, respectively. The predicted adiabatic strength for concrete with 20 and 50% GGBS can be found in Figures E-15 and E-16 in Appendix E. Similarly in the prediction of the adiabatic strength for mortars, the four models are used to predict the adiabatic strength of concrete. Generally, all the models predict the adiabatic strength inaccuracy particularly for GGBS concretes. All the models predict the strength quite well at early age only, but overestimate them at later ages.

In PC concrete grade C45 (Figure 6.9), both the C-NS and TPE-NS models predict the adiabatic strength quite well up to an age of 4-days. However, both the models then overestimate the strength at later ages up to age 128-days, because the concrete experienced a detrimental effect due to a high early-age curing temperature. On the other hand, the two other models based on the Arrhenius formula in calculating the maturity i.e. the C-Arr and TPE-Arr models, predict the strength quite well until the age of 2-days, the models then overestimate the strength at later ages, which is shown clearly in Figure 6.11. All the models however, predict the adiabatic strength of PC mortar grade C75 reasonably well, except the predicted strength at very early age i.e. the first 12-hours after casting, as shown in Figure 6.10. The differences between the actual and the predicted strength during the ages from 1-day to 365-ages are less than 10% as shown in the Figure 6.12 that was obtained from the TPE-NS model and it is only slightly different with the other models.

Generally, in GGBS concretes grade C45, the C-NS and TPE-NS models, which are based on the Nurse-Saul function, are better at predicting the adiabatic strength of concretes. This particularly the case at early ages with the cement replacement levels by GGBS up to 35% when compared to the models based on the Arrhenius equation (Figures 6.9 and 6.11). However, for concrete with high levels of GGBS such as 50 and 70%, the C-Arr and TPE-Arr models appears to be

better in predicting the strength compared to the models developed based on the Nurse-Saul maturity function.

As can be seen in the Figure 6.11, the predicted strength obtained from the TPE-Arr and C-Arr models overestimate the strength more than that of the C-NS and TPE-NS models for GGBS levels in concrete up to 35%. However, in the higher levels GGBS concrete, although, the C-Arr and TPE-Arr models appear to overestimate the strength, the predicted strengths are better than that of the two other models (C-NS and TPE-NS). These are much more likely to underestimate the strength at early ages up to 4-days. Nevertheless, the predicted strength of both these models is much better than that of the C-Arr and TPE-Arr models from the age 4-days and later on.

In GGBS concretes grade C75 (Figure 6.12), the C-Arr and TPE-Arr models seem to better predict the strength for concrete with high levels of GGBS such as 50 and 70% at early age i.e. up to 4-days rather than the C-NS and TPE-NS models. However, after the age of 4-days, the C-NS and TPE-NS models appear much better than the other two models (C-Arr and TPE-Arr).

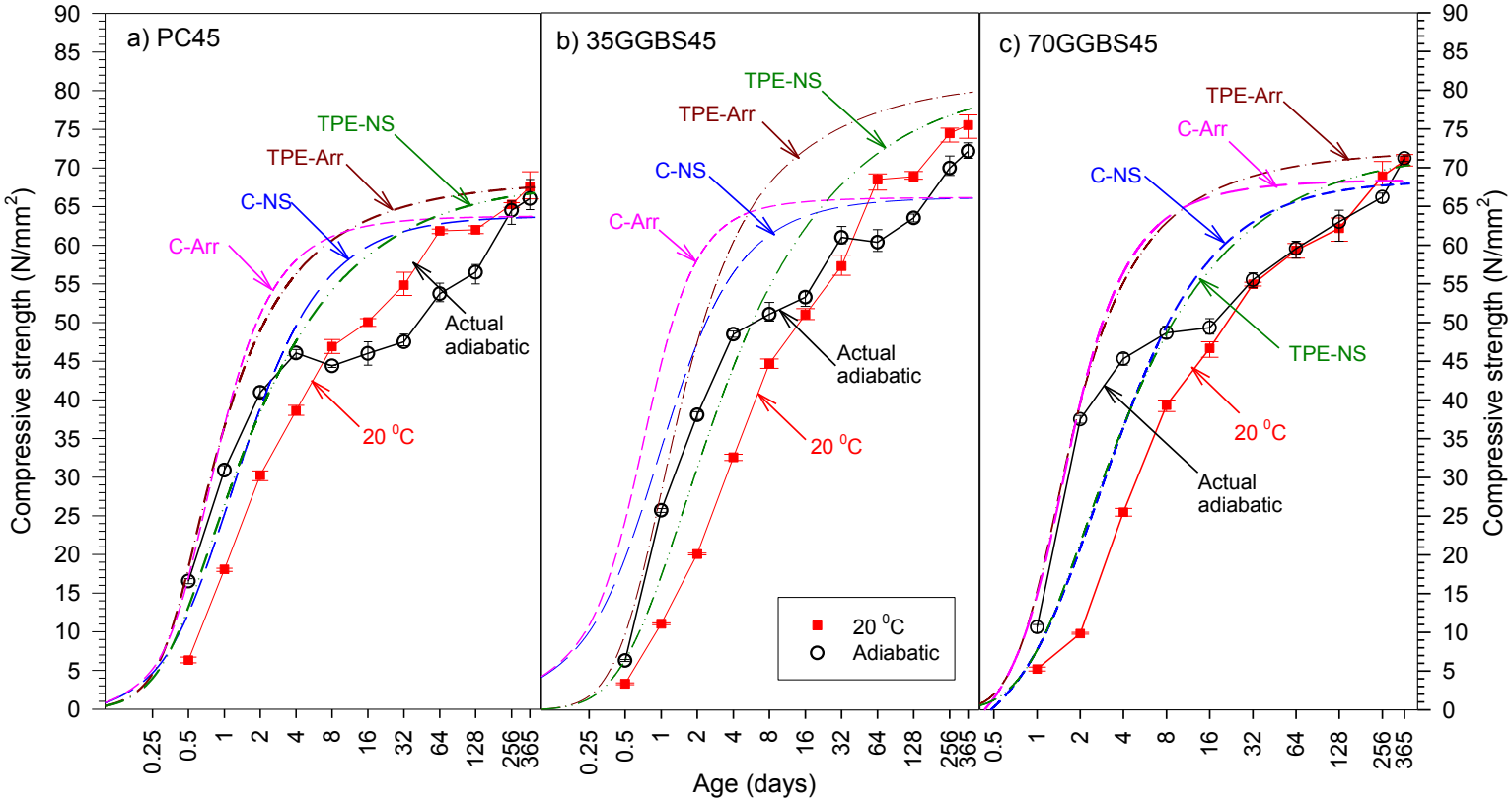

Figure 6.9: Predicted adiabatic strength development based on the Carino and TPE equation using a datum temperature of -11^{0}C concrete with 0, 35 and 70% GGBS **grade C45**

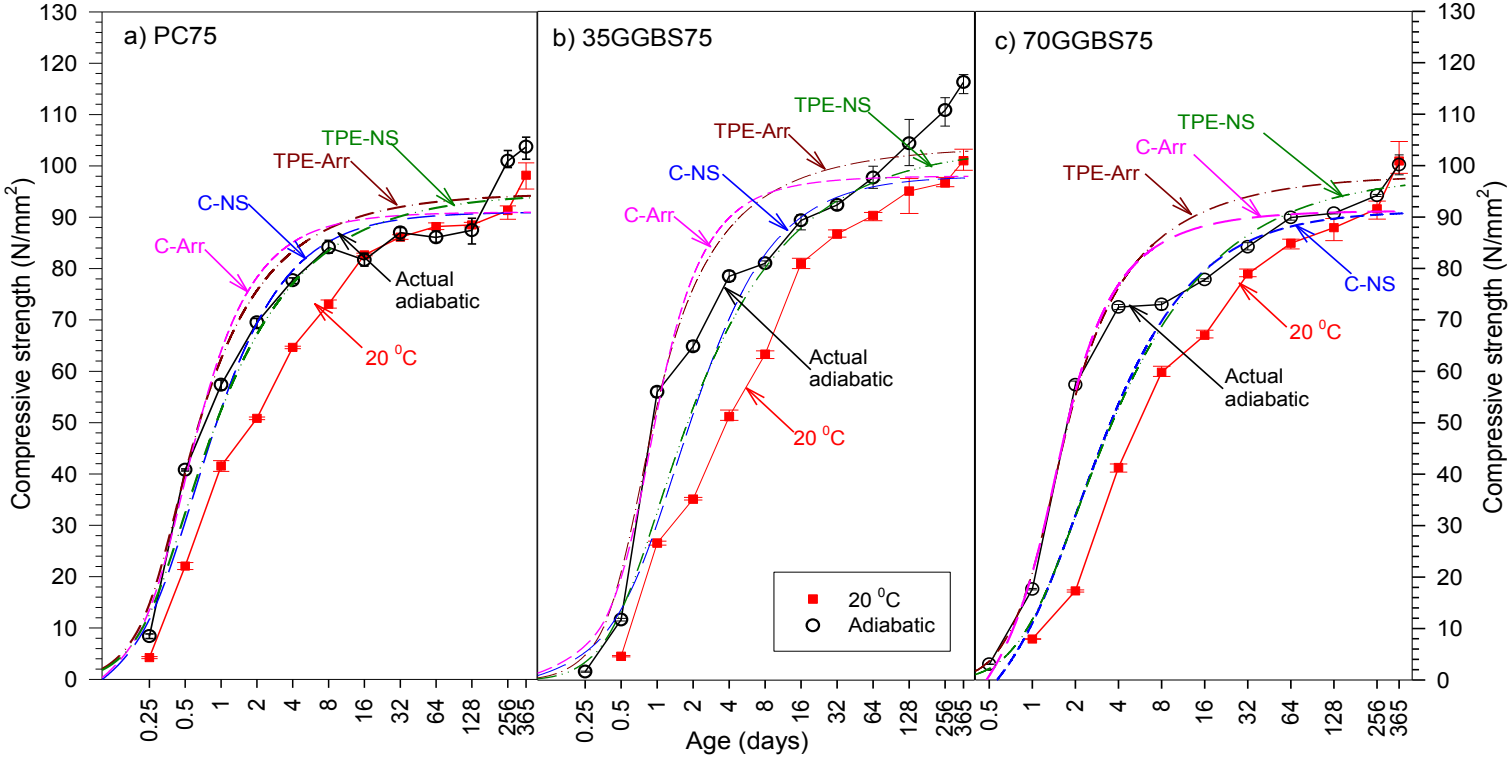

Figure 6.10: Predicted adiabatic strength development based on the Carino and TPE equation using a datum temperature of -11^{0}C Concrete with 0, 35 and 70% GGBS **grade C75**

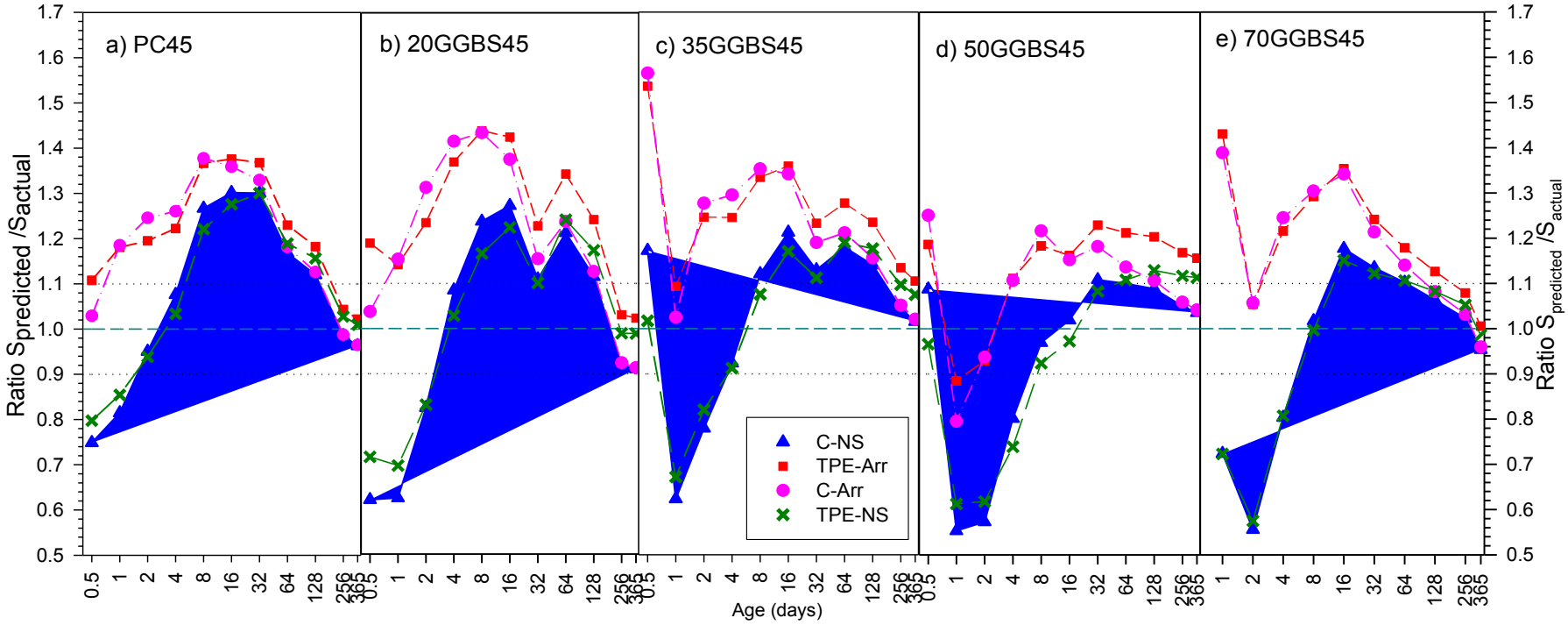

Figure 6.11: Ratio predicted adiabatic strength (obtained from C-NS, TPE-Arr, C-Arr and TPE-NS models) to the actual adiabatic strength concrete **grade C45**

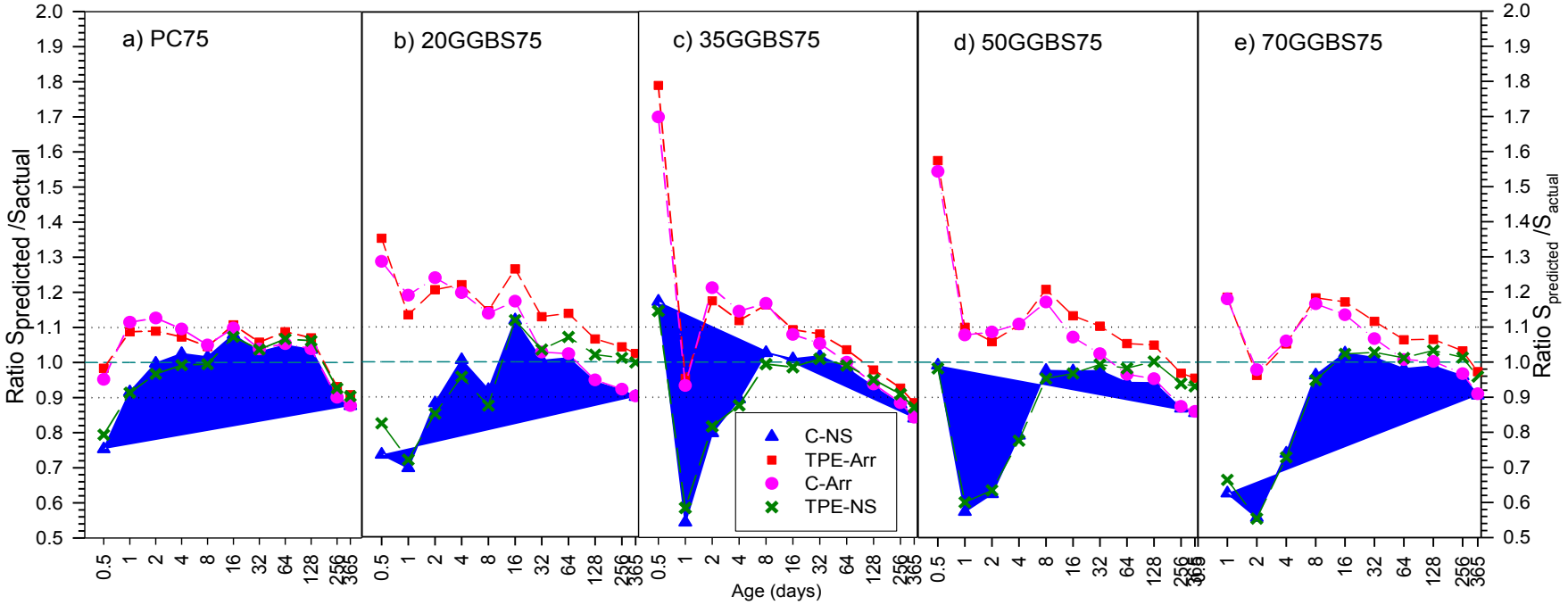

Figure 6.12: Ratio predicted adiabatic strength (obtained from C-NS, TPE-Arr, C-Arr and TPE-NS models) to the actual adiabatic strength concrete **grade C75**

Figures 6.13 and 6.14 show the predicted strength of concretes both grade C45 and C75 using the C-NS and TPE-NS models; with GGBS levels of 0, 35% and 70% of GGBS. The figures of 20 and 50% GGBS for both grade C45 and C75 can be found in Appendix E (Figures E-15 and E-16). The C-NS and TPE-NS models that were developed based on the Nurse-Saul maturity function were used to predict the strength. The maturities are calculated by using two different datum temperatures; one that was calculated according to ASTM C 1074 shown in Table 6.1 and another one that was recommended from previous works i.e. -11^0C.

In all grades of concrete, both the Carino and TPE equations (C-NS and TPE-NS models) that used the datum temperature calculated according to ASTM C 1074, predict the adiabatic strength to be more accurate than that using a recommended datum temperature of -11^0C up to ages 4-day, particularly for predicting strength of GGBS concretes at an early age. The predicted strengths of these models are more accurate than that of models developed based on the Arrhenius maturity function (C-Arr and TPE-Arr). The datum temperatures calculated according to ASTM C 1074 are higher than that recommended from previous work i.e. -11^0C, which could be explained in the higher in strength prediction.

For GGBS concretes both grades C45 and C75, it could be suggested to take the datum temperature that was calculated according to ASTM C-1074 to predict the strength up to age 4-days and from the age of 4-days, use the datum temperature of -11^0C to predict the strength more accurately, as shown in Figures 6.13 and 6.14.

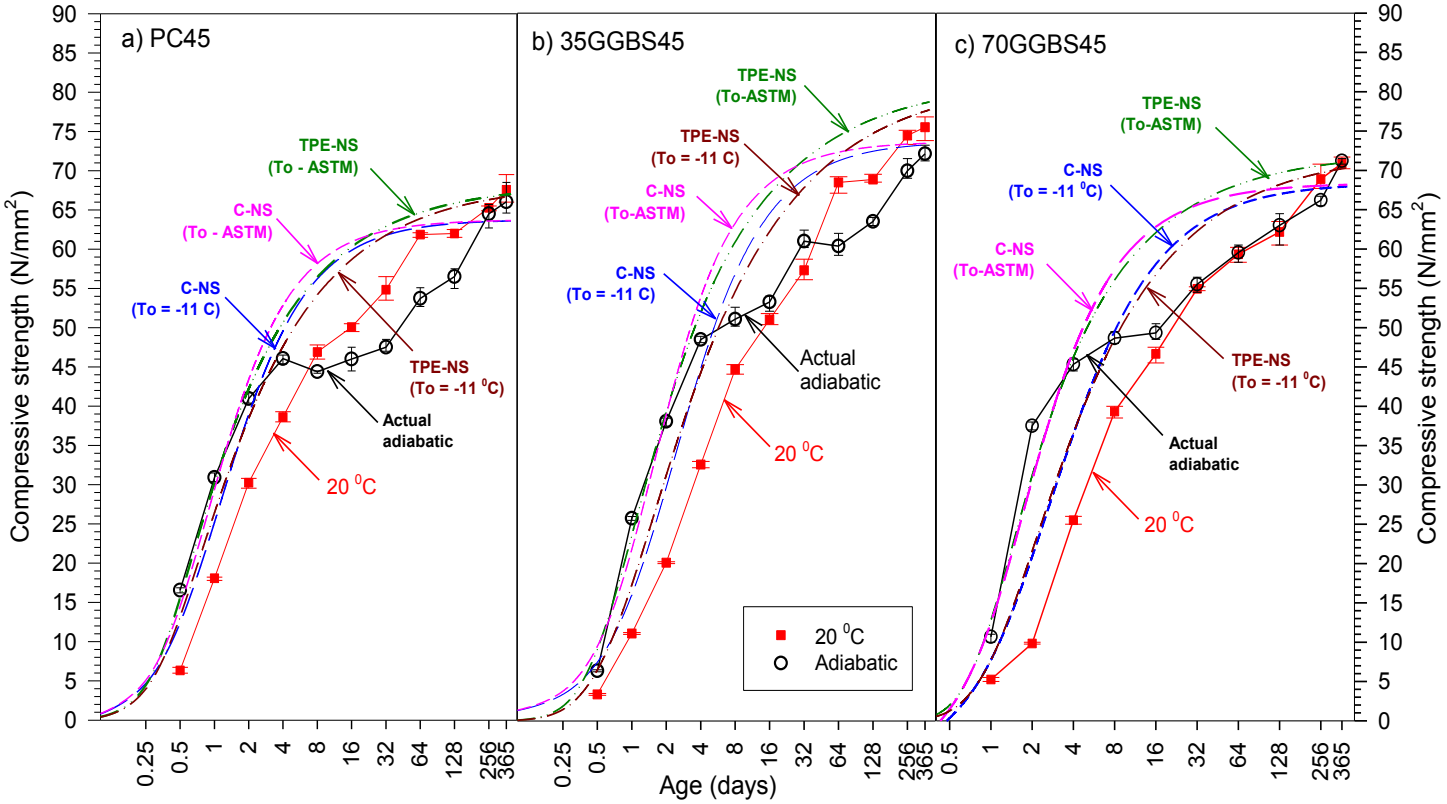

Figure 6.13: Predicted adiabatic strength development using the Carino and TPE equations with a datum temperature based on ASTM C 1074 concretes with 0, 35 and 70% GGBS **grade C45**

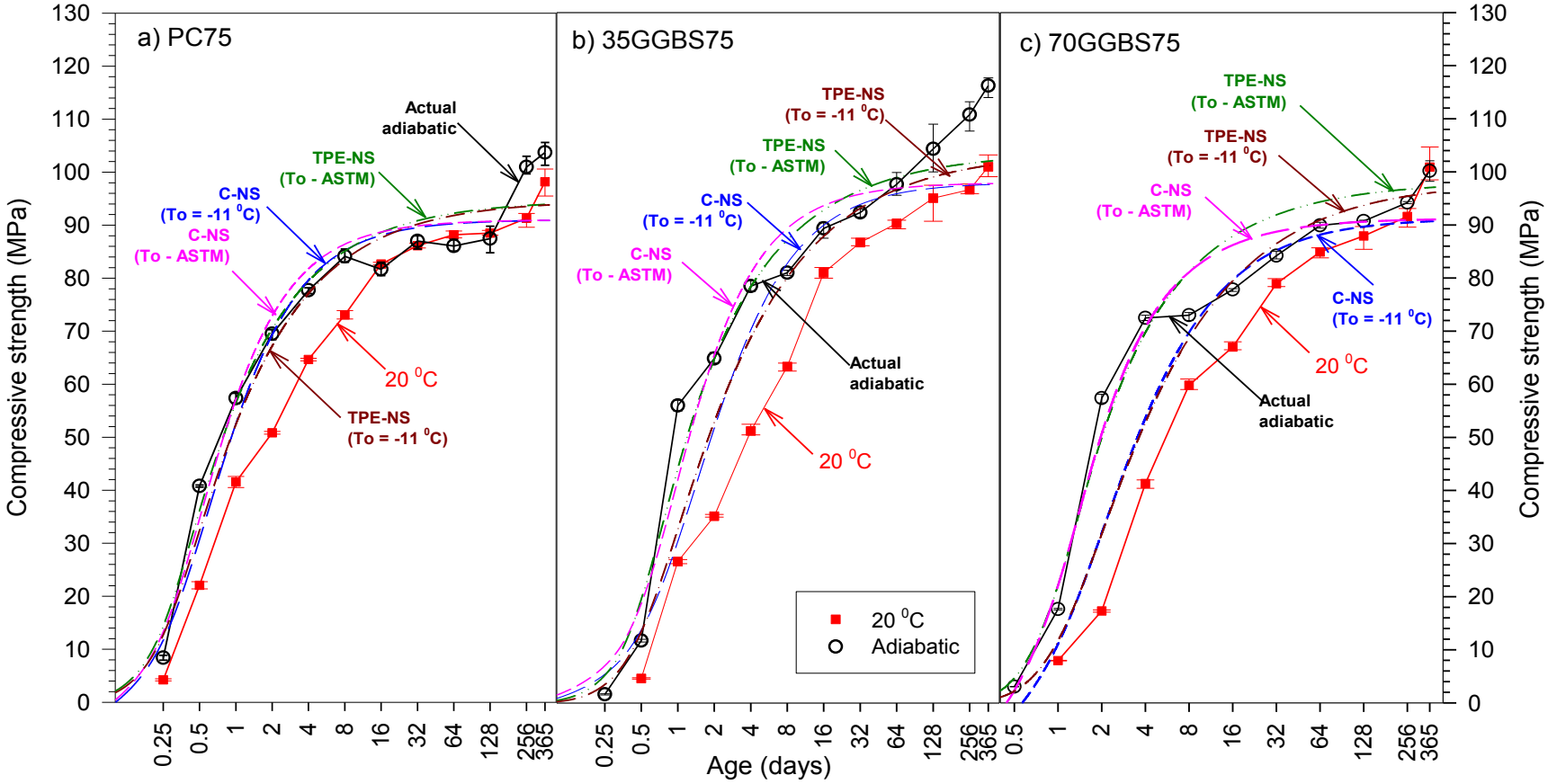

Figure **6. 14:** Predicted adiabatic strength development using the Carino and TPE equations with a datum temperature based on ASTM C 1074 concretes with 0, 35 and 70% GGBS **grade C75**

6.4. Strength prediction using recent improvements of the maturity functions

This section will assess four methods, which have been recently developed to predict the strength of concrete like Carino and TPE equations, mentioned in the literature chapter and the introduction to this section. The methods are those proposed by Y.A. Abdel Jawad in 2005 and 2006 (AJ-05 and AJ-06), Kjellsen and Detwiler (K&D), and Chanvillard and D'Aloia (C&D). The predicted strength value was obtained using the four-models and one model as modification by combining the AJ-05 and AJ-06 models. The model proposed by Addel Jawed 2006[164] as in Equation 2.90, appears to underestimate the adiabatic strength development of the mortars. This is believed to be due to a reduction of strength that was taken into account in this model as the effect of the high earlier-age curing temperature on the strength at later ages. $(T - T_r)$ is too high as adiabatic temperature is high and therefore, its predicted strength becomes much lower than the actual strength at later ages. It is found that dividing $(T - T_r)$ by T_r can improve the AJ-06 model, where it was presented in the previous model proposed by Addel Jawed 2005[163] (AJ-05 model). The modification of the AJ-06 model is presented as Modified-AJ in Figures 6.15 and 6.16. The equation for the Modified-AJ model (Equation 6.2) is as follows:

$$S(T,t) = S(T_r, t_e)\left[1 - 0.01(1 - e^{-0.05t_e})\left(\frac{T - T_r}{T_r}\right)\right] \quad \text{Equation 6.2}$$

where:

S (T, t) = the compressive strength of concrete at age t cured at temperature T.

S (T_r, t_e) = the compressive strength of the same concrete at equivalent age t_e and cured at reference temperature T_r.

All the models take into account the detrimental effect of the high earlier-age curing temperature on the strength at later-ages. The suitability of these models for GGBS mortars and concretes under different isothermal (constant) curing temperatures have been investigated.

6.4.1. Adiabatic Strength Prediction of Equivalent GGBS Mortars

The parameters used to predict the strengths are obtained from the Carino strength-age regression linear analysis presented in Tables 6.5 and 6.6 for mortars grade C45 and C75, respectively. The apparent activation energies are determined according to the ASTM C-1074 standard[6] and TPE method, where the values obtained are shown in Table 6.2. These values are also used as the initial apparent activation energies in predicting the strength, using the model proposed by Kjellsen and Detwiller[157] (K&D). Determination of the constant *p* in the model proposed by Chanvillard and D'Aloia[162] (C&D model) based on the results of the mortars, which produced a value close to 0.01, was recommended for use with this model. The values of p used in each case are given in Table 6.13.

Table 6.13: Parameters of the constant *p* mortars **grade C45** and **C75**

Grade C45	p value	Grade C75	p value
PC45	0.0096	PC75	0.0052
20GGBS45	0.0067	20GGBS75	0.0064
35GGBS45	0.0090	35GGBS75	0.0048
50GGBS45	0.0099	50GGBS75	0.0046
70GGBS45	0.0102	70GGBS75	0.0060

The AJ-05 model is based on the Nurse-Saul equation by considering the role of the water-cement ratio to better account for the equivalent age of concrete cured at different curing temperatures of the reference temperature. On the other hand, the AJ-06 model is based on the Arrhenius equation proposed by Freiesleben, Hansen and Pedersen. The model uses the apparent activation energy, which varies with w/c ratio and curing temperature according to parameter β as described in the literature review. The parameters to calculate the β values obtained from linear regression are given in Table 6.14.

Table 6.14: Parameters to calculate β values for mortars and concretes **grade C45** and **C75**

Grade	GGBS level (%)	Parameters obtained from regression analysis		
		a	b	r^2
C45	0	1.0942	-0.0057	0.98
	20	1.0976	-0.0042	0.90
	35	1.0716	-0.0044	0.97
	50	1.1073	-0.0053	0.99
	70	1.0992	-0.0052	0.99
C75	0	1.0644	-0.0039	0.94
	20	1.1131	-0.0058	0.98
	35	1.0929	-0.0048	1.00
	50	1.1353	-0.0058	0.98
	70	1.0222	-0.0033	0.77

Figures 6.15 and 6.16 show the predicted adiabatic strengths used in recent methods for mortar grades C45 and C75, respectively with 0, 35 and 70% GGBS. Trends for mortars with 20 and 50% of GGBS are similar, as can be seen in Appendix E (Figures E-19 and E-20). The predicted strengths obtained from the models were compared with the actual strengths of cubes cured adiabatically to assess the accuracy of the five models in predicting strength.

In all mortars, the AJ-05 and AJ-06 models underestimated the strength to be much lower than the actual strength at all testing ages, apart from mortar with PC only for grades C45 and C75. However, the models predict the strength quite well up to the age of 1-day only and then predict the strengths to be much lower than the actual strengths at later ages. The Modified-AJ model, however, appears to allow improved prediction of strength in all mortars, except in mortars grade C75 with 35, 50 and 70% of GGBS, where the modified models predict the strengths to be lower than the actual strength during the testing ages. However, this method seems to have the potential to be modified to produce more accurate strength predictions.

In mortar grade C45 with all levels of GGBS, the model proposed by Kjellsen and Detwiler (K&D) predicts the strength reasonably well from early age to later age. The model appears to account well for the detrimental effect of high earlier-age curing temperature on later age strength. However, in the mortars grade C75, the K&D model predicts the strength quite well at earlier-ages up to 1-day, where the model then underestimates the strength of the mortars at later ages. It can be deduced that the use of activation energy as a function of relative strength is better than as a constant value, as discussed in the literature review chapter. The model has potential to be improved by introducing a new formula to calculate the required activation energy more accurately, as the existing one was originally introduced for mortar or concrete with Portland cement only.

The C&D model, proposed by Chanvillard and D' Aloia, predicts the strength of mortars reasonable well at a very early age up to 2-days for PC and GGBS mortar with levels of GGBS up to 20% for both grades C45 and C75. However, in the mortars with higher levels (35 to 70%) of GGBS, the model appears to underestimate the strength from early ages to later ages. The model also seems to have potential to be modified to have a more accurate result in predicting the strength.

There is no single model of the five investigated that produces an accurate prediction of strength development of the mortars. All the models need to be improved, particularly in way of the activation energy calculation is taken into account to predict the effect of high earlier-age curing temperature on the strength at later ages.

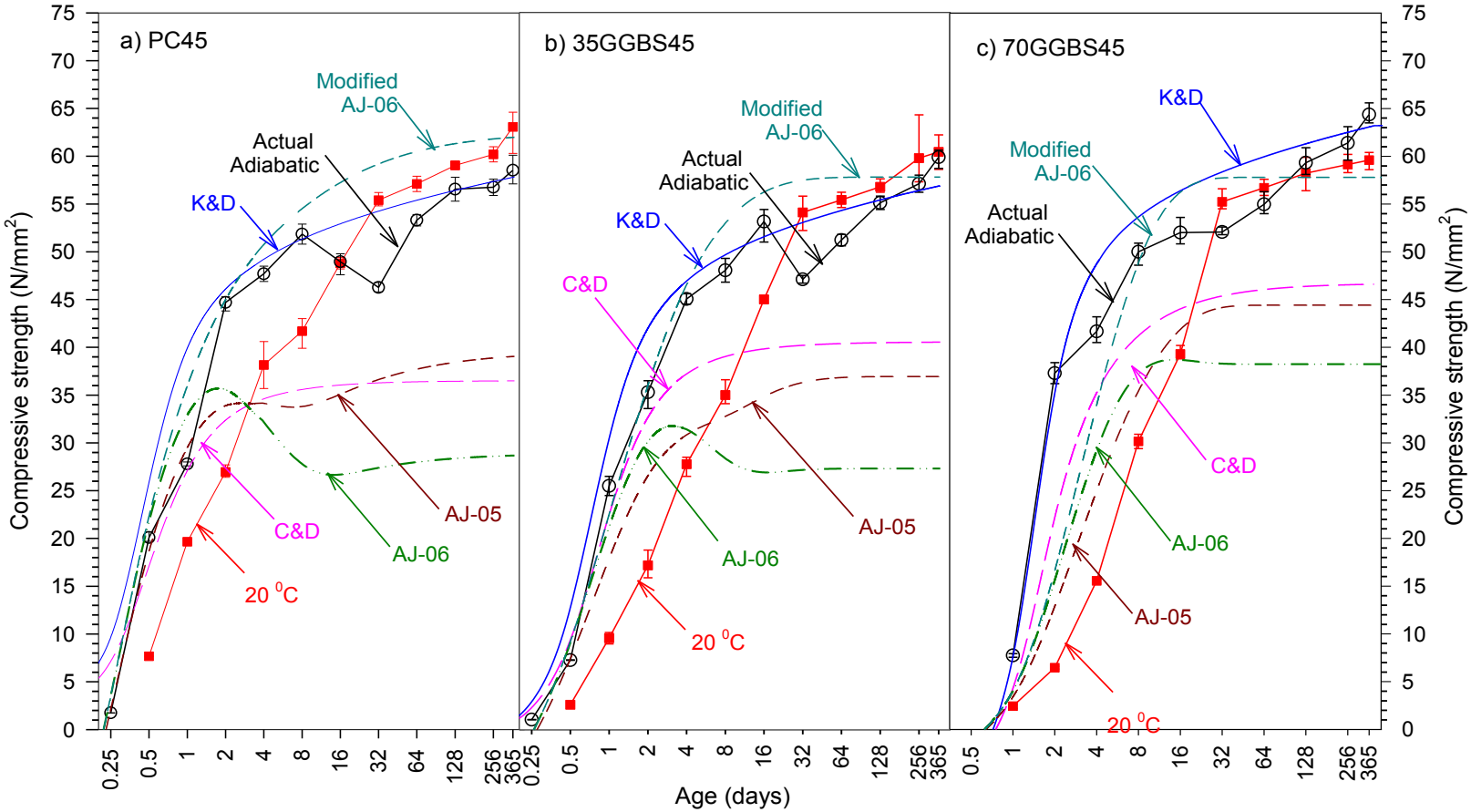

Figure 6.15: Predicted adiabatic strength development of mortars with 0, 35 and 70% GGBS **grade C45** using recent maturity equations

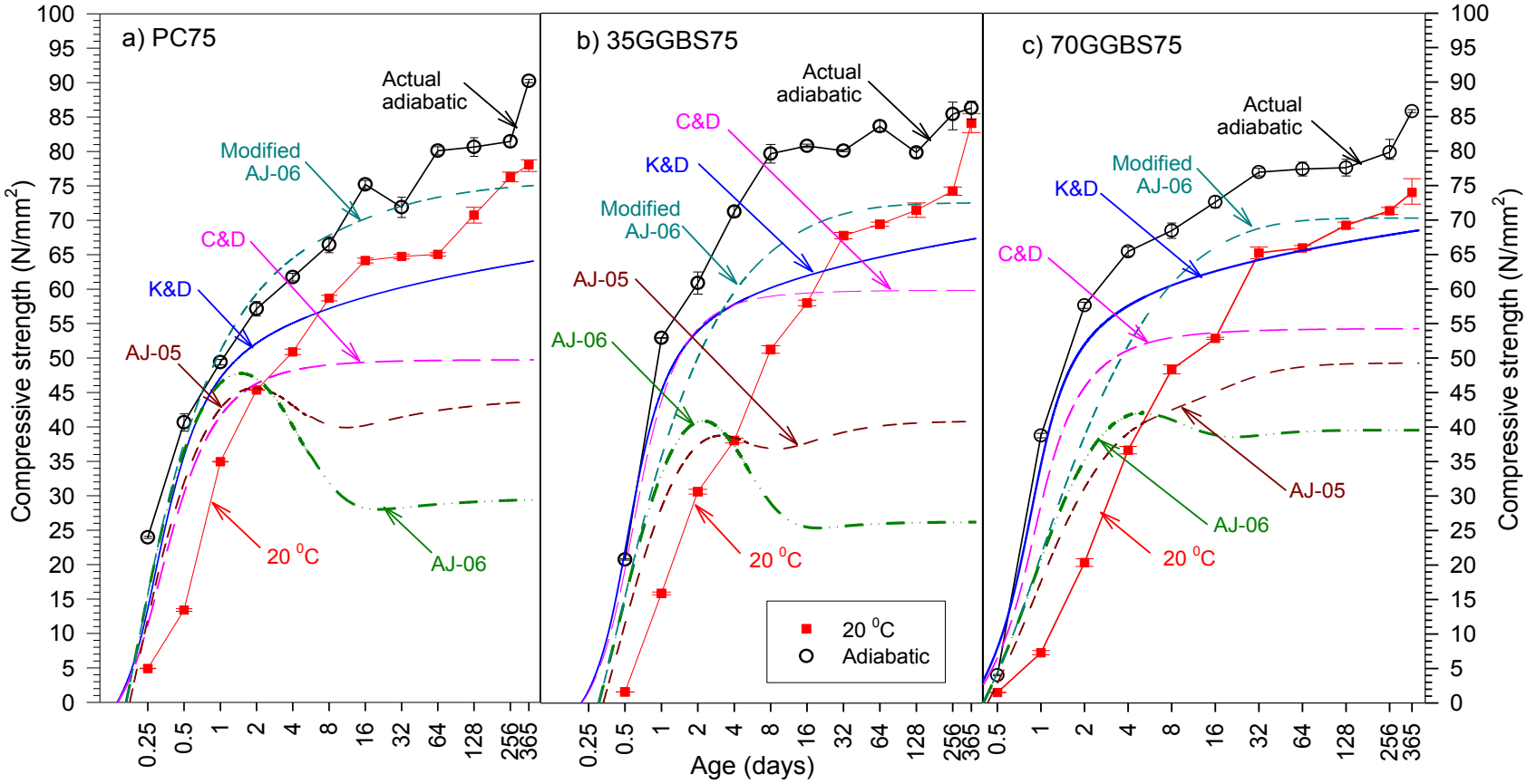

Figure 6.16: Predicted adiabatic strength development of mortars with 0, 35 and 70% GGBS **grade C75** using recent maturity equations

The accuracy of the five models in predicting the strength of mortar is shown in Figures 6.17 and 6.18. Generally, in PC mortar grade C45, the Modified-AJ and K&D models appear to predict the strength reasonable well (Figure 6.17a). The K&D model overestimates the strength up to age 1-day. The model then accurately predicts the adiabatic strength of the mortar, where the errors are within 10% from age 2-days to age 16-days. The model then overestimates the predicted strength at age 32-days, i.e. 17% higher than actual strength. This is due to the actual adiabatic strength of the mortar reducing as a result of a fundamental change in the hydration products formed due to high curing temperature at early-age. The model then predicts the strength very accurately from age 64-days onwards, where the prediction is within 5 % of actual at later ages.

The Modified-AJ model also predicts the strength of the mortar quite well, where the accuracy of the model is to within 10 % of actual strengths from age 2-days to age 8-days. The actual strength development of the mortar decreases from age 16-days to 32-days, as a result the model overestimates the strength up to 30% higher than the actual strength at age 32-days as the actual strength reduces. The actual strength of the mortar, however, increases again from age 64-days onwards, where the accuracy of the strength prediction improves again to within 10% of actual from age 128-days onwards. The predicted strength of the other three models i.e. C&D, AJ-05 and AJ-06 are much lower than the actual strength, where the accuracy ranges from 36% (AJ-06 model) to 63% (C&D model).

In GGBS mortar grade C45 (Figure 6.17) for levels of GGBS in mortar up to 35%, the K&D and Modified-AJ models predict the strengths to be higher than the actual strength from early age onwards, and then underestimates them at later ages. On the other hand, generally, the other three models (C&D, AJ-05 and AJ-06) underestimate the strength during the testing ages for all levels of GGBS. Furthermore, in mortars with high levels of GGBS i.e. 50 and 70%, both the K&D and Modified-AJ models predict the strength to be lower than the actual strength, except for the Modified-AJ models in 70% GGBS mortar.

In 20% GGBS mortar, the predicted strength using the K&D model appears to be more accurate in comparison to the other four models investigated. K&D model predicts the strength of mortar with 20% GGBS reasonably well, where the accuracy of the strength prediction to within 10% of actual from age 12-hours to age 128-days. The predicted strength at age 256-days and 365-days is a little bit low but the accuracy is still within 20% of actual as can be seen in Figure 5.53b.

The Modified-AJ model predicts the strength quite accurately until an age of 2-days. The model then overestimates the strength from age 4-days until age 128-days with a 22% error at age 16-days. The model underestimates the strength at later ages, where the accuracy of the model reduces to more than 10% of actual, i.e. 12 and 13% errors at age 256-days and 365-days, respectively. This is believed to be due to the strength of the GGBS mortar continuously growing at those ages and exceeded the limited strength that was used in the model to predict the strength.

The C&D model predicted the strength quite well only at age 4-days to 16-days to the predicted strengths were within 10% of actual. The predicted strength of the model reached 37% lower than of the actual strength at ages 256-days onwards. On the other hand, the predicted strength obtained from the AJ-05 and AJ-06 models at the same age only reached 53 and 36% of the actual strength, respectively, which meant the errors of the models to predict the strength at the age reached 47 and 64% for the AJ-05 and AJ-06 models, respectively.

Figure 6.17c shows that the predicted strength using both the K&D and Modified-AJ models in mortar with 35% of GGBS (35GGBS45 mortar) appears to be more accurate than that of in mortar with 20% of GGBS. The K&D model overestimates the strength up to an age of 2-days. The models then predicted the strength reasonable well, where the errors less than 10% from age 4-days to age 365-days, apart from the predicted strength at age-32 days when the actual strength reduced, the error of prediction reached 13%. The Modified-AJ model

predicts the strength fluctuation with age; however, the errors are within 15%, except the predicted strength at age 32-days with an error of 22%.

The accuracy of strength prediction for mortars with high levels of GGBS such as 50 and 70% are shown in Figures 6.17d and 6.17e. These figures show that the accuracy of the K&D and C&D models in predicting the strength decrease with increased levels of GGBS in mortar. In contrast, the models proposed by Abdel Jawad (AJ-05 and AJ-06) and the Modified-AJ model predict the strength more accurately by increasing the GGBS levels in mortar. This is due to the use of GGBS as a replacement for cement in mortar or concrete that allows a reduced temperature rise in the mortar or the concrete.

In mortar with 50% GGBS grade C45; the K&D model predicts the strength quite well from age 2-days to age 32-days with the errors of less than 10%. However, the model then slightly underestimates the strength from age 64-days onwards, although the errors are still within 20%. The accuracy of this model in predicting the strength of 70% GGBS mortar is slightly decreased compared with that of 50% GGBS mortar at early age, however, the accuracy of this model in predicting the strength of both 50 and 70% GGBS mortar at age 64-days onwards is the same.

The strength prediction obtained from the Modified-AJ model for 70% GGBS mortar seems to be better than that of 50% GGBS mortar. This model predicts the strength reasonably well at age 8-days onwards where the errors are within 10%, except the predicted strength at age 32-days, where the error of the predicted strength is 11%. In comparison, the accuracy of strength prediction of this model in predicting the strength of 50% GGBS mortar is slightly less than that of 70% GGBS mortar; particularly at a later age i.e. from age 128-days onwards. The accuracy of strength predictions in both mortars vary between 83 to 87% and 90 to 97% for 50 and 70% GGBS mortars, respectively.

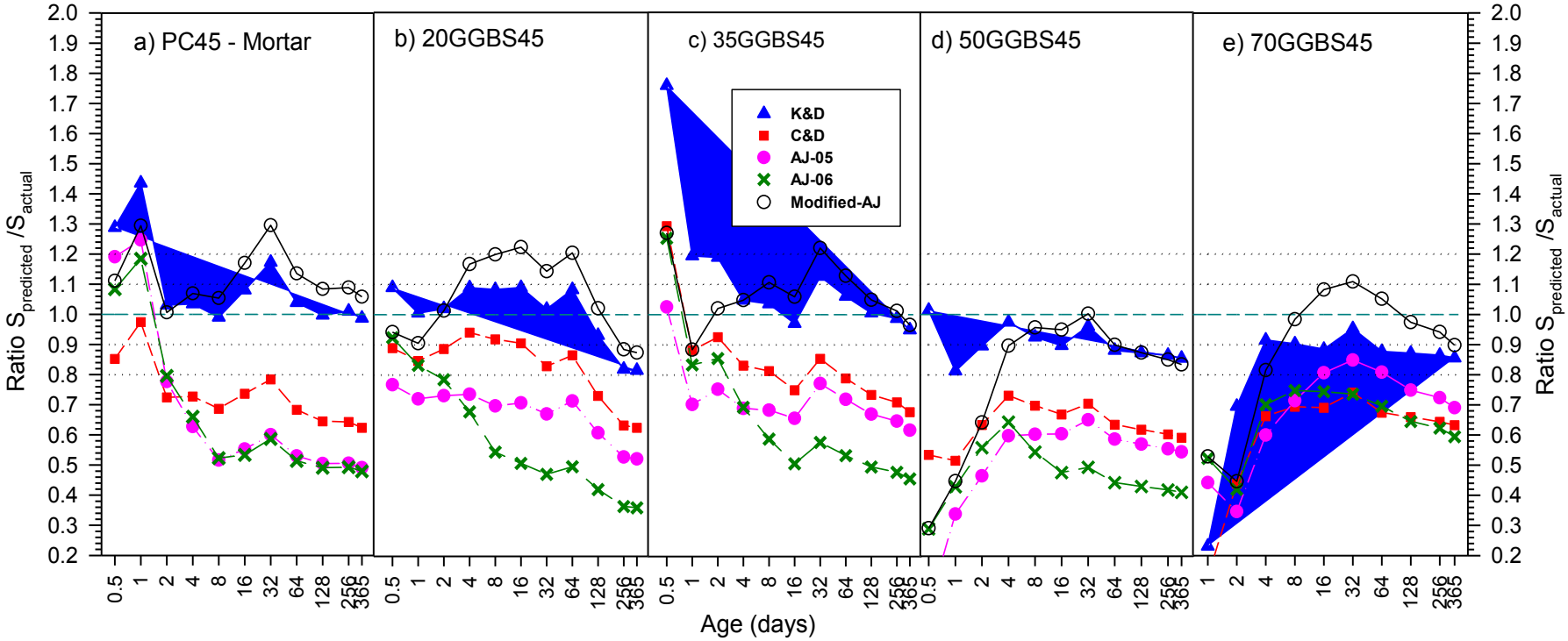

Figure 6.17: $S_{predicted}/S_{actual}$ of adiabatic strength development of mortar **grade C45** using recent maturity equations

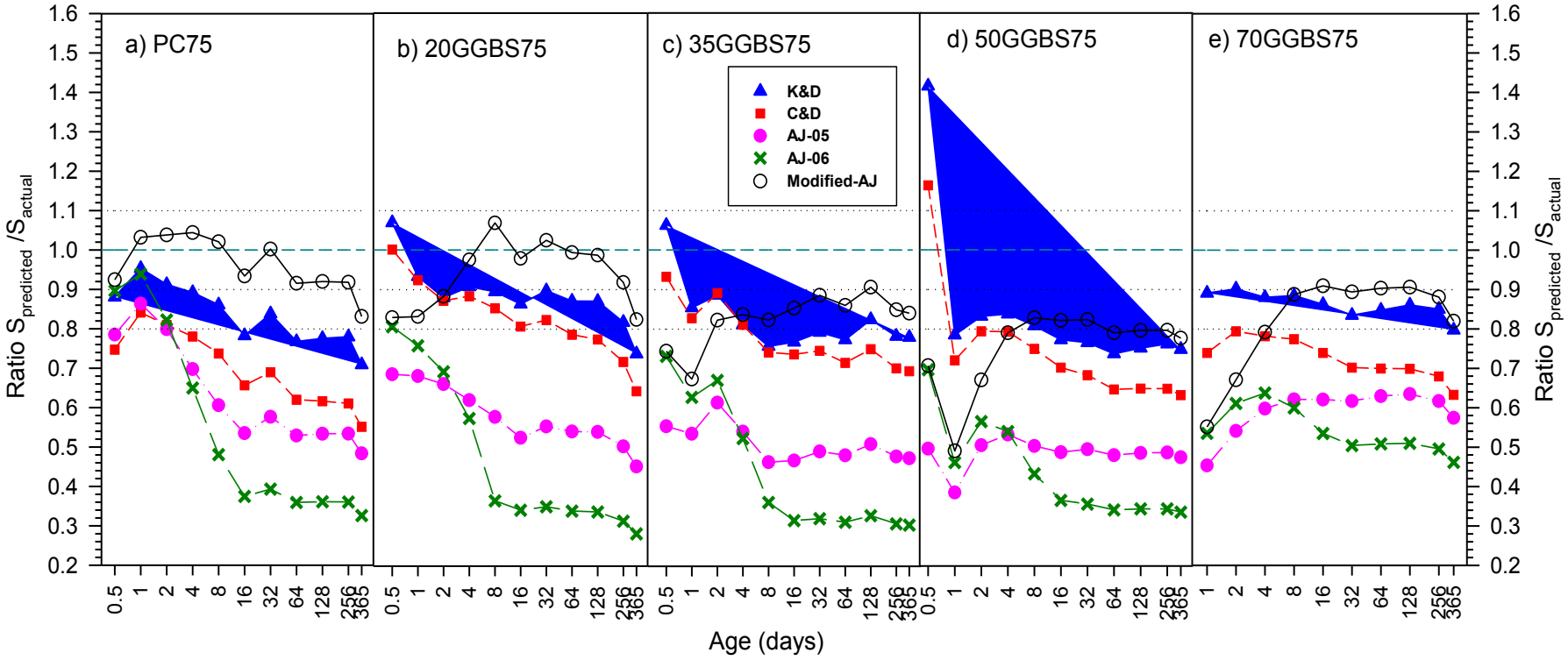

Figure 6.18: $S_{predicted}/S_{actual}$ of adiabatic strength development of mortar **grade C75** using recent maturity equations

The accuracy of all models in predicting the strength of mortar grade C75 is less than that of their accuracy in predicting the strength of mortar grade C45. Generally, as shown in Figure 6.18, all the models underestimate strength for all mortars, except the Modified-AJ model in PC mortar grade C75. This is believed mainly to be due the limiting strength of mortars that were used in the models, which were lower than that of expected. Figure 6.18 shows that there are three models i.e. K&D, C&D and Modified-AJ, which have potential to be improved to give good results when predicting the strength of mortar.

In PC mortar grade C75 (PC75 mortar), the Modified-AJ appears reasonably good at predicting the strength of this mortar at age 1-day onwards, where the errors of the prediction are within 10%, except the strength prediction at age 365-days. The predicted strength of this mortar reaches only 83% of the actual strength at that age. Figure 6.16a shows that the adiabatic strength still increased sharply at age 256 to 365-days, as the strength development of the mortar at early age was too late. This could also explain the errors in the strength prediction, as all the models expect the increase of strength mortar at later ages will be very small; therefore, the strength developments of mortar at later ages will tend to be constant.

The K&D and Modified-AJ models appear less accurate for predicting the strength of the mortar grade C75 with levels of GGBS of 35, 50 and 70% compared to mortars with PC only and 20% GGBS, while the accuracy of the C&D model seem to be similar in all mortars and GGBS levels. In addition, the accuracies of the other two models (AJ-05 and AJ-06) seem to be similar in all mortars and levels of GGBS, except their accuracy in the mortar with 70% GGBS. The accuracy of both the models in predicting strength of the mortar is slightly increased compared to their accuracies in mortar with other levels of GGBS. This is thought to be due to the temperature rise in this mortar being lower than that in mortars with other levels of GGBS, as the high temperature is very sensitive in the predicted strength of the models.

6.4.2. Adiabatic Strength Prediction of GGBS Concretes

Figures 6.19 and 6.20 show the predicted adiabatic strength of concretes with the GGBS levels of 0, 35 and 70 % for grades C45 and C75, respectively. Trends for concretes with GGBS levels of 20 and 50% are similar and they can be found in Appendix E (Figures E-21 and E-22). This aims to examine whether the activation energies determined based on equivalent mortars can be used for concretes. The parameters used in predicting the strengths are obtained from regression linear analysis based on the Carino strength-age relationship. The parameters are given in Tables 6.9 and 6.10 for concrete grades C45 and C75, respectively.

The apparent activation energies used in predicting the strength of concrete were determined according to the ASTM C-1074 standard, which used the equivalent mortar mixes, as shown in Table 6.2. The values are also used as the initial apparent activation energies in predicting the strength, using the model proposed by Kjellsen and Detwiller[157] (K&D). The constant p that is needed in the C&D model proposed by Chanvillard and D'Aloia[162] are given in Table 6.13.

In concretes grade C45, the K&D, C&D and Modified-AJ models appear to predict strengths of the concretes quite well and also have potential to be improved in predicting the strength. On the other hand, both the AJ-05 and AJ-06 models overestimate the strength up to age 12-hours from casting time, the models then underestimate the strength from age 1-day onwards. The K&D model predicts the strength reasonably well for concretes with PC only and GGBS concrete with levels of GGBS as cement replacement up to 35%, except the predicted strength of concrete with 35% GGBS at age 12-hours. This model overestimates the strength at this age i.e. 47% higher than the actual strength of the concrete as shown in Figure 6.21. The model predicts the strength of the concretes up to age 128-days accurately enough, where the errors are within 10%, except for predicted strength of concrete with 35% GGBS at age 12-hours. The model predicts the strength at later ages i.e. at age 256-days onwards to be lower than the actual strength. For example, the strength prediction of concrete with

20% GGBS at age 365-days reached only 72% of the actual strength. A reason for this may be that the strength of concrete at the later age was still continuous and significantly increasing, particularly for GGBS concrete; while the model expects the strength of concretes at later ages to be very small or even constant.

The accuracies of this model in predicting the strength development of concrete with a high-level of cement replacement with GGBS i.e. of 50 and 70% are slightly decreased compared to that of concrete with lower levels of GGBS. The model overestimates the strength of the concrete with 50% GGBS to be 16% higher than the actual strength at a very earlier age i.e. 12-hours, while in concrete with 70% GGBS the predicted strength is 37% higher than the actual strength at age 1-day. The model then underestimates the strength from age 12-hours and 1-day onwards for the concretes designated 50GGBS45 and 70GGBS45, respectively. The accuracy of the K&D model reduced in predicting strength development of concrete grade C45 with increasing the levels of GGBS in the concrete. However, the accuracy of the predicted strength of the concrete with 70% GGBS is slightly better than that of the concrete with 50% GGBS. The errors in the model when predicting strength development of concrete at age 2-days to 32-days in concrete with 70% GGBS are still less than 10%, while the errors in the concrete with 50% GGBS are over 10%, as shown in Figures 6.21d and 6.21e.

On the contrary, in concrete grade C75 (Figure 6.20), the K&D model predicts the strength development reasonably well for concrete with higher level of GGBS such as 50 and 70%, while the predicted strength development of this model for concrete with lower levels of GGBS, i.e. 0. 20 and 30% of GGBS, are slightly less accurate as shown in Figure 5.58. Figure 6.22a shows that the K&D model overestimates the strength by 54% more than the actual strength at age 6-hours for PC concrete grade C75. The model then underestimates the strength from age 12-hours onward. The errors in the strength prediction from age 12-hours to 128-days are within 20%, which is a higher than that of PC concrete grade C45, i.e. within 10% at similar ages.

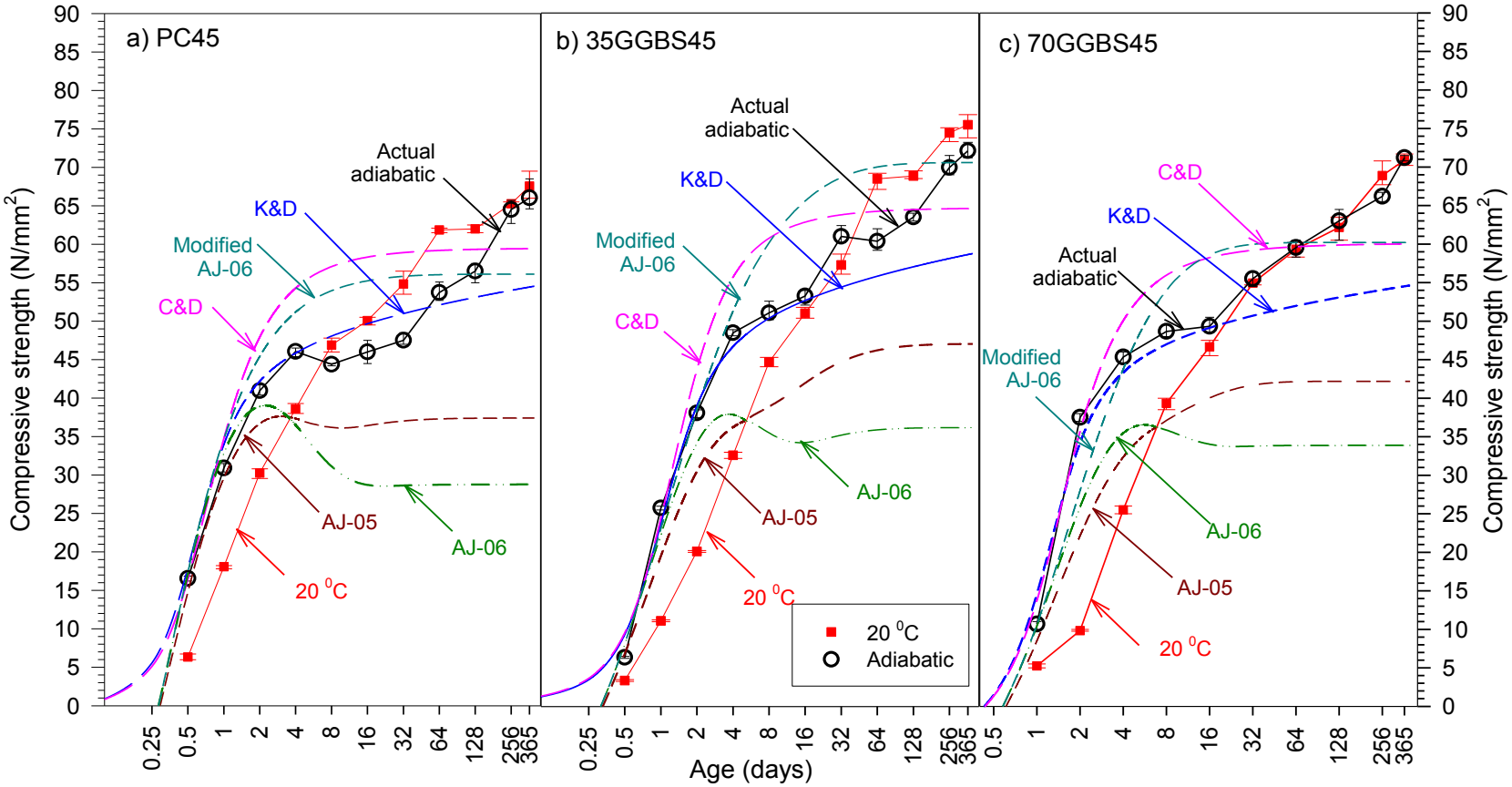

Figure 6.19: Predicted adiabatic strength development of concrete **grade C45** using recent maturity equations

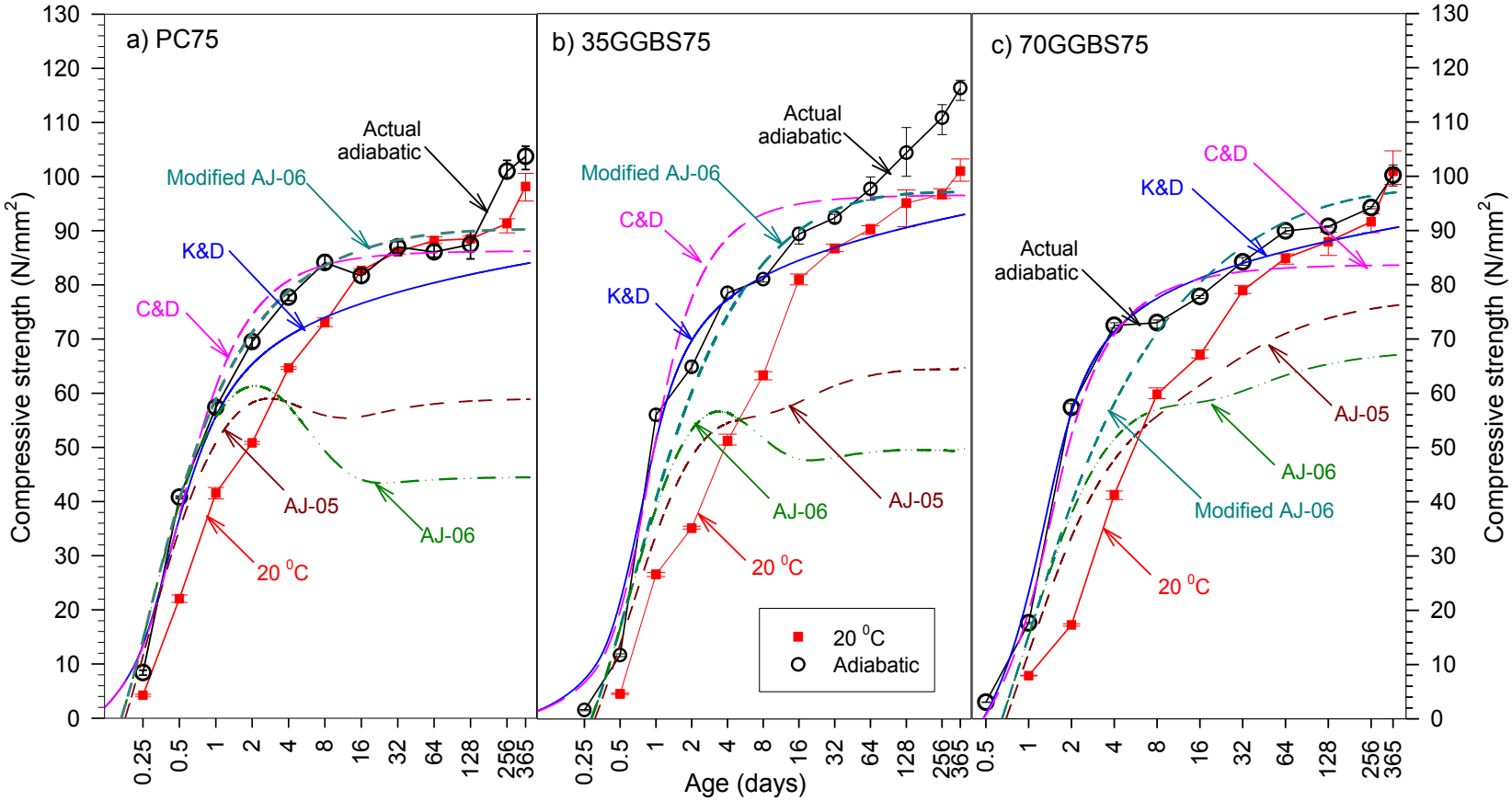

Figure 6.20: Predicted adiabatic strength development of concrete **grade C75** using recent maturity equations

The accuracy of this model in predicting the strengths of GGBS concretes grade 75 also appears to dependent on the levels of GGBS in the concrete, as shown in Figure 6.20. The model is considerably more accurate in predicting the strength development of the concrete with 20% GGBS, where the errors are less than 10% from age 1-day to age 16-days (Figure 5.58). In comparison, this model predicts the strength of the concrete with 70% GGBS with errors less than 10% from age 2-days to 128-days.

Figures 6.19 and 6.20 show that the C&D model appears to predict the strength development of concrete reasonably well for PC concrete and 70% GGBS concrete grade C75. The level of agreement with the experimental data is not dependent on age. In concrete PC45 (PC concrete grade C45), this model overestimates the strength of the concrete from 1-day to age 64-days, where the errors are less than 30%. This model then predicts the strength reasonably well from age 128-days onward with errors are within 10%. The model appears more accurate in predicting the strength development of the concrete PC75 (PC concrete grade C75) than that of the PC45concrete. In the PC75concrete, this model predicts the strength of the concrete considerably accurately from age 12-hours to 128-days, where the errors are less than 10%.

In 20 and 35% GGBS concretes for both grades C45 and C75 (Figures 6.21 and 6.22), the model overestimates the strengths at age 2-day to 16-days, where the errors are within 30%. The model then underestimates the strength from age 32-days onward where the errors to within 20%. However, the model predicts the strengths of 50% GGBS for both grades C45 and C75 reasonably well where the errors are within 10% at age 4-days to 128-days.

The strengths prediction using the C&D model in concretes with 70% GGBS grade C75 appears to be more accurate than that of the concrete with the same GGBS level but grade C45. The model predicts the strength of 70% GGBS concretes grade C75 considerably more accurately at age 2-days to 128-days with errors of less than 10%, while the strength prediction of the concrete 70% GGBS

grade C45 is overestimated from age 1-day to 16-days where the errors are within 20%. The model then accurately predicted the strength at age 32-days to 265-days where the errors were within 10%.

The other two models proposed by Abdel-Jawad, i.e. the AJ-05 and AJ-06 models, appear to underestimate the strengths of all concretes and grades, as was seen in the mortars. Both the models are highly affected by the temperature rise in the concrete. The more the discrepancy between the temperature rise in concrete and the reference temperature, the more the reduction in strength prediction of the concrete. This is believed to be due to the models being highly sensitive to the effect of the high early-age curing temperature on the later ages of concrete.

Generally, both the models predicted the strengths accurately up to age 2-days for PC concrete, while for GGBS concretes strengths vary up to 1-day depending on the levels of GGBS in the concrete. Both the models then underestimate the strengths at later ages. The models are more underestimate the strength of PC concrete compared to GGBS concretes, particularly for concretes with higher levels of GGBS. A reason for this might be that the temperature rise in the concrete with the higher levels of GGBS was much lower than that of the concrete with lower levels of GGBS, especially in PC concrete.

In concrete grade C45 (Figure 6.21), the AJ-05 model predicts the strength quite well at early ages up to age 2-days for concrete with PC only, where the errors are within 10%. The model then underestimates the strength at the later ages, where the predicted strength is highly dependent on the ages and reached only 57% of the actual strength at age 365-days. At an early age, the accuracy decreased as the percentage of GGBS in the concrete increased; however, the accuracy then increased at later age.

Although the AJ-06 model was developed based on the Arrhenius equation, the model underestimated the strength for all concretes and grades. The model underestimates the strength more compared to the AJ-05 model. Figures 6.21 and

6.22 clearly show that the accuracy of strength prediction is increased as the level of GGBS increased, particularly the strength prediction at later ages.

The Modified-AJ model is a proposed model that is found by combining the AJ-05 and AJ-06 models, which is more accuracy than its original models. The model predicts the strength quite well for PC concrete grades C45 and C75 at age 12-hours to age 365-days, where the errors are within 20%, except the predicted strength of PC concrete grade C45 at age 8-days, where the model predicted the strength 22% higher than the actual strength. In concrete with GGBS levels up to 35%, the model predicts the strength reasonably well, where the errors are on average within 20%. In concrete with higher levels of GGBS such as 50 and 70%, the model underestimates the strength up to 2-days and then predicts the strength reasonably well from age 4-days to age 365-days, where the errors are within 10 and 20% for concrete with 50 and 70% GGBS, respectively.

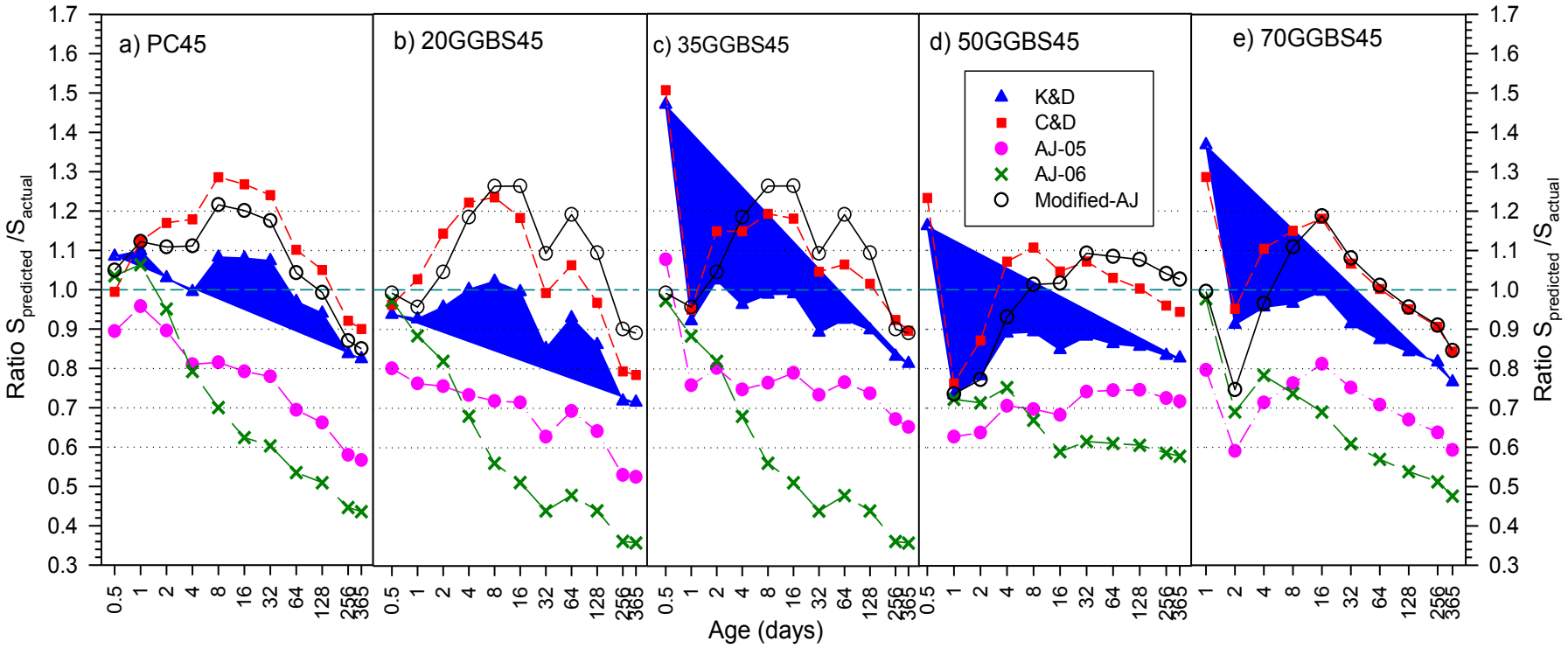

Figure 6.21: $S_{predicted}/S_{actual}$ of adiabatic strength development of concrete **grade C45** using recent maturity equation

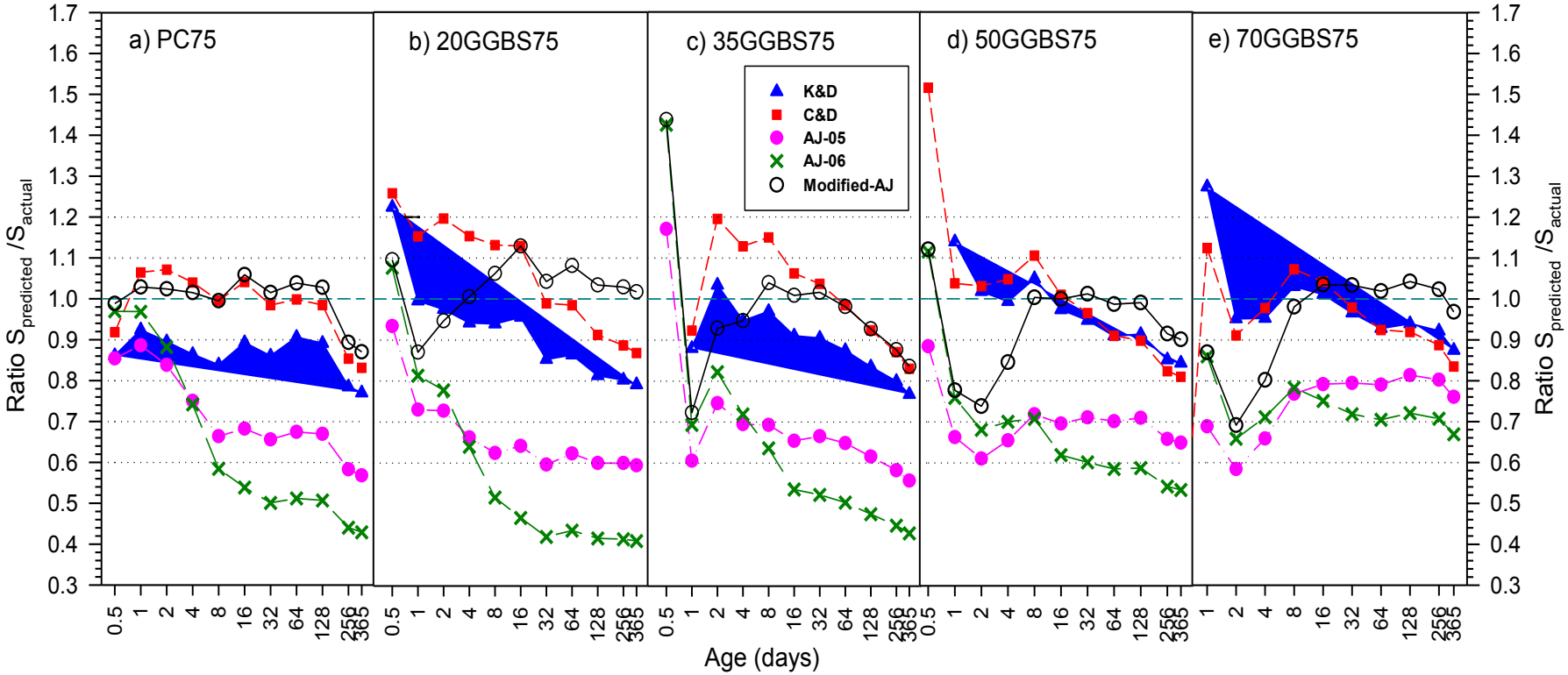

Figure 6.22: $S_{predicted}/S_{actual}$ of adiabatic strength development of concrete **grade C75** using recent maturity equation

6.5. Strength Prediction Using the Modification Nurse-Saul Method

6.5.1. Introduction

The assessment of all the maturity methods examined in this study shows that there is no one single method of making an accurate prediction of concrete strength development. This section discusses a relatively new method called the Modified Nurse-Saul (MNS) method proposed by Soutsos[166]. This method is an improvement of the existing maturity methods i.e. the Nurse-Saul and Freiesleben Hansen and Pedersen methods, as has been discussed in the literature review chapter, Section 2.4.7.4 Chapter 2.

Regression analyses using the TPE equation had been carried out to obtain the parameters such as S_∞, τ, and a, which were needed in the strength prediction. The parameters that were obtained from equivalent mortars could be used to predict the concrete strength development. The effects of higher curing temperatures on the acceleration and compression factors were determined based on the age conversion factor (ACF).

The strength prediction for both mortars and concretes cured under isothermal and adiabatic conditions is presented in this section. This aims to evaluate the accuracy of this method in predicting the strength of concrete/mortar.

6.5.2. Modified Nurse-Saul (MNS) Method

Differentiation of Equation 2.21 results[166] in the following:

$$\frac{dS}{dt} = \frac{a\tau^a\,(T - T_0)}{M^{a+1}}\, S_\infty\, e^{-(\frac{\tau}{M})^a} \qquad \text{Equation 6.3}$$

or

$$\frac{1}{S}\frac{dS}{dt} = \frac{\alpha\tau^a\,(T - T_0)}{M^{a+1}} \qquad \text{Equation 6.4}$$

The strength development was differentiated with respect to maturity rather than time, therefore, the Equation 6.4 then can be written:

$$\frac{1}{S}\frac{dS}{dM} = \frac{a\tau^a}{M^{a+1}} \qquad \text{Equation 6.5}$$

Equation 6.4 can be solved in an *"iterative procedure"* to calculate the strength rate of mortar/concrete cured under non-isothermal curing temperatures or cured at temperatures other than the reference temperature. The equation below illustrates Saul's principle:

$$\frac{1}{S_r}\left(\frac{dS}{dM}\right)_r = \frac{1}{S}\frac{dS}{dM} \qquad \text{Equation 6.6}$$

It is necessary to transform the strength rate when cured under the reference temperature to temperatures other than the reference temperature. The transformation strength rate could provide an understanding of the hydration kinetics of cement or the combination of cement and GGBS in mixture, where the hydration rate is part of the hydration kinetics. Therefore, an investigation of hydration kinetics should consider the strength rate, which it directly related to the hydration rate.

The regression analysis results are presented in Figures 6.23 and 6.24 for mortar grades C45 and C75, respectively. Many trials have been carried out to obtain the best-fit curve by changing the "*a*" value. It was found that if the shape parameter "*a*" was left as a variable in the regression analysis; this results in a much better fit curve. However, it did not produce any consistent relationship with curing temperature. Therefore, the shape parameter "*a*" was set as unity for all curing temperatures as was recommended by Soutsos.

Both the figures show that at same law value of maturity, the higher curing temperature result in a higher compressive strength. However, it conversely results in lower strength at later age/high maturity, as the strength was detrimentally affected by the higher curing temperature, which shows that Saul's maturity rule is not applicable. The parameters obtained from the regression analysis were used to calculate the strength rate for each curing temperature in respect to maturity. The tables for the parameters obtained can be found in Appendix E (Tables E-7 and E-8).

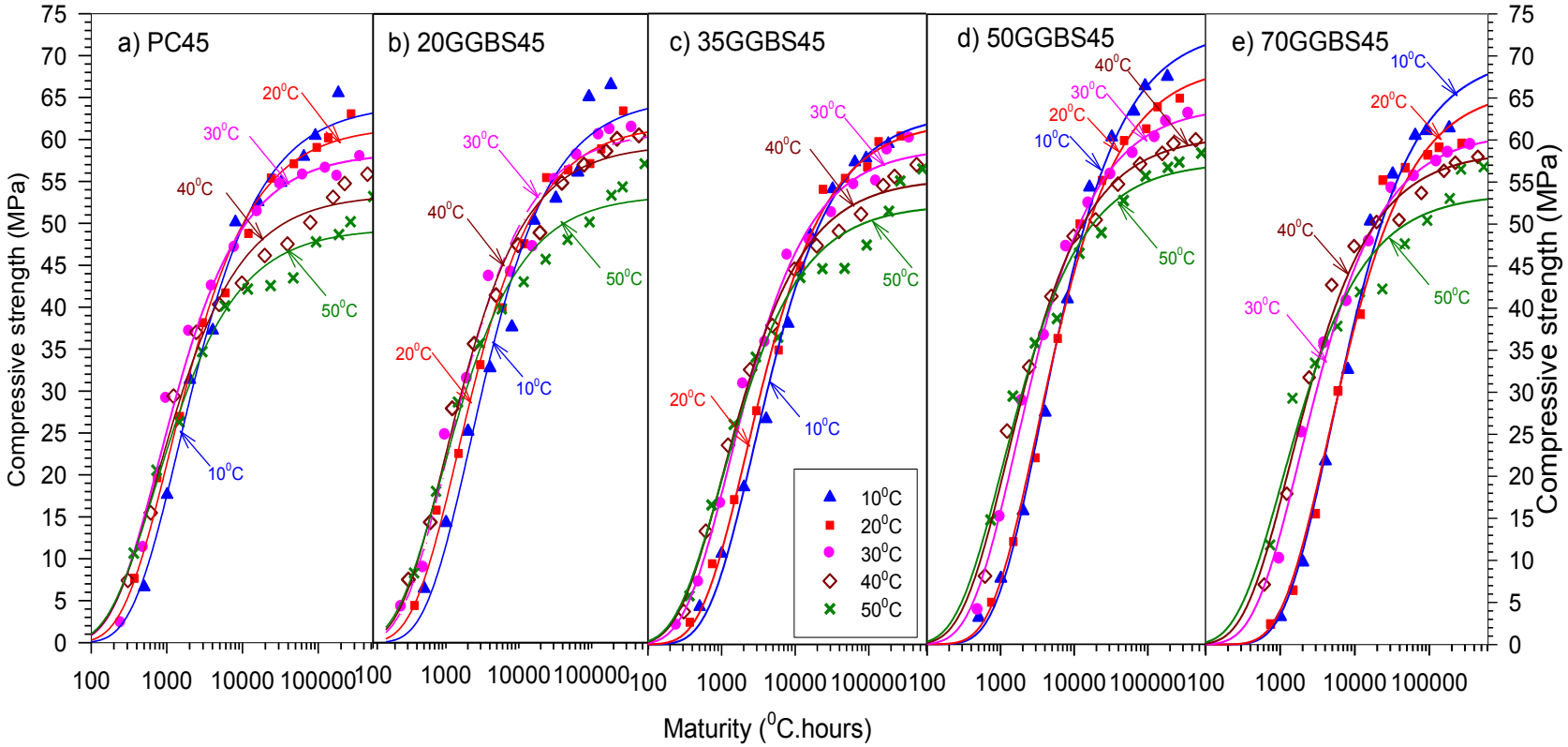

Figure 6.23: Linear Regression compressive strength vs. maturity for mortar **grade C45**

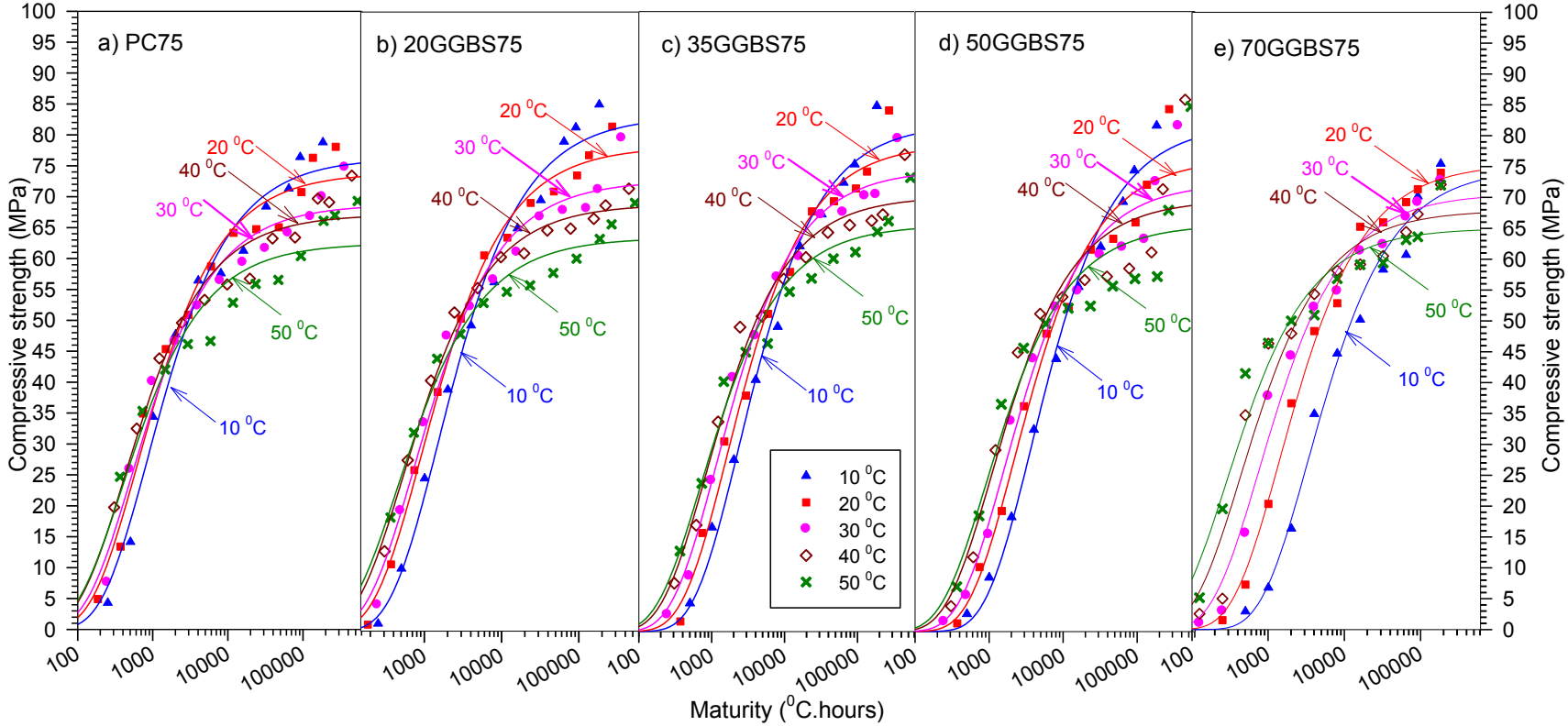

Figure 6.24: Linear regression compressive strength vs. maturity for mortar **grade C75**

Figures 6.25 shows the maximum rates of strength development in respect to maturity for mortar grade C45, while the rate for mortar grade C75 can be seen in Figure E-23 in Appendix E. The effect of temperature on the rate of hydration should be in respect to maturity rather than time, as this is required for Equation 6.5. The figures show that the peak value of dS/dM of the curves, which is the maximum rates of strength development, that not only occurred at earlier maturity values with higher curing temperature, but they are also numerically higher as this reaction is accelerated at the higher temperature. For example, for PC mortar grade C45 (Figure 6.25a), as the higher curing temperature accelerates the reaction, it compresses a certain maturity interval into a smaller one, e.g., the reaction until it reaches the peak of maturities at 310 and 193.17 ^{0}C.hours, for 20 and 50^{0}C curing temperatures respectively. Figure 6.26 is similar to Figure 6.25, where they have the same rates of reaction; however, the maturity axis of Figure 6.26 is plotted on a logarithmic scale to accentuate the differences at early ages/maturities. Equation 6.5 can be expressed as:

$$\log\left(\frac{1}{S}\frac{dS}{dM}\right) = \log(\alpha\tau^{a}) - (a+1)\log(M) \qquad \text{Equation 6.7}$$

by applying a logarithm on the both sides of the equation. Equation 6.7 indicates that plots should result in straight lines with gradients of - (a + 1). The value of all the gradients will be minus 1.7, as the shape parameter "a" that is used for the regression analysis for both strength versus age and strength versus maturity was set as unity i.e. 0.7.

If all the lines in Figures 6.27 follow the Saul's maturity rule, then the predicted and the actual data will overlap, as Saul's maturity rule is valid. It is necessary to understand how the rate of reaction is affected by the temperature. The rate of reaction is in terms of maturity rather than time is plotted against maturity in Figure 6.28 for mortar grade C45, while for mortar grade C75 can be seen in Appendix E (Figure E-26). The two hydration curves of two different curing temperatures i.e. 20 and 50^{0}C do not coincide.

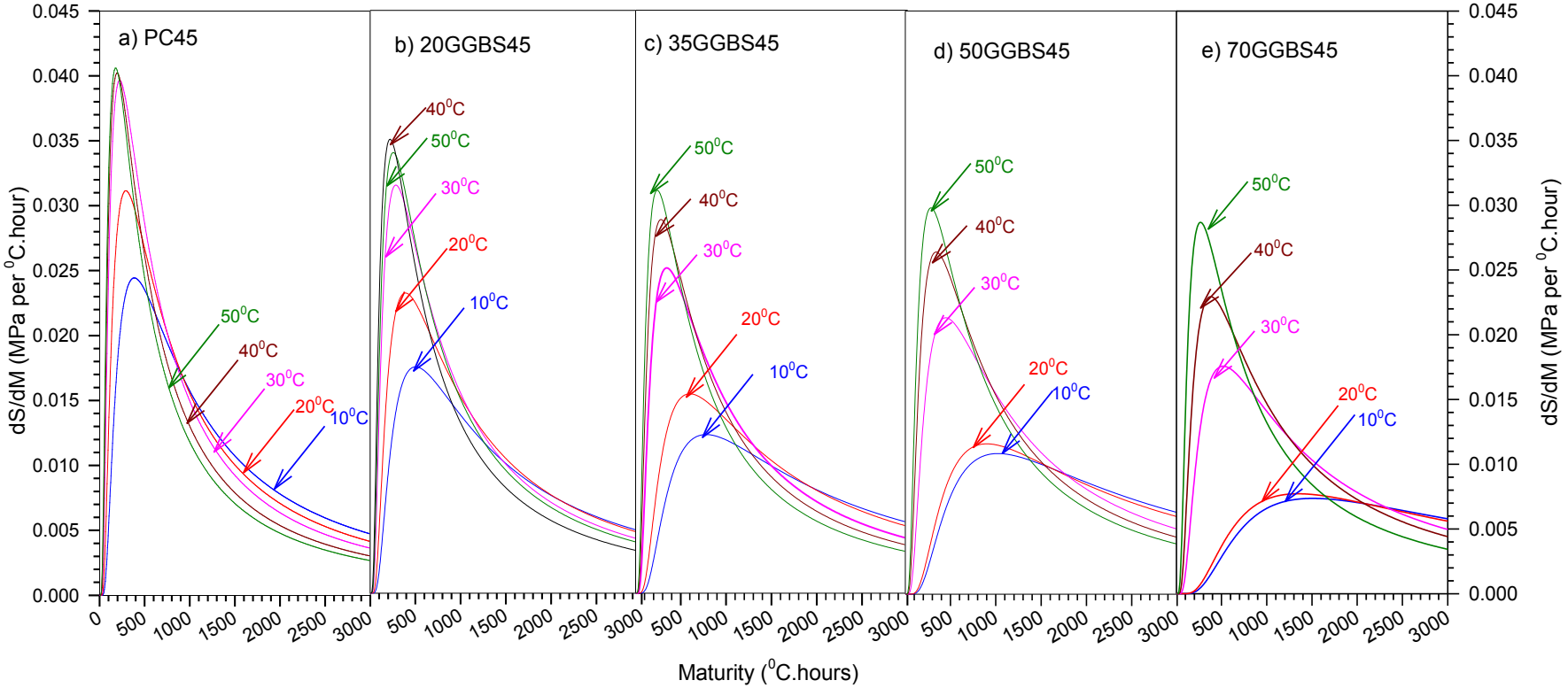

Figure 6.25: Rate of compressive strength gain with respect to maturity (dS/dM) vs. maturity (^{0}C.hours) mortar grade C45

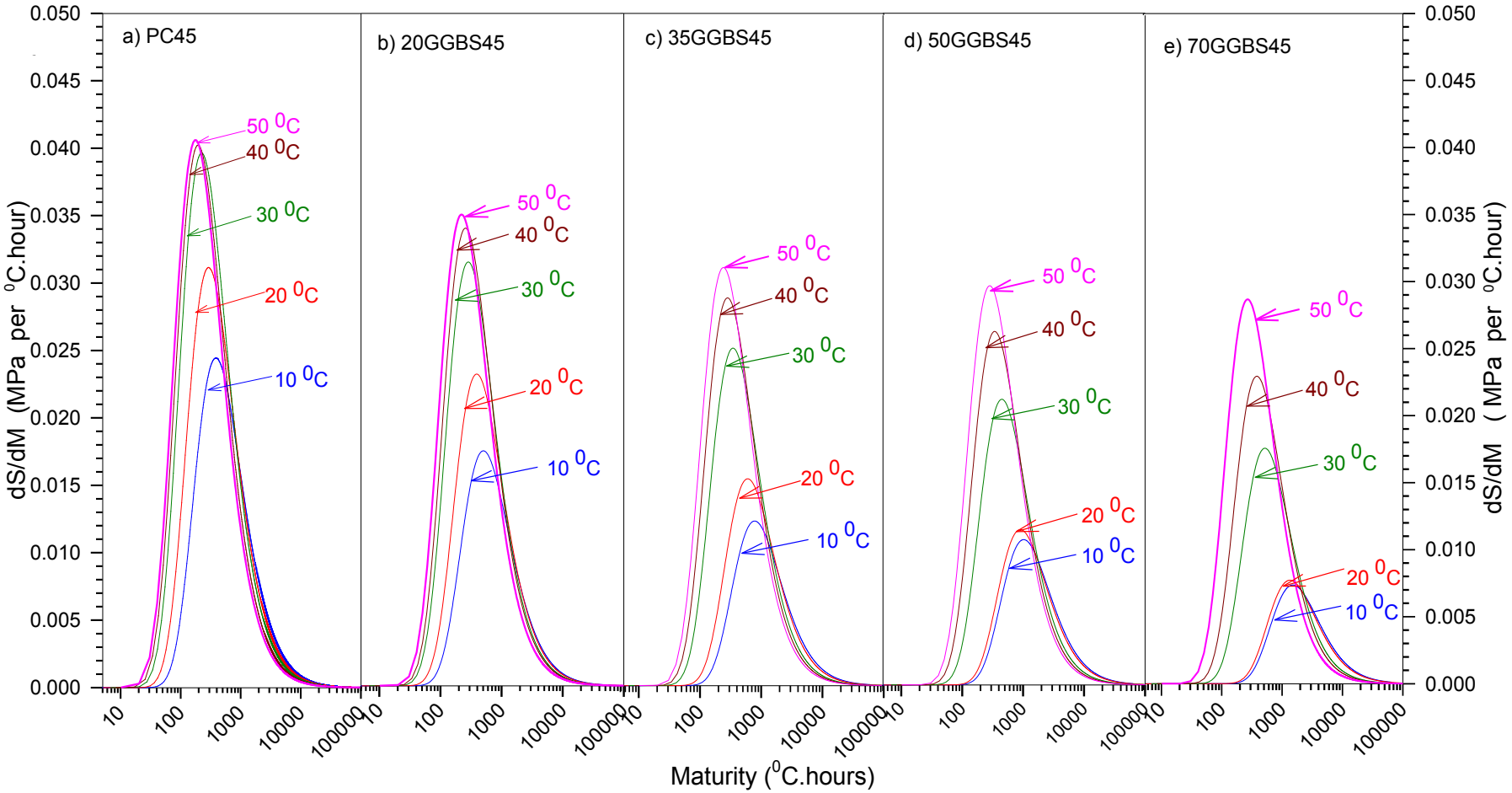

Figure 6.26: Rate of compressive strength gain with respect to maturity (dS/dM) vs. maturity (^{0}C.hours) plotted on a logarithmic axis for mortar **grade C45**

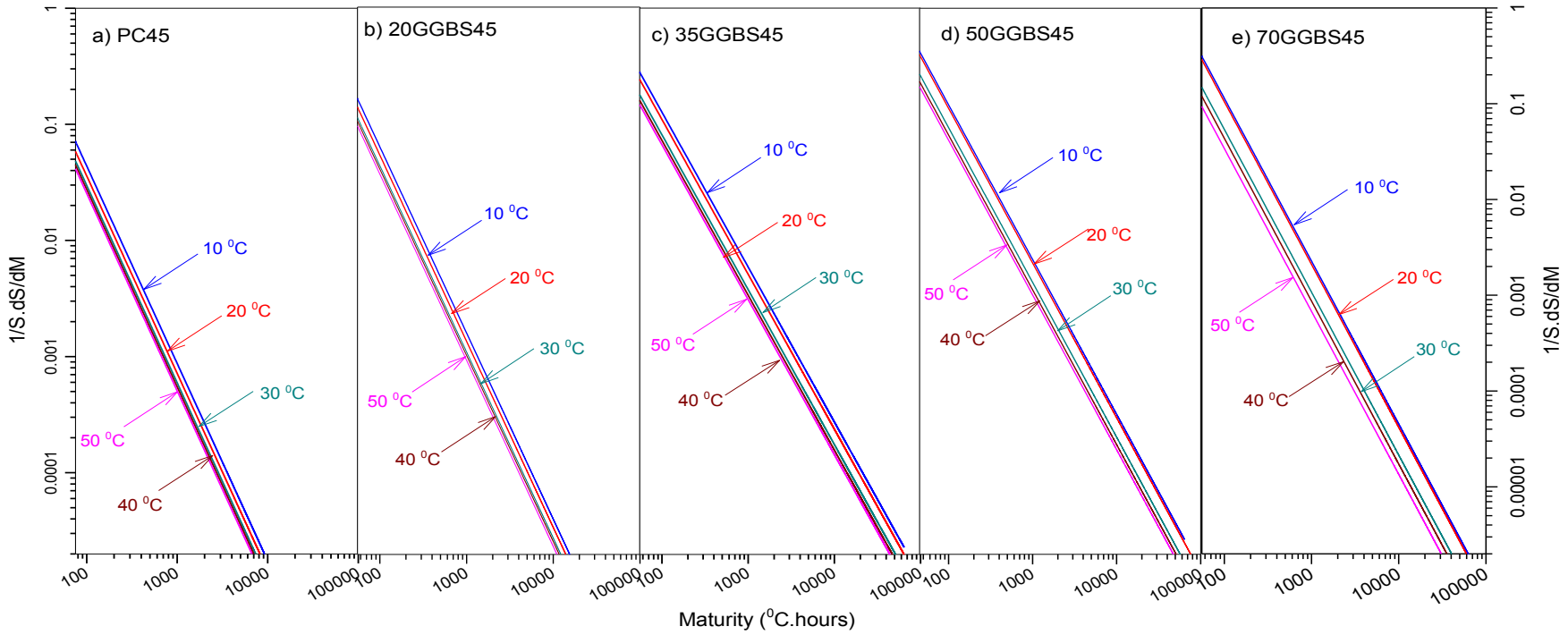

Figure 6.27: Relationship of 1/S.dS/dM with maturity for different curing temperatures mortar **grade C45**

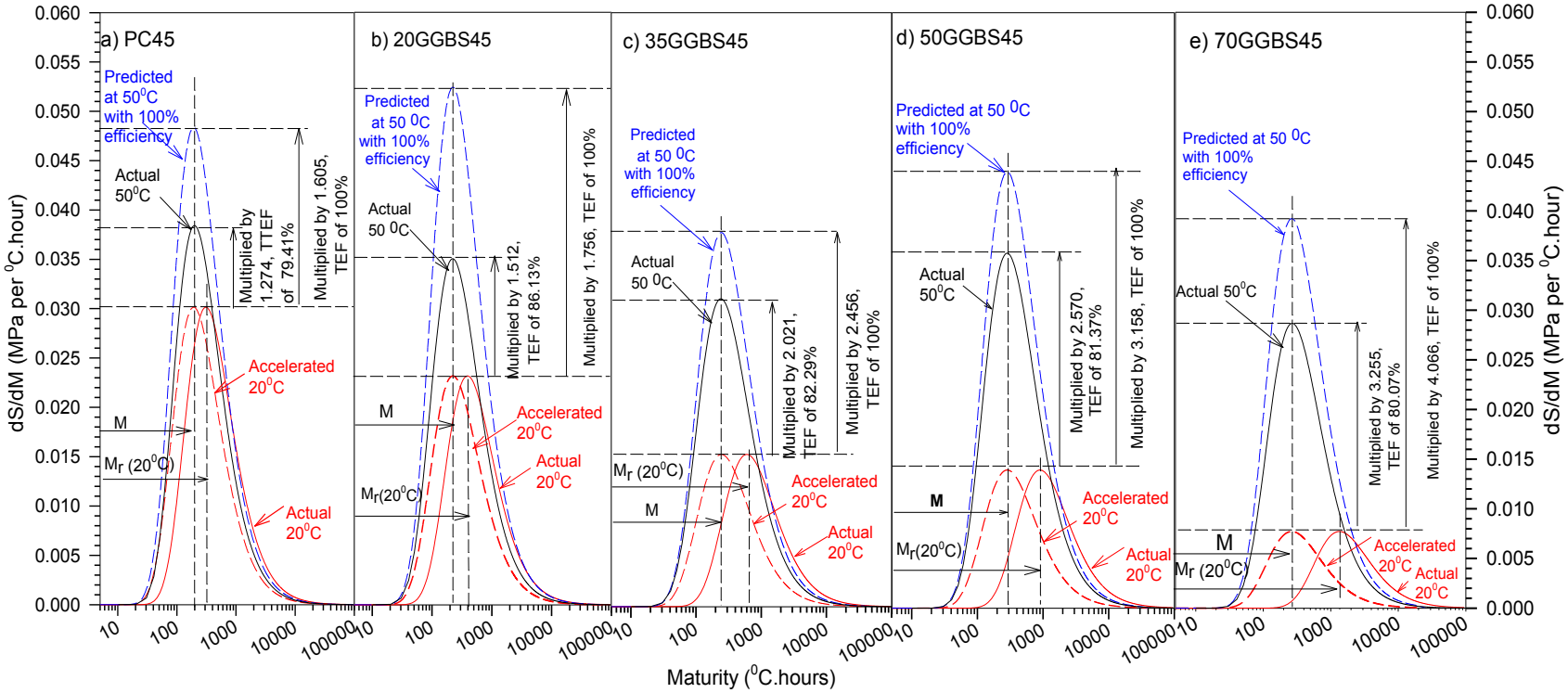

Figure 6.28: "Acceleration (M_r/M)" and "temperature efficiency" factors used to transform the 20^0C rate of compressive strength gain (dS/dM) to that 50^0C for mortar **grade C45**

The age conversion factor (ACF) i.e. $\beta = \frac{(T - T_0)}{(T_r - T_0)} = \frac{(50 + 11)}{(20 + 11)} = 1.97$, implied by Nurse-Saul's maturity rule, is not enough to cause the reaction curves of 50 and 20^0C curing temperature to overlap. Figure 6.28a shows that the peak dS/dM for 20^0C occurs at a maturity of 310^0C.hours, while the peak dS/dM of hydration under 50^0C occurs at an earlier maturity than that of 20^0C i.e. 193.17 ^{0}C.hours. These are related to 10 and 3.17 hours for 20 and 50^0C, respectively. Therefore, the age conversion factor β should be 3.15 instead of 1.97. The strength-maturity relationship at 20^0C can be brought to 50^0C by introducing an "acceleration" factor, which is introduced by Soutsos[166]. The acceleration is specified as the ratio of the maturity at the peak dS/dM of 20^0C to the maturity at the peak dS/dM of a curing temperature, which can be expressed:

$$a_M = \frac{M_r}{M} \qquad \text{Equation 6.8}$$

where:

a_M = acceleration factor

M_r = the maturity at the peak dS/dM at reference temperature (20^0C)

M = the maturity at the peak dS/dM at curing temperature

The function of the acceleration factor is to compress a certain maturity interval into a smaller one. Therefore, the numerical value of dS/dM is increased. Another factor needs to be introduced is a factor that brings the peak dS/dM at 20^0C to the peak dS/dM at a curing temperature, which can be mathematically written as follows:

$$a_C = \frac{dS/dM_{peak,\ curing\ temp.}}{dS/dM_{peak,\ reference\ temp.}} \qquad \text{Equation 6.9}$$

where:

a_C = compression factor

$dS/dM_{peak,\ curing\ temp.}$ = peak dS/dM at curing temperature

$dS/dM_{peak,\ reference\ temp.}$ = peak dS/dM at reference curing temperature

The facts show that the strength of concrete mixtures that cured at higher curing temperature at early-age is higher than that of concretes cured at lower temperature, but this is reversed at later age. This means that the reaction at the

higher curing temperature was not as efficient as at the lower curing temperature. Therefore, the temperature efficiency factor (TEF) "η", can then be defined as the ratio of the compression factor and the acceleration factor as follows[166]:

$$\eta = \frac{a_C}{a_M} \text{ X } 100\% \qquad \text{Equation 6.10}$$

So, when the rate of hydration at the higher curing temperature is the same as that of the standard curing temperature (20^0C), the acceleration factor should also be the same as the compression factor. The prediction of the strength rate development assuming 100% temperature efficiency is shown as a blue dashed line in Figure 6.28. The actual and the prediction of the strength rate with temperature efficiency at higher curing temperature of 50^0C coincide, which is shown as solid black line in the figures. This is therefore believed to enable the accurate prediction of the strength development of mortar and concrete. Furthermore, the actual and the acceleration of the strength rates of 20^0C are shown as solid and dashed red lines in the figures.

Figure 6.29 shows the effect of the acceleration and the temperature efficiency factors in terms of the 1/S.dS/dM relationship with the maturity. It is difficult to distinguish between the actual and the predicted value of 1/S.dS/dM as they coincide. Therefore, this relationship enables the prediction of the strength development of mortar/concrete cured under non-isothermal or changing curing temperatures.

Similarly, analyses have been done for the mortar specimens cured at different curing temperatures i.e. 10, 30 and 40^0C. These aim to find the relationship between the curing temperatures and the acceleration and the temperature efficiency factors in terms of strength rate. It appears that a direct correlation between the curing temperature and the acceleration and also the temperature efficiency factors, results in inaccurate strength prediction.

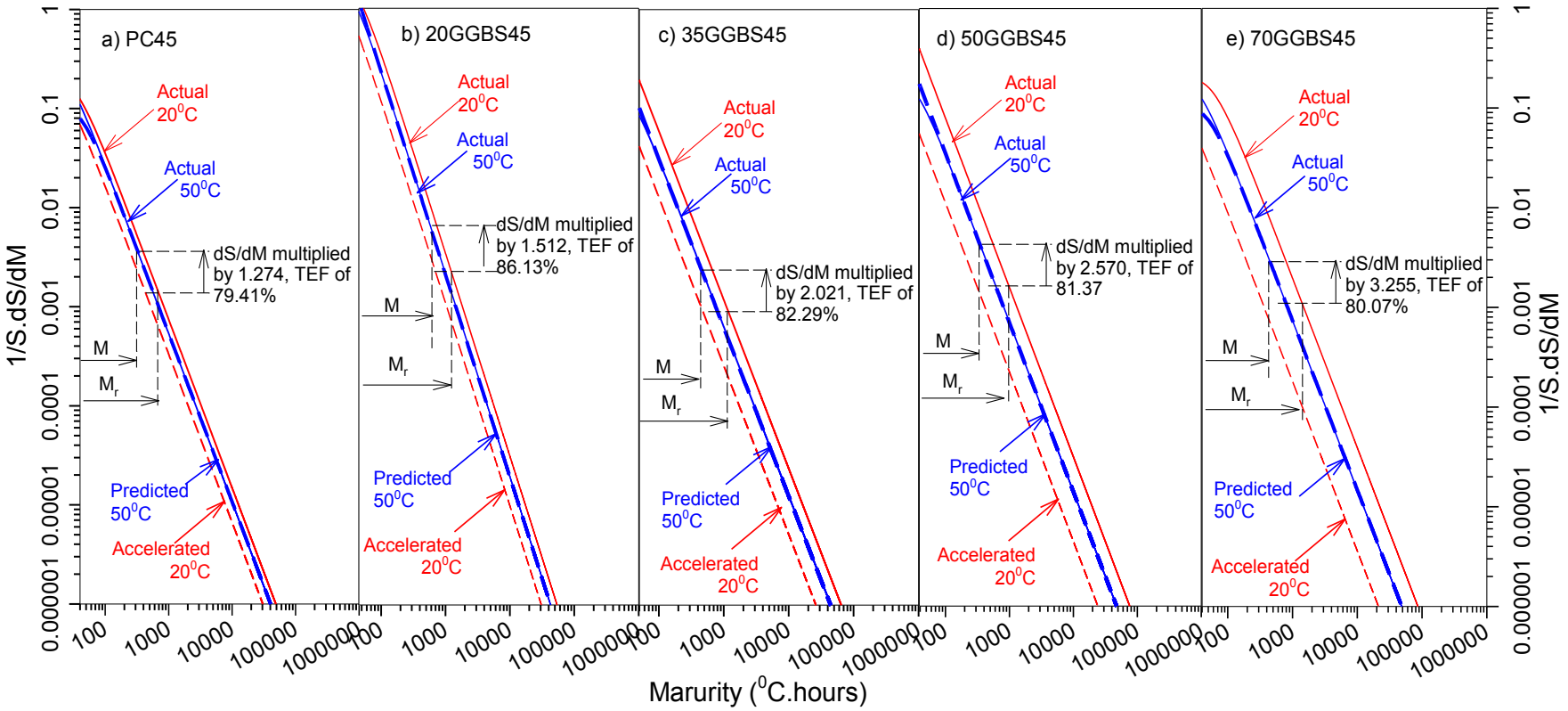

Figure 6.29: "Acceleration (M_r/M)" and "temperature efficiency" factors used to transform the 20^0C relationship between 1/S.dS/dM and maturity to that of specimens cured at 50^0C for mortar **grade C45**

This can be explained that the high curing temperature results in a lower efficiency factor, even if it can be reduced to less than 50%, while it does not happen, particularly in GGBS concrete. It is found that a correlation between the age conversion factor (β) and both the acceleration and temperature efficiency factors results in much better strength prediction.

Table 6.15: Parameters obtained from transformation the strength rate at 20^0C to other curing temperatures i.e. 10, 30, 40 and 50^0C for PC mortar **grade C45**

Temp. (^{0}C)	Age conversion factor (β)	Maturity at peak dS/dM	(dS/dM)max	a_C	a_M
10	0.6774	409.5000	0.0236	0.7839	0.7570
20	1.0000	310.0000	0.0301	1.0000	1.0000
30	1.3226	225.5000	0.0400	1.3256	1.3747
40	1.6452	212.5000	0.0386	1.2794	1.4588
50	1.9677	193.1667	0.0384	1.2745	1.6048

Table 6.15 presents the parameters obtained from transformation of the strength rate at 20^0C to the other curing temperatures i.e. 10, 30, 40 and 50^0C. Parameters for the other mortars grade C45 and C75 can be seen in Appendix E (Tables E-9 and E-10). Regression analyses had been carried out for all mortars grade C45 and C75 as shown in Figures 6.30 and 6.31, respectively. This aims to find out the best-fit line of the relationship between the age conversion factor (β) and both the acceleration factor (a_M) and compression factor (a_C).

The relationships between the age conversion factor (β) and both the acceleration and compression factors can be expressed mathematically as follows:

$$a_M = a\,.\,\beta + b \qquad \text{Equation 6.11}$$

and

$$a_C = a\,.\,\beta + b \qquad \text{Equation 6.12}$$

where a and b are parameters obtained from the regression analysis given in Table 6.16.

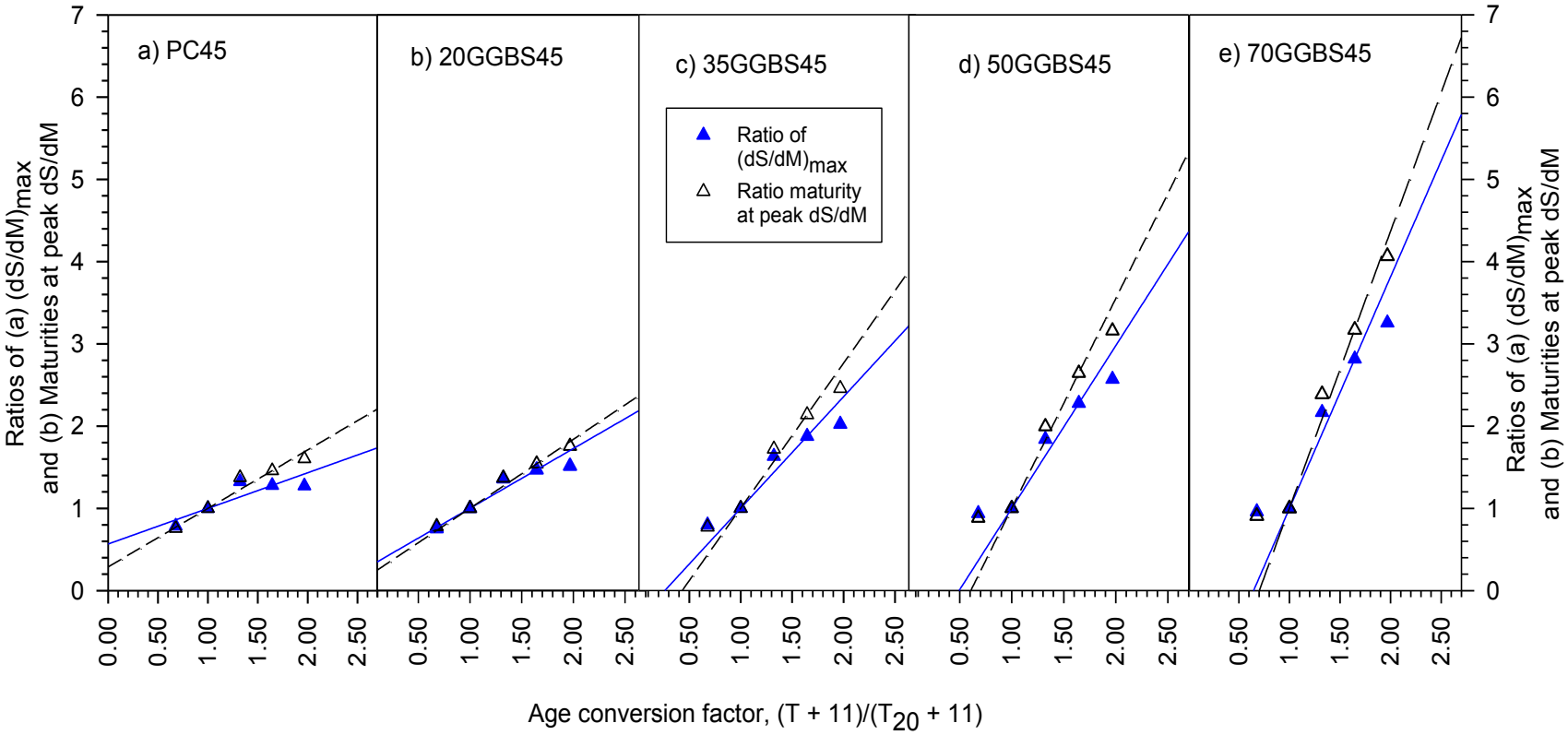

Figure 6.30: Ratios of $(dS/dM)_{max}$ and maturities at peak dS/dM versus age conversion factor (ACF) mortar **grade C45**

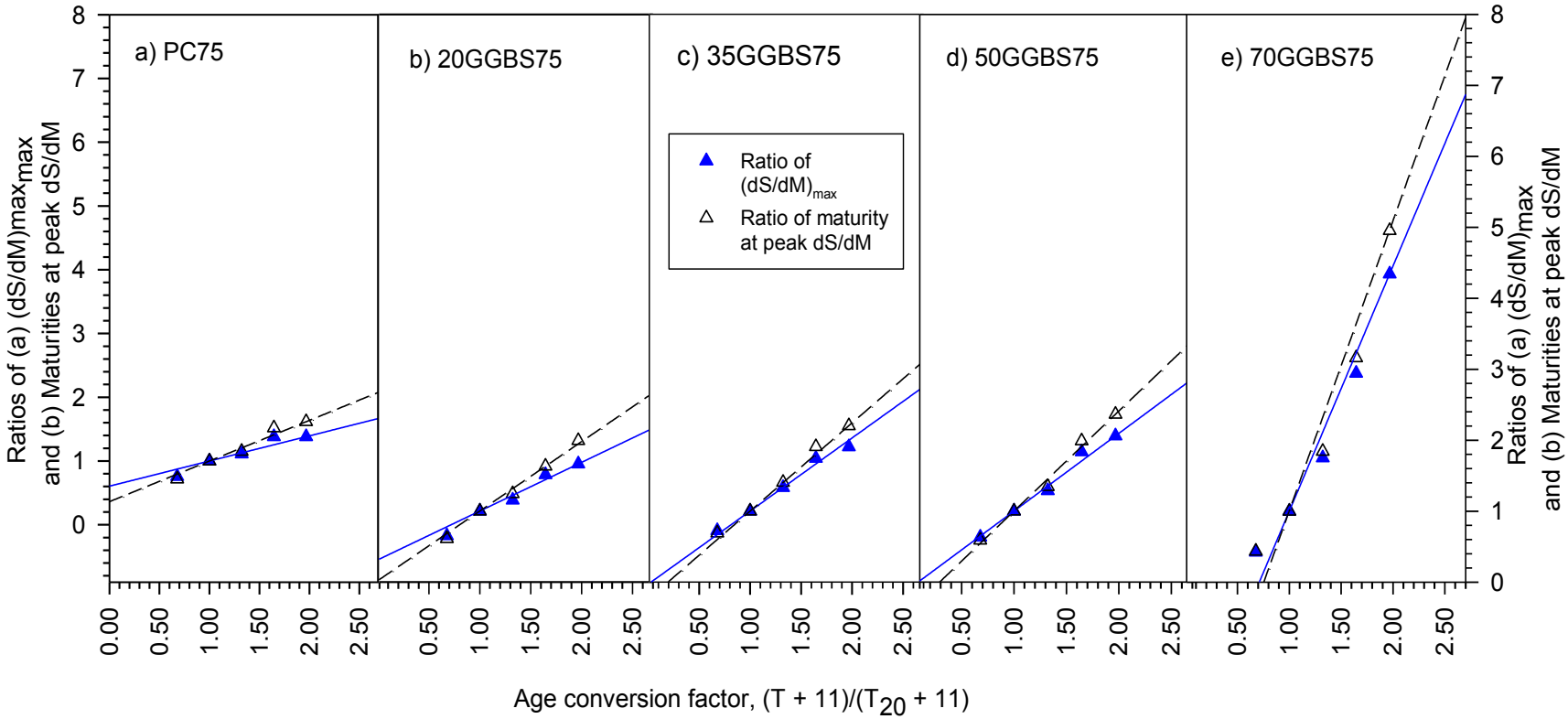

Figure 6.31: Ratios of $(dS/dM)_{max}$ and maturities at peak dS/dM versus age conversion factor (ACF) mortar **grade C75**

Table 6.16: Parameters for the accelerator and compression factors obtained from linear regression mortar grade C45 and C75

Mortars grade	GGBS level (%)	$a_C = (dS/dM)/(dS/dM)_{20}$			$a_M = M_{20}/M$		
		a	b	R^2	a	b	R^2
C45	0	0.3908	0.6159	0.9120	0.6679	0.3558	0.9473
	20	0.6150	0.4050	0.9460	0.7730	0.2660	0.9860
	35	1.0310	0.1010	0.9480	1.3970	-0.2310	0.9760
	50	1.4090	-0.1390	0.9540	1.9200	-0.6040	0.9630
	70	2.3240	-0.8900	0.9410	3.3720	-1.8440	0.9510
C75	0	0.4220	0.6050	0.8940	0.6620	0.3620	0.9660
	20	0.7020	0.3130	0.9870	1.0200	-0.0270	0.9980
	35	0.9290	0.0840	0.9970	1.2410	-0.2400	1.0000
	50	1.1100	-0.1380	0.9950	1.4350	-0.4820	0.9920
	70	3.0130	-2.0130	1.0000	3.3490	-2.3490	1.0000

There is no one single method that can be used to predict the strength development of all the mortars and concretes investigated and so produce an accurate prediction. Therefore, it is necessary to develop a new method of predicting the strength development of mortar/concrete that uses GGBS as the cement replacement material. The Modified Nurse-Saul (MNS) method is a method that has been developed by combining the Three Parameter Exponential (TPE) and Nurse-Saul equations. The strength is calculated using the modified TPE equation by applying a time efficiency factor. The Nurse-Saul's maturity method is modified by applying an acceleration factor *"a_M"*, as the age conversion factor (β) is not enough to transform a strength rate as cured under the reference temperature to another curing temperature.

The following procedures are used to predict the strength development of mortar/concrete cured under non-isothermal conditions using the MNS method:

1. Determine $S = S_\infty e^{-(\frac{\tau}{M})^a}$ (Equation 2.21) using the parameters obtained from the linear regression analysis for mortar/concrete cured at the reference temperature, in this study taken as 20^0C.

2. Determine the acceleration factor a_M and predict the strength for temperature efficiency factor (TEF), η = 100%, using the equation:

   $S = S_\infty e^{-\left(\frac{\tau}{a_M M}\right)^a}$, where *"a"* is taken as 1.

3. Determine the rate of strength development dS/dM for η = 100%.
4. Predict the strength development for η being a function of temperature, η(T) using the equation:

$$S = \sum \frac{dS}{dM} \eta(T)\, \Delta M$$

   η(T) is determined based on Equation 6.10, where a_M and a_C are calculated using Equations 6.11 and 6.12, respectively. The values of a_M and a_C are changed as the curing temperature is changed as shown in both Equations 6.11 and 6.12, where they are a function of the age conversion factor, β. The age conversion factor is calculated using Equation 2.9 in Chapter 2.

6.5.3. Modified MNS Method Proposed in This Study

If the shape parameter *"a"* is left as a variable in the regression analysis it produces a better-fit curve. It is found that the shape parameter *"a"* has an important role in producing a good strength prediction. By simulation of the value of *"a"* on the mortar specimens cured under an isothermal curing temperature, it is found that taking a higher *"a"* value at lower curing temperatures resulted in good strength prediction. Therefore, this shows that the *"a"* value should be decreased as temperature increases or it should be changed by changing the curing temperature. The adiabatic curing temperature is increased with time; but conversely, the temperature efficiency factor (η) is decreased by increasing temperature, which is similar to the *"a"* value. Taking into account the effect of high curing temperatures, the *"a"* value is then multiplied by the temperature efficiency factor (η). This produces a reasonably good prediction of concrete strength development rather than directly multiplying the temperature efficiency factor (η) by the ultimate strength.

The procedure of the modified MNS method proposed in this study to predict the strength development of concrete cured under non-isothermal as follows:

1. Determine $S = S_\infty e^{-(\frac{\tau}{M})^a}$ using the parameters obtained from the linear regression for mortar/concrete cured at the reference temperature, in this study taken as 20^0C.

2. Determine the acceleration factor a_M and predict the strength for temperature efficiency factor (η), using the equation:

   $S = S_\infty e^{-\left(\frac{\tau}{a_M M}\right)^{a\,\eta}}$, where *"a"* is taken as 1.

3. Determine the rate of strength development dS/dM for η(T)
4. Predict the strength development for η being a function of temperature, η(T) using the equation:

$$S = \sum \frac{dS}{dM} \eta(T)\, \Delta M$$

6.5.4. Adiabatic Strength Prediction of Equivalent Mortars Grade C45 and C75

Figures 6.32 and 6.33 present the predicted strength of mortar cured at 50^0C using the MNS method. The best-fit curve obtained from the linear regression analysis illustrates the best relationships between the strength and maturity. Therefore, the strength predictions of all the mortars for both grades C45 and C75 that cured at 50^0C using the MNS method are reasonably accurate, as all the curves of the predicted strength almost overlap with the curves obtained from the linear regression analyses. Furthermore, it is believed that the method can also be applied for mortar/concrete cured under adiabatic conditions, even to predict the in-situ strength development of mortar/concrete.

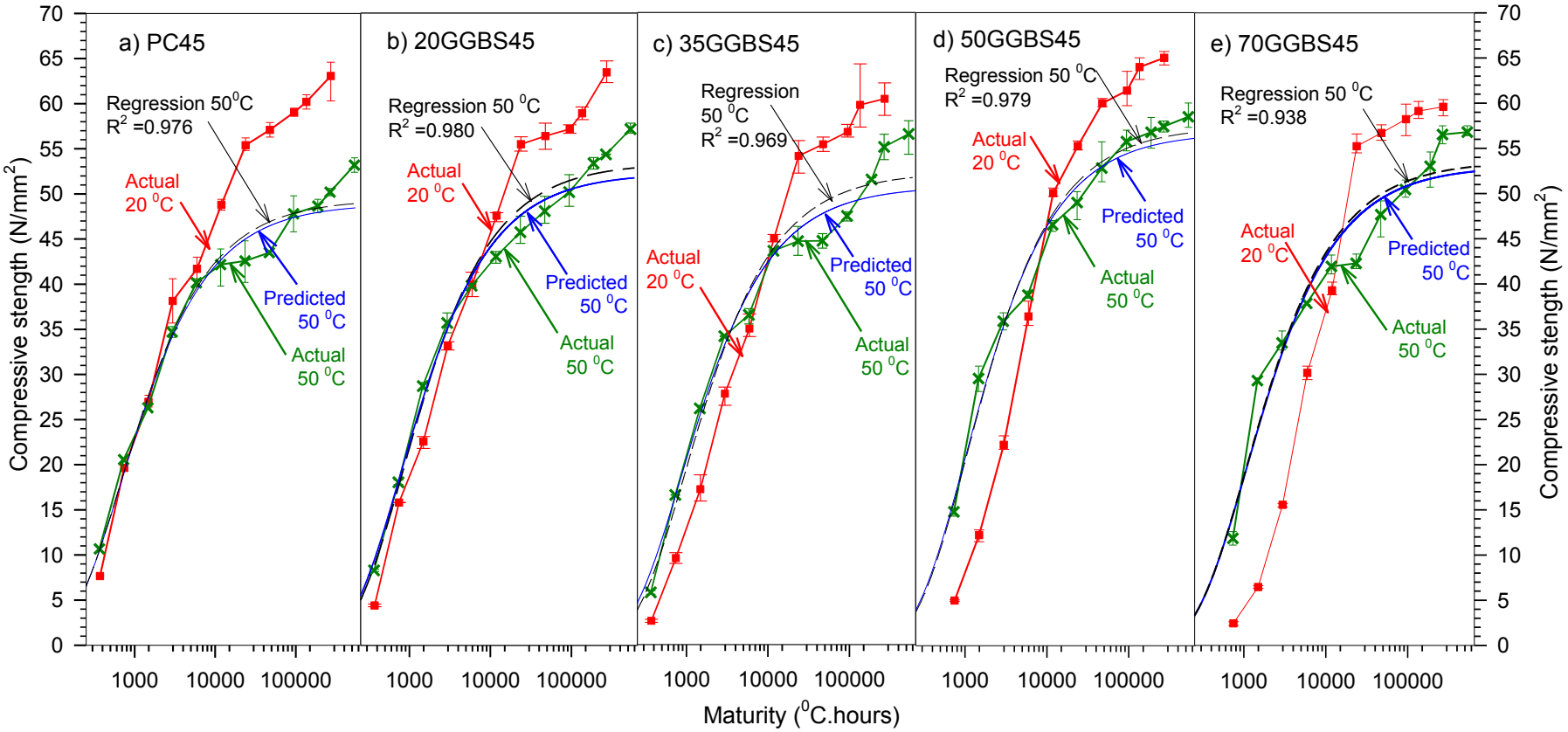

Figure 6.32: Predicted strength of mortar cured at 50^{0}C mortar **grade C45** using the Modified Nurse Saul (MNS) method

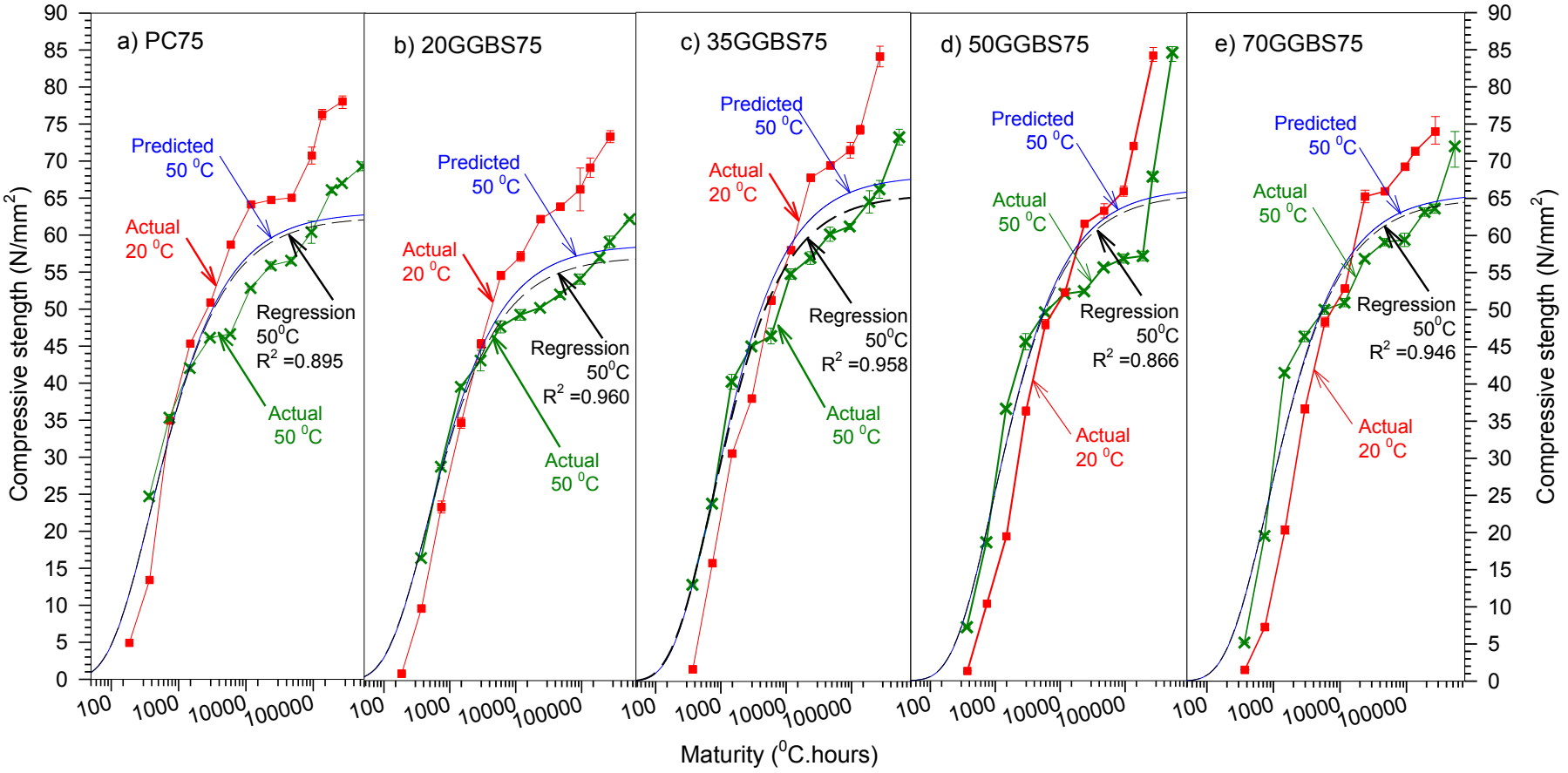

Figure 6.33: Predicted strength of mortar cured at 50^{0}C mortar **grade C75** using the Modified Nurse Saul (MNS) method

The strength predictions of mortar cured at 50^0C at lower maturity are very good, where the predicted strength lines almost overlap with the actual strength line. However, the predicted strength at the higher maturities is a little bit higher than that of the actual strength. This is due to the detrimental effect of the high curing temperature at early-age on the strength development of mortar/concrete at later ages.

In mortar grade C75 (Figure 6.33), the discrepancy between the predicted strength and the actual strength at higher maturity or at later ages is much higher than that for mortar grade C45. This is due to the limiting strength of mortar grade C75 being obtained from linear regression and used in predicting the strengths are lower than that of expected ones. The results of the strength predictions are lower than the actual strengths. The significant increase of the strength of mortars at later ages was unexpected for all the maturity methods in predicting the strength, therefore, their prediction of strength at later ages are inaccurate as shown in Figure 6.33d for mortar 50% GGBS grade C75.

The predicted adiabatic strength of equivalent mortar for both grades C45 and C75 with all levels of GGBS are presented in Figures 6.34 and 6.35, respectively. The figure presents the predicted strength development using the MNS method proposed in the earlier work and the modified MNS method proposed in this study.

Figure 6.34 shows that the model proposed in the earlier work (MNS method) and the Modified MNS proposed in this study slightly overestimate the adiabatic strength development of all mortars grade C45 at later age, except the mortar with 20 and 50% of GGBS. It is believed that both the models overestimate the strength at later ages due to the detrimental effect of high curing temperature at earlier ages. The model proposed in this study (Modified MNS), however, predicts the adiabatic strength for all mortars grades C45 more accurately than that of earlier work (MNS).

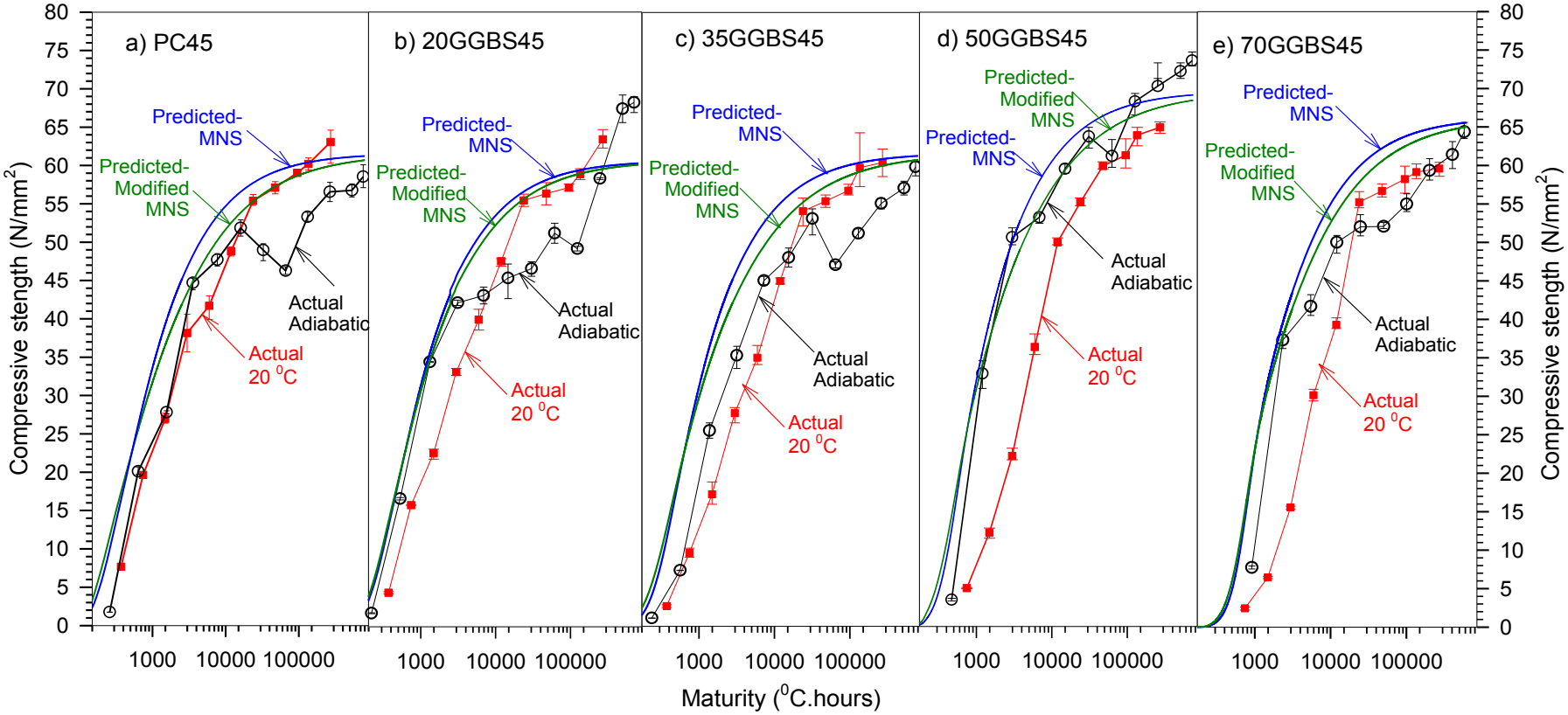

Figure 6.34: Predicted strength mortar cured under adiabatic conditions mortar **grade C45** using the MNS method and the Modified MNS proposed in this study

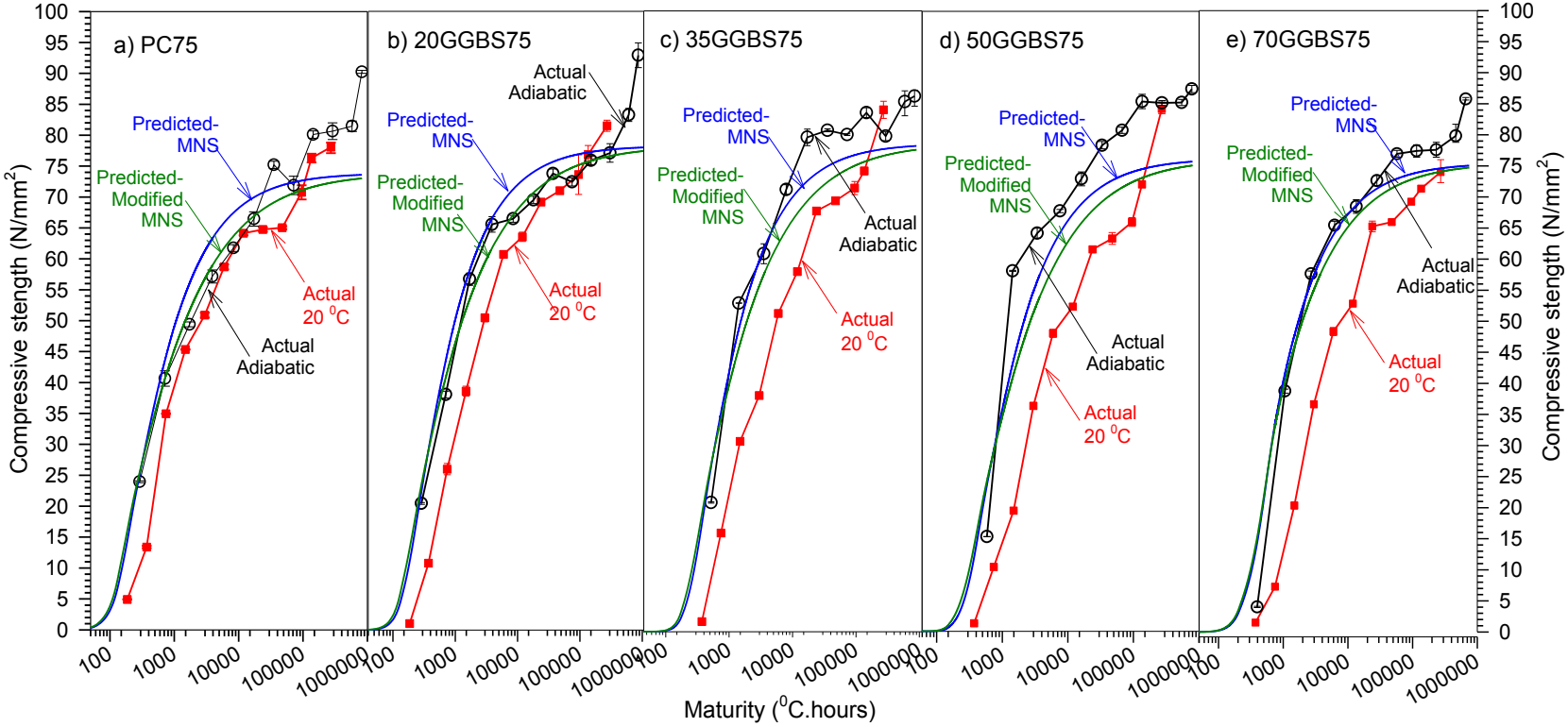

Figure 6.35: Predicted strength mortar cured under adiabatic conditions mortar **grade C75** using the MNS method and the Modified MNS proposed in this study

In mortar grade C75 (Figure 6.35), both the models that were proposed in the earlier work and in this study appear reasonably accurate for predicting the adiabatic strength development at low maturity values or early ages; however, they both underestimate the strength at high maturity values or later ages. This is due to the ultimate strength of all the mortars being lower than expected. The strength development of the mortars was lower than the expected values, as the casting temperatures of the mortars slightly higher, this caused the mortars quickly dried; the lack of water prevented further hydration. The result was the strength development of the mortars was slower, even the target mean strengths at age 32-days i.e. 85 MPa were not achieved. However, the strength development of the mortars after age 32-days continuously increases until the later ages. It could be also explained that the inaccuracy of the prediction of the model is due to the strength development of mortars cured under the reference temperature being lower than that of mortars cured under adiabatic conditions. Therefore, the predicted strength, which is based on the parameters obtained from the regression analysis on the mortars cured at the reference temperature, will be underestimated.

Figures 6.36 and 6.37 present the ratio of predicted adiabatic strength to actual adiabatic strength for all mortars grade C45 and C75, respectively. In general, both the models underestimate the strength of mortars grade C45 at early ages, except for GGBS mortar with 35% GGBS. However, the predicted strength from age 4-days and later are reasonably good, where the error are within 10%, except the predicted strength at the age when the strength development of the mortars drop as a result of the detrimental effect of high curing temperatures at earlier ages. The accuracy of the predicted strength of the model proposed in this study, when the actual strengths drop due to thermal shock also decreases but they still reach 80% or the errors are within 20%. In comparison to the model proposed in the earlier work, the model proposed in this study is more accurate.

Generally, both the models that were proposed in the earlier work and in this study appear to underestimate the adiabatic strength development of all mortars grade C75 as shown in Figure 6.37, except for PC75 and 20GGBS75 mortars.

Both the models predict the adiabatic strength of the two mortars quite well, where the errors on average are within 20% during the testing age. However, the predicted strength of GGBS mortar with 35, 50 and 70% of GGBS are underestimated at early ages up to age 8-days, particularly for 35% GGBS mortar (Figure 6.37d) where the errors are over 20%.

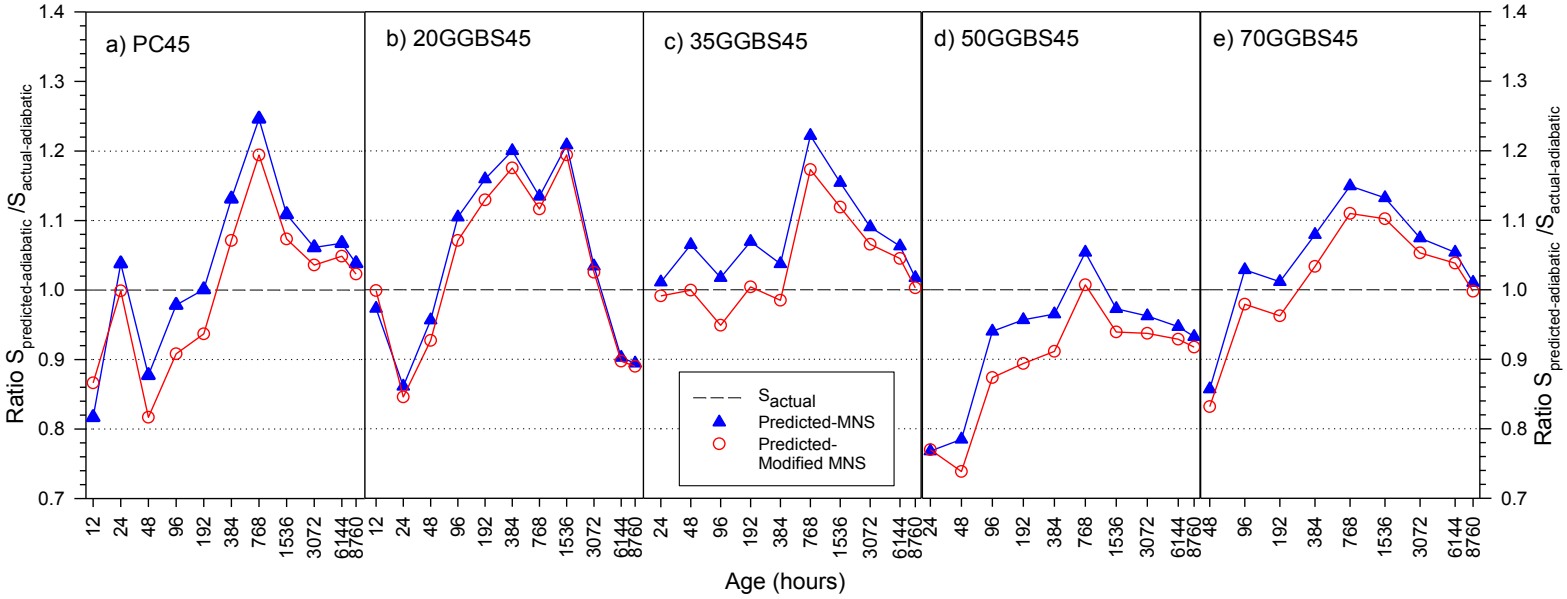

Figure 6.36: $S_{predicted}/S_{actual}$ of adiabatic strength development of mortar **grade C45** using the MNS method and the Modified MNS proposed in this study

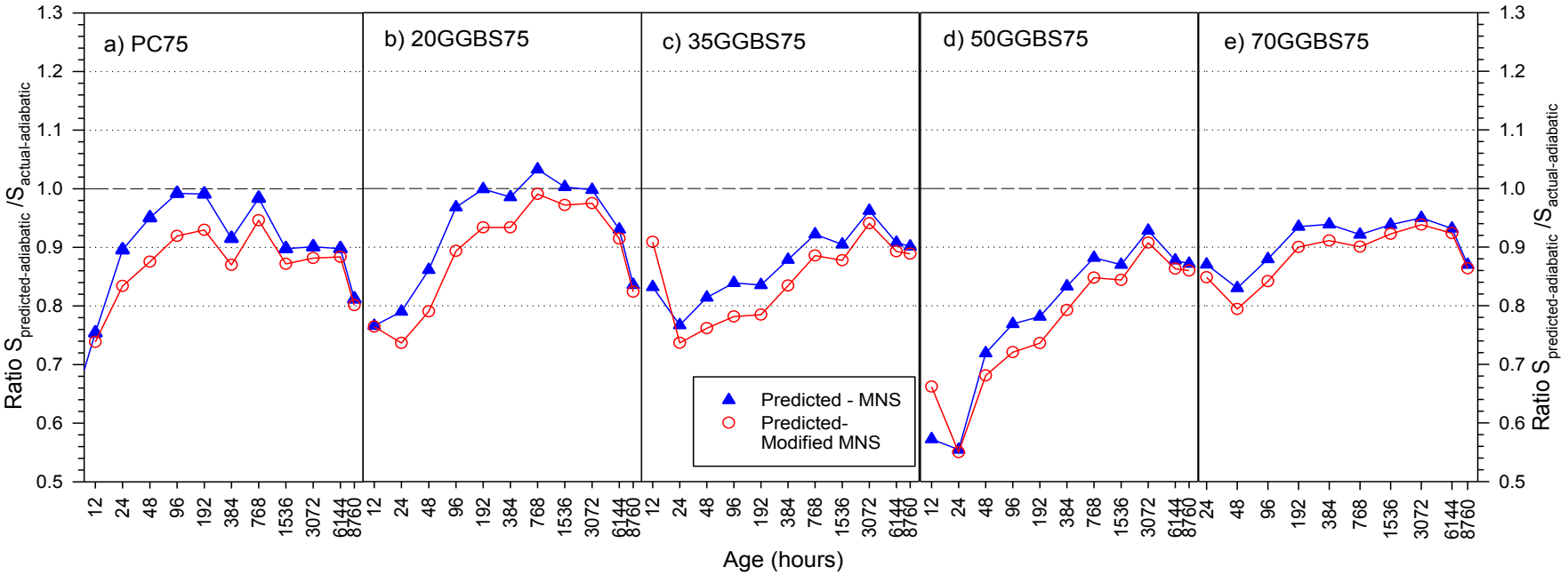

Figure 6.37: $S_{predicted}/S_{actual}$ of adiabatic strength development of mortar **grade C75** using the MNS method and the Modified MNS proposed in this study

6.5.5. Adiabatic Strength Prediction for Concretes Grade C45 and C75

Regression analyses, which are based on the strength-maturity relationship; using the TPE method, were carried out on all concrete mixtures as shown in Figures 6.38 and 6.39 for grades C45 and C75, respectively. This aims to obtain the parameters such as the ultimate strength (S_∞) and time characteristic (τ), as they are needed to predict the adiabatic strength development of the concrete. The parameters that are needed in the prediction of the adiabatic strength can be seen in Appendix E.

The other parameters such as acceleration, compression and time efficiency factors (TEF), which are used to predict strength development of the mortars, will be used to predict the strength development of concrete as the mortar mixtures were designed to be an equivalent mixture of each investigated concrete. Figure 6.38 shows that the concretes also experienced the crossover effect, as happened in mortars; however, it appears to happen at later ages than in mortar. Furthermore, it seems the crossover effect is delayed in GGBS concrete, where the higher level of GGBS in concrete results in a longer time delay for crossover to happen.

In addition, Figure 6.39 shows that the crossover effect in concretes with lower water-binder ratio happened at later ages than that of concrete with higher water-binder ratios such as concrete grade C45 (Figure 6.38). This might be explained by Figure 5.25 of Chapter 5. The total binder in all concretes grade C75 was more than that of in concretes grade C45 for concrete with the same level of GGBS. Therefore, the temperatures rise in higher-grade concretes is expected to be higher than in lower-grade concretes. However, the temperature rise in lower-grade concretes is higher than that in higher-grade concretes. It is believed that some of the heat produced in the hydration process of higher-grade concretes was converted into activation energy, which is used for further hydration. As a result, the temperatures rise in higher-grade concretes is slightly lower than that in lower-grade concretes and delays the crossover effect.

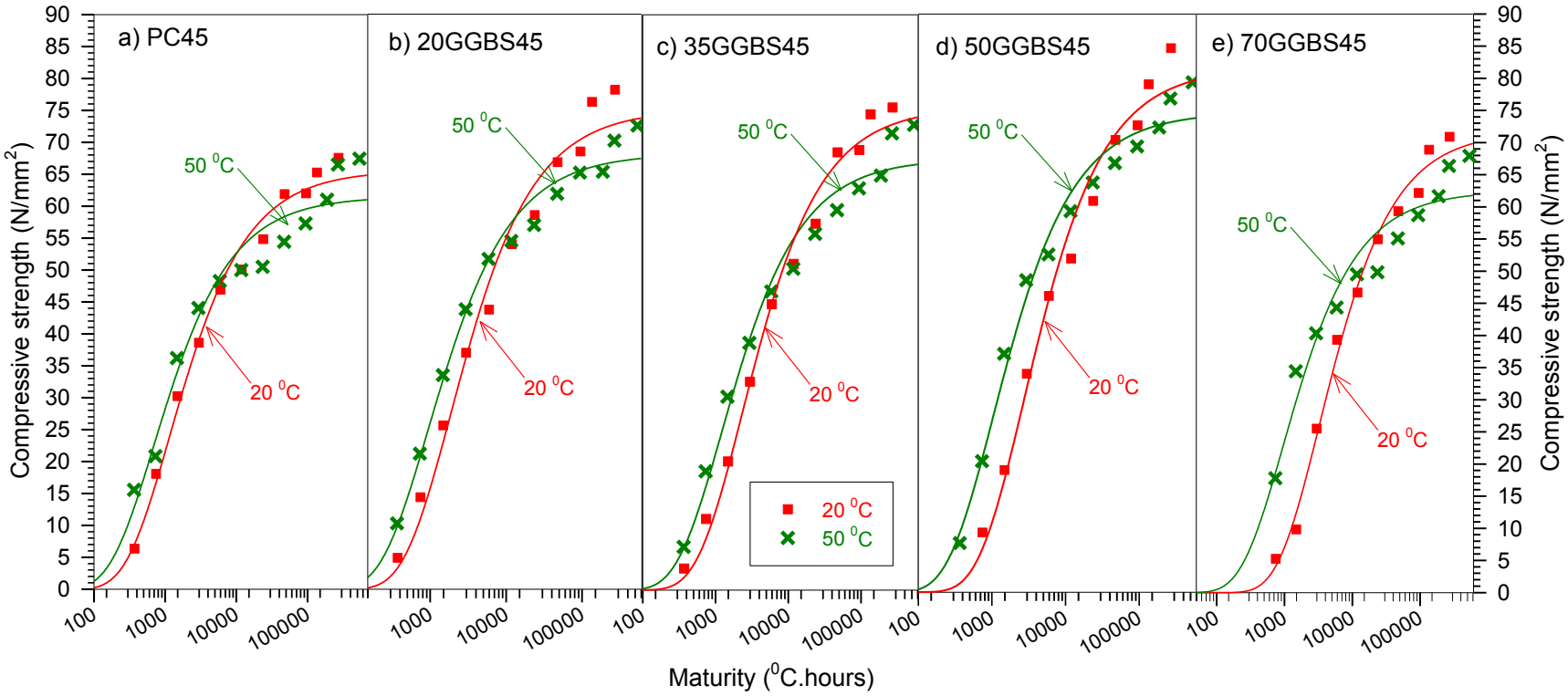

Figure 6.38: Linear regression strength – maturity for concrete **grade C45**

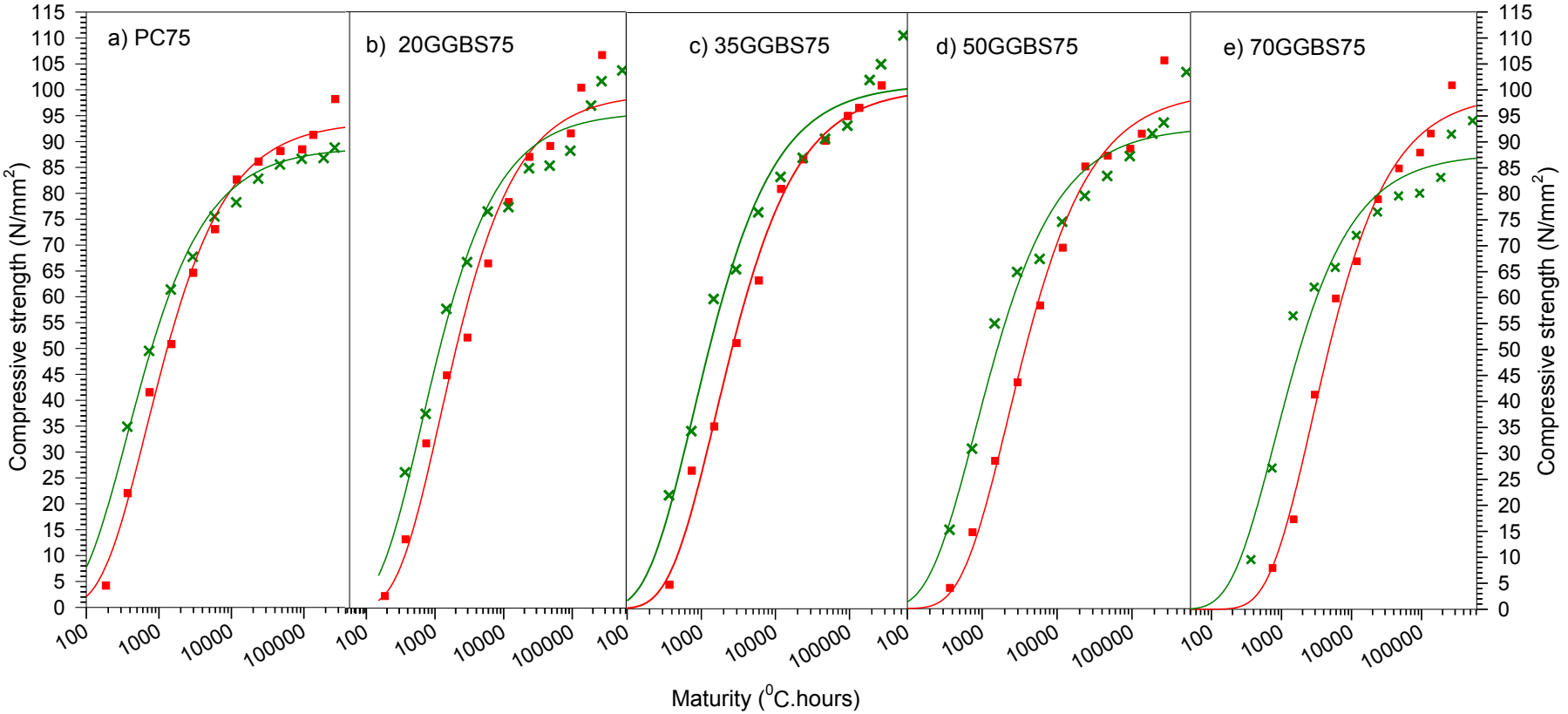

Figure 6.39: Linear regression strength – maturity for concrete **grade C75**

The predicted strengths of concrete cured under isothermal conditions, i.e. at 50^0C, are presented in Figures 6.40 and 6.41 for concrete grade C45 and C75 respectively. The model proposed in this study, predicts the strength development of all concretes both grade C45 and C75 cured at 50^0C reasonably well. All the predicted strength lines almost overlap with the regression analysis lines, which have extremely good R^2 values, except the strength prediction of concrete with Portland cement only grade C45 (Figure 6.40a). The strength development of the concrete from age 4-days until 16-days slowly increased, leading one to expect a detrimental effect, which is due to the high curing temperature at early age.

The strength development of GGBS concretes appear to be less affected by the high early age curing temperature than in PC concrete. The model overestimates the strength of all concretes grade C45 and C75 cured at 50^0C at later ages, but as unexpected the strength of concrete still significantly increased at later ages.

Figures 6.43 and 6.44 present the predicted adiabatic strength for concretes grade C45 and C75, respectively. The proposed model predicts the adiabatic strength reasonably well up to age 4-days for concretes grade C45; however, the model overestimates the adiabatic strength from this age until later ages, where the predicted strength and actual strength are close.

In concretes grade C75, the proposed model in this study predicts the adiabatic strength development reasonable well from age 4-days until later ages, i.e. after age 128-days, except for the 70% GGBS concrete. The predicted strength from the age 128-days and later are lower than the actual strength, as the strengths of the concretes are still significantly developed at this age.

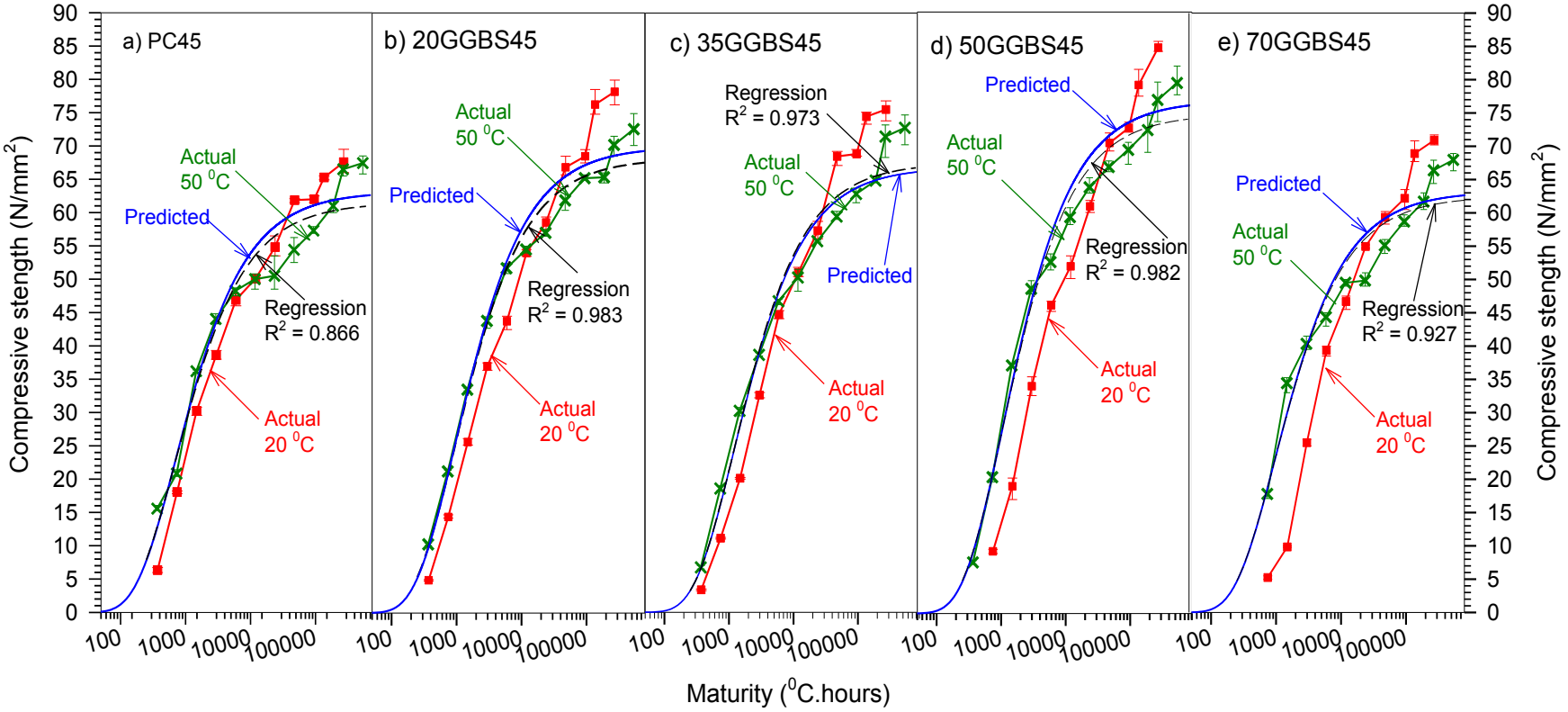

Figure 6.40: Predicted strength concrete cured at 50^{0}C **grade C45** using the Modified Nurse Saul (MNS) method

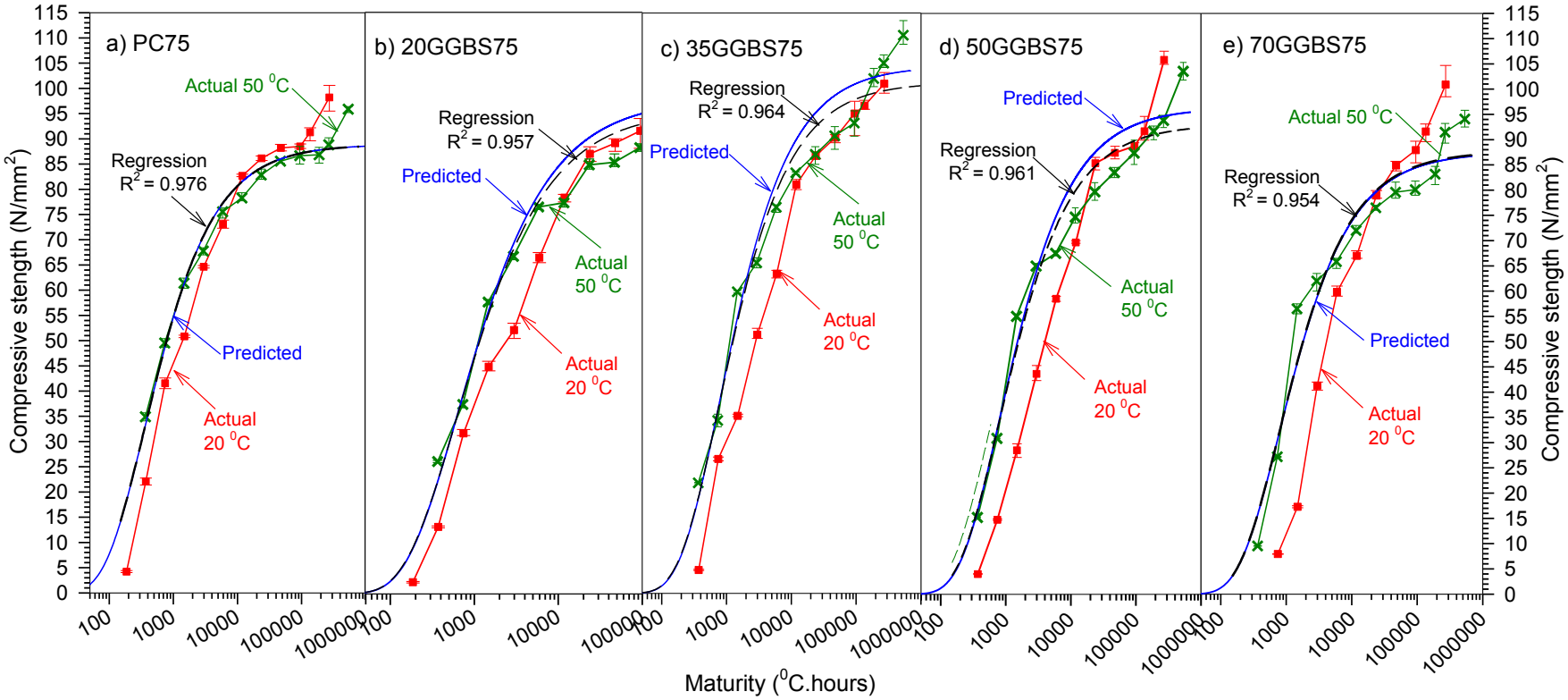

Figure 6.41: Predicted strength concrete cured at 50^0**C grade C75** using the Modified Nurse Saul (MNS) method

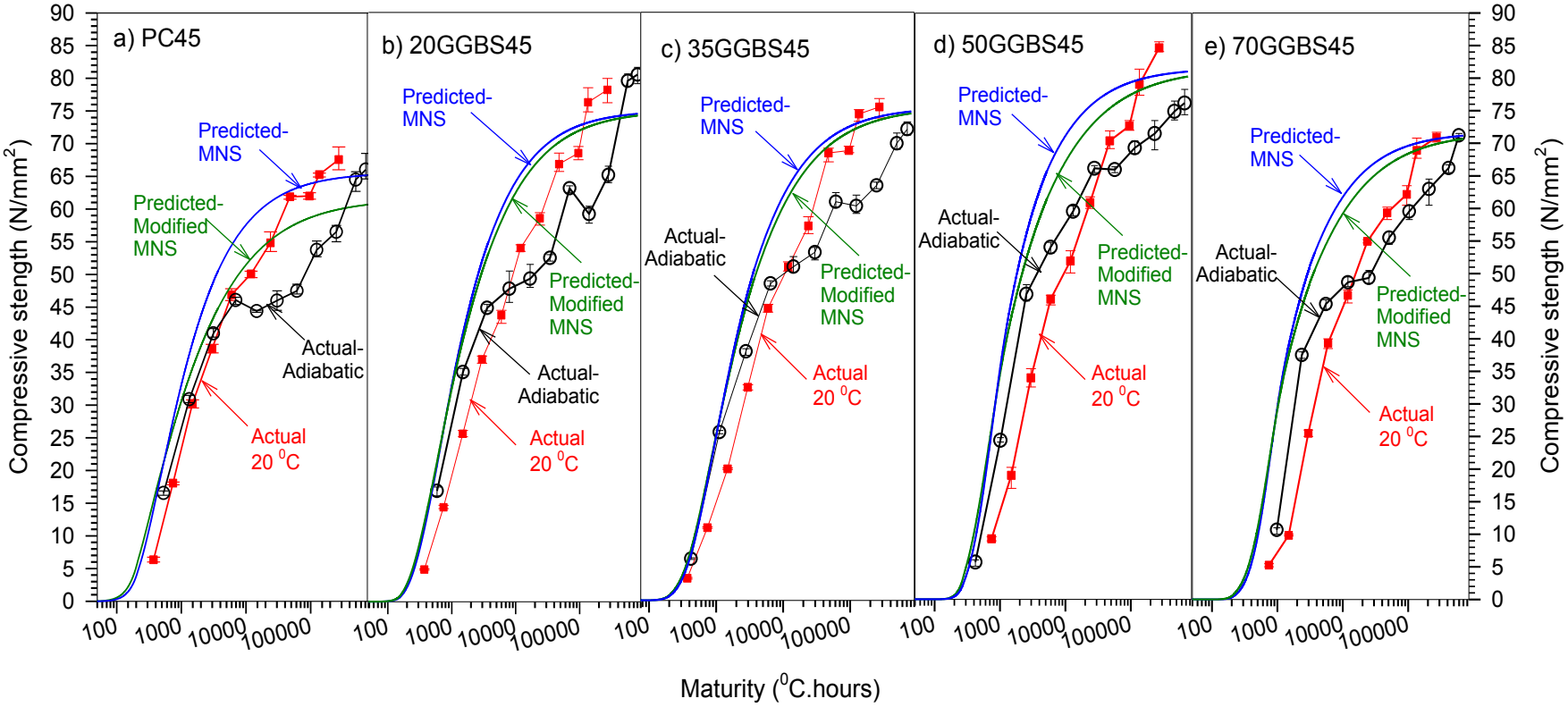

Figure 6.42: Predicted strength of concrete cured under adiabatic condition concrete **grade C45** using the MNS method and the Modified MNS proposed in this study

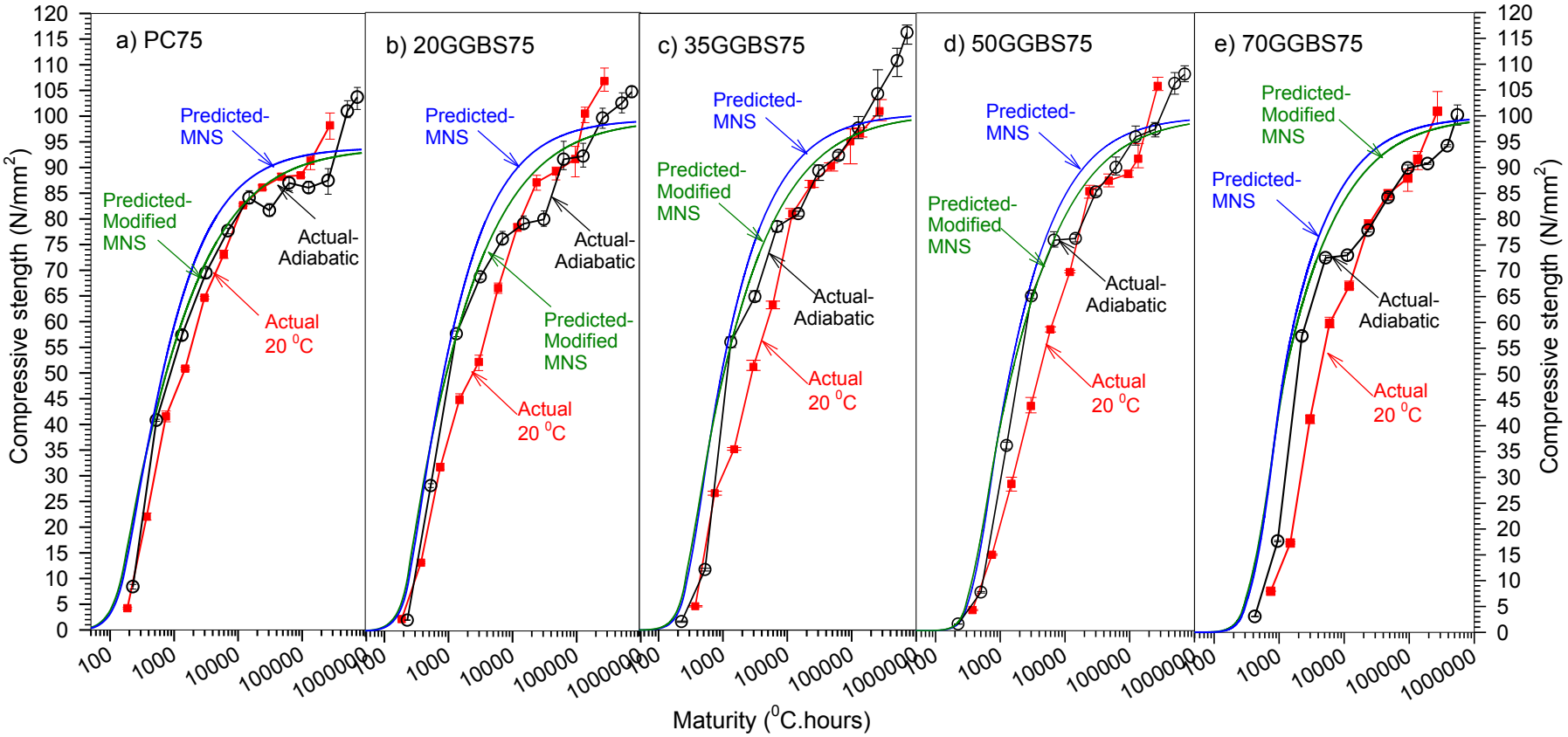

Figure 6.43: Predicted strength of concrete cured under adiabatic condition concrete **grade C75** using the MNS method and the Modified MNS proposed in this study

The strength ratio between the predicted and the actual adiabatic strength of all concretes are presented in Figures 6.44 and 6.45 for concretes grade C45 and C75, respectively. The model seems to be more accurate in predicting GGBS concretes.

In Portland cement concrete grade C45, the model predicts the adiabatic of the concrete strength good enough from age 4-days until 8-days, where the predicted strength reaches over 90% of actual strength. The predicted strength is then higher than the actual strength, as the actual adiabatic strength development of the concrete drops from the age to 16-days, while the model predicts the strength to continue increasing. This is believed to be due to the detrimental effect of the high early age curing temperature. However, the actual adiabatic strength of the concrete increases again from age 32-days and later, even if it is higher than that predicted at later ages.

Similar in concrete with 20, 35 and 70% of GGBS, the model predicts the adiabatic strength quite well up to age 8-days, even for 20% GGBS concrete up to 4-days, where the errors are within 10%; the model then overestimates the strength at later ages. In the 50% GGBS concrete, the model predicts the strength reasonably well from age 2-days until age 365-days, where the errors are less than 10%.

There is an indication that the inaccuracy of the proposed model in predicting the strength due to the detrimental effect of the high early age curing temperature, where the strengths development after 4-days or later ages increase slowly. Even the strength is decreased as happened in Portland cement concrete at age 8-days, 20% GGBS concrete at age 64-days, etc.

The predicted adiabatic strengths of grade C75 concretes appear to be more accurate than that of grade C45. The model predicts the adiabatic strength development reasonably well from age 4-days until age 365-days, where the errors are within 10%, except the predicted strength of the 50% GGBS concrete at age 4-days. The model underestimates the strength of the concrete at this age and

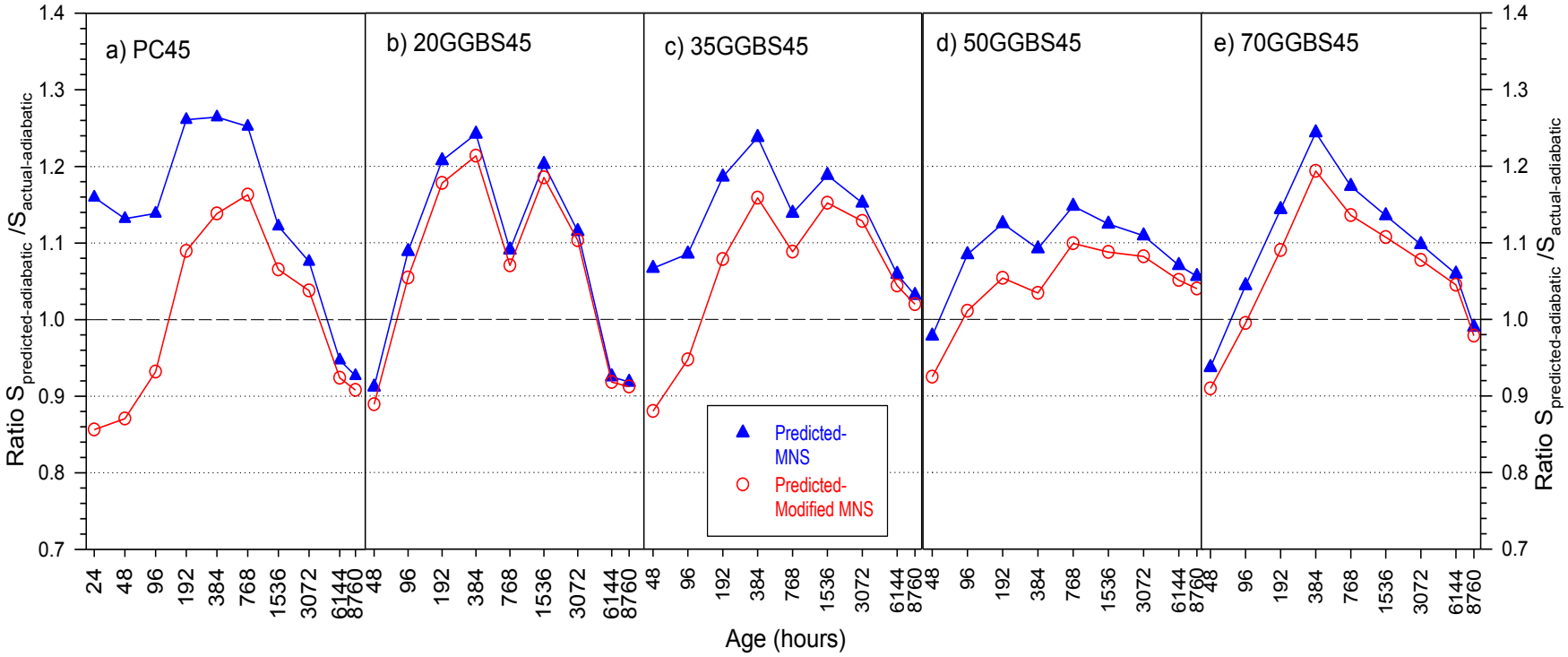

Figure 6.44: $S_{predicted}/S_{actual}$ of adiabatic strength development of concrete **grade C45** using the MNS method and the Modified MNS proposed in this study

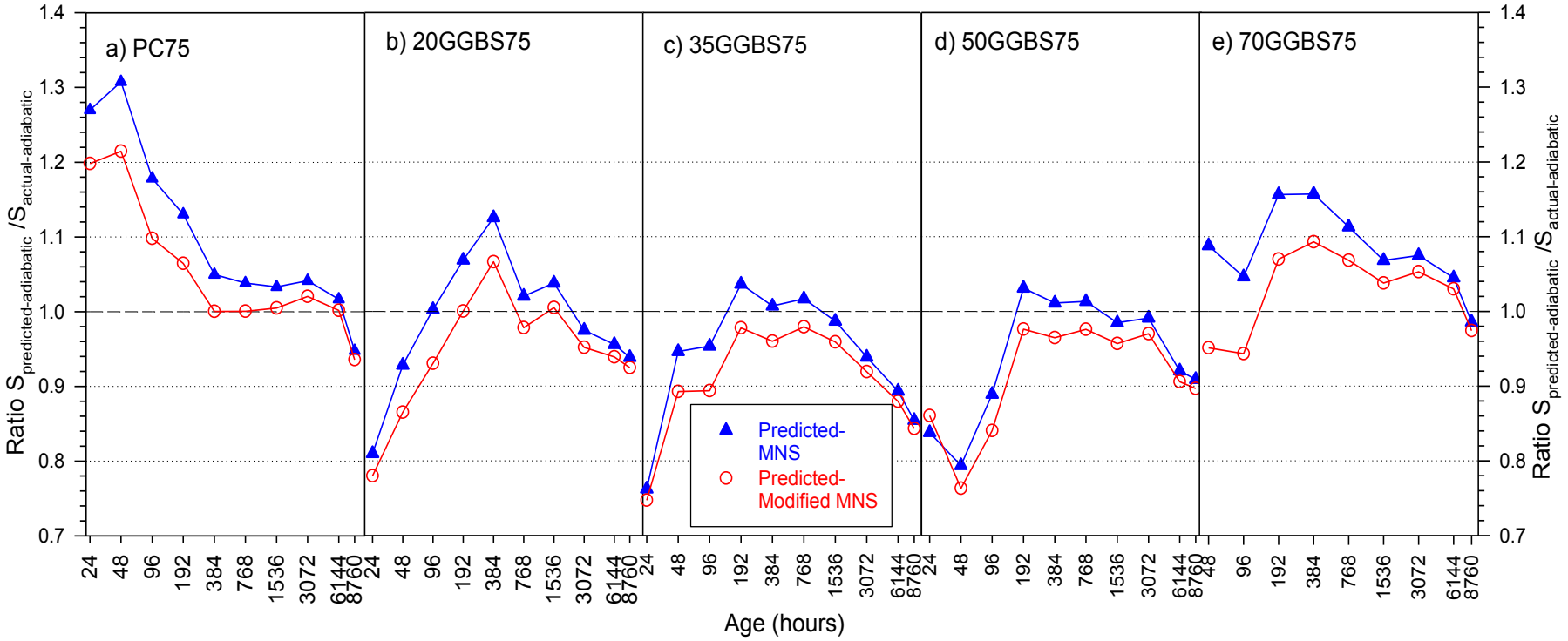

Figure 6.45: $S_{predicted}/S_{actual}$ of adiabatic strength development of concrete **grade C75** using the MNS method and the Modified MNS proposed in this study

the accuracy of the predicted strength only reaches 84%. However, the model predicts the strength development of the concrete from age 8-days to age 128-days very well, where the errors are less than 5%. It is believed that the detrimental effect of the high early age curing temperature to the concrete grade C45 seem to be less than that in grade C75.

6.6. Summary

The summary of this chapter can be drawn as follows:

- The apparent activation energy (Ea) values for both the grades of concrete (C45 and C75) determined from the two methods (ASTM standard and TPE) were found to be similar. For the concrete that have the same grade, the higher levels of GGBS, the higher the activation energy values.
- The C-NS model predicts the strength of concrete more accurately using the datum temperature (T_0) calculated according to ASTM C-1074 at very early age to 4-days, which is similar with the predicted strength using the TPE-Arr model.
- Both AJ-05 and AJ-06 models overestimate the strength up to age 12-hours from casting time, both the models then underestimate the strength from age 1-day onward.
- The K&D, C&D and Modified AJ-06 models appear to predict the strength of concrete quite well up to age 8-days and look to have potential to be improved in predicting strength development of concrete.
- The predicted strength of concrete using the MNS method proposed by Soutsos[166] and the improved MNS method proposed in this study seems to be more accurate in predicting the strength of GGBS concrete. Both the methods predict the strength of concrete following the actual strength curve. The modified MNS method proposed in this study take into account the effect of higher curing temperature to the time efficiency factor (η), which it improves the accuracy of predicted strength.

CHAPTER 7 – HEAT OUTPUT OF HYDRATION – RESULTS AND ANALYSIS

7.1. Introduction

The heat output of hydration of the equivalent mortar mixes of the concrete grades C45 and C75 are presented in this chapter. The mortars were cured under isothermal curing conditions for temperatures: 20, 30, 40 and 50^0C. The effect of GGBS on the heat output of hydration at different curing temperatures was also investigated. The results of heat output could also be used to determine the apparent activation energy and compared to that obtained using strength data. The recorded heat of hydration under varying isothermal temperature conditions is used to predict the heat output and adiabatic temperature rise. The in-situ temperature rise could be predicted using the estimated heat of hydration.

7.2. Recording the Heat Output of Hydration Using an Isothermal Calorimeter

The isothermal Tam-Air calorimeter equipment was used to measure the heat output of hydration of mortar mixes cured at different temperatures, as mentioned in Chapter 4. The mixtures of the mortars used to measure the heat output of hydration are the same to that of used to investigate the strength development of the mortars cured at different temperatures, which are presented in Tables 4.6 and 4.7 in Chapter 4.

The isothermal calorimeter recorded the heat output rate of the mortars in milli watts. The recorded heat outputs were then converted into the mortar's heat output rate per kg of binder, which depended on the weight of specimens and the density of the mortar calculated from the following equation:

$$q_M = \frac{heat\ output\ recorded\ (Watt)}{weight\ of\ specimens\ (kg)\ X\ \frac{binder\ content\ of\ mortar\ (\frac{kg}{m^3})}{mortar\ density\ (\frac{kg}{m^3})}} \quad \text{Equation 7.1}$$

where q_M is the heat output rate per kilogram binder of mortar, in W/kg.

The heat output per kilogram binder of mortar for both mortar grades C45 and C75 are presented in Figures 7.1 and 7.2, respectively. Generally, both figures show that the higher the curing temperature, the earlier and higher of the peak of hydration reached. The heat output of the same mix, as expected, depends on the curing temperature. A similar trend was observed for the mortar strength development under isothermal conditions discussed in Chapter 5, where at the earlier age the higher curing temperature has the higher strength rate.

The peaks of heat output of hydration of mortars cured at the same temperature decreased by increasing the replacement levels of GGBS. For the same mix of mortar, the higher isothermal curing temperature resulted in higher peaks of heat output and also reached the peak of hydration earlier. At a curing temperature of 20^0C for all mortars, there were two peaks observed. The first peak was slightly lower than the second peak as the level of GGBS increased. This is believed to be due to the heat output produced by the secondary reaction of the hydration of GGBS, as has been discussed in Section 2.4.3.5. Furthermore, the second peak heat output for the C45 mortars with lower replacement levels of GGBS i.e. less than 50%, were not as clear as that of the higher replacement levels of GGBS.

Conversely, the second peak of the hydration of both mortars C45 and C75 with 70% of GGBS cured at 50^0C were lower than that of the first peak. This is believed to be due to the hydration of GGBS being immediately followed the hydration of cement when the mixing water added. However, at a curing temperature of 20^0C, the hydration of GGBS was delayed, as the mortar needed time to achieve the activation energy to start the GGBS reaction.

Both Figures 7.1 and 7.2 show that the use of GGBS in concrete can reduce the heat output rate of hydration, and consequently reduce the rise of temperature produced in the hydration process of concrete. This can reduce the cracking risk of the concrete at earlier age by reducing the temperature gradient between the surface and the inside of the concrete. The higher the level of GGBS replacing the cement in concrete, the more the temperature rise can be reduced. In addition, the

rate of heat output is highly dependent on temperature, time and the levels of cement replacement by GGBS.

It is important to note that the data recorded during the first 1.5 hours after the mortar was put into the isothermal calorimeter is not used in the analysis as the isothermal calorimeter was still equilibrating. This means that only the heat output produced in the main reaction phase was analysed.

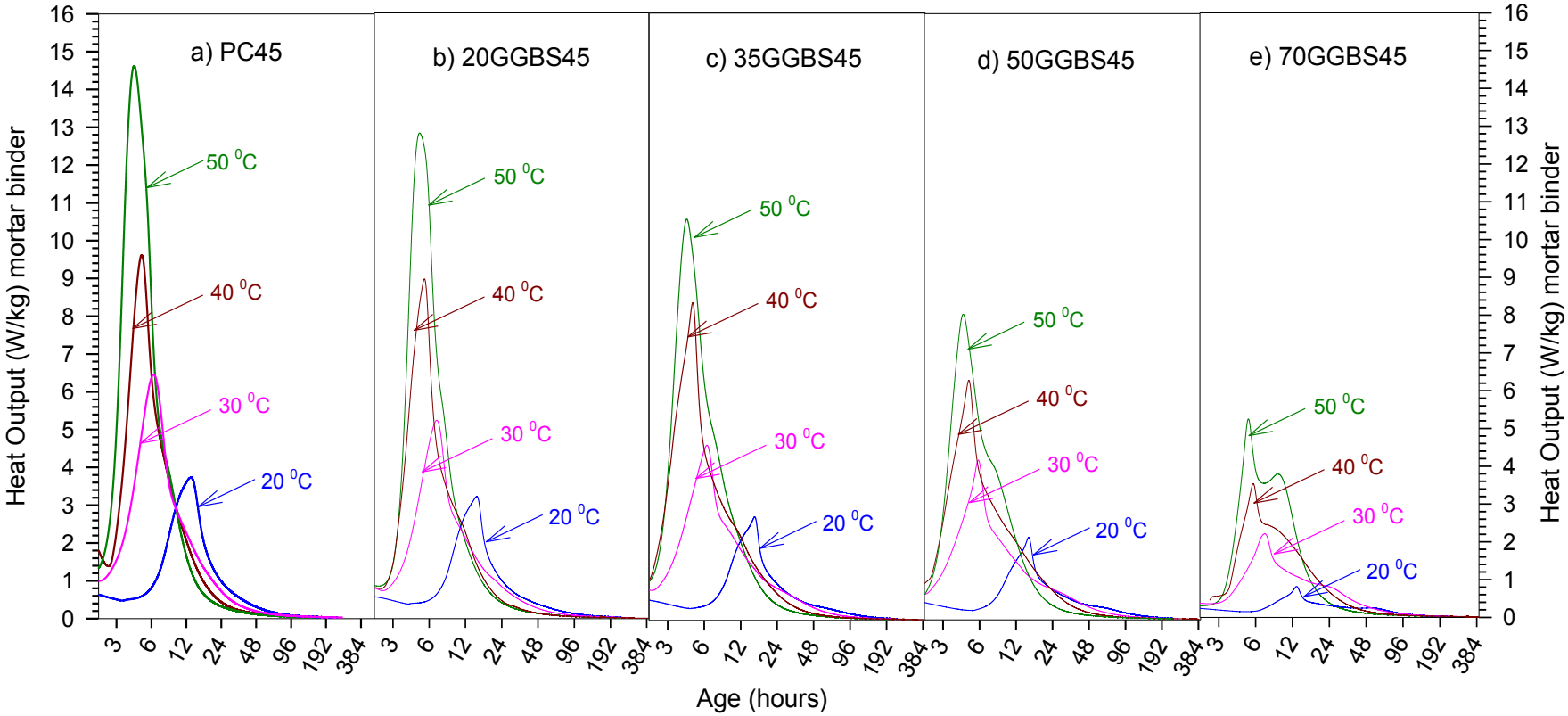

Figure 7.1: Heat output per kilogram binder of mortar **grade C45** cured at 20, 30, 40 and 50^{0}C

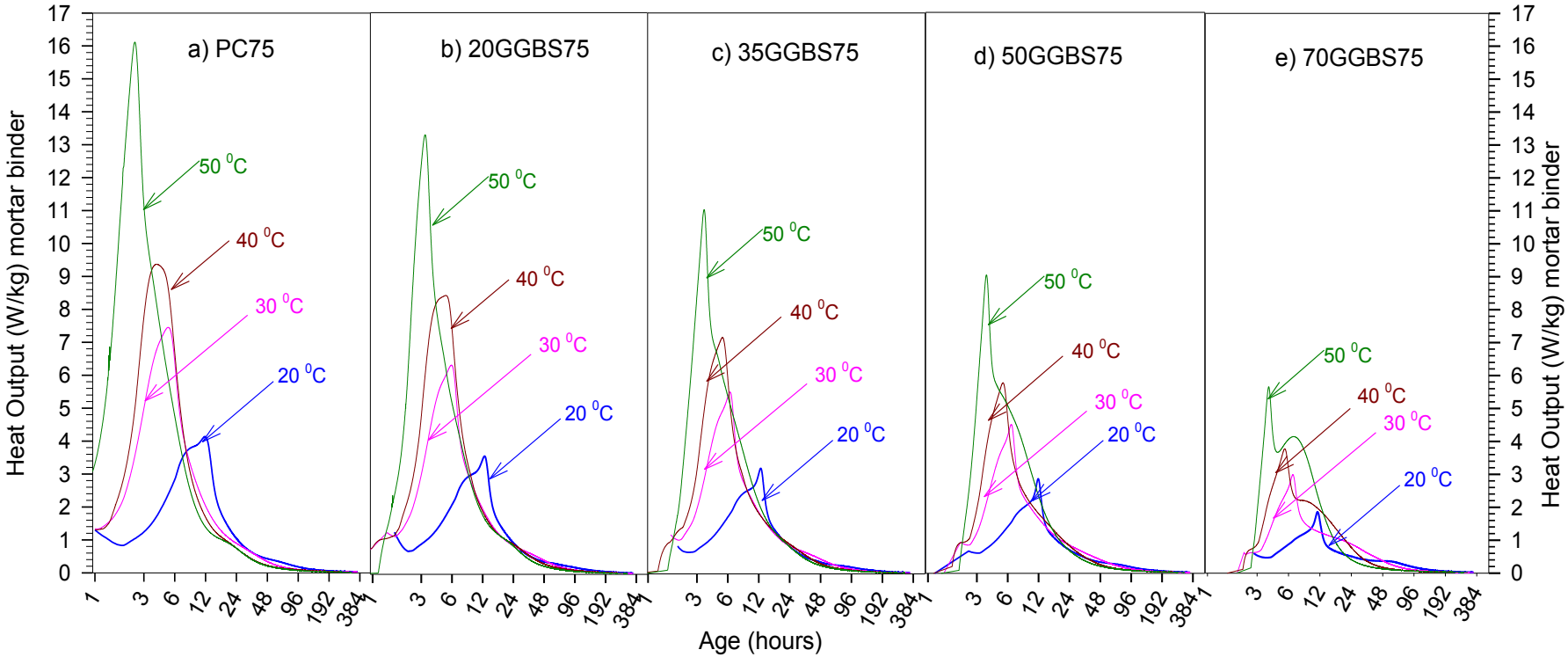

Figure 7.2 Heat output per kilogram binder of mortar **grade C75** cured at 20, 30, 40 and 50^{0}C

7.3. Heat Output of Concrete Cured Under Adiabatic Condition

The heat outputs of the mortar cured under isothermal conditions recorded by the isothermal calorimeter were converted into the heat output per kilogram binder of the concrete that was equivalent to the mortar using the equation as follows[144]:

$$q_C = \frac{B_C}{\gamma_C}\ q_M \qquad \text{Equation 7.2}$$

where:

q_c = heat output per kilogram binder of concrete (W/kg).

B_C = binder content of concrete (kg/m^3)

γ_c = density of concrete (kg/m^3)

q_M = heat output per kilogram binder of mortar (W/kg).

The rate of heat output of concrete per cubic meter cured under isothermal condition was then calculated using the following equation[144]:

$$Q_C = q_C\,\gamma_C \qquad \text{Equation 7.3}$$

where:

Q_C = the rate of heat output of concrete (W/m^3)

Assuming that the specific heat capacity of concrete, $C_{p,}$ remains constant, the rate of heat output of concrete cured under adiabatic conditions can be determined using the equation as follows:

$$Q_C = \frac{\Delta T\ C_P\ \rho}{\Delta t} \qquad \text{Equation 7.4}$$

where:

Q_C = Heat output rate of concrete (W/m^3)

ΔT = difference temperature (adiabatic temperature) during time interval Δt (^{0}C)

Cp = specific heat capacity of concrete (880 J/^{0}C kg)

Δt = time interval (seconds)

ρ = density of concrete (kg/m^3)

The specific heat capacity which was used for all the concrete mixes, was 880 $J/^0C$ kg taken from literature reviews[144]. As the specific heat capacity and density used remained constant during the test, the trends of heat output rate of concrete is identical to the adiabatic temperature rise of the concrete.

The adiabatic concrete heat output rates (shown as green curves) were smoothened using Sigma Plot to remove the data noise as shown in Figures 7.3 and 7.4 for concrete grades C45 and C75, respectively. Many trials have been carried out to find the best fit-curve of the smoothed data. It was found that the negative exponential smoother with the value of sampling proportion of 0.035 and using the 3^{rd} order polynomial regression was the best way to smoothen or remove the data noise. The results are shown as black curves in both figures.

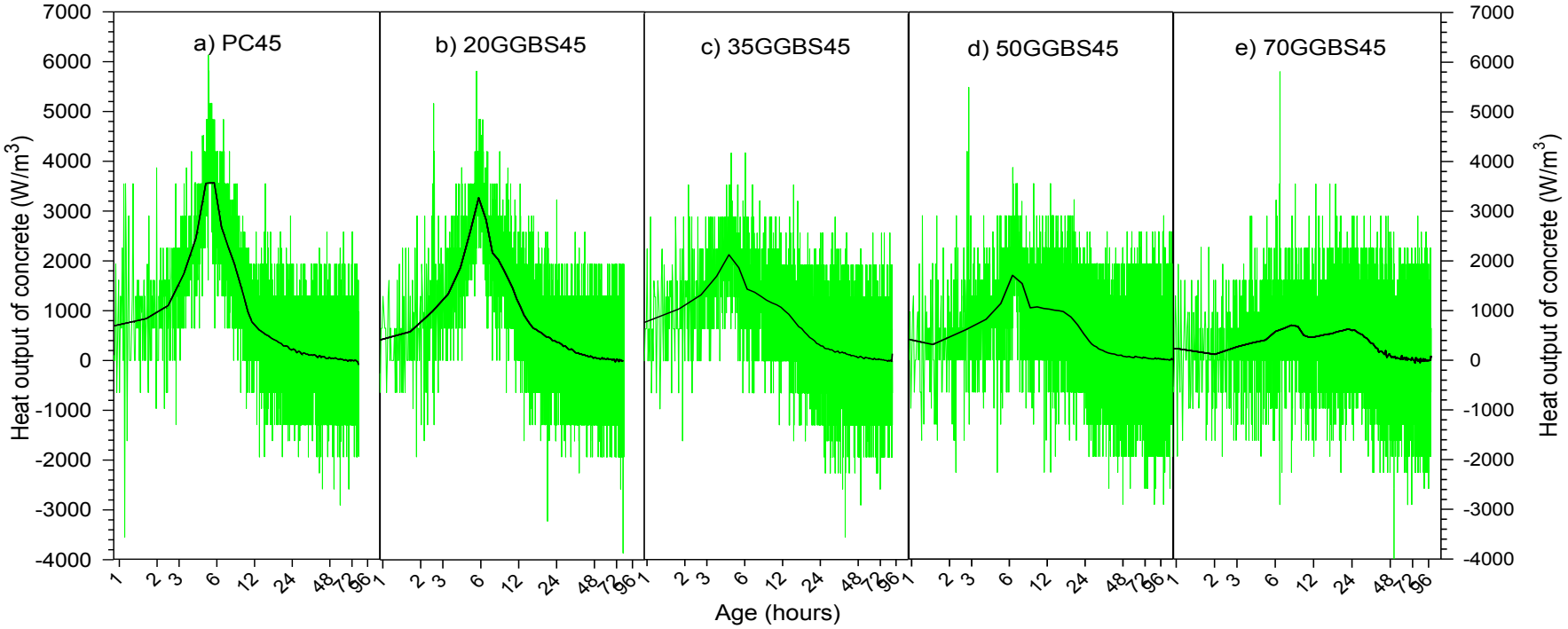

Figure 7.3: Smoothing the adiabatic heat output rate for concretes **grade C45**

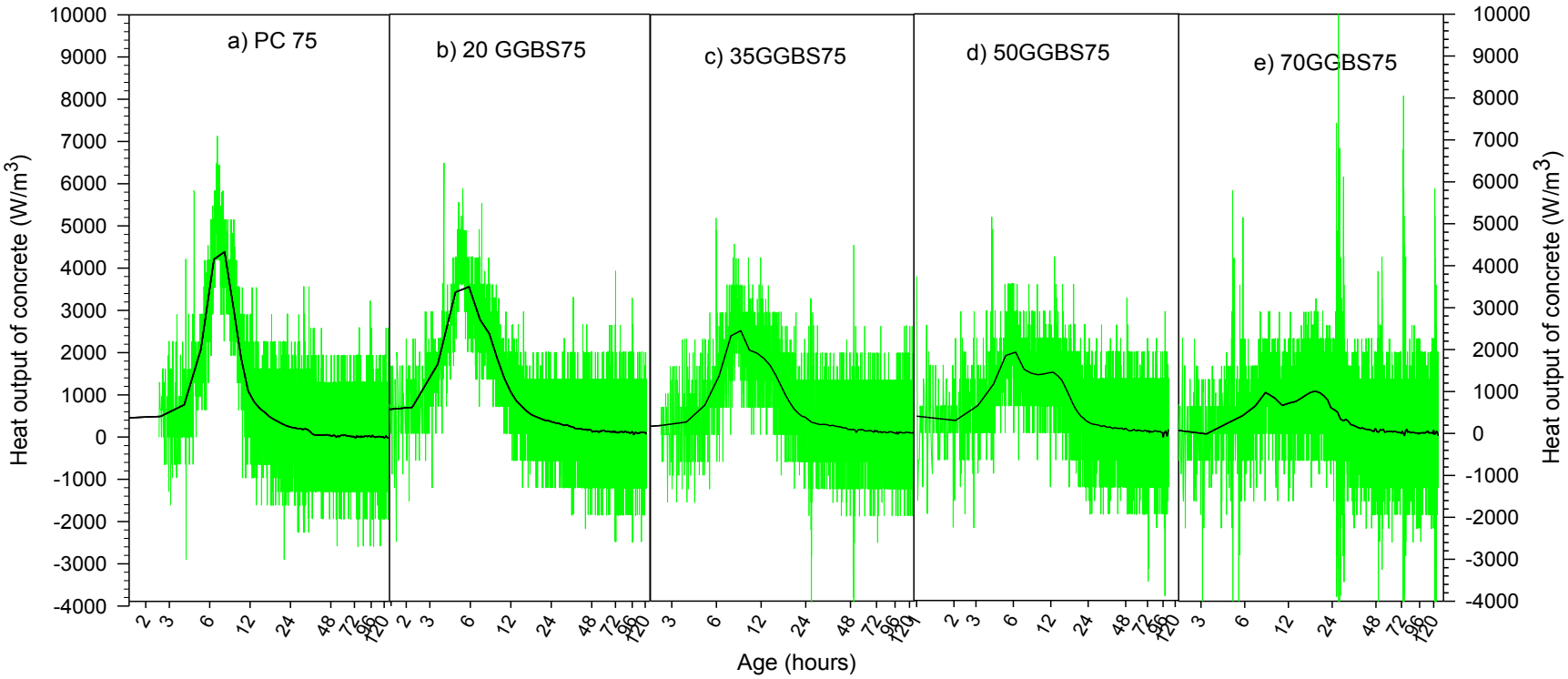

Figure 7.4: Smoothing the adiabatic heat output rate for concretes **grade C75**

The rate of heat output of concrete cured under adiabatic condition was then plotted with that obtained from the equivalent mortar mixes using isothermal calorimeter cured under isothermal temperatures. The results are presented in the Figures 7.5 and 7.6 for concretes grades C45 and C75, respectively.

The peak of heat output of concretes cured under adiabatic conditions appeared later than the peak of heat output of the same concrete mix cured at higher isothermal temperatures i.e. 40 and 50^0C. The exception is for PC mortar grade C75 cured at 40^0C, as shown in Figure 7.6a. The peak of the adiabatic heat outputs for all mortars, however, appeared earlier than that of the same concrete mix cured at 20^0C. Although the second peak of the adiabatic heat outputs were reached after the peak of the heat outputs of the same concrete mix cured at 20^0C. These occurred particularly for concretes grades C45 and C75 with 70% of GGBS as shown in Figures 7.5e and 7.6e.

For concrete grade C45 cured under adiabatic curing conditions, the replacement of 70% of the cement with GGBS decreased the peak of heat output significantly, by about 80%. It was decreased from 3600 W/m^3 (mortar with PC only) to 700 W/m^3 (mortar with 70% GGBS). In comparison to the heat of output mortar cured under standard temperature (20^0C), the replacement of cement with GGBS by 70% reduced the peak of heat output by 43.75%. It was decreased from 1600 W/m^3 (concrete with PC only) to 900 W/m^3 (concrete with 70% GGBS).

For concretes grade C75 cured under adiabatic condition, the replacement of 70% of the cement by GGBS resulted in a reduction of the peak of heat output. This was decreased from 4700 W/m^3 (concrete with PC only) to 1000 W/m^3 (concrete with 70% GGBS); a decreased of 78.70%. While for the concrete cured at 20^0C, the replacement of 70% of the cement with GGBS decreased the peak heat output by 68.75%. It was decreased from 1600 W/m^3 for concrete with PC only to 500 W/m^3 for 70% GGBS concrete. These indicate that GGBS concrete is highly dependent on the curing temperature. The lower curing temperatures result in the lower rates of heat output.

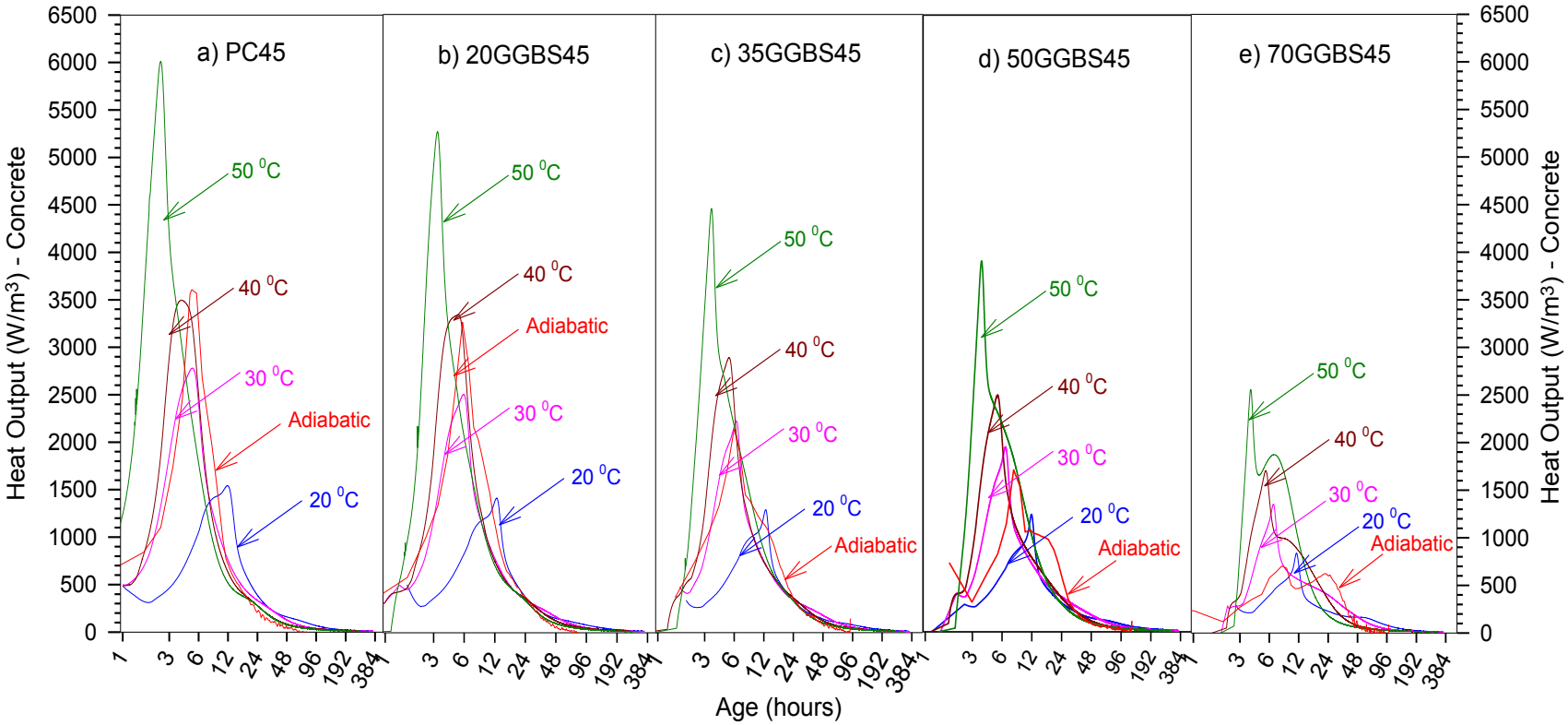

Figure 7.5: Comparison the heat output rate obtained from adiabatic curing conditions to that of cured under isothermal condition for concrete **grade C45**

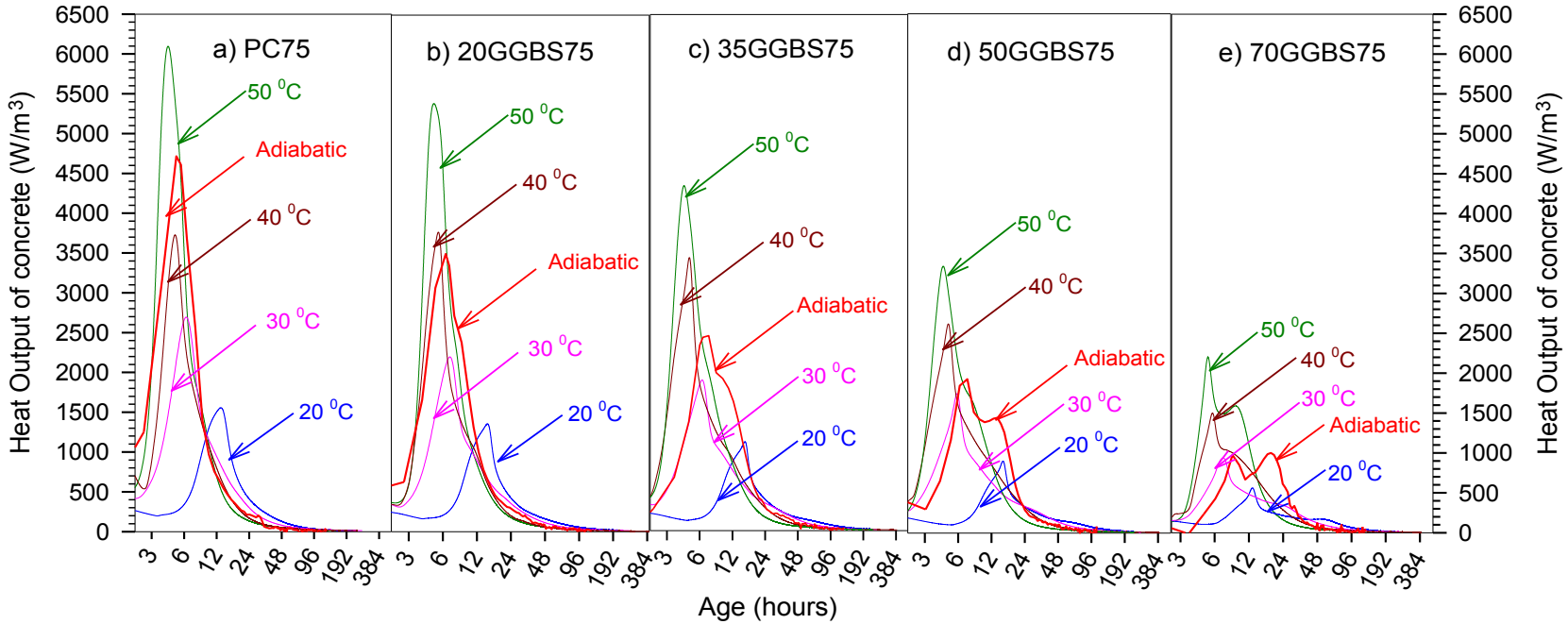

Figure 7.6: Comparison the heat output rate obtained from adiabatic curing conditions to that of cured under isothermal condition for concrete **grade C75**

In addition, the rate of heat output of the PC concrete mixes were higher than that of GGBS concrete mixes. For the same curing temperature, the higher the level of GGBS replacing the Portland cement, the lower the rate of heat output. For the same concrete mix, the higher curing temperature, the higher the rate of heat output obtained. The rate of the heat output of a GGBS concrete mix cured under adiabatic conditions was generated between the heat outputs of the same concrete mix cured isothermally between 20 and 40^0C.

7.4. Estimation of Cumulative Heat Output

The cumulative heat output of concrete that were cured under adiabatic conditions and isothermal temperatures of 20, 30, 40 and 50^0C can be seen in Figures 7.7 and 7.8 for concrete grade C45 and C75 respectively. The cumulative heat outputs of the concrete cured under adiabatic conditions were calculated using the following equation:

$$Q_{cum,adb} = \sum_0^t \Delta T \,.\, C_p \qquad \text{Equation 7.5}$$

where:

$Q_{cum,\,adb}$ = Cumulative heat output of concrete cured under adiabatic conditions, during time, t (J/kg)

The cumulative heat output of concrete cured under isothermal temperature was calculated using the equation as follows:

$$Q_{cum,ish} = \sum_0^t q_C \, \Delta t \qquad \text{Equation 7.6}$$

where:

q_c = heat output rate in W/kg of concrete binder , using Equation 7.2.

Δt = time interval of recording data, (seconds)

$Q_{cum,\,ish}$ = Cumulative heat output of concrete cured under isothermal temperature, J/kg.

Generally, the heat outputs of the concretes with GGBS cement replacement levels up to 50% were similar to that of concrete with Portland cement only. Exceptions are for GGBS concrete for grades C45 and C75 with replacement level of cement by GGBS of 70%. The heat output of concrete cured under adiabatic

conditions with 70% GGBS decreased significantly compared to that of PC concrete for both concrete grades C45 and C75. The heat output decreased from 41,484 to 25,971 J/kg (37.4%) and from 44,540 to 29,454 J/kg (33.8%) for concrete grades C45 and C75, respectively as shown in Figures 7.7 and 7.8.

The crossover effects on the heat output of the concrete, which was due to a higher curing temperature at earlier age, appeared similar to that which occurred in the strength development. The crossover effect appeared to be occurring much later, as the level of GGBS in concrete increased.

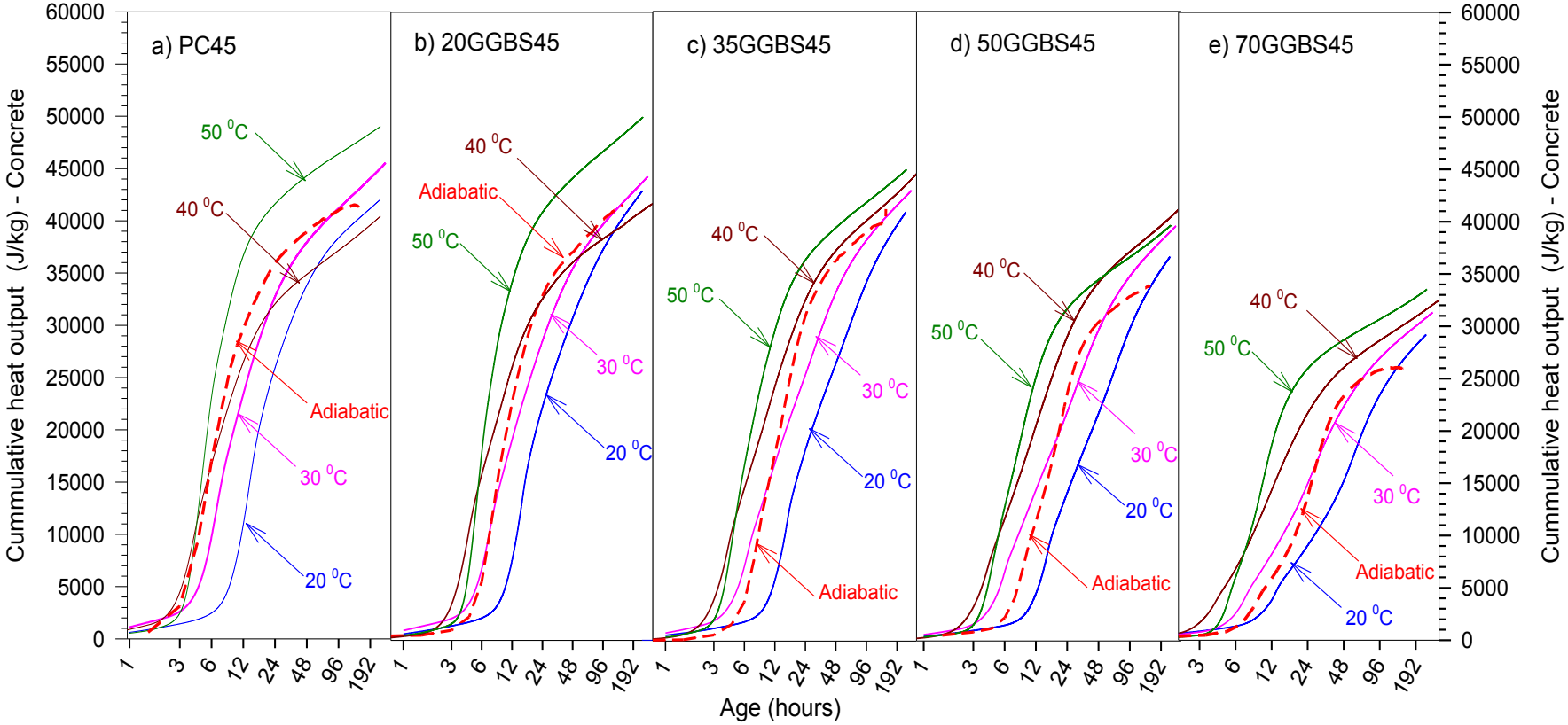

Figure 7.7: Cumulative heat output (J/kg) of concrete **grade C45** obtained from specimens cured under adiabatic conditions and under isothermal temperatures of 20, 30, 40 and 50^{0}C

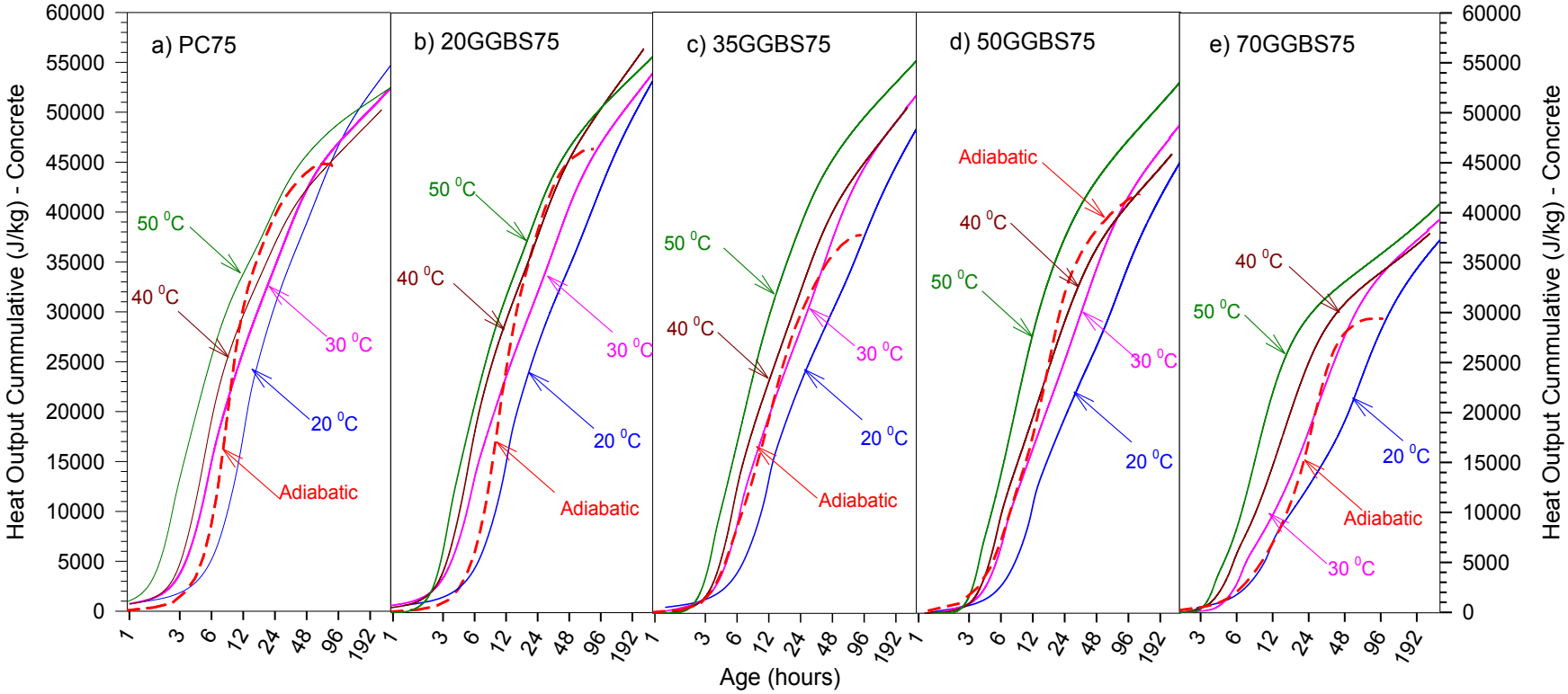

Figure 7.8: Cumulative heat output (J/kg) of concrete **grade C75** obtained from specimens cured under adiabatic conditions and under isothermal temperatures of 20, 30, 40 and 50^{0}C

7.5. Estimation of the Apparent Activation Energy

The heat outputs that were measured using the isothermal calorimeter can be used to estimate the apparent activation energy. The heat output describes the rate of the reaction of concrete, therefore, the relationship between the degree of hydration and the curing temperature follows Arrhenius' law. The relationship can be expressed by rewriting Equation 2.38 discussed earlier in the literature review chapter, as follows[144, 145]:

$$q(T) = A\, e^{-\frac{E_a}{R\,T}} \qquad \text{Equation 7.7}$$

$$\ln\,(q(T)_{max}) = \ln A\; x\; (-\frac{E_a}{R\,T}) \qquad \text{Equation 7.8}$$

Wadso[410] reported that the maximum heat output rate of a mix cured at any temperature occurs at the same degree of hydration. Therefore, the apparent activation energy can be determined by plotting *ln* (q_{max}) versus *1/T* as shown in Equation 7.8. A regression analysis was then carried out to find the best-fit line as shown in Figure 7.9. The slope of the best-fit line is equal to $-E_a/R$, where R is the universal gas constant. The results are presented in Table 7.1 as follow:

Table 7.1: Apparent activation energy based on the maximum of the heat output data

Grade C45		**Grade C75**	
Mix	**Activation Energy, Ea (J/mol)**	**Mix**	**Activation Energy, Ea (kJ/mol)**
PC45	34.80	PC75	33.91
20GGBS45	36.84	20GGBS75	33.33
35GGBS45	36.80	35GGBS75	31.35
50GGBS45	34.32	50GGBS75	29.06
70GGBS45	35.93	70GGBS75	20.96

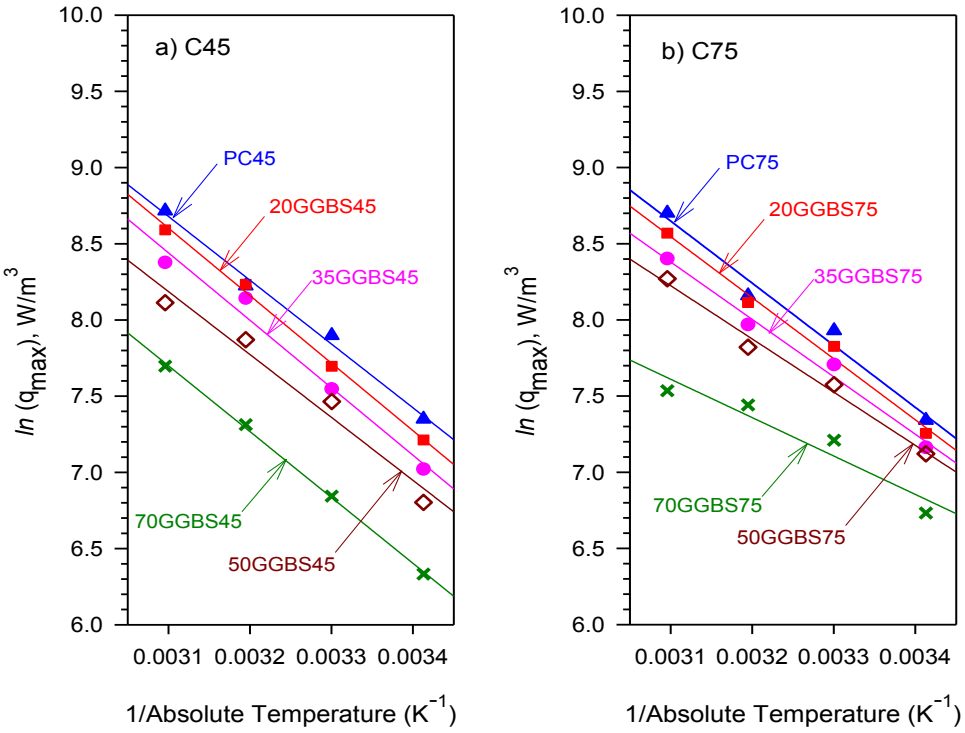

Figure 7.9: *ln* (q_{max}) versus *1/T*

The results of activation energies for both concrete grades C45 and C75 in Table 7.1 above appeared to be slightly lower than those determined based on the strength development of the mortar, as shown in Table 6.2 of Chapter 6. Exceptions were for concrete with Portland cement only, where the activation energies of the mortar were similar.

The accuracy of the activation energies for the GGBS concrete grade C75 was not satisfactory. It appears to be hampered by the fact that the maximum (peak) of the heat output of GGBS concrete cured at different temperatures was not too different compared to that of concrete with Portland cement only. As a result, the slopes of the best fit line of the peak of heat output for the GGBS mortar obtained from linear regression were small. Therefore, the activation energy of the GGBS mortar decreased as the GGBS levels increased, which was the inverse of that obtained using the strength development data.

The activation energies of the mortar grade C45 obtained from the heat output data, however, appeared to be still comparable to that obtained from the strength development data; although the activation energy for GGBS mortar with higher replacement levels appeared slightly lower than that obtained from the strength development data.

An alternative method uses the Three Parameter Exponential (TPE), based on the rate constant, τ, was recommended by Pole et al[146] and Schindler[154] for estimating the apparent activation energy. Hansen, Freiesleben and Pedersen[121] proposed Equation 2.143 to determine the degree of hydration at an equivalent age.

The degree of hydration could be described as the development of the cumulative heat output, which was developed by using the data obtained from the isothermal calorimeter. Equation 2.143 in Chapter 2 can then be rewritten as follows[154]:

$$Q(t_e) = Q_u . \exp\left(-\left(\frac{\tau}{t_e}\right)^a\right) \qquad \text{Equation 7.9}$$

where:

$Q(t_e)$ = the cumulative heat output at equivalent age, t_e

Q_u = the ultimate cumulative of heat output (J/kg)

Linear regressions were carried out to determine the parameters of hydration time, hydration shape and the ultimate cumulative heat output of hydration by fitting the TPE equation on the cumulative heat output data. The *ln (τ)* is then plotted against *1/T* as shown in Figure 7.10 to find out the best fit line through the data points plotted. The slope of the best fit line is equal to *Ea/R*.

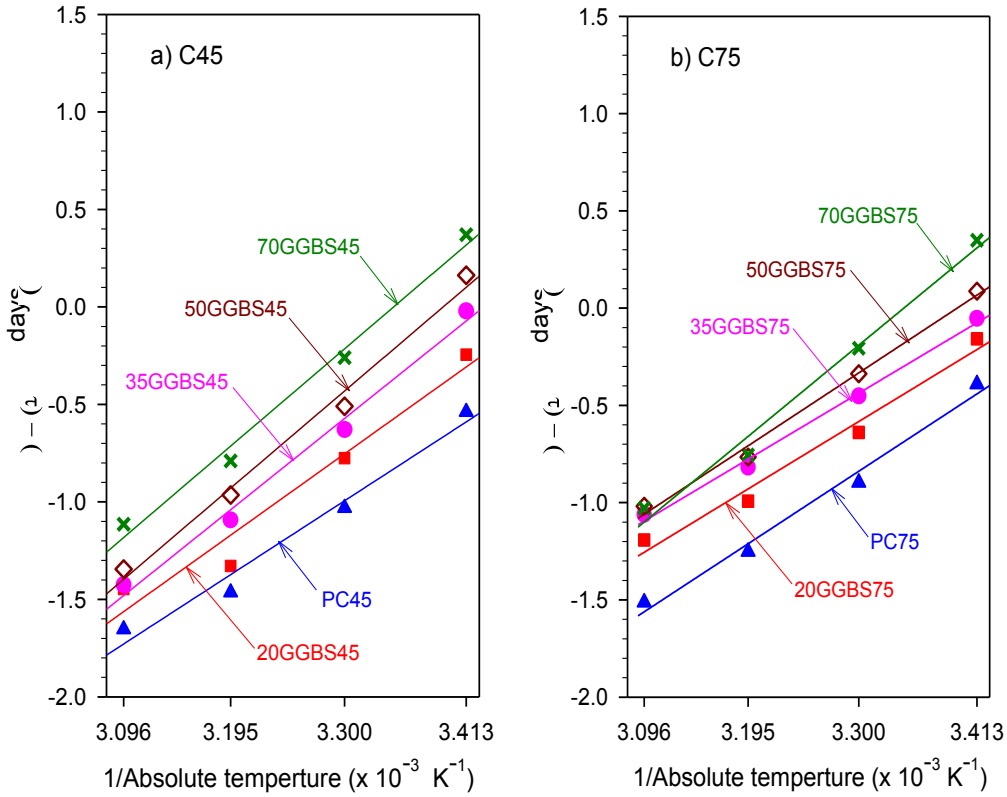

Figure 7.10: *ln (τ)* versus *1/T*

The apparent activation energies, which are obtained using the TPE equation are presented in Table 7.2.

Table 7.2: The apparent activation energy based on the cumulative heat output of hydration using the TPE equation

Grade C45		**Grade C75**	
Mix	**Activation Energy, Ea (J/mol)**	**Mix**	**Activation Energy, Ea (J/mol)**
PC45	29.87	PC75	29.39
20GGBS45	32.90	20GGBS75	27.33
35GGBS45	36.93	35GGBS75	26.74
50GGBS45	39.27	50GGBS75	29.54
70GGBS45	39.34	70GGBS75	36.96

The results that are shown in Table 7.2 appear more comparable to the values of activation energy obtained from strength development data (Table 6.2), compared to those presented in Table 7.1, which were determined based on the peak of heat output. The values of the apparent activation energy shown in Table 6.2 Chapter 6 varied from 28 to 55 kJ/mol.

7.6. Prediction of the Cumulative Heat Output of Concrete

The heat outputs of the specimens cured under isothermal temperature could be used to predict the heat output for concrete cured under non-isothermal curing regimes such as adiabatic conditions. The procedure that was used to predict the heat output of the concrete cured under adiabatic conditions was similar to that used to predict the adiabatic strength development, which has been discussed in the Section 6.5 Chapter 6.

Freiesleben Hansen and Pedersen[121] suggested the Three Parameter Equation (TPE) to describe the heat cumulative output (J/kg) as follows:

$$Q = Q_{\infty}\, e^{-(\frac{\tau}{M})^{a}} \qquad \text{Equation 7.10}$$

where:

Q_{∞} = the ultimate of heat output, J/kg

M = maturity index, calculated using Equation 2.28

τ = characteristic time of hydration

a = shape factor of hydration

Regression analyses were carried out based on the Equation 7.10 for all mixes curing temperatures to determine the parameters of Q_{∞}, τ, and a (presented in the Appendix E). The parameters of acceleration, compression and temperature efficiency factors, which were obtained from the mortar strength development curves, has been discussed in Chapter 6 (Table 6.16). The parameters can be used to transform the cumulative heat output from the curing temperature of 20^0C to the temperatures of 30, 40 and 50^0C.

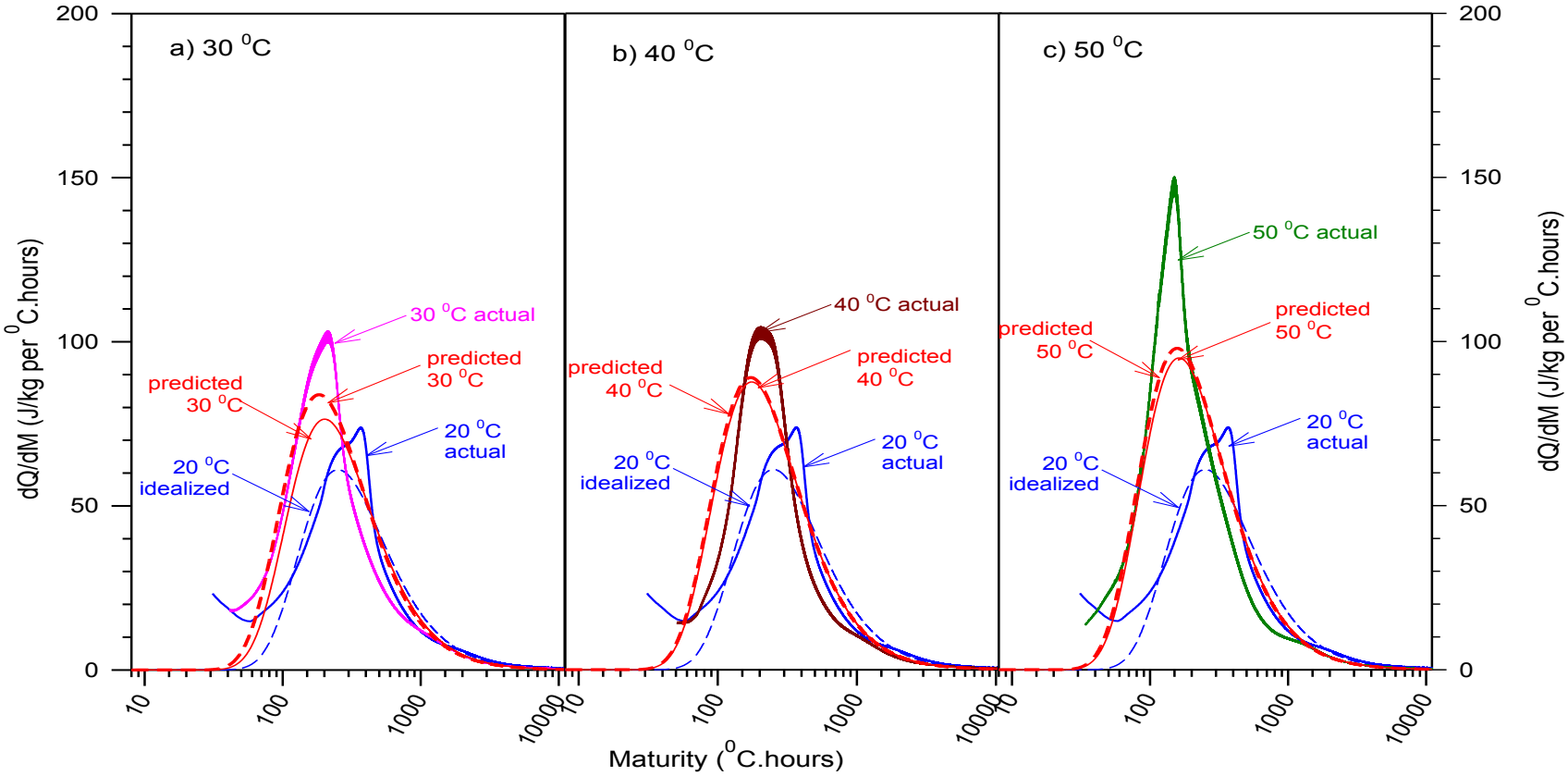

Figure 7.11: Comparison the prediction of heat output rate using the acceleration and compression factors obtained from the heat output (solid line) to that of obtained from strength development (dash line), PC mortar **grade C45**

The predicted heat output rates were described in Figure 7.11 for PC mortar grade C45 by the red solid and dash lines for the predictions using the parameters obtained from the heat output and strength development, respectively. The prediction of the heat output rates using the strengths data were compared to those using the heat outputs and were seen to be similar. However, when the parameters obtained from the strength data was used to predict the heat output of GGBS concrete cured at temperatures higher than 20^0C, the results showed an overestimate the actual heat outputs.

A transformation of the heat output of the concrete cured at 20^0C to those cured at 30, 40 and 50^0C using the heat outputs data was carried out to determine the acceleration, compression and temperature efficiency factors, as was done for strength data in Chapter 6. The acceleration and compression factors were a function of the age conversion factor (ACF) β, as shown in Equations 6.11 and 6.12. The regression analyses were carried out to find out the best relationship between the parameters and the β value. The results are presented in the Table 7.3 and for both grades C45 and C75.

Table 7.3: Parameters accelerator and compression factors obtained from linear regression based on the heat output data.

Mortars grade	**GGBS level (%)**	**$a_C = (dQ/dM)/(dQ/dM)_{20}$**			**$a_M = M_{20}/M$**		
		a	b	R^2	a	b	R^2
C45	0	0.5717	0.4373	0.9881	0.4586	0.5748	0.9750
	20	0.5744	0.4683	0.8984	0.5921	0.4519	0.9125
	35	0.4799	0.5240	0.9942	0.5858	0.4171	0.9825
	50	0.2894	0.6994	0.9839	0.4154	0.5825	0.9764
	70	-0.0303	1.0384	0.9935	-0.0917	1.0995	0.9712
C75	0	0.7501	0.2633	0.9977	0.5586	0.4593	0.9753
	20	0.3275	0.6771	0.9943	0.3275	0.6771	0.9943
	35	1.1196	-0.1192	0.9962	1.0695	-0.0622	0.9937
	50	1.2605	-0.2314	0.9943	1.2818	-0.2736	0.9849
	70	1.2733	-0.2969	0.9880	1.2546	-0.2637	0.9908

The procedures of the MNS method to predict the cumulative heat output of concrete are similar to that of used to predict the strength of concrete. The procedures are as follows:

1. Determine $Q = Q_\infty e^{-(\frac{\tau}{M})^a}$ for the reference temperature, in this case 20^0C, where the shape parameter, *a,* was taken as 1.
2. Predict the cumulative heat output with the acceleration factor a_M, for η = 100%, using the equation as follows:

$$Q = Q_\infty e^{-(\frac{\tau}{a_M M})^a}$$

3. Determine the rate of heat output, dQ/dM for η = 100%.
4. The cumulative heat output Q can then be calculated from the following equation:

$$Q = \sum \frac{dQ}{dM} \eta \Delta M$$

where η is the temperature efficiency factor.

Figures 7.12 and 7.13 show the predicted cumulative heat output for concrete grades C45 and C75, respectively. They were then compared to the actual heat outputs obtained from the isothermal calorimeter. Generally, the method predicted the cumulative heat output accurately as shown in both Figures 7.12 and 7.13 for all mixes and curing temperatures. The accuracy of the predicted cumulative heat outputs, however, appeared slightly decreased as the curing temperature increased. This is believed to be due to the hydration process in concrete with a high level of GGBS reacting more slowly than that of with a low level of GGBS.

The predicted cumulative heat output lines and the idealized/regression lines of the same mix and curing temperature almost overlapped when they were plotted. The idealized data using the regression equation was carried out to fit the actual data obtained from the isothermal calorimeter.

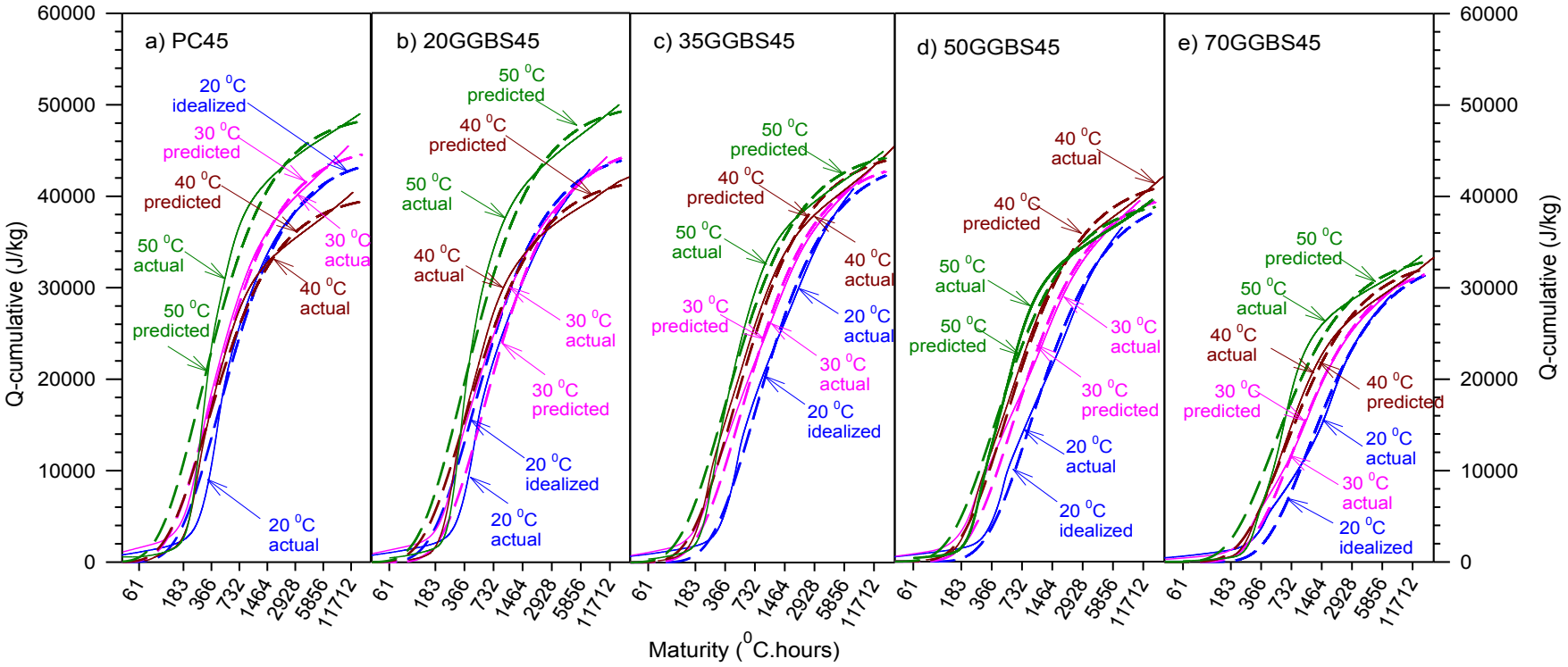

Figure 7.12: Predicted cumulative heat output for curing temperature of 30, 40 and 50^{0}C concrete **grade C45**

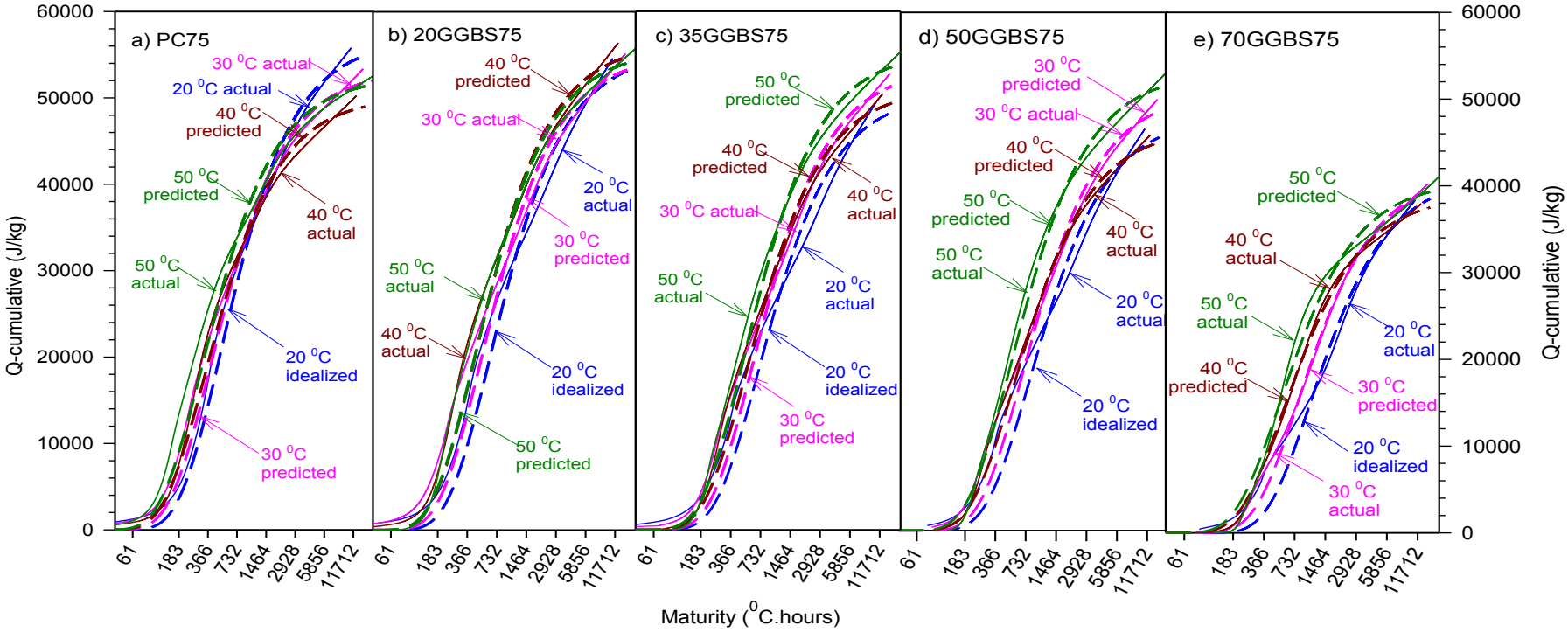

Figure 7.13: Predicted cumulative heat output for curing temperature of 30, 40 and 50^{0}C concrete **grade C75**

Generally, both Figures 7.12 and 7.13 show that the predicted cumulative heat output of concrete with GGBS up to 50% is similar to that of concrete with the Portland cement only. However, the replacement of cement by 70 % with GGBS resulted in a significant reduction in the cumulative heat output. The cumulative heat output of the concrete with Portland cement only that was cured at 50^0C, decreased by 33% and 23% for concrete grades C45 and C75, respectively. This is similar to the temperature rise in the adiabatic test, where the temperature rise of the concrete with the replacement of cement by up to 50% with GGBS did not affect the temperature rise significantly.

The rates of heat output (dQ/dM) in Joule/kg per ^{0}C.hour for concrete at all curing temperatures for concrete grade C45 with GGBS levels of 0, 35 and 70% are presented in Figures 7.14 to 7.16. The other levels of concretes grade C45 and all concretes grade C75 can be found in the Appendix E.

All the results in these figures show that the rates of heat output of a concrete mix cured at different curing temperatures increased as the curing temperature increased. However, the increase of the heat output rates for concrete with high levels of GGBS by increasing of the curing temperature was much higher than that of concrete with lower levels of GGBS.

The peak of the heat output rate of concrete PC45 increased by 197.3% when the curing temperature was elevated from 20 to 50^0C. This increased from 74 to 146 J/kg per ^{0}C.hour. The peak of the heat output rate of concrete with 70% GGBS of the same grade concrete was slightly higher i.e. it increased by 211.5%. The peak of heat output rates of the concrete increased from 26 to 54 J/kg per ^{0}C.hour when the curing temperature elevated from 20 and 50^0C. Under the standard curing temperature (20^0C), the higher levels of GGBS in concrete resulted in lower values of the peak rate of heat output. The effect of the water binder ratio on the heat output rate was less significant compared to that of temperature and the GGBS levels in the concrete.

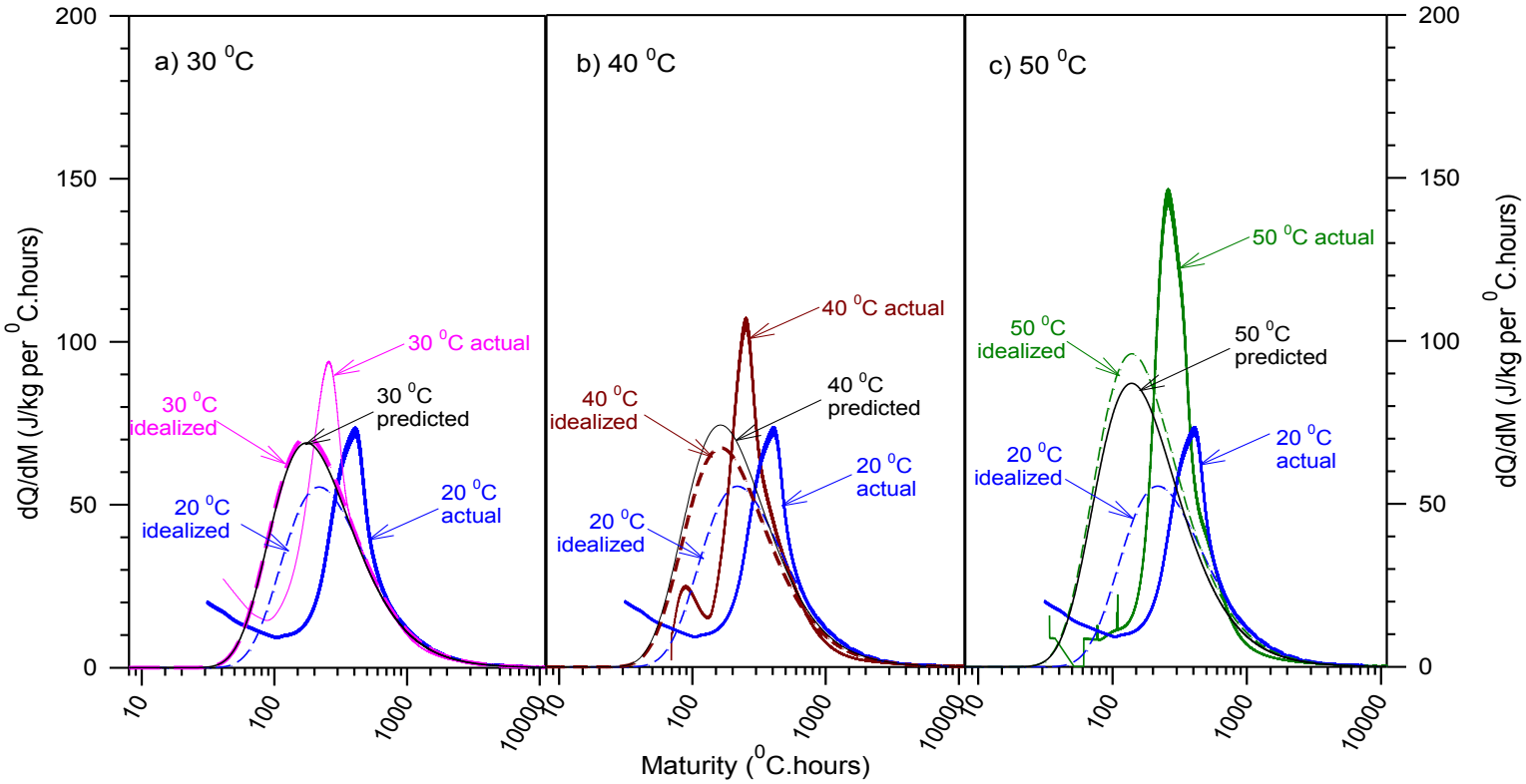

Figure 7.14: Transformation of rate of heat output dQ/dM for 30, 40 and 50^{0}C vs. maturity on a logarithmic scale for concrete **PC45**

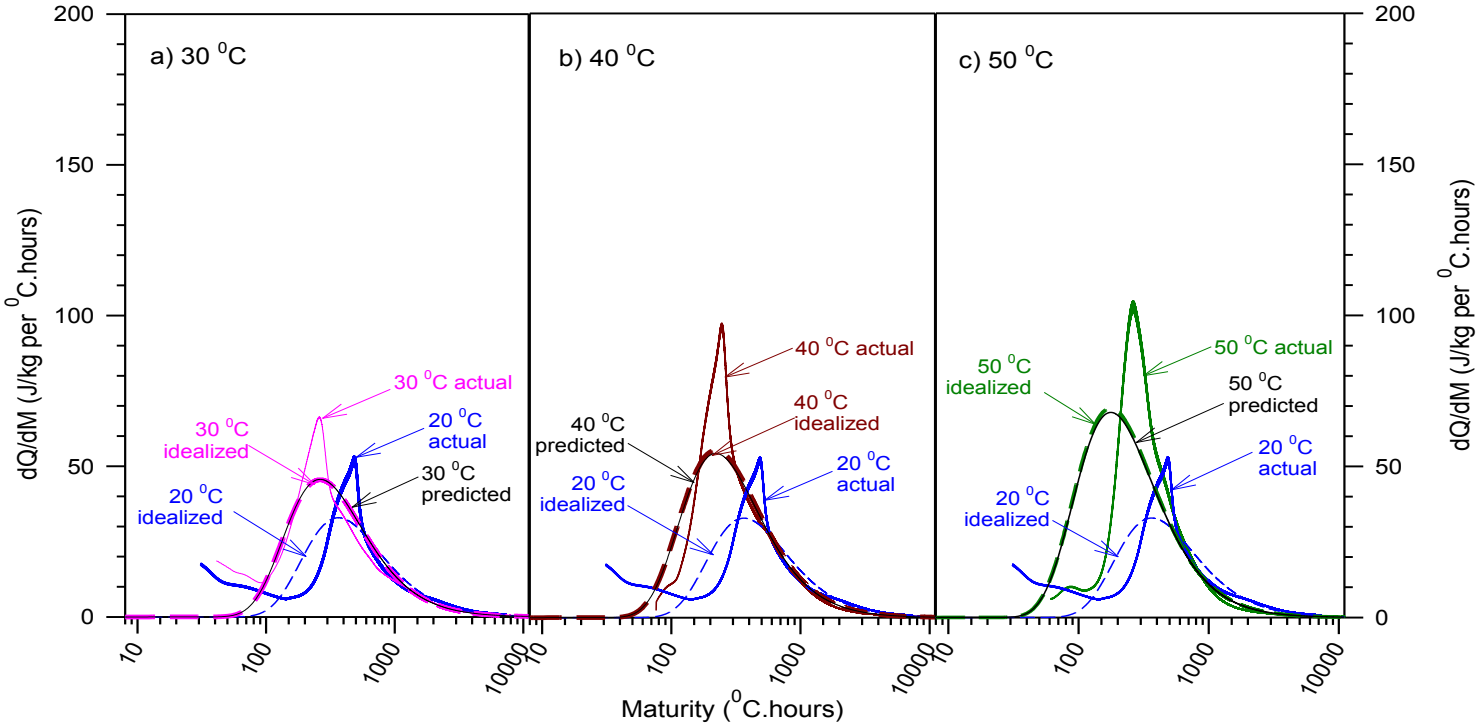

Figure 7.15: Transformation of rate of heat output dQ/dM for 30, 40 and 50^{0}C vs. maturity on a logarithmic scale for concrete **35GGBS45**

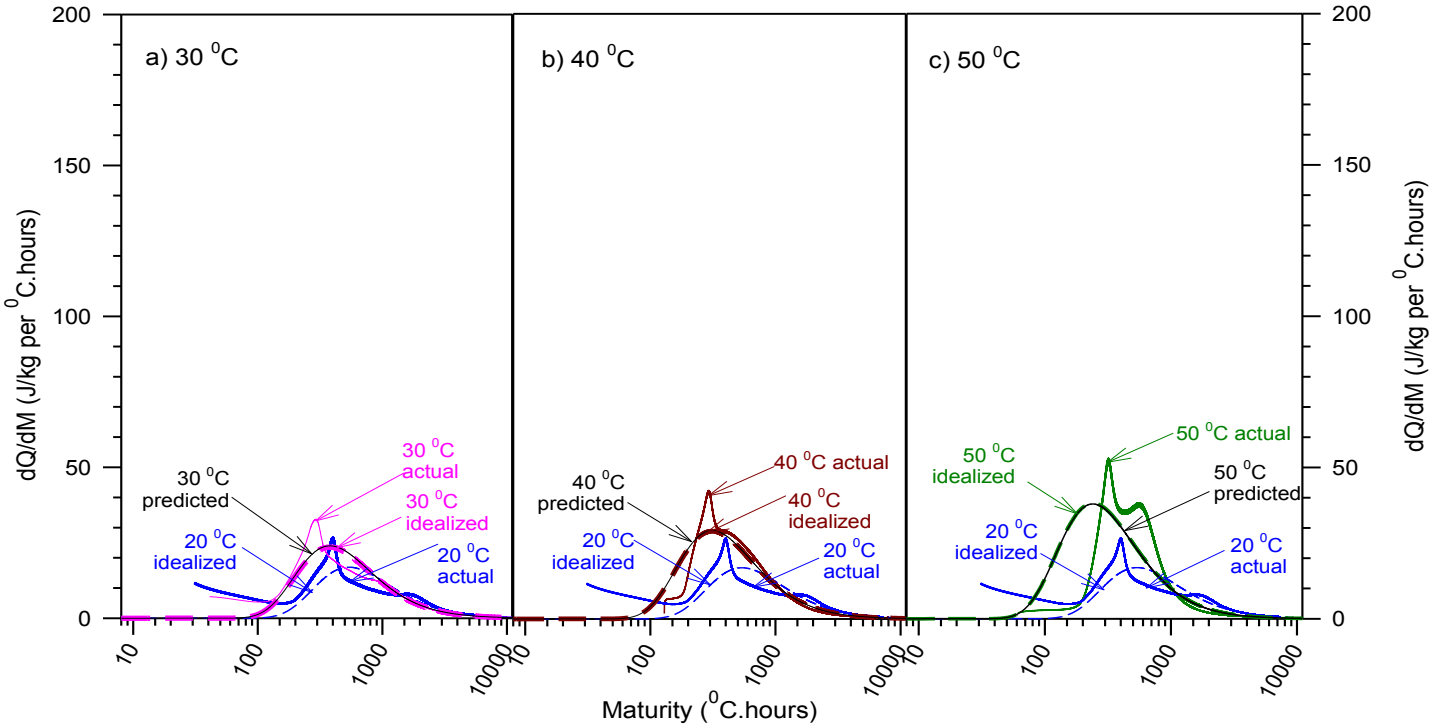

Figure 7.16: Transformation of rate of heat output dQ/dM for 30, 40 and 50^{0}C vs. maturity on a logarithmic scale for concrete **70GGBS45**

Figures 7.17 and 7.18 show the relationship between *1/Q.dQ/dM* and *maturity* for concrete grades C45 and C75, respectively. The figures show the effect of different curing temperatures on the acceleration of the cement hydration in concrete. The predicted acceleration lines overlapped with the lines obtained from the equation from linear regression on actual data for all mixes and curing temperatures.

The higher curing temperatures greatly affect the acceleration of the cement hydration, particularly at very earlier ages or at lower maturity as shown clearly in both figures. At early ages, the acceleration curves of the different curing temperatures can be clearly seen, but when compared to those at later ages it is a little difficult to distinguish them, particularly for those cured at higher temperatures. This proves that the influence of higher curing temperatures at early ages is more significant than at later ages.

The acceleration of hydration in concrete with higher levels of GGBS appeared to be more affected by the higher curing temperatures compared to that of concrete with Portland cement only. This can describe the sensitivity of GGBS concrete to the curing temperature.

For the GGBS concrete, the effect of curing temperature on the acceleration of hydration of concrete with higher water-binder ratios was more significant than that of GGBS concrete with lower water-binder ratios. This is believed due to the concrete with lower water-binder ratio contain cement much more than that of concrete with higher water-binder ratio. Therefore, the heat that was produced by Portland cement in concrete with a lower water-binder ratio when it had contact with water was enough to activate the GGBS reaction.

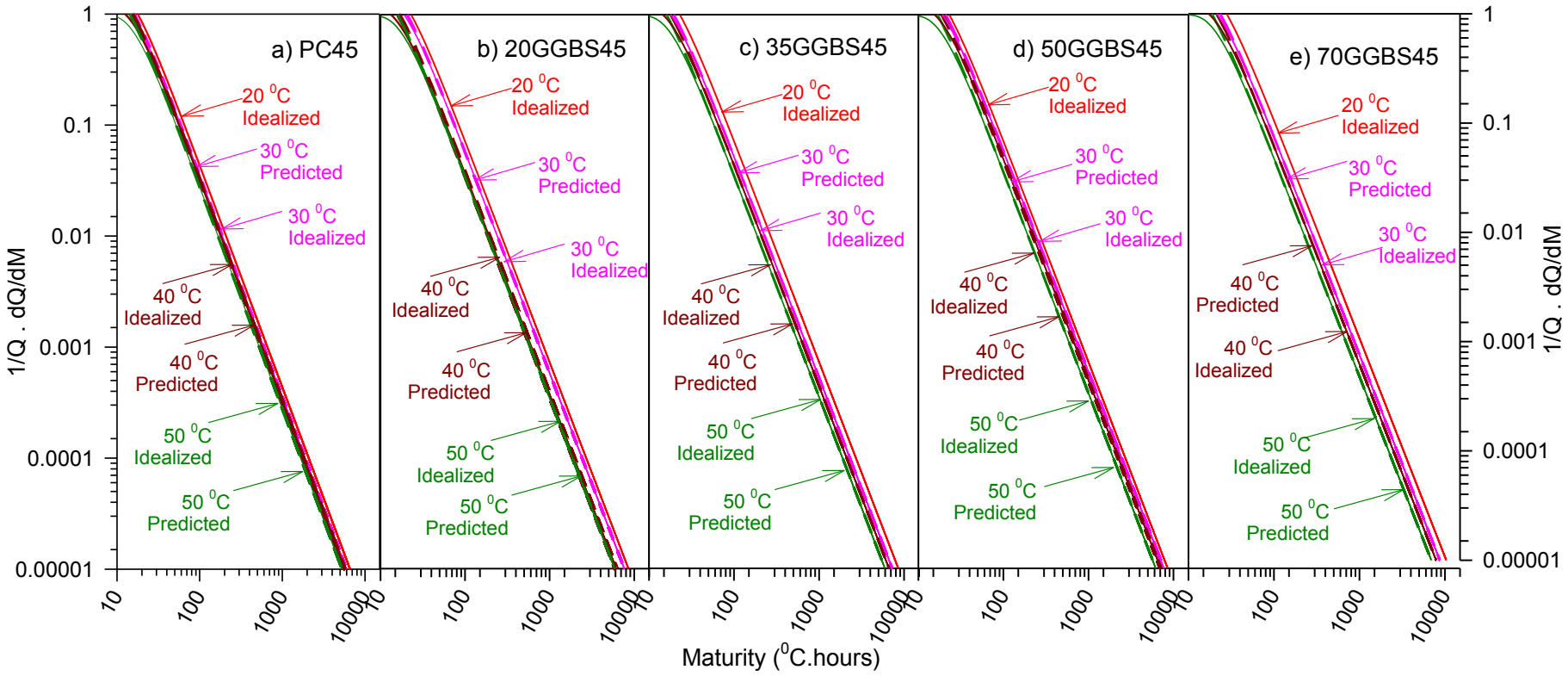

Figure 7.17: Relationship 1/Q.dQ/dM versus maturity on logarithmic scale at different curing temperatures for concrete **grade C45**

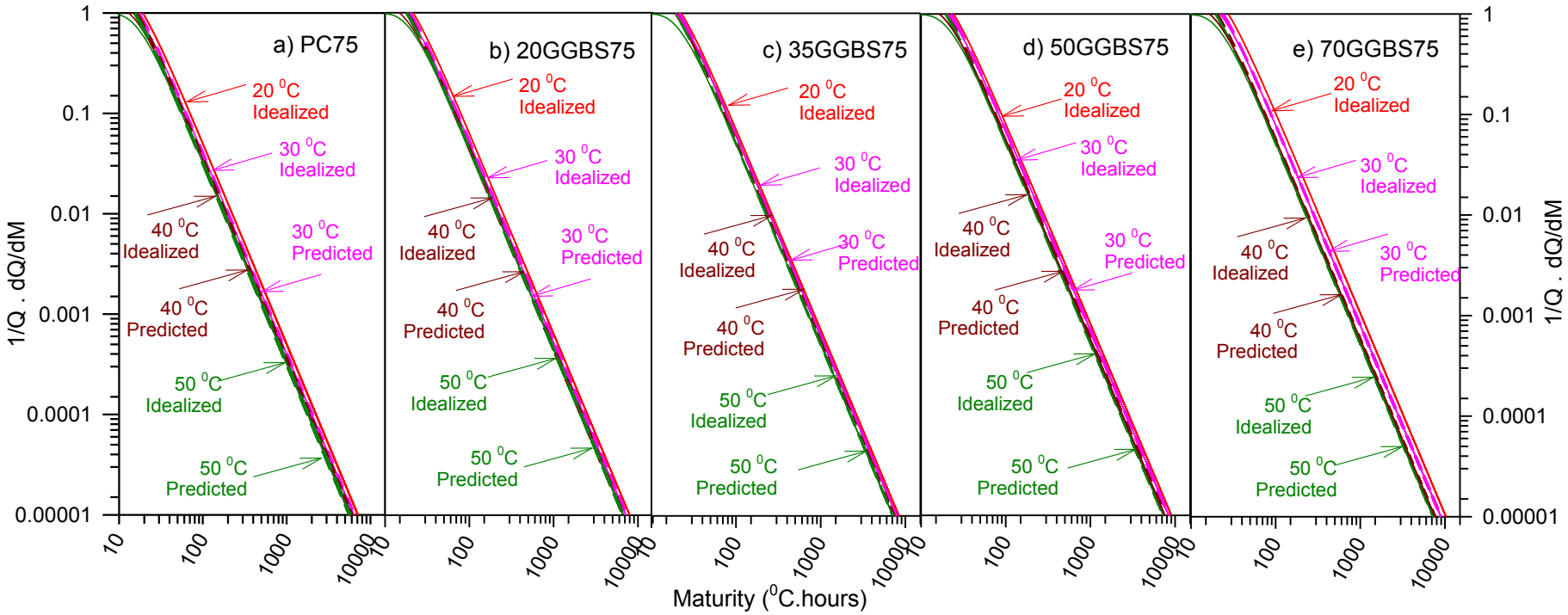

Figure 7.18: Relationship 1/Q.dQ/dM versus maturity on logarithmic scale at different curing temperatures for concrete **grade C75**

The procedures of the Modified MNS method to predict the cumulative heat output of concrete cured under non-isothermal conditions was similar to that used to predict the strength development of concrete cured under non-isothermal curing temperature in Chapter 6. The procedures are as follows:

1. Determine the parameters of Q_∞, τ and a for reference temperature, in this case 20^0C, where shape parameter *"a"* was taken as 1.

2. Predict the cumulative heat output with the acceleration factor a_M, for η, using the equation as follows:

$$Q = Q_\infty e^{-(\frac{\tau}{a_M M})^{\eta a}}$$

3. Determine dQ/dM using the heat output obtained in Step 2 above for η(T)

4. The cumulative heat output Q can then be calculated from the following equation:

$$Q = \sum \frac{dQ}{dM} \eta \Delta M$$

The results then were compared to the results obtained from the model proposed in an earlier study (MNS method)[356].

Generally, the model proposed in this study predicted the heat output quite well for all mixes of both grades C45 and C75. The increase of GGBS levels in concrete, however, appears to decrease the accuracy of the prediction of the adiabatic cumulative heat output. In order to confirm that the model could be reliably used for predicting the adiabatic cumulative heat output, the results obtained using the model will be used to model the adiabatic temperature rise, using a finite element model.

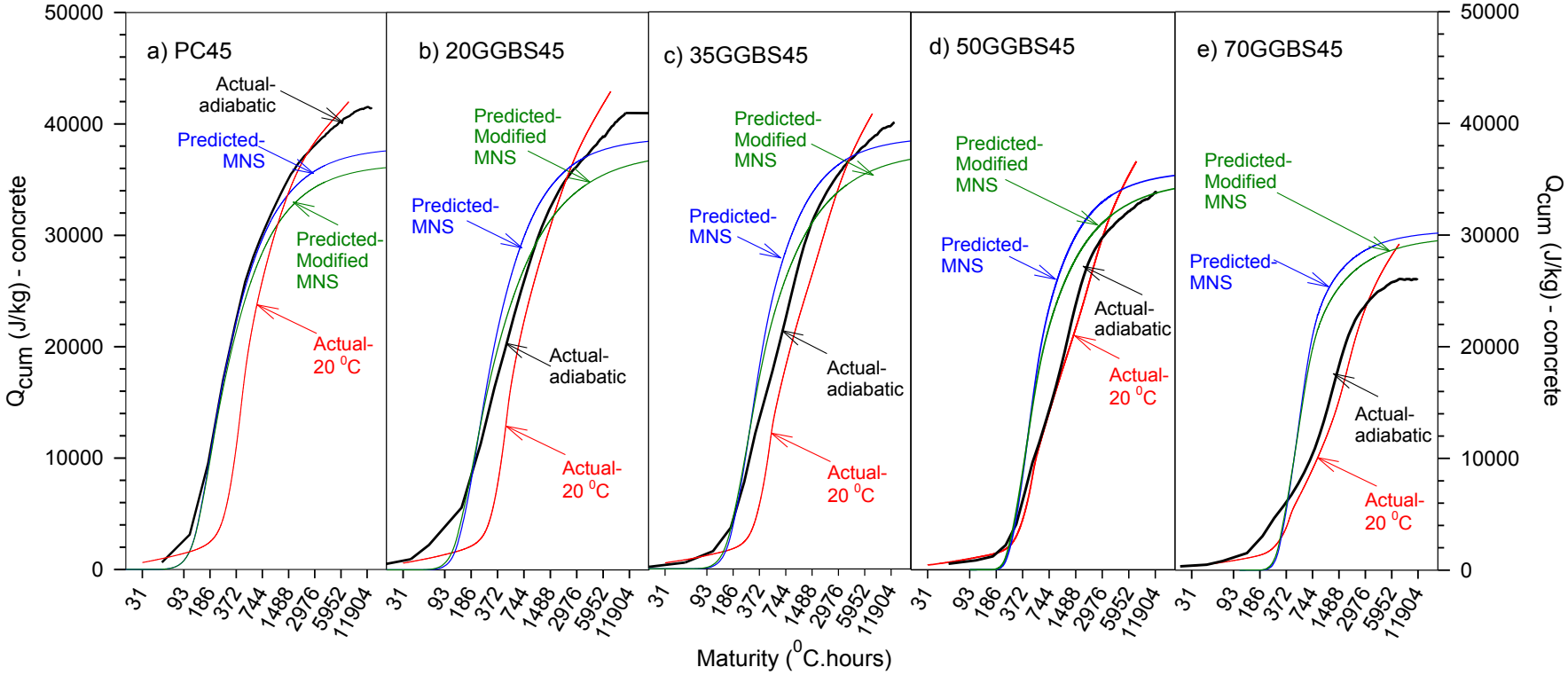

Figure 7.19: Predicted adiabatic cumulative heat output (J/kg) for concretes **grade C45**

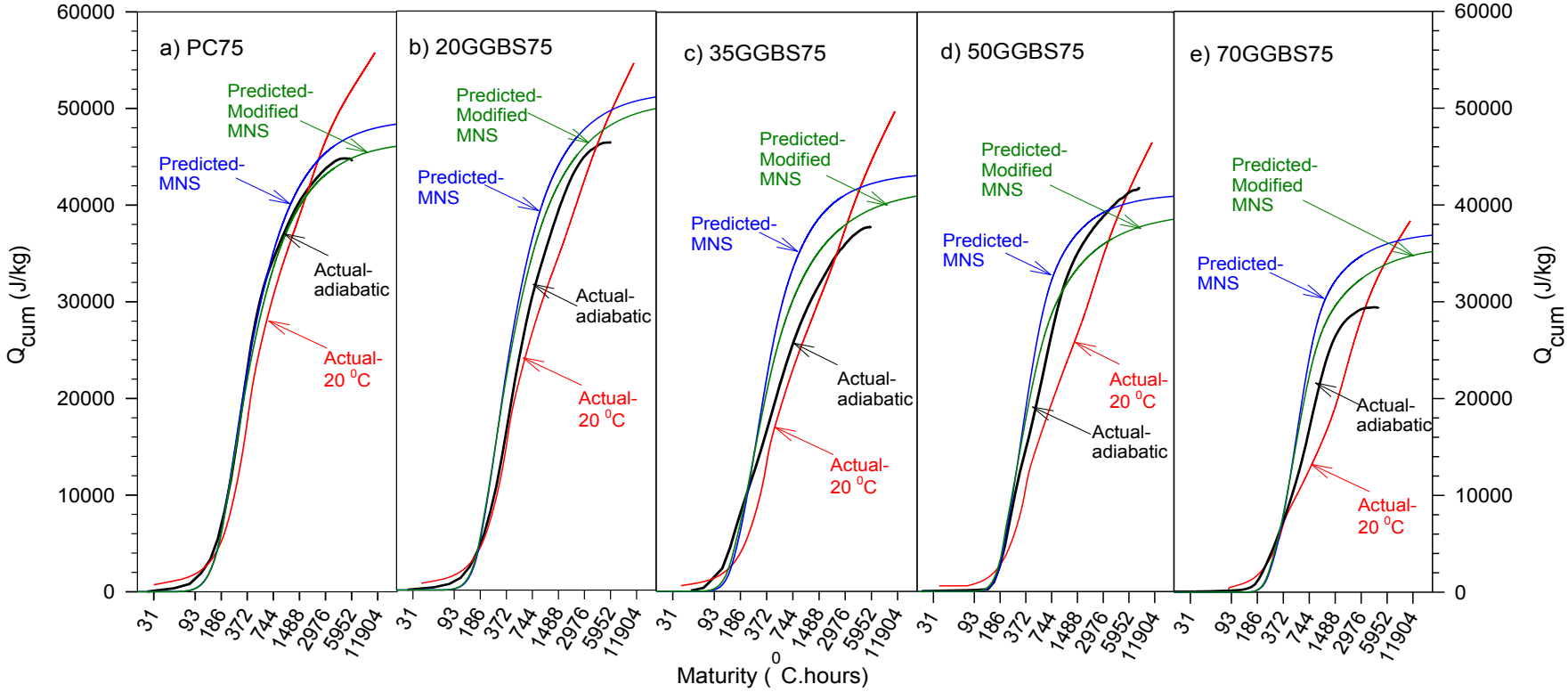

Figure 7.20: Predicted adiabatic cumulative heat output (J/kg) for concretes **grade C75**

7.7. Contribution of GGBS to the heat output

In order to quantify the contribution of GGBS to the heat output, mortar mixes without GGBS were prepared for both grades C45 and C75. The mix proportions for mortars with GGBS that were presented in Tables 4.6 and 4.7, were recalculated for mix proportion of mortars without GGBS. The mortars without GGBS had the same water-cement ratios and the same paste volume as those mortars with GGBS. The quantities of each material in kg per cubic metre of the equivalent mortar without GGBS are presented in Tables 7.4 and 7.5, for mortar grades C45 and C75, respectively.

Table 7.4: Quantity of each material (kg) per cubic metre of mortar **grade C45**

Mix	PC45	20GGBS45	35GGBS45	50GGBS45	70GGBS45
Cement	455	385	319	261	147
GGBS	0	96	172	261	344
Free water	232	231	230	229	206
Total Water	242	241	240	238	215
Superplasticier	0	0	0	0	0
Sand	1505	1476	1470	1439	1494
w/c	0.51	0.60	0.72	0.88	1.40
w/b	0.51	0.48	0.47	0.44	0.42
Equivalent mortars without GGBS					
Mix	**PC45**	**Equivalent of 20GGBS45**	**Equivalent of 35GGBS45**	**Equivalent of 50GGBS45**	**Equivalent of 70GGBS45**
Cement	455	422	377	337	217
GGBS	0	0	0	0	0
Free water	232	253	272	296	304
Total Water	242	263	282	305	313
Superplasticier	0	0	0	0	0
Sand	1505	1516	1541	1558	1604
w/c	0.51	0.60	0.72	0.88	1.40

The heat output of the mortars cured at 20 and 50^{0}C for both mortar grades C45 and C75 are presented in Figures 7.21 to 7.24. For heat outputs of the mortars cured at 30 and 40^{0}C can be found in the Appendix E. As expected, the heat output per kg binder increased when the GGBS was removed from the mix composition and cement was added to maintain the water cement ratio to be the

same to that of mortar with GGBS. This is due to the increase of the amount of cement in the mortar without GGBS compared to that of mortar with GGBS.

Table 7.5: Quantity of each material (kg) per cubic metre of mortar **grade C75**

Mix	PC75	20GGBS75	35GGBS75	50GGBS75	70GGBS75
Cement	502	406	324	251	154
GGBS	0	101	174	251	358
Free water	166	162	164	160	154
Total Water	173	169	171	167	160
Superplasticier	4.016	4.056	3.785	3.808	3.891
Sand	1521	1523	1529	1527	1523
w/c	0.33	0.40	0.51	0.64	1.00
w/b	0.33	0.32	0.33	0.32	0.30
Equivalent mortars without GGBS					
Mix	**PC75**	**Equivalent of 20GGBS75**	**Equivalent of 35GGBS75**	**Equivalent of 50GGBS75**	**Equivalent of 70GGBS75**
Cement	502	455	398	342	249
GGBS	0	0	0	0	0
Free water	166	182	201	218	249
Total Water	173	189	209	226	257
Superplasticier	4.016	4.056	3.785	3.808	3.891
Sand	1521	1549	1587	1625	1689
w/c	0.33	0.40	0.51	0.64	1.00

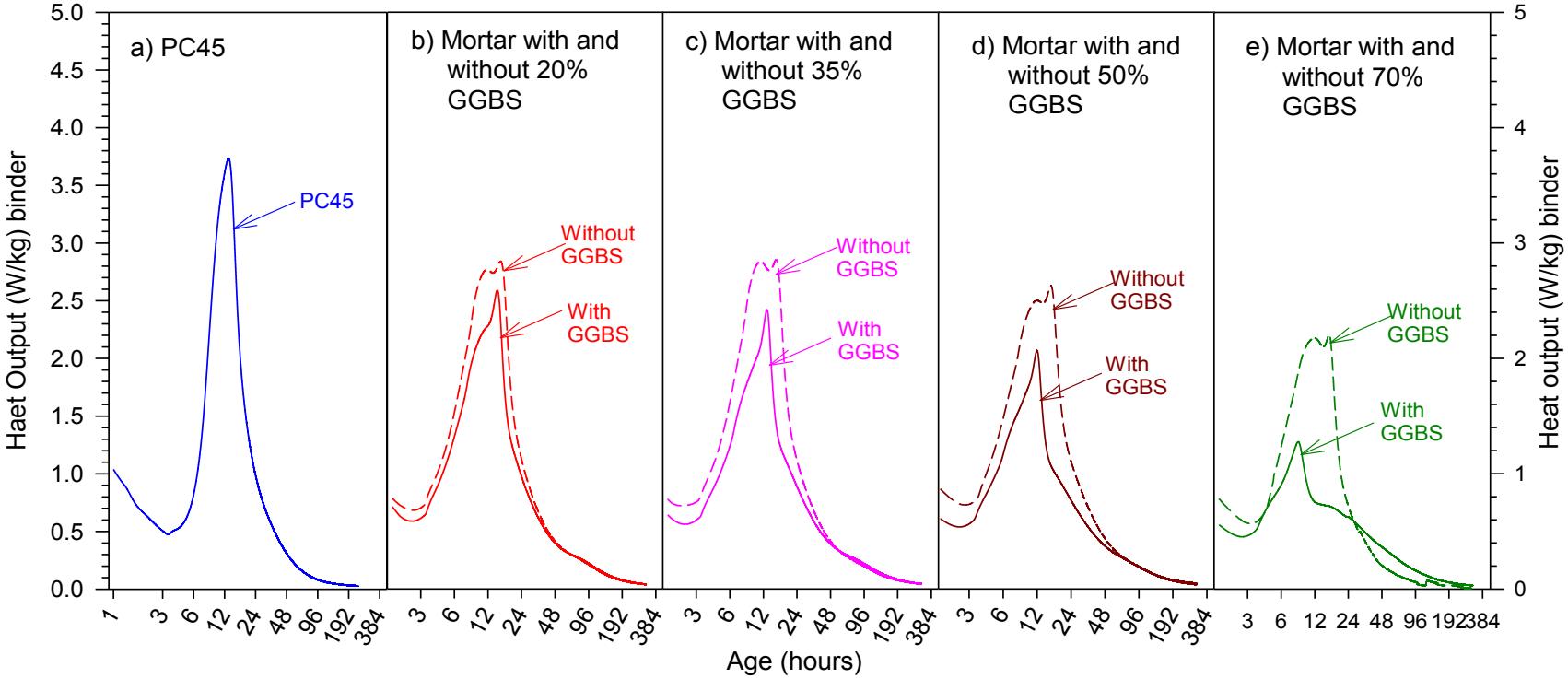

Figure 7.21: Comparison of heat output in W/kg of binder of mortars **grade C45** of 20, 35, 50 and 70% GGBS with their equivalent mortars without GGBS cured at 20^0C

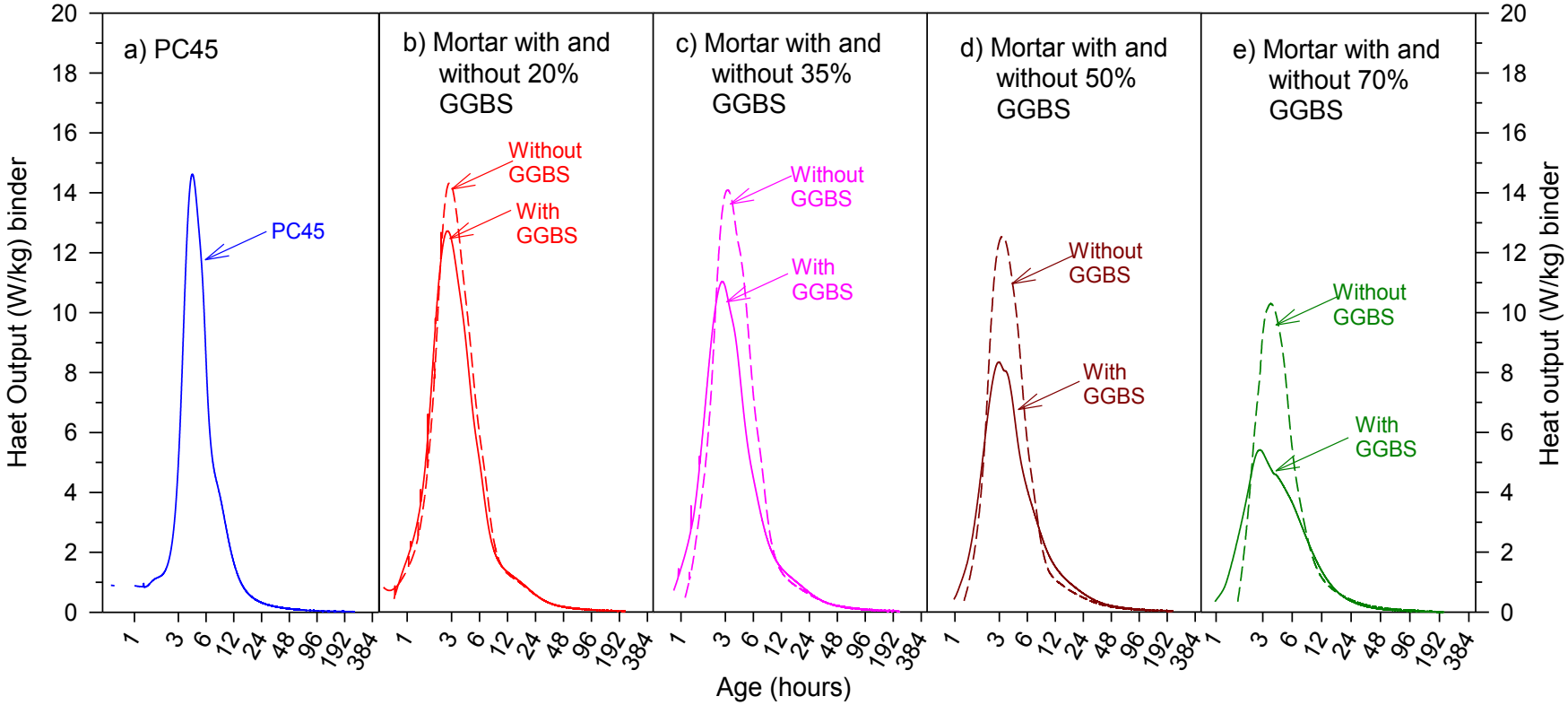

Figure 7.22: Comparison of heat output in W/kg of binder of mortars **grade C45** of 20, 35, 50 and 70% GGBS with their equivalent mortars without GGBS cured at 50^0C

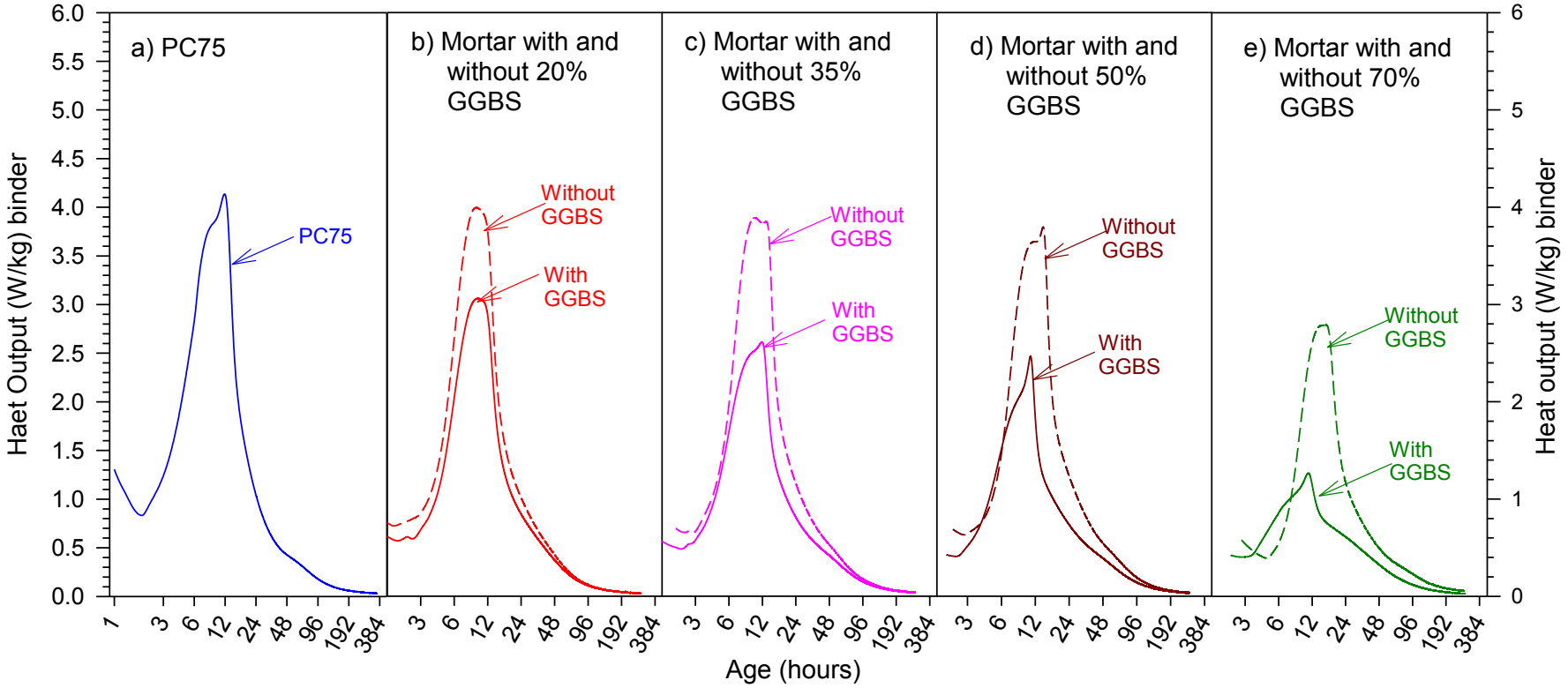

Figure 7.23: Comparison of heat output in W/kg of binder of mortars **grade C75** of 20, 35, 50 and 70% GGBS with their equivalent mortars without GGBS cured at 20^0C

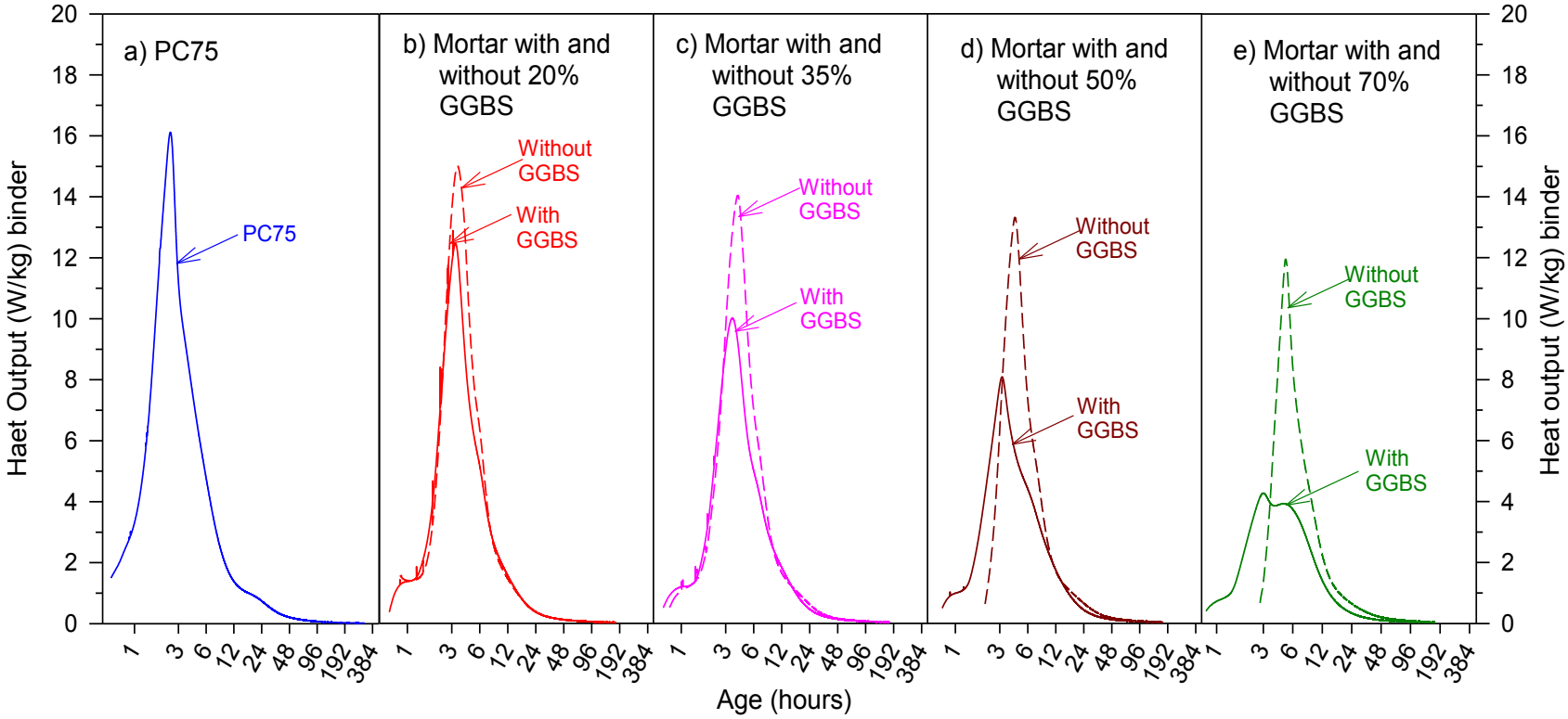

Figure 7.24: Comparison of heat output in W/kg of binder of mortars **grade C75** of 20, 35, 50 and 70% GGBS with their equivalent mortars without GGBS cured at 50^0C

Figures 7.25 to 7.28 show the contribution of GGBS to the cumulative heat output of mortar grades C45 and C75 cured at 20 and 50^0C. The other figures for mortar cured at 30 and 40 ^{0}C can be found in Appendix E. The total heat output of cement that was used in this study was 1214 J/g, which was calculated according to Equation 2.139 proposed by Bogue[219]. This was 2.6 times more than that of the total heat output of GGBS, i.e. 461 J/g recommended by Kishi and Maekawa[220] as discussed in Chapter 2. The comparison between the cumulative heat output of mortars with GGBS for all levels and grades to that of their equivalent mortars without GGBS show that the use of GGBS in concrete to replace a part of cement can reduce the heat output produced in hydration process.

The higher levels of cement replacement result in higher differences between the cumulative heat outputs of mortars with and without GGBS, except for mortar grade C45 with 70% GGBS. The water-cement ratio of this mortar was 1.40 (shown in Table 6.4), therefore when the GGBS in this mortar was removed and cement was added to maintain its water-cement ratio, this mortar was still able to flow. The mix of the mortar was then modified by increasing the paste volume to allow adding more cement and confirming that the cement paste could be set.

At curing the temperature 20^0C, the replacement of cement by 70% GGBS can reduce the cumulative heat output of mortar by 30 and 44.8% for mortar grades C45 and C75, respectively, in comparison to the cumulative heat output of mortar with Portland cement only to that of mortar with 70% GGBS of the same grade. The cumulative heat output of mortar PC45 of 250,000 J/kg can be reduced to 175,000 J/kg by replacing 70% of the cement with GGBS. While the cumulative heat output of mortar PC75 of 362,500 J/kg can be reduced to 200,000 J/kg when 70% of the cement is replaced with GGBS. The cumulative heat output of PC mortar and the mortars without GGBS, which were equivalent to the GGBS mortars, were similar. The exception is for the equivalent mortar of 70% GGBS grade C45.

`

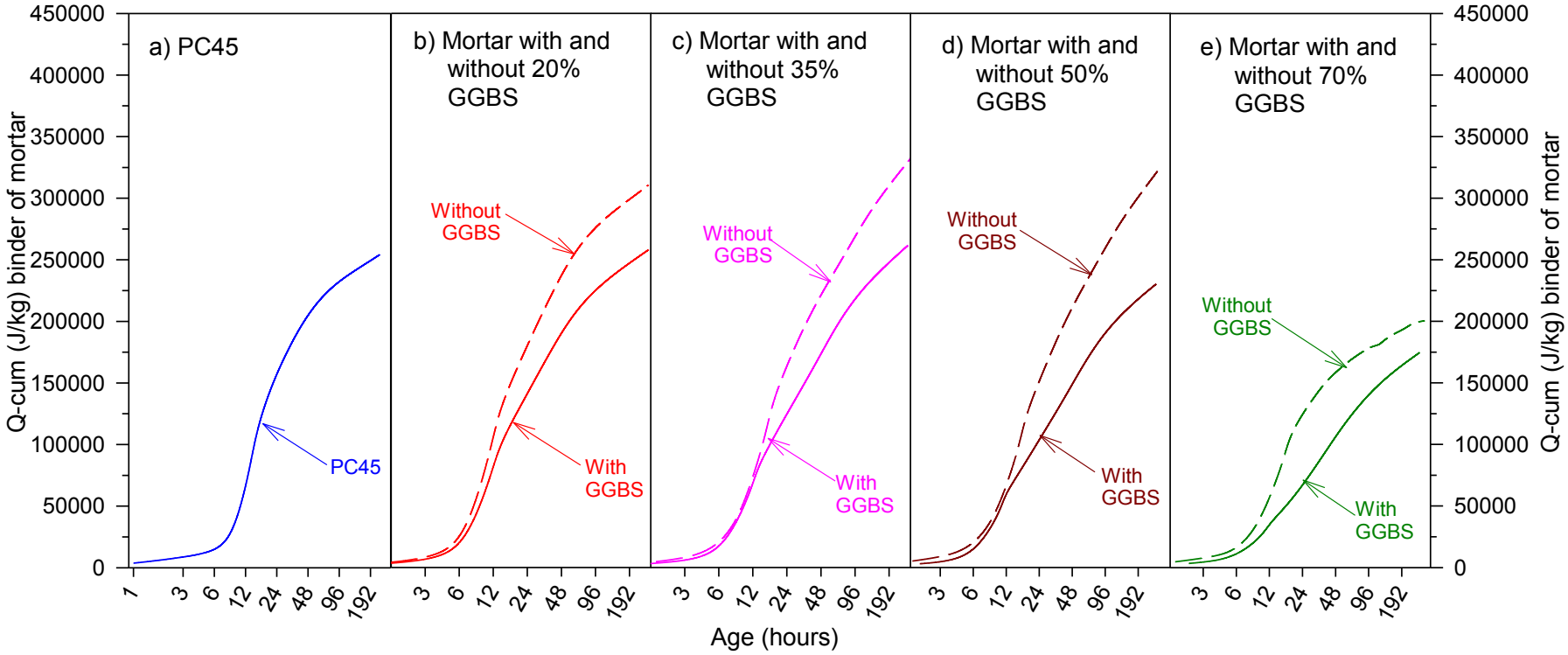

Figure 7.25: Comparison of the cumulative heat output in J/kg of binder of mortars **grade C45** of 20, 35, 50 and 70% GGBS with their equivalent mortars without GGBS cured at 20^0C

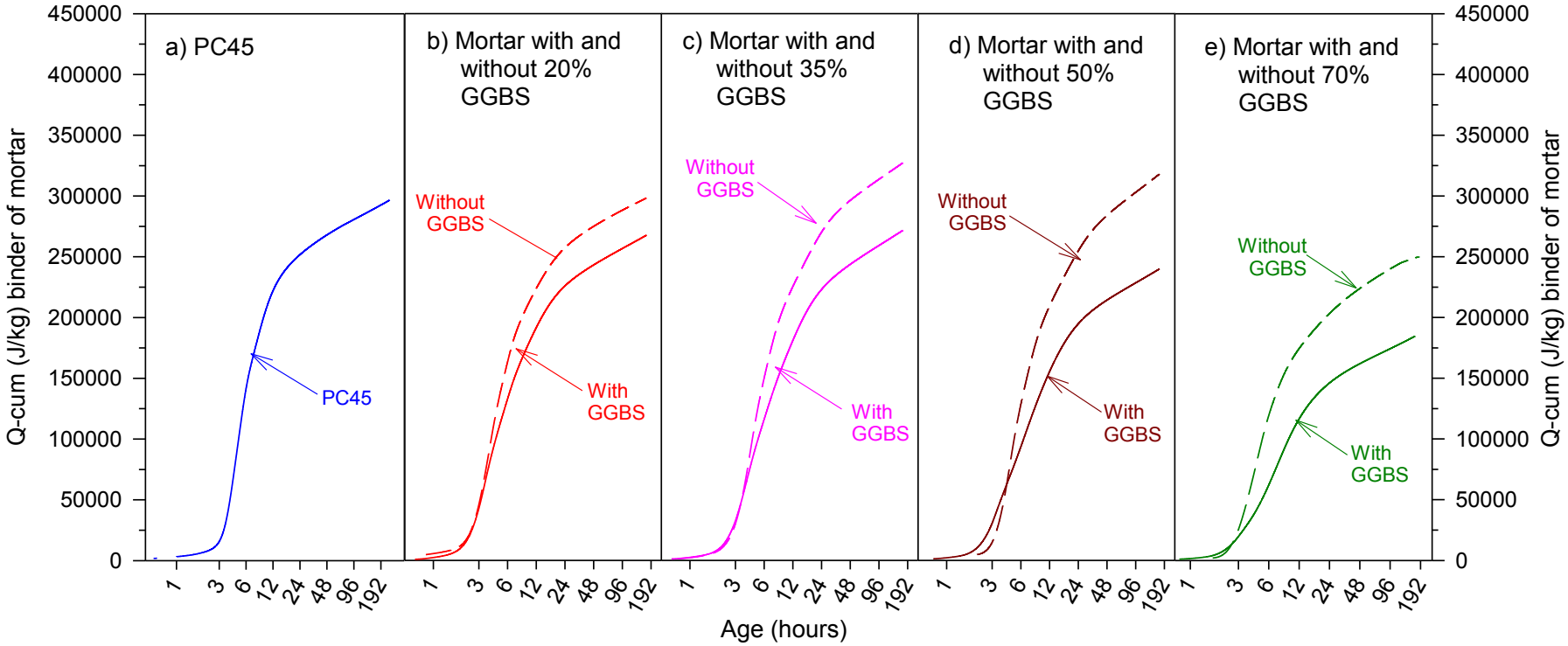

Figure 7.26: Comparison of the cumulative heat output in J/kg of binder of mortars **grade C45** of 20, 35, 50 and 70% GGBS with their equivalent mortars without GGBS cured at 50^0C

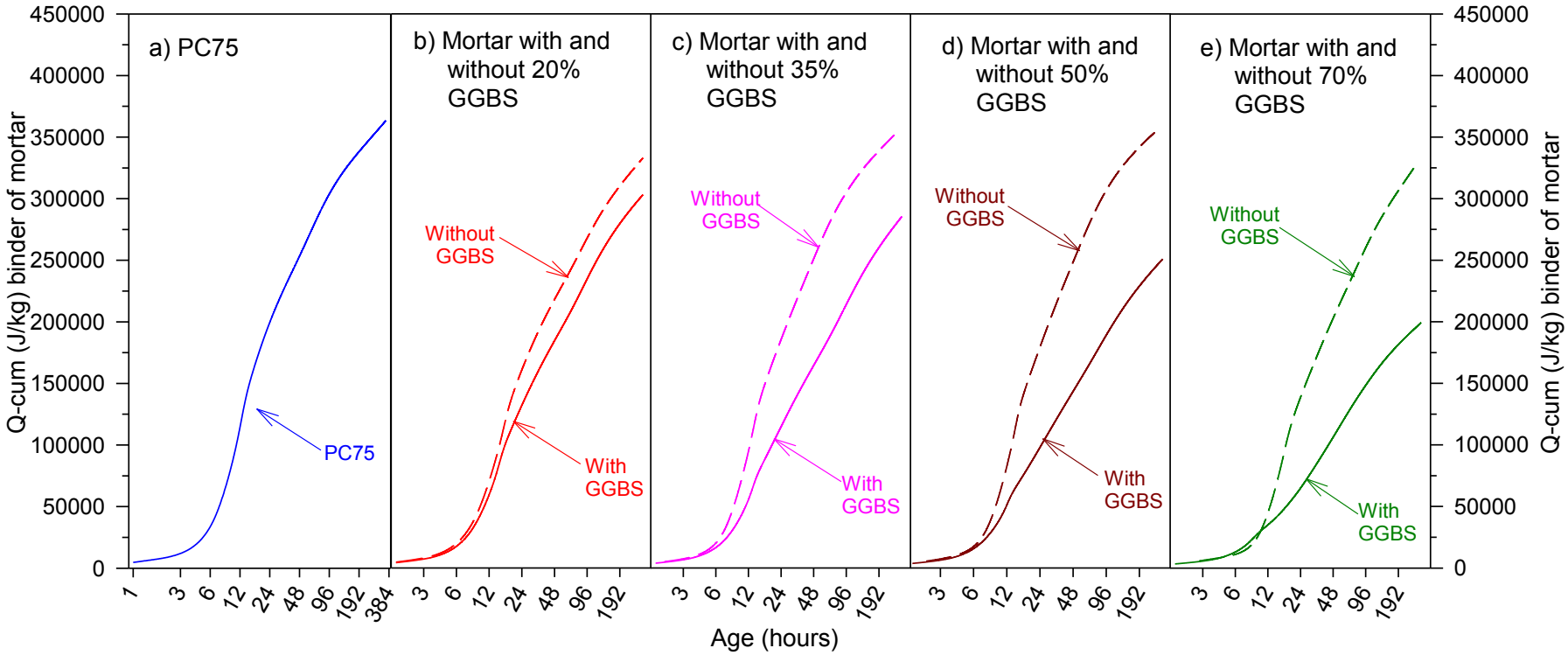

Figure 7.27: Comparison of the cumulative heat output in J/kg of binder of mortars **grade C75** of 20, 35, 50 and 70% GGBS with their equivalent mortars without GGBS cured at 20^0C

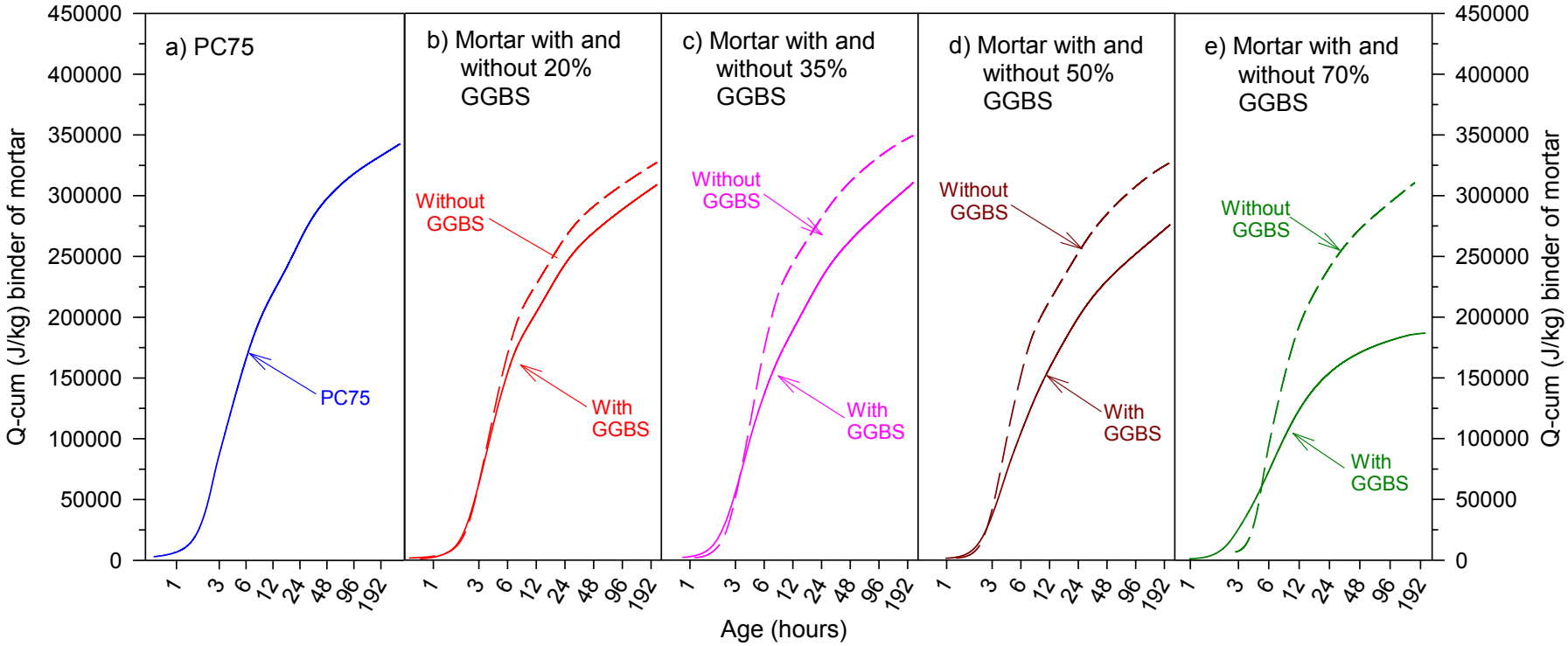

Figure 7.28: Comparison of the cumulative heat output in J/kg of binder of mortars **grade C75** of 20, 35, 50 and 70% GGBS with their equivalent mortars without GGBS cured at 50^0C

Therefore, the differences between the cumulative heat outputs of the GGBS mortars to that of their equivalent mixes without GGBS were the contributions of the GGBS to the heat output of the hydration.

The rate of heat output of the GGBS concrete and that of their equivalent mortars without GGBS cured at 20^0C were very similar for the first six hours, as shown in Figures 7.25 and 7.27. Both curves of the cumulative heat output of the GGBS mortars and their equivalent mortars without GGBS almost overlapped for the first six hours of hydration process. The curves appear to develop separately from the age of six hours onwards, which were occurred earlier on mortars cured at higher curing temperatures. This proves that the GGBS mortars react quicker under higher curing temperature than those cured under lower temperatures. The higher curing temperature causes the GGBS to contribute more to the cumulative heat output.

7.8. Summary

This chapter can be concluded as follows:

- The activation energies calculated using the heat output obtained from calorimeter test appeared to be less reliable than that of determined using strength test results. However, the activation energy values are still in the range of value that of obtained using strength data test results.
- The use of GGBS in concrete can reduce the heat output rate of hydration and consequently, reduce the rise temperature resulted in the hydration process of cement, where the higher levels of GGBS replaced cement, the higher the temperature rice can be reduced.
- The modified MNS method proposed in this study predicted the heat output of cement hydration quite well for all mixes of both concrete grades C45 and C75.
- The higher levels of cement replacement with GGBS result in higher differences between the cumulative heat outputs of mortars with and without GGBS.

CHAPTER 8 – PREDICTION OF TEMPERATURE HISTORY IN CONCRETE USING FINITE ELEMENT METHOD

8.1. Introduction

This chapter discuss the procedure that uses the finite element analysis (FEA) method, with the COMSOL software package, for predicting the temperature history of concrete structural elements. The accurate prediction of temperature rise of the concrete structural elements could be used to accurately predict the strength development of the concrete. It can then be used to optimise the construction schedules. The temperature rise development in the concrete block that is cured under adiabatic condition is very similar to that of the in-situ condition. The temperature rise development of both the conditions is changed by time, which is a function of time. The adiabatic temperature rise obtained from the modelling was then compared to the experimental results. The accuracy of the modelling results using the COMSOL package software can then be assessed.

8.2. Modelling of Structural Element

A concrete block with a size of 200 x 200 x 200 mm was modelled. The concrete block was cured inside an environmental chamber. The temperature of the chamber was set to the same or a maximum difference of one degree to that of the temperature inside the concrete block. This aimed to confirm that there is no loss of the heat produced in the process of hydration. The temperature histories inside the concrete were recorded by inserting two thermocouples into the centre of the concrete block as has been discussed in Chapter 4.

8.3. COMSOL Multiphysics Software Modelling

8.3.1. Creating Model in COMSOL

A drawing menu is provided in COMSOL software to draw the element of structure that will be modelled. The COMSOL software also provided the mesh menu to create meshes on the element. A mesh is a partition of the geometry

model into small units of simple shapes. For a 3D geometry, the COMSOL software allow to choose between creating a free mesh containing tetrahedral elements, or a swept mesh containing prism elements or hexahedral elements shown in Figure 8.1.

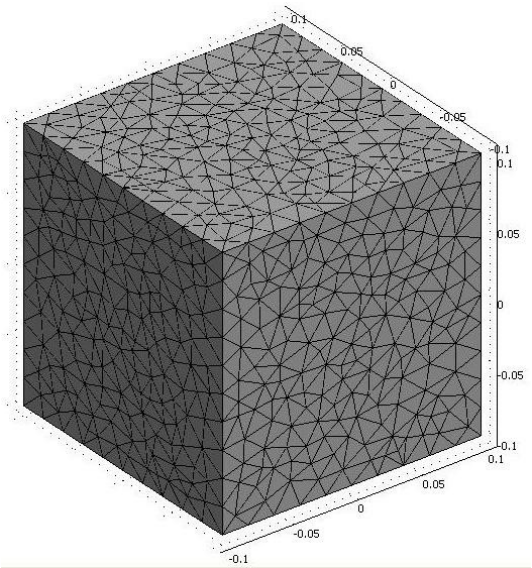

Figure 8.1: Creating mesh on an element

In COMSOL, unless stated otherwise the "Normal" predefined mesh size and non-uniformly was used for all the structural elements. The maximum element size scaling factor was equal to 1, the element growth rate was 1.3, the mesh curvature factor 0.3 and the mesh curvature cut off 0.001[247].

8.3.2. Thermal Properties of Concrete

This section discusses the procedure of modelling the adiabatic temperature rise in the concrete block using the COMSOL package software. The mathematical model for heat transfer by conduction that was expressed in the Equation 2.117 can be re-written as follows[247]:

$$\delta_{ts}\ \rho\ C_p \frac{\partial T}{\partial t} - \nabla(k\nabla T) = Q + h_{trans}(T_{ext} - T) + C_{trans}(T_{amb}^4 - T^4) \qquad \text{Equation 8.1}$$

where:

δ_{ts} = time scaling coefficient

ρ = density of the concrete, kg/m^3

C_p = specific heat, J/kg ^{0}K

T = temperature of the material, ^{0}K

k = thermal conductivity, W/m^{0}K

Q = heat source, W/m^3

h_{trans} = convective heat transfer coefficient, W/m^2 ^{0}K

C_{trans} = user-defined constant, W/m^2 K^4

T_{ext} = external temperature, ^{0}K

T_{amb} = ambient temperature, ^{0}K

The concrete specific heat capacity for all mixes was taken as 880 J/kg ^{0}K. In the literate review, the thermal conductivity of concrete typically ranged from 1.0 to 3.2 W/m.K, which depends on the type of aggregates that were used in the concrete[16]. The thermal conductivity of concrete mixes with pozzolanic replacement materials were lower than concrete with Portland cement only, as shown in Table 8.1.

Table 8.1: Thermal conductivity values for pozzolanic and Portland cement concretes[336]

Mixes	Thermal Conductivity (W/m ^{0}C)	Mixes	Thermal Conductivity (W/m ^{0}C)
PC 90	2.0	PC 30	1.6
35GGBS90	1.9	PC 50	1.8
50GGBS90	1.8	FA 30	1.5
PC 30	1.6	FA 50	1.7
35GGBS30	1.5	GGBS 30	1.5
50GGBS30	1.4	GGBS 50	1.7

The accurate value of the thermal conductivity of concrete that is used in modelling is very important to predict the temperature rise in the concrete during its hydration process, particularly when the formwork is still in place. The reason

is the heat and subsequently temperature distribution in the structural elements of the concrete, which were heavily insulated, will depend mainly on the concrete thermal conductivity.

The density of concrete of each mix, which was used in the COMSOL modelling, was measured from experimental work along with the concrete compression strength of cubes. The heat source (Q), which is generated inside the concrete, was released from the hydration reaction. The heat output was measured in the adiabatic test carried out using the TAS chamber connected to a computer as has been discuss in Chapter 4. In the modelling of the adiabatic temperature rise, the heat outputs used were those, which were obtained from adiabatic tests and the predicted adiabatic heat output. The predicted heat output was calculated using the heat output at 20^0C obtained from isothermal experimental work, as has been discussed in Chapter 7.

8.3.3. Boundary Conditions

In order to simulate the concrete heat output exchanges within its environment accurately; the boundary conditions, therefore, should be defined accurately. When modelling the in-situ temperature of concrete, the effect of the sun on the heat development of the concrete as the concrete absorbs the heat from the sun due to the effect of solar radiation. It was different when modelling the adiabatic temperature rise, where the effect of the solar radiation was not considered. The inward heat flux due to the solar radiation q_0, can be determined using the equation as follows[247, 248]:

$$q_0 = \beta_c \, q_{solar} \qquad \text{Equation 8.2}$$

where:

q_0 = solar absorption heat flux, W/m^2

β_c = concrete's solar absorptivity

q_{solar} = instantaneous solar radiation, W/m^2

A white-body would have a value of 0 and a black one would have a value of 1.0[248]. The solar absorptivity of concrete is a function of the surface colour, which is typically in the range from 0.5 to 0.6. It is expected that the GGBS concretes will have a slightly smaller absorptivity than that of concrete with Portland cement only as the GGBS concretes have a lighter colour than Portland cement. On the other hand, FA concretes that have darker colour are expected to have a higher absorptivity.

Similarly, the solar radiation is a function of cloud cover (sky conditions), as presented in Table 8.2, where the solar radiation during night time will be negligible.

Table 8.2: Solar radiation values[248]

Sky Conditions	Solar Radiation (W/m^2)
Sunny	1000
Partly Cloudy	700
Cloudy (Overcast)	300

The irradiation heat transfer of concrete is accomplished by electromagnetic waves between a surface and its surroundings. The heat flux due to irradiation can be calculated according to the Stefan-Boltzmann equation as follows[247-249]:

$$q_r = C_{const} \left(T_c^4 - T_{inf}^4 \right) \qquad \text{Equation 8.3}$$

where:

q_r = heat radiated from the concrete surface, W/m^3

T_c = concrete surface temperature, ^0C

T_{inf} = temperature of the surrounding radiating environment, ^0C

C_{const} = the radiation transfer coefficient, $W/m^2\ ^0C^4$

C_{const} is the radiation heat coefficient, which can be determined as follows[249]:

$$C_{const} = \varepsilon\, \sigma \qquad \text{Equation 8.4}$$

where:

ε = surface emissivity (without units)

σ = Stefan-Boltzmann constant, 5.669 x10^{-8}W/m^2 $^0C^4$

The surface emissivity is a function of the concrete surface colour. An idealized black surface would have a value of 1.0. In modelling temperature rise in concrete using HIPERPAV software, a value of 0.88 was selected for all concrete mixes[249].

The temperature of the surrounding radiating environment, T_{inf}, will possibly differ from the ambient temperature, T_{amb}. The temperature of the surrounding radiating environment can be determined as follows[249]:

$$T_{inf} = \varepsilon_s^{\frac{1}{4}} T_{amb} \qquad \text{Equation 8 5}$$

where:

ε_s = sky emissivity

The sky emissivity is determined as the following equation:

$$\varepsilon_s = 0.787 + 0.764\, x\, \ln(\frac{T_{dew}}{273})\, x\, F_{cloud} \qquad \text{Equation 8.6}$$

where F_{clouds} can be calculated as follows:

$$F_{cloud} = 1.0 + 0.024\, N - 0.0035\, N^2 + 0.00028\, N^3 \qquad \text{Equation 8.7}$$

where N is the *"tenths cloud cover"* ranging from 0 and 1. Branco et al[180] simplified Equation 8.3 to become the following equation:

$$q_r = \varepsilon \{ 4.8 + 0.75\, (T_{amb} - 5)\} (T_c - T_{amb}) \qquad \text{Equation 8.8}$$

The total radiation heat transfer effect that was specified by the inward heat flux can be determined as follows:

$$q = q_s - q_r \qquad \text{Equation 8.9}$$

where:

q_s = heat transferred through solar radiation, W/m^3

q_r = heat radiated from the concrete surface, W/m^3

The effect of irradiation was not considered when the surface of the structural element was insulated. The heat transfer coefficient in Equation 8.1 can be defined as the convective heat transfer coefficient. The wind speed is very important in determining the heat loss due to convection. It has a significant effect on the in-situ concrete temperature development. The relation between the convective heat transfer coefficient and the velocity of wind is expressed in the following equations[225]:

$$h = 5.6 + 4.0\,V_{wind} \quad \text{for } V_{wind} \leq 5 \text{ m/s} \qquad \text{Equation 8.10}$$

$$h = 7.2\,V_{wind}^{0.78} \quad \text{for } V_{wind} > 5 \text{ m/s} \qquad \text{Equation 8.11}$$

where:

h = convective heat transfer coefficient, $W/m^2\ ^0K$

In addition, the ambient temperatures were changed by time according to the following equation[249]:

$$T_{amb} = T_0 + a \sin\left(\frac{2\pi t}{b}\right) \qquad \text{Equation 8.12}$$

where:

T_{amb} = ambient temperature, ^0C

T_0 = average ambient temperature, ^0C

= (T_{max} + T_{min}) / 2

a = (T_{max} - T_{min}) / 2

b = 24 (hours)

The procedures to modelling temperature rise in concrete cured under adiabatic conditions can be found in Appendix F.

8.4. Predicted Adiabatic Temperature History

The heat outputs that were used in the modelling of the adiabatic temperature rise were the actual adiabatic heat output and the predicted adiabatic heat. The actual adiabatic heat output was obtained from the adiabatic test and the predicted

adiabatic heat output was the predicted adiabatic heat output using the heat output of mortar cured at 20^0C from isothermal calorimeter test, as has been discussed in Chapter 7.

The predicted adiabatic cumulative heat output obtained in Chapter 7 was in units of J/kg. Therefore, the adiabatic cumulative heat output should be transferred into the unit of W/m^3 as required in the COMSOL software using the following equation:

$$Q_n = \left[\frac{Q_{cum,n} - Q_{cum,n-1}}{t_{n-} t_{n-1}}\right] x\, \gamma_c \qquad \text{Equation 8.13}$$

where:

Q_n = Heat output at the age n, W/m^3

$Q_{cum, n}$, $Q_{cum, n-1}$ = Cumulative heat output, J/kg

t_n, t_{n-1} = age, seconds

γ_c = density of concrete, kg/m^3

The heat output was accompanied by the data noise; therefore, the heat output data should be smoothed, as shown in Figures 8.2 and 8.3 for concrete grades C45 and C75, respectively. The predicted adiabatic heat outputs with the data noise were presented by the green curves, while the smoothed adiabatic heat outputs were presented by the black curves.

The smoothing data were carried out using the SigmaPlot software. It was found that the negative exponential smoother with the value of sampling proportion of 0.035 and using the 3rd order polynomial regression was the best way to smooth or remove the data noise. The smoothed adiabatic heat outputs can then be used as the heat sources in modelling the adiabatic temperature rise.

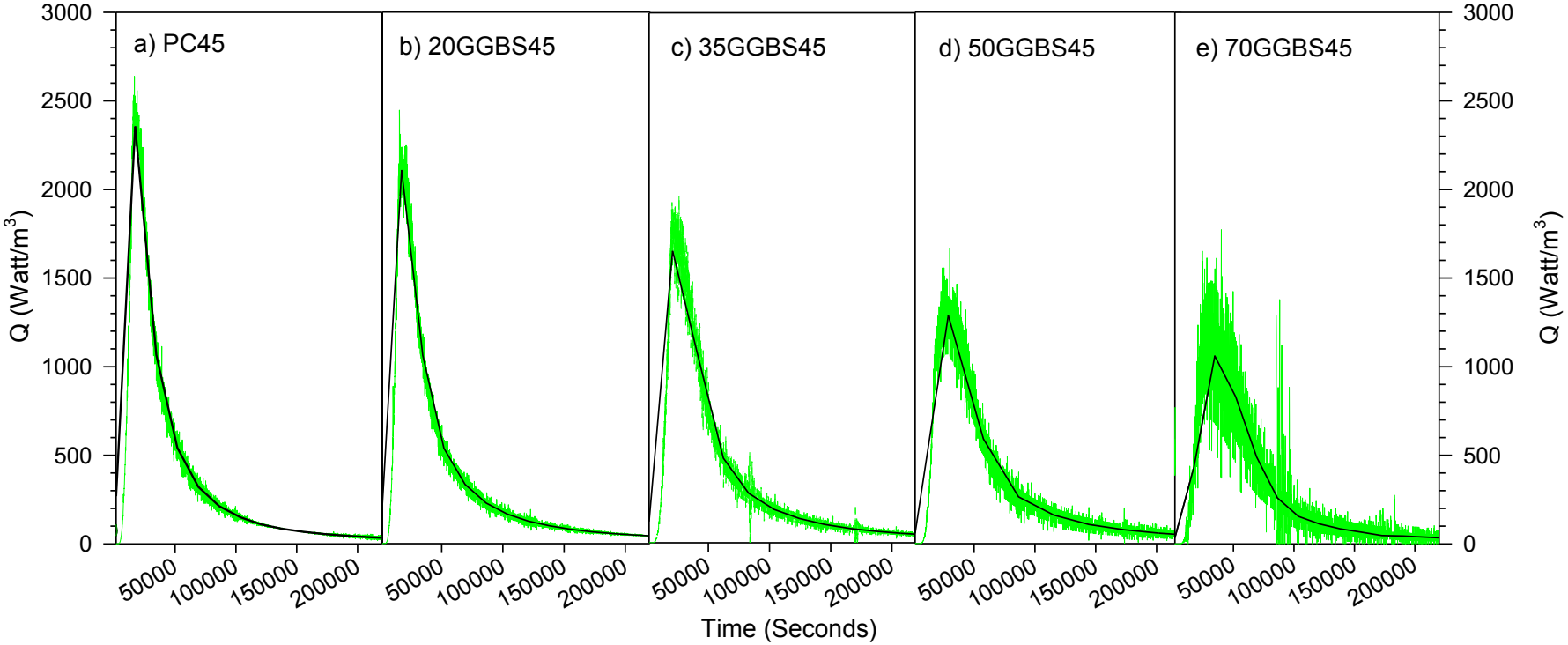

Figure 8.2: Smoothing the predicted adiabatic heat output concrete **grade C45**

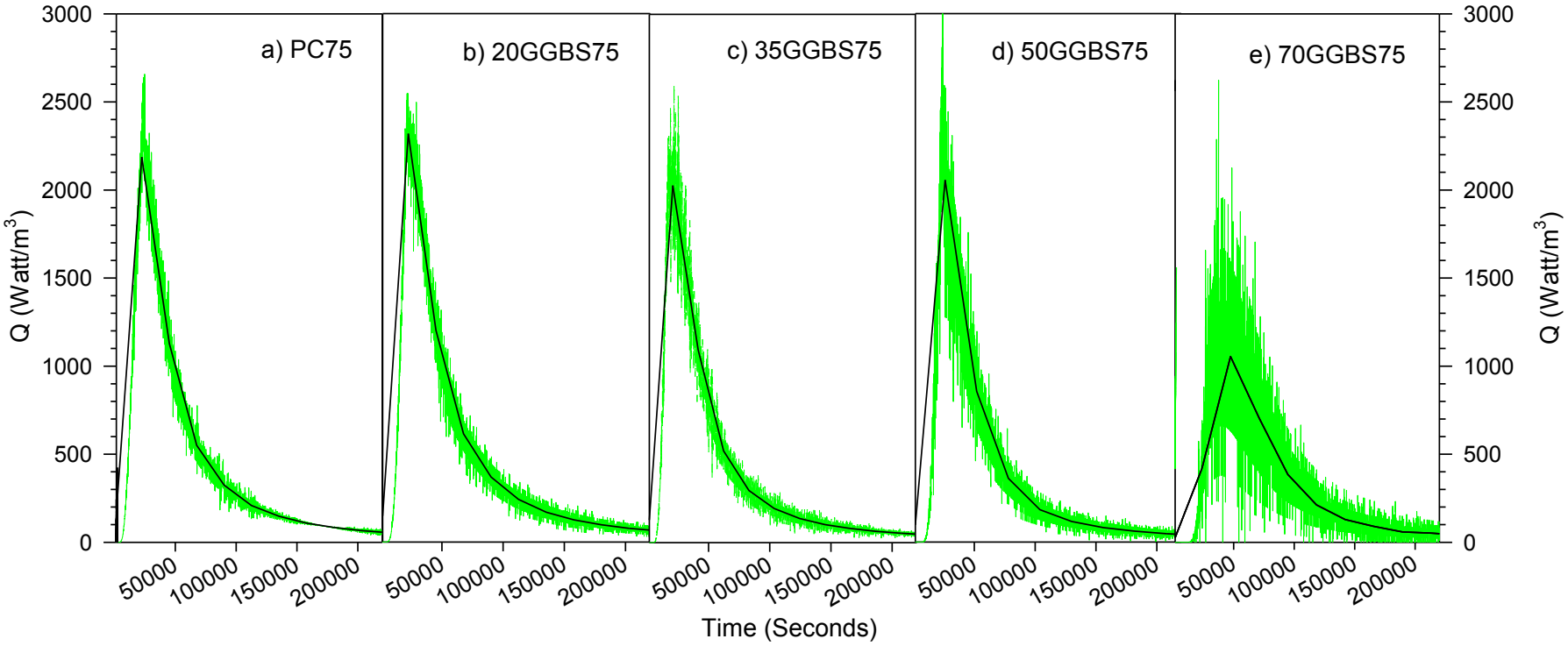

Figure 8.3: Smoothing the predicted adiabatic heat output concrete **grade C75**

Although the predicted cumulative heat outputs were higher than that of the actual measurements as presented in Figures 7.5 and 7.6 of Chapter 7 for concrete grades C45 and C75, respectively; the smoothed heat output in units of W/m^3, however, appeared to be much less than the actual heat output. It is believed to be due to the data noise, which resulted in a reduction in heat output when it was smoothed.

The more noise of the heat output data, the more reduction in the heat output when it was smoothed as shown in the Figures 8.1 and 8.2. A reduction in the heat output used in the modelling of the temperature rise in the concrete, might result in a less accurate prediction of temperature.

The predicted adiabatic temperatures, which resulted from the modelling using the two heat outputs data, were then compared to the actual adiabatic temperatures, which were measured during the adiabatic tests.

The predicted adiabatic temperatures are shown in the Figures 8.3 and 8.4 for concrete grades C45 and C75, respectively. The solid blue lines represent the actual adiabatic temperatures, while the red dash and green das dot lines represent the predicted adiabatic temperatures using the heat outputs, which were obtained from the adiabatic tests and the isothermal calorimeter tests, respectively.

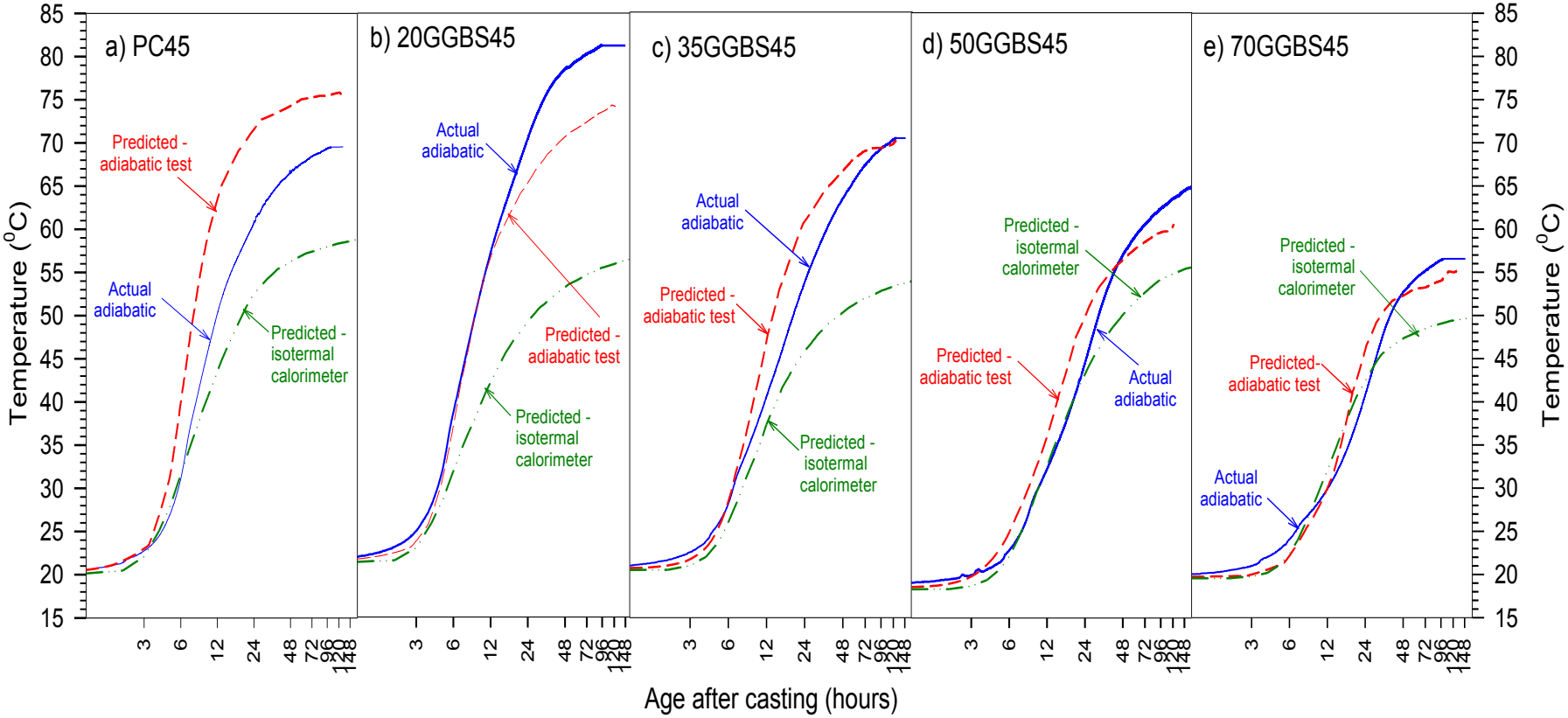

Figure 8.4: Predicted adiabatic temperature concrete **grade C45**

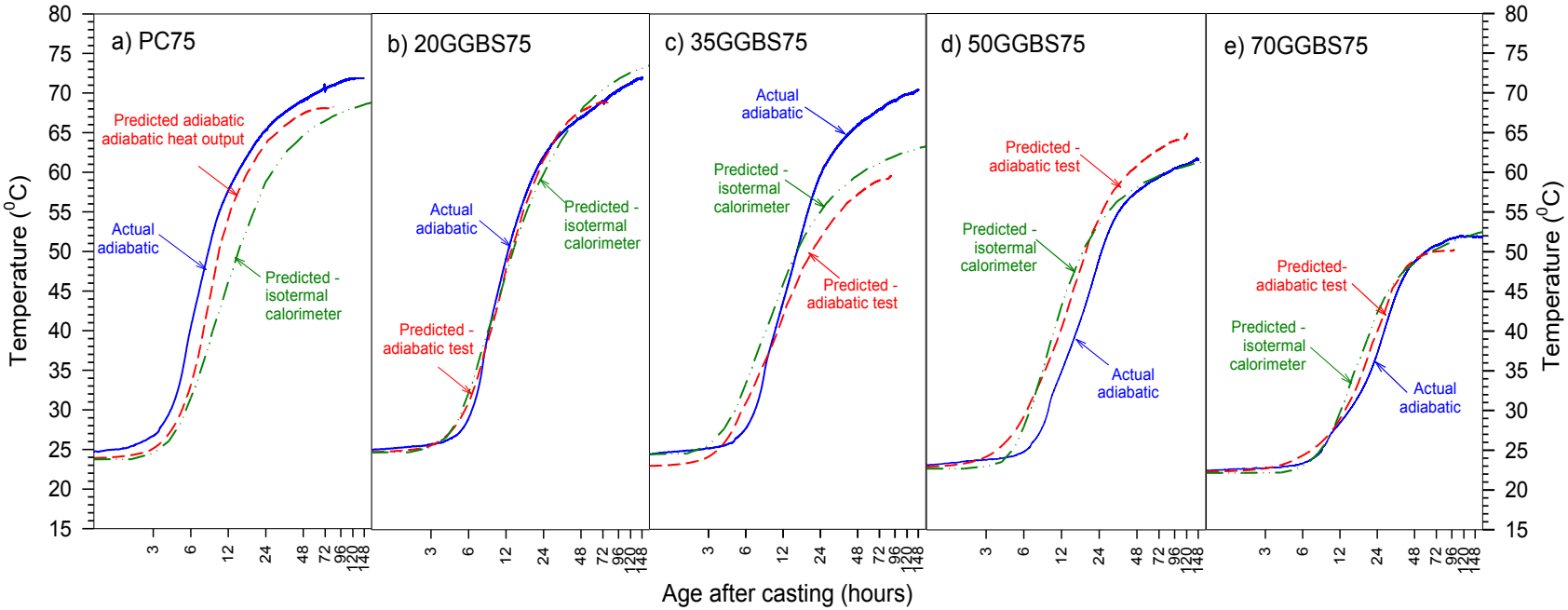

Figure 8.5: Predicted adiabatic temperature concrete **grade C75**

In the 20% GGBS concrete grade C45 (20GGBS45), although the amount of binder in the concrete mixture was not significantly different compared to that of concrete with Portland cement only of the same grade (PC45), the result was unexpected; as the actual adiabatic temperature of the 20GGBS45 concrete was much higher than that of PC45 concrete. As has been discussed in Chapter 4, the adiabatic temperature was measured using thermocouples and a data logger connected to a computer. The computer was then used to control the temperature of the adiabatic chamber. In comparison with the adiabatic temperature obtained from the modelling, it is expected that the actual adiabatic temperature of the 20GGBS45 concrete would be higher as data logger and thermocouples might be produce a false reading.

In general, the predicted adiabatic temperature used the heat output obtained from adiabatic test were very good for all concretes grade C45 and C75, as shown in Figures 8.3 and 8.4, respectively. The dormant or induction period discussed in Chapter 2, was also shown clearly in both these figures. The higher the GGBS level in the concrete, the longer the dormant period. The periods needed for the concrete to begin developing the temperature rise were similar for the actual and the predicted temperatures.

The predicted adiabatic temperatures of concretes grade C45, that used the heat output obtained from the isothermal calorimeter as the heat source in modelling, were reasonably good. This was particularly so for the concretes containing higher levels of GGBS. For the Portland cement and GGBS concretes with level up to 35%, the predicted adiabatic temperatures were much lower than the actual adiabatic temperature of the concretes. It is believed this is due to the smoothed heat output used in the model as the heat source, which appears to play a major role in producing an accurate prediction. Figures 8.1 and 8.2 show that when the heat outputs with any data noise were smoothed, the value of the heat output would reduce. Consequently, the predicted adiabatic temperature resulting from a smoothed heat output in the model will be lower than the actual adiabatic temperature.

The predicted adiabatic temperatures for concretes grade C45 with GGBS levels of 50 and 70%, however, were reasonably accurate. The difference between the predicted and the actual temperatures were not significant up to the age of 3-days, where the effect of curing temperature during the period on the strength development of concrete is much more significant than that at later ages.

In general, the predicted adiabatic temperature for all concretes grade C75 were reasonably accurate. Even the predicted and the actual temperature curves for 20 and 70% GGBS concretes were almost overlapping. The dormant period for the actual and the predicted temperatures are similar, where they also show the higher GGBS levels in concrete having the longer the dormant period.

The accuracy of the predicted adiabatic temperature using the COMSOL software package is very dependent on the heat output used in the modelling. In addition, some values of material properties used in the modelling were taken from the literature review instead of being measured experimentally.

CHAPTER 9 – STRENGTH DEVELOPMENT OF LIGHTWEIGHT AND SELF-COMPACTING CONCRETE – RESULTS AND ANALYSIS

Portions of the material presented in this chapter (i.e. the strength prediction of lightweight and self compacting concretes using the Carino-NS method) have been published in a journal: Soutsos, M. N., Turu'allo, G., Owens, K., Kwasny, J., Barnett, S. J., and Basheer, P. A. M., *Maturity testing of lightweight self-compacting and vibrated concretes.* Construction and Building Materials, 2013. **47**: p. 118-125.

9.1. Introduction

This chapter aims to analyze and investigate the strength development of lightweight and lightweight self compacting concretes that cured at different temperatures. There were five lightweight concretes and three lightweight self compacting concrete mixes cast and tested. The mix designs of the concretes were derived from Queen's University Belfast (QUB) through a research collaboration, developed between QUB and the University of Liverpool.

The five lightweight concrete mixes were: Lightweight Portland cement concrete (LW-PC), Lightweight Fly Ash concrete (LW-FA), Lightweight Fly Ash concrete with activator (LW-FA act), Lightweight Ground Granulated Blast Furnace Slag concrete (LW-GGBS), and Lightweight Ground Granulated Blast Furnace Slag concrete with activator (LW-GGBS act). The three self compacting concrete mixtures were: Normal Weight Self Compacting Concrete with Portland cement as a control (NWSCC-PC), Lightweight Self Compacting Concrete with Ground Granulated Blast Furnace Slag concrete (LWSCC-GGBS), and Lightweight Self Compacting Concrete with Limestone Powder concrete (LWSCC-LSP).

The concretes were cured at different curing temperatures and three cubes were made from samples of each mix for each testing age. Analyses were done to investigate the apparent activation energy and strength development of the

lightweight and self compacting concretes. The results obtained from the analyses were used to assess the suitability of maturity methods for predicting concrete strength development of the lightweight and self compacting concretes.

9.2. Strength Development

9.2.1. Strength Developments of Lightweight Concrete at Curing Temperatures of 20, 30, 40 and 50^0C

The effect of curing temperature on strength development of lightweight concrete was investigated by casting and testing the concretes at certain ages in a similar approach to the testing regimes discussed in the Chapter 4. The results were plotted and regression analyses were carried out using Sigmaplot on the strength development of each curing temperature as shown in Figure 9.1. All the points are the experimental data, while the lines are results that were obtained from a linear regression. The concrete mixtures and strength results are shown in Table C-2 in Appendix C and Tables D-21 to D-25 in Appendix D.

Generally, the effects of curing temperature on the strength development of lightweight concretes at early age are similar to that of the normal concrete. Concretes that cured at higher temperatures had higher strength development at earlier- ages; however, the strength development at later ages is much less affected by higher curing temperatures (up to 40^0C) than that of the normal concretes, which is due to the 'crossover effect'.

Figure 9.1 shows that the strength development of FA and GGBS lightweight concretes cured at 30 and 40^0C at age 28-days are higher than that of concretes cured at the standard curing temperature (20^0C) and appear to be continuously increased after 28-days. The strength development the concretes cured at 50^0C from the ages of 4 to 28-days only increased very slowly, particularly for the concretes that used activator.

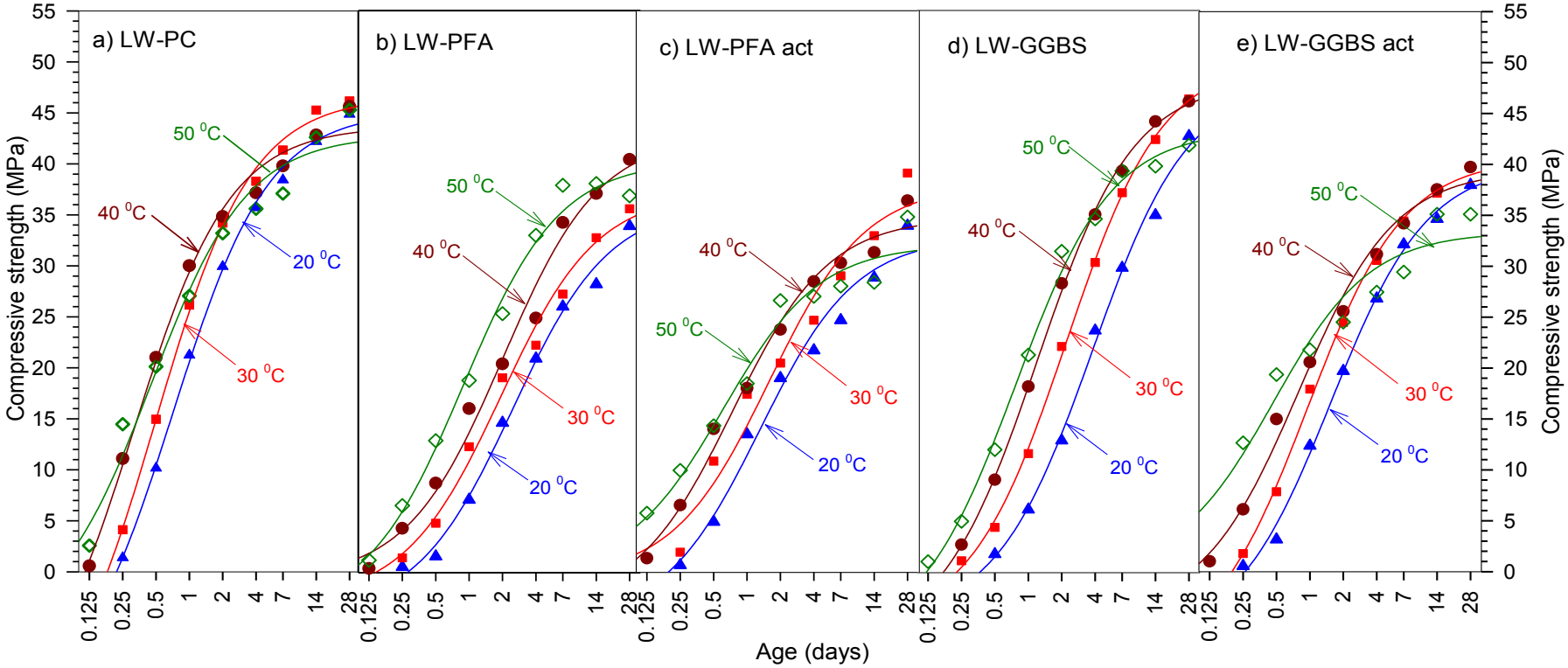

Figure 9.1 : Strength development of **LW-PC, LW-FA, LW-FA act, LW-GGBS** and **LW-GGBS act** concretes cured at 20, 30, 40 and 50^{0}C.

Figure 9.2 shows the ratio of strength development of lightweight concrete with FA and GGBS (with and without activator) and lightweight concrete with Portland cement only that were cured at higher curing temperatures; i.e. 30, 40 and 50^0C to the strength development of concretes, which were cured under the standard curing temperature (20^0C). The strength development of concretes cured at higher curing temperatures is higher compared to that of concretes cured under the standard curing temperature (20^0C). The graph shows that concretes with the higher curing temperature have the higher strength ratio at an early age.

In the lightweight concrete with Portland cement only (LW-PC) that was cured at 50^0C (shown in Figure 9.2a), the strength ratio of the concrete cured at 50^0C compared to that of concrete cured at 20^0C at age six hours (0.25 day) after casting is 10.0. However, the strength ratio then decreases to about 2.0 at the age of twelve hours (0.5 day) after casting. It is believed that 12 hours after casting, the hydration rate of concrete cured at 50 ^{0}C has already reached the peak of hydration. The next hydration phases developed more slowly after the first peak of hydration occurred. On the other hand, the first hydration process in the concrete that was cured at 20^0C was just about to reach the peak of hydration rate.

Figure 9.2 also shows that the ratio of strength development of concrete cured at higher curing temperatures i.e. at 50^0C for GGBS lightweight concrete with activator, to that of concrete cured at 20^0C at earlier age is much higher than the other lightweight concretes. The strength ratios of GGBS lightweight concrete with activator that cured at 30, 40 and 50^0C to that cured at 20^0C at the age of 6 hours (0.25 day), are 3.2, 11.2 and 22.7, respectively. However, the strength ratios significantly decreased at the age of 12 hours (0.5 day), i.e. 2.49, 4.74 and 6.08 for curing temperatures of 30, 40 and 50^0C, respectively. This is similar to the strength ratio of GGBS lightweight concrete without activator; namely 2.47, 5.07 and 6.70 for curing temperatures of 30, 40 and 50^0C, respectively. This means that the effect of activator on the strength development of GGBS concrete cured at 50^0C is significant only at a very early age, i.e. up to the first six hours. The

strength development of both the GGBS concretes with and without activator at a later age was similar.

The effect of higher curing temperature on strength development of FA lightweight concrete is similar to that of GGBS lightweight concrete. Concrete that cured at a higher curing temperature had higher strength development at earlier-age. The ratios of the strength development of FA lightweight concrete with activator that cured at 30, 40 and 50^0C to that of concrete cured at 20^0C at the age of 6 hours (0.25 day) are 2.8, 9.4 and 14.3, respectively. These ratios are quite similar to that of FA lightweight concrete without activator; where the values of the ratio are 2.7, 8.0, and 12.1 for concrete cured at temperature of 30, 40 and 50^0C respectively.

All strength developments of lightweight concrete with Portland cement only that cured at 30, 40 and 50^0C at an age of 2-days, are less than 20% higher than that of concrete cured at 20 ^{0}C. The ratio of strength of concrete cured at 50^0C to that of 20^0C is 0.96, while for concretes cured at 30 and 40^0C are 1.07 and 1.04 respectively. In comparison to FA and GGBS lightweight concretes (with and without activator), the strength of concretes that cured at 30, 40 and 50^0C are 20% higher than the strength of concretes cured at 20 ^{0}C. The exception is for FA lightweight concrete with activator that had been cured at 30^0C, where the ratio of the strength of the concrete to that of cured at 20 ^{0}C is 1.08. Even the strength of FA and GGBS lightweight concretes that cured at 50^0C at an age of 4-days are still 20% higher than that of concrete cured at 20^0C; except for GGBS lightweight concrete with activator, which had a strength ratio of 1.01.

Ratios of strength development of lightweight concretes cured at 20, 30, 40 and 50^0C to the strength of concrete at 28-days that cured under standard curing temperature (20^0C) are shown in Figure 9.3. The strength of PC, FA and GGBS lightweight concretes with activator cured at 50^0C at an age of 6 hours after casting are 30.97%, 29.43% and 32.73% respectively of their strength at an age of 28-days cured at 20^0C. On the other hand, the strengths of both LW-FA and LW-

GGBS concretes without activator at the same age only reached 19.35% and 11.76% of their strength at 28-days. The ratio of the strength of LW-FA act and LW-FA concretes cured at 50^0C at age 1-day to their strength at age 28-days cured at 20^0C is similar, i.e. 0.55 and 0.56 respectively, where the strength of both the concretes cured at 20^0C at 28-days was the same i.e. 33.9 MPa. On the other hand, the ratio of strength of LW-GGBS act and LW-GGBS concretes at age 1-day to their strength at age 28-days cured at 20^0C were 0.57 and 0.50, respectively. The strength development of LW-FA and LW-GGBS concretes that had cured at 50^0C at later ages, however, was higher than that of the concretes with activator. This is believed to be due to the formation of dense hydrated phase around the unreacted binder particles preventing further hydration. The use of activator in concrete that was cured at a higher temperature increased the rate of hydration compared to the concrete cured at a lower temperature at an earlier age. However, the hydration products were not well distributed and resulted in preventing water reaching the unreacted binder for further reaction.

The strength of FA concrete without activator that cured at 40^0C at age 28-days was 19.27% higher than that cured at 20^0C. While the strength of GGBS concrete without activator cured at the same curing temperature and age was only 7.96% higher than the strength of the concrete cured at 20^0C. However, the strength development of all concretes at all curing temperatures appears to increase continuously after 28 days. This proves that lightweight concrete cured at higher temperature does not affect the strength development of the concrete too much, unlike what was seen with normal weight concrete.

In LW-PC concrete, the *'crossover effect'* occurred due to an earlier-age high curing temperature. The strength of the LW-PC concrete cured at 30 and 40^0C were higher than that of cured at 50^0C, from the age of 2-days until 28-days, as shown in Figure 9.1. The figure also shows that the detrimental effect of the high curing temperature, i.e. 50^0C, at early age occurred earlier in the FA and GGBS concretes with activator than that in the FA and GGBS concretes without activator.

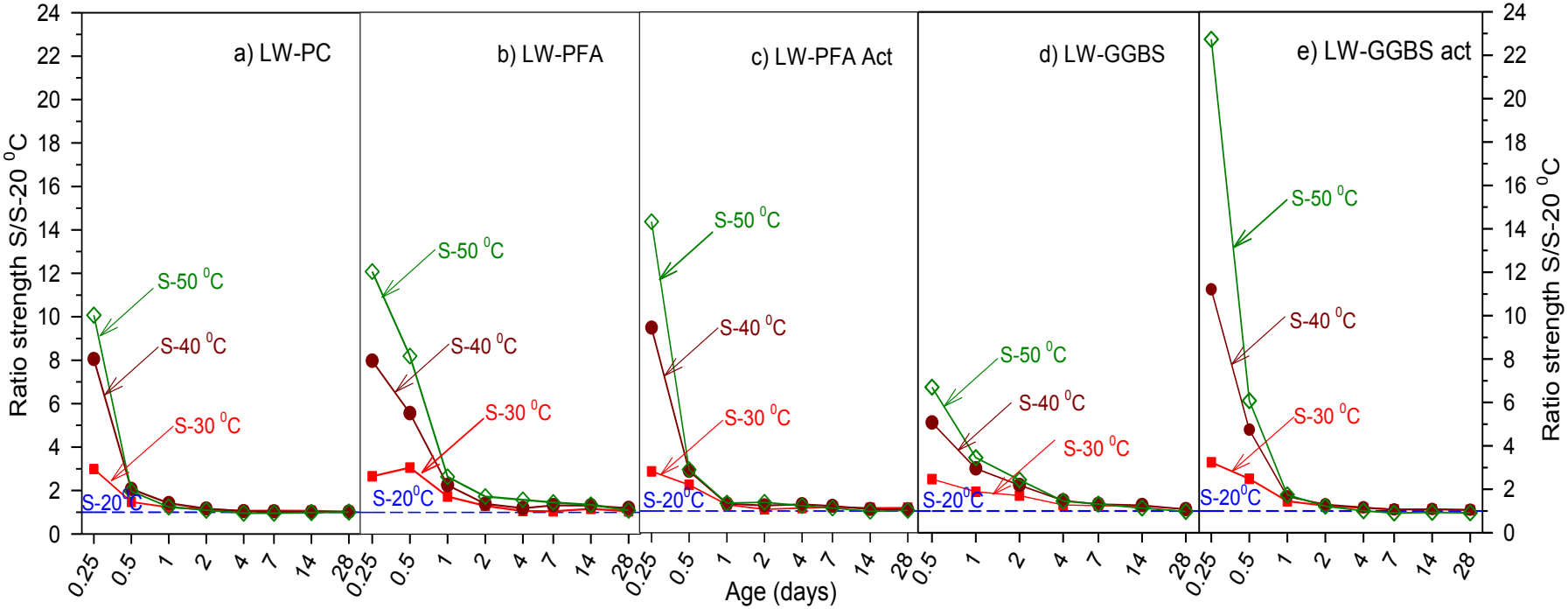

Figure 9.2: Ratios strength development of **LW-PC, LW-FA, LW-FA act, LW-GGBS** and **LW-GGBS act** concretes cured at higher temperatures i.e. 30, 40 and 50 ^{0}C to that of the concretes cured under standard curing temperature (20^{0}C).

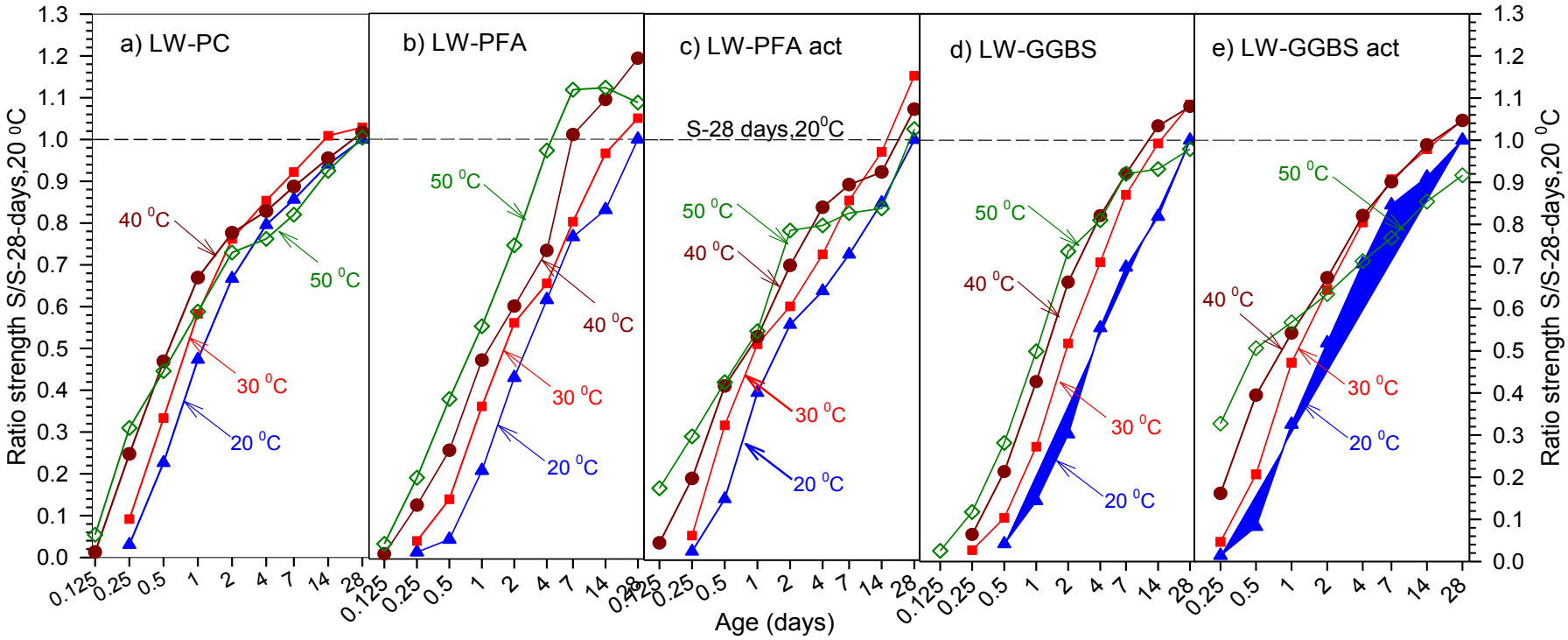

Figure 9.3: Ratios strength development of **LW-PC, LW-FA, LW-FA act, LW-GGBS** and **LW-GGBS act** concretes cured at 20, 30, 40 and 50 ^{0}C to the strength of the concretes at 28-days cured under standard curing temperature (20^{0}C).

The water-binder ratios of FA and GGBS lightweight concretes (with and without activator) were the same as that of lightweight concrete with Portland cement only, i.e. 0.42; which were expected to have similar target mean strength at 28-days. Figure 9.4 shows the ratio of strength development of FA and GGBS concretes (with and without activator) to the strength development of lightweight concrete with Portland cement only. The figure shows that the strengths of FA (with and without activator) and GGBS lightweight concretes with activator at 28-days are lower than that of lightweight concrete with Portland cement only at the same age. The exception is for GGBS concrete without activator (LW-GGBS) cured at 30 and 40^0C, where the strength of the concrete at age 28-days are similar, even slightly higher than that of lightweight concrete with Portland cement only.

It is shown in Figure 9.4 that the strength development of FA concrete with activator is very slow after the age of 6 hours (0.25 day) which is similar to the strength development of GGBS concrete with activator. The ratios of strength of FA lightweight concretes (with and without activator) cured at all temperatures to the strength of Portland cement lightweight concrete at 28-days were lower than 1.0. It ranged from 0.76 to 0.89, where the lowest and the highest ratio are FA concrete (with and without activator) cured at 20^0C and FA concrete without activator cured at 40^0C, respectively.

The strength development of FA lightweight concrete without activator that was cured at 20, 30 and 40^0C appears to be still continuously increasing at later ages (after 28-days). In contrast to the concrete that had cured at 50^0C, the strength development of the concrete seems to be affected by a high curing temperature at an early age. The strength development of the concrete cured at 50^0C appears to be very slow from the age of 7 to 14-days and then goes up again from the age 14 days until 28-days. The strength development of FA concrete with activator is very different than that of FA concrete without activator. The strength development of LW-GGBS act concrete was lower than that of LW-PC concrete during 28-days testing, where its strength at age 28-days varies between 77.2%

and 87.1% of the strength of lightweight concrete with Portland cement only that had been cured at the same curing temperature. This is on average 15% lower than that of lightweight concrete with Portland cement. The strength development of GGBS concrete without activator was higher than that of GGBS concrete with activator after age 7-days. Even the strength of GGBS concrete without activator was similar to the strength of lightweight concrete with Portland cement only at age 28-days. The strength of the concrete reached 95.2% and 92.8% of the strength of Portland cement concrete at age 28-days that had been cured at 20 and 50^0C respectively, and 100.4% and 101.0% for GGBS concrete without activator cured at 30 and 40 ^{0}C.

Except for the use of an activator, the ingredient mixture of FA concrete with and without activator was the same as for GGBS concrete with and without activator. Figure 9.5 shows the ratio of strength development of FA and GGBS concretes (with and without activator). The strength development of both FA and GGBS concretes that was cured at 50^0C rapidly increased at very early age. The strength ratio of concrete with activator compared to that of concrete without activator that cured at 50 ^{0}C at the age of 3-hours (0.125 day) are 4.79 and 3.39 for FA and GGBS concretes, respectively. The strengths of FA concrete at the same age are 5.79 MPa and 1.21 MPa for concrete with and without activator, respectively. On the other hand, the strength of GGBS concrete that was cured at 50 ^{0}C at age 3 hours, are 3.65 and 1.07 MPa for the GGBS concrete with and without activator, respectively.

The strength of both FA and GGBS concretes with activator appears to be similar to the strength of FA and GGBS concretes without activator at age 1-day. Even the strength of both FA and GGBS concretes with activator are lower than that of concretes without activator at later ages. This is believed to be due to the effect of using the activator and high curing temperature at an early age.

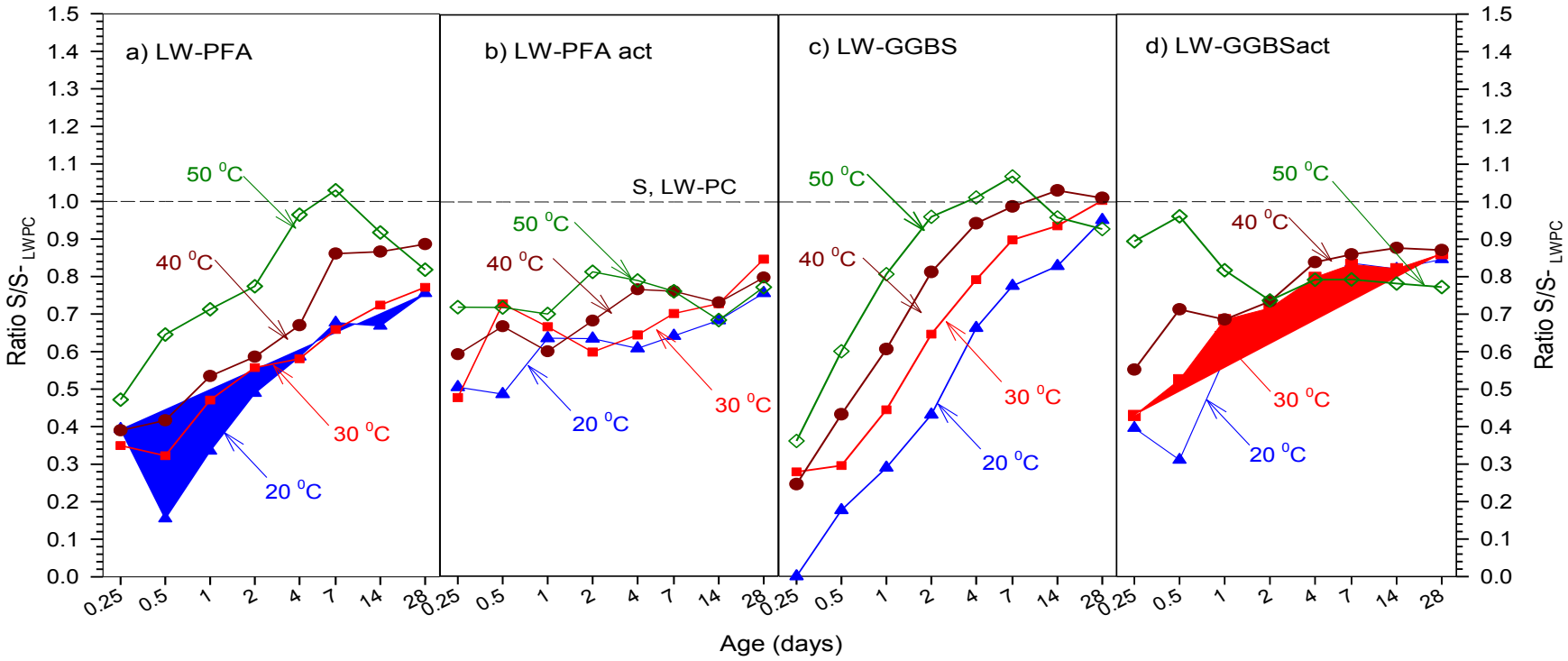

Figure 9.4: Ratio strength developments of **LW-FA, LW-FA act, LW-GGBS** and **LW-GGBS act** concretes to the strength of LW-PC concrete cured at 20, 30, 40 and 50^{0}C.

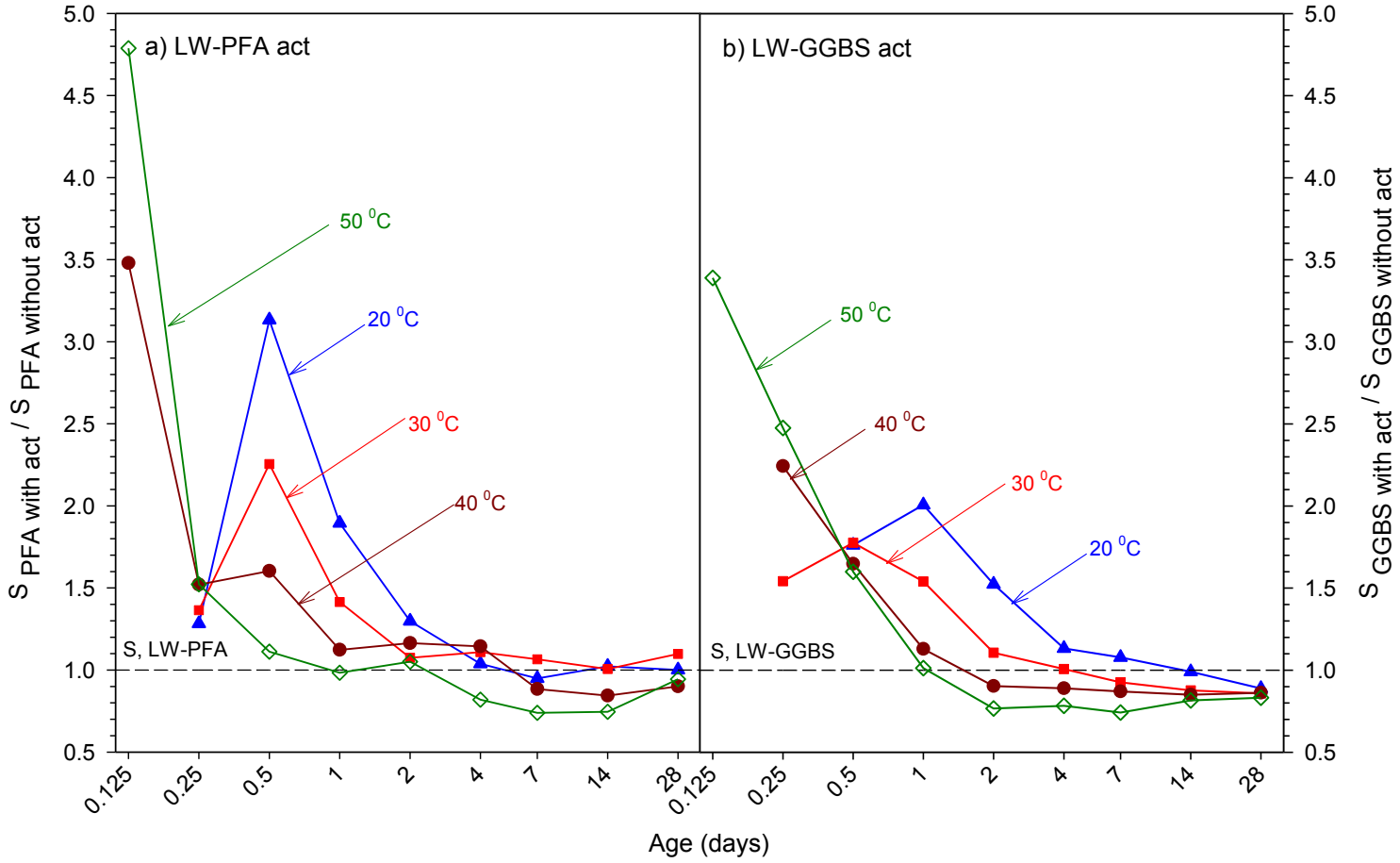

Figure 9.5: Ratio strength developments of **FA** and **GGBS lightweight** concretes with activator compared to that of without activator

The use of activator significantly increases the strength development of concrete, particularly at an earlier age. However, the increase in hydration products at earlier age leads to more large pores due to the reaction products not having time to become uniformly distributed within the pores of the hardened paste. Furthermore, "shell" made up of low permeability hydration products builds up around the un-hydrated cement grains. This shell therefore, prevents further hydration of the un-reacted portion of the grains at later ages. As a result, concrete with activator has a lower strength than that of concrete without activator even when they were cured at the same temperature.

Figure 9.6 presents the effect of curing temperature on the time taken for each concrete to reach 50% of its calculated ultimate strength *(t_{50})*. Commonly, the highest curing temperature had the shortest time taken to reach 50% of its calculated ultimate strength. The figure shows that the '*t_{50}*' increases with decreasing curing temperature. The '*t_{50}*' of Portland cement, FA and GGBS lightweight concretes (without activator) cured under the standard curing temperature are 27.6, 72.7 and 107.9 hours, respectively. All the lightweight concrete mixes have the same water-binder ratio; therefore, the results prove that the strength development of GGBS lightweight concrete is slower than the other two mixes. However, at the temperature 50^0C, the '*t_{50}*' of PC, FA and GGBS lightweight concretes (without activator) were significantly decreased to become 50.3%, 34.5% and 22.2% of their t_{50} of the concrete that cured at 20^0C.

The increase of curing temperature by 10^0C, significantly shortened the time taken to reach the calculated ultimate strength of concrete. For example, the increased curing temperature from 20 to 30^0C for the FA and GGBS concretes can shorten the 't_{50}' to 53.19 and 63.54 hours, respectively. However, it appeared that there was no significant decrease of the '*t_{50}*' by increasing the curing temperature by 10 ^{0}C for the FA concrete without activator (from 30 to 40^0C) and the PC concrete (from 40 to 50^0C).

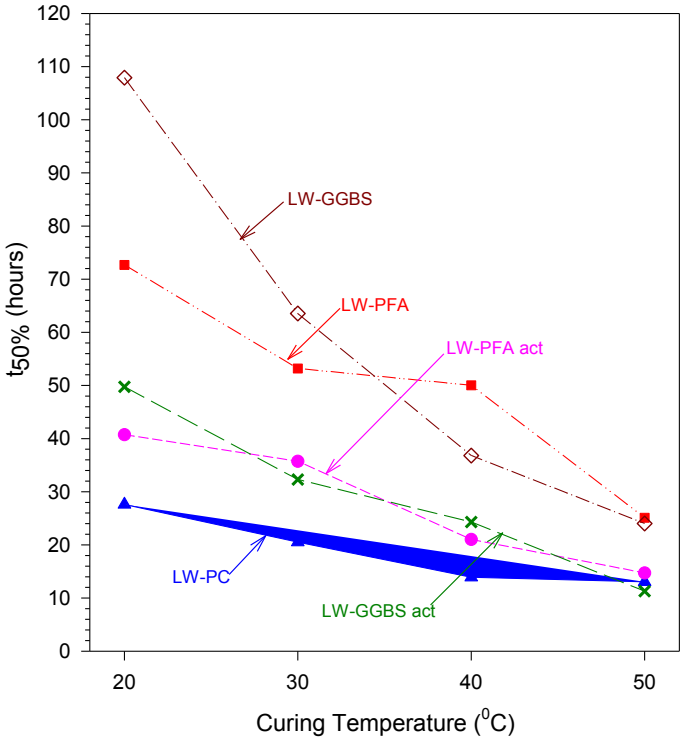

Figure 9.6: Effect of curing temperature on the time taken to reach 50% of ultimate strength of **LW-PC, LW-FA, LW-FA act, LW-GGBS** and **LW-GGBS act** concretes

It is useful to investigate the effect of activator on the time taken of each concrete to reach 50% of its calculated ultimate strength. For the FA concrete, the use of activator can decrease the 't_{50}' by 30 hours, from 72.7 to 40.7 hours for concrete cured at 20^0C. Furthermore, the use of activator for FA concrete cured at 50^0C still reduces the 't_{50}'. However, this was not as more to that of concrete cured at 20^0C, which only cuts about ten hours from the curing time i.e. from 25.11 to 14.72 hours.

The use of activator for GGBS concrete appears to be much more significant particularly for concrete cured at 20^0C. The use of activator can shorten the 't_{50}' as much as 58.1 hours, from 107.9 to 49.8 hours; this is about 2.2 times shorter than that of GGBS concrete without activator. The effect is similar to that of concrete cured at higher temperatures, for example at 50^0C, the use of activator can reduce the 't_{50}' by about 2.13 times than that of GGBS concrete without activator; i.e. from 24.03 to 11.29 hours.

9.2.2. Strength Developments of Self Compacting Concrete at Curing Temperatures of 20, 30, 40 and 50^0C

To investigate the effect of curing temperature on the strength development of normal and lightweight self compacting concrete, three mixes were produced, i.e. normal weight self compacting concrete with Portland cement, GGBS lightweight self compacting, and limestone powder (LSP) lightweight self compacting concretes. All of these were cast, cured at different curing temperatures, and tested. The water binder ratio of normal weight concrete with Portland cement, i.e. 0.45 is higher than that of GGBS and LSP lightweight self compacting concretes, where both the concretes have the same water binder ratio i.e. 0.35.

Figure 9.7 presents the effect of curing temperature on strength development of normal and lightweight self compacting concretes cured at 20, 30, 40 and 50^0C. All the points are the experimental data, while the lines are the results that obtained from linear regression. The concrete mixtures and strength results are shown in Table C-2 of Appendix C and in Tables 26 to 28 in Appendix D, respectively.

The strength development of self compacting concrete depends greatly on curing temperature as it does with normal concrete. As expected, the strength development of concrete cured at higher curing temperature at early ages was faster than that of concrete cured at lower temperature; however, they have lower strength at later ages. Conversely, strength development of concretes that cured at lower temperature is slower than that of concrete cured at higher temperature, but they have higher strength at later ages. The figure shows that the 'crossover effect' occurred at an earlier age than that in normal concrete. This is believed to be due to the influence of the use of high doses of superplasticizer which result in the concrete having a high workability. The superplasticizer accelerates the hydration process; therefore, concretes that use superplasticizer, which are cured at higher curing temperatures produce much greater degrees of hydration product at an earlier age. Furthermore, the formation of a dense hydrated phase around

the un-hydrated cement particles, preventing further hydration, this will lead to lower strength at later ages.

The effect of higher curing temperature on lightweight self compacting GGBS concrete (LWSCC-GGBS) appears to be slightly less than that on normal weight self compacting concrete with Portland cement only (NWSCC-PC) and lightweight self compacting concrete with limestone powder (LWSCC-LSP). It is expected that the heat produced in the hydration process of LWSCC-GGBS was absorbed and used as activation energy for further hydration. Therefore, the effect of the use high doses of superplasticizer can be minimized in both others concretes. The strength development of the concretes cured at 20^0C appears to develop continuously after age 28-days for all concretes.

The LWSCC-GGBS and LWSCC-LSP concretes have the same water binder ratio and the same replacement level of cement with GGBS and LSP of 30%. Therefore, they were expected to have a similar target mean strength at age 28-days, but in fact, the strength of LWSCC-LSP concrete ranged between 21% and 30% lower than that of LWSCC-GGBS concrete, where the maximum difference occurred in concrete cured at 50^0C.

Figure 9.8 presents the strength ratio of normal and lightweight self compacting concrete that cured at 30, 40 and 50^0C to the strength of concrete cured at the standard curing temperature. The figure shows that the highest curing temperature results in the highest strength ratio at very early ages. For concrete NWSCC-PC, the ratio of strength of concrete cured at 30, 40 and 50^0C to the strength of concrete cured at the standard curing temperature at age 6 hours after casting are 3.9, 6.0 and 7.77, respectively. The strength ratio of LWSCC-GGBS concrete at that age is similar to that of NWSCC-PC, but it is higher than that of LWSCC-LSP concrete, even though they have the same water binder ratio and the same replacement level of cement with these materials. The ratios for LWSCC-GGBS concrete were 3.14, 4.90, and 6.62 for 30, 40 and 50^0C respectively, and 2.42, 3.18, and 3.44 for the LWSCC-LSP concrete.

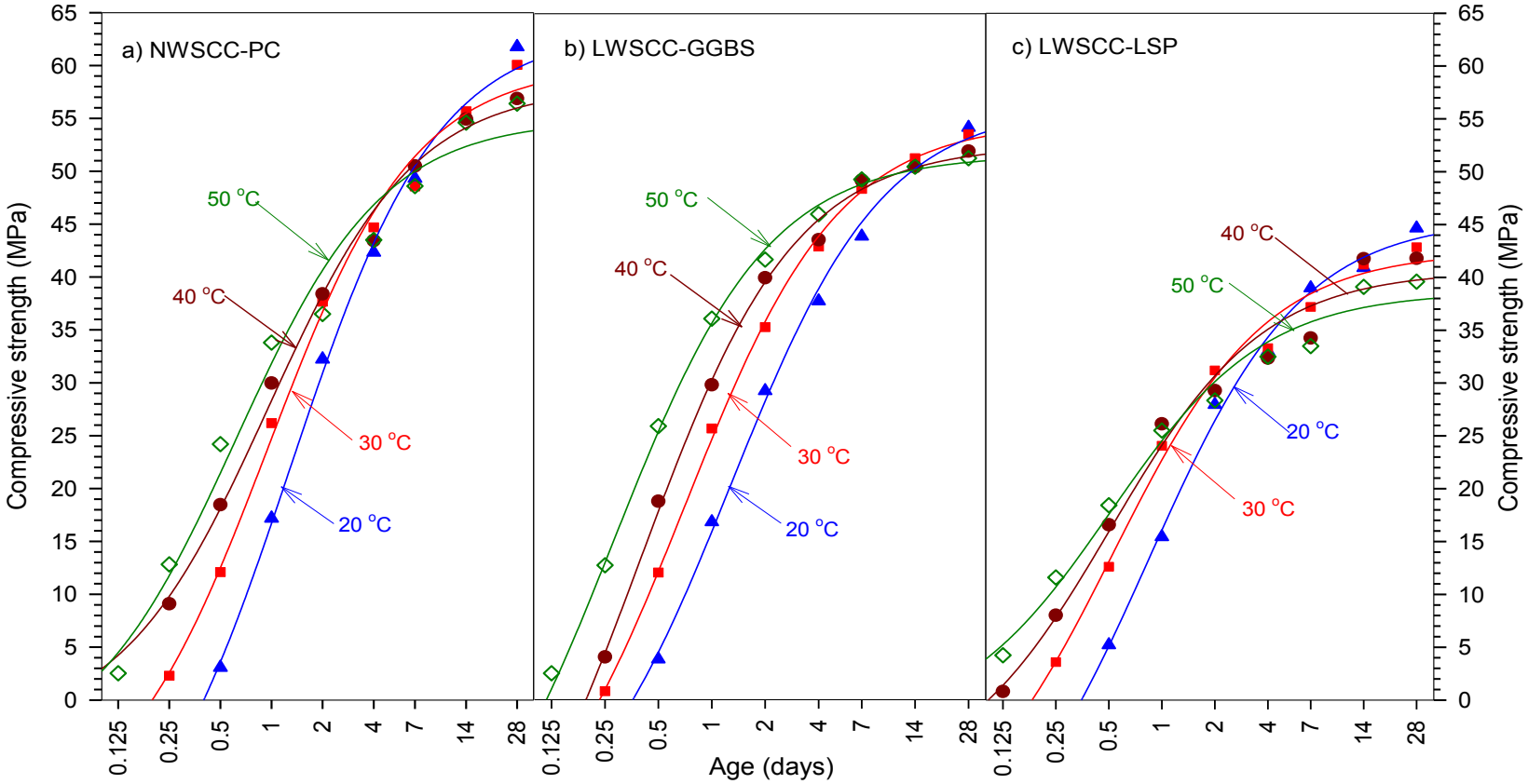

Figure 9.7: Strength development of **NWSCC-PC, LWSCC-GGBS** and **LWSCC-LSP** concretes cured at 20, 30, 40 and 50^{0}C.

The *"crossover effect"* in the NWSCC-PC and LWSCC-LSP concretes occurred earlier than that in the LWSCC-GGBS. This proves that the hydration process in concrete that used GGBS occurs slowly. The ratios of the strength of concrete cured at higher temperatures to that of concrete cured at the standard curing temperature at age 28-days for all concretes were quite similar, with ranges from 0.88 to 0.99. The ratio of 0.88 was for LWSCC-LSP cured at 50^0C, while 0.99 was for LWSCC-GGBS concrete that cured at 30^0C.

The ratios of strength of concrete cured at 20, 30, 40 and 50^0C to the strength of the concrete cured under the standard curing temperature (20^0C) at age 28-days are presented in Figure 9.9. All self compacting concretes at age 1-day that were cured at 50^0C reached about 50% of their strength at age 28-days, i.e. 53.6%, 65.7% and 56.5% for NWSCC-PC, LWSCC-GGBS and LWSCC-LSP concretes, respectively. These are significantly higher than that for concrete cured at 20^0C, where the percentage strength of concrete at age 1-day to the strength at age 28-days are 27.8%, 31.1% and 34.6% for NWSCC-PC, LWSCC-GGBS and LWSCC-LSP concretes, respectively.

The strength percentage of NWSCC-PC concrete is lower than that of both other self compacting concretes even though its strength is the highest among the three concretes. This is due to the strength of NWSCC-PC concrete at age 28-days being higher than that of the LWSCC-GGBS and LWSCC-LSP concretes. For the concrete cured at 30 and 40^0C, the percentage of strength of concrete at age 1-day to the strength of the concrete at age 28-day cured at 20^0C varies from 42.4% to 53.9 % for curing temperature 30^0C and from 48.5% to 58.5% for 40^0C.

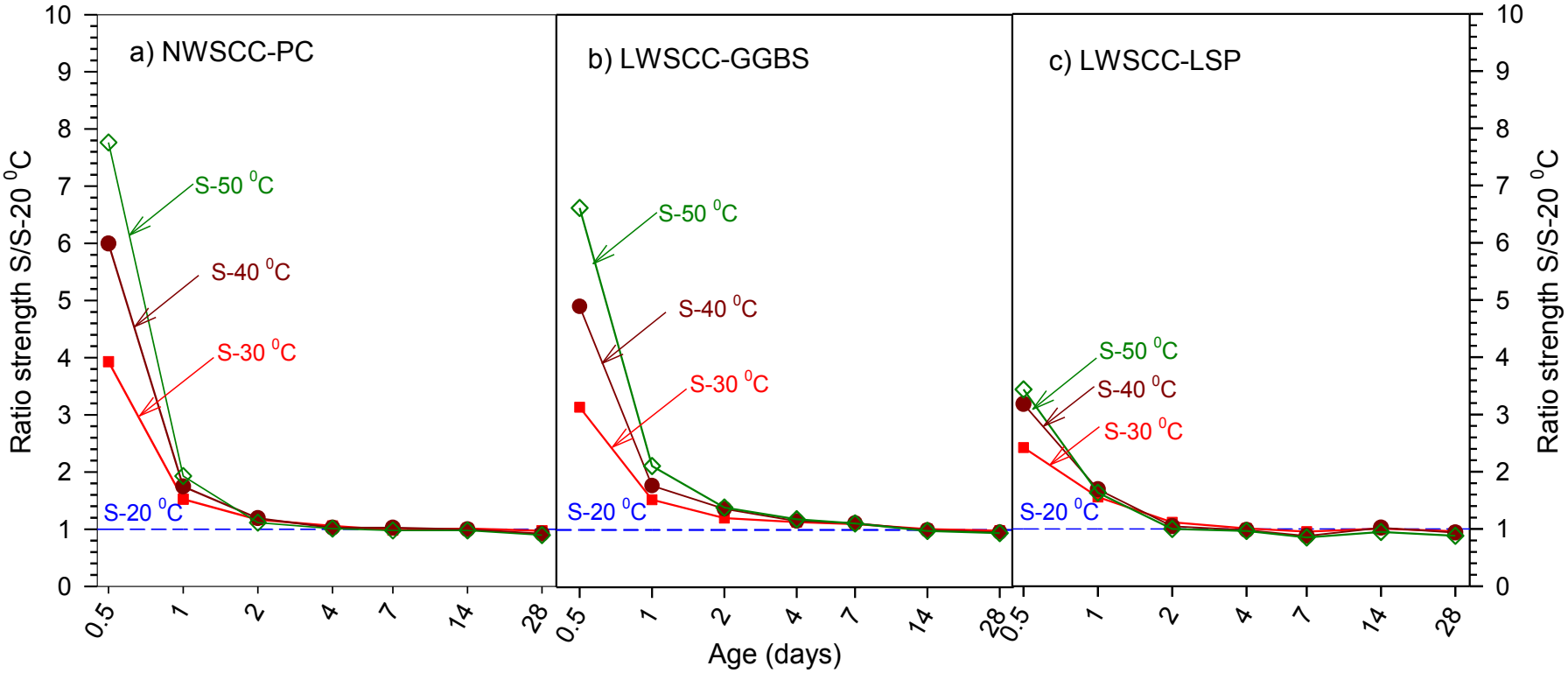

Figure 9.8: Ratios strength development of **WNSCC-PC, LWSCC-GGBS** and **LWSCC-LSP** concretes cured at 30, 40 and 50^{0}C to that of the concretes cured 20^{0}C.

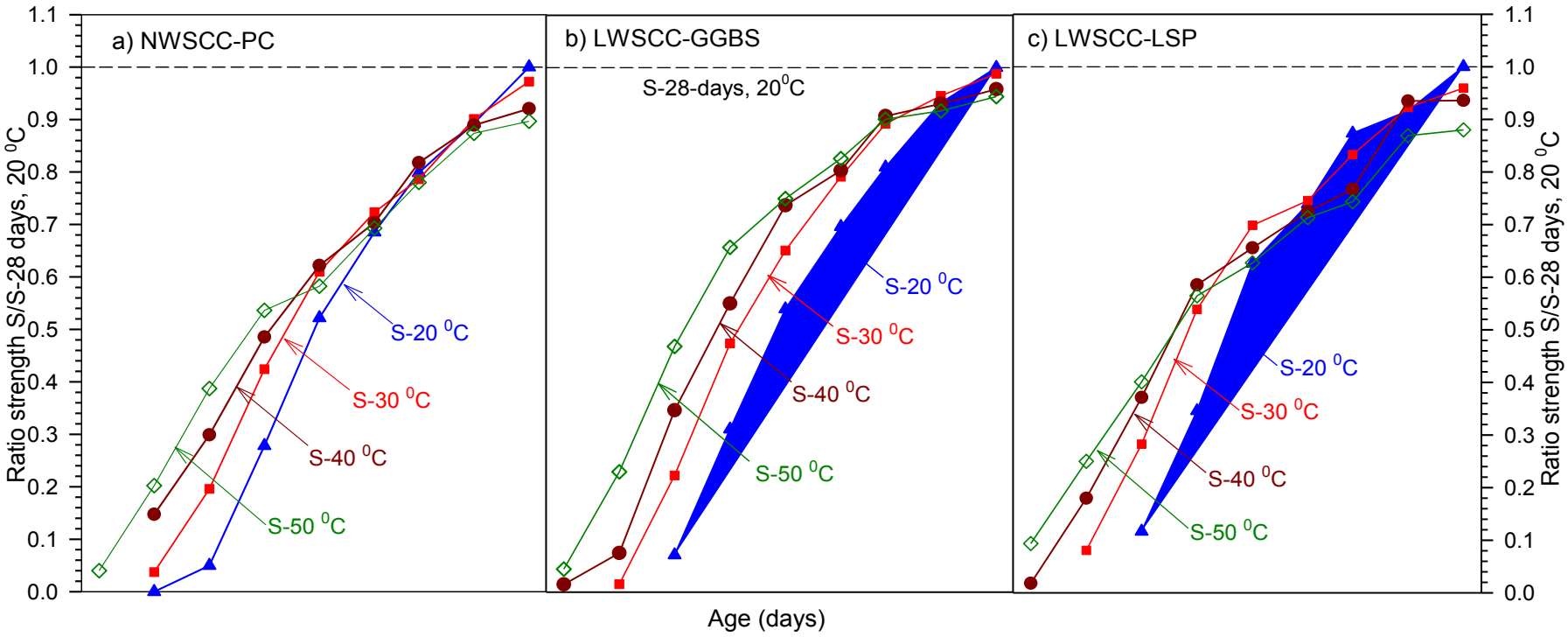

Figure 9.9: Ratios strength development of **WNSCC-PC, LWSCC-GGBS** and **LWSCC-LSP** concretes cured at 20, 30, 40 and 50^{0}C to the 28-days strength of the concretes cured at 20^{0}C.

Figure 9.10 shows the effect of curing temperature to the time taken for concrete to reach 50% of its calculated ultimate strength, t_{50}. The figure shows that the highest curing temperature resulted in the shortest time taken to reach 50% of its calculated ultimate strength, and the 't_{50}' increases with decreasing of curing temperature. The 't_{50}' of NWSCC-PC, LWSCC-GGBS and LWSCC-LSP concretes cured under the standard curing temperature are 49.89, 47.67 and 37.02 hours respectively. NWSCC-PC concrete has a water-binder ratio higher than that of both LWSCC-GGBS and LWSCC-LSP concretes, and LWSCC-GGBS and LWSCC-LSP concretes have the same water-binder ratio. Therefore, it was acceptable if the time taken to reach 50% of its calculated ultimate strength of NWSCC-PC concrete is longer than that of the two other concretes. The result also shows that although the water-binder ratio of LWSCC-GGBS and LWSCC-LSP concretes are the same, however, the 't_{50}' of LWSCC-GGBS concrete cured at 20^0C takes 10.65 hours longer than that of LWSCC-LSP concrete. This was because the hydration process in the LWSCC-LSP concrete was faster than that in the LWSCC-GGBS concrete.

The increase in curing temperature by10^0C significantly shortened the time taken to reach its calculated ultimate strength of concrete particularly from 20 to 30^0C, where it reduced the 't_{50}' by 17.59, 19.57 and 25.58 hours for NWSCC-PC, LWSCC-GGBS and LWSCC-LSP concretes, respectively. However, the increase in temperature by 10^0C is not so significant when the temperature increases 10^0C from 40 to 50^0C. The reduction of 't_{50}' is not much compared to the increasing from 20 to 30^0C. The 't_{50}' were reduced to only 7.28, 6.62 and 3.04 hours for NWSCC-PC, LWSCC-GGBS and LWSCC-LSP concretes respectively.

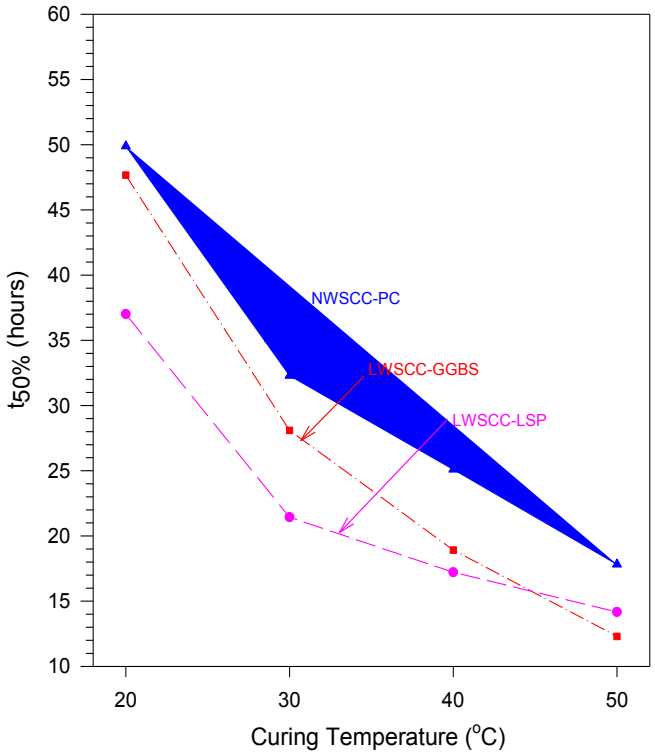

Figure 9.10: Effect of curing temperature on the time taken to reach 50% of ultimate strength of **LW-PC, LW-FA, LW-FA act, LW-GGBS** and **LW-GGBS act** concretes

9.3. Adiabatic Temperatures Rise

9.3.1. Adiabatic Temperatures Rise of Lightweight Concrete

Figure 9.11 presents the adiabatic temperature rise of lightweight concretes. The casting temperatures varied from 22 to 23^{0}C. As expected, the temperature rise of lightweight concrete with Portland cement only was the highest, which increased by 59^{0}C from its casting temperature, i.e. 23^{0}C, as the concrete contained two times more cement than the other concretes.

It is important to investigate the different temperature rise of GGBS lightweight concrete with and without activator. This is expected to have a similar temperature rise as they have the same binder content and water-binder ratios. The presence of activator is the only significant difference between them. The temperature rise in GGBS lightweight concrete without activator i.e. 74^{0}C; is

10^0C higher than that of GGBS lightweight concrete without activator. This is believed that as the activator accelerates the hydration process of cement, therefore, the hydration product of concrete with activator at early ages is much greater than that of concrete without activator. This is as a result of the formation of dense hydrated phases around the un-hydrated cement particles obstructing further hydration. This means that there is still un-hydrated cement inside the concrete, which will lower the temperature rise in the concrete.

The temperature rise of lightweight FA concrete with and without activator was similar, i.e. 38 and 37^0C, respectively. However, the temperature rise in FA concrete with activator rapidly increases at earlier age compared to that of FA concrete without activator.

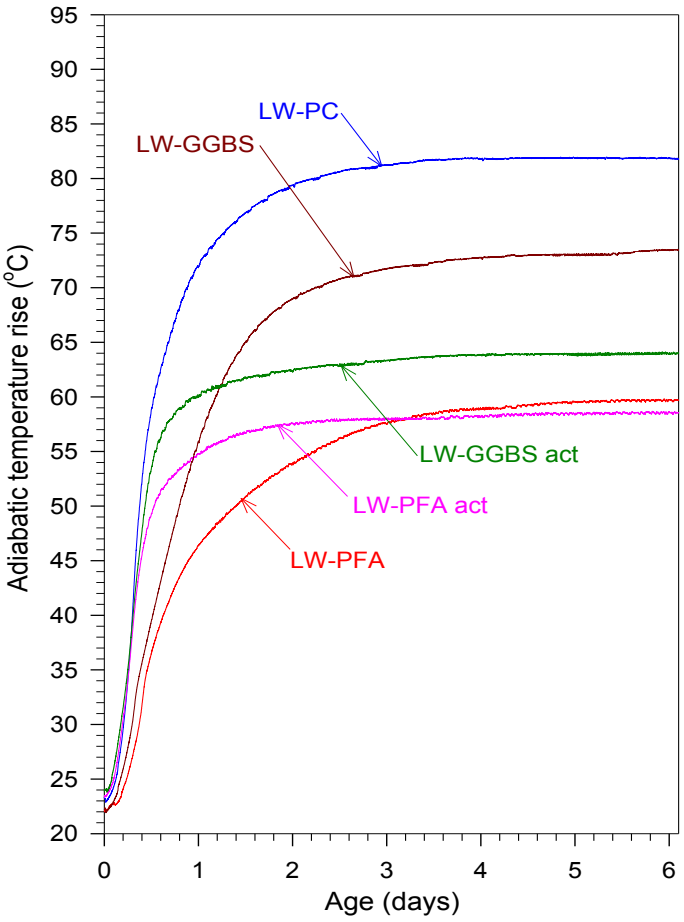

Figure 9.11: Adiabatic temperature rises of **LW-PC, LW-FA, LW-FA act, LW-GGBS** and **LW-GGBS act** concretes

9.3.2. Adiabatic Temperatures Rise of Self Compacting Concrete

Figure 9.12 presents the adiabatically temperature rise of normal and lightweight self compacting concretes. The casting temperature varies from 20 and 22^{0}C.

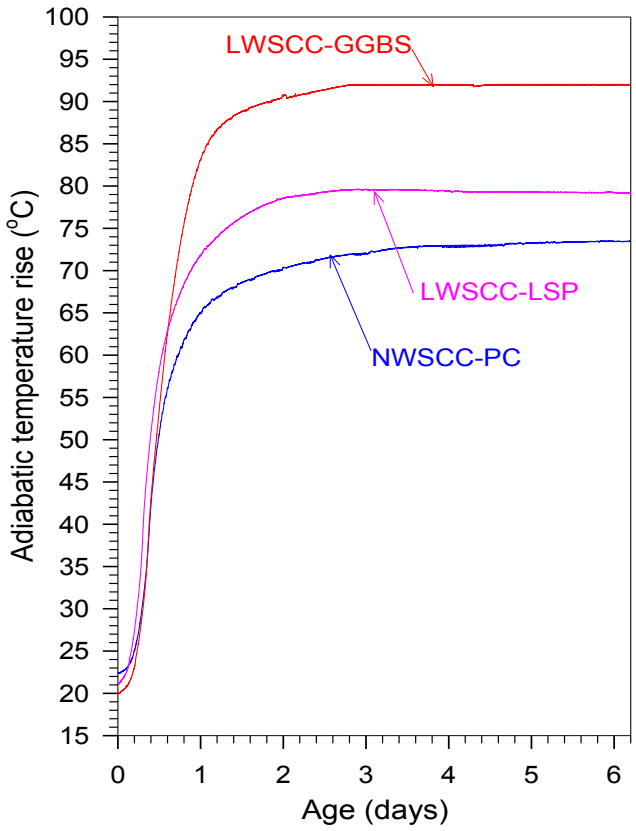

Figure 9.12: Adiabatic temperature rises of NWSCC-PC, LWSCC-GGBS and LWSCC-LSP concretes

The maximum temperature rise occurred in LWSCC-GGBS concrete i.e. 72^{0}C from its casting temperature. This was as expected, as the LWSCC-GGBS concrete contains more binder with a lower water-binder ratio than that of NWSCC-PC concrete. Although both the LWSCC-GGBS and LWSCC-LSP concretes have similar contents of binder, however, the temperature rise in LWSCC-GGBS is 12.8^{0}C higher than that of LWSCC-LSP concrete.

9.4. Strength Development of Lightweight and Self Compacting Concrete under Standard Curing Temperature and Adiabatic Condition

9.4.1. Strength Development of Lightweight Concrete under Standard Curing Temperature and Adiabatic Conditions

Figure 9.13 shows the strength development of lightweight concretes cured under adiabatic conditions. In general, the adiabatic strength development is higher than that of the strength development of concrete cured at standard curing temperature. Apart from LW-FA, all the strengths of lightweight concrete at age 28-days are similar to their strength for concrete that was cured at the standard curing temperature, while the adiabatic strength for LW-FA concrete (without activator) is 32.15% higher than the strength of concrete cured at the standard curing temperature. There is not much negative effect on adiabatic strength development of lightweight concrete as sometimes happens in normal concrete.

At an early age (1-day), the ratio of adiabatic strength of LW-GGBS to the strength of the concrete that was cured at 20^0C, was higher than that of other lightweight concretes, i.e. 2.86, compared to that of LW-FA act and LW-FA (with and without activator), i.e. 1.52 and 2.36, respectively, as shown in Figure 9.14. This is due to the strength development of LW-GGBS concrete under the standard curing temperature being slower than that of the other lightweight concretes.

Except for LW-GGBS act concrete, all other lightweight concretes cured under adiabatic condition during the testing have a strength higher than that of the strength of concrete cured at 20^0C.

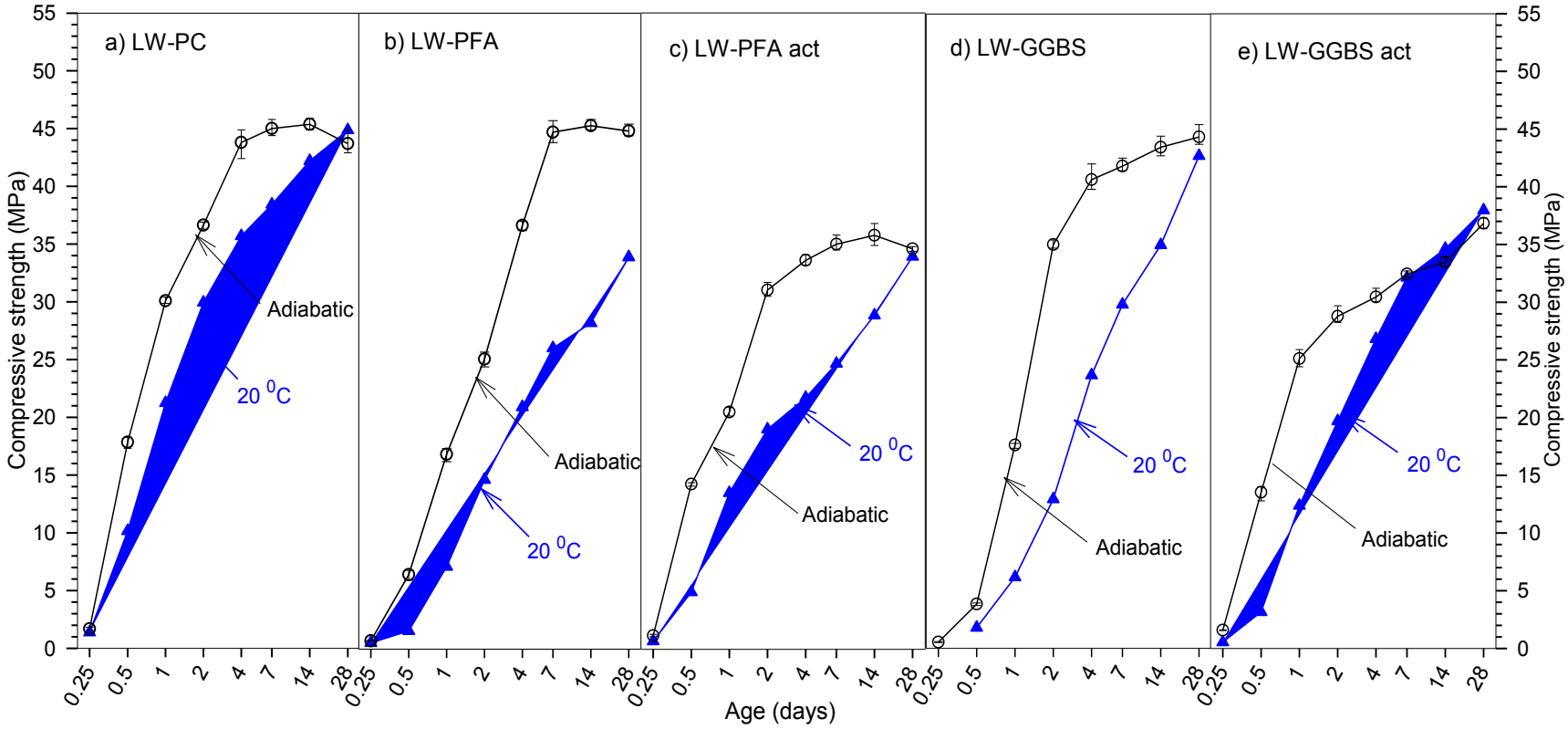

Figure 9.13: Strength developments of **LW-PC, LW-FA, LW-FA act, LW-GGBS** and **LW-GGBS act** concretes cured at standard curing temperature curing temperature (20^0C) and under adiabatic curing condition

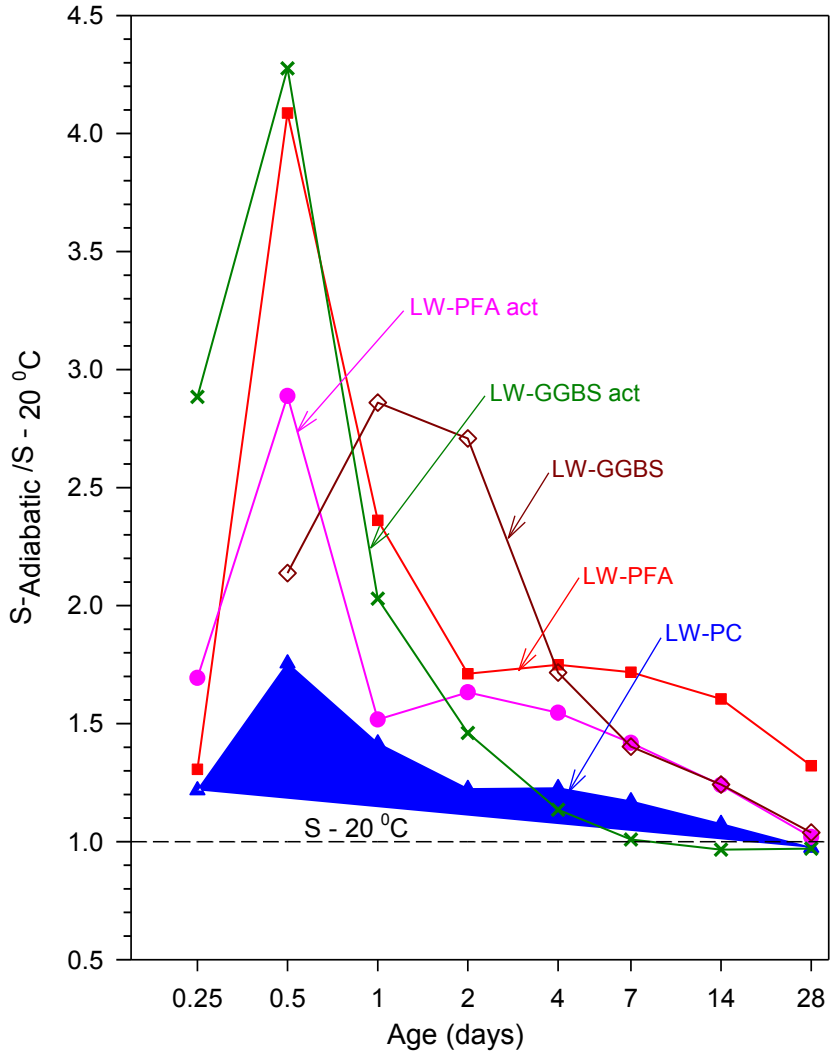

Figure 9.14: Ratio S-adiabatic/S-20^{0}C of **LW-PC, LW-FA, LW-FA act, LW-GGBS** and **LW-GGBS act** concretes

The ratio between the strength of concrete cured under adiabatic condition to the strength of concrete at age 28-days cured at the standard curing temperature is shown in Figure 9.15. At age 1-day, the strength of LW-PC reached 67.07% of the strength of concrete at age 28-days that had been cured at the standard curing temperature. The result shows that activator contributes to strength development of concrete. The strength of LP-FA act and LW-FA concretes (with and without activator) at age 1-day are 60.41 and 49.67% respectively of the strength of concrete at age 28-days cured at 20^{0}C.

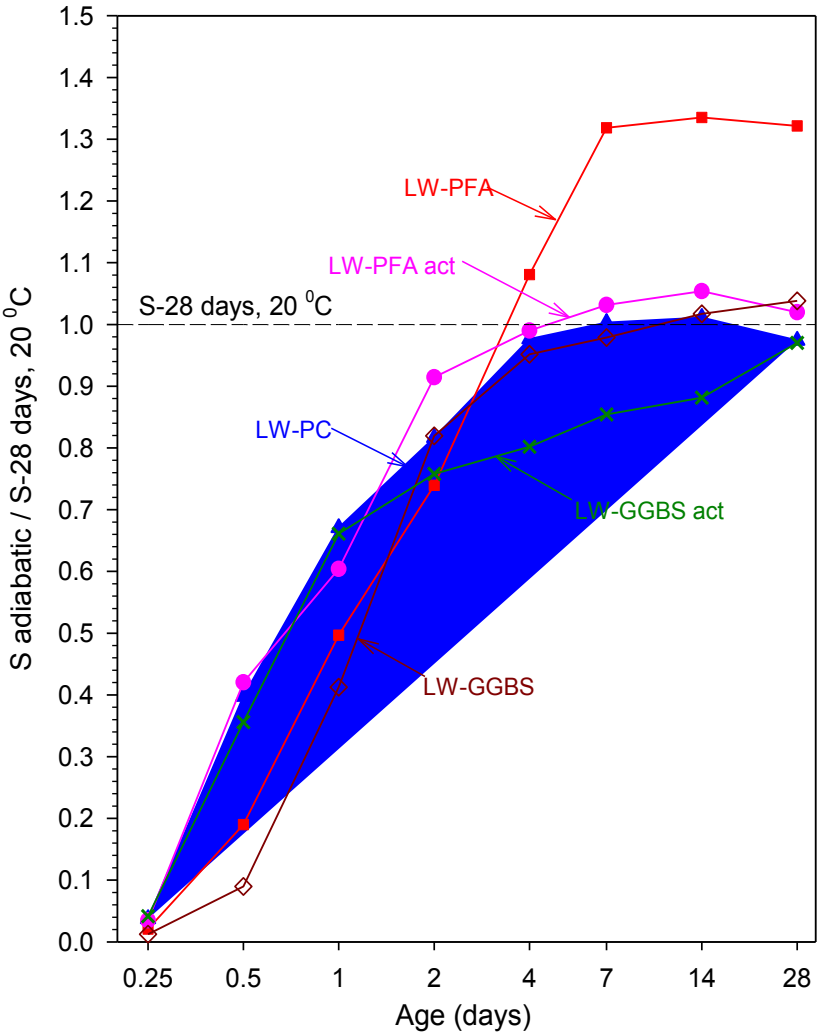

Figure 9.15: Ratio S-adiabatic/S-28 days, 20^{0}C of **LW-PC, LW-FA, LW-FA act, LW-GGBS** and **LW-GGBS act** concretes

9.4.2. Strength Development of Self Compacting Concrete under Standard Curing and Adiabatic Condition

Figure 9.16 presents the strength development of normal and lightweight self compacting concretes cured under adiabatic conditions. At an early age (1-day), the strength of NWSCC-PC is two times higher than the strength of the concrete cured at 20^{0}C, while LWSCC-GGBS and LWSCC-LSP concretes cured under adiabatic conditions have strength 2.54 and 1.88 times higher respectively than that of the concretes cured at 20^{0}C. At age 28-days however, the strength of all

self compacting concretes cured under adiabatic conditions are similar to the strength of concretes cured at 20^0C.

The ratio of strength of concrete cured under adiabatic conditions to the strength of the concrete cured at standard curing temperature can be seen in Figure 9.17. At age 0.5 day (12 hours), the strength of NWSCC-PC cured under adiabatic conditions reached 5.20 times higher than that of concrete cured at 20^0C. The ratios of the adiabatic strength of LWSCC-GGBS and LWSCC-LSP concretes compared to the strengths of the concretes cured at 20^0C at the same age are slightly lower than that of NWSCC-PC concrete, i.e. 3.27 and 3.02 times higher than the strength of the concretes cured at 20^0C. The graph shows that the strength of normal and lightweight self compacting concrete compared the strength of the concrete that was cured at 20^0C at age 14-days.

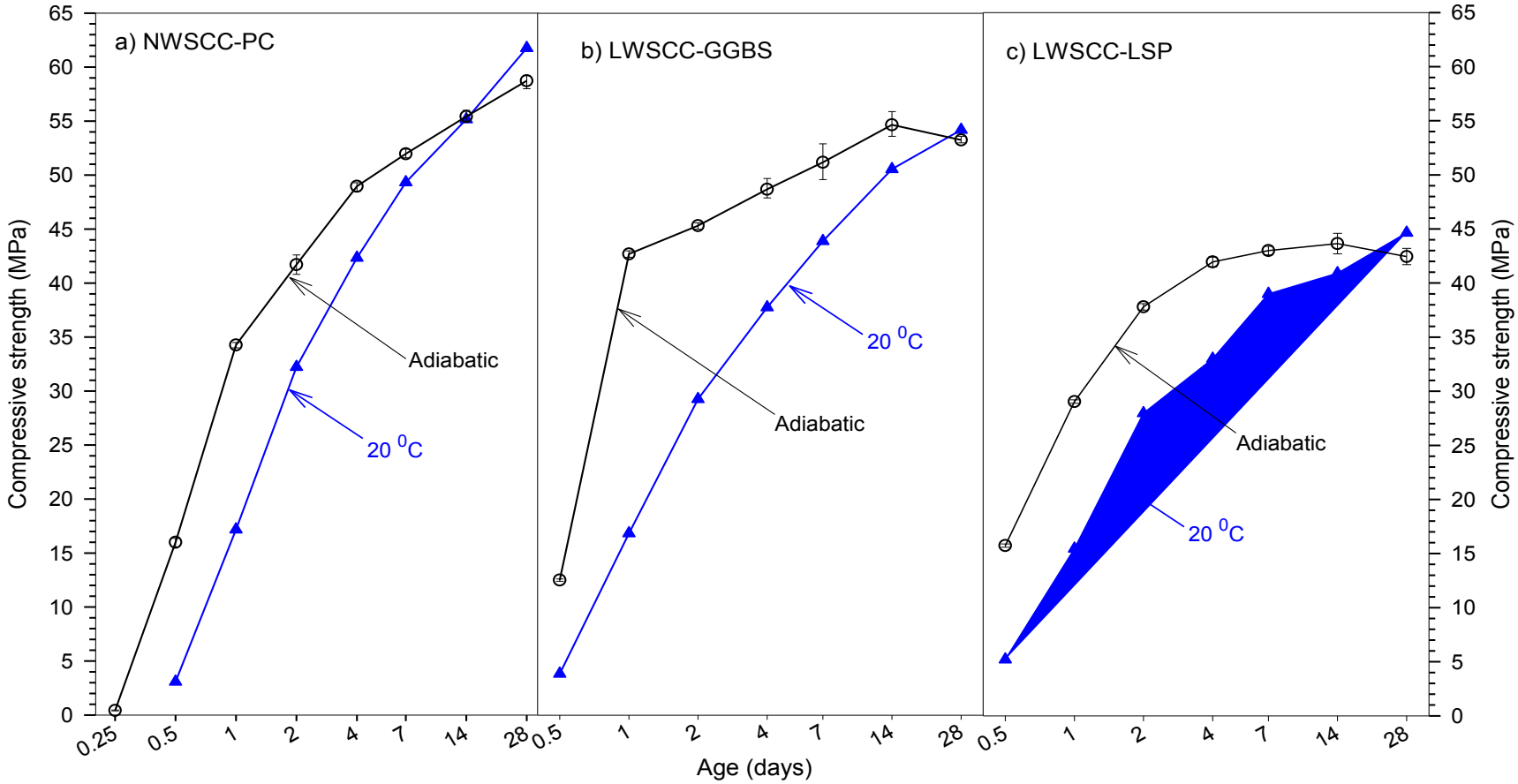

Figure 9.16: Strength developments of **NWSCC-PC, LWSCC-GGBS** and **LWSCC-LSP** concretes cured at standard curing temperature curing temperature (20^0C) and under adiabatic curing conditions

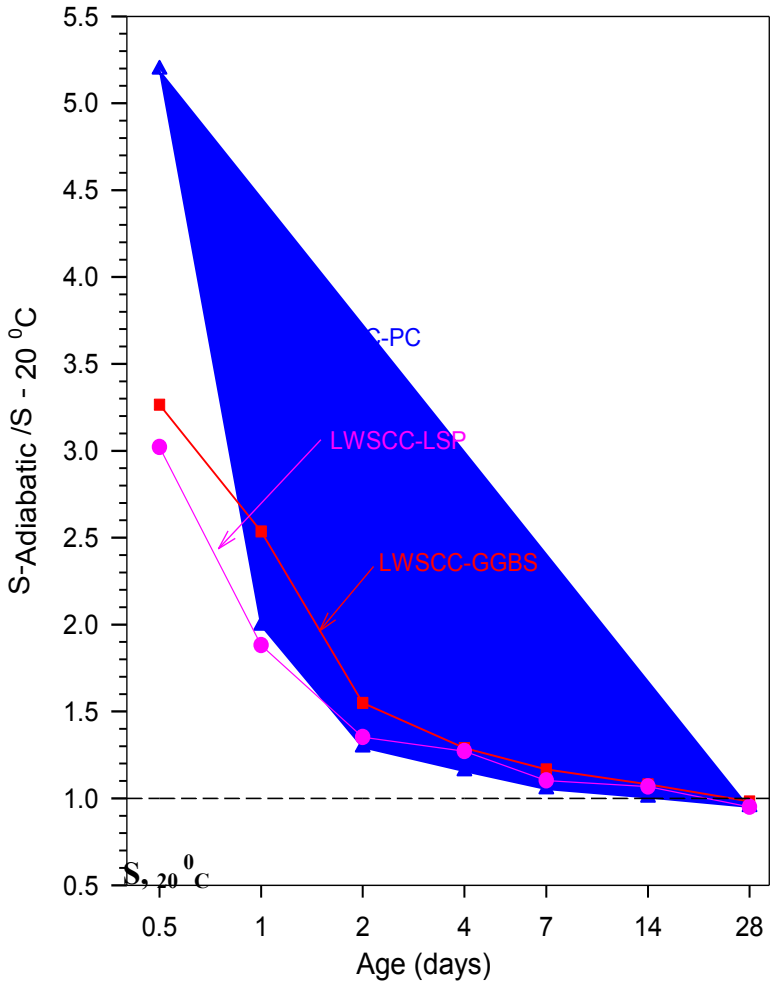

Figure 9. 17: Ratio S-adiabatic/S-20^{0}C of **NWSCC-PC, LWSCC-GGBS** and **LWSCC-LSP** concretes

Ratio of concrete cured under adiabatic conditions to the strength of concrete at age 28-days, cured at 20^{0}C is shown in Figure 9.18. At age 1-day, NWSCC-PC, LWSCC-GGBS and LWSCC-LSP concretes cured under adiabatic conditions reached 55.48%, 78.78% and 65.05%, respectively, of the strength of the concretes at age 28-days cured at 20^{0}C. At age 28-days, the ratios of the strength of NWSCC-PC, LWSCC-GGBS and LWSCC-LSP concretes cured under adiabatic conditions compared to the strength of concrete cured at 20^{0}C ranged from 0.95 to 0.98. This meant the effect of high curing temperature under adiabatic conditions has a less negative effect on the later age compared to the strength of concrete cured at constant high temperature.

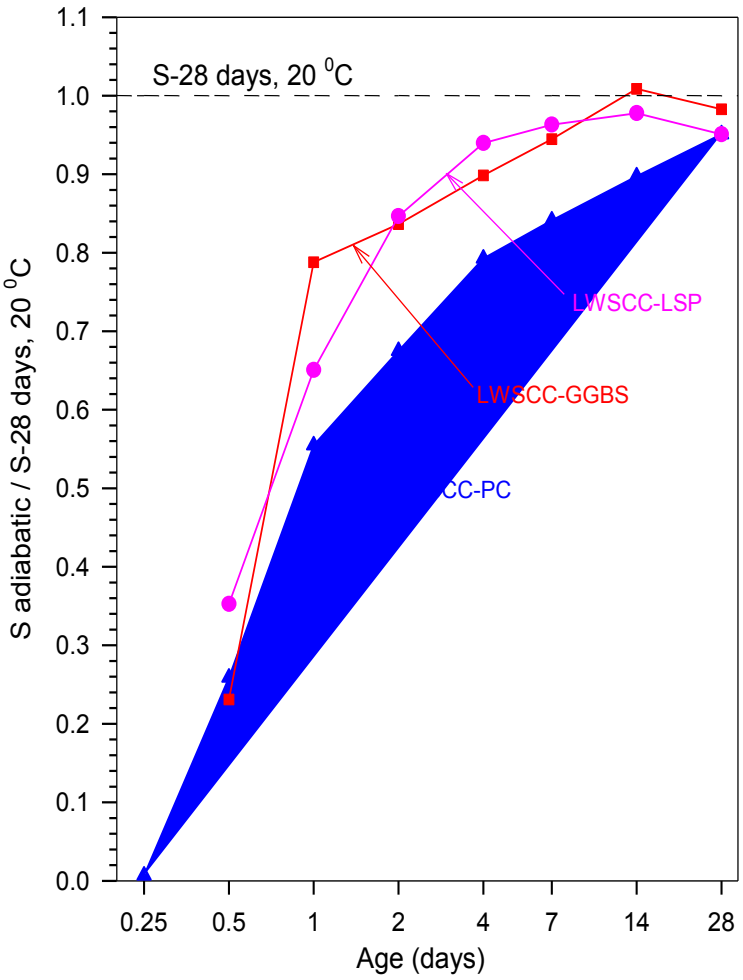

Figure 9. 18: Ratio S-adiabatic/S-28 days, 20^{0}C of **NWSCC-PC, LWSCC-GGBS** and **LWSCC-LSP** concretes

9.5. Adiabatic Strength Prediction

The parameters, which are needed in the prediction of adiabatic strength development, should be determined first before predicting the adiabatic strength of concrete. The parameters are the activation energy of concrete, ultimate strength of the concrete cured at 20^0C, adiabatic temperature histories, etc.

The results of concrete compressive strength test for all curing temperatures were plotted against the curing temperatures. A regression analysis was carried out, which was based on two different methods i.e. ASTM method and TPE equation to obtain the parameters needed in determining the activation energy of the concretes. The parameters obtained from regression analysis can be found in Table E-19 in Appendix E.

9.5.1. Determination of Activation Energy based on ASTM C-1074 Standard

The values of ln k were plotted against the reciprocal of absolute temperatures ($^0K^{-1}$) for all lightweight and self compacting concretes, as shown in Figure 9.19. The regression analyses were carried out to find out the best-fit straight line of each mix.

The slope of the best-fit straight line, therefore, is equal to $-E_a/R$ as shown in Equation 2.57 in Chapter 2. The activation energy of the concretes then can be calculated as presented in Table 9.1.

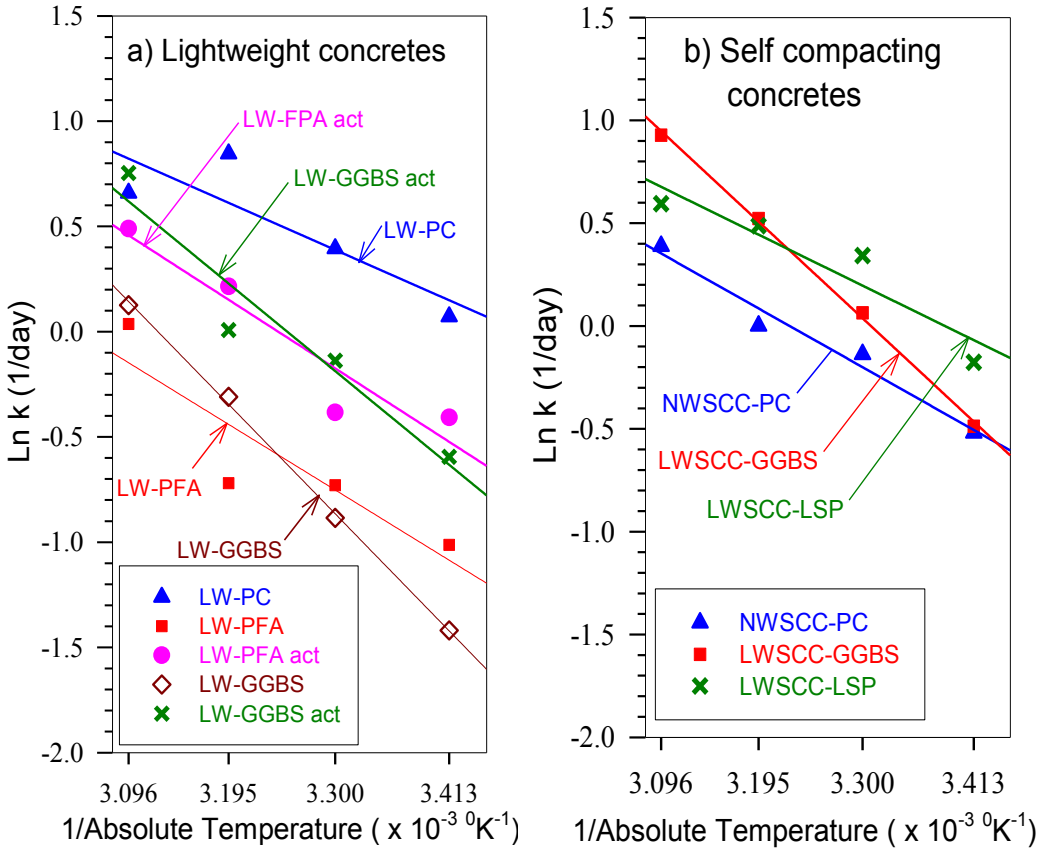

Figure 9.19: Natural logarithms of the rate constant *(k)* versus the reciprocal of absolute temperature

9.5.2. Determination of Activation Energy based on the Three Parameter Equation (TPE)

The parameters such as S_∞, τ and a were obtained from a regression analysis based on Three Parameter Equation as shown in Equation 2.36 in Chapter 2. The parameter obtained from the regression analysis can be seen in Table E-20 in Appendix E.

Figure 9.20 shows the graphs obtained by plotting the "ln τ" values against the age for each lightweight concrete and self compacting concrete that was cured at curing temperatures of 20, 30, 40 and 50^{0}C.

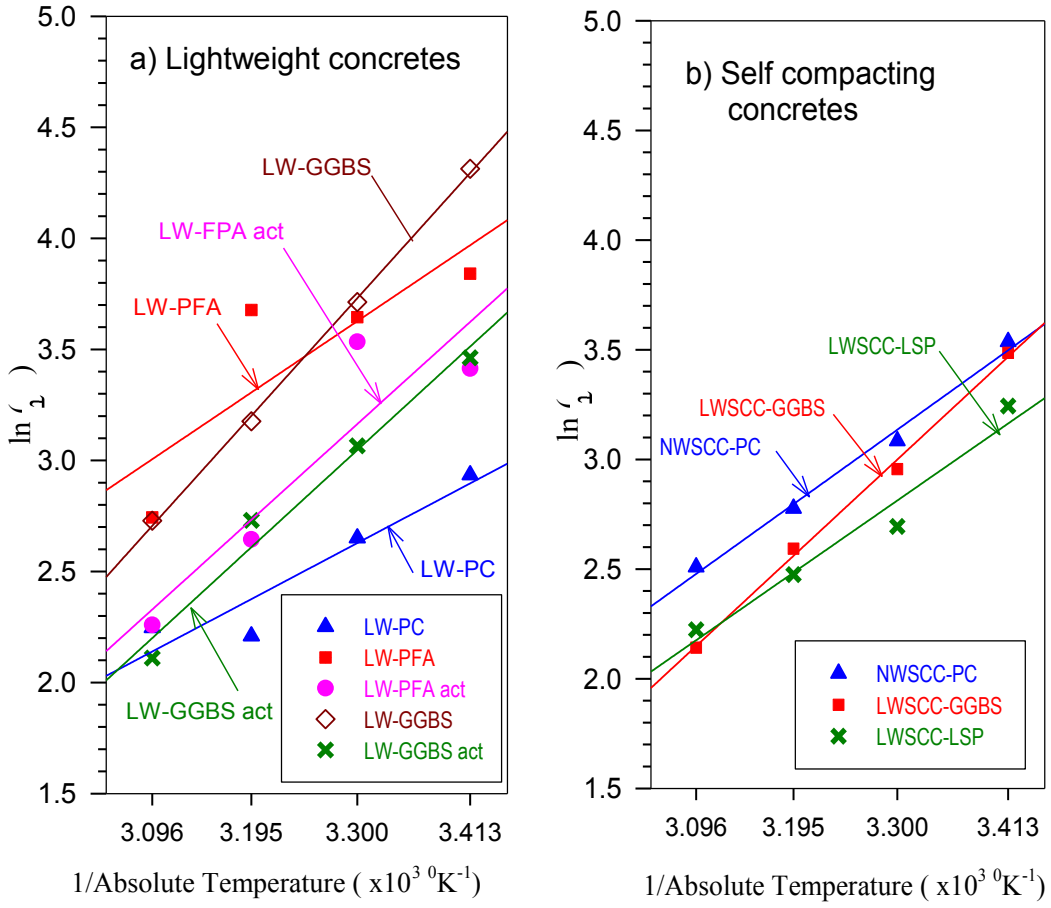

Figure 9.20: Natural logarithms of the characteristic time (τ) versus the reciprocal of absolute temperature.

Figure 9.20 a plot of *ln (τ)* values against *1/T* based on Equation 2.65 for lightweight and self compacting concretes. A linear regression analysis was carried out based on Equation 2.65 to find out the best-fit straight line. The slope of the best-fit line is equal to E_a/R. Accordingly, the value of the apparent activation energies can be calculated for each concrete as presented in Table 9.1.

The values vary from 17 to 42 kJ/mol. As has been discussed previously in Chapter 5, the activation energies found in literature vary a lot from 18 to 60 kJ/mol, therefore, the values of apparent activation energy presented in Table 9.1 was in the range of apparent activation energy found in literature.

Table 9.1: Activation energy for lightweight and self compacting concretes

Concrete	Activation energy (kJ/mol)	
	ASTM Method	TPE Equation
LW-PC	17.636	19.863
LW-PFA	24.591	25.277
LW-PFA act	25.724	33.964
LW-GGBS	41.032	41.679
LW-GGBS act	32.811	34.435
NWSCC-PC	22.501	26.752
LWSCC-GGBS	37.041	34.599
LWSCC-LSP	19.549	25.916

The value of activation energy for GGBS concretes seems to be the higher than that of other concretes, which vary from 32 to 42 kJ/mol. The activation energy values for GGBS concretes that were found in literature varied from 35 to 60 kJ/mol. It is interesting to note that the activation energy value of GGBS concrete with activator determined in this work using both the ASTM and TPE methods i.e. 32.8 and 34.4 kJ/mol respectively. These values are lower than that of the range of values reported in the literature. These values are also lower than that of the others GGBS mixes without activator in this work. This is expected as the activator accelerates the hydration reaction. Therefore, it reduces the activation energy that was needed to start the reaction between water and binder in the concrete.

9.5.3. Adiabatic Strength Prediction for Lightweight and Self Compacting Concretes

The parameters that were obtained from a regression analysis on the strength development of the concrete cured at 20^0C (used as the reference temperature) with the recorded adiabatic temperature and the activation energy that were previously determined were used to estimate the adiabatic strength development.

Figures 9.21 and 9.22 show the predicted adiabatic strength for lightweight and self compacting concretes, respectively.

The strength development of the concretes that were cured at higher isothermal temperature than 20^0C was predicted well using the values of activation energy that had been previously determined. This increased confidence to use the values of the activation energy in predicting adiabatic strength development.

In general, both the NS-Carino and TPE methods predict the adiabatic strength of the lightweight concretes relatively accurately at early age. However, both the methods predict the adiabatic strength inaccurately at later ages. The exception is for lightweight concrete with Portland cement only (LW-PC), where the adiabatic strength of the concrete was predicted reasonably well using both methods, as shown in Figure 9.21a. The adiabatic strength prediction for the FA lightweight concretes with and without activator (LW-FA act and LW-FA) was under estimated during the testing ages as shown in Figures 9.21b and c. On the other hand, the adiabatic strength prediction of both the GGBS lightweight concretes with and without activator (LW-GGBS act and LW-GGBS) was predicted quite accurately at early ages using the TPE method. The TPE method, however, overestimated the adiabatic strength of both the concretes at later ages. The NS-Carino method underestimated the adiabatic strength at earlier ages for both the GGBS lightweight concretes with and without activator. Furthermore, it overestimated the adiabatic strength of the concretes at later ages as did that of the TPE method that can be seen in Figures 9.21c and d. This was similar to that used to predict the adiabatic strength of normal concrete with GGBS.

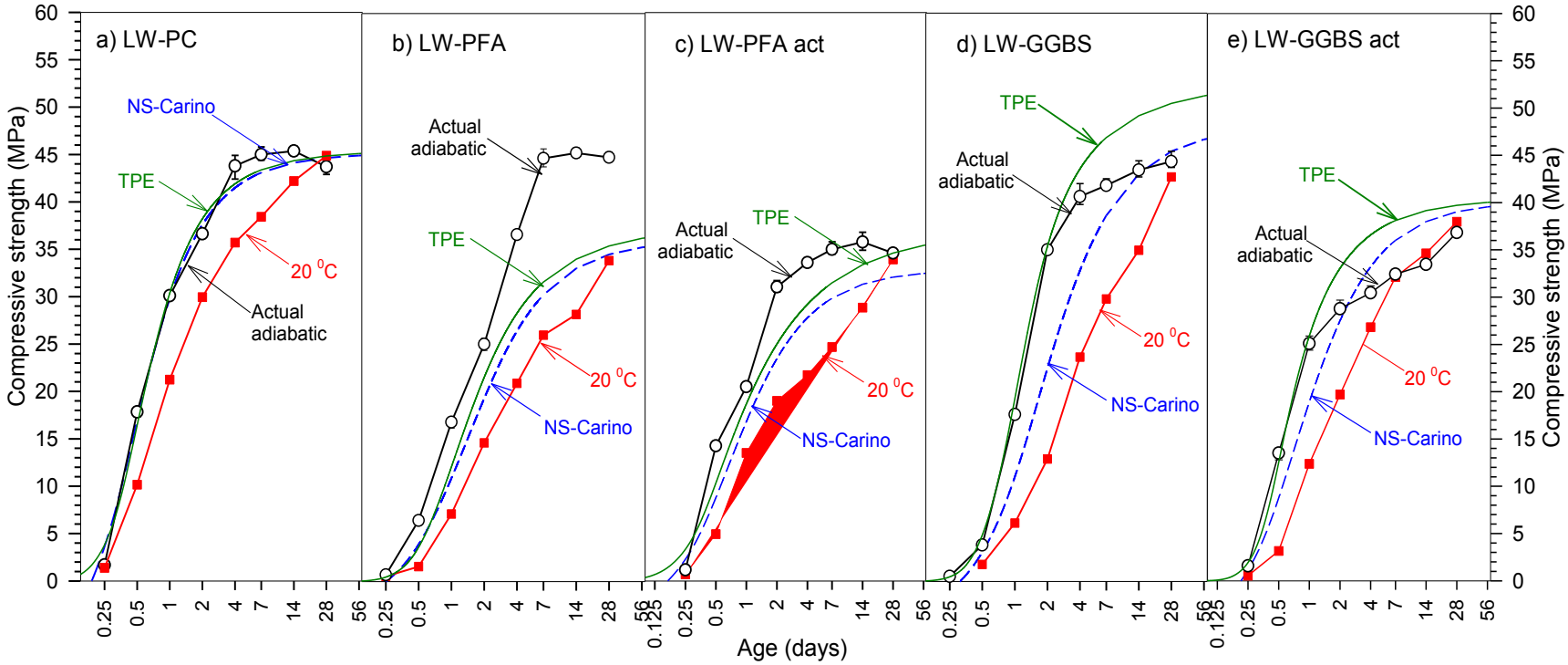

Figure 9.21: Adiabatic strength prediction for **LW-PC, LW-FA, LW-FA act, LW-GGBS** and **LW-GGBS act** concretes

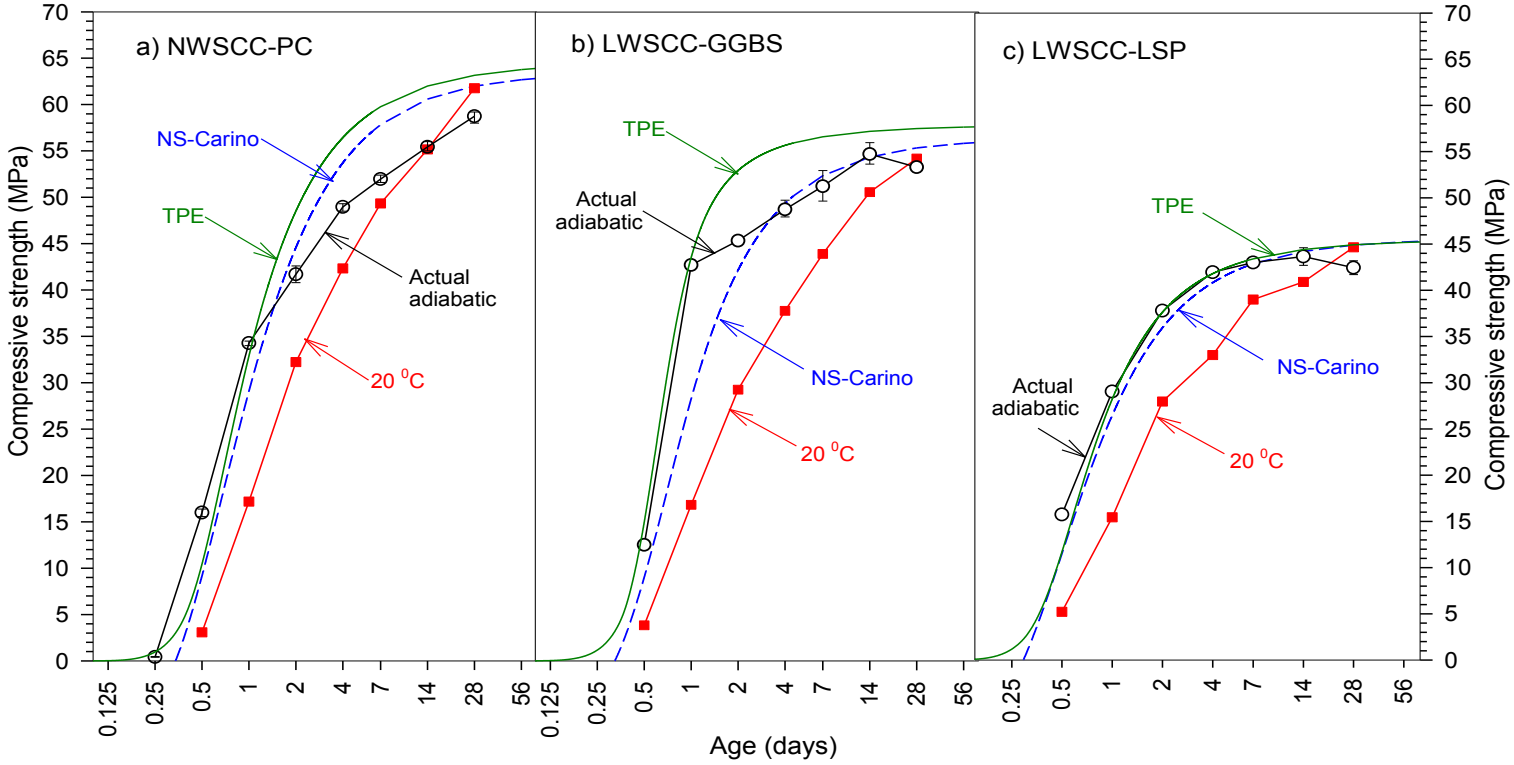

Figure 9.22: Adiabatic strength prediction for **NWSCC-PC, LWSCC-GGBS** and **LWSCC-LSP** concretes

For the PC and GGBS self compacting concretes (NWSCC-PC and LWSCC-GGBS), shown in Figures 9.22a and b, both the NS-Carino and TPE methods underestimated the adiabatic strength. Conversely, both methods overestimated the adiabatic strength of the NWSCC-PC and LWSCC-GGBS concretes at later ages. However, Figure 9.22c shows that both the methods were reasonably good predicting the adiabatic strength of LWSCC-LSP concrete during the testing ages. Particularly the TPE method, as the curve of the adiabatic strength using this method from the age of 1-day to 14-days almost overlaps with the curve of the actual adiabatic strength of the concrete.

9.6. Summary

This chapter can be summarised as follows:

- The values of activation energy for lightweight and self compacting concretes vary between 17 to 42 kJ/mol. The values are in the same range of apparent activation energy of normal weight concrete found in literatures, ranges from 18 to 60 kJ/mol.
- The effects of curing temperature on the strength development of lightweight concretes at early age are similar to that of the normal weight concrete. However, the 'crossover effect' on the strength development of lightweight concrete due to higher curing temperatures (up to 40^0C) at early age is much less than that of the normal weight concretes.
- The predicted strength of lightweight and self compacting concrete using both Carino-NS and TPE methods for lightweight concretes with GGBS are similar to that of normal weight concrete. The TPE method predicted well the strength of LW-GGBS concretes with and without activator up to two days and then overestimates the strength at later on. Both the methods underestimated the fly ash - lightweight concrete (LW-PFA) with and without activator. However, the methods predicted the strength development of lightweight concrete with PC only (LW-PC) and self compacting concrete with limestone powder (LWSCC-LSP) very well during the testing ages.

CHAPTER 10 – CONCLUSIONS AND RECOMMENDATION FOR FUTURE RESEARCH

Both the fresh and hardened properties of Portland cement concrete improved when the cementitious materials such as GGBS were used to replace part of the Portland cement in concrete. Using GGBS as a partial cement replacement can enhance the workability more than that of concrete with Portland cement only. This is because the particle size of GGBS is finer than that of Portland cement. Also the relative density of GGBS is slightly lower than that of Portland cement. The glassy surface and smoother surface texture of GGBS powder also enhances the workability of the concrete made using GGBS. Therefore, for the same water-binder ratio, the GGBS concrete exhibits a much higher level of workability than Portland cement concrete. This allows a small reduction in the amount of water, without any loss in workability, which results in an increase in strength and durability of the GGBS concrete.

Like Portland cement, GGBS reacts when in contact with water. However, its reaction rate is slower than that of Portland cement, and GGBS needs an activator to start the reaction. When Portland cement reacts with water, calcium hydroxide is released; this activates the reaction of the GGBS. GGBS concrete has more smaller gel pores and fewer larger capillary pores than that in Portland cement concrete. As a result, GGBS concrete has a much lower permeability than Portland cement concrete, where contributes to the improvement in the durability.

The use of GGBS with a level above 50% in concrete can significantly reduce the temperature rise in concrete. Using GGBS with levels that are less than 50% (by weight with Portland cement) resulted in temperature rises that were similar to that in Portland cement concrete as shown in Figures 5.24 and 5.25 in Chapter 5. In addition, the use GGBS in concrete as a partial cement replacement gives both environmental and economic benefits. The production of GGBS releases much less CO_2 than that which is produced in the normal cement making process. Therefore, using GGBS in concrete to replace a part of the cement content can

reduce the CO_2 emission into the atmosphere by reducing the production of cement. This improves the sustainability of the concrete structure. The use of GGBS in concrete is cheaper than Portland cement as the GGBS is essentially a waste material. It can then give economic benefits when used to replace a proportion of the cement.

Its use in fast track construction however has not been popular due to its slower strength development at the standard curing temperature at early ages. The mix design of GGBS concrete when used in fast track construction depends on the accuracy of the method used to predict and to monitor its strength development on site.

A new method called Modified MNS method to predict the strength development of GGBS concrete has been developed in this study. The new method predicted the strength development of GGBS concrete more accurate, compare to the existing methods. This is the result as the existing methods were developed based on the strength data obtained from concrete with Portland cement only.

10.1. Conclusions

Based on the results of this study, the following conclusions can be drawn:

- The early age strength of GGBS mortars/concretes cured under the standard curing temperature (20^0C), which have a similar 28-day strength to that of mortars/concretes with Portland cement only, decrease as the levels of GGBS in the mortars/concretes increase. At higher curing temperatures, however, the early age strength gain is much faster and the improvement of the early strength is more pronounced for concretes with higher levels of GGBS. For example, when the curing temperature was raised from 20 to 50^0C, the improved strength was much more significant especially in 70% GGBS concrete compared to concretes containing lower GGBS levels. This can be seen in Figures 5.11 and 5.12 in Chapter 5 for concrete grades C45 and C75,

respectively. This proves that the higher the levels of GGBS in concrete, the more sensitive the strength development is to temperature. This is a consequence of their higher apparent activation energy. The values of apparent activation energy increase linearly with GGBS levels, as shown in Figure 6.4 in Chapter 6.

- The activation energies that were determined based on the cubes' strength data were comparable to that determined based on the heat output data using the Three Parameter Equation. The activation energy values were determined from the cubes' strength in this study, and these were used to predict the strength development of the mortars/concretes cured under adiabatic conditions. The existing models for the prediction of the strength development, which generally have been developed based on the concrete with Portland cement only, were assessed for use with GGBS concrete.

- Under the standard curing temperature, the strengths of GGBS concretes designed to have similar 28-days strengths to Portland cement concrete were normally achieved when using GGBS at up to 50% as cement replacement. Concrete with the GGBS contents above this level have a strength slightly lower than that of Portland cement concrete at the same age. However, their long-term strengths were greater than that of Portland cement concrete as shown in Figures 5.9 and 5.10 in Chapter 5 for concrete grades C45 and C75, respectively.

- The levels of GGBS which can be used for fast-track construction is dependent on many factors, such as: curing temperature during casting, type of formwork used, striking times, and the size of the concrete structural element. Under the standard curing temperature, Figures 5.16 and 5.17 in Chapter 5 show that there is no delay for fast-track construction when GGBS was used at levels up to 50% in concrete, even if it needs the removal of the formwork two days after casting. The use of GGBS levels up to or above of

70% (except for mass concrete) possibly needs special curing such as an elevated curing temperature.

- The 28-days strengths of the GGBS concretes not very sensitive to the levels of GGBS and seem to be highly dependent on the water-binder ratio only. Conversely, the strength development of mortars/concrete at an early age is highly dependent on the curing temperature. The casting temperature affects the hydration process at early ages, when the hydration products highly influence the subsequent hydration reaction. This is particularly true for GGBS concrete as the product of cement hydration i.e. calcium hydroxide, at early age will activate the GGBS and cause it to react earlier.

- Elevated curing temperatures enhanced the strength development of GGBS mortars/concrete at an early age. However, mortars/concretes cured at higher curing temperatures at early age have a strength lower than that of concrete cured at lower temperature; this is called the *'crossover effect'*. This is explained by the limited strength obtained of each mortar/concrete cured at different temperatures which can be found in Appendix E. The concretes cured at higher curing temperatures have a lower strength than that of concrete cured at lower temperatures at later ages. The detrimental effect on the strength development of mortars is more pronounced for mortar with Portland cement only compared to GGBS mortar. In addition, the detrimental effect that the concrete experienced was less than that of mortar, which is shown in Figures 5.18 and 5.19. The *'crossover effect'* occurred in concretes at much later ages than in mortars.

- Figures 5.1 and 5.2 present the strength development of mortars cured at different curing temperatures for mortar grades C45 and C75, respectively. The strength development of the mortars cured at 30^0C compared to that cured at the standard curing temperature are significant for mortars with high levels of GGBS in terms of utilising GGBS in fast track construction. The strength development of mortars with higher levels of GGBS such as 50 and 70% are comparable to the strength of the concrete cured at higher

temperatures at age 2-days onwards. Furthermore, the detrimental effect on the strength development of mortar cured at 30 ^{0}C at later ages due to higher temperature at early age, is not as much as that of mortars cured at higher temperatures.

- The strengths development of GGBS mortars/concretes cured under adiabatic conditions are comparable to the strength of concrete with Portland cement only from the age of 2-days onwards. This can be seen in Figures 5.27 and 5.28 for mortars grades C45 and C75, respectively. For concrete this is presented in Figures 5.32 and 5.33 for grades C45 and C75, respectively. It is important to note that the improved strengths obtained under adiabatic conditions are also relevant to mass concreting. The temperature conditions of mass concreting cured on site may be very close to adiabatic conditions.

- It is believed that the temperature rise inside larger structural elements with lower heat dissipation is high enough to produce similar improvements in early age strength to those concretes investigated in this study under adiabatic conditions. In smaller structural elements such as thin slabs or walls where heat dissipation is expected to be high, the use of GGBS in fast-track construction is possible when applying thermal insulation at an early age.

- The predicted adiabatic strength in this study is presented in Chapter Six. The existing maturity methods were developed based on the data obtained from mortars or concretes with Portland cement only. Therefore, the predicted strengths of GGBS concretes using the methods were less accurate - as can be seen in Figures 6.9 and 6.10. Generally, the predicted adiabatic strength of GGBS concretes using the Three Parameter Equation (TPE)[121] is accurate only at an early age. However, the method overestimates the adiabatic strength of GGBS concretes at later ages. On the other hand, the Carino-Nurse Saul (C-NS)[6, 101] method underestimates the adiabatic strength of GGBS concretes at an early age but overestimates the adiabatic strength at later ages. It is believed that both methods overestimate the strength of

concrete at later ages as they both do not consider the effect of higher curing temperature at early ages on the strength at later ages.

- The accuracy of the modified maturity methods recently proposed by Chanvillard and D'Loia[162], Kjellsen and Detwiler[157], and Jawad[163, 164] to predict the adiabatic strength of GGBS concrete were also evaluated in this study. The model proposed by Canvillard and D'Loia (CD)[162] as shown in Figure 6.19 in Chapter Six predicts the adiabatic strength of GGBS concrete grade C45 very well up to the age of 2-days. The model then overestimates the adiabatic strength of GGBS concrete from the age to the age of 64-days and underestimated the strength at later age. The model, however, predicted the adiabatic strength for concrete grade C75 quite better as shown in Figure 6.20.

- Both models proposed by Jawad (AJ-05 and AJ-06)[163, 164] underestimate the adiabatic strength for all concretes from the age of 2-days onwards. It was found that when the temperature rise was starting to get higher, the model started to underestimate the strength. The modified AJ-06 model (Modified AJ-06), which is proposed in this study, seems to be more accurate in predicting the adiabatic strength of all concretes at early ages similar to the model proposed by Kjellsen and Detwiler (KD)[157].

- The predicted adiabatic strength using the C-NS model[6, 101] for all concretes at early ages is reasonably good when the maturity was calculated using the datum temperature (T_0) determined from the ASTM[6] method compared to that suggested from previous work (-11^0C). This can be seen in Figures 6.13 and 6.14 in Chapter Six for concrete grades C45 and C75, respectively.

- The Modified MNS method proposed in this study seems to be more accurate in predicting the strength of GGBS concrete, as shown in Figures 6.42 and 6.43 in Chapter 6. The model has the potential to be improved to produce more accurate strength development predictions as its predicted strength curves follow the actual adiabatic strength curves. In addition, the predicted

strength of concretes cured at 50^0C is extremely good as can be seen in Figures 6.40 and 6.41 for concrete grades C45 and C75, respectively. The curves of predicted strengths almost overlap with the regression curves. This proves that the prediction of the strength of concrete in the field can be developed to obtain more accurate results.

- The use of GGBS in concrete contributes to lower the heat output or temperature rise in concrete when used above 50% of the total binder in concrete (Figures 5.24 and 5.25). At higher curing temperatures the contribution of GGBS to the cumulative heat output increases. The predicted adiabatic temperature rise using the predicted heat output obtained from adiabatic tests is more accurate when compared to the predicting method that used the predicted heat obtained from the isothermal calorimeter.

- The strength development of lightweight concretes and self compacting lightweight concrete cured under different curing temperatures were similar to that of normal concrete. The higher the curing temperature at early ages, the greater was the strength development gain compared to concrete cured under standard curing temperatures. However, their strengths at later ages were lower than that of concrete cured under the standard curing temperature. The "*crossover effect"* also occurred on those concretes.

- Activation energies for the lightweight and self compacting concretes obtained in this study appear to be similar to that of normal concretes with similar binder contents. The measured adiabatic temperature rise can be used to predict the adiabatic strength development of those concretes.

10.2. Recommendations for Future Research

Recommendations for further study are as follows:

- Investigation of the strength development of mortars or concretes cured at temperatures other than those applied in this study is needed. Particularly for

GGBS mortar or concrete cured at higher curing temperatures, as the GGBS is more sensitive to the higher curing temperatures than Portland cement. This would allow an improvement in the accuracy of the acceleration, compression and efficiency factors, which are the parameters were used in the MNS method proposed in this study to predict the strength development of concrete.

- Further study of the real activation energy that is needed when concrete is cured at elevated temperatures, even when the temperature changes over time. This can also improve the predicted strength of concrete using the maturity method.

- A comprehensive study on the heat output is needed. A standard of procedure to do the test is needed. A study on the accuracy of maturity methods used to predict the strength of concrete using the activation energy determined based on the heat output is also needed. Some of the existing maturity methods appear have the potential to be improved by considering the activation energy that was used in predicting the strength of concrete.

- An investigation into the effect of superplasticizer to the hydration of cement or binder is needed. It would be very useful to determine their influence on the activation energy of the concrete. This can improve the accuracy of the predicted strength of concrete that uses a superplasticizer.

- Further study of establishing a relationship between cement replacement levels and type, strength development, curing conditions and formwork striking times for typical reinforced concrete structures in the UK is required.

- Further investigation is required to observe the effect of ambient conditions, type of formwork used and structural element types on the temperature rise in concrete.

- Further study required regarding to the thermal shock effect on the strength development of concrete.

References

1. Soutsos, M. N., Barnett, S. J., Bungey, J. H., and Millard, S. G. *Fast track construction with high strength concrete mixes containing ground granulated blast furnace slag*. in *Proceedings of ACI Seventh International Symposium on High Strength/High Performance Concrete, ACI SP-228*. 2005.
2. McCullough, B. F. and Rasmussen, R. O., *Fast-track paving: concrete temperature control and traffic opening criteria for bonded concrete overlays.* Task G, Final Report, FHWA, US Department of Transportation, 1999.
3. Harrison, T. A., *Formwork striking times - criteria, prediction and methods of assessment, CIRIA vol. Report 136*, 1995.
4. Carino, N. J. and Lew, H. S. *Temperature effects on strength-maturity relations of mortar*. in *ACI Journal Proceedings*. 1983. ACI.
5. Roy, D. M. *Hydration, structure, and properties of blast furnace slag cements, mortars, and concrete*. 1982. ACI.
6. ASTM C 1074, *Standard Practice for Estimating Concrete Strength by the Maturity Method,".* Annual Book of ASTM Standards, 2004. **4**.
7. Carino, N. J., Jennings, H. M., and Snell, L. M., *Properties of concrete at early ages.* Concrete International, 1989. **11**(4): p. 51-54.
8. Bergström, S. G. and Byfors, J., *Properties of concrete at early ages.* Materials and Structures, 1980. **13**(3): p. 265-274.
9. Wang, K., Ge, Z., Grove, J., Ruiz, J.M., and Rasmussen, R.O., *Developing a simple and rapid test for monitoring the heat evolution of concrete mixtures for both laboratory and field applications* 2006.
10. Glišić, B. and Simon, N., *Monitoring of concrete at very early age using stiff SOFO sensor.* Cement and Concrete Composites, 2000. **22**(2): p. 115-119.
11. Reinhardt, H. W. *Relevence of testing during construction*. 1990. Routledge.
12. Neville, A. M., *Properties of concrete*. Fourth ed 2004: Prentice Hall.
13. Al-Khaiat, H. and Fattuhi, N., *Long-term strength development of concrete in arid conditions.* Cement and Concrete Composites, 2001. **23**(4): p. 363-373.

14. Gonen, T. and Yazicioglu, S., *The influence of mineral admixtures on the short and long-term performance of concrete.* Building and environment, 2007. **42**(8): p. 3080-3085.

15. Rodriguez-Camacho, R. E. and Uribe-Afif, R., *Importance of using the natural pozzolans on concrete durability.* Cement and Concrete Research, 2002. **32**(12): p. 1851-1858.

16. Naik, T. R., Singh, S. S., and Hossain, M. M., *Enhancement in mechanical properties of concrete due to blended ash.* Cement and Concrete Research, 1996. **26**(1): p. 49-54.

17. Mullick, A. K., *Performance of concrete with binary and ternary cement blends.* Indian Concrete Journal, 2007. **81**(1): p. 15.

18. Malhotra, V. M., Zhang, M. H., Read, P. H., and Ryell, J., *Long-term mechanical properties and durability characteristics of high-strength/high-performance concrete incorporating supplementary cementing materials under outdoor exposure conditions.* ACI materials journal, 2000. **97**(5).

19. Kaid, N., Cyr, M., Julien, S., and Khelafi, H., *Durability of concrete containing a natural pozzolan as defined by a performance-based approach.* Construction and Building Materials, 2009. **23**(12): p. 3457-3467.

20. Sata, V., Jaturapitakkul, C., and Kiattikomol, K., *Influence of pozzolan from various by-product materials on mechanical properties of high-strength concrete.* Construction and Building Materials, 2007. **21**(7): p. 1589-1598.

21. Targan, S., Olgun, A., Erdogan, Y., and Sevinc, V., *Effects of supplementary cementing materials on the properties of cement and concrete.* Cement and Concrete Research, 2002. **32**(10): p. 1551-1558.

22. Papadakis, V. G., *Effect of supplementary cementing materials on concrete resistance against carbonation and chloride ingress.* Cement and Concrete Research, 2000. **30**(2): p. 291-299.

23. Thomas, M. D. A, Shehata, M. H, Shashiprakash, S. G, Hopkins, D. S, and Cail, K., *Use of ternary cementitious systems containing silica fume and fly ash in concrete.* Cement and Concrete Research, 1999. **29**(8): p. 1207-1214.

24. Memon, A. H., Radin, S. S., Zain, M. F. M., and Trottier, J. F., *Effects of mineral and chemical admixtures on high-strength concrete in seawater.* Cement and Concrete Research, 2002. **32**(3): p. 373-377.

25. Toutanji, H., Delatte, N., Aggoun, S., Duval, R., and Danson, A., *Effect of supplementary cementitious materials on the compressive strength and*

durability of short-term cured concrete. Cement and Concrete Research, 2004. **34**(2): p. 311-319.

26. Wood, S. L., *Evaluation of the long-term properties of concrete.* ACI materials journal, 1992. **88**(6).
27. Aitcin, P. C., Miao, B., Cook, W. D., and Mitchell, D., *Effects of size and curing on cylinder compressive strength of normal and high-strength concrete.* ACI materials journal, 1994. **91**(4).
28. Neville, A. M. and Brooks, J. J., *Concrete Technology*, 2nd edition, 2010, Malaysia: Prentice Hall.
29. Li, Zongjin, *Advanced Concrete Technology* 2011, United States of America: John Wiley & Sons, Inc.
30. ASTM C 39M - 03, *Standard Test Method for Compressive Strength of Cylindrical Concrete Specimens* 2003, ASTM International.
31. BS EN 12390-3, *Testing Hardened Concrete Part 3: Compressive strength of test specimens*, 2009, British Standard Institution: London.
32. Gee, K. H. *The potential for slag in blended cements*. 1979.
33. Siddique, R., *Waste materials and by-products in concrete* 2007: Springer Verlag.
34. Siddique, R. and Khan, M. I., *Supplementary cementing materials* 2011: Springer Verlag.
35. Hogan, F. J. and Meusel, J. W., *Evaluation for durability and strength development of a ground granulated blast furnace slag.* Cement, Concrete and Aggregates, 1981. **3**(1).
36. Barnett, S.J., Soutsos, M. N., Bungey, J. H., and Millard, S.G. *The effect of ground granulated blast furnace slag on the strength development and adiabatic temperature rise of concrete mixes*. 2005. Thomas Telford.
37. Aldea, C. M., Young, F., Wang, K., and Shah, S. P., *Effects of curing conditions on properties of concrete using slag replacement.* Cement and Concrete Research, 2000. **30**(3): p. 465-472.
38. Hwang, C.L. and Lin, C.Y., *Strength development of blended blast-furnace slag-cement mortars.* Journal of the Chinese Institute of Engineers, 1986. **9**(3): p. 233-239.
39. Miura, T. and Iwaki, I., *Strength development of concrete incorporating high levels of ground granulated blast-furnace slag at low temperatures.* ACI materials journal, 2000. **97**(1).

40. Barnett, S. J., Soutsos, M. N., Millard, S. G., and Bungey, J. H., *Strength development of mortars containing ground granulated blast-furnace slag: Effect of curing temperature and determination of apparent activation energies.* Cement and Concrete Research, 2006. **36**(3): p. 434-440.

41. Çakır, Ö. and Aköz, F., *Effect of curing conditions on the mortars with and without GGBFS.* Construction and Building Materials, 2008. **22**(3): p. 308-314.

42. Rajamane, N. P., PETER, J. A., Dattatreya, J. K., Neelamegam, M., and Gopalakrishnan, S., *Improvement in properties of high performance concrete with partial replacement of cement by ground granulated blast furnace slag.* Journal of the Institution of Engineers. India. Civil Engineering Division, 2003. **84**(mai): p. 38-42.

43. Regourd, M., *Slags and slag cements.* Cement Replacement Materials, 1986. **3**: p. 73-99.

44. Roy, D. M. and Malek, R. I. A., *Hydration of slag cement.* Progress in Cement and Concrete–Mineral Admixtures in Cement and Concrete (Ed. SN Ghosh), 1993. **4**: p. 84-117.

45. Reeves, C. M., *The use of ground granulated blast furnace slag to produce durable concrete: Improvement of concrete durability.* Proceedings of Association of Engineers and Institution of Civil Engineers, Thomas Telford, London, 1986: p. 59-95.

46. Austin, S. A., Robins, P. J., and Issaad, A., *Influence of curing methods on the strength and permeability of ggbfs concrete in a simulated arid climate.* Cement and Concrete Composites, 1992. **14**(3): p. 157-167.

47. Robins, P. J., Austin, S. A., and Issaad, A., *Suitability of ggbfs as a cement replacement for concrete in hot arid climates.* Materials and Structures, 1992. **25**(10): p. 598-612.

48. ACI Committee 213, *Guide for Structural Lightweight Aggregate Concrete*, 2003, America Concrete Institute: Farmington.

49. ASTM C 330-04, *Standard Specification for Lightweight Aggregates for Structural Concrete*, 2004, ASTM International: Farmington Hills.

50. Chandra, S. and Berntsson, L., *Lightweight aggregate concrete: science, technology, and applications* 2002: William Andrew.

51. NRMCA. *CIP 36 Structural Lightweight Concrete*. Technical information 2003 [cited 2012 October]; Available from: http://www.nrmca.org/aboutconcrete/cips/36p.pdf.

52. Ke, Y., Beaucour, AL, Ortola, S., Dumontet, H., and Cabrillac, R., *Influence of volume fraction and characteristics of lightweight aggregates on the mechanical properties of concrete.* Construction and Building Materials, 2009. **23**(8): p. 2821-2828.

53. Swamy, R. N. and Lambert, G. H., *The microstructure of Lytag aggregate.* International Journal of Cement Composites and Lightweight Concrete, 1981. **3**(4): p. 273-282.

54. Bai, Y., Ibrahim, R., and Basheer, P. A. M. *Properties of lightweight concrete manufactured with fly ash, furnace bottom ash, and lytag*. 2004.

55. Lo, T. Y., Tang, W. C. P., and Cui, H. Z., *The effects of aggregate properties on lightweight concrete.* Building and environment, 2007. **42**(8): p. 3025-3029.

56. Cui, HZ, Lo, T.Y., Memon, S.A., and Xu, W., *Effect of lightweight aggregates on the mechanical properties and brittleness of lightweight aggregate concrete.* Construction and Building Materials, 2012. **35**: p. 149-158.

57. Ramamurthy, K. and Harikrishnan, K. I., *Influence of binders on properties of sintered fly ash aggregate.* Cement and Concrete Composites, 2006. **28**(1): p. 33-38.

58. Wasserman, R. and Bentur, A., *Effect of lightweight fly ash aggregate microstructure on the strength of concretes.* Cement and Concrete Research, 1997. **27**(4): p. 525-537.

59. Kockal, N. U. and Ozturan, T., *Optimization of properties of fly ash aggregates for high-strength lightweight concrete production.* Materials & Design, 2011. **32**(6): p. 3586-3593.

60. Lo, T. Y. and Cui, H. Z., *Effect of porous lightweight aggregate on strength of concrete.* Materials Letters, 2004. **58**(6): p. 916-919.

61. Kockal, N. U. and Ozturan, T., *Strength and elastic properties of structural lightweight concretes.* Materials & Design, 2011. **32**(4): p. 2396-2403.

62. Lo, T. Y., Nadeem, A., Tang, W. C. P., and Yu, P. C., *The effect of high temperature curing on the strength and carbonation of pozzolanic structural lightweight concretes.* Construction and Building Materials, 2009. **23**(3): p. 1306-1310.

63. Zhang, M. H. and Gjorv, O. E., *Characteristics of lightweight aggregates for high-strength concrete.* ACI materials journal, 1991. **88**(2).

64. Zhang, M. H. and Gjvorv, O. E., *Mechanical properties of high-strength lightweight concrete.* ACI materials journal, 1991. **88**(3).

65. Ge, Y., Kong, L., Zhang, B., and Yuan, J., *Effect of lightweight aggregate pre-wetting on microstructure and permeability of mixed aggregate concrete.* Journal of Wuhan University of Technology--Materials Science Edition, 2009. **24**(5): p. 838-842.

66. Lo, Y., Gao, X. F., and Jeary, A. P., *Microstructure of pre-wetted aggregate on lightweight concrete.* Building and environment, 1999. **34**(6): p. 759-764.

67. Lo, T. Y., Cui, H. Z., and Li, Z. G., *Influence of aggregate pre-wetting and fly ash on mechanical properties of lightweight concrete.* Waste Management, 2004. **24**(4): p. 333-338.

68. Loudon, A. G., *The thermal properties of lightweight concretes.* International Journal of Cement Composites and Lightweight Concrete, 1979. **1**(2): p. 71-85.

69. Demirboğa, R. and Gül, R., *The effects of expanded perlite aggregate, silica fume and fly ash on the thermal conductivity of lightweight concrete.* Cement and Concrete Research, 2003. **33**(5): p. 723-727.

70. Kockal, N. U. and Ozturan, T., *Durability of lightweight concretes with lightweight fly ash aggregates.* Construction and Building Materials, 2011. **25**(3): p. 1430-1438.

71. Chia, K. S. and Zhang, M. H., *Water permeability and chloride penetrability of high-strength lightweight aggregate concrete.* Cement and Concrete Research, 2002. **32**(4): p. 639-645.

72. ACI Committee 237R-07, *Self-Consolidating Concrete*, 2007, American Concrete Institute: Farmington Hills.

73. Brouwers, H. J. H. and Radix, H. J., *Self-compacting concrete: Theoretical and experimental study.* Cement and Concrete Research, 2005. **35**(11): p. 2116-2136.

74. NRMCA. *CIP 37 - Self Consolidating Concrete (SCC)*. Technical information 2004 [cited 2012 October]; Available from: http://www.nrmca.org/aboutconcrete/cips/37p.pdf.

75. Okamura, H., *Self-compacting high-performance concrete.* Concrete International-Design and Construction, 1997. **19**(7): p. 50-54.

76. Okamura, H. and Ouchi, M., *Self-compacting concrete.* Journal of Advanced Concrete Technology, 2003. **1**(1): p. 5-15.

77. Ouchi, M., *Self-Compacting Concrete-Development, Applications and Investigations.* Nordic Concrete Research Publications, 2000. **23**: p. 29-34.

78. Okamura, H. and Ouchi, M. *Applications of Self-Compacting Concrete in Japan*. in *3rd International RILEM Symposium on Self-Compaction Concrete*. 2003. Reykjavik, Iceland: RILEM Publications S.A.R.L.

79. Rich, D., Glass, J., Gibb, A. G. F., and Goodier, C. I., *UK contractors' views on self-compacting concrete in construction.* 2012.

80. Skarendahl, Å. *The present - the future*. in *3rd International RILEM Symposium on Self-Compacting Concrete*. 2003. Reykjavik, Iceland: RILEM Publications S.A.R.L.

81. Skarendahl, Å. and Billberg, P., *Report 35: Casting of self-compacting concrete - Final Report of RILEM TC 188-CSC*. Vol. 35. 2006: RILEM publications.

82. Khayat, K. H., *Workability, testing, and performance of self-consolidating concrete.* ACI materials journal, 1999. **96**: p. 346-353.

83. EFNARC. *European SCC Guidelines*. 2005 [cited 2012 October]; Available from: http://www.efnarc.org/publications.html.

84. Jawahar, J.G., Sashidhar, C., Ramana Reddy, I.V., and Annie Peter, J., *Effect of coarse aggregate blending on short-term mechanical properties of self compacting concrete.* Materials & Design, 2012.

85. Jawahar, J. G., Premchand, M. M., Sashidhar, C., Reddy, I. V. R., and Peter, J. A., *Effect of coarse aggregate blending on fresh properties of self-compaction concrete.* 2012.

86. Gesoğlu, M., Güneyisi, E., and Özbay, E., *Properties of self-compacting concretes made with binary, ternary, and quaternary cementitious blends of fly ash, blast furnace slag, and silica fume.* Construction and Building Materials, 2009. **23**(5): p. 1847-1854.

87. Ravindrarajah, R.S., Siladyi, D., Adamopoulos, B., Wallevik, O., and Nielsson, I. *Development of high-strength self-compacting concrete with reduced segregation potential*. 2003. RILEM Publications SARL.

88. Bouzoubaa, N. and Lachemi, M., *Self-compacting concrete incorporating high volumes of class F fly ash: preliminary results.* Cement and Concrete Research, 2001. **31**(3): p. 413-420.

89. Boukendakdji, O., Kenai, S., Kadri, EH, and Rouis, F., *Effect of slag on the rheology of fresh self-compacted concrete.* Construction and Building Materials, 2009. **23**(7): p. 2593-2598.

90. Ye, G., Liu, X., De Schutter, G., Poppe, A.M., and Taerwe, L., *Influence of limestone powder used as filler in SCC on hydration and microstructure of cement pastes.* Cement and Concrete Composites, 2007. **29**(2): p. 94-102.

91. Schutter, G. De, *Effect of limestone filler as mineral addition in self-compaction concrete*, in *36th Conference on Our World in Concrete & Structures* 2011, CI-Premier PTE Ltd: Singapore.

92. Ravindrarajah, R. S., Farrokhzadi, F., Lahoud, A., Wallevik, O., and Nielsson, I. *Properties of flowing concrete and self-compacting concrete with high-performance superplasticizer*. 2003. RILEM Publications SARL.

93. Melo, K. A. and Repette, W. L., *Optimization of superplasticizer content in self-compacting concrete.* Measuring, Monitoring and Modeling Concrete Properties, 2006: p. 469-477.

94. Bateman, C. S. *The Use of superplasticizers to enhance the durability of concrete*. 1985. Institution of Engineers, Australia.

95. Boukendakdji, O., Kadri, E.H., and Kenai, S., *Effects of granulated blast furnace slag and superplasticizer type on the fresh properties and compressive strength of self-compacting concrete.* Cement and Concrete Composites, 2012. **34**(4): p. 583-590.

96. Şahmaran, M., Christianto, H. A., and Yaman, İ. Ö., *The effect of chemical admixtures and mineral additives on the properties of self-compacting mortars.* Cement and Concrete Composites, 2006. **28**(5): p. 432-440.

97. Papanicolaou, C. G. and Kaffetzakis, M. I., *Lightweight aggregate self-compacting concrete: State-of-the-art and pumice application.* Journal of Advanced Concrete Technology, 2011. **9**(1): p. 15-29.

98. Kim, Y. J., Choi, Y. W., and Lachemi, M., *Characteristics of self-consolidating concrete using two types of lightweight coarse aggregates.* Construction and Building Materials, 2010. **24**(1): p. 11-16.

99. Wu, Z., Zhang, Y., Zheng, J., and Ding, Y., *An experimental study on the workability of self-compacting lightweight concrete.* Construction and Building Materials, 2009. **23**(5): p. 2087-2092.

100. Rahman, M. M., Rashid, M. H., Hossain, M. A., Adrita, F. S., and Hossain, T., *Mixing time effects on properties of self compacting concrete.* Journal of Engineering and Applied Sciences, 2006. **6**.

101. Malhotra, V. M. and Carino, N. J., *Handbook on nondestructive testing of concrete* 2004: ASTM International.

102. McIntosh, J. D., *Electrical curing of concrete.* Magazine of Concrete Research, 1949. **1**(1): p. 21-28.

103. Nurse, R. W., *Steam curing of concrete.* Magazine of Concrete Research, 1949. **1**(2): p. 79-88.

104. Saul, A. G. A, *Principles underlying the steam curing of concrete at atmospheric pressure.* Magazine of Concrete Research, 1951. **2**(6): p. 127-140.

105. McIntosh, J. D. *The effects of low-temperature curing on the compressive strength of concrete*. in *Proceedings*. 1956.

106. Carino, N. J. and Lew, H. S., *The maturity method: From theory to application.* Cement, Concrete, and Aggregates, 1984. **6**(2): p. 61-73.

107. Kehl, R. J., Constantino, C. A., and Carrasquillo, R. L., *Match-Cure and Maturity: Taking Concrete Strength Testing to a Higher Level* 1998: Center for Transportation Research, Bureau of Engineering Research, The University of Texas at Austin.

108. De Vree, R. T. and Tegelaar, R. A., *Gewichtete reife des betons, beton 48.* H, 1998. **11**: p. 674-678.

109. Papadakis, M. and Bresson, J., *Contribution to the study of the maturity of hydraulics binder. Application to the prefabricated concrete industry.* Revue Mater Constr & Trav Pub'Ciments & Betons', 1973(678).

110. Han, N., *Advanced testing of cement-based materials during setting and hardening-final report of RILEM TC 185-ATC chapter 6 maturity method*, 2005, RILEM Publications SARL, 2005: 277,284-292.

111. CUR-Recommendation, *9 Determining the strength of young concrete on the basis of Weighted maturity.*, 1986, The Dutch Centre for Civil Engineering, Research, Codes and Specifications: Grouda, the Netherlands.

112. Luo, Q. L. and Wang, W. L., *Accelerated test method for cement strength based on the weighted maturity theory.* Applied Mechanics and Materials, 2012. **105**: p. 897-901.

113. Rastrup, E., *Heat of hydration in concrete.* Magazine of Concrete Research, 1954. **6**(17): p. 127-140.

114. Bergström, S. G., *Curing temperature, age and strength of concrete.* Magazine of Concrete Research, 1953. **5**(14): p. 61-66.

115. Weaver, J. and Sadgrove, B. N., *Striking times of formwork-tables of curing periods to achieve given strength* 1971.

116. Harrison, T. A., *Mechanical damage to concrete by early removal of formwork*, 1975.

117. Clear, C. A., *Fact Sheet 5: Self-Compacting Concrete (SCC).* British Cement Association, Camberley, UK, 2006.

118. Wimpenny, D. and Ellis, C. *The effect of ggbs on the temperature and strength development in concrete elements under low ambient temperatures*. 1991.

119. Sadgrove, B. M., *Prediction of strength development in concrete structures.* Transportation Research Record, 1975(558).

120. Copeland, L. E., Kantro, D. L., and Verbeck, G. J., *Chemistry of hydration of Portland cement* 1960: Portland Cement Association, Research and Development Laboratories.

121. Hansen, P. F. and Pedersen, E. J., *Maturity computer for controlled curing and hardening of concrete*, 1977.

122. Byfors, J., *Plain concrete at early ages* 1980: Swedish Cement and Concrete Research Institute.

123. Naik, T. R., *Maturity functions for concrete cured during winter conditions.* Temperature effects on concrete, ASTM STP, 1985. **858**: p. 107.

124. Alexander, K. M. and Taplin, J. H., *Concrete strength, paste strength, cement hydration and the maturity rule.* Australian journal of applied science, 1962. **13**(4): p. 277-84.

125. Verbeck, G.J. and Helmuth, R.H. *Structures and physical properties of cement paste*. 1968.

126. Hudson, S. B. and Steele, G. W., *Prediction of Potential Strength of Concrete from the Results of Early Tests.* Highway Research Record, 1971.

127. Hudson, S. B. and Steele, G. W., *Developments in the prediction of potential strength of concrete from results of early tests.* Transportation Research Record, 1975(558).

128. ASTM C 918-02, *Standard Test Method for Measuring Early-Age Compressive Strength and Projecting Later-Age Strength*, 2002, International ASTM.

129. Nykanen, A. *Hardening of concrete at different temperatures, especially below the freezing point*. in *Proc. RILEM Symp. on Winter Concreting, Session BII*. 1956. Conpenhagen.

130. Plowman, J. M., *Maturity and the strength of concrete.* Magazine of Concrete Research, 1956. **8**(22): p. 13-22.

131. Bernhardt, C. J., *Hardening of concrete at different temperatures*, in *Proc. RILEM Symp. on Winter Concreting, Session BII* 1956, Danish Institute for Building Research: Conpenhagen.

132. Goral, M. L. *Empirical time-strength relations of concrete*. in *ACI Journal Proceedings*. 1956. ACI.

133. ACI Committee 209, *Prediction of Creep, Shrinkage, and Temperature Effects in Concrete Structures*, 2008: Farmington.

134. Chin, F. K. *Relation between strength and maturity of concrete*. in *ACI Journal Proceedings*. 1971. ACI.

135. Chin, F. K., *Strength tests at early ages and at high setting temperatures.* Transportation Research Record, 1975(558).

136. Carino, N. J., Lew, H. S., and Volz, C. K. *Early age temperature effects on concrete strength prediction by the maturity method*. 1983. ACI.

137. Carino, N. J., *Closure to discussion of Reference 32.* Journal of American Concrete Institute, 1984. **81**(1): p. 98.

138. Lew, H. S. and Reichard, T. W., *Prediction of strength of concrete from maturity.* Accelerated Strength Testing, 1978: p. 229-248.

139. Hansen, P. F. and Pedersen, E. J., *Curing of concrete structures* 1984.

140. Tank, R. C. and Carino, N. J., *Rate constant functions for strength development of concrete.* ACI materials journal, 1991. **88**(1).

141. Brooks, A. G., Schindler, A. K., and Barnes, R. W., *Maturity method evaluated for various cementitious materials.* Journal of Materials in Civil Engineering, 2007. **19**(12): p. 1017-1025.

142. Carino, N.J. and Tank, R.C., *Maturity Function for Concretes Made With Various Cements and Admixtures.* ACI materials journal, 1992. **89**(2).

143. Wikipedia. *Activation energy*. [cited 2012 October]; Available from: http://en.wikipedia.org/wiki/Activation_energy.

144. Hatzitheodorou, A., *Insite strength development of concretes with supplementary cementitious materials*, 2007, University of Liverpool.

145. Chanvillard, G. and D'Aloia, L., *Determination of the Apparent Activation Energy of Concrete: Ea. Semi-Adiabatic Tests of Heat Development.* ACI Special Publications, 1998. **179**: p. 561-586.

146. Poole, J. L., Riding, K. A., Folliard, K. J., Juenger, M. C. G., and Schindler, A. K., *Methods for calculating activation energy for portland cement.* ACI materials journal, 2007. **104**(1): p. 303-311.

147. Kada-Benameur, H., Wirquin, E., and Duthoit, B., *Determination of apparent activation energy of concrete by isothermal calorimetry.* Cement and Concrete Research, 2000. **30**(2): p. 301-305.

148. Copeland, L. E. and Kantro, D. L., *Chemistry of hydration of portland cement at ordinary temperature.* The Chemistry of Cements, 1964. **1**: p. 313-370.

149. Carino, N. J., *Temperature Effects on the Strength–Maturity Relation of Mortar, Report No.* NBSIR 81-2244, 1981. **81**.

150. Regourd, M. and Mortureux, B. *Characterization of thermal activation of slag cements*. in *Proceedings of the 7th International Congress on the chemistry of cements (Paris)*. 1980.

151. Gauthier, E. and Regourd, M., *The hardening of cement in function of temperature.* Proceedings, RILEM, France, 1982: p. 145-150.

152. Geiker, M., *Studies of Portland cement hydration by measurements of chemical shrinkage and a systematic evaluation of hydration curves by means of the dispersion model*, 1983, Technical University of Denmark.

153. Geiker M. and Knudsen T., *Chemical Shrinkage of Portland Cement Pastes.* Cement and Concrete Research, 1982. **12**(5): p. 603-610.

154. Schindler, A. K., *Effect of temperature on hydration of cementitious materials.* ACI materials journal, 2004. **101**(1): p. 72-81.

155. Jonasson, J. E., Groth, P., and Hedlund, H. *Modelling of temperature and moisture field in concrete to study early age movements as a basis for stress analysis*. in *Rilem Proceedings*. 1995. Chapman & Hall.

156. Rilem, TC119-TCE, *Avoidance of thermal cracking in concrete at early ages - Adiabatic and semi-adiabatic calorimetry to determine the temperature increase in concrete due to hydration heat of the cement.* Materials and Structures, 1997. **30**: p. 451-464.

157. Kjellsen, K. O. and Detwiler, R. J., *Later-age strength prediction by a modified maturity model.* ACI materials journal, 1993. **90**(3).

158. Kim, J. K., Han, S. H., and Lee, K. M., *Estimation of compressive strength by a new apparent activation energy function.* Cement and Concrete Research, 2001. **31**(2): p. 217-225.

159. Pane, I. and Hansen, W., *Concrete hydration and mechanical properties under nonisothermal conditions.* ACI materials journal, 2002. **99**(6).

160. Han, S .H., Kim, J. K., and Park, Y. D., *Prediction of compressive strength of fly ash concrete by new apparent activation energy function.* Cement and Concrete Research, 2003. **33**(7): p. 965-971.

161. Barnett, S. J., Soutsos, M.N., Bungey, J.H., and Millard, S.G., *Fast-track construction with slag cement concrete: Adiabatic strength development and strength prediction.* ACI materials journal, 2007. **104**(4): p. 388.

162. Chanvillard, G. and D'Aloia, L., *Concrete strength estimation at early ages: modification of the method of equivalent age.* ACI materials journal, 1997. **94**(6).

163. Abdel-Jawad, Y. A., *The maturity method: Modifications to improve estimation of concrete strength at later ages.* Construction and Building Materials, 2005. **20**(10): p. 893-900.

164. Abdel-Jawad, Y. A., *Estimating concrete strength using a modified maturity model.* Proceedings of the ICE-Construction Materials, 2006. **159**(1): p. 33-37.

165. Abdel-Jawad, Y. A. and Hansen, W. *The effect of temperature on hydration kinetics of Portland cement*. in *Proceedings of the 1st International Conference on Reinforced Concrete Materials in Hot Climates, Al Ain, UAE. UAE University Press, United Arab Emirates*. 1994.

166. Soutsos, M. N., *The effect of curing temperature on the rate of cement hydration*, 2009.

167. Waller, V., d'Aloïa, L., Cussigh, F., and Lecrux, S., *Using the maturity method in concrete cracking control at early ages.* Cement and Concrete Composites, 2004. **26**(5): p. 589-599.

168. Ryell, J. and Bickley, J. A. *Scotia Plaza: High strength concrete for tall buildings*. in *Proceedings Utilization of High Strength Concrete, Stavanger, Norway*. 1987.

169. Con-Cure. *Concrete maturity solutions*. [cited 2012 November]; Available from: http://www.con-cure.com/customer-case-study.html.

170. Roy, D. M., Scheetz, B. E., Sabol, S., Brown, P. W., Shi, D., Licastro, P. H., Idom, G. M., Andersen, P. J., and Johanson, V., *Maturity model and curing technology*. SHRP-C-625 Vol. 100. 1993.

171. Pinto, R. C. A. and Hover, K. C., *Application of maturity approach to setting times.* ACI Materials Journal, 1999. **96**(6): p. 686-691.

172. Schindler, A. K. *Prediction of concrete setting*. in *International RILEM Symposium on Concrete Science and Engineering: A Tribute to Arnon Bentur*. 2004. RILEM Publications SARL.

173. Han, M.C. and Han, C.G., *Use of maturity methods to estimate the setting time of concrete containing super retarding agents.* Cement and Concrete Composites, 2010. **32**(2): p. 164-172.

174. Anderson, K. W., Uhlmeyer, J. S., Kinne, C., Pierce, L. M., and Muench, S., *Use of the maturity method in accelerated PCCP construction* 2009.

175. Bamforth, P. B., *Early-age thermal crack control in concrete.* CIRIA 660, London, 2007.

176. Holman, J. P., *Heat Transfer*, ed. th 1990, New York: McGraw Hill. Inc.

177. Ballim, Y. and Graham, P. C., *A maturity approach to the rate of heat evolution in concrete.* 2003.

178. Branco, F. A., Mendes, P., and Mirambell, E., *Heat of hydration effects in concrete structures.* ACI materials journal, 1992. **89**(2).

179. Ge, Z., Wang, K., and Gao, Z., *Prediction of Pavement Concrete Strength Development, Joint Sawing, and Opening Time Using FEMLAB.* Journal of Performance of Constructed Facilities, 2012. **26**(2): p. 162-169.

180. Ruiz, J., Schindler, A. K., Rasmussen, R., and Johnson, T. *Prediction of heat transport in concrete made with blast furnace slag aggregate*. in *9th conference on Advances in Cement and Concrete, Colorado, USA*. 2003.

181. Jeong, J.H. and Zollinger, D.G., *Finite-element modeling and calibration of temperature prediction of hydrating Portland cement concrete pavements.* Journal of Materials in Civil Engineering, 2006. **18**(3): p. 317-324.

182. Larsson, O. and Thelandersson, S., *Estimating extreme values of thermal gradients in concrete structures.* Materials and Structures, 2011: p. 1-10.

183. Nevander, L.E. and Elmarsson, B., *Fukthandbok: Praktik och teori* 1994: Svensk Byggtjänst.

184. Incropera, F. P. and DeWitt, D. P., *Fundamentals of Heat and Mass Transfer* 1996, Wiley, New York.

185. Mehta, P. K. and Monteiro, P. J. M., *Concrete: microstructure, properties and materials* 2006: McGraw-Hill.

186. Kim, K. H., Jeon, S. E., Kim, J. K., and Yang, S., *An experimental study on thermal conductivity of concrete.* Cement and Concrete Research, 2003. **33**(3): p. 363-371.

187. Khan, M. I., *Factors affecting the thermal properties of concrete and applicability of its prediction models.* Building and environment, 2002. **37**(6): p. 607-614.

188. Campbell-Allen, D. and Thorne, C. P., *The thermal conductivity of concrete.* Magazine of Concrete Research, 1963. **15**(43): p. 39-48.

189. Khan, A. A., Cook, W. D., and Mitchell, D., *Thermal properties and transient thermal analysis of structural members during hydration.* ACI materials journal, 1998. **95**(3).

190. Demirboğa, R., *Thermal conductivity and compressive strength of concrete incorporation with mineral admixtures.* Building and environment, 2007. **42**(7): p. 2467-2471.

191. Morabito, P., *Thermal properties of concrete.* Variations with the temperature and during the hydration phase. IPACS document, Subtask, 2001. **2**.

192. Marshall, A. L., *The thermal properties of concrete.* Building Science, 1972. **7**(3): p. 167-174.

193. Brown, T. D. and Javaid, M. Y., *The thermal conductivity of fresh concrete.* Materials and Structures, 1970. **3**(6): p. 411-416.

194. De Schutter, G. and Taerwe, L., *Specific heat and thermal diffusivity of hardening concrete.* Magazine of Concrete Research, 1995. **47**(172): p. 203-208.

195. RILEM-TC-42-CEA, *Properties of set concrete at early ages - State-of-the-art report*, in *Materials and Structures* 1981. p. 399-402.

196. O'Donnell, J. J. and O'Brien, E. J., *A new methodology for determining thermal properties and modelling temperature development in hydrating concrete.* Construction and Building Materials, 2003. **17**(3): p. 189-202.

197. Yoshida, T., *Studies on cooling of fresh concrete in freezing weather.* 1921.

198. Rousan, A. A. and Roy, D. M., *A thermal comparator method for measuring thermal conductivity of cementitious materials.* Industrial & Engineering Chemistry Product Research and Development, 1983. **22**(2): p. 349-351.

199. Davey, N. *Concrete mixes for various building purposes*. in *Proceedings*. 1954.

200. Mass, G. R., Burgess, W. L., Abdun-Nur, E. A., Cannon, R. W., Groner, D., Price, W. H., Schrader, E. K., Anderson, F. A., Carlson, R. W., and Hansen, K. D., *Mass Concrete*, 1997, ACI.

201. Mindess, S. and Young, J. F., *Concrete* 1981, Englewoods Cliffs: Prentice Hall Inc.

202. Whiting, D., Litvin, A., and Goodwin, S. E. *Specific heat of selected concretes*. in *ACI Journal Proceedings*. 1978. ACI.

203. Bamforth, P., Chisholm, D., Gibbs, J., and Harrison, T., *Properties of Concrete for use in Eurocode 2*, 2008, The Concrete Centre, CCIP-026.

204. Lofqvist, B., *Temperature effekter i hardnande betong.* Tekniskt Meddelande Fran KungI , Vatterfallsstyrelsen Stockholm, 1946: p. 195.

205. Van Breugel, K., *Numerical simulation of hydration and microstructural development in hardening cement-based materials:(II) applications.* Cement and Concrete Research, 1995. **25**(3): p. 522-530.

206. Bentz, D. P., Garboczi, E. J., Haecker, C. J., and Jensen, O. M., *Effects of cement particle size distribution on performance properties of Portland cement-based materials.* Cement and Concrete Research, 1999. **29**(10): p. 1663-1671.

207. Lerch, W., *The influence of gypsum on the hydration and properties of Portland cement pastes* 1946: Portland Cement Association.

208. Ben-Bassat, M. and Paillere, A. M., *Water reducing/retarding admixtures.* Application of Admixtures in Concrete, 1995.

209. Nagataki, S., *Hardening accelerators.* Application of Admixtures in Concrete, 1995.

210. Wang, J. C. and Yan, P. Y., *Influence of initial casting temperature and dosage of fly ash on hydration heat evolution of concrete under adiabatic condition.* Journal of thermal analysis and calorimetry, 2006. **85**(3): p. 755-760.

211. Gruyaert, E., Robeyst, N., and De Belie, N., *Study of the hydration of Portland cement blended with blast-furnace slag by calorimetry and thermogravimetry.* Journal of thermal analysis and calorimetry, 2010. **102**(3): p. 941-951.

212. Coole, M. J., *Heat release characteristics of concrete containing ground granulated blast furnace slag in simulated large pours.* Magazine of Concrete Research, 1988. **40**(144): p. 152-158.

213. Bamforth, P. B., *Early-age thermal crack control in concrete*, in *CIRIA Report C660* 2007: London.

214. Dhir, R. K., Paine, K. A., and Zheng, L., *Design data for use where low heat cements are used. Final Report to Department of Trade and Industry, CTU/2704.* Final Report to Department of Trade and Industry, 2004.

215. De Schutter, G. and Taerwe, L., *General hydration model for Portland cement and blast furnace slag cement.* Cement and Concrete Research, 1995. **25**(3): p. 593-604.

216. Bogue, R.H., *The chemistry of Portland cement* 1947: Reinhold publishing corporation.

217. ASTM C 150-04, *Standard specification for Portland cement*, 2004, ASTM International: West Conshohocken, PA 19428-2959, United States.

218. Schindler, A. K., *Concrete hydration, temperature development, and setting at early-ages.* 2011.

219. Schindler, A. K. and Folliard, K. J. *Influence of supplementary cementing materials on the heat of hydration of concrete*. 2003.

220. Kishi, T. and Maekawa, K. *Thermal and mechanical modelling of young concrete based on hydration process of multi-component cement minerals*. in *Rilem Proceedings*. 1995. Chapman & Hall.

221. Bensted, J., *Hydration of Portland cement.* Advances in cement technology: chemistry, manufacture and testing, 2003: p. 31.

222. Taplin, J. H., *A method for following the hydration reaction in portland cement paste.* Australian journal of applied science, 1959. **10**(3): p. 329-345.

223. Mills, R. H., *Factors influencing cessation of hydration in water cured cement pastes.* Highway Research Board Special Report, 1966(90).

224. Wadsö, L., *An experimental comparison between isothermal calorimetry, semi-adiabatic calorimetry and solution calorimetry for the study of cement hydration.* Nordtest report TR, 2003. **522**.

225. Bentz, D. P., *A computer model to predict the surface temperature and time-of-wetness of concrete pavements and bridge decks* 2000: US Department of Commerce, Technology Administration, National Institute of Standards and Technology.

226. Ruiz, J., Schindler, A., Rasmussen, R., and Johnson, T. *Prediction of heat transport in concrete made with blast furnace slag aggregate*. in *9th conference on Advances in Cement and Concrete, Colorado, USA*. 2003.

227. Schindler, A. K., Ruiz, J. M., Rasmussen, R. O., Chang, G. K., and Wathne, L. G., *Concrete pavement temperature prediction and case studies with the FHWA HIPERPAV models.* Cement and Concrete Composites, 2004. **26**(5): p. 463-471.

228. Ge, Z. and Wang, K., *Predicting field concrete temperature using an integrated model*, in *Rilem International Conference on Microstructure Related Durability of Cementitious Composites* 2008: nanjing, China. p. 1125 - 1138.

229. Teychenne, D. C., Franklin, R. E., Erntroy, H. C., Nicholls, J. C., HOBBS, D. W., and MARSH, D. W., *Design of normal concrete mixes* 1997: Building Research Establishment.

230. Domone, P. L. and Soutsos, M. N., *An approach to the proportioning of high-strength concrete mixes.* Concrete International-Design and Construction, 1994. **16**(10): p. 26-31.

231. Domone, P. L. and Soutsos, M. N., *Properties of high-strength concrete mixes containing PFA and ggbs.* Magazine of Concrete Research, 1995. **47**(173): p. 355-367.

232. Fosroc. *Structuro 11180*. 2007 [cited 2009 January]; Available from: http://www.resapol.com/datasheets/data500.pdf.

233. Castle-Cement, *Laboratory Chemical Report*, Limited, C. C., Editor 2009: Lancashire, UK.

234. BS EN 197-1*, Cement - Part 1: Composition, specifications and conformity criteria for common cements*, 2000, British Standard Institution: London.

235. Civil+Marine, *Chemical Analysis Report of GGBS*, 2009.

236. BS 6110, *Pozzolanic-fuel ash cement*, 1996, British Standard Institution: London.

237. BS 882, *Specification for aggregates from natural sources for concrete* 1992, British Standard Institution: London.

238. BS EN 1097-6, *Tests for mechanical and physical properties of aggregates - Part 6: Determination of particle density and water absorption*, 2000, British Standards Institution: London.

239. BS EN 13055 - 1: 2002, *Lightweight aggregates*, in *Part 1: Lightweight aggregates for concrete, mortar and grout* 2002, British Standards Institution: London.

240. Lytag. *Ltd, Technical Manual - Section 2 Introduction to Lytag lightweight aggregate concrete - LWAC* 2009 [cited 2009 July]; Available from: http://www.lytag.co.uk/uploads/techdocs/Section%202%20-%20Introduction%20to%20Lytag%20lightweight%20aggregate%20concrete%20LWAC.pdf.

241. BS EN 1008, *Mixing water for concrete - Specification for sampling, testing and assessing the suitability of water, including water recovered from processes in the concrete industry, as mixing water for concrete*, 2002, British Standard Institution: London.

242. BS 1881-125, *Testing concrete - Part 125: Methods for mixing and sampling fresh concrete in the laboratory*, 1986, British Standard Institution: London.

243. Taylor, R. L. and Associates, *Thermometric 3114/3236 TAM Air Isothermal Calorimeter: A multichannel isothermal calorimeter for heat flow measurements in the milliwatt range,* 2000: Instructions Manual, Thermometric AB, Sweden.

244. Pico. *Technology USB TC-08 Thermocouple Data Logger: User's Guide*. [cited 2012 September]; Available from: http://www.picotech.com/thermocouple.html?source=feat.

245. Soutsos, M. N., *Mix design,workability, adiabatic temperature and strength development of high strength concrete, PhD Thesis*, 1992, College London.

246. ACI Committee 207.1R-96, *Mass Concrete*, 1996, America Concrete Institute: Farmington.

247. COMSOL, *Comsol Multyphysics Modeling Guide Version 3.4,* 2007: COMSOL AB.

248. Ruiz, J. M., Schindler, A. K., Rasmussen, R. O., Nelson, P. K., and Chang, G. K. *Concrete temperature modeling and strength prediction using maturity concepts in the FHWA HIPERPAV software*. in *Seventh International Conference on Concrete Pavements. The Use of Concrete in Developing Long-Lasting Pavement Solutions for the 21st Century*. 2001.

249. Incropera, F. P. and De Witt, D. P., *Fundamentals of heat and mass transfer*. 1985.

250. Soutsos, M. N., Turu'allo, G., Owens, K., Kwasny, J., Barnett, S. J., and Basheer, P. A. M., *Maturity testing of lightweight self-compacting and vibrated concretes.* Construction and Building Materials, 2013. **47**: p. 118-125.

251. Raphael, J. M. *Tensile strength of concrete*. 1984. ACI.

252. Oluokun, F., *Prediction of concrete tensile strength from its compressive strength: an evaluation of existing relations for normal weight concrete.* ACI materials journal, 1991. **88**(3).

253. BS EN 12390-6, *Testing hardened concrete - Part 6: Tensile splitting strength test specimens*, 2009, British Standard Institution: London.

254. ASTM C 496M-04, *Standard Test Method for Splitting Tensile Strength of Cylindrical Concrete Specimens*, 2004, ASTM International.

255. Oluokun, F. A., Burdette, E. G., and Deatherage, J. H., *Splitting tensile strength and compressive strength relationships at early ages.* ACI materials journal, 1991. **88**(2).

256. Oluokun, F.A., Burdette, E.G., and Deatherage, J.H., *Elastic modulus, Poisson's ratio, and compressive strength relationships at early ages.* ACI materials journal, 1991. **88**(1).

257. ACI Committee 318-05, *Building code requirements for structural concrete (ACI 318-05) and commentary (ACI 318R-05)*, 2005, American Concrete Institute: Farmington Hills, Mich.

258. Van Breugel, K., *Modelling of strength development in hardening concrete.* IPACS, 2001: p. 13-16.

259. Klieger, P. *Effect of mixing and curing temperature on concrete strength*. 1958. ACI.

260. Bentz, D. P., Sant, G., and Weiss, J., *Early-age properties of cement-based materials. I: Influence of cement fineness.* Journal of Materials in Civil Engineering, 2008. **20**: p. 502.

261. Dhir, R. K. and Jackson, N., *Civil Engineering Materials* 1990: Macmillan.

262. Somayaji, S., *Civil engineering materials, 2nd ed*. Great Bretain: Prentice Hall 2001.

263. Ashraf, W. B. and Noor, M. A., *An experimental comparative study on the effects of cement types on concrete properties.* 2011.

264. Aitcin, P. C. and Mehta, P. K., *Effect of coarse aggregate characteristics on mechanical properties of high-strength concrete.* ACI materials journal, 1990. **87**(2).

265. de Larrard, F. and Belloc, A., *The influence of aggregate on the compressive strength of normal and high-strength concrete.* ACI materials journal, 1997. **94**(5).

266. Cordon, W. A. and Gillespie, H. A. *Variables in concrete aggregates and Portland cement paste which influence the strength of concrete*. 1963. ACI.

267. Yaqub, M. and Bukhari, I. *Effect of Size of Coarse Aggregate on Compressive Strength of High Strength Concrete*. in *31st Conference on Our World in Concrete & Stuctures*. 2006. Singapore.

268. Goto, S. and Roy, D. M., *The effect of w/c ratio and curing temperature on the permeability of hardened cement paste.* Cement and Concrete Research, 1981. **11**(4): p. 575-579.

269. Popovics, S. and Ujhelyi, J., *Contribution to the concrete strength versus water-cement ratio relationship.* Journal of Materials in Civil Engineering, 2008. **20**: p. 459.

270. Popovics, S. *New formulas for the prediction of the effect of porosity on concrete strength*. 1985. ACI.

271. Popovics, S. *Effect of curing method and final moisture condition on compressive strength of concrete*. 1986. ACI.

272. ACI Committee 308R-01*, Guide to Curing Concrete*, in *Field Reference Manual: Standard Specifications for Structural Concrete with Selected ACI and ASTM References* 2005, America Concrete Institute: Farmington. p. 487.

273. BS EN 12390-2, *Testing hardened concrete. Part 2: Making and curing specimens for strength tests*, 2000, British Standard Institution: London.

274. ASTM C192/C 192M, *Standard Practice for making and curing concrete test specimens in laboratory*, 2004, ASTM International.

275. Newman, J. B. and Choo, B. S., *Advanced Concrete Technology, Volume 2: Concrete Properties* 2003: Elsevier Science & Technology.

276. Price, W. H. *Factors influencing concrete strength*. 1951. ACI.

277. Hayri, U. N. and Baradan, B., *The effect of curing temperature and relative humidity on the strength development of Portland cement mortar.* Scientific Research and Essays, 2011. **6**(12): p. 2504-2511.

278. Turuallo, G., and Soutsos, M. N., *Prediction of concrete strength development using maturity function* in *The 3rd International Conference of European Asian Civil Engineering Forum (EACEF)* 2011: Jogjakarta, Indonesia.

279. Soutsos, M. N., Barnett, S. J., Millard, S. G., and Bungey, J. H., *The effect of temperature on the rate of strength development of slag cement.* ACI Special Publication, 2009. **263**: p. 111-126.

280. Kim, J. K., Moon, Y. H., and Eo, S. H., *Compressive strength development of concrete with different curing time and temperature.* Cement and Concrete Research, 1998. **28**(12): p. 1761-1773.

281. Husem, M. and Gozutok, S., *The effects of low temperature curing on the compressive strength of ordinary and high performance concrete.* Construction and Building Materials, 2005. **19**(1): p. 49-53.

282. Ezziane, K., Bougara, A., Kadri, A., Khelafi, H., and Kadri, E., *Compressive strength of mortar containing natural pozzolan under various curing temperature.* Cement and Concrete Composites, 2007. **29**(8): p. 587-593.

283. Escalante-Garcia, J.L. and Sharp, J.H., *The microstructure and mechanical properties of blended cements hydrated at various temperatures.* Cement and Concrete Research, 2001. **31**(5): p. 695-702.

284. Escalante-Garcia, J. L. and Sharp, J. H., *Effect of temperature on the hydration of the main clinker phases in Portland cements: Part I, neat cements.* Cement and Concrete Research, 1998. **28**(9): p. 1245-1257.

285. Daveis, R. E., Carlson, R. W., Troxell, G. E., and Kelly, J. W. *Cement Investigations for Boulder Dam with the Results up to the Age of One Year*. 1934. ACI.

286. Moranville, M. *Implications of curing temperatures for durability of cement based systems, Curing temperatures and durability*. 1995.

287. Rostasy, F. S., Weiβ, R., and Wiedemann, G., *Changes of pore structure of cement mortars due to temperature.* Cement and Concrete Research, 1980. **10**(2): p. 157-164.

288. ACI Committee 308.1-11, *Specification for Curing Concrete*, 2011, American Concrete Institute: Farmington.

289. Branson, D. E. and Christiason, M. L., *Time-Dependent Concrete Properties Related to Design—Strength and Elastic Properties, Creep and*

Shrinkage. Designing for Effects of Creep, Shrinkage and Temperature in Concrete Structures, 1971: p. 27-13.

290. CEB-FIP, *Design of concrete structures. CEB-FIP Model Code 1990*, 1993, Thomas Telford.

291. ASTM C 494, *Standard Spesification for Chemical Admixtures for Concrete*, in *in Annual Book of ASTM Standards* 2004, ASTM International.

292. BS EN 934-2, *Admixtures for Concrete, Mortar and Grout*, in *Part 2: Concrete admixtures - Definitions, requirements, comformity, marking and labelling* 2009, British Standard Institution: London.

293. Hewlett, P. C., *Lea's chemistry of cement and concrete* 2004: A Butterworth-Heinemann.

294. Pan, L. S., Qiu, X. Q., Pang, Y. X., and Yang, D. J., *Effect of water-reducing chemical admixtures on early hydration of cement.* Advances in cement research, 2008. **20**(3): p. 93-100.

295. Paillere, A. M., Ben Bassat, M., and Akman, S., *Guide for use of admixtures in concrete.* Materials and Structures, 1992. **25**(1): p. 49-56.

296. Paillère, A. M., *Application of admixtures in concrete* 1995: Taylor & Francis.

297. Barnett, S.J., Soutsos, M.N., Bungey, J.H., and Millard, S.G. *Fast-track concrete construction using cement replacement materials*. in *Proceedings of the Eighth CANMET/ACI International Conference on Fly Ash, Silica Fume, Slag, and Natural Pozzolans in Concrete, ACI SP-221, American Concrete Institute, Farmington Hills, Mich*. 2004.

298. Eren, Ö., *Strength development of concretes with ordinary Portland cement, slag or fly ash cured at different temperatures.* Materials and Structures, 2002. **35**(9): p. 536-540.

299. Jackson, N., Dhir, R. K., *Civil Engineering Materials* 1996: Macmillan.

300. Weaver, J. and Sadgrove, BN, *Striking Time oh Formwork-Tables of Curing Periods to Achieve Given Strength*, 1971.

301. BS 1881 Part 130, *Method for temperature-matched curing of concrete specimens*, 1996, British Satandard Institution: London.

302. Clear, C. A., *Formwork Striking Times for Ground Granulated Blast Furnace Slage Concrete : Test and Site Results.* Proceedings of the ICE-Structures and Buildings, 1994. **104**(4): p. 441-448.

303. Luke, A., Konon, W., and Punurai, S., *Maturity method in prestressed concrete applications.* Submitted to New Jersey Department of Transportation, New Jersey Institute of Technology, 2004.

304. Association, American Concrete Pavement, *Maturity testing of concrete pavements: Applications and benefits.* Publication IS257P, 2002.

305. Humboldt. *Windsor Probe for Testing Concrete Compressive Strength, .* [cited 2012 September]; Available from: http://www.humboldtmfg.com/c-3-p-248-id-3.html.

306. Hansen, A.J., *Method and a device for measuring concrete maturity*, 1984, Google Patents.

307. Instruments, Germann. *COMA - Meter.* [cited 2012 September]; Available from: http://www.germann.org/Brochures/COMA-Meter.pdf.

308. Malhotra, V. M., *Evaluation of the Windsor probe test for estimating compressive strength of concrete.* Materials and Structures, 1974. **7**(1): p. 3-15.

309. Humboldt. *Windsor Probe for Testing Concrete Compressive Strength, Construction Materials Testing Equipment.* [cited 2012 Sepetember]; Available from: http://www.humboldtmfg.com/c-3-p-248-id-3.html.

310. Keiller, A. P., *A preliminary investigation of test methods for the assessment of strength of in situ concrete, Cement and Concrete Association*, 1982, Technical Report 511, London.

311. Di Maio, A., Giaccio, G., and Zerbino, R., *Break-Off Test for High-Strength Concrete.* Cement, Concrete and Aggregates, 1996. **18**(1).

312. Dilly, R.L and Vogt, W.L., *Pullout Test, Maturity, and PC Spreadsheet Software.* Nondestructive Testing, 1989: p. 193-218.

313. Poulsen, Claus Germann Petersen and Ervin, *Pull-out testing by Lock-test and CAPO-test*, 1993, Dansk Beton Institut A/S.

314. Petersen, Claus Germann, *Lok-Test and Capo-Test Pullout Testing Twenty Years Experience*, in *Non-Destructive Testing in Civil Engineering* 1997, The British Institute of Non-Destructive Testing: Liverpool.

315. Instruments, Germann. *NDT Systems.* [cited 2012 September]; Available from: http://www.germann.org/Brochures/Catalog-NDT-2010.pdf.

316. Soutsos, M. N, Bungey, J. H, Long, A. E, and Henderson, G. D, *In-situ strength assessment of concrete-The European concrete frame building project.* Insight-Wingston Then Northampton, 2000. **42**(7): p. 432-435.

317. BS EN 12504-2, *Testing concrete in structures, Part 2: Non-destructive testing — Determination of rebound number*, 2001, British Standard Institution: London.

318. ASTM C 805-97, *Standard Test Method for Rebound Number of Hardened Concrete; Annual Book of ASTM Standards, Vol 14.02*, 1997, ASTM International.

319. ACI Committee 228.1R-95, *In-Place Methods to Estimate Concrete Strength*, 1995: Farmington.

320. BS EN 12504-1, *Testing concrete in structures, Part 1: Cored specimens — Taking, examining and testing in compression*, 2009, Brtish Standard Institution: London.

321. BS EN 13791, *Assessment of in-situ compressive strength in structures and precast concrete components*, 2007, British Standard Institution: London.

322. Malhotra, V. M., *Role of supplementary cementing materials in reducing greenhouse gas emissions.* Concrete technology for a sustainable development in the 21st century, 2000: p. 226-235.

323. Penttala, V., *Concrete and sustainable development.* ACI materials journal, 1997. **94**(5): p. 409-416.

324. Meyer, C., *Concrete and sustainable development.* ACI SPECIAL PUBLICATIONS, 2002. **206**: p. 501-512.

325. Mehta, P. K. *Role of pozzolanic and cementious material in sustainable development of the concrete industry*. 1998.

326. Berry, E. E. and Malhotra, V. M. *Fly ash for use in concrete-A critical review*. 1980. ACI.

327. Papadakis, V. G. and Tsimas, S., *Supplementary cementing materials in concrete:: Part I: efficiency and design.* Cement and Concrete Research, 2002. **32**(10): p. 1525-1532.

328. ASTM C 595-03, *Standard Specification for Blended Hydraulic Cements*, 2003, ASTM International.

329. Antiohos, S., Maganari, K., and Tsimas, S., *Evaluation of blends of high and low calcium fly ashes for use as supplementary cementing materials.* Cement and Concrete Composites, 2005. **27**(3): p. 349-356.

330. Gosh, S. N., Sarkar, S. L., and Harsh, S., *Mineral admixtures in cement and concrete.* Advances in cement research, 1995. **7**(25): p. 43-46.

331. Malhotra, V. M. and Mehta, P. K., *Pozzolanic and cementitious materials*. Vol. 1. 1996: Taylor & Francis.

332. Safiuddin, M. and Zain, M. F. M., *Supplementary cementing materials for high performance concrete.* 2006.

333. Pandey, S. P. and Sharma, R. L., *The influence of mineral additives on the strength and porosity of OPC mortar.* Cement and Concrete Research, 2000. **30**(1): p. 19-23.

334. Khatri, R. P., Sirivivatnanon, V., and Gross, W., *Effect of different supplementary cementitious materials on mechanical properties of high performance concrete.* Cement and Concrete Research, 1995. **25**(1): p. 209-220.

335. Siddique, R., *Performance characteristics of high-volume Class F fly ash concrete.* Cement and Concrete Research, 2004. **34**(3): p. 487-493.

336. Turner Fairbank Highway Resarch Centre. Recycled Materials in the Highway Environment, User Guidelines for Waste and Byproduct Materials in Pavement Construction. *Fairbank Highway Resarch Centre, User Guidelines for Waste and By-product Materials in Pavement Construction*. 2007.

337. Bilodeau, A. and Malhotra, V. M., *High-volume fly ash system: concrete solution for sustainable development.* ACI materials journal, 2000. **97**(1).

338. Bilodeau, A., Sivasundaram, V., Painter, KE, and Malhotra, VM, *Durability of concrete incorporating high volumes of fly ash from sources in the USA.* ACI materials journal, 1994. **91**(1).

339. Bijen, J., *Benefits of slag and fly ash.* Construction and Building Materials, 1996. **10**(5): p. 309-314.

340. Zhang, M.H., Bilodeau, A., Malhotra, V.M., Kim, K.S., and Kim, J.C., *Concreteincorporating supplementary cementing materials: Effect of curing on compressive strength and resistance to chloride-ion penetration.* ACI materials journal, 1999. **96**(2).

341. ACI Committee 226.3R-87, *Use of Fly Ash in Concrete*, in *ACI materials journal* 1987: Farmington.

342. ASTM C 618-03, *Standard Specification for Coal Fly Ash and Raw or Calcined Natural Pozzolan for Use in Concrete*, 2003, ASTM International.

343. BS EN 450-1, *Fly ash for concrete - Part 1: Definition, specifications and conformity criteria*, 2012, Britih Standard Institution: London.

344. Newman, J. B. and Choo, B. S., *Advanced Concrete Technology, Volume 1: Constituent Materials* 2003: Elsevier Science & Technology.

345. Roy, D. M., *Hydration of blended cements containing slag, fly ash or silica fume.* Lecture presented to the Institute of Concrete technology, London, 1987.

346. Dhir, R. K., Munday, J. G. L., and Ong, L. T. *Investigations of the engineering properties of OPC/pulverised fuel ash concrete: strength development and maturity*. 1984.

347. Dhir, R. K., Hubbard, F. H., Munday, J. G. L., Jones, M. R., and Duerden, S. L., *Contribution of PFA to concrete workability and strength development.* Cement and Concrete Research, 1988. **18**(2): p. 277-289.

348. McCarthy, M. J. and Dhir, R. K., *Development of high volume fly ash cements for use in concrete construction.* Fuel, 2005. **84**(11): p. 1423-1432.

349. Ravina, D. and Mehta, P. K., *Properties of fresh concrete containing large amounts of fly ash.* Cement and Concrete Research, 1986. **16**(2): p. 227-238.

350. Sivasundaram, V., Carette, G. G., and Malhotra, V. M., *Properties of concrete incorporating low quantity of cement and high volumes of low calcium fly ash.* ACI Special Publication SP-114, 1989. **1**: p. 45-71.

351. Joshi, R. C. and Lohtia, R. P., *Fly ash in concrete: production, properties and uses* 1997: Taylor & Francis.

352. Naik, T. R. and Singh, S. S., *Influence of fly ash on setting and hardening characteristics of concrete systems.* ACI materials journal, 1997. **94**(5).

353. Ballim, Y. and Graham, P. C., *The effects of supplementary cementing materials in modifying the heat of hydration of concrete.* Materials and Structures, 2009. **42**(6): p. 803-811.

354. Jun-yuan, H., Scheetz, B. E., and Roy, D. M., *Hydration of fly ash-portland cements.* Cement and Concrete Research, 1984. **14**(4): p. 505-512.

355. Glasser, F. P., Diamond, S., and Roy, D. M. *Hydration reactions in cement pastes incorporating fly ash and other pozzolanic materials*. 1986. Cambridge Univ Press.

356. Joshi, R. C. *Sources of pozzolanic activity in fly ashes–A Critical Review*. 1979.

357. Joshi, R. C., *Experimental production of synthetic fly ash from kaolinite*, 1968, Iowa State University.

358. Chindaprasirt, P., Jaturapitakkul, C., and Sinsiri, T., *Effect of fly ash fineness on compressive strength and pore size of blended cement paste.* Cement and Concrete Composites, 2005. **27**(4): p. 425-428.

359. Ravina, D. *Efficient concrete utilization of coarse and fine fly ash in precast concrete by incorporating thermal curing*. 1981. ACI.

360. Mehta, P. K. *Concrete Technology*. 1994.

361. Swamy, R. N., Ali, S. A. R., and Theodorakopoulos, D. D. *Early strength fly ash concrete for structural applications*. 1983. ACI.

362. William, J. T. and Owens, P. L. *The implications of a selected grade of United Kingdom pulverized fuel ash on the engineering design and use in structural concrete*. 1982.

363. Haque, M. N. and Gopalan, M. K. *Temperature and humidity effect on the strength of plain and fly ash concrete*. 1987. Ice Virtual Library.

364. Dhir, R.K., *Pulverized fuel ash.* Cement Replacement Materials (Ed. RN Swamy), Survey University Pres, London, 1986.

365. Balendran, R. V. and Pang, H. W., *Strength development, deformation properties and mix design of pulverized fuel ash concrete.* Structural Survey, 1995. **13**(1): p. 7-11.

366. Sivasundaram, V., Carette, GG, and Malhotra, VM, *Long-term strength development of high-volume fly ash concrete.* Cement and Concrete Composites, 1990. **12**(4): p. 263-270.

367. Hansen, T. C., *Long-term strength of high fly ash concretes.* Cement and Concrete Research, 1990. **20**(2): p. 193-196.

368. Tikalsky, P. J. , Carrasquillo, P. M., and Carrasquillo, R. L., *Strength and durability considerations affecting mix proportioning of concrete containing fly ash.* ACI materials journal, 1988. **85**(6).

369. Bamforth, P. B. *In situ measurement of the effect of partial Portland cement replacement using either fly ash or ground granulated blast-furnace slag on the performance of mass concrete*. 1980. Ice Virtual Library.

370. Naik, T. R., Singh, S. S., and Hossain, M. M., *Permeability of concrete containing large amounts of fly ash.* Cement and Concrete Research, 1994. **24**(5): p. 913-922.

371. Thomas, M. D. A. and Matthews, J. D., *The permeability of fly ash concrete.* Materials and Structures, 1992. **25**(7): p. 388-396.

372. Shafiq, N., *Effects of fly ash on chloride migration in concrete and calculation of cover depth required against the corrosion of embedded steel reinforcement.* Structural concrete, 2004.

373. Society, Concrete, *The use of ggbs and pfa in concrete, Concrete Society Technical Report No. 40*, 1991, The Concrete Society.

374. ACI Committee 233, *Ground Granulated Blast-Furnace Slag as a Cementitious Constituent in Concrete.* ACI materials journal, 1995. **84**(4).

375. Kumar, R., Kumar, S., Badjena, S., and Mehrotra, SP, *Hydration of mechanically activated granulated blast furnace slag.* Metallurgical and Materials Transactions B, 2005. **36**(6): p. 873-883.

376. Kumar, S., Kumar, R., Bandopadhyay, A., Alex, TC, Ravi Kumar, B., Das, S.K., and Mehrotra, SP, *Mechanical activation of granulated blast furnace slag and its effect on the properties and structure of portland slag cement.* Cement and Concrete Composites, 2008. **30**(8): p. 679-685.

377. Slag Cement Association,. *Slag cement in concrete*. 2002 [cited 2012 September]; Available from: http://www.slagcement.org/News/pdf/No1_Slag_Cement.pdf.

378. Euroslag. *Granulated Blastfurnace Slag*. Technical Leaflet No. 1 2003 [cited 2012 September]; Available from: http://www.euroslag.com/fileadmin/_media/images/Research/FACT_SHEETS/LeafletGBS.pdf.

379. Higgins, D. *Portland cement replacement: within-mixer or factory-blend?* 2009 [cited 2012 September]; Available from: http://www.ukcsma.co.uk/files/mixervsfactory_concrete_may09.pdf.

380. ASTM C 989-04, *Standard Specification for Ground Granulated Blast-Furnace Slag for Use in Concrete*, 2004, ASTM International.

381. BS EN 15167–1, *Ground granulated blast furnace slag for use in concrete, mortar and grout —*, in *Part 1 : Definitions, specifications and conformity criteria,* 2006: London.

382. Virgalitte, S. J., Luther, M. D., Rose, J. H., Mather, B., Bell, L. W., Ehmke, B. A., Klieger, P., Roy, D. M., Call, B. M., and Hooton, R. D., *Ground granulated blast-furnace slag as a cementitious constituent in concrete.* 1995.

383. Taylor, H. F. W., *Cement chemistry* 1997: Thomas Telford Services Ltd.

384. Alizadeh, R., Beaudoin, J. J., and Raki, L., *Mechanical properties of calcium silicate hydrates.* Materials and Structures, 2011. **44**(1): p. 13-28.

385. Bullard, J.W., Jennings, H.M., Livingston, R.A., Nonat, A., Scherer, G.W., Schweitzer, J.S., Scrivener, K.L., and Thomas, J.J., *Mechanisms of cement hydration.* Cement and Concrete Research, 2011. **41**(12): p. 1208-1223.

386. Brunauer, S., Kantro, D. L., and Copeland, L. E., *The Stoichiometry of the Hydration of -Dicalcium Silicate and Tricalcium Silicate at Room Temperature.* Journal of the American Chemical Society, 1958. **80**(4): p. 761-767.

387. Maage, M. and Smeplass, S. *37 A practice-matrix model for prediction of workability of concrete*. 1996. Taylor & Francis.

388. ACI Committee 225, *Guide to the Selection and Use of Hydraulic Cements*. 2009. ACI.

389. PCA (Portland Cement Association), *Portland cement, concrete, and heat of hydration, Concrete Technology Today*, 1997. p. 1-8.

390. Alexander, K. M., *The relationship between strength and the composition and fineness of cement.* Cement and Concrete Research, 1972. **2**(6): p. 663-680.

391. ASTM C 150, *Standard Specification for Portland Cement*, in *in Annual Book of ASTM Standards, 2004, ASTM International* 2004, ASTM international.

392. Sandberg, P., Porteneuve, C., Serafin, F., Boomer, J., LoConte, N., Gupta, V., Dragovic, B., Doncaster, F., Alioto, L., and Vogt, T. *Effect of Admixture on Cement Hydration Kinetics by Synchrotron XRD and Isothermal Calorimetry*. 2007.

393. Peschard, A., Govin, A., Pourchez, J., Fredon, E., Bertrand, L., Maximilien, S., and Guilhot, B., *Effect of polysaccharides on the hydration of cement suspension.* Journal of the European Ceramic Society, 2006. **26**(8): p. 1439-1445.

394. Cheung, J., Jeknavorian, A., Roberts, L., and Silva, D., *Impact of admixtures on the hydration kinetics of Portland cement.* Cement and Concrete Research, 2011.

395. Ramachandran, V. S. and Feldman, R. F., *Effect of calcium lignosulfonate on tricalcium aluminate and its hydration products.* Materials and Structures, 1972. **5**(2): p. 67-76.

396. Massazza, F. and Costa, U. *Effect of superplasticizers on the C3A hydration*. 1980.

397. Dodson, V.H., *Concrete admixtures*. Vol. 115. 1990: Van Nostrand Reinhold New York.

398. Samarai, M., Popovics, S., and Malhotra, V. M., *Effect of high temperatures on the properties of fresh concrete.* Transportation Research Record, 1983(924).

399. Smolczyk, H.G., *The effect of chemistry of slag on the strength of blast furnace cements.* Zem-Kalk-Gips, 1978. **31**(6): p. 294-296.

400. Connell, M. D., *Ground Granulated Blast Furnace Slag (GGBS)*, in *Concrete Durability: A practical guide to the design of durable concrete structures*, Soutsos, M., Editor 2010, Thomas Telford Limited: London. p. 186-206.

401. Bakker, R. F. M. *Permeability of blended cement concretes*. 1983.

402. Cheron, M. and Lardinois, C. *The role of magnesia and alumina in the hydraulic properties of blast-furnace slag*. 1968.

403. Pal, S. C., Mukherjee, A., and Pathak, S. R., *Investigation of hydraulic activity of ground granulated blast furnace slag in concrete.* Cement and Concrete Research, 2003. **33**(9): p. 1481-1486.

404. Zhu, J., Zhong, Q., Chen, G., and Li, D., *Effect of particle size of blast furnace slag on properties of portland cement.* Procedia Engineering, 2012. **27**: p. 231-236.

405. Öner, M., Erdoğdu, K., and Günlü, A., *Effect of components fineness on strength of blast furnace slag cement.* Cement and Concrete Research, 2003. **33**(4): p. 463-469.

406. Zhou, J., Ye, G., and van Breugel, K. *Hydration of Portland cement blended with blast furnace slag at early stage*. 2006. RILEM Publications SARL.

407. Cyr, M., Lawrence, P., and Ringot, E., *Mineral admixtures in mortars: quantification of the physical effects of inert materials on short-term hydration.* Cement and Concrete Research, 2005. **35**(4): p. 719-730.

408. Wainwright, P. J and Ait-Aider, H., *The influence of cement source and slag additions on the bleeding of concrete.* Cement and Concrete Research, 1995. **25**(7): p. 1445-1456.

409. Wainwright, P. J. and Rey, N., *The influence of ground granulated blastfurnace slag (GGBS) additions and time delay on the bleeding of concrete.* Cement and Concrete Composites, 2000. **22**(4): p. 253-257.

410. Wood, K. *Twenty years of experience with slag cement*. 1981.

411. Fulton, F.S., *The Properties of Portland Cements Containing Milled Granulated Blast-furnace Slag* 1974: Portland Cement Institute.

412. Meusel, J. W. and Rose, J. H., *Production of granulated blast furnace slag at sparrows point, and the workability and strength potential of concrete incorporating the slag.* Fly Ash, Silica Fume, Slag & Other Mineral By-Products in Concrete, ACI Sp-79, 1983: p. 867-890.

413. ACI Committee 201.2R-08, *Guide to Durable Concrete*, 2008, American Concrete Institute: Farmington.

414. Osborne, G. J., *Durability of Portland blast-furnace slag cement concrete.* Cement and Concrete Composites, 1999. **21**(1): p. 11-21.

415. Song, H.W. and Saraswathy, V., *Studies on the corrosion resistance of reinforced steel in concrete with ground granulated blast-furnace slag—An overview.* Journal of hazardous materials, 2006. **138**(2): p. 226-233.

416. Pavia, S., *A comparative study of the moisture transfer properties and durability of PC and GGBS mortars.* 2007.

417. Jain, D. K., Prasad, J. and Ahuja, A. K., *Latest issues: Ground granulated blast furnace slag*, in *New Building Material & Construction World* 2007, NBM Media: India.

418. Kwon, Y., *A study on the alkali-aggregate reaction in high-strength concrete with particular respect to the ground granulated blast-furnace slag effect.* Cement and Concrete Research, 2005. **35**(7): p. 1305-1313.

419. Lee, S. T., *Effects of curing procedures on the strength and permeability of cementitious composites incorporating GGBFS.* Journal of ceramic processing research, 2008. **9**(4): p. 358-361.

420. Li, K. L., Huang, G. H., Lin, J., and Tang, X. S., *Durability of High-Volume GGBS Concrete.* Advanced Materials Research, 2011. **261**: p. 338-343.

421. Pavía, S. and Condren, E., *Study of the durability of opc versus ggbs Concrete on exposure to silage effluent.* Journal of Materials in Civil Engineering, 2008. **20**(4): p. 313-320.

422. Ramezanianpour, A. A. and Malhotra, V. M., *Effect of curing on the compressive strength, resistance to chloride-ion penetration and porosity of concretes incorporating slag, fly ash or silica fume.* Cement and Concrete Composites, 1995. **17**(2): p. 125-133.

423. Basheer, P. A. M., Gilleece, P. R. V., Long, A. E., and Mc Carter, W. J., *Monitoring electrical resistance of concretes containing alternative cementitious materials to assess their resistance to chloride penetration.* Cement and Concrete Composites, 2002. **24**(5): p. 437-449.

424. Ecocem. *Cementitous Reaction*. [cited 2012 September]; Available from: http://www.ecocem.ie/technical,ggbs,reaction.htm.

425. Lewis, D. W. *Blast-furnace slag as a mineral admixture for concrete*. 1982 [cited 2012 September]; Available from: http://www.concreteconstruction.net/images/Blast-Furnace%20Slag%20as%20a%20Mineral%20Admixture%20for%20Concrete_tcm45-340933.pdf.

426. Association, Slag Cement. *High volume substitution of Portland cement*. 2006 [cited 2012 September]; Available from: http://slagcement.org/pdf/no28%20Slag%20Cement%20and%20LEED.pdf.

427. Domone, P. L. and Illston, J. M., *Construction materials: their nature and behaviour* 2010: Spons Architecture Price Book.

428. Kett, I., *Engineered Concrete Mix Design and Test Methods* 2009: CRC.

429. Day, K., *Concrete mix design, quality control and specification* 2006: Routledge.

430. Illston, J. M. and Domone, P. L. J., *Construction materials: their nature and behaviour*. 2001.

431. Beshr, H., Almusallam, A A., and Maslehuddin, M., *Effect of coarse aggregate quality on the mechanical properties of high strength concrete.* Construction and Building Materials, 2003. **17**(2): p. 97-103.

APPENDIX - A

A. DETAIL LITERATURE REVIEW

A. 1. Concrete Tensile Strength

The tension strength of concrete is much lower than its compressive strength. The measurement of tensile strength of concrete can be carried out in three ways i.e. direct tension, splitting tension and flexural tests, which give different results[251, 252]. The indirect tension test, which is also called the splitting test or Brazilian test, is the simplest way to measure the tensile strength of concrete. The test is carried out to measure the tension strength of the concrete. The standard specimen for the splitting test is a cylinder with a size of 150 X 300 mm[253, 254]. The tensile strength, therefore, is calculated using the following equation:

$$f_t = \frac{2P}{\pi DL} \qquad \text{Equation A.1}$$

where: f_t = tensile splitting strength (MPa or N/mm^2)
P = maximum load (N)
D = diameter of cylinder (mm)
L = length of cylinder (mm)

Assuming that the tensile strength of the concrete is proportional to its compressive strength, it is important to establish a method of describing this relationship. In 1991, Oluokun et al[255] developed the relationship between concrete compressive strength and its splitting tensile strength. They found that that the 0.5 power of the compressive strength proposed by ACI 318-83 was not proportional to the splitting tensile strength. Therefore, they suggested using the 0.79 power, which is much more realistic. Specifically,

$$f_t = 0.584\,(f'_c)^{0.79} \qquad \text{Equation A.2}$$

where f'c is the compressive strength of concrete in unit of MPa or N/mm^2.

A. 2. Modulus of Elasticity of Concrete

The modulus of elasticity of concrete is essential parameters required in structural analysis for the determination of the strain distributions and displacements, especially when the design is based on elasticity considerations. Therefore, knowledge of the modulus of elasticity of concrete for the designer is very important in estimating the deformation of structural elements under service conditions in structural concrete.

The relation between the compressive strength and the modulus of elasticity of concrete can be mathematically expressed as[28, 256]:

$$E_c = 33\, w^{1.5}\, (f_c')^{0.5} \qquad \text{(in-lb units)} \qquad \text{Equation A.3}$$

or

$$E_c = 0.043\, w^{1.5}\, (f_c')^{0.5} \qquad \text{(SI units)} \qquad \text{Equation A.4}$$

where: E_c = modulus of elasticity of concrete (kip/in^2 or MPa)
w = unit weight of concrete (lb/ft^3 or kg/m^3)
f'_c = compressive strength of concrete (kip/in^2 of MPa)

Furthermore, the equation above can be simplified, when using normal weight concrete i.e. between 90 and 155 lb/ft^3 or between 1500 and 2500 kg/m^3, i.e.[28, 257]:

$$E_c = 57{,}000\, (f_c')^{0.5} \qquad \text{(in-lb units)} \qquad \text{Equation A.5}$$

$$E_c = 4700\, (f_c')^{0.5} \qquad \text{(SI units)} \qquad \text{Equation A.6}$$

A. 3. Factors Influencing Concrete Strength Development

Factors affecting the strength development of concrete are: cement type, aggregates, water-binder ratio, curing temperature, admixture and the use of cementitious as a part replacement of cement in concrete[258]. Even in 1958,

Klieger[259], pointed out that the mixing techniques such as adding materials in a different sequence can influence the concrete strength development.

A.3. 1. Cement type

The fineness and chemical composition of cement and binder greatly affect the strength of concrete with given mix proportion of the same water-binder ratio. Bentz et al[206, 260] carried out researches, which are related to the effect of cement type, fineness and Portland cement particle size distribution (PSD) on the strength development of concrete. They found that using the finer cement results in higher compressive strength than that of the coarser cement at all testing ages up to the age of 28-days, which have the same water-cement ratio of 0.5.

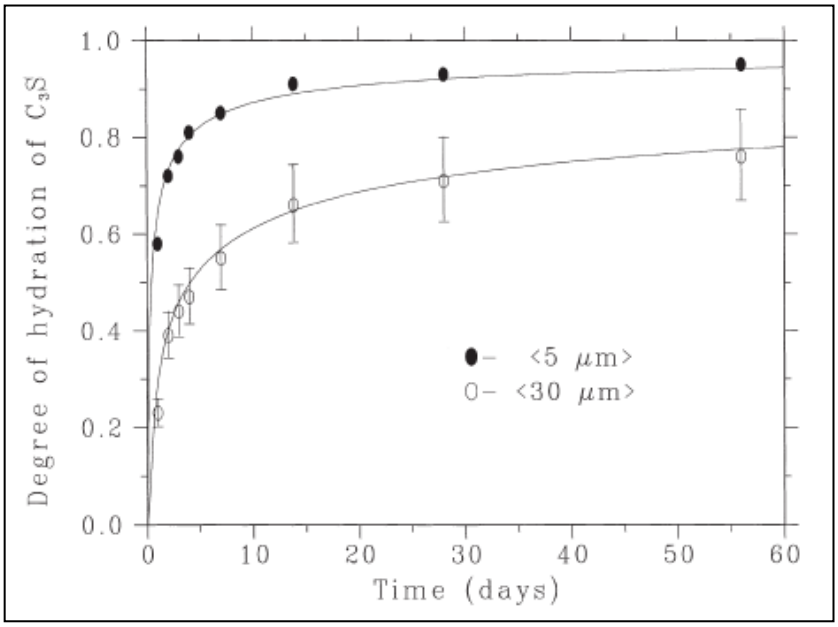

Figure A.1: Hydration of cement compound tricalcium silicate or alite (C_3S) with different size[206]

Figure A.1 shows the hydration of one of the main compound of cement i.e. tricalcium silicate with different fineness. It is clearly seen from the figure that for the same water-cement ratio, the finer grinding of the tricalcium silicate compound results in increased hydration at all ages investigated in the study.

Many researchers investigated the influence of the composition of the main chemical compound of cement that is used in the strength development of concrete. They highlighted that cements, which were containing a higher percentage of tricalcium silicate or alite (C_3S) gained strength much more rapidly at early age than that of cements with a higher percentage of declaim silicate or belite (C_2S). The difference in the strength gained however, is very small at later age[261, 262].

Furthermore, in 2011, Ashraf and Noor[263] investigated the influence of cement types and water-binder ratio on concrete properties such as the compressive strength of concrete. Using two different types of cement i.e. CEM I and CEM II/B-M that refer to BS EN 197-1 with five different water-binder ratios, they found that the compressive strength of both cements at the same age of 28-days were different even though they were the same water-binder ratio as shown in Figure A.2.

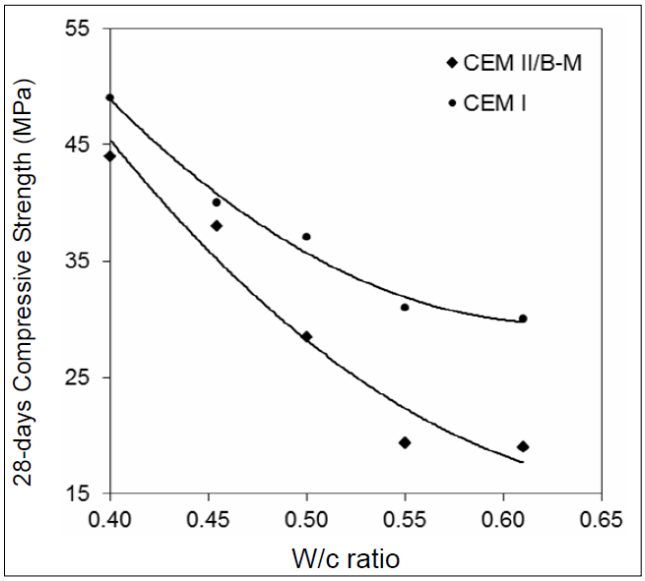

Figure A.2: Compressive strength of different cement type and water-binder ratio at the age of 28-days[263]

A.3. 2. Aggregate

The effect of aggregate on concrete strength is not commonly ignored due to an overemphasis of the influence of water-cement ratio to the strength development of concrete. It is true that the aggregate is not considered as a factor that affects the strength of normal concrete because the aggregate particle is usually stronger than the matrix and the interfacial transition in zone concrete, except lightweight aggregates[185, 264, 265].

However, there are other characteristics of aggregate than strength, such as the size, shape, surface texture, particle size distribution and mineralogy, which can affect concrete strength in varying degree. For example, for maximum size of coarse aggregate of a given mixtures with the same cement content and consistency, concrete mixtures containing larger aggregate particles need less mixing water than that of containing smaller aggregate. On the contrary, larger aggregates appear to form weaker interfacial transition zone containing more microcracks[185, 266].

The shape and texture of aggregate affects the properties of fresh concrete more than hardened concrete. The smooth and rounded aggregates produce concrete more workable than that of rough angular or elongated aggregates. Natural aggregates that are commonly taken from riverbeds or seashores are smooth and rounded, and a given mix will produce a better workability of concrete rather than the use of crushed stone aggregates. The crushed stone aggregates are more angular and elongated aggregates, which have a higher surface to volume ratio, therefore, need more cement paste to produce a workable concrete. However, the types of coarse aggregates have a better bond.

Furthermore, Yaqub and Bukhari[267] investigated the effect of size of coarse aggregate on compressive strength of high strength concrete. They found that the combination coarse aggregate of size 5mm and 10mm give optimum strength compare to other combinations, as shown in Figure A.3.

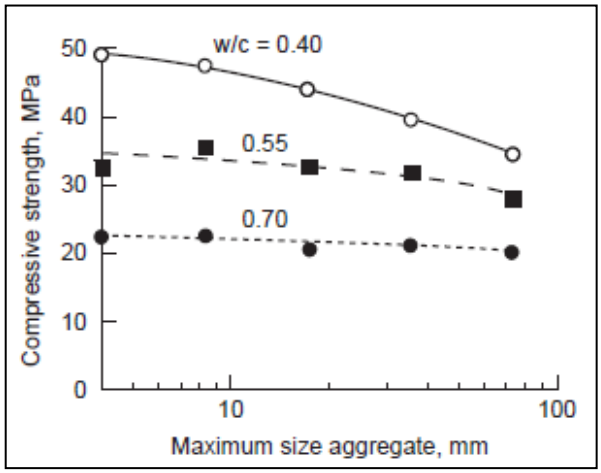

Figure A.3: Influence of the aggregate size and the water-cement ratio on concrete strength[185]

A.3. 3. Water-cement (binder) ratio

The water-binder ratio and the degree of compaction are primary factors that affect the strength of concrete, at a given age and cured in water at a prescribed temperature. Under full compaction, compressive strength is inversely proportional to water-cement ratio as shown in Figure A.4 and is given by the relationship developed by Duff Abrams (1919) as follow[12, 28]:

$$f_c = \frac{K_1}{K_2^{w/c}} \qquad \text{Equation A.7}$$

where: f_c = compressive strength (MPa)

K_1 and K_2 = empirical constant

w/c = water-cement ratio

An exception to the theory proposed by Abrams is the behaviour of strength at very low water-cement ratio as has been discussed by Mehta and Monteiro[185]. They state that, *"In low and medium-strength of concrete made with normal aggregate, both the transition zone porosity and the matrix porosity determine the strength, and direct relation between the water-cement ratio and the concrete strength"*. However, this appears no longer to be the case in high-strength concrete.

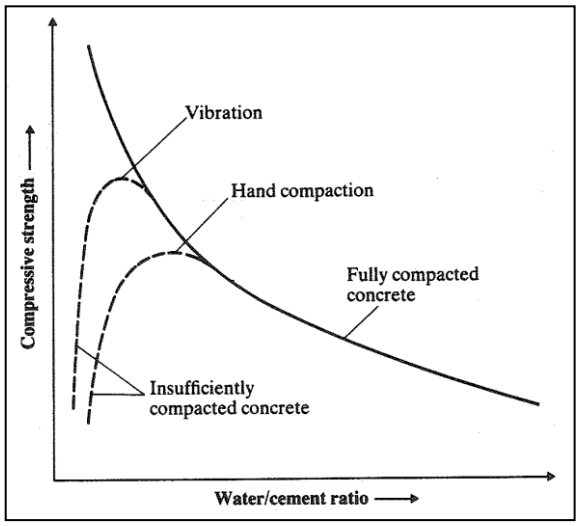

Figure A . 4: Relation between strength and water-cement ratio of concrete[28]

Goto and Roy[268] reported the effect of water-cement ratio and curing temperature on the permeability of concrete. They found that, at a constant curing temperature, the permeability values decrease exponentially with decreasing water-cement ratio. However, concrete that was cured at higher curing temperature had higher permeability.

In 2008 Popovics[269] stated that the fundamental assumptions that can clearly describe the relationship between strength and water-cement ratio are:

- ❖ The strength of structural concrete is controlled by the strength of the cement paste in it.
- ❖ The strength of a cement paste depends strongly on the porosity in it.
- ❖ The porosity (capillary) is a function of the water-cement ratio.

He proposed the relationships between porosity and paste composition mathematically written as[269-271]:

$$p = 0.01a + \frac{w/c}{w/c + 1/G} \qquad \text{Equation A.8}$$

where: p = total porosity in the fresh cement paste, 0.01% by volume.

a = air content, % by volume

w/c = water cement ratio by mass

G = specific gravity of the cement, 3.15

It is clear that concrete with the higher water-cement ratio has the higher porosity. He agreed with Abrams' formula, however, it should be improved by the augmentation of the earlier formula with a second independent variable, such as the cement content or water content or paste content, etc.

A.3. 4. Curing Temperature and Curing Time

The ACI 308R-01[272] identified term *'curing'* to describe the process by which hydraulic cement concrete matures and develops hardened properties over time as the continued hydration of cement in the presence of sufficient water and heat. The term is also used to describe the effort taken to maintain moisture and temperature conditions in a freshly placed cementitious mixture to allow hydraulic-cement hydration and, if applicable, pozzolanic reactions to occur so that the potential properties of the mixture may develop. Mehta and Monteiro[185] defined the term 'curing' of concrete as a combination of time, humidity and temperature conditions immediately after placing concrete into formwork.

In order to obtain good concrete, the placing of a given mix must be cured in a suitable environment during the early age stages of hardening. The British European standard[273] and the ASTM standard[274] required the procedure for making and curing concrete specimens test.

The purpose of curing is to protect concrete against[275]:

- premature drying out, particularly due to solar radiation and wind (plastic shrinkage)
- leaching out by rain and flowing water
- rapid cooling during the first few days after placement
- high internal thermal gradients

- ❖ low temperature or frost
- ❖ vibration and impact

Many researchers studied the effect of curing method and final moisture condition on compressive strength of concrete. They concluded that the compressive strength of concrete is greatly affected by moisture content of hardened concrete. Although the changes in the overall moisture content are relatively small, the effect on the compressive strength of concrete, results in considerable changes[271, 276, 277].

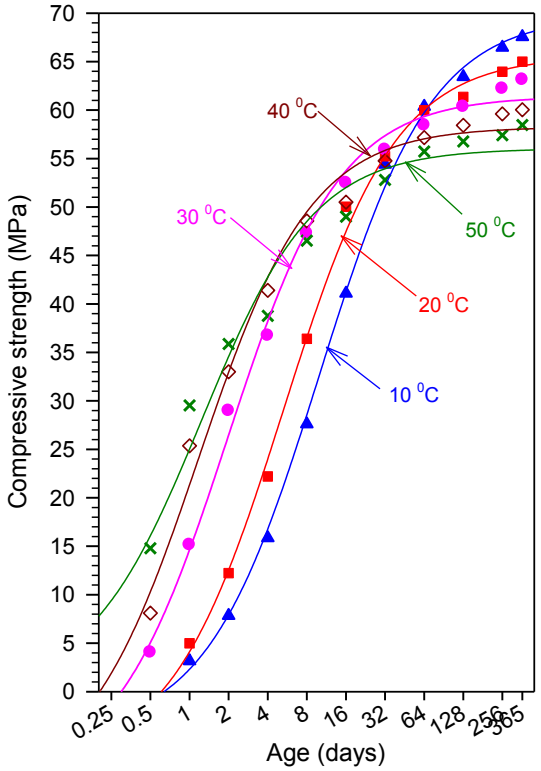

Figure A .5: Relation between compressive strength and curing timeat different curing temperature[278]

At an early age, the strength development of concrete is higher at higher curing temperature as the rate of reaction is greater. The strength development of concrete, however, is lower at later age. Conversely, the strength development of concrete cured at lower curing temperature at early age is lower, but it is higher at later ages [40, 125, 276, 279-281], which is called *"crossover effect"*, as is presented in

Figure A.5. This is due to the creation of dense hydrated phases around the unreacted cement particles avoiding water to reach the unhydrated cement grain for further hydration. The reaction products not having time to become uniformly distributed within the pores of the hardening paste. The larger pores in microstructure could be the result of the non-uniform distribution of hydration products[5, 40, 120, 282-284].

The temperatures of casting and curing of concrete highly affect the development of concrete strength with time. Starting from the early 1930's, many researchers have investigated the effect of temperature on the strength development of concrete.

In 1934, Davis et al[285] concluded that low initial curing temperatures resulted in higher ultimate strength. However, higher curing temperatures normally have a detrimental effect on concrete at later ages, as discussed before. At low curing temperatures, the rate of reaction is slower, which means the concrete needs to be cured for a longer period to attain the required degree of reaction. The fast rate of reaction at high temperature gives relatively high early strengths but the long-term strength and durability are usually reduced[272, 275, 276].

Moranville[286] and Rostasy et al[287], observed the changes in microstructure of cement pastes, which is due to elevated curing temperature. They found that the elevated curing temperature affect the stability of hydration products, such as changes in porosity, bound water and ionic pore solutions. Furthermore, they added that the higher curing temperature caused a delayed formation of ettringite in pre-existing micro cracks and the aggregate interface in the paste, where voids were presumed to effect from thermally induced drying shrinkage or mechanical stresses.

Neville and Brooks[28, 275] suggested the optimum temperature of curing, which is needed to obtain the maximum 28-day strength for small laboratory specimens, is

approximately 13^0C; while the ambient temperatures that ranged from 15-25^0C to be most suitable for concreting work.

At curing temperatures down to as low as –10°C, the hydration of cement will occur to some degree. Even so, little strength will develop below 0°C, and below 5°C, the early strength development is significantly retarded. Even in the range of temperature 5–10°C are poor curing conditions for the development of early strength. These effects mostly happen in thin sections, in the surface area of larger sections, and in concrete with lower rate of hydration cements. The strength of bigger sections will not be affected much as the internal temperature will be elevated by the heat produced in hydration process[272, 275, 288].

Factors affecting the temperature rise in concrete during curing are[275]:

- the dimensions of the element
- the weather (ambient conditions)
- cement type
- cement content
- admixtures (accelerators, retarders)
- the fresh concrete temperature
- formwork type/insulation formwork stripping time

Some recommendations about the relationships between strength and age were suggested. The ACI committee 209 recommends the relationship between strength-time for Portland cement at moisture curing condition as follow[133, 289]:

$$f_{cm}(t) = f_{c,28}\left(\frac{t}{4+0.85t}\right) \qquad \text{Equation A.9}$$

where: $f_{cm}(t)$ = mean compressive strength at age t (days)

$f_{c,28}$ = compressive strength at age 28-days

t = age of concrete (days)

Comite Euro-International du Beton expressed the relation between the strength and age of concrete, which is cured at 20^0C[290]:

$$f_{cm}(t) = f_{cm}\ exp\left(s\left(1 - \sqrt{\frac{28}{(\frac{t}{t_1})}}\right)\right) \qquad \text{Equation A.10}$$

where: $f_{cm}(t)$ = mean compressive strength at age t (days)

f_{cm} = mean compressive strength at age of 28 days

s = coefficient depending on the cement type

s = 0.20 for higher early strength cements, Type 42.5R and 52.5

s = 0.25 for normal hardening cements, Type 32.5R and 42.5

s = 0.38 for slow hardening cements, Type 32.5

t_1 = 1 day

A.3. 5. Admixture

The effects of admixtures on the strength development of concrete depend on the type of admixtures added to the concrete mixture, which is possible to change some of the properties of concrete of the more commonly used cements.

Chemical admixture is added into mortar/concrete mixture to achieve the desired properties of fresh concrete such as workability, delay or accelerate setting time of the mortar/concrete, reducing used water, etc. The chemical admixtures are classified based on their function in concrete as following[9, 291]:

- Type A for water-reducing
- Type B for retarding
- Type C for acceleration
- Type D for water-reducing and retarding
- Type E for water-reducing and accelerating
- Type F for high range water-reducing or superplasticizing, and
- Type G for high water reducing and retarding or superplasticizing and retarding.

The British Standard[292] for admixtures, classified them more specifically based on their functions, and combined them to have a multi function. There are eight types of single function and the other three types are multi functions. The presence of chemical admixtures in mortars/concretes affects the heat generation in hydration process of the mortars/concrete. The effect of admixture on the hydration of cement depends on the type of the admixture that is used in the mortar/concrete mix.

Water reducers are defined as admixtures that enable to decrease the required amount of water to achieve a required workability. These types of admixtures are used in mortars/concretes for three purposes as following[9, 12, 28, 29, 293, 294]:

- To enhance strength and durability of concrete by reducing the water-cement ratio at the same workability as the mortar/concrete without admixture.
- To achieve the same workability by decreasing the cement content to reduce the heat of hydration in mass concrete.
- To increase workability or to make the concrete flowable, the water-cement ratio is held constant.

Both ASTM standard and British standard classify this admixture type into two categories: normal and high range water reducing. The normal water reducers are called plasticizers, while the high-range water reducers are called superplasticizers[29, 291-296]. The normal water reducers can reduce the required water by 5-10%, while the high-range water reducers can reduce the required water more by15-40%[29].

The admixture can also be used to control the setting time of mortar/concrete, either to extend or to shorten the plastic stage of concrete to meet the requirement of the construction of the concrete structures. The admixture is called an accelerator, when it is used to shorten the plastic period, and is called a retarder, when it is used to extend the plastic period of the mortars/concretes[29, 291, 292].

The retarding admixtures can be used to delay the setting time of mortars/concretes due to the high ambient temperature, particularly in hot weather. It is also used as setting control of large structural element units, to keep the concrete workable during placing the concrete throughout the structural element and as well as keeping the workability of concrete during transportation from concrete plant to the construction site.

On the other hand, the accelerator admixtures are needed when concrete is to be placed at low temperatures, in the production of precast concrete, a busy infrastructure repairing such as a road pavement construction, where a rapid removal formwork is desirable or needs early finishing; allowing accesses the road.

A.3. 6. The Use of Supplementary Materials

Barnett et al[40, 297] and Soutsos et al[1, 279] investigated the strength development of concrete containing GGBS with various levels of cement replacement. They reported that the strength development of GGBS mortar is highly dependent on temperature, particularly at the early age. Therefore, the strength development of GGBS concrete cured under the standard curing temperature (20^0C) is lower than that of equal-grade concrete with Portland cement only. The higher cement replacement levels the lower the strength at early age. This is due to the reaction of GGBS is much slower than that of Portland cement. However, they found that at elevated curing temperatures, the strength development of GGBS concrete could be as high as that of PC concrete.

Similar to GGBS concrete, Eren[298] reported that at early ages, the strength development of FA concrete is much slower than that of concrete with Portland cement only cured at the standard curing temperatures. The higher cement replacement level with FA the lower the strength development obtained at early age.

In addition, Jackson and Dhir[299] summarised factors that affect the strength of concrete as shown in Figure A.6. As can be seen in the diagram, the primary factors influence the strength of concrete in general are constituent materials, methods of preparation, curing, and testing conditions.

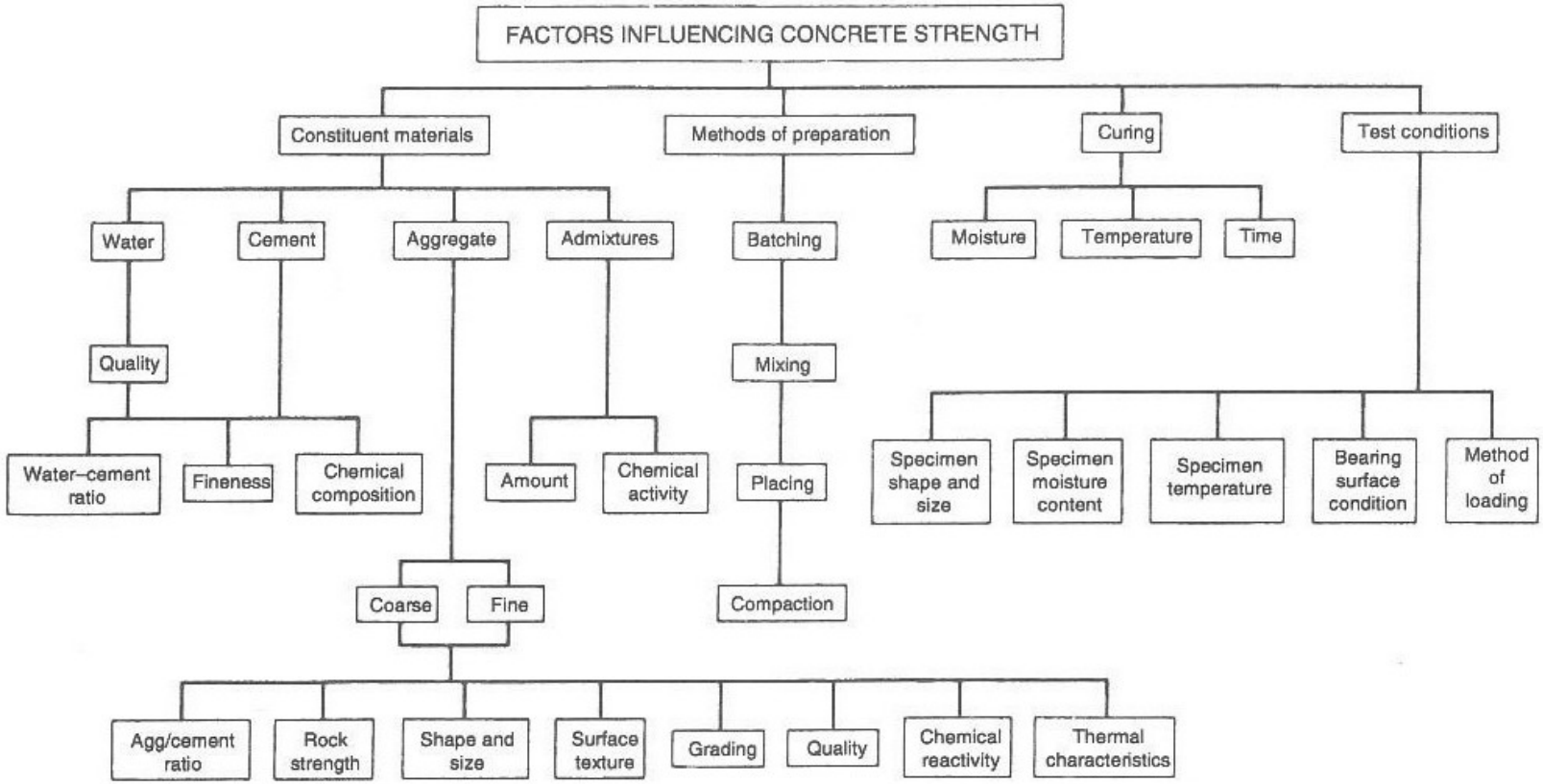

Figure A .6: Factors affecting strength of concrete[299]

A. 4. Methods of Assessment of the Concrete Strength Development

The strength development of concrete achieved in structural elements will be different from the strength of specimens that cured under standard curing condition, even though they are the same mixture for the following reasons[275]:

- differences in maturity
- differences in compaction and curing
- water and cement migration within the cast element

The large size of the structural element will have significant temperature gradients across the section and the temperature history and maturity will vary in the each point of structural element. The lack of water for hydration on the upper surface zone of structural element makes it weaker than the bottom surface zone. Even in suspended slabs, there will be significant differences. For example, the measurement strength by using the pullout test on the upper surface and the bottom surface of the structural element can be different by about 10 percent. For structural elements that getting heat from outside, the lowest maturity and strength will be at the points of around upper surface.

The differences between the strength of concrete specimens cured under standard curing conditions and that of in-situ strength obtained even though they are the same mix make it difficult to decide whether the quality of concrete supplied to the site was of the required quality. Therefore, it is necessary to determine whether the structural element is adequately strong enough to withstand the intended loading, and allowing the contractor to remove the formwork. The methods listed below are some of the most popular and widely used methods of estimating the early-age concrete strength development during construction for formwork striking purposes[275]:

- cured specimens alongside the structure
- tables of formwork striking times
- temperature matching curing bath

- maturity
- penetration tests
- break-off tests
- pull-out tests
- rebound-hammer test
- coring test

The first two methods are frequently used in the UK for formwork striking time, but they have their strengths and weakness[275]. The British Cement Association suggested using the LOK-test for the assessment of formwork striking times because of the benefits it gives to process efficiency.

A.4.1. Cured Specimens Alongside the Structural Element

The cube specimens are typically cast from fresh concrete alongside the structural elements being cast. The cubes were covered with plastic sheeting or similar material to prevent premature drying, which is also done on the structural element as well. The temperature rise in concrete is also affected by the size and the surrounding environment such as ambient temperature, relative humidity, wind velocity, and solar radiation. Therefore, the cubes were expected to underestimate the structural element concrete strength as the cubes have a tendency to follow the ambient temperature rather than the temperature rise in the structural element. As the result, the maturity of cube specimens is lower than that of structural element. Finally, the cube specimens do not estimate the strength of a structural element accurately[12, 275].

This overview, however, may not be true, depending on the size of the structural element. With thin section, this method is reasonable and safe for estimating in-situ strength of concrete. Nevertheless, with large sections, or well-insulated sections, this method can result in significantly underestimating the in-situ concrete strength.

A.4.2. Tables of Formwork Striking Times

For a given set of conditions and a known strength/maturity relationship, it is possible to produce tables of when the concrete should achieve a certain strength[275]. CIRIA Report 136[3] described this method in detail. In this method, tables are developed based on the assumption that the concrete achieves its characteristic strength at 28-days. The tables are applicable to concretes that satisfy the rates of strength development that is determined in CIRIA Report 136[3]. The equation proposed by Sadgrove[300] for maturity is realistic enough to be used.

CIRIA Report 136 tables are conservative as they are based on the lowest probable rate of strength development for a Portland cement and the assumption that the concrete only attains the specified characteristic strength. The rate of strength development at 20^{o}C has been given in the report to allow the tables to be applied to other concretes that gain these rates of strength development[3, 275].

A.4.3. Temperature Match Curing (TMC) of Concrete Specimens

This method is described in British Standard[301] and ASTM, which appears to overcome the limitation of the method of concrete specimens cured alongside structures. The concrete specimens are cast from samples of concrete and stored immediately in a water bath as shown in Figure 2.8. This equipment consist of a temperature sensor that is placed in the freshly cast element, a water-filled tank with stirrer, heater and temperature sensor and a control system. When it detects a difference in temperature between the sensor in the cast element concrete and the water tank, it will heat the water to make the temperatures of them both the same. By using this tool, any cubes kept in the tank will have the same maturity to the point in the cast element, where the sensor is placed.

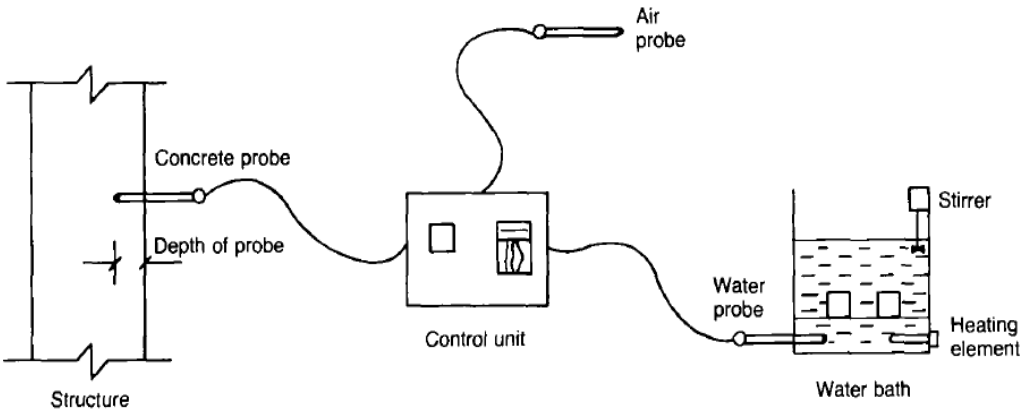

Figure A .7: Temperature matched curing (TMC) equipment[302]

A.4.4. Maturity Methods

The term *'maturity or maturity index'* can be defined as a *'temperature-time factor'* that describes the combined effect of temperature and time on the development of concrete strength. The method developed is based on the principle that concretes cast from the same mix that have equal maturity will have equal strength regardless of their actual temperature-time history. This section presents a brief discussion of the maturity method and its application to predict the strength of in-situ concrete. A more detailed discussion of this method is presented in Section 2.4.

The maturity method is one of the most reliable methods of assessing early-age in-situ concrete strength, particularly for fast-track construction applications. Many methods have been proposed to determine the maturity of concrete empirically[119, 121, 142, 275]. In recent years, however, many methods have been developed based on the concept of activation energy and the Arrhenius law on the rate of reaction[275]. This method has a wide variety of applications in the precast concrete industry that include the assessment of strength of prestressed heat accelerated concrete elements. Luke et al[303] verified the efficiency of the

maturity method in determining the time needed for the concrete to achieve adequate strength to permit the release of the pre-stressing force.
The in-situ concrete maturity can be determined using one of the following procedures:

1. Analysing in-situ temperature recordings using maturity functions.
2. Using electronic maturity meters
3. Using a commercial maturity probe, which is based on the evaporation of a volatile liquid

The maturity index is determined from the temperature history of concrete by a maturity function; such as the Nurse-Saul[103, 104] or the Arrhenius formulation proposed by Freiesleben Hansen and Pedersen[121]. Once the maturity index or the equivalent age at a reference temperature, is determined the strength development of concrete cured at other than reference or standard curing temperature can be determined as well.

The index maturity of concrete at standard curing temperature; can then be used to determine the strength of concrete using the strength-maturity correlations of concrete cured at standard temperature. The strength-maturity correlations is developed by statistically analysing the strength data of cubes, which are cast from the same mix and cured isothermally at the reference temperature. The maturity testing procedure is described in Figure A.8.

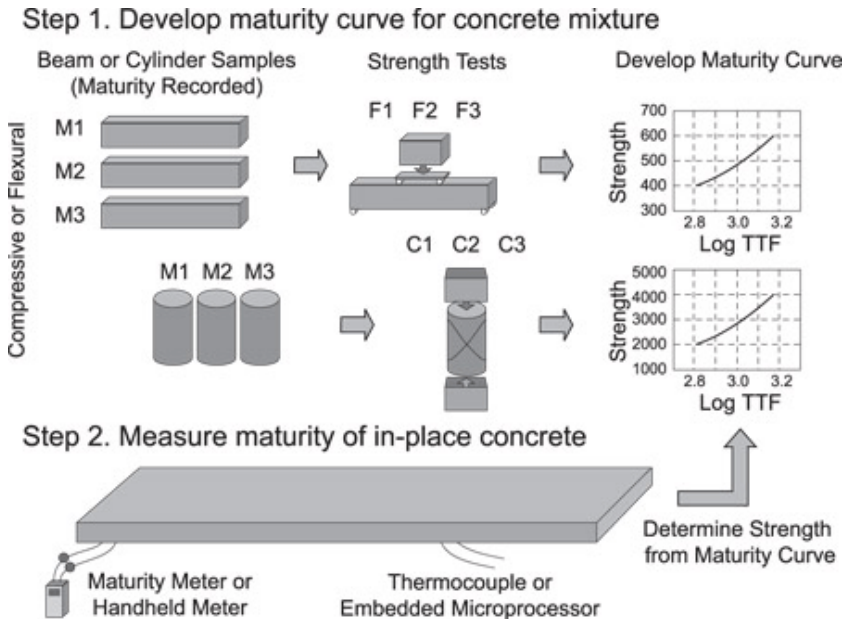

Figure A .8: Maturity testing procedure[304]

The maturity meter can directly measure the maturity of concrete by analysing the recorded temperature obtained from a temperature-sensing probe or thermocouples. One of the ends of the thermocouple is connected to the maturity meter, while the other one is embedded in the structural element while the concrete is still fresh. The strength of concrete cubes is calculated using the maturity obtained from maturity meter[3].

Multichannel maturity computers have been developed, which use thermocouple wires as sensors to calculate the maturity of concrete automatically. The equipment allows either the Nurse-Saul function or the Arrhenius equation to calculate the maturity of concrete. These multichannel meters, as shown in Figure A.9, allow each channel to separately record the temperature as the corresponding thermocouple embedded in fresh concrete[101].

Figure A .9: Multichannel maturity meter[101, 305]

The equipment provides a predictable strength determination of in-situ concrete based on ASTM standard[6]. It uses inexpensive, disposable, T-type thermocouple wire with quick-connect jacks, which can be embedded directly into a concrete structure to measure temperature at timed intervals.

These reading can then be used to document the maturity process within the structure in order to[305]:

- predict the time for form and shoring removal
- estimate loading and post-tensioning time
- control winter heating/insulation requirements
- reduce construction time and costs through accurate maturity readings.

The maturity meter is quite expensive; therefore, engineers may opt for a cheaper one and more simple. Hansen[306] developed mini maturity meter called COMA meter, which is disposalable equipment as shown in Figure A.10. The equipment was developed based on the principle that the rate constant of evaporation of the fluid from the capillary due to varying of temperatures follows the Arrhenius equation, which is the same function used to determine maturity of concrete from the temperature history. The mini meter maturity includes a fluid, which is

accounted to have activation energy of 40 kJ/mol. The capillary tube of the mini-maturity meter is attached to a card that is noticeable in units of equivalent age at 20°C. This equipment is activated by taking away the cap and breaking the capillary at the zero days mark. The cap is then replaced on the plastic container and it is then inserted into the fresh concrete. The temperature inside the container will quickly stabilize with the temperature of the surrounding concrete. The liquid in the capillary tube evaporates at a rate determined by the temperature and time. The level of the liquid, readable on the scale, measures the maturity of the concrete stated in M_{20} units, which is the number of equivalent days of curing at 20ºC[101, 307].

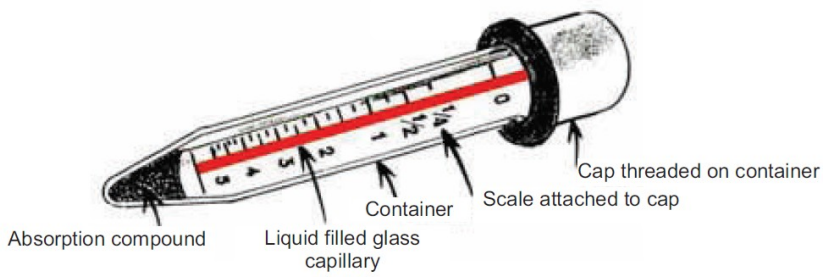

Figure A .10: COMA maturity meter[307]

A.4.5. Penetration Tests

The most popular and widely used penetration test is the Windsor Probe test. There are at least three hardened steel probes fired into the concrete under strength development investigation as presented in Figure A.11. To make the measurement easy, all the probes have the same length and the length of probe projecting from the concrete is measured and thereby the depth of penetration. The depth it penetrates into the concrete is correlated to the concrete strength. The benefits of the testing are simple to operate, rugged and low cost maintenance except for cleaning of the gun barrel. The correlation between the results of the test and concrete strength is affected by a relatively less number of variables[275]. The Probe test, however, has limitations that should be fulfilled, such as minimum size

requirements for the concrete member to be tested. The minimum distance required from a test location to any edges of the concrete member or between two given test location are 150 and 200 mm respectively[101, 308].

Figure A .11: Windsor Probe test apparatus[309]

A.4.6. Break-Off Tests

The Break-off test is developed based on breaking off a cylindrical specimen of in-situ concrete with size of 55 and 70 mm for diameter and height respectively. The specimens are made in the concrete by means of a disposable tubular plastic sleeve that is cast into the fresh concrete, which is then removed prior to test or by drilling the hardened concrete at the time just before testing[101]. A hydraulic ram is used to apply hydraulic pressure and eventually break the cylinders. This break-off force has correlation to the strength of cubes. Keiller[3, 310] reported that the 90% confidence limits for a range of mature concrete is about 8 N/mm2. Di Maio et al[311] convinced that the break-off test could give results reasonable well to assess the in-situ strength of concrete with strength grade up to 100 MPa. The procedure of break-off test is shown in Figure A.12.

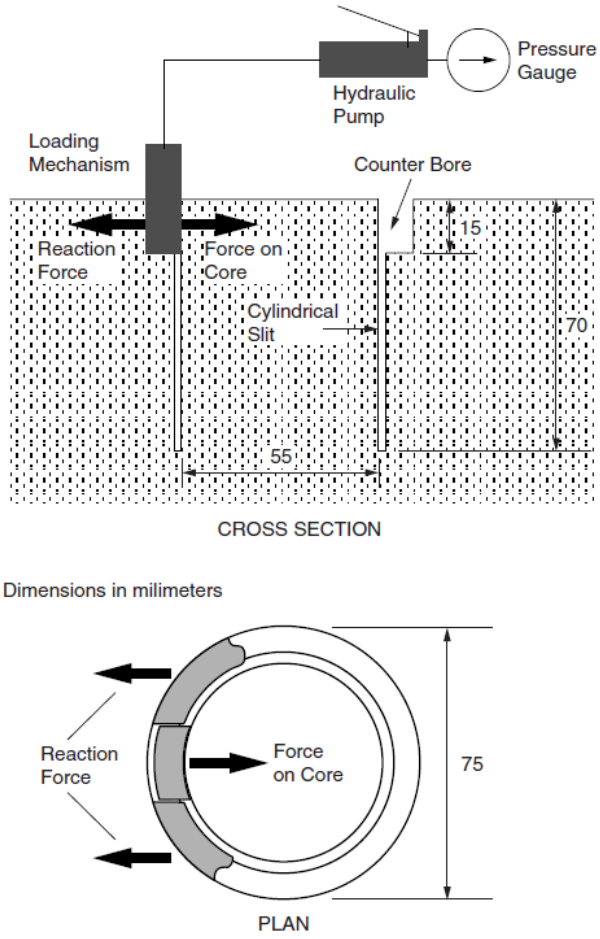

Figure A .12: Break-off test apparatus[101]

A.4.7. Pull-Out Test

The pullout test measures the force needed to pull an embedded metal with a large heat inserted in a concrete specimen or a structure. The equipment developed based on the concept that the force required to pullout the embedded metal in concrete, is directly correlated to the compressive strength of concrete[101]. The most widely used pullout test is the LOK test, which was designed and introduced in 1962 by Peter Kierkegaard-Hansen in Denmark. Pullout testing is an effective method to determine the in-place strength. Furthermore, it can be used to

determine the variability in concrete strength, especially in vertical elements and easily to perform[312-314].

For this test, a 25mm diameter of steel disk is cast at a depth 25mm below the concrete surface as presented in Figure A.13. The pullout force at which concrete rapture occurs is measured and the compressive strength of concrete is approximated by relating this result to a calibration graph. The actual time needed to perform each LOK test is equal or less than 2 minutes[314].

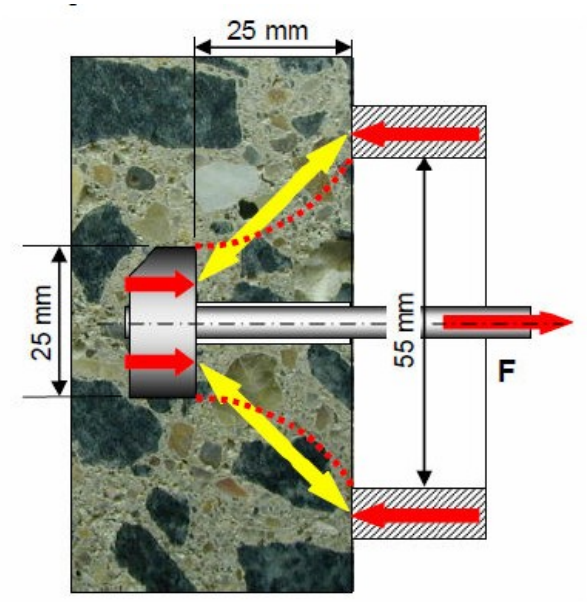

Figure A .13: Pullout test[315]

Generally, engineers convert LOK test results into concrete strength using a linear strength correlation, which is provided by the manufacturer of LOK test apparatus. Soutsos et al[316], however, found that the pullout test appeared less sensitive to changes in compressive strength at high levels. Furthermore, they concluded that for concrete with strength over than 50 MPa might require a non-linear strength relationship. In addition, Soutsos et al also reported that even though a progress has been found in assessing the in-place strength, there is still no agreement regarding the statistical procedure that should be followed to change it into characteristic strength.

A.4.8. Rebound-Hammer

This test is also known Schmidt hammer test, impact hammer or sclera meter test, which is one of non-destructive testing of concrete as shown in Figure A.14[28]. The procedure to perform the test is described in the British standard[317] and ASTM standard[318]. The test is based on the principle that the rebound of an elastic mass depends on the hardness of surface against which the mass imposes. It is a practical test for measure the uniformity strength of an element and it is easy to select points for more detailed investigation. The results can be used to estimate the strength of concrete when it is calibrated to the concrete being tested[275]. In ACI 228 (1995)[319], it is concluded that although the rebound number test is simple to perform, there are many factors other than concrete strength, however, which influence the test results. As a result, estimated strengths are not as reliable as those are obtained from other in-place test methods have been discussed earlier.

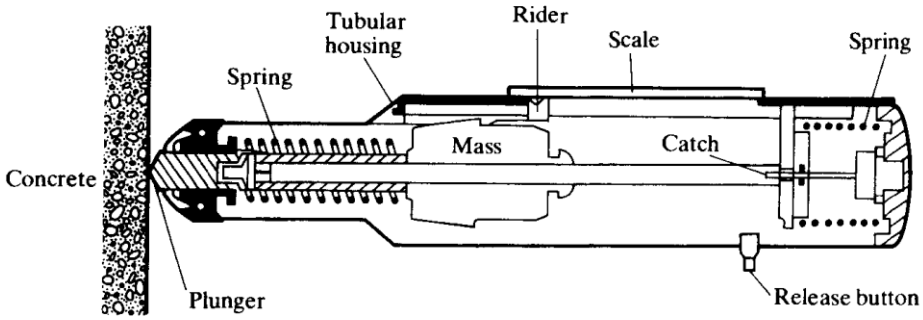

Figure A .14: Rebound hammer test[28]

A.4.9. Coring

Coring is a direct assess of the in-place strength. Cores extracted from hardened concrete using a core drill are carefully examined, prepared by grinding or capping and tested in compression using standard procedures. The test is rarely used for determining the rate of strength gain. However, it is frequently used to

assess the in-place strength of hardened concrete. The procedure to perform the test is described in the British European standard[320, 321].

A. 5. Supplementary Cementing Materials (SCMs) and Sustainability

A.5.1. Introduction

The environmental concern will play a most important role in the sustainable development of the cement and concrete industry in the 21st century. The World Earth Summits in Rio de Janeiro, Brazil (1992) and in Kyoto, Japan (1997) have made it very clear that uncontrolled increase in the emission of the greenhouse gases to the atmosphere is environmentally and socially no longer allowable for the overall sustainable development. The CO_2 emission is the primary greenhouse gas emission that was discussed in the conferences. The process of cement productions significantly contributes to the amount of the emission gas. Therefore, the use of large volume of supplementary cementing materials such as fly ash (FA) and ground granulated blast furnace slag (GGBS) in the construction industry can play an important role in solving the problem[322].

A suitable development supports the use of energy and natural resources in means that confirms long-term survival of human life. This survival is intimidated by consuming energy and raw material resources and unacceptable levels of ecological pollution from solid, liquid and gaseous waste products[323, 324]. The sustainable development of the cement and construction industries can be achieved by maximizing of the use of cementitious and pozzolanic by-products[325-327]. The reasons to use supplementary cementing materials to replace part of cement in concrete are the lack of cement, the high amounts of energy used to manufacture cement, and the need to conserve the natural resources that are needed to produce cement.

A pozzolana is a natural or artificial material containing silica in a reactive form. By themselves, pozzolana has little or no cementitious value. However, in a finely

divided form and in the presence of moisture they will chemically react with calcium hydroxide to form cementing compounds[328]. Pozzolanas must be finely divided in order to expose a large surface area to the alkali solutions for the reaction to proceed. Thus, a pozzolanic material requires $Ca(OH)_2$ in order to form strength products, whereas a cementitious material itself contains quantities of CaO and can exhibit a self-cementitious (hydraulic) activity.

Many waste materials are by-products of industry such as siliceous and aluminous materials (fly ash, silica fume, slag, etc.). The others are natural pozzolanic materials such as volcanic tuffs, diatomaceous earth, etc. All the materials have the similar properties of cementitious and/or pozzolanic materials. The materials, therefore, are categorized as supplementary cementing materials (SCM)[327]. The use of these materials not only gives economic and ecological benefits, but also imparts technological improvements to the final product[325, 329-331].

The use of supplementary cementing materials in concrete improves the properties for both fresh and hardened state, such as workability, strength and durability of the concrete[20-22, 25, 332-334]. It can reduce the porosity and refinement of microstructure in concrete. Therefore, it enables a decrease in the ingress of water and other harmful salt solutions that can deteriorate the concrete. Strength improvements due to the added minerals, results in an increase of calcium silicate hydrate (C-S-H) gel, which is the main component of concrete strength development. The C-S-H gel is produced in the pozzolanic reaction of the supplementary cementing materials; following the pozzolanic reaction of cement.

A.5.2. Pulverised Fuel Ash (FA)

A.5.2.1. Introduction

FA is produced from burning pulverized coal in electric power generating plants. During the combustion process, mineral impurities in the coal (clay, feldspar, quartz, and shale) fuse in suspension and float out of the combustion chamber along with exhaust gases. As the fused material rises, it cools and solidifies into

spherical glassy particles called FA. FA has been widely used as a partial replacement of cement in concrete for over half a century[33, 34, 335]. Figure A.15 shows a schematic diagram describing the FA production process.

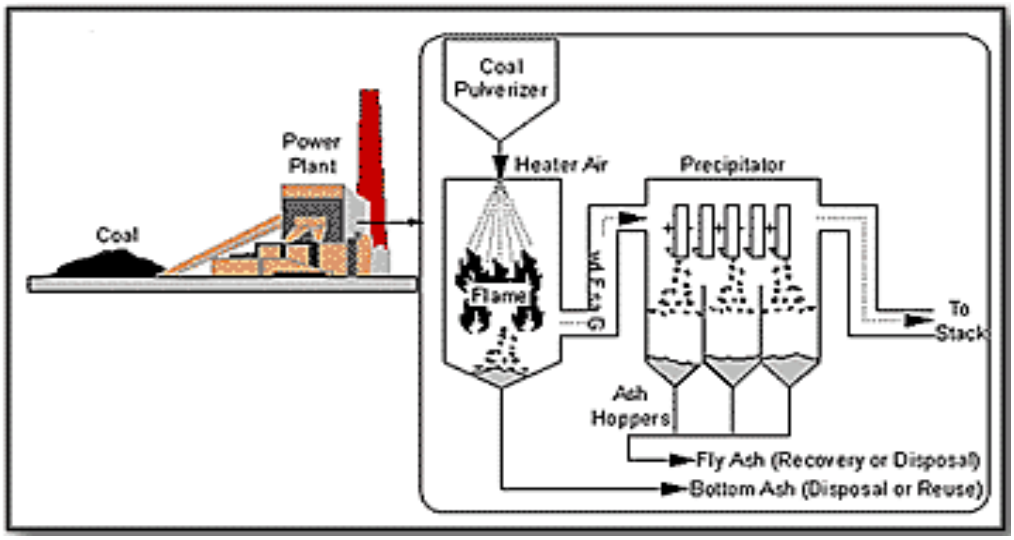

Figure A .15: Schematic diagram of production of FA in a dry-bottom utility boiler with electrostatic precipitator[336]

Besides the economic benefits as FA is a waste material, the FA also gives benefits of three different aspects. First, for sustainable development, the use of FA can save cement or natural resources in making the concrete. Another aspect is ecology, where the use of FA reduces the land use for disposal and avoids harmful impurities in the material to environment. Finally, the using of FA can lower the heat of hydration in mass concrete, as well as increase the performance of concrete in fresh and hardened state, such as increased workability, strength and durability of concrete for technical benefits[337-340].

FA is an amorphous glassy material that is mainly composed of silica, alumina and iron oxides. The largest fraction of FA, 60 – 90% of the total mass, consists of glassy spheres, solid or hollow. The rest of the FA is made out of crystalline phases. The interdependency between the amorphous and crystalline phases makes FA a complex material to classify. The chemical composition of UK FA presented in Table A.1.

Table A. 1: UK typical chemical analysis of FA[341]

Composition	Percent %
Aluminium (% as Al_2O_3)	20 - 40
Calcium or lime (% as CaO)	1.8 - 10
Chloride (% as Cl)	0.01 - 0.02
Free calcium oxide (%)	<0.1 - 1.0
Iron (% as Fe_2O_3)	6 - 16
Loss on ignition (%)	3 - 20
Magnesium (% as MgO)	1.0 - 3.5
pH	9 - 12
Potassium (% as K_2O)	2.3 - 4.5
Silica (% as SiO_2)	38 - 52
Sodium (% as Na_2O)	0.8 - 1.8
Sulfate (% as SO_3)	0.35 - 2.5
Titanium (% as TiO_2)	0.9 - 1.1
Water soluble sulphate (g/l as SO_4)	1.3 - 4.0 using 2:1 water solid extract

ASTM standard[342] classify FA into two classes i.e. class F and class C, depending on their chemical composition resulting from the type of coal burned and CaO content. Class F FA contains lime of less than 10% and a combination of Silicon (SiO_2), Aluminium (Al_2O_3) and Iron (Fe_2O_3) should not be less than 70% of the total weigh of FA. It is generally a product of combustion of anthracite and bituminous coals. Class C FA, on the other hand, is a product of the combustion of lignite and sub-bituminous coals, containing 15 to 40% of lime and a combination of Silicon (SiO_2), Aluminium (Al_2O_3) and Iron (Fe_2O_3) should not less than 50% of the total weight of FA. The class F FA has pozzolanic properties, while the class C FA has both pozzolanic and cementations properties.

The British European standard[234] also classifies FA into two classes. The FA with low content of calcium was classified as siliceous FA (V), which is the most used in the UK. Another class is calcareous FA (W), which contains reactive Calcium (CaO), reactive Silicon (SiO_2) and reactive Aluminium (Al_2O_3) that has

some cementations properties, in addition to pozzolanic properties. The British European standard classified two Portland siliceous FA (V) cements: class CEM II/A-V with FA content of 6 to 20 percent, and CEM II/B-V with a FA content of 21 to 35 percent[12].

The existence of unburned carbon in ash can affect the durability of concrete, where it may have an influence on the effect of air-entraining admixtures used for the manufacture of concrete resistant to freezing and thawing. Therefore, the measurement of unburned carbon (coal) remaining in ash by term of loss on ignition (LOI) is needed. British European standard, limits the maximum of unburned carbon remaining in ash, which is categorized as follows[343]:

- Category A:LOI ≤ 5%
- Category B:LOI ≥ 2% ≤ 7%
- Category C:LOI ≥ 4% ≤ 9%

A.5.2.2. Pozzolanic Reaction of Fly Ash (FA)

The calcium hydroxide ($Ca(OH)_2$) that was formed during the hydration reaction of cement reacts with FA when the water available to form additional calcium silicate hydrate (C-S-H) with the reaction as follows[33, 34, 344]:

Cement reaction : $C_3S + H \longrightarrow C\text{-}S\text{-}H + CaOH$ Equation A.11

Pozzolanic reaction : $CaOH + S \longrightarrow C\text{-}S\text{-}H$ Equation A.12
Silicate from FA

When FA is added to concrete, the pozzolanic reaction happens between the silica glass (SiO_2) and the calcium hydroxide ($Ca(OH)_2$) or lime, which is produced in the hydration of Portland cement. The permeability of the matrix reducing as the hydration products that were produced fill the pores[344]. Roy[345] states *'the reaction products are highly complex involving phase solubility, synergetic accelerating and retarding effects of multiphase, multi-particle materials and the surface effects at the solid liquid interface'*.

The products of the reaction are different from the products produced in the reaction in the concretes with Portland cement only. A very much finer pore structure is produced with time when there is access to water to keep the hydration process. In 1984, Dhir *et al*.[346] reported that the addition of FA enhances the dispersion of the Portland cement particles, which improves their reactivity.

A.5.2.3. Properties of Fresh and Hardened Concrete Containing FA

As mentioned before, one of the benefits using FA in concrete is that it can improve the workability of concrete. Use of FA in a concrete mix as replacement cement, increases the volume of cementitious material (cement and FA) in the concrete mix, compared to the mix without FA. Therefore, the volume of paste increases, which leads to a reduction in aggregate particle interference and the workability of concrete[347-349]. Some researchers studied and reported that the setting time of FA concrete for both classes of FA and all levels increased when compared to concrete with Portland cement, depends on the level of cement replacement with FA[349-351]. Naik and Singh[352] measured the initial and final setting of FA concrete using FA from different sources. They reported that in addition to the level of FA, source of FA also significantly affects the initial and final setting of FA concrete.

The hydration process of cement paste is an exothermic reaction, which is accompanied by the liberation of heat, raising the temperature of the concrete. FA has slower pozzolanic reactions; therefore, partial replacement of cement by FA results in a reduction of heat over a longer period of time and keeps the temperature of concrete remains lower. This is of huge importance in mass concrete avoiding early cracking, which is due to cooling, following a large temperature rise. Use of Class F of FA can reduce the rate of temperature rise more than that of Class C, as the Class C of FA has cementitious properties as well[344, 353-355]. Furthermore, Ballim and Graham[353] reported the effects of FA to hydration of concrete using an adiabatic calorimeter. They concluded that the use

of FA in concrete as replacement cement could reduce the peak rate of heat evolution linearly with increasing the level of replacement as clearly shown in the Figure A.16.

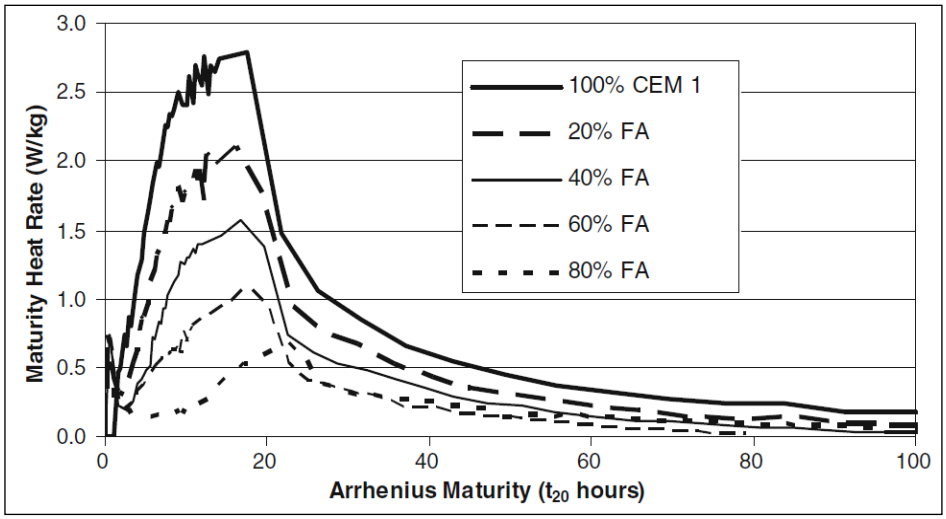

Figure A .16: Heat hydration of CEM I and FA concretes[353]

Wang and Yan[210] reported the influence of initial casting temperature and level of FA on the hydration of concrete under adiabatic conditions. They concluded that the heat hydration and heat hydration rates of binder in concrete were significantly affected by the temperature of which concrete was cast. The higher initial casting temperature the shorter the hydration reaction time and the lower the liberated heat amount of binder at early age. However, the heat hydration rate of binder increases. Moreover, they reported that the level of FA in concrete has different effects on the different water-binder ratio of concrete. At high water-binder ratio, the increase of level of FA decreases the heat hydration of binder as presented in the Figure A.17.

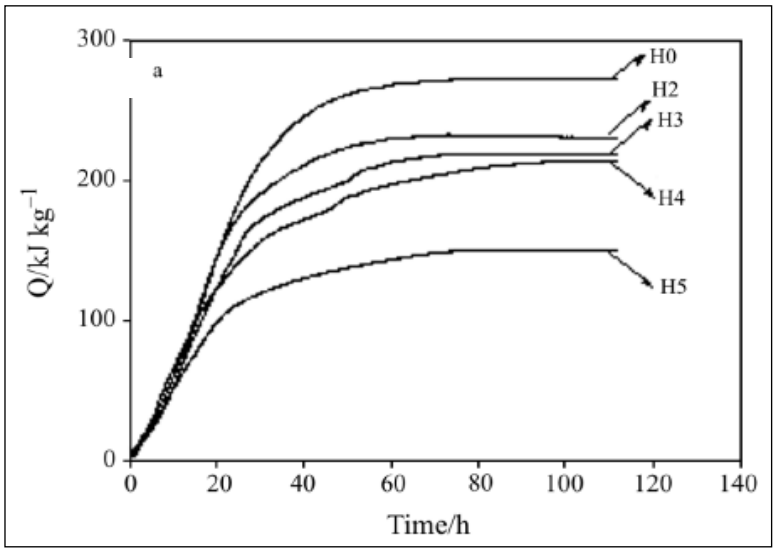

Figure A .17: Influence of dosage of FA on the heat hydration of binder for water-binder ratio of 0.53; H0-0%, H2-20%, H3-30%, H4-40% and H5-50% FA under adiabatic condition [210]

On the other hand, at low water- binder ratio, the increase of level of FA in concrete up to 40% of total quantity of binder increases the heat hydration of binder as shown in the Figure A.18. It is important to note that when the level of FA in concrete reaches 50% of the total of binder, the heat hydration of binder (with FA) is lower than that of with Portland cement only.

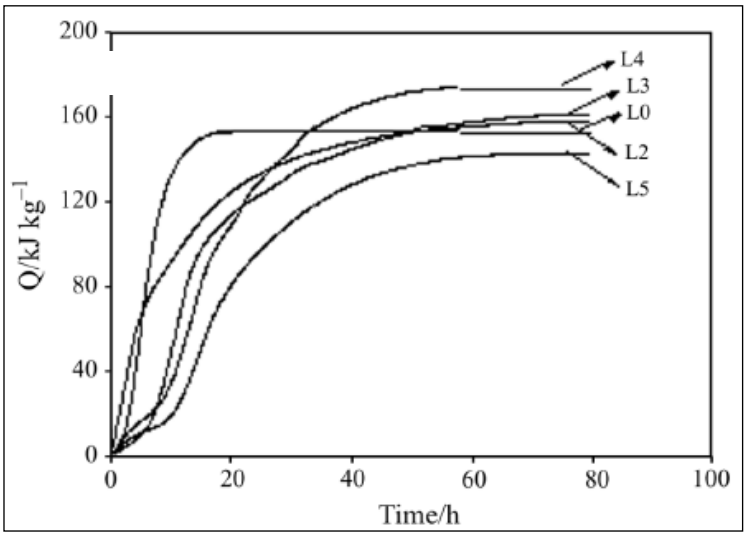

Figure A .18: Influence of dosage of FA on the heat hydration of binder for water-binder ratio of 0.25; L0-0%, L2-20%, L3-30%, L4-40% and L5-50% FA under adiabatic condition[210]

The strength rate development of FA concrete is affected by many factors such as[34, 185, 344]:

a) FA characteristics (chemical and mineralogical composition, fineness, pozzolanic reactivity)
b) Type of cement
c) Replacement level of cement with FA
d) Mixture proportions
e) Ambient temperature
e) Curing environment

Pozzolanic reactivity is the property of FA to react with calcium oxide in the presence of water and result highly cementitious water insoluble products. Factors affect the pozzolanic activity of a FA are: fineness, calcium content, specific surface, particle size distribution, and LOI content[356]. Several researchers have reported that when FA is pulverized to increase fineness, its pozzolanic activity increases significantly[33, 34, 344]. It is reported, however, that the effect of increase in specific surface area beyond 6,000 cm^2/g to be insignificant.

ASTM standard[342] limits the maximum amount of FA retained on the 45 μm (#325) mesh sieve on wet sieving as 34%. Generally, a large fraction of ash particle is smaller than 3-μm in size. The particle sizes range from less than 1 to over 100μm in bituminous ash. Joshi[357] reported that average size of FA lies between 7–12μm. The more fineness of the FA the more reaction between FA particles and calcium hydroxide occur, resulting in an increase of concrete strength. Furthermore, Chindaprasirt et al.[358] reported that the strength of FA concrete with more fineness of FA is higher than that of concrete with coarser FA.

The content and fineness of FA in concrete significantly affects the strength gain.

The low-calcium FA (Class F) do not exhibit significant pozzolanic activity to affect strength until about 2 weeks after hydration, but the high-calcium (Class C), which is highly pozzolanic FA, start their contribution to strength development almost from the onset of Portland cement hydration. The high-calcium FA, which have calcium oxide content of more than 15%, may begin to contribute to compressive strength development from the age of 3-days after mixing as they have self-hardening and pozzolanic properties.

The rate of pozzolanic reaction of FA in cement concrete is significantly influenced by curing temperatures at early ages, as discussed earlier. At elevated curing temperature, Ravina[359] reported that the strength development of FA concretes increase at early age. It is believed this is to due to the higher rate of pozzolanic reactions as the higher curing temperature. When concrete is cured at elevated temperatures, large quantities of FA may be incorporated with a significant improvement in strength development. Therefore, the strength development of FA concrete cured at elevated temperature is higher, compared to that cured under standard curing temperature (20^0C) up to 28 days.

For the type of class F FA (low calcium FA), Mehta (1994)[360] found that the pozzolanic reaction started at 11 days after hydration at curing temperature 20^0C and the significant contribution on strength development seems to occur after the age of 28-days of curing. He reported that the use of low calcium FA in concrete has no significant contribution to strength development up to 7 days. At 28 days and beyond most FA concretes with the cement replacement by FA up to 30% by cement weight, reached the strength of control concrete, which is normally equal and even higher than that of control concrete with cement only[33, 34, 361].

William and Owens (1982)[362] found that the strength development of FA concrete is significantly different from concrete with Portland cement only; particularly when they are cured at elevated temperature as shown in Fig. A.19. Conversely the reduction of strength that occurred with Portland cement concrete exposed to high temperatures, FA concretes showed strength gains because of

heating[363]. Elevated temperature at early age has a detrimental effect to Portland cement concrete but has less effect on FA concrete at later-age. Dhir[364] found that curing temperature at 60^0C can reduce strength in Portland cement concrete by up to 30%, but it can increase the strength of FA concrete by over 10 %. The beneficial effects of FA in concrete when it is exposed to elevated temperatures, therefore, can give benefits when it is used in the construction of mass concrete or concrete construction at elevated temperatures.

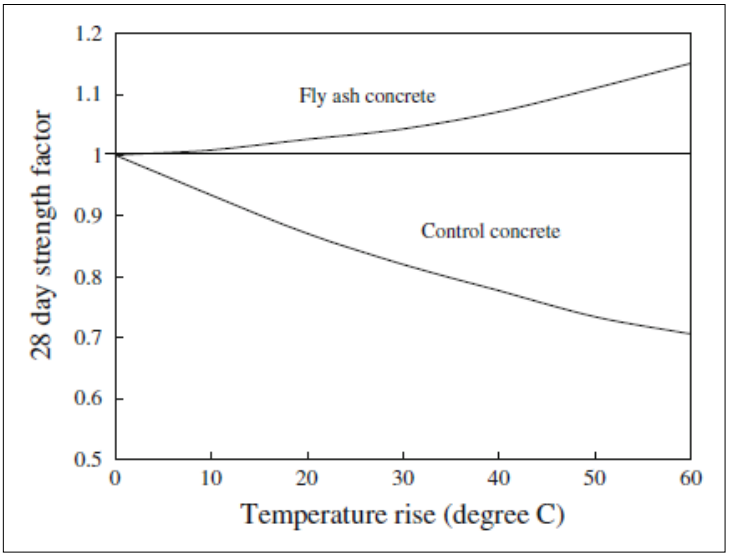

Figure A .19: Effect of temperature rise during curing on the compressive strength development of concretes[362]

Normally, the strength development of FA concrete is slightly lower than that of concrete with Portland cement only at early age. However, its strength reaches an equal strength or even higher than that of concrete with Portland cement only at later age (beyond 28-days) due to pozzolanic reaction, as mentioned before. Such a reaction continues to contribute to the strength development of the FA concrete for up to three to ten years as shown in Figure A.20[365]. The additional binder produced by the FA reaction with available lime allows FA concrete to continue to gain strength over time, and improve long term compressive and flexural strength[366-368].

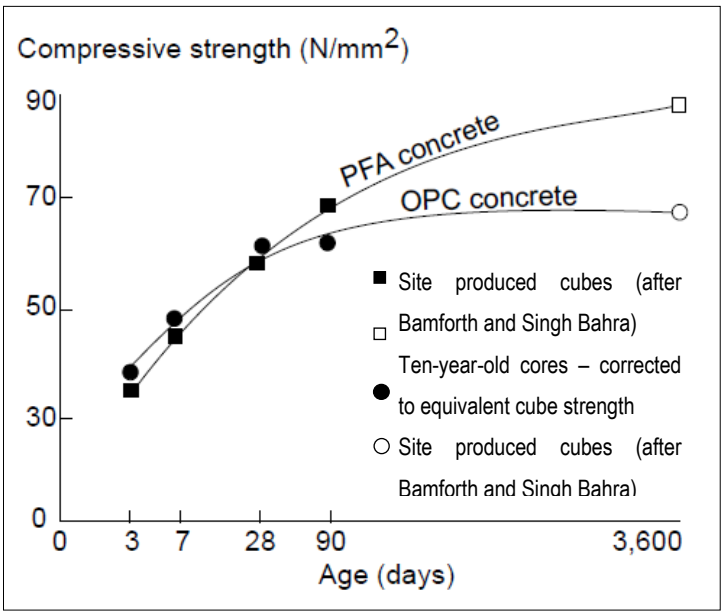

Figure A .20: Strength development of ordinary Portland cement (OPC) and pulverised fuel ash (FA)[365, 369]

A.5.2.4. Durability Properties of Concrete Containing FA

The durability of concrete exposed to harsh environments depends highly on the permeability of concrete[370]. The permeability of concrete primarily depends on the size, distribution and continuity of the pores of the hydrated paste of the concrete, which are highly affected by the quality of curing. Movement of aggressive solutions into concrete or the removal of the dissolved reaction products out of concrete is very important in the determination of the rate of progress of concrete deterioration caused by chemical attack[33, 34].

Thomas and Matthews[371] concluded that concretes containing FA, which were cured for 28-days in water, have lower permeability than that of equal-grade concrete with Portland cement only. The differences increase with FA level. They reported that the shortest curing time, the highest permeability of examined concrete, particularly when the ambient relative humidity was low. Under standard curing temperature (20^0C), the permeability of FA concrete is lower than

that of equal-grade concrete with Portland cement only, even under poor curing and storage conditions.

In 1994, Bilodeau et al.[338] reported that the high volume of fly ash (HVFA) concrete gave excellent resistance to chloride-ion penetration. It is probably due to the porosity in concrete decreases, as the additional product from pozzolanic reaction of FA continuously occurs filling the pores in concrete. Shafiq[372] reported that using FA as a partial replacement of cement in concrete reduces the rate of chloride migration, which yields a smaller cover depth for a longer specified service of structure exposed to chloride environment.

The Concrete Society[373] suggests the use of FA in concrete (refer to BS EN 450-1[343]) to reduce shrinkage. They reported that drying shrinkage has a linear relation with the equivalent cement of paste volume of concrete.

A.5.3. Ground Granulated Blast Furnace Slag (GGBS)

A.5.3.1. Introduction

Currently, there has been an increased trend for the use of supplementary cementitious materials, whether natural, waste, or by-products, in the manufacture of composite cements because of ecological, economical and diversified product quality reasons.

Ground granulated blast furnace slag (GGBS) is a by-product from the blast furnaces used to produce iron. Blast furnaces are filled up with the raw materials of iron ore, coke and limestone, and they are then heated up to 1,500 ^{0}C. Two products are produced i.e. molten iron and molten slag when the raw materials melt. The molten slag floats on the top of the molten iron because it is lighter. The molten slag, which is a by-product in the process, comprises mostly silicates and alumina from the original iron ore, combined with some oxides from the limestone. The major oxides SiO_2, CaO, Al_2O_3, and MgO constitute the bulk of the slag, which appears to be similar to the primarily content of cement constituent.

The procedure of granulating the slag involves the rapid cooling of molten slag through high-pressure water jets. This then quickly quenches the slag and forms granular particles, which are normally no larger than 5 mm in diameter. This rapid cooling is needed to prevent the slag from forming larger crystals. The obtained granular material consists of approximately 95% of non-crystalline calcium-alumino silicates. A further process of the granulated slag is the drying and then grinding of the slag to a very fine powder, which is called ground granulated blast furnace slag (GGBS)[33, 34, 374-376].

In 1774, the slag cement or ground granulated blast furnace slag was started to be used in producing mortar, when Loriot used it to make a mortar, and mixed it with lime. This was continued until 1862, when Emil Langen recommended a way to facilitate removal and handling of iron blast furnace slag when leaving the blast furnace. Further investigations on the glassy GGBS slag were carried out by Michaelis, Prussing, Tetmayer, Prost, Feret, and Green, where their investigations were along with that of Pasow, who introduced the process of air granulation

The Portland blast furnace slag cement was first produced in Germany in 1892, while in America it was introduced in 1896. Until 1950's, the GGBS was utilized in two ways; either as an ingredient in the manufacture of Portland cement or as a cementitious material mixed with Portland cement, hydrated lime, and gypsum. Since the end of 1950's, the GGBS was produced to be used as a separate cementitious material, which was added to the concrete/mortar mixtures. This procedure has been accepted in Australia, South Africa, The United Kingdom, Japan, Canada and the United States. The advantages of splitting the GGBS and Portland cement and combining them with others materials in the mixing are to allow both Portland cement and GGBS to be ground until its own optimum fineness is achieved and to adjust the desired replacement levels of cement with GGBS, in particular when it is requested in construction. Since then, it has been used extensively in many European countries such as Netherlands, France and Germany. In the UK it was first included into the British standard in 1923[374, 377].

A.5.3.2. Ground Granulated Blast Furnace Slag (GGBS) Production

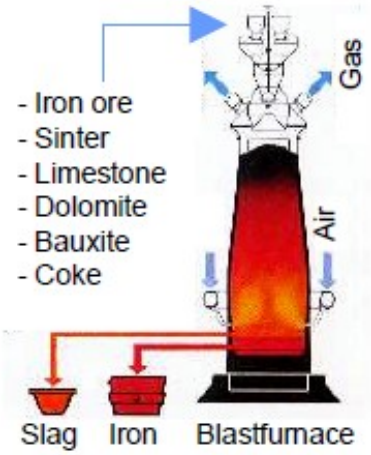

Figure A .21: Schematic diagram of production of GGBS[378]

Iron ores blended with limestone and/or dolomite and coke are used to manufacture iron or steel. The blended materials are sintered to remove moisture, some sulphur, and other materials, which cause the formation of nodules. Lump ore, sinter cake, fine ore pellets and additives from the blast furnace burden. The blast furnace is continuously fed with precise mixtures of burden and coke. The temperature of the blast furnace is kept at around 1500 ^{0}C. The products of molten iron and slag are periodically drawn off from tap holes at the base of the blast furnace as shown in Figure A.21. Furthermore, all processes to obtain the powder of granulated blast furnace slag, which is called GGBS; are described in Figure A.22.

Currently, the UK uses 2.5 million tonnes of GGBS and FA as cement replacements every year, saving over 2 million tonnes of carbon dioxide emissions[379]. Euroslag reports that about 230 – 300 kg of slag can be produced from the production of one tonne of iron[378]. For producing each ton of iron, it consumes about 1.6 tons of raw material, 330 kg coke, 150 kg coke coal powder and 900 m³ hot air are necessary. The quality production of iron greatly affects the quality of blast furnace slag that is produced.

The colour of GGBS varies, ranging from beige to dark to off-white, which depending on moisture content, chemistry and efficiency of granulation. However, it has usually white colour after it has been grounded.

A.5.3.3. Activity Index of GGBS

The activity index (the term in BS EN) or slag activity index (SAI, the term in ASTM) is determined as the ratio (in percent) of the compressive strength of the mortar with combination (by mass) of 50% of ground granulated blast furnace slag (GGBS) and 50% of test cement, to the compressive strength of mortar with the Portland cement only. It can be mathematically expressed as follow[380-382]:

$$Activity\ index, \% = \frac{SP}{P}\ X\ 100 \qquad \text{Equation A.13}$$

Where: SP = the compressive strength of concrete with GGBS and Portland cement.

P = the compressive strength of concrete with Portland cement only.

The British European standard BS EN 15167–1[381] is not identical with the American standard, ASTM C-989-04, the British European standard does not classify the GGBS in different class, whereas the ASTM standard classifies it as grades 80, 100 and 120 based on the slag activity index (SAI). However, both the standards require the minimum activity index of GGBS that can be used as partly replacement of cement as shown in Table A.2.

Table A. 2: Minimum activity index of GGBS[380, 381]

Age (days)	**Minimum activity index (%)**			
	ASTM C 989 – 04			BS EN 15167–01
	Grade 80	Grade 100	Grade 120	
7	-	70	90	45
28	70	90	100	70

Measures to influence the quality of the slag

Process stage	Measures to influence the quality	Influenced properties
Raw material preparation	Selection, arrangement and pre-treatment of raw materials related to the chemical comp. of the blast furnace slag	Chemical composition e.g. CaO, SiO2, Al2O3, MgO, alkalis
Melting process	Selection of suitable process conditions (blast furnace temp., minimization of carbon rate, gas flow, etc …)	temperature, composition of the products
Heat treatment	Different cooling rates a) quick: - blowing - granulation - pelletizing	glass content, structure, porosity
	b) moderate - foaming	bulk density, strength, porosity
	c) slow - air-cooling	strength, porosity, resistance to polishing, grain size
Processing	crushing sieving grading milling	grain size, shape, grain size distribution

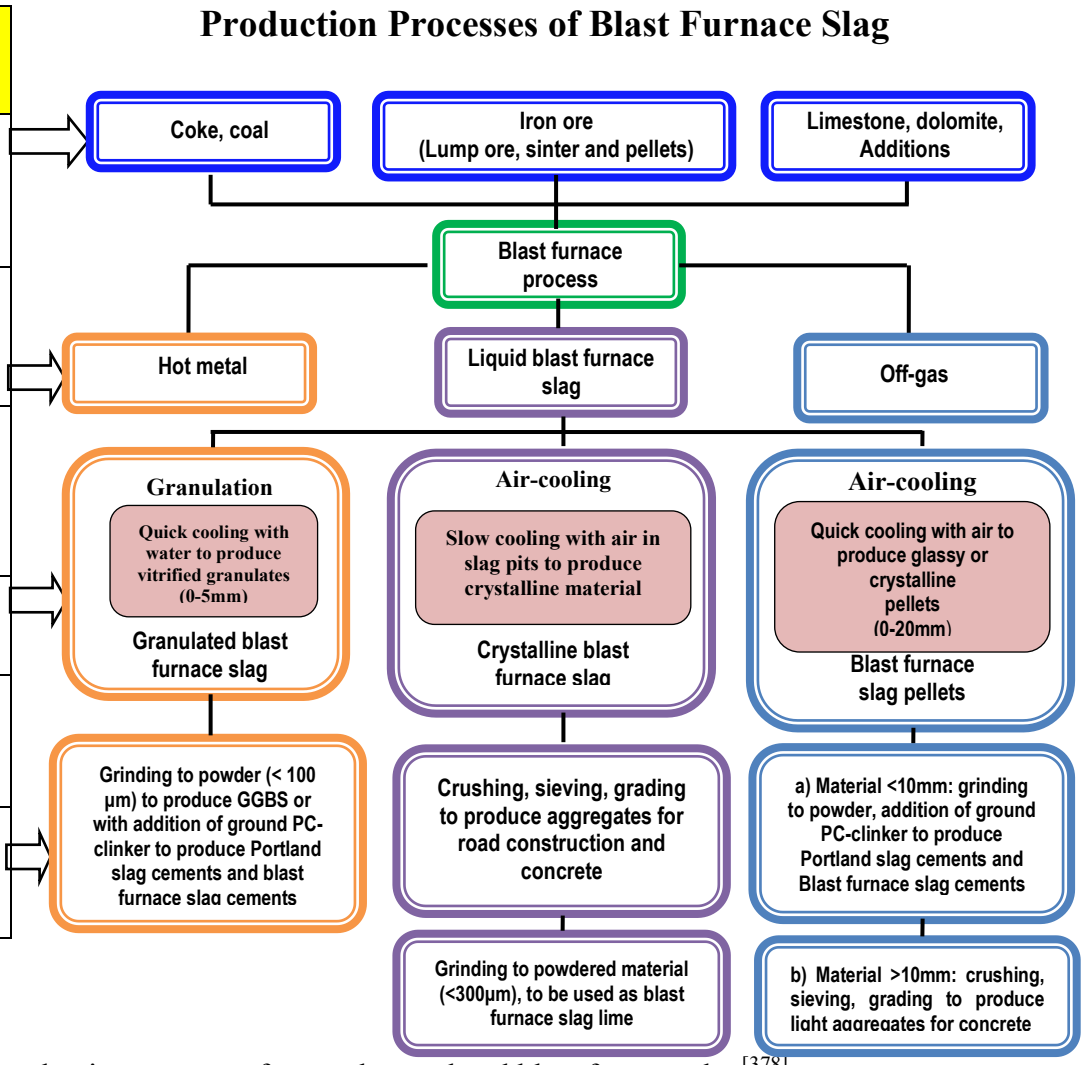

Figure A .22: Flow chart of production process of ground granulated blast furnace slag[378]

A.5.3.4. Hydration of Cement

Hydration of cement is the reaction between cement particles and water, including both chemical and physical process. The hydration products are directly related to the properties of fresh concrete, such as setting time and hardening.

There four major compounds of cement as presented in Table 2.3. The abbreviation of all oxides in the main compounds are CaO = C; SiO_2 = S; Al_2O_3 = A; Fe_2O_3 = F and H_2O = H.

Table A. 3: Main compounds in Portland cement[12, 28, 29, 216, 293]

No	Name of compound	Oxide composition	Abbreviation
1	Tricalcium silicate	$3CaO.SiO_2$	C_3S
2	Dicalcium silicate	$2CaO.SiO_2$	C_2S
3	Tricalcium aluminate	$3CaO.Al_2O_3$	C_3A
4	Tetracalcium aluminoferrite	$4CaO.Al_2O_3.Fe_2O_3$	C_4AF

The most important of the compounds are the two silicates C_3S and C_2S, which are responsible for the strength of hydrated cement paste. It is found that the silicate compounds in cement are not pure compounds. They also contain minor oxides in solid solution such as MgO, TiO_2, Mn_2O_3, K_2O and N_2O, where they usually amount to not more than a few per cent of the mass of cement. Two of the minor compounds are of interest: the oxides of sodium and potassium (N_2O and K_2O), where they are well known as the alkalis. Furthermore, they are found to react with some aggregates, where the products of the reaction cause disintegration of the concrete and can also affect the rate of strength of the cement.[12, 216].

The presence of C_3A and C_4AF compounds in cement contribute little even nothing to the strength of hydrated cement. However, the C_3A compound in the manufacture of cement facilitates the combination of lime and silica. Similarly, the C_4AF compound does not contribute to cement strength, but it reacts with

gypsum to form calcium sulfoferrite, which may accelerate the hydration of the silicates.

Bogue proposed a method to calculate the composition of compounds in cement as follow[12, 28, 29, 216, 293, 383]:

$$C_3S = 4.07(CaO) - 7.60(SiO_2) - 6.72(Al_2O_3) - 1.43(Fe_2O_3) - 2.85(SO_3) \quad \text{Equation A.14}$$

$$C_2S = 2.87(SiO_2) - 0.75(3CaO.SiO_2) \quad \text{Equation A.15}$$

$$C_3A = 2.65(Al_2O_3) - 1.69(Fe_2O_3) \quad \text{Equation A.16}$$

$$C_4AF = 3.04(F_2O_3) \quad \text{Equation A.17}$$

The terms in brackets, refer to the percentage of the given oxide in the total mass of cement. The products of hydration processes of the two silicate compounds, C_3S and C_2S are similar i.e. the microcrystalline hydrate ($C_3S_2H_3$ or C-S-H) with some lime separating out as crystalline $Ca(OH)_2$. The C-S-H compound has variable stoichiometry, which is affected by water-cement ratio, curing conditions, and use of supplementary cementitious materials.[384-386]. However, the main parameter that controls the various forms of the C-S-H structures is the molar ratio of CaO to SiO_2 (C/S ratio).

The amount of lime that was produced from C_2S hydration is less than that of C_3S as shown in the reaction equation below. The hydration reactions as follow[12, 28, 29, 293, 383, 386, 387].

$$2C_3S + 6H \rightarrow C_3S_2H_3 + 3Ca(OH)_2 \quad \text{Equation A.18}$$

$$2C_2S + 4H \rightarrow C_3S_2H_3 + Ca(OH)_2 \quad \text{Equation A.19}$$

The hydration reaction of the other two compounds is as follows:

$$C_3A + 6H \rightarrow C_3AH_6 \quad \text{Equation A.20}$$

$$C_4AF + 3(CSH_2) + 21H \rightarrow C_6(A,F)S_3H_{32} + (F,A)H_3$$ Equation A.21

The reaction of tricalcium aluminates in the Equation 2.21 occurs, when there is no gypsum available. In the case, of the gypsum being present with water the reaction will take place as follow:

$$C_3A + 3(CaSO4.2H_2O) + 26H_2O \rightarrow 3CaO.Al_2O_3.CaSO_4.32H_2$$ Equation A.22

$$C_3AH_6 + 3(CaSO_4.2H_2O) + 20H_2O \rightarrow 3CaO.Al_2O_3.CaSO_4.32H_2O$$ Equation A.23

The primary products from the hydration of Portland cement are shown in the Table A.4.

Table A. 4: Primary products of cement Portland hydration[388]

Formula	Name	Abbreviation
$3CaO{\cdot}2SiO_2 \cdot xH_2O$, ($x \approx 3$)	Calcium-silicate hydrate	CSH
$6CaO{\cdot}Al_2O_3{\cdot}32H_2O$	Ettriginite	$C_6AS_3H_{32}$
$6CaO{\cdot}Fe_2O_3{\cdot}3SO_3{\cdot}32H_2O$	Iron ettriginite	$C_6FS_3H_{32}$
$4CaO{\cdot}Al_2O_3{\cdot}SO_3{\cdot}12H_2O$	Calcium monosulfoaluminate 12-hydrate	C_4ASH_{12}
$Ca(OH)_2$	Calcium hydroxide	CH
$Mg(OH)_2$	Magnesium hydroxide	MH

The primary hydration products, which is most effect on the strength development of concrete is calcium-silicate hydrate as discuss earlier.

The rate of hydration of individual compound of cement in the order from the highest to the lowest is C_3A, C_3S, $C4_AF$ and C_2S respectively[29, 120, 148], can be shown in Figure A.23.

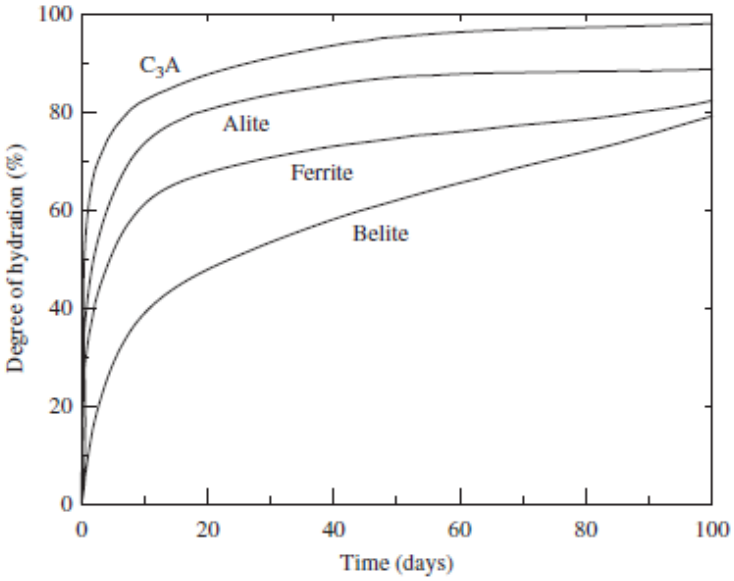

Figure A .23: Hydration process of main compounds of Portland cement[29]

The figure shows the hydration of dicalcium oxide is very slow at the early age, but it becomes faster at later ages, which opposite of the other main compounds of cement. Furthermore, the mechanism of hydration of Portland cement is presented in the Figure A.24. As we can see from the figure, the hydration process of Portland cement consists of five stages: dissolution (stage 1), dormant period (stage 2), acceleration (stage 3), deceleration (stage 4) and steady (stage 5). The two peaks in the figure correspond to the leading effect of C_3S and C_3A in hydration process, where their order of occurrence can be reversed, depends on cement type.

Immediately, when the cement has a contact with water, the reaction between C_3A and water with the presence of gypsum dissolving the ions in water. The reaction results in a rapid heat evolution. At the same time, the calcium ions and hydroxide ions are rapidly released from the C_3S grain, which is a hydrolysis reaction generates a heat evolution as well. A very short period of rapid heat evolution occurs in few minutes, which is known as stage 1 or sometimes called pre-induction period. Generally, this stage is not captured by the calorimeter test due to the very short reaction time.

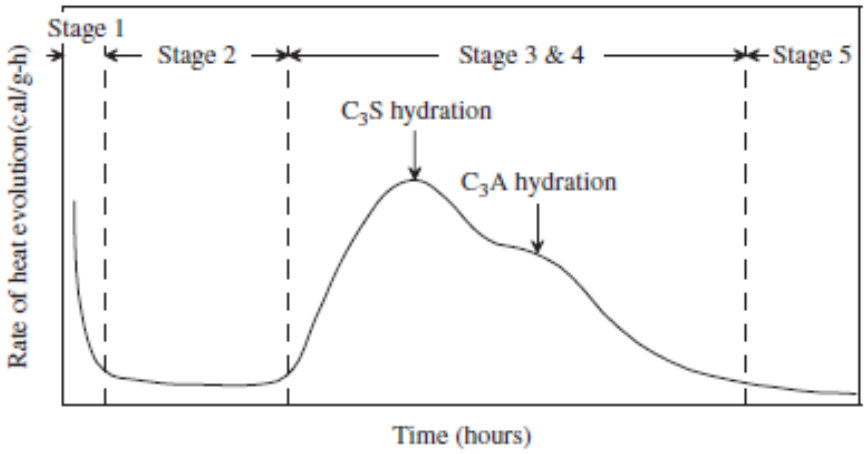

Figure A .24: The different stages in the cement hydration process [9, 29, 385]

Normally, the heat evolution is measured from the beginning of the dormant period or induction period (stage 2). The concrete is flowable in this period and the hydrations of all main compounds are very slow; a small amount of heat is generated. The ion dissolution continues during the time, which results in the increasing the ion concentrations of C_3S and C_2S in system. This period usually lasts a few hours - approximately five hours. The dormant stage is followed by the acceleration stage. In this stage, the heat evolution generated significantly increases as the hydration of C_3S and C_2S are started again. Temperature rise in concrete increases rapidly during this stage.

The deceleration period (stage 4) follows the acceleration period, which is started once the first peak of the rate of evolution is reached. The rate of heat evolution in this stage gradually slows. The products of hydration i.e. C-S-H in the acceleration stage develop on the surface of un-hydrated cement (C_3S and C_2S grains), which forms a covering of these grains. The hydration occurs continuously, which results in the thickness of the hydrated layer increasing. Therefore, the hydrated layer hinders water, which must reach the unhydrite C_3S for continuing hydration. Furthermore, the hydration process reaches the steady period (stage 5), where the hydration becomes a diffusion process, as occurs in the deceleration stage.

The factors affecting the strength development of concrete affect the hydration of cement as well, as the strength of concrete is the product of the hydration of cement/binder in the concrete. The type of cement affects the heat of hydration. Cement with higher content of tricalcium silicate (C_3S) and tricalcium aluminate (C_3A) with the higher fineness, such as Type III cements, generate the heat of hydration higher and at faster rate than other cements[389, 390]. The fine cement has a greater surface area to be wetted, which results in an acceleration of the reaction between cement and water. As a result, it increases the rate of heat generation at early ages, but may not affect to the total amount of head liberation after few weeks. The Type II cement should be chosen, when the heat generation must be minimized in concrete. This cement type contents low C_3S and C_3A in order to low the heat out of hydration of the cement by limiting the amount of the two compounds in cement[234, 389, 391].

Chemical admixture is added into mortar/concrete in order to adjust to the weather conditions or to meet construction requirements. The admixture interacts with cement and cement hydrates during the hydration process. The mechanisms of the interactions include adsorption, dispersion, chelation and solubilization. All the mechanisms may affect cement hydration kinetics, phase composition and hydrates morphology[392]. The effects of admixtures to the hydration process highly depend on the type and dosage of admixture added into a given mixture.

Peschard et al (2006) [393] and Cheung et al (2011) [394] investigated the impact of retarder admixtures on the hydration kinetic of silicates compounds in Portland cement. They reported that retarder admixtures delayed the induction period of hydration and in some cases, increased hydration rate after hydration accelerates. The large absorption of calcium lignosulfonate on the C_3A result in an increase of induction period or delay time of hydration[395]. On the other hand, the accelerator admixtures are used to speed up the hydration process of cement in mortar/concrete, in order to accelerate the strength development of the mortars/concretes at early age[296, 396, 397].

The ASTM type C admixtures are referred to as accelerators, which is has function to accelerate the hydration process of cement at early age. Calcium chloride ($CaCl_2$) is commonly used as accelerator for many decades. It is effective to accelerate the hydration of the calcium silicates, particularly C_3S compound, possibly by a slight change in the alkalinity of the pore water or as catalyst in the reactions of hydration[12].

In 1960, Copeland at al.[120], point out the effect of water-cement ratio to the heat generation of hydration. Enhancing in the water-cement ratio from 0.30 to 0.50 increased the head of hydration by 14% at 3-days and 23% at 28-days. Furthermore, they found that the hydration of cement is come with an increase in the volume of solids within the hydrating paste, where the volume of the hydration products is greater than that of what was produced.

Many researchers have investigated the effect of temperature on hydration process of cement in mortar/concrete. The rates of hydration process of cement in mortars/concretes cured at higher temperatures are greatly accelerated over than that of those cured at lower temperatures. The curing temperature of the concrete is arguably the variable that has the most significant effect on the setting time of concrete.

In 1975, Samarai et al[398] reported that elevated temperatures in hot climates accelerated the setting time of mortar/concrete. The higher the curing temperatures are, the quicker the reactions between cement and water are, and as a result, the setting time becomes shorter or it accelerates the hydration process as shown in Figure A.25.

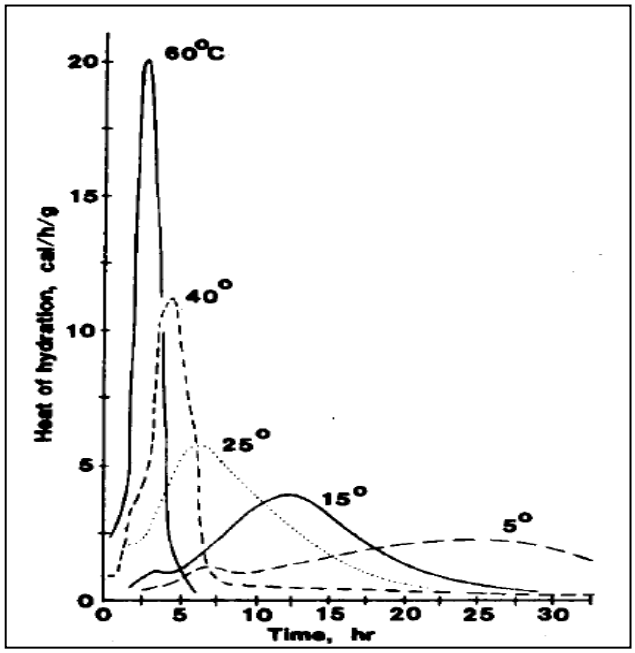

Figure A .25: Heat of hydration for tricalcium silicate (C_3S) under different curing temperatures[398]

Conversely, Wang et al.[9], reported that the rate of cement hydration of mortars/concretes cured under higher temperatures, is decelerated at later ages. This is due to the products of the hydration in mortars/concretes cured at higher curing temperatures forming a "shell" or a coat layer surrounding the un-hydrated cement grain, which delays further hydration.

A.5.3.5. Hydration of GGBS

Many researchers agreed that the principal hydration products that are formed, when GGBS is mixed with Portland cement and water are the same as the product of the hydration of Portland cement only, i.e. calcium silicate hydrate (C-S-H)[399]. The Portland cement and GGBS are found in the same field in the ternary diagram; however, Portland cement is fundamentally in the tricalcium silicate (C_3S) field, while GGBS is found essentially in the dicalcium silicate (C_2S) field on the ternary diagram as shown in Figure A.26. The GGBS hydration, however, is found to be more gel-like than the products of hydration of Portland cement. Therefore, it increases the denseness of cement paste[382].

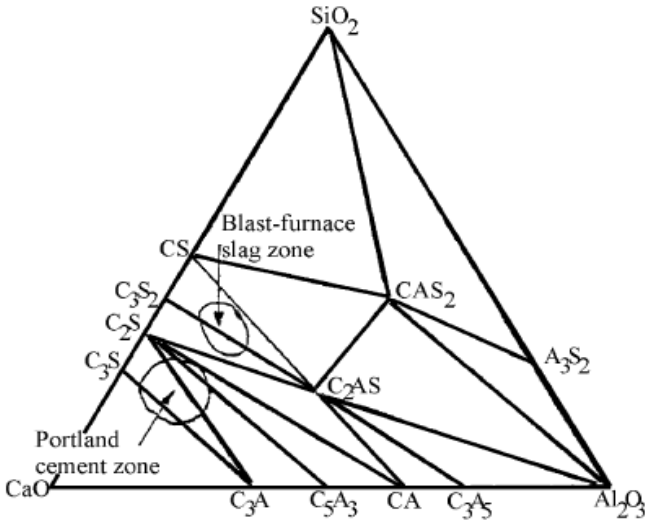

Figure A .26: Ternary diagram indicating composition of Portland cement and GGBS in the system CaO-SiO_2-Al_2O_3.[382]

In general, the chemical composition of GGBS is similar to that of Portland cement. It comprises of the main oxides such as lime, silica and alumina, which are constituents of Portland cement; however, they are different in proportions. The typical range of chemical composition of GGBS in the United States and Canada in 1988 and in the UK are presented in Table 2.5

Table A. 5: Range of Chemical Composition of GGBS in the United States and Canada[374] and in the UK[400]

Chemical Constituent		**Range of Composition (% by mass)**	
Name	**Formula**	**US and Canada**	**UK**
Silicate oxide	SiO_2	32 – 42	34-36
Aluminium oxide	Al_2O_3	7-16	12-14
Calcium oxide	CaO	32 – 45	38-42
Magnesium oxide	MgO	5 – 15	7-9
Sulphur	S	0.7 – 2.2	-
Iron oxide	Fe_2O_3	0.1 – 1.5	-
Manganese oxide	MnO	0.2 – 1.0	-

GGBS generally has a higher silica content. This is clearly seen in the phase diagram shown in Figure A.26. The diagram was based on work carried out by Lea[293] and Bakker[401], which shows the composition of Portland cement and blast-furnace slag in the systems CaO-SiO_2-Al_2O_3. Cheron and Lardinois[402] found a linear relationship between mechanical strength and the hydraulic index, which can be defined as follow:

$$Hydraulic\ activity\ index = \frac{(CaO + 1.4\ MgO + 0.56\ Al_2O_3)}{SiO_2} \quad \text{Equation A.24}$$

where the value of hydraulic activity index is between 1.65 and 1.85 are considered normal. However, Pal et al[403] suggested a value of the hydraulic activity index of 2.0 to obtain a good performance of GGBS.

As mentioned before, GGBS has a similar compound that of Portland cement, therefore, it reacts, when it is mixed with water. However, the initial hydration is much slower than that of Portland cement. Roy and Idorn[5] state that the temperature rise during the early hydration of cement provides energy to activate alkali-hydroxide attack on the GGBS particles. Therefore, it is needed the Portland cement or alkali salts or lime as an activator to increase the reaction rate.

The rate of hydration of GGBS in presence of Portland cement greatly relies on breakdown and dissolution of the glassy GGBS structure by hydroxyl ions released during the hydration of the Portland cement, which occurred before GGBS hydration[211, 374]. In the hydration of GGBS, the GGBS reacts with alkali and calcium hydroxide ($Ca(OH)_2$), to produce additional C-S-H.

The model for earlier hydration of GGBS assumes that sufficient heat of cement hydration is available for initial alkali-activation of GGBS[5] as shown in Figure A.27. The model related to the following is typical of the hydration mechanism and structure formation:

a) Dilution of Portland cement by GGBS decreases the quantity of calcium hydroxide to be precipitated in the pores formed from cement hydration and the GGBS portion hydrates along with the Portland cement portion.

b) The Portland cement fraction releases alkalis and lime during the hydration, while the GGBS fraction preserves lime and alkalis in its hydration products.
c) The lower the lime concentration the more alkalis can be accommodated by the C-S-H.
d) The more participation of GGBS in the hydration process results in a hardened paste of greater denseness with less pores and a smaller size of pore that that of the equivalent mix with Portland cement only.

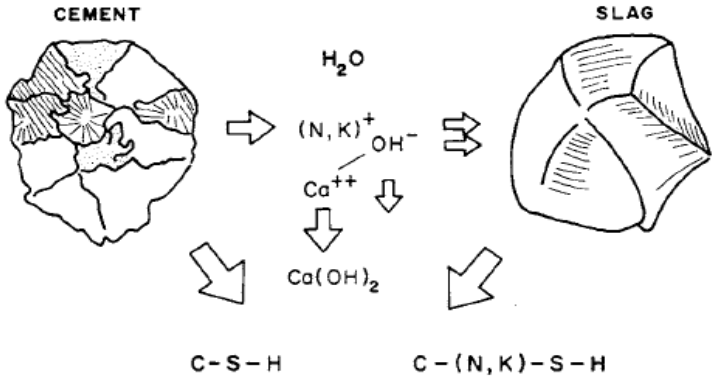

Figure A .27: Model for early hydration of slag cement[5]

Furthermore, Roy and Idorn found that the secondary or long-term hydration of Portland cement continuously produces crystalline $Ca(OH)_2$ in the pores of cement paste or concrete. On the other hand, long-term hydration of GGBS occurs in different ways, where calcium is kept during reaction of the glassy GGBS structure and C-S-H phase. In a saturated solution of $Ca(OH)_2$, the pozzolanic reaction of GGBS consumes the $Ca(OH)_2$ to produce additional C-S-H.

The model of the long-term hydration of GGBS is shown in Figure A.28. A system, which has the continuous capability to increase the amount of C-S-H compound, creates fineness of pores of microstructure by consuming the crystalline $Ca(OH)_2$; has been formed. Therefore, the hydration of GGBS will carry on through the performance periods of concrete and at the same time keep alkalis and calcium hydroxyl to enhance strength, density and chemical resistance.

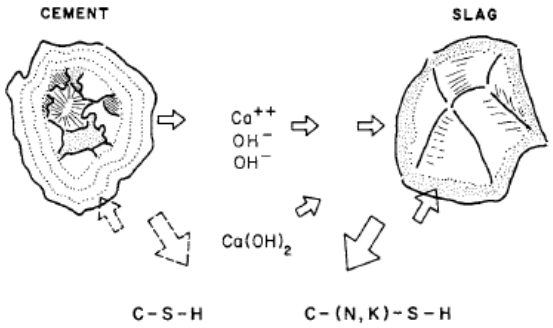

Figure A .28: Model for long-term hydration of slag cement[5]

The mechanism of GGBS hydration can be clearly expressed as follow[344]:

- Primary reaction:

$$OPC + water \longrightarrow C\text{-}S\text{-}H + Ca(OH)_2 \quad \text{(Na(OH), KOH)} \qquad \text{Equation A.25}$$

$$GGBS + water + Ca(OH)_2 \ (Na(OH), KOH) \longrightarrow C\text{-}(N,K)\text{-}S\text{-}H \qquad \text{Equation A.26}$$

- Secondary reaction:
  a) OPC primary reaction products + GGBS
  b) OPC primary reaction products + GGBS primary reaction products

The hydration mechanism of Portland cement is much simpler than that of binder with a combination of GGBS and Portland cement. Many researchers found that the hydration of GGBS at early age is much slower than that of Portland cement only as mentioned before, where the higher replacement levels of cement with GGBS, the slower the rate of hydration. Therefore, Portland cement or alkalis salts or lime is needed as activator to increase the reaction rate. However, there are many other factors, which affect the rate of hydration.

Zhu at al.[404] investigated the effect of particle size distribution (PSD) of slag on mixing water, setting time, and strength. They found that the decrease of particle size of GGBS increased the strength, mixing water and density of concrete. Oner et al[405] studied the strength development of concretes with 50% of GGBS with

the fineness varied from 3000 to 6000 cm^2/g. They added that it is not only the fineness of the clinker slag, which affect the strength of concrete. However, it is also determined by the individual components, which govern the mix composition for a desired strength.

Zhou at al.[406] investigated the influence of GGBS content on the hydration of blended cement using an isothermal conduction calorimeter. Their experimental works revealed that the addition of GGBS accelerates the hydration of Portland cement at the early stage. It is believed that the acceleration was due to the "dilution effect", where the consumption of CH by GGBS and the nucleation site for the formation of CH presented by GGBS particles. However, the higher GGBS content, the lower C-S-H and CH content in blended cement paste due to the low degree of hydration of GGBS.

Furthermore, SEM images obtained from the experiment show that GGBS affects the formation and distribution of hydration product, where CH crystals are mainly formed surrounding GGBS particles. Similarly, Lawrence et al (2005)[407] also reported that when the inert mineral admixtures were used as cementitious materials, they could improve the degree of hydration.

The higher early age temperatures developed within the structural elements due to heat hydration of binders, appear to be sufficient in supplying the activation energy that is the minimum energy required to start a chemical reaction needed for the pozzolanic reaction to kick-in earlier. This advantage has not been explored properly, but it can enhance the strength development of GGBS concrete at early age[1, 40, 161, 279].

A.5.3.6. Fresh Properties of GGBS Concrete

Bleeding can be defined as the movement of water to the surface of the freshly placed concrete, which is a form of settlement as the water is being forced to the surface as the heavier solids in the concrete begin to settle. Wainwright and Aider[408] reported that all concrete bleeds to some extent, the bleed of water,

however, is only investigated on the surface, once the rate of bleeding exceeds the rate of evaporation. Replacing Portland cement by GGBS up to 55% increased the bleed capacity by 30% higher than that of Portland cement only, but still has little effect on the bleed rate. However, there is no significant effect on bleeding, when the replacement cement with GGBS up to 85%[409].

Wood[410] reported that the workability of GGBS concrete improved, when compared to the concrete with Portland cement only of the same water-binder ratio. He further reported that this result was due to GGBS being much finer than Portland cement. In 1974, Fulton[411] concluded that the improvement of workability of GGBS concrete, is due to the increased paste content and cohesiveness of the paste.

Meusel and Rose[412] investigated the effect of highly active slag with cement replacement of 30–50% with GGBS on the workability of concrete. They found that the addition of GGBS could improve the workability of concrete. The higher replacement levels with GGBS, the greater improvement in workability. The fineness of slag did not have significant effect on the workability.

Normally, the setting time of concrete with GGBS is generally greater than that of the same water-binder ratio concrete with Portland cement only. Setting time increased with the increase in GGBS. Wainwright and Aider[408] observed the effect of GGBS additions on the setting times and consistency of cements. Three different sources of cement and single source of GGBS were used. The replacement levels of cement were 40 and 70% of GGBS. They concluded as follows:

(a) The consistency and setting times results were almost similar for all the three sources of cements.
(b) The addition of GGBS affected the consistency of cements, and it was reduced with the increase in GGBS content.
(c) The setting time of cements was increased with the increase in GGBS content.

A.5.3.7. Durability of GGBS Concrete

The term 'durability' of concrete can be defined as the ability of a concrete structure to resist weathering action, chemical attack, abrasion, or any other process of deterioration. A durable concrete will retain its original appearance, quality, and serviceability when exposed to its environment. Many factors affect the durability of concrete such as: properly designed, proportioned, placed, finished, tested, inspected, and curing[185, 400, 413].

It is well known that the durability of concrete greatly depends on its permeability or diffusion to liquids, gases and its resistance to penetration by ions such as chlorides and sulphates. Many researchers[37, 231, 339, 414-421] agreed that the using of GGBS in concretes can improve the durability of the concretes, when adequate curing is allowed. Ramezanianpour and Malhotra[422] investigated the influence of curing method on the strength of concrete; resistance to penetration of chloride ions and porosity of concretes that using cementitious materials such as GGBS, FA and silica fume to the strength of concrete. They found that to gain the highest strength, lowest porosity and highest resistant to the penetration of chloride ions of given concrete mix, it is essential to continuously cure the concrete under moist curing condition.

Bijen[339] and Aldea et al[37]found that the effect of GGBS on permeability and chloride diffusivity is strongly dependent on the levels of cement replacement. Osborne[414] suggest the use of GGBS up to 70% as cement replacement, when chemical resistance to sulphates, chlorides and sea-water is required. In common construction, however, it is suggested that for small sections special attention on both curing and cover of reinforcement should be given. Furthermore, he found that there is a significant reduction in temperature rise in mass concrete with high GGBS content, which can minimise the risk thermal cracking.

Song and Saraswathy[415] investigated the corrosion resistance of reinforced steel in GGBS concrete. They stated that there is no detrimental effect, due to a

reduction of pH value by using GGBS in concrete. Even, an increase in replacement levels of GGBS decreases the rate of corrosion of reinforced steel bars in GGBS concrete.

In 2002, Basheer et al[423] reported that GGBS can be effectively incorporated with Portland cement to minimise the quantity and the size of pores in concrete. The higher replacement levels of cement with GGBS, the denser microstructures that are formed, and prevent the concrete from water penetration[424]. The resulting hardened cement paste using GGBS is more chemically stable, as it remains much less free lime, which can lead to a further reaction forming other compounds causing a reduction in concrete durability[34].

Kwon[418] observed the effect of GGBS, which is used in corporation with Portland cement to reduce the risk of alkali aggregate reaction. He found that the replacement of cement by 30% with GGBS and using a low-alkali cement could avoid the alkali-aggregate reaction from causing large expansion in concrete. Li et al[420] investigated the durability of Cao'e River Floodgate structure in China, which is used high-volume of GGBS. They found that high-volume GGBS concrete had better capability to resist chloride ion penetration, where concrete with high-volume GGBS had lower diffusion coefficient of chloride ion that that of concrete with Portland cement only.

A.5.3.8. Application of GGBS Concrete in Construction

There are two ways that GGBS can be used in concrete. Firstly, it can be as raw material, which is blended with Portland cement to produce blended cement. Another way is using it as a separate 'addition, which is combined with the Portland cement in the concrete mixer[379].

The percentages of GGBS in blended cement should be in accordance to the British European standard[234]. In the production of Portland-composite cement, i.e. Portland-slag cement for both CEM II/A-S and CEM II/B-S types, the GGBS content is between 6 – 20% and 21 – 35% respectively. The content of GGBS

required to produce cement type III or blast furnace cements are higher than that of cement type II. They are between 36 – 65%, 66 – 80% and 81 – 95% for types of CEM III/A, CEM III/B and CEM III/C respectively. Cement type V or composite cement is a combination of Portland cement and more than two cementitious materials. These cement types contain GGBS between 18 – 30% and 31 – 49% for types of CEM V/A and CEM V/B respectively.

Lewis[425] reported that the use of separate GGBS, as a mineral admixture to replace a part of Portland cement in concrete was started in South Africa in 1958. The Portland cement was replaced by 50% and 70% of GGBS for ordinary concrete and marine structural concrete respectively. This application began in the UK after a decade i.e. in 1970 and a little bit later in Canada in 1976. The advantages of the separate grinding of GGBS and the adding it at the mixer are:

- The ability to adjust the proportion of GGBS to that required of the project.
- To enable the grinding of both GGBS and Portland cement to the optimum of fineness.
- To improve the workability of concrete.

Normally, GGBS is used as cement replacement at levels from 20 to 80 percent, which is varied depending on the application. Cement replacement levels are generally much lower in cold weather applications. Conversely, in hot weather concreting, the levels of GGBS used in concrete might be higher in order to delay the setting time of the concrete[426]. Table 2.6 presented the levels of GGBS suggested for different applications and environmental conditions.

Table A. 6: Suggested slag cement replacement levels[426]

Concrete application	Percentage of GGBS
Concrete paving	25-50%
Exterior flatwork not	25-50%
Exposed to deicer salts	
Exterior flatwork exposed to deicer salts with w/cm < 0.45	25-50%
Interior flatwork	25-50%
Basement floors	25-50%
Footings	30-65%
Walls & columns	25-50%
Tilt-up panels	25-50%
Pre-stressed concrete	20-50%
Pre-cast concrete	20-50%
Concrete blocks	20-50%
Concrete pavers	20-50%
High strength	25-50%
ASR mitigation	25-70%
Sulfate resistance	
Type II equivalence	25-50%
Type V equivalence	50-65%
Lower permeability	25-65%
Mass concrete	50-80%

A. 6. Mix Design of Portland Cement and GGBS Concretes

The mix design can be defined as a process to select the correct proportions of cement, fine and coarse aggregate and water to produce concrete having the specified properties[229, 427]. Sometimes, additional ingredients such GGBS, FA or other admixtures are added into concrete mix, when they are needed to obtain the desired properties of the concrete.

Generally, the properties, which are mostly taken into account in determining the proportion of concrete mixes, are:

- The workability of the fresh concrete.
- The compressive strength at a specified age.
- The durability, by means of specifying the minimum cement content and/or the maximum free-water/cement ratio, which is dependent on the purpose for which the concrete will be used or the conditions/environment, where concrete will be placed[229, 428, 429].

A concrete mix proportion can be determined from the existing statistical data using the same materials, proportions and concreting conditions. However, when there are no recorded data or they are not enough, the concrete mix must be determined by trial mixes. The trial mixes then can be checked, and it is normally found that the proportions have to be adjusted according to experience gained from the trial mixes[229, 429].

The procedures in the mix design process are shown in Figure 2. 30. The required properties of the concrete – freshness and hardness, which are required in the structural design process, will determine the mix proportion of the concrete. The required strength is usually specified as the strength of concrete at the age of 28-days and is called characteristic strength[430].

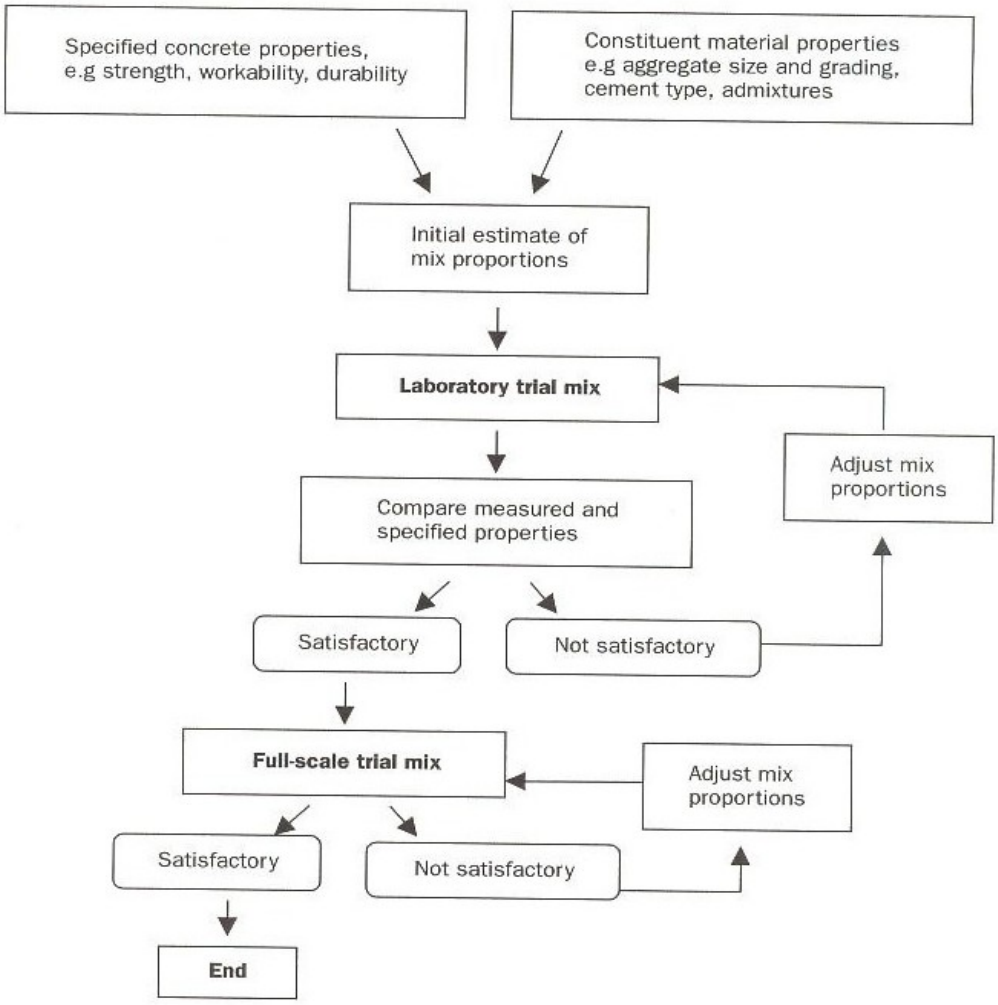

Figure A .29: The mix design process[430]

There are many methods with different steps of procedures to estimate the mix proportion of concrete. Many countries like the UK have their own preferred method to estimate the proportion of concrete mix. However, it is important to recognise that whichever method is used, the result is only a best estimate, perhaps even only a good guess. The reason is that the constituent materials are not exactly the same as assumed and their interaction cannot be predicted with any great certainty[429, 430]. Therefore, it is unlikely to meet the requirements precisely of a desired concrete.

A.6.1. Normal Concrete Mixes Design (BRE Method)

The Building Research Establishment (BRE) method offers a good procedure of the process of an initial estimate of the mix proportions. The procedures are simple and provide reasonable results, where all the materials needed most commonly are available in the UK.

The main part of the BRE method is concerned with the design of mixes incorporating Portland cement, water, and normal density coarse and fine aggregates only, and with characteristic strengths of concrete up to 70 N/mm^2, which is considered as normal or medium strength of concrete[229, 430]. Furthermore, the method includes modifications to estimate the mix proportion for the concrete containing entrained air, FA and GGBS. The principle behind the method is that the restricted data usually available at the mix design stage, and the mix proportions are derived in an attempt to produce a concrete having the required workability and strength.

The BRE method prepares the stages in estimation of the mix proportion. Each of these stages deals with a particular aspect of the design and ends with an important parameter or final unit proportions. The stages are as follow[229]:

- Stage 1 determines target mean strength based on characteristic strength leading to the free-water/cement ratio.
- Stage 2 selection of workability that leads to the determination of the free water content.
- Stage 3 combines the results of Stages 1 and 2 to give the cement content by dividing the free water content with the free water/cement ratio
- Stage 4 determines of the total aggregate content
- Stage 5 selection of the fine and coarse aggregate contents

GGBS complying with BS EN 15167-1[381] can be added in the mixer, incorporation with Portland cement class 42.5 and 52.5 complying with BS EN 197-1[234]. This aims to obtain similar properties of the concrete, which uses

Portland-blast furnace cement or other composites cement between Portland cement and GGBS. Normally, the GGBS acts as water-reducing agent, when it is added in a concrete mix as a replacement of cement. It enables the reduction of water by 5 kg/m^3 of concrete of that is used by its equivalent concrete mix with Portland cement only. Guidance such as the maximum amount of GGBS required in the varying conditions may be needed in estimating the mix proportion of the GGBS concrete.

A.6.2. Modified Maximum Density Theory (MMDT) Method

The main principle of the maximum density method in concrete mix design is the requirement that the aggregate occupies as large a part of volume of mix as possible, which results in minimum required volume of cement paste. Therefore, the mix needs less cement, which leads to an economic mix deign. The theory has been developed since the 1920s, which is based on the assumption that a concrete mix with the density of the maximum value will result in maximum strength and imperviousness of concrete[245].

Beshr et al[431] investigated the effect of coarse aggregate quality on the strength of high strength concrete using four different types of coarse aggregate. They found that the quality of coarse aggregate has a significant effect on the compressive strength of high strength concrete rather than that in normal strength of concrete.

Domone and Soutsos[230] reported that in order to obtain high-strength in concrete, some essential factors is required such as:

- A low water-cement ratio (w/c) or water-cementitious-material ratio (w/(c+m)), however, achieving this by increasing the cementitious materials content will not in itself guarantee a high strength concrete.
- Good quality of aggregate includes its grading and maximum size, where the fine aggregate is recommended to have fineness modulus of 3.0 and it should be free of clay or silt.

- The use of plasticizers or superplasticizers is vital to have an adequate workability of concrete, without an over cementitious content.
- The strength of the transition zone between the aggregate's surface and the hardened cement paste should be improved.

As has been mentioned before the maximum density theory results in minimum cement or cementitious paste, as most of the volume of concrete is aggregate, where the voids are filled with cement or cementitious paste. It is interesting to note that in high strength concrete, to obtain a high strength, an increase of cement content is not necessary[230, 245].

Domone and Soutsos[230] further reported that the increase of cement content will result in: increased stickiness and loss of workability, enhanced temperature rise in concrete during hydration, the possibility of risk thermal cracking at early age, as well as creep and shrinkage.

The use of aggregate as large a relative volume of concrete with a minimum of cement or cementitious paste will result in a workability problem. To overcome this problem, the maximum density theory needs a modification that takes into account the effect of the aggregate surface area and void content. The method has been established since 1992, which is called *'modified maximum density theory'* (MMDT). The modified method takes into account the volume of paste that is needed not only to fill the voids in the aggregate system. An excess over and above this amount (overfill) is also needed to provide a lubrication between the particles of aggregate, which then increases the workability[245].

The modified maximum density theory is an approach to design the high strength of concrete. The proportion of the constituent materials of the concrete is estimated by assuming that the total volume of all the ingredients of the concrete including the overfill paste is one cubic metre. The procedures to estimate the mix proportion of concrete is as follow:

- Stage 1: determine the void content of the combined aggregates (fine and coarse aggregates) of selected proportion of the fine and coarse aggregates.
- Stage 2: select the percentage of overfill cement paste.
- Stage 3: select the free water-cement ratio or free water-binder ratio.
- Stage 4: determine the proportion by volume of both paste and aggregate total.
- Stage 5: estimate the mass of cement or binder and water in the needed volume of paste per cubic meter of concrete.
- Stage 6: estimate the mass of fine and coarse aggregates based on the volume of aggregate total per cubic meter of concrete.
- Stage 7: adjust the mass of each aggregate for water absorption.
- Stage 8: adjust the mass of water for absorption and reducing water by using the superplasticizier in concrete.

APPENDIX B

Email from Peter Seymour asking for the data obtained from this study

Turu'allo, Gidion

From: Peter Seymour [pete.seymour@ecocem.ie]
Sent: 13 February 2013 07:04
To: Turu'allo, Gidion
Cc: Marios Soutsos
Subject: RE: Data for Ecocem

Hi Gidion,

Apologies for the delay in this response.

Thank you for the data you have supplied. This is a useful data set, as it gives a good view on how temperature affects early strength of concrete with varying levels of GGBS. We are using it as base data in an evaluation of how the use of heated water (20°C and above) can be used in the precast concrete manufacturing industry to counteract the slower early age strength gain that can occur when GGBS is used.

As the demand for lower carbon construction materials increases, it is necessary to find new solutions for some of the technical difficulties posed by these materials.

Your data has been a useful reference in studying this problem.

Many thanks for your assistance,

Kind regards,

Peter

Peter Seymour C.Eng., M.I.E.I.
Business Development Director
Ecocem Ireland Ltd
Portview House (Third Floor)
Thorncastle Street
Ringsend
Dublin 4

tel: +353 (0)1 667 0900
mob: +353 (0)87 258 9783

www.ecocem.ie
www.carbonneutralconcrete.com
www.emissionzero.ie

From: Peter Seymour
Sent: 10 January 2013 11:14

To: 'Turu'allo, Gidion'
Subject: RE: Data for Ecocem

Hi Gideon,

Got those. Many thanks.

I'll read through them now, and come back to you with any queries.

Thanks again,

Regards,

Peter

tel: +353 (0)1 667 0900
mob: +353 (0)87 258 9783

From: Turu'allo, Gidion [mailto:Gidion.Turuallo@liverpool.ac.uk]
Sent: 10 January 2013 11:03
To: Peter Seymour
Cc: 'Marios Soutsos'
Subject: RE: Data for Ecocem

Hi Peter,

I attach the data we talked about by telephone.

Thanks,

Best regards

Gidion

From: Peter Seymour [mailto:pete.seymour@ecocem.ie]
Sent: 10 January 2013 10:40
To: Turu'allo, Gidion
Subject: Data for Ecocem

Hi Gideon,

Further to correspondence with Marios, could you mail me your phone number, land-line or mobile, so I can discuss with you our requirement.

Many thanks,

Regards,

Peter

Peter Seymour C.Eng., M.I.E.I.
Business Development Director
Ecocem Ireland Ltd
Portview House (Third Floor)
Thorncastle Street
Ringsend
Dublin 4

tel: +353 (0)1 667 0900
mob: +353 (0)87 258 9783

www.ecocem.ie
www.carbonneutralconcrete.com
www.emissionzero.ie

CASTLE CEMENT
HEIDELBERGCEMENT Group

Laboratory Chemical Report

Castle Cement Limited
Technical Services
Ribblesdale Works
Clitheroe
Lancashire
BB7 4QF
Tel: 01200 422401
Fax: 01200 414172

Composition of Ribble Rapid Hardening PC, BS EN 197-1:2000, CEM I 52,5N
Manufactured at Ribblesdale.
Chemical analysis for week ending 11 Jan 2009 (Week No. 2)

Compound	%
SiO_2	19.88
Al_2O_3	5.06
Fe_2O_3	2.66
CaO	62.12
MgO	2.09
SO_3	3.19
K_2O	0.59
Na_2O	0.27
Cl	0.06
Loss on Ignition	2.93
Not Detected	1.15
Total	100.00

	%
Insol Residue	0.71
Free CaO	1.4
Total Alkali Na_2O (Equiv)	0.66
LSF (x 100)	93.5

Clinker compounds by calculation	
C_3S	51.9
C_2S	21.9
C_3A	10.2
C_4AF	8.2

For and on behalf of
CASTLE CEMENT LIMITED

S D Pepper FICT
National Technical Manager (Commercial)

Registered Office: Park Square, 3160 Solihull Parkway, Birmingham Business Park, Birmingham B37 7YN Registered in England No 2182762

Civil + Marine

CHEMICAL ANALYSIS RESULTS

The sample was tested following the methods given in BS EN 196-2 : 2005.
Additions and modifications have been made in accordance with the Civil + Marine Testing Manual.

Scunthorpe Spot Sample

Sample Period :	January 2009	

Chemical Composition %

SiO_2	35.82	S^t	0.83
Al_2O_3	13	S^{2-}	0.81
Fe_2O_3	0.53	SO_3	0.05
CaO	40.62	L.O.I.	0.66
MgO	8	I.R.	0.36
MnO	0.51	C	0.07
Mn_2O_3 Calc.	0.57	Cl	0.02
TiO_2	0.53	Glass Count	n/a

Relative Density g/cm³	n/a

Slag 'Rapid Cooling' Method

The majority of the feed is manufactured by Granulation, though on occasion a proportion of it may be by Pelletisation.

The GGBS contained no additional materials other than those permitted. The above results and other tests demonstrate the conformity of the material sold during the month to the requirements of EN 15167-1:2006

BSI REGISTERED UKAS QUALITY MANAGEMENT 003 FM 507625

BSI REGISTERED UKAS ENVIRONMENTAL MANAGEMENT 003 53307

Signed: *M D Connell*

M D Connell MICT, MIAT, FIHIE, I Eng. National Technical Manager

Telephone 01724 282211

Appendix C

Table C-1: Trial mixes proportion

Water/ Binder ratio	GGBS of total binder %	Mixture Proportion							Slump mm
		Kg / m³						SPA, %	
		Portland cement	GGBS	Granite	Sand	Free water	Total water		
0.25	0	475	-	1270	685	119	126	0.50	165
	20	377	94	1270	685	118	128	0.27	65
	35	304	164	1270	685	117	126	0.35	200
	50	232	232	1270	685	116	126	0.3	100
	70	138	322	1270	685	115	125	0.25	45
0.30	0	437	-	1270	685	131	140	0.40	flowing
	20	347	87	1270	685	130	142	0.22	70
	35	280	151	1270	685	129	140	0.25	75
	50	214	214	1270	685	128	139	0.25	75
	70	127	297	1270	685	127	138	0.25	flowing
0.35	0	405	-	1270	685	142	154	0.19	65
	20	321	80	1270	685	141	153	0.12	50
	35	259	140	1270	685	140	152	0.15	55
	50	198	198	1270	685	139	152	0.07	55
	70	118	275	1270	685	138	151	0.07	60
0.40	0	377	-	1270	685	151	163	0.16	120
	20	299	75	1270	685	149	163	0.2	175
	35	242	130	1270	685	149	161	0.15	120
	50	185	185	1270	685	148	161	0.07	75
	70	110	257	1270	685	147	160	0.07	85
0.45	0	352	-	1270	685	159	173	-	60
	20	280	70	1270	685	157	172	-	65
	35	226	122	1270	685	157	171	-	70
	50	173	173	1270	685	156	170	-	65
	70	103	240	1270	685	155	169	-	75
0.56	0	339	-	1264	623	190	204	-	120
	20	271	68	1264	623	190	204	-	125
	35	220	119	1264	623	190	204	-	175
	50	169.5	169.5	1264	623	190	204	-	120
	70	102	237	1264	623	190	204	-	140
0.63	0	302	-	1289	636	190	204	-	125
	20	242	60	1289	636	190	204	-	137
	35	196	106	1289	636	190	204	-	190
	50	151	151	1289	636	190	204	-	170
	70	91	211	1289	636	190	204	-	160
0.69	0	275	-	1306	644	190	204	-	150
	20	220	55	1306	644	190	204	-	165
	35	179	96	1306	644	190	204	-	170
	50	137.5	137.5	1306	644	190	204	-	175
	70	82.5	192.5	1306	644	190	204	-	165

Table C-2: Mixture proportions for lightweight and self compacting concretes

Mix / Ingredients	kg /m³							
	LW-PC	LW-FA	LW-FA act	LW-GGBS	LW-GGBS act	NWSCC-PC	LWSCC-GGBS	LWSCC-LSP
Cement type I 42.5	450	225	225	225	225	460	424	419
Fly ash	-	154	154	-	-	-	-	-
GGBS	-	-	-	211	211	-	181.5	-
LSP	-	-	-	-	-	-	-	180
SIKA-SPA	2.25	1.89	1.89	2.18	2.18	-	-	-
Lytag 4-14 mm	561	561	561	561	561	-	351	351
Sand	787	787	787	787	787	781	819	819
Granite	-	-	-	-	-	954	-	-
Na_2SO_4	-	-	15.15	-	17.43	-	-	-
LARSEM Chemcrete HP3	-	-	-	-	-	2.5	3.3	3.3
Free water	189	159	159	183	183	209	208	210
w/b	0.42	0.42	0.42	0.42	0.42	0.45	0.35	0.35

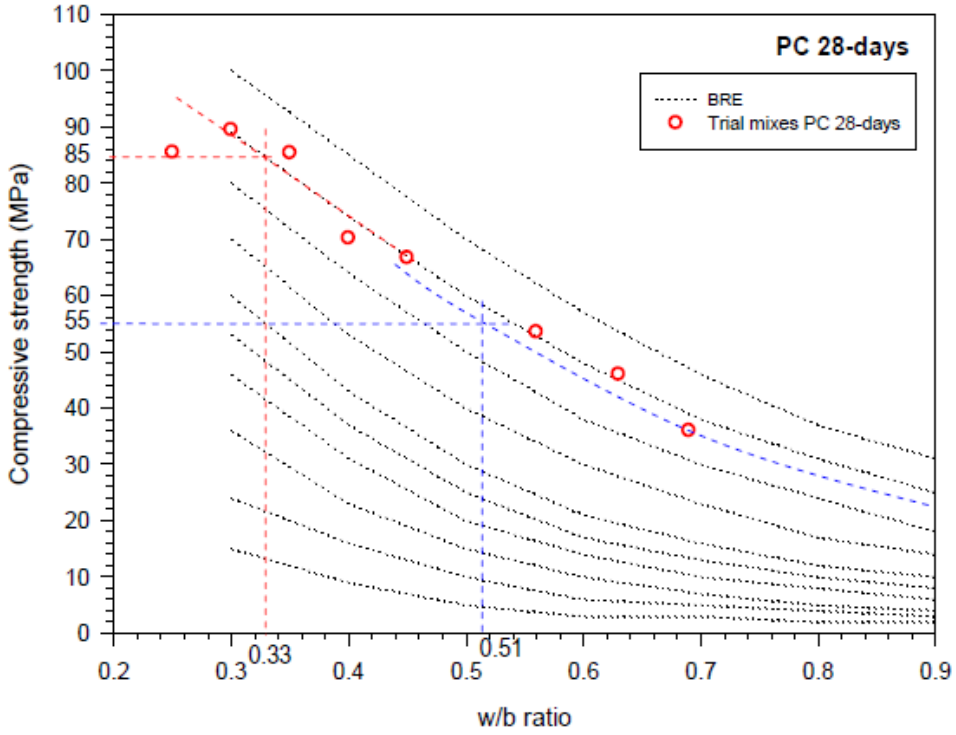

Figure C -1: Determination water-cement ratio for PC concrete investigated

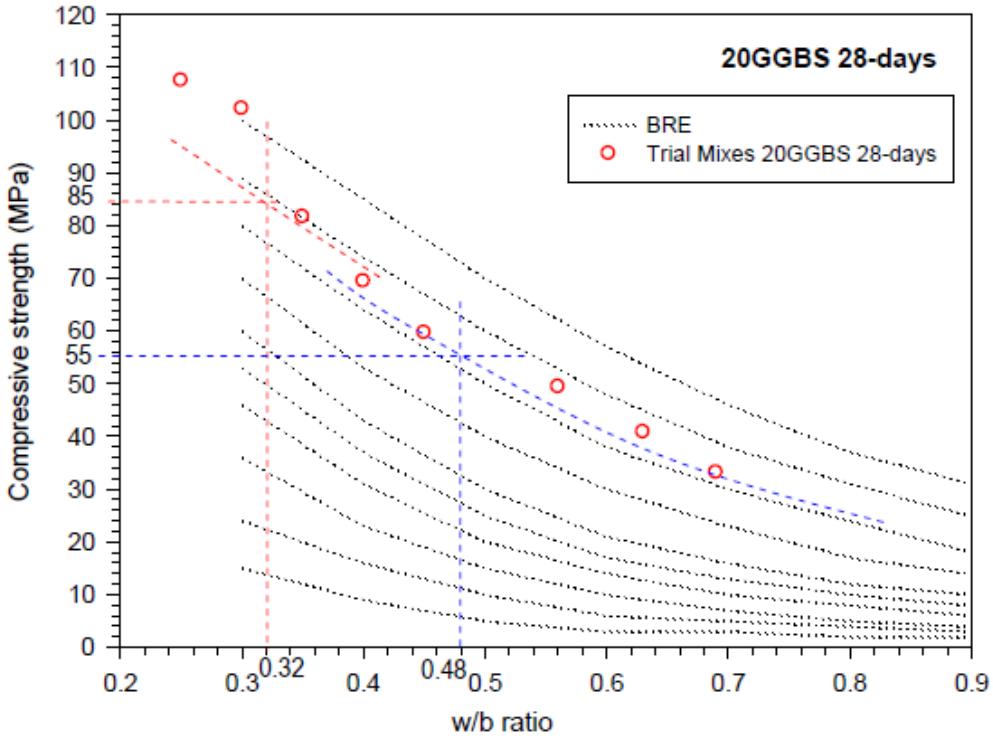

Figure C-2: Determination water-cement ratio for 20GGBS concrete investigated

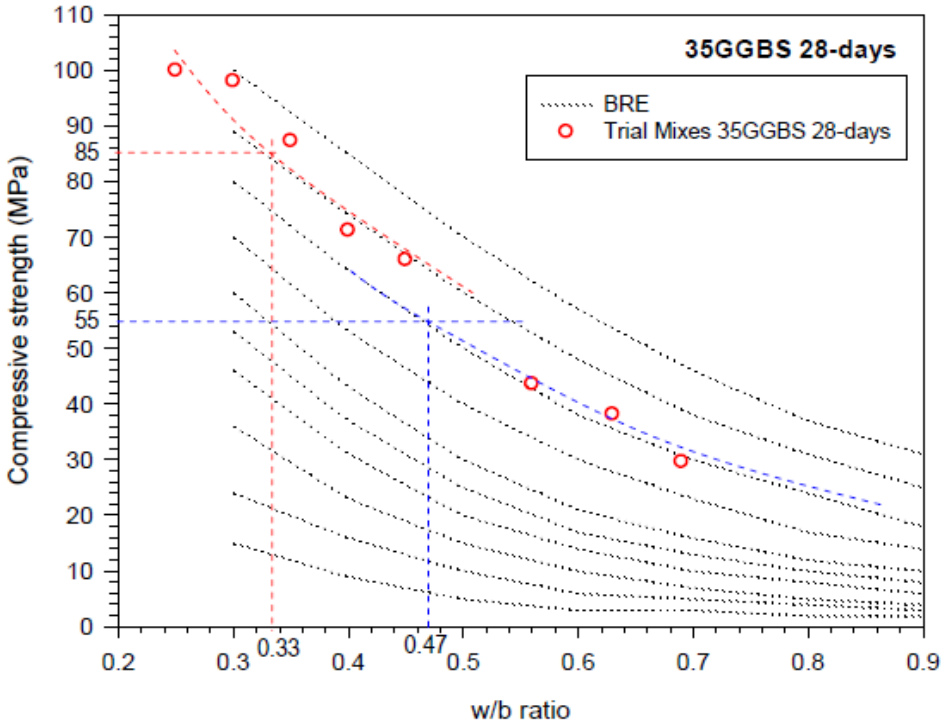

Figure C-3: Determination water-cement ratio for 35GGBS concrete investigated

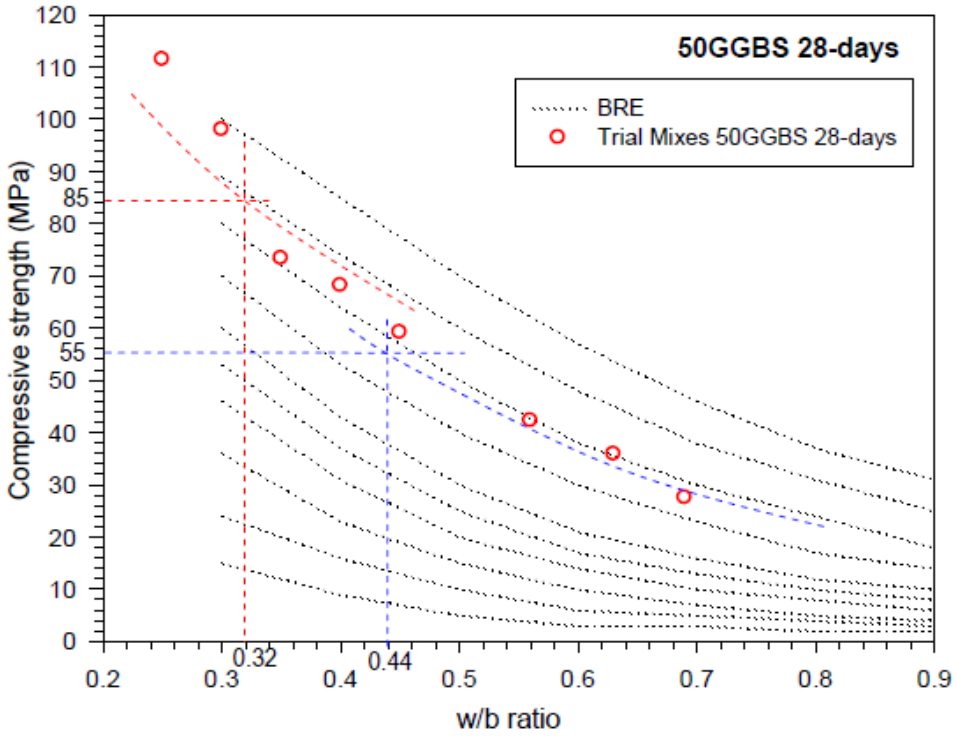

Figure C-4: Determination water-cement ratio for 50GGBS concrete investigated

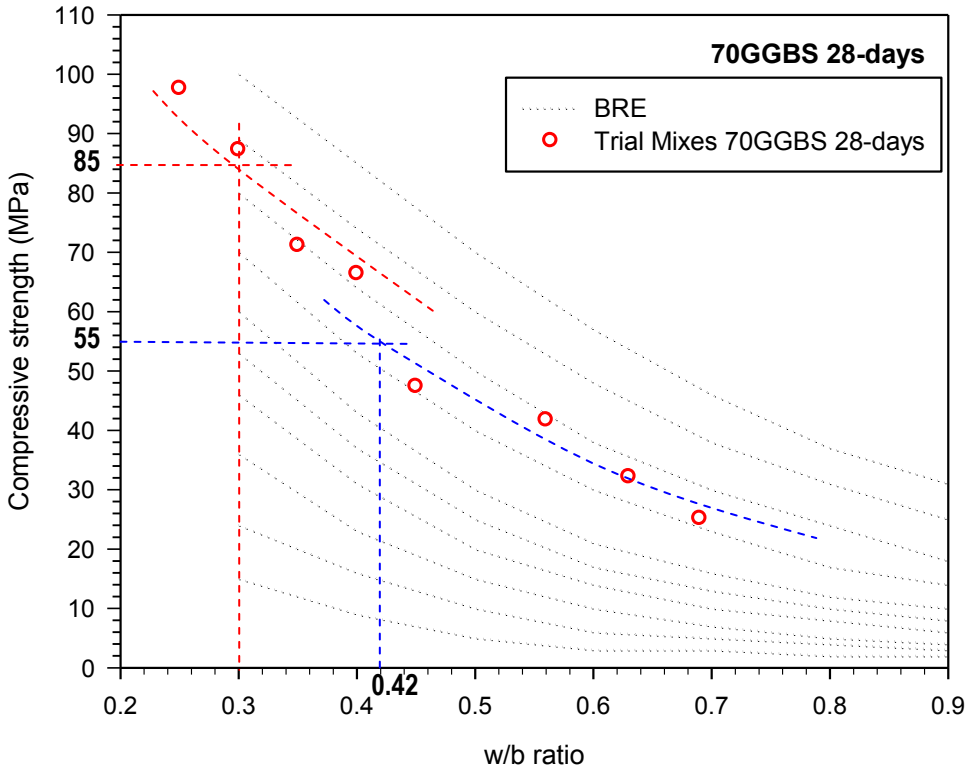

Figure C - 5: Determination water-cement ratio for PC concrete investigated

Table D - 1: Compressive test results for mortar **PC45** cured at 10, 20, 30, 40 and 50^{0}C and adiabatic condition

Age (Days)	Strength at different curing temperature (N / mm^2) - Mortar PC45																	
	10 ^{0}C			20 ^{0}C			30 ^{0}C			40 ^{0}C			50 ^{0}C			adiabatic		
	avr	min	max	avr	min	max	avr	min	max	avr	min	max	avr	min	max	avr	min	max
0.25							2.35	2.18	2.54	7.43	7.39	7.47	10.67	10.48	10.84	1.75	1.74	1.76
0.5				7.67	7.64	7.71	11.33	10.65	12.09	15.47	14.50	16.40	20.57	20.40	20.70	20.10	19.70	20.70
1	6.63	5.77	7.48	19.65	19.40	19.90	29.10	28.40	29.80	29.40	28.60	30.20	26.30	26.20	26.40	27.80	27.60	28.00
2	17.63	16.80	19.20	26.97	26.40	27.70	37.10	34.30	38.60	37.00	35.20	38.30	34.70	34.10	35.30	44.70	43.80	45.30
4	31.35	30.00	32.70	38.15	35.70	40.60	42.50	41.60	43.40	40.35	39.40	41.30	40.15	39.70	40.60	47.70	46.90	48.50
8	37.23	35.80	39.30	41.70	39.90	43.00	47.10	46.80	47.40	42.87	42.20	43.80	42.17	39.80	43.90	51.85	50.80	52.90
16	50.13	48.40	51.60	48.80	48.20	49.40	51.37	49.50	53.20	46.17	45.30	46.70	42.57	40.20	44.80	48.97	47.60	49.80
32	52.53	50.40	54.30	55.40	54.80	56.20	54.67	53.50	55.90	47.53	46.50	49.30	43.50	43.30	43.70	46.27	45.80	46.80
64	54.85	54.50	55.20	57.10	56.30	57.90	55.75	54.60	56.90	50.10	49.90	50.30	47.80	45.80	49.80	53.30	52.70	53.90
128	57.95	57.60	58.30	59.05	58.60	59.50	56.55	54.90	58.20	53.10	52.60	53.60	48.65	47.90	49.40	56.55	55.30	57.80
256	60.45	59.50	61.40	60.20	59.40	61.00	55.60	54.70	56.50	54.75	54.40	55.10	50.20	49.80	50.60	56.75	55.90	57.60
365	65.53	64.20	66.60	63.07	60.30	64.60	57.93	56.30	59.70	55.87	53.60	57.30	53.20	52.40	54.00	58.53	57.10	60.10

Table D - 2: Compressive test results for mortar **20GGBS45** cured at 10, 20, 30, 40 and 50^{0}C and adiabatic condition

Age (Days)	Strength at different curing temperature (N / mm^2) - Mortar 20GGBS45																	
	10 ^{0}C			20 ^{0}C			30 ^{0}C			40 ^{0}C			50 ^{0}C			adiabatic		
	avr	min	max	avr	min	max	avr	min	max	avr	min	max	avr	min	max	avr	min	max
0.25							4.26	4.11	4.41	7.53	7.43	7.62	8.30	8.18	8.42	1.755	1.7	1.81
0.5				4.43	4.28	4.57	8.94	8.76	9.11	14.36	13.92	14.80	18.05	17.80	18.30	16.67	16.50	16.80
1	6.44	6.24	6.77	15.81	15.80	15.82	24.75	24.50	25.00	27.93	25.60	30.40	28.70	28.30	29.10	34.45	34.40	34.50
2	14.30	14.10	14.50	22.57	21.80	23.11	31.47	30.30	32.80	35.65	34.80	36.50	35.70	34.60	36.80	42.15	41.80	42.50
4	25.20	24.80	25.60	33.15	32.70	33.60	43.65	43.00	44.30	41.45	40.00	42.90	39.80	39.60	40.00	43.10	42.00	44.20
8	32.77	32.30	33.50	39.95	38.60	41.30	44.15	43.50	44.80	47.40	47.10	47.70	43.03	42.30	43.60	45.37	42.70	47.20
16	37.65	36.80	38.50	47.57	46.90	47.90	47.20	45.50	49.90	48.90	48.60	49.30	45.73	44.50	47.50	46.60	45.60	47.50
32	50.37	48.80	53.20	55.47	54.70	56.30	55.20	54.20	56.70	54.83	53.10	56.70	48.07	46.72	49.70	51.20	49.90	52.50
64	53.00	52.50	53.80	56.37	54.90	57.80	58.15	56.60	59.70	57.00	56.10	57.90	50.17	48.60	52.10	49.20	48.90	49.50
128	56.10	55.32	56.88	57.15	56.68	57.62	60.56	59.96	61.16	58.62	56.63	60.60	53.36	52.72	54.00	58.32	58.20	58.44
256	65.10	63.80	66.40	58.90	58.20	59.60	61.20	60.50	61.90	60.10	58.90	61.30	54.35	54.30	54.40	67.40	65.60	69.20
365	66.53	64.50	67.60	63.43	62.30	64.70	61.43	59.50	63.00	60.50	58.50	62.50	57.13	56.70	57.80	68.23	66.90	69.00

Table D - 3: Compressive test results for mortar **35GGBS45** cured at 10, 20, 30, 40 and 50^{0}C and adiabatic condition

Age (Days)	Strength at different curing temperature (N / mm^2) - Mortar 35GGBS45																	
	10 ^{0}C			20 ^{0}C			30 ^{0}C			40 ^{0}C			50 ^{0}C			adiabatic		
	avr	min	max	avr	min	max	avr	min	max	avr	min	max	avr	min	max	avr	min	max
0.25							2.28	2.21	2.34	3.91	3.90	3.91	5.77	5.57	5.97	1.07	1.06	1.08
0.5				2.63	2.45	2.80	7.41	7.21	7.61	13.45	12.90	14.00	16.57	16.53	16.60	7.29	7.27	7.31
1	4.47	4.46	4.47	9.58	8.98	10.18	16.75	14.90	18.60	23.67	22.20	25.10	26.15	25.80	26.50	25.50	24.50	26.50
2	10.79	10.38	11.19	17.20	15.90	18.80	30.95	30.10	31.80	32.65	32.60	32.70	34.15	34.10	34.20	35.30	33.60	36.50
4	18.70	18.30	19.10	27.77	26.50	28.50	35.90	34.60	36.60	37.90	35.90	40.10	36.50	35.50	37.20	45.05	44.50	45.60
8	26.80	25.80	27.90	35.00	34.10	36.60	46.25	45.40	47.10	44.60	43.30	45.90	43.60	43.50	43.70	48.05	46.80	49.30
16	38.13	35.40	40.90	45.00	44.60	45.40	48.03	46.20	49.30	47.40	46.10	48.20	44.67	43.10	46.30	53.13	51.00	54.40
32	48.63	47.20	49.60	54.10	52.20	55.80	51.30	48.60	54.00	49.10	48.30	49.90	44.70	43.90	45.50	47.10	46.70	47.50
64	54.13	51.80	55.80	55.40	54.60	56.20	54.63	54.10	55.50	51.15	50.20	52.10	47.47	46.90	47.90	51.20	50.60	51.80
128	57.33	56.40	58.20	56.77	56.20	57.60	55.07	53.70	57.20	54.55	53.90	55.20	51.50	51.30	51.70	55.10	54.40	55.80
256	57.80	56.40	59.20	59.77	57.30	64.30	58.75	56.10	61.40	55.63	53.60	56.70	55.10	53.70	56.50	57.10	56.20	58.00
365	59.50	58.00	61.30	60.43	58.60	62.20	60.17	58.80	61.50	57.03	56.20	58.00	56.53	54.30	58.00	59.87	58.70	60.60

Table D - 4: Compressive test results for mortar **50GGBS45** cured at 10, 20, 30, 40 and 50^{0}C and adiabatic condition

Age (Days)	Strength at different curing temperature (N / mm^2) - Mortar 50GGBS45																	
	10 ^{0}C			20 ^{0}C			30 ^{0}C			40 ^{0}C			50 ^{0}C			adiabatic		
	avr	min	max	avr	min	max	avr	min	max	avr	min	max	avr	min	max	avr	min	max
0.25																		
0.5							4.05	3.68	4.33	8.11	8.07	8.16	14.79	14.31	15.20	3.48	3.30	3.65
1	3.17	3.11	3.28	4.99	4.90	5.06	15.13	14.60	15.60	25.37	24.80	26.00	29.53	28.10	30.90	32.93	31.00	34.60
2	7.84	7.51	8.09	12.23	11.49	12.80	28.97	27.80	29.60	33.00	31.20	34.50	35.87	34.90	36.80	50.67	49.70	51.90
4	15.87	14.70	16.50	22.20	21.70	23.20	36.73	35.50	38.40	41.40	38.70	43.00	38.77	38.40	39.20	53.27	52.50	53.80
8	27.60	26.40	28.50	36.40	35.40	38.10	47.30	46.80	48.20	48.57	48.50	48.60	46.53	45.80	47.00	59.60	59.00	60.20
16	41.10	39.60	42.30	50.03	49.70	50.60	52.47	50.00	54.10	50.50	49.20	52.50	49.00	47.10	50.20	63.80	62.30	65.00
32	54.40	53.20	56.40	55.23	54.80	55.80	55.90	54.60	57.30	54.77	52.30	57.40	52.80	51.30	55.70	61.27	59.80	63.40
64	60.37	60.00	60.90	59.97	59.60	60.50	58.43	57.30	59.30	57.17	56.20	58.80	55.73	54.70	57.00	68.37	66.60	69.40
128	63.43	62.40	64.00	61.37	59.70	63.50	60.33	58.60	62.30	58.43	56.80	60.10	56.77	55.00	58.40	70.37	71.36	73.40
256	66.47	65.60	67.80	63.97	62.60	65.00	62.20	61.70	62.60	59.60	58.40	61.00	57.40	56.80	58.00	72.31	71.36	73.40
365	67.57	66.00	69.40	65.00	64.20	65.70	63.13	62.50	63.70	60.03	58.20	61.50	58.47	57.30	60.00	73.70	73.00	74.80

Table D - 5: Compressive test results for mortar 70GGBS45 cured at 10, 20, 30, 40 and 50^{0}C and adiabatic condition

Age (Days)	Strength at different curing temperature (N / mm^2) - Mortar 70GGBS45																	
	10 ^{0}C			20 ^{0}C			30 ^{0}C			40 ^{0}C			50 ^{0}C			adiabatic		
	avr	min	max	avr	min	max	avr	min	max	avr	min	max	avr	min	max	avr	min	max
0.25																		
0.5										7.13	6.86	7.40	11.85	11.10	12.60			
1				2.44	2.20	2.61	10.19	9.59	10.84	17.93	17.60	18.40	29.30	29.00	29.60	7.75	7.55	7.94
2	3.30	3.25	3.34	6.47	6.32	6.61	25.20	25.00	25.40	31.77	30.30	33.40	33.47	32.70	34.80	37.30	36.20	38.40
4	9.80	9.72	9.87	15.56	15.30	15.70	35.80	35.10	36.50	42.75	42.70	42.80	37.85	37.70	38.00	41.67	40.50	43.20
8	21.83	20.80	22.50	30.15	29.40	30.90	40.80	39.70	42.80	47.37	46.30	48.40	41.93	41.10	43.20	50.00	48.60	50.90
16	32.69	31.48	33.80	39.30	38.80	40.20	47.90	46.90	49.00	50.24	48.90	52.70	42.28	41.70	43.30	52.01	50.84	53.60
32	50.33	49.30	51.60	55.23	54.50	56.60	54.23	52.90	55.10	50.50	49.40	51.20	47.67	45.20	49.20	52.07	51.80	52.60
64	55.93	54.10	57.90	56.70	55.90	57.60	55.67	55.00	56.80	53.70	52.80	54.60	50.43	49.60	51.50	54.97	54.00	56.30
128	60.53	59.90	61.50	58.23	56.40	59.90	57.43	55.60	58.80	56.33	55.60	57.10	53.03	50.70	54.60	59.33	58.10	60.90
256	61.10	59.50	62.80	59.13	58.30	60.20	58.47	57.90	59.00	57.30	56.90	57.60	56.53	55.50	57.50	61.40	59.60	63.10
365	61.43	59.30	63.50	59.60	58.60	60.40	59.40	58.70	60.10	58.00	56.90	59.60	56.80	56.40	57.50	64.37	63.50	65.60

Table D - 6: Compressive test results for mortar **PC75** cured at 10, 20, 30, 40 and 50^{0}C and adiabatic condition

Age (Days)	Strength at different curing temperature (N / mm^2) - Mortar PC75																	
	10 ^{0}C			20 ^{0}C			30 ^{0}C			40 ^{0}C			50 ^{0}C			adiabatic		
	avr	min	max	avr	min	max	avr	min	max	avr	min	max	avr	min	max	avr	min	max
0.25				4.915	4.88	4.95	7.63	7.36	7.9	19.75	19.6	19.9	24.70	24.30	25.10	23.95	23.8	24.1
0.5	4.30	4.24	4.36	13.40	13.20	13.60	25.90	25.20	26.60	32.50	32.30	32.70	35.35	34.90	35.80	40.65	39.40	41.90
1	14.15	13.80	14.50	34.95	34.90	35.00	40.10	39.50	40.70	43.85	43.70	44.00	42.05	41.60	42.50	49.40	49.00	49.80
2	34.40	34.30	34.50	45.35	45.30	45.40	46.55	46.40	46.70	49.60	48.80	50.40	46.15	46.10	46.20	57.15	56.10	58.20
4	47.70	47.30	48.10	50.90	50.50	51.30	52.35	52.00	52.70	53.30	52.80	53.80	46.65	46.50	46.80	61.75	61.20	62.30
8	56.42	56.30	56.54	58.70	58.30	59.10	56.45	56.10	56.80	55.80	55.20	56.40	52.85	52.70	53.00	66.45	65.30	67.60
16	57.60	56.80	58.40	64.15	63.80	64.50	59.40	59.10	59.70	56.75	56.40	57.10	55.90	55.40	56.40	75.20	74.60	75.80
32	61.25	60.80	61.70	64.75	64.40	65.10	61.65	60.80	62.50	63.25	62.50	64.00	56.55	56.10	57.00	71.88	70.40	73.36
64	68.40	68.00	68.80	65.05	64.80	65.30	64.15	64.00	64.30	63.40	62.90	63.90	60.40	58.90	61.90	80.10	79.50	80.70
128	71.30	69.40	73.20	70.75	69.60	71.90	66.80	65.50	68.10	69.70	68.40	71.00	66.10	65.70	66.50	80.65	79.30	82.00
256	76.40	74.60	78.20	76.30	75.60	77.00	70.00	69.60	70.40	69.10	68.20	70.00	67.00	66.80	67.20	81.45	80.60	82.30
365	78.80	78.30	79.10	78.07	77.10	78.80	74.77	73.90	75.60	73.40	72.90	74.00	69.30	68.70	69.90	90.24	90.00	90.48

Table D - 7: Compressive test results for mortar **20GGBS75** cured at 10, 20, 30, 40 and 50^{0}C and adiabatic condition

Age (Days)	Strength at different curing temperature (N / mm^2) - Mortar 20GGBS75																	
	10 ^{0}C			20 ^{0}C			30 ^{0}C			40 ^{0}C			50 ^{0}C			adiabatic		
	avr	min	max	avr	min	max	avr	min	max	avr	min	max	avr	min	max	avr	min	max
0.25				1.035	1.03	1.04	4.26	4.19	4.33	12.90	12.6	13.2	18.35	18.00	18.70	20.45	20.3	20.6
0.5	1.21	1.15	1.26	10.79	10.55	11.03	19.45	19.40	19.50	27.60	27.30	27.90	32.05	31.90	32.20	38.05	37.50	38.60
1	10.09	9.43	10.74	26.00	25.10	26.90	33.65	33.00	34.30	40.45	40.10	40.80	44.00	43.60	44.40	56.70	55.70	57.70
2	24.65	24.60	24.70	38.60	37.80	39.40	47.65	46.60	48.70	51.45	50.50	52.40	47.95	46.40	49.50	65.55	64.30	66.80
4	39.00	38.60	39.40	50.45	49.80	51.10	52.40	52.30	52.50	55.40	54.40	56.40	53.00	52.10	53.90	66.45	65.90	67.00
8	49.35	48.50	50.20	60.70	60.10	61.30	56.75	56.60	56.90	60.40	60.00	60.80	54.80	54.00	55.60	69.50	68.90	70.10
16	56.35	55.30	57.40	63.55	62.80	64.30	61.20	60.20	62.20	61.00	60.70	61.30	55.85	55.60	56.10	73.77	73.04	74.50
32	65.05	64.70	65.40	69.15	69.10	69.20	66.90	66.50	67.30	64.70	64.50	64.90	57.85	57.40	58.30	72.41	71.76	73.06
64	69.60	68.40	70.80	71.00	70.60	71.40	67.95	67.20	68.70	65.00	64.80	65.20	60.15	59.40	60.90	75.90	75.20	76.60
128	79.05	77.80	80.30	73.60	70.40	76.80	68.25	67.40	69.10	66.60	64.90	68.30	63.35	62.90	63.80	77.10	75.60	78.60
256	81.35	79.20	83.50	76.85	75.40	78.30	71.30	69.50	73.10	68.75	68.40	69.10	65.70	64.80	66.60	83.25	82.20	84.30
365	85.03	83.80	86.40	81.50	80.60	82.40	79.65	78.20	81.10	71.45	69.30	73.60	69.15	69.00	69.30	92.88	90.88	94.88

Table D - 8: Compressive test results for mortar **35GGBS75** cured at 10, 20, 30, 40 and 50^{0}C and adiabatic condition

Age (Days)	Strength at different curing temperature (N / mm^2) - Mortar 35GGBS75																	
	10 ^{0}C			20 ^{0}C			30 ^{0}C			40 ^{0}C			50 ^{0}C			adiabatic		
	avr	min	max	avr	min	max	avr	min	max	avr	min	max	avr	min	max	avr	min	max
0.25							2.72	2.67	2.77	7.79	7.51	8.07	12.99	12.87	13.10			
0.5				1.63	1.62	1.63	8.99	8.87	9.10	17.15	16.80	17.50	23.90	23.60	24.20	20.80	20.70	20.90
1	4.55	4.41	4.69	15.90	15.70	16.10	24.35	23.90	24.80	33.80	33.30	34.30	40.30	39.30	41.30	52.92	52.88	52.96
2	16.80	16.30	17.30	30.65	30.30	31.00	40.95	40.40	41.50	49.10	48.40	49.80	45.05	45.00	45.10	60.88	59.28	62.48
4	27.70	26.80	28.60	38.05	37.70	38.40	47.70	46.70	48.70	50.85	49.90	51.80	46.45	45.40	47.50	71.22	70.44	72.00
8	40.60	39.20	42.00	51.25	50.70	51.80	57.15	56.20	58.10	56.85	55.90	57.80	54.80	54.10	55.50	79.62	78.28	80.96
16	49.15	48.20	50.10	58.00	57.60	58.40	60.50	60.00	61.00	60.35	59.10	61.60	56.95	56.10	57.80	80.76	80.52	81.00
32	62.15	61.80	62.50	67.75	67.30	68.20	67.25	66.90	67.60	64.35	63.20	65.50	60.15	59.20	61.10	80.06	79.92	80.20
64	67.30	65.60	69.00	69.40	69.10	69.70	67.65	66.80	68.50	65.55	64.80	66.30	61.20	60.80	61.60	83.60	82.80	84.40
128	72.40	71.80	73.00	71.45	70.40	72.50	70.30	68.90	71.70	66.25	65.10	67.40	64.50	63.00	66.00	79.80	79.10	80.50
256	75.35	74.30	76.40	74.20	73.60	74.80	70.50	69.60	71.40	67.25	65.90	68.60	66.20	65.00	67.40	85.37	83.10	87.10
365	84.77	82.24	86.28	84.06	82.68	85.44	79.50	77.60	81.40	76.90	75.40	78.70	73.20	72.16	74.28	86.25	84.64	87.20

Table D - 9: Compressive test results for mortar **50GGBS75** cured at 10, 20, 30, 40 and 50^{0}C and adiabatic condition

Age (Days)	Strength at different curing temperature (N / mm^2) - Mortar 50GGBS75																	
	10 ^{0}C			20 ^{0}C			30 ^{0}C			40 ^{0}C			50 ^{0}C			adiabatic		
	avr	min	max	avr	min	max	avr	min	max	avr	min	max	avr	min	max	avr	min	max
0.25							1.61	1.55	1.66	4.08	4.07	4.09	7.22	7.18	7.25			
0.5				1.30	1.24	1.36	5.81	5.74	5.87	11.99	11.89	12.09	18.65	18.10	19.20	15.26	15.24	15.28
1	2.85	2.58	3.11	10.38	10.34	10.42	15.65	15.40	15.90	29.25	29.00	29.50	36.65	36.40	36.90	58.12	58.04	58.20
2	8.70	8.69	8.71	19.45	19.20	19.70	33.95	33.70	34.20	45.00	44.90	45.10	45.70	44.60	46.80	64.20	63.40	65.00
4	18.45	17.50	19.40	36.35	35.80	36.90	44.00	43.60	44.40	51.25	50.90	51.60	49.65	49.30	50.00	67.78	67.52	68.04
8	32.55	31.90	33.20	48.05	47.40	48.70	52.35	52.00	52.70	53.95	53.80	54.10	52.15	51.80	52.50	72.96	71.84	74.08
16	43.95	43.70	44.20	52.35	51.90	52.80	54.95	54.10	55.80	56.70	56.30	57.10	52.50	52.20	52.80	78.37	77.80	79.00
32	55.60	55.50	55.70	61.60	61.30	61.90	60.80	58.60	63.00	57.25	56.90	57.60	55.70	55.40	56.00	80.80	80.30	81.30
64	62.05	60.80	63.30	63.35	62.40	64.30	62.00	61.80	62.20	58.55	57.80	59.30	56.90	56.30	57.50	85.44	84.28	86.60
128	69.30	68.50	70.10	66.00	65.30	66.70	63.25	62.80	63.70	61.15	60.40	61.90	57.25	56.60	57.90	85.20	84.80	85.60
256	74.38	73.68	75.08	72.07	71.76	72.56	72.56	71.48	73.64	71.34	70.52	72.16	67.95	67.30	68.60	85.28	84.80	85.76
365	81.61	81.36	81.80	84.27	83.48	85.36	81.57	79.40	83.32	85.78	85.60	85.96	84.68	83.48	85.48	87.46	86.88	88.04

Table D - 10: Compressive test results for mortar **70GGBS75** cured at 10, 20, 30, 40 and 50^{0}C and adiabatic condition

Age (Days)	Strength at different curing temperature (N / mm^2) - Mortar 70GGBS75																	
	10 ^{0}C			20 ^{0}C			30 ^{0}C			40 ^{0}C			50 ^{0}C			adiabatic		
	avr	min	max	avr	min	max	avr	min	max	avr	min	max	avr	min	max	avr	min	max
0.25							1.04	1.02	1.06	2.56	2.44	2.67	5.18	5.13	5.22			
0.5				1.52	1.51	1.53	3.01	2.99	3.02	5.02	2.28	7.75	19.55	19.40	19.70	4.02	3.92	4.12
1	2.94	2.88	3.00	7.28	6.96	7.60	15.60	15.30	15.90	34.75	34.60	34.90	41.50	41.10	41.90	38.76	38.44	39.08
2	6.78	6.72	6.84	20.35	19.80	20.90	37.80	37.50	38.10	46.30	45.50	47.10	46.40	45.70	47.10	57.64	57.20	58.08
4	16.36	15.88	16.84	36.65	36.10	37.20	44.30	43.10	45.50	47.95	47.00	48.90	50.00	49.40	50.60	65.44	64.80	66.08
8	34.93	34.76	35.10	48.35	47.70	49.00	52.20	51.40	53.00	54.35	53.60	55.10	50.95	50.40	51.50	68.46	67.36	69.56
16	44.70	44.40	45.00	52.85	52.70	53.00	54.85	54.70	55.00	58.15	57.50	58.80	56.85	56.50	57.20	72.62	71.80	73.44
32	50.20	49.40	51.00	65.25	64.40	66.10	61.35	59.40	63.30	59.15	58.70	59.60	59.10	58.60	59.60	76.95	76.40	77.50
64	58.30	57.70	58.90	65.95	65.60	66.30	62.35	60.80	63.90	60.50	58.80	62.20	59.40	58.50	60.30	77.40	76.40	78.40
128	60.70	59.50	61.90	69.25	68.80	69.70	66.85	66.10	67.60	64.40	63.60	65.20	63.15	62.60	63.70	77.60	76.40	78.80
256	70.17	69.76	70.48	71.35	70.80	71.84	69.22	68.84	69.60	67.28	66.44	68.12	63.62	63.00	64.24	79.83	78.80	81.70
365	75.47	74.30	76.20	74.00	72.30	76.00	72.73	72.30	73.00	72.10	69.90	73.40	72.00	69.20	74.00	85.77	85.60	86.00

Table D - 11: Compressive test results for Concrete **PC45** cured at 20, 50^{0}C and adiabatic condition

Age (Days)	Strength at different curing temperature (N / mm2) - Concrete PC45								
	20 ^{0}C			50 ^{0}C			adiabatic		
	avr	min	max	avr	min	max	avr	min	max
0.25				15.56	15.30	16.06			
0.5	6.35	5.99	6.74	20.83	20.40	21.40	16.56	16.22	16.87
1	18.08	17.81	18.23	36.20	36.00	36.40	30.90	30.40	31.50
2	30.25	29.56	30.80	44.03	43.30	44.80	40.97	40.40	41.70
4	38.60	38.00	39.30	48.27	47.50	48.70	46.07	45.40	46.50
8	46.90	46.00	47.80	50.00	48.50	50.80	44.40	44.20	44.50
16	50.08	49.50	50.50	50.50	48.50	53.50	46.00	44.50	47.50
32	54.83	53.50	56.50	54.42	52.50	56.25	47.50	47.00	48.50
64	61.87	61.50	62.10	57.30	56.90	57.90	53.73	52.70	55.10
128	62.00	61.50	62.50	61.00	60.00	62.00	56.50	55.00	57.50
256	65.27	64.90	65.50	66.50	65.50	67.10	64.50	62.70	65.70
365	67.57	66.00	69.50	67.43	65.80	68.50	66.03	64.60	68.50

Table D - 12: Compressive test results for Concrete **20GGBS45** cured at 20, 50^{0}C and adiabatic condition

Age (Days)	Strength at different curing temperature (N / mm2) - Concrete 20GGBS45								
	20 ^{0}C			50 ^{0}C			adiabatic		
	avr	min	max	avr	min	max	avr	min	max
0.25				10.30	10.11	10.48			
0.5	4.92	4.79	5.03	21.22	20.90	21.40	16.92	16.15	17.51
1	14.41	14.21	14.72	33.50	33.30	33.70	35.07	34.60	35.60
2	25.64	25.19	26.15	43.80	42.70	44.40	44.87	44.40	45.40
4	37.00	36.40	37.50	51.70	50.90	52.40	47.80	45.70	50.50
8	43.75	42.50	44.50	54.50	54.00	55.00	49.33	48.00	51.50
16	54.00	53.50	54.50	57.00	56.50	57.50	52.50	52.00	53.00
32	58.57	57.50	59.40	61.87	60.40	63.90	63.13	62.50	63.50
64	66.83	65.70	68.50	65.20	64.90	65.70	59.20	57.80	60.40
128	68.50	67.50	69.50	65.33	64.50	66.00	65.17	64.00	66.50
256	76.27	74.80	78.50	70.20	68.50	71.50	79.53	78.70	80.60
365	78.17	76.20	79.90	72.57	70.10	74.90	80.50	79.10	81.60

Table D - 13: Compressive test results for Concrete **35GGBS45** cured at 20, 50^{0}C and adiabatic condition

Age (Days)	Strength at different curing temperature (N / mm2) - Concrete 35GGBS45								
	20 ^{0}C			50 ^{0}C			adiabatic		
	avr	min	max	avr	min	max	avr	min	max
0.25				6.75	6.50	7.00			
0.5	3.38	3.25	3.50	18.58	18.25	19.00	6.38	6.25	6.50
1	11.13	11.00	11.25	30.25	29.50	30.75	25.75	25.50	26.00
2	20.13	20.00	20.25	38.67	38.50	39.00	38.08	37.50	38.50
4	32.60	32.20	33.00	46.70	46.20	47.00	48.50	48.10	48.90
8	44.70	44.10	45.30	50.27	48.20	51.50	51.07	50.20	52.60
16	51.03	50.40	51.80	55.73	55.60	55.90	53.27	52.10	54.00
32	57.30	56.10	58.70	59.43	59.00	60.20	61.00	60.20	62.40
64	68.47	67.10	69.20	62.83	61.50	63.70	60.37	59.20	62.00
128	68.83	68.50	69.50	64.83	64.50	65.50	63.50	63.00	64.00
256	74.43	73.30	75.10	71.43	68.30	73.20	69.93	69.00	71.50
365	75.50	73.80	76.80	72.77	70.20	74.70	72.10	71.20	73.20

Table D - 14: Compressive test results for Concrete **50GGBS45** cured at 20, 50^{0}C and adiabatic condition

Age (Days)	Strength at different curing temperature (N / mm2) - Concrete 50GGBS45								
	20 ^{0}C			50 ^{0}C			adiabatic		
	avr	min	max	avr	min	max	avr	min	max
0.25				7.64	7.36	7.92			
0.5				20.39	19.70	21.07	5.70	5.06	6.04
1	9.30	8.97	9.59	37.10	36.90	37.30	24.39	24.15	24.82
2	19.03	17.04	20.26	48.57	47.80	49.80	46.83	45.80	48.30
4	34.00	32.60	35.40	52.57	51.40	53.80	54.07	53.10	54.80
8	46.10	45.20	46.70	59.30	58.20	60.70	59.57	58.90	60.40
16	51.93	50.10	53.50	63.77	62.90	65.20	66.17	65.50	66.60
32	60.90	60.00	61.80	66.80	66.10	67.70	65.97	65.50	66.40
64	70.40	69.20	71.90	69.37	67.20	70.50	69.30	68.40	70.40
128	72.67	72.00	73.50	72.33	69.00	74.50	71.50	69.00	73.50
256	79.07	77.40	81.40	76.83	73.60	79.50	74.90	73.60	76.50
365	84.67	84.10	85.60	79.37	77.60	81.90	76.20	74.40	78.30

Table D - 15: Compressive test results for Concrete **70GGBS45** cured at 20, 50^0C and adiabatic condition

Age (Days)	Strength at different curing temperature (N / mm2) - Concrete 70GGBS45								
	20 ^{0}C			50 ^{0}C			adiabatic		
	avr	min	max	avr	min	max	avr	min	max
0.25									
0.5				17.78	17.11	18.19			
1	5.25	5.00	5.50	34.42	33.00	35.25	10.67	10.00	11.00
2	9.83	9.75	10.00	40.33	39.50	41.50	37.50	37.00	38.00
4	25.50	25.00	26.00	44.33	43.00	45.00	45.33	44.50	46.00
8	39.33	38.50	40.00	49.50	49.00	50.00	48.67	48.00	49.50
16	46.67	45.50	47.50	49.83	49.00	51.00	49.33	48.50	50.50
32	54.95	54.70	55.20	55.10	53.90	56.00	55.50	54.50	56.40
64	59.33	58.30	60.20	58.70	58.00	59.70	59.53	58.30	60.50
128	62.17	60.50	63.50	61.67	60.50	63.00	63.00	60.50	64.50
256	68.90	67.70	70.80	66.37	64.40	67.90	66.20	65.50	66.70
365	70.90	70.20	71.70	67.93	66.30	68.90	71.20	70.80	71.50

Table D - 16: Compressive test results for Concrete **PC75** cured at 20, 50^0C and adiabatic condition

Age (Days)	Strength at different curing temperature (N / mm2) - Concrete PC75								
	20 ^{0}C			50 ^{0}C			adiabatic		
	avr	min	max	avr	min	max	avr	min	max
0.25				9.55	9.50	9.60			
0.5				27.20	27.10	27.30	3.05	3.00	3.10
1	7.95	7.90	8.00	56.50	55.50	57.50	17.65	17.50	17.80
2	17.30	17.10	17.50	62.00	60.00	63.50	57.37	56.50	58.10
4	41.30	40.40	42.00	65.83	64.50	66.50	72.50	72.00	73.00
8	59.83	59.00	61.00	72.00	71.50	73.00	73.00	72.00	73.50
16	67.00	66.50	68.00	76.50	76.00	77.00	77.83	77.50	78.00
32	78.93	78.40	79.90	79.60	78.40	81.60	84.20	83.60	85.00
64	84.90	83.80	85.70	80.10	79.00	81.80	89.90	89.40	90.50
128	87.93	85.40	89.70	83.17	81.10	84.70	90.73	90.60	90.90
256	91.60	89.60	93.10	91.47	89.30	93.20	94.20	94.00	94.40
365	100.90	98.50	104.70	94.07	92.50	95.80	100.17	98.20	102.10

Table D - 17: Compressive test results for Concrete **20GGBS75** cured at 20, 50^{0}C and adiabatic condition

Age (Days)	Strength at different curing temperature (N / mm2) - Concrete 20GGBS75								
	20 ^{0}C			50 ^{0}C			adiabatic		
	avr	min	max	avr	min	max	avr	min	max
0.25	2.30	2.14	2.46	26.18	25.96	26.40	2.08	2.04	2.12
0.5	13.24	13.05	13.43	37.45	36.80	38.10	28.18	27.80	28.55
1	31.73	31.30	32.50	57.70	57.20	58.20	57.65	57.10	58.20
2	44.90	44.10	46.00	66.73	66.10	67.30	68.67	68.20	69.30
4	52.17	50.50	53.50	76.50	76.00	77.00	76.00	75.00	77.50
8	66.50	65.50	67.50	77.33	76.50	78.00	79.00	78.00	80.50
16	78.33	77.50	79.00	84.83	84.00	86.00	79.83	78.50	81.50
32	87.03	85.50	88.40	85.33	84.50	87.00	91.50	89.50	95.00
64	89.13	87.50	90.00	88.23	87.50	89.00	92.10	90.00	94.60
128	91.57	88.10	94.00	96.93	95.00	98.40	99.50	97.50	101.40
256	100.37	98.60	101.60	101.63	99.30	103.00	102.40	100.50	104.40
365	106.67	104.70	109.20	103.70	103.00	104.30	104.60	103.50	105.60

Table D - 18: Compressive test results for Concrete **35GGBS75** cured at 20, 50^{0}C and adiabatic condition

Age (Days)	Strength at different curing temperature (N / mm2) - Concrete 35GGBS75								
	20 ^{0}C			50 ^{0}C			adiabatic		
	avr	min	max	avr	min	max	avr	min	max
0.25				21.88	21.75	22.00	1.625	1.5	1.75
0.5	4.63	4.50	4.75	34.25	33.00	35.50	11.75	11.50	12.00
1	26.63	26.25	27.00	59.75	59.50	60.00	56.00	55.00	57.00
2	35.17	35.00	35.50	65.50	64.50	66.50	64.83	64.00	66.00
4	51.23	50.50	52.50	76.50	75.50	77.00	78.50	77.50	79.50
8	63.33	62.50	64.00	83.33	83.00	83.50	81.00	80.50	81.50
16	81.00	80.00	82.00	87.00	85.00	88.50	89.33	87.50	90.50
32	86.70	86.10	87.50	90.67	88.00	92.50	92.33	91.50	93.00
64	90.30	89.30	90.90	93.20	90.60	95.60	97.67	95.60	99.90
128	95.07	90.70	97.50	102.00	100.40	104.00	104.33	100.00	109.00
256	96.63	95.90	97.70	105.07	104.20	106.70	110.77	107.70	113.20
365	100.97	99.10	103.20	110.60	108.80	113.50	116.23	114.00	117.70

Table D - 19: Compressive test results for Concrete **50GGBS75** cured at 20, 50^{0}C and adiabatic condition

Age (Days)	Strength at different curing temperature (N / mm2) - Concrete 50GGBS75								
	20 ^{0}C			50 ^{0}C			adiabatic		
	avr	min	max	avr	min	max	avr	min	max
0.25		0	0	15.20	15.15	15.25	1.275	1.25	1.3
0.5	4.00	3.90	4.10	30.85	30.80	30.90	7.45	7.30	7.60
1	14.75	14.60	14.90	55.00	54.50	55.50	35.95	35.30	36.60
2	28.50	27.10	29.80	64.97	64.40	65.50	65.00	64.50	65.50
4	43.63	42.30	45.30	67.50	67.00	68.00	75.83	74.50	77.50
8	58.50	58.00	59.00	74.67	73.50	76.50	76.17	75.50	77.00
16	69.67	69.50	70.00	79.67	78.00	81.50	85.20	84.50	85.70
32	85.33	84.00	86.50	83.50	82.50	84.50	90.00	88.50	92.00
64	87.40	86.20	88.70	87.33	85.10	89.90	95.90	94.30	98.00
128	88.73	88.10	89.40	91.67	90.00	92.70	97.37	95.90	98.70
256	91.67	89.90	94.60	93.80	92.40	94.80	106.27	104.20	108.40
365	105.80	104.90	107.50	103.53	101.80	105.30	108.10	106.60	109.70

Table D - 20: Compressive test results for Concrete **70GGBS75** cured at 20, 50^{0}C and adiabatic condition

Age (Days)	Strength at different curing temperature (N / mm2) - Concrete 70GGBS75								
	20 ^{0}C			50 ^{0}C			adiabatic		
	avr	min	max	avr	min	max	avr	min	max
0.25				9.55	9.50	9.60			
0.5				27.20	27.10	27.30	3.05	3.00	3.10
1	7.95	7.90	8.00	56.50	55.50	57.50	17.65	17.50	17.80
2	17.30	17.10	17.50	62.00	60.00	63.50	57.37	56.50	58.10
4	41.30	40.40	42.00	65.83	64.50	66.50	72.50	72.00	73.00
8	59.83	59.00	61.00	72.00	71.50	73.00	73.00	72.00	73.50
16	67.00	66.50	68.00	76.50	76.00	77.00	77.83	77.50	78.00
32	78.93	78.40	79.90	79.60	78.40	81.60	84.20	83.60	85.00
64	84.90	83.80	85.70	80.10	79.00	81.80	89.90	89.40	90.50
128	87.93	85.40	89.70	83.17	81.10	84.70	90.73	90.60	90.90
256	91.60	89.60	93.10	91.47	89.30	93.20	94.20	94.00	94.40
365	100.90	98.50	104.70	94.07	92.50	95.80	100.17	98.20	102.10

Table D - 21: Compressive strength results for **LW-PC** concrete

Age (Days)	20 ^{0}C			30 ^{0}C			40 ^{0}C			50 ^{0}C			adiabatic		
	avr	min	max	avr	min	max	avr	min	max	avr	min	max	avr	min	max
0.125							0.573	0.540	0.600	2.437	2.360	2.570			
0.25	1.380	1.350	1.420	4.127	3.950	4.310	11.100	10.930	11.310	13.897	12.770	14.470	1.680	1.560	1.810
0.5	10.160	9.830	10.500	14.963	14.630	15.510	21.027	20.570	21.670	20.003	19.940	20.120	17.833	17.320	18.270
1	21.247	20.340	21.790	26.163	25.460	26.650	30.013	29.640	30.400	26.383	25.960	27.060	30.090	29.870	30.400
2	29.943	29.530	30.400	34.200	33.800	34.600	34.833	34.300	35.500	32.733	32.000	33.200	36.633	36.300	36.900
4	35.700	35.000	36.500	38.300	37.600	39.200	37.167	36.300	38.500	34.200	33.400	35.600	43.800	42.400	44.900
7	38.433	36.800	39.800	41.367	40.800	41.800	39.800	39.000	40.400	36.800	36.500	37.100	45.000	44.400	45.800
14	42.200	41.400	43.100	45.267	44.500	45.700	42.833	41.400	43.600	41.500	40.100	42.600	45.367	44.900	45.900
28	44.867	44.100	45.300	46.167	45.800	46.400	45.633	44.900	46.200	45.067	44.800	45.300	43.700	42.900	44.900

Table D - 22: Compressive strength results for **LW-FA** concrete

Age (Days)	20 ^{0}C			30 ^{0}C			40 ^{0}C			50 ^{0}C			adiabatic		
	avr	min	max	avr	min	max	avr	min	max	avr	min	max	avr	min	max
0.125							0.397	0.380	0.410	1.210	1.120	1.280			
0.25	0.543	0.530	0.560	1.443	1.280	1.560	4.327	4.310	4.350	6.560	6.460	6.710	0.710	0.690	0.740
0.5	1.577	1.490	1.690	4.827	4.650	5.170	8.757	8.640	8.940	12.913	12.210	13.550	6.443	5.960	6.820
1	7.130	6.660	7.480	12.320	11.710	13.080	16.050	15.640	16.780	18.800	18.360	19.450	16.837	16.210	17.340
2	14.650	13.960	15.270	19.063	18.820	19.340	20.417	19.730	21.420	25.333	25.060	25.610	25.070	24.410	25.690
4	20.940	20.600	21.200	22.250	21.900	22.610	24.900	24.620	25.190	32.993	32.680	33.400	36.633	36.200	37.000
7	26.020	25.640	26.270	27.247	26.810	27.850	34.267	33.600	34.700	37.900	37.600	38.300	44.700	43.800	45.700
14	28.207	27.790	28.620	32.767	32.500	33.200	37.100	36.400	37.500	38.067	37.800	38.400	45.267	44.900	45.800
28	33.900	33.600	34.300	35.600	35.000	36.300	40.433	39.800	41.000	36.867	36.000	37.700	44.800	44.400	45.400

Table D - 23: Compressive strength results for **LW-FA act** concrete

Age (Days)	20 ^{0}C			30 ^{0}C			40 ^{0}C			50 ^{0}C			adiabatic		
	avr	min	max	avr	min	max	avr	min	max	avr	min	max	avr	min	max
0.125							1.380	1.350	1.410	5.793	5.630	6.050			
0.25	0.697	0.680	0.710	1.970	1.900	2.060	6.580	6.290	6.880	9.987	9.770	10.150	1.180	1.080	1.300
0.5	4.940	4.880	5.010	10.883	10.670	11.100	14.037	13.680	14.250	14.360	13.830	14.710	14.267	14.090	14.400
1	13.510	13.290	13.790	17.433	16.540	18.280	18.030	17.630	18.620	18.483	17.980	18.750	20.500	20.150	20.900
2	19.010	18.650	19.460	20.483	20.180	20.800	23.773	22.820	24.720	26.620	26.080	27.300	31.033	30.500	31.700
4	21.733	21.350	22.180	24.680	24.140	24.970	28.480	28.060	28.880	27.023	26.720	27.540	33.600	33.200	34.100
7	24.683	24.220	25.310	29.040	28.790	29.410	30.300	29.800	30.800	28.017	27.820	28.310	35.000	34.500	35.800
14	28.853	28.350	29.300	32.967	32.000	33.500	31.330	30.900	31.850	28.393	27.980	28.640	35.767	34.900	36.800
28	33.933	33.400	34.600	39.100	38.600	39.500	36.400	36.200	36.600	34.800	34.600	35.000	34.600	34.400	34.800

Table D - 24: Compressive strength results for **LW-GGBS** concrete

Age (Days)	20 ^{0}C			30 ^{0}C			40 ^{0}C			50 ^{0}C			adiabatic		
	avr	min	max	avr	min	max	avr	min	max	avr	min	max	avr	min	max
0.125										1.077	0.960	1.150			
0.25				1.150	1.090	1.210	2.730	2.640	2.840	5.020	4.770	5.150	0.533	0.490	0.580
0.5	1.793	1.680	1.900	4.423	4.380	4.490	9.090	8.840	9.340	12.020	11.790	12.260	3.833	3.710	3.930
1	6.160	5.850	6.320	11.637	11.120	12.090	18.210	17.850	18.800	21.293	20.350	22.000	17.620	17.340	17.770
2	12.923	12.450	13.430	22.113	21.800	22.470	28.300	27.640	28.900	31.433	31.200	31.700	35.000	34.700	35.400
4	23.677	23.280	24.130	30.333	29.800	31.200	35.033	34.600	35.700	34.600	34.300	35.000	40.633	39.800	42.000
7	29.807	28.920	30.500	37.167	36.500	37.900	39.300	38.300	39.900	39.300	39.200	39.400	41.800	41.400	42.500
14	34.967	34.700	35.200	42.367	41.800	42.700	44.133	43.200	44.900	39.767	39.400	40.300	43.433	42.700	44.400
28	42.700	42.300	43.000	46.333	45.500	47.000	46.100	45.600	46.400	41.800	41.600	42.100	44.333	43.700	45.400

Table D - 25: Compressive strength results for **LW-GGBS act** concrete

Age (Days)	20 ^{0}C			30 ^{0}C			40 ^{0}C			50 ^{0}C			adiabatic		
	avr	min	max	avr	min	max	avr	min	max	avr	min	max	avr	min	max
0.125							1.017	0.990	1.040	3.650	3.550	3.740			
0.25	0.547	0.510	0.590	1.773	1.760	1.790	6.123	5.740	6.430	12.427	12.280	12.650	1.577	1.540	1.620
0.5	3.160	3.020	3.270	7.857	7.690	8.120	14.983	14.720	15.120	19.223	18.960	19.360	13.513	12.790	14.010
1	12.367	12.020	12.590	17.923	17.430	18.650	20.573	20.200	20.920	21.557	21.230	21.790	25.100	24.400	25.890
2	19.700	19.390	20.190	24.480	23.750	25.030	25.557	25.140	26.200	24.103	23.400	24.500	28.777	28.250	29.690
4	26.820	25.890	27.500	30.567	30.300	31.100	31.167	30.700	32.100	27.077	26.420	27.460	30.450	30.050	31.200
7	32.133	31.900	32.500	34.433	33.900	34.800	34.200	33.500	34.800	29.163	28.790	29.420	32.433	32.200	32.700
14	34.633	34.200	35.100	37.167	36.600	37.700	37.533	36.900	38.000	32.433	31.400	33.400	33.467	33.100	33.900
28	37.967	36.800	38.700	39.767	38.900	40.300	39.733	39.400	40.300	34.800	34.500	35.100	36.833	36.400	37.300

Table D - 26: Compressive strength results for **NWSCC-PC** concrete

Age (Days)	20 ^{0}C			30 ^{0}C			40 ^{0}C			50 ^{0}C			adiabatic		
	avr	min	max	avr	min	max	avr	min	max	avr	min	max	avr	min	max
0.125										2.470	2.360	2.530			
0.25				2.303	2.290	2.320	9.100	8.780	9.500	12.477	12.160	12.830	0.420	0.390	0.460
0.5	3.080	3.060	3.100	12.103	11.960	12.220	18.463	18.270	18.580	23.917	23.550	24.200	16.000	15.560	16.370
1	17.180	16.340	18.310	26.190	25.800	26.850	29.973	29.220	30.500	33.133	32.500	33.800	34.267	34.000	34.500
2	32.233	31.600	33.300	37.667	37.500	37.800	38.400	37.800	38.800	35.967	35.500	36.500	41.700	40.800	42.600
4	42.333	41.600	43.300	44.700	44.400	44.900	43.433	43.100	43.700	42.800	42.300	43.500	48.967	48.500	49.300
7	49.333	48.400	50.800	48.567	48.300	48.900	50.500	49.900	51.200	48.200	47.900	48.600	51.967	51.600	52.400
14	55.167	54.300	56.500	55.667	54.300	56.800	54.933	54.500	55.500	53.967	53.200	54.600	55.433	55.000	56.000
28	61.767	60.800	63.400	60.067	59.600	60.500	56.867	56.400	57.700	55.400	54.300	56.400	58.733	58.000	59.200

Table D - 27: Compressive strength results for **LWSCC-GGBS** concrete

Age (Days)	20 ^{0}C			30 ^{0}C			40 ^{0}C			50 ^{0}C			adiabatic		
	avr	min	max	avr	min	max	avr	min	max	avr	min	max	avr	min	max
0.125							0.780	0.740	0.810	2.370	2.200	2.540			
0.25				0.810	0.780	0.840	4.037	3.940	4.120	12.427	12.100	12.740			
0.5	3.833	3.780	3.910	12.053	11.960	12.110	18.793	18.440	19.260	25.387	25.090	25.920	12.517	12.400	12.610
1	16.837	16.650	17.040	25.693	25.560	25.880	29.823	29.470	30.100	35.633	35.300	36.100	42.700	42.400	43.000
2	29.257	29.060	29.580	35.300	34.600	36.100	39.967	39.200	40.800	40.667	39.700	41.700	45.333	45.000	45.600
4	37.767	37.000	38.400	42.933	42.500	43.200	43.567	42.800	44.500	44.800	43.800	46.000	48.700	47.900	49.700
7	43.900	43.200	44.500	48.400	47.000	49.300	49.200	48.900	49.600	48.867	48.600	49.300	51.200	49.600	52.900
14	50.567	49.900	51.000	51.300	50.500	52.400	50.467	49.100	51.500	49.733	48.600	50.500	54.667	53.600	55.900
28	54.200	53.100	55.900	53.567	53.000	54.400	51.967	51.300	53.200	51.200	51.100	51.300	53.267	53.000	53.600

Table D - 28: Compressive strength results for **LWSCC-LSP** concrete

Age (Days)	20 ^{0}C			30 ^{0}C			40 ^{0}C			50 ^{0}C			adiabatic		
	avr	min	max	avr	min	max	avr	min	max	avr	min	max	avr	min	max
0.125							0.805	0.790	0.820	4.185	4.130	4.240			
0.25				3.600	3.520	3.680	8.015	8.000	8.030	11.155	10.710	11.600			
0.5	5.210	5.110	5.310	12.620	12.600	12.640	16.580	16.410	16.750	17.910	17.380	18.440	15.740	15.590	15.890
1	15.445	15.240	15.650	24.065	23.640	24.490	26.135	26.120	26.150	25.205	24.900	25.510	29.045	28.890	29.200
2	27.965	27.680	28.250	31.200	30.800	31.600	29.275	29.010	29.540	28.015	27.670	28.360	37.800	37.500	38.100
4	33.000	32.700	33.300	33.300	32.900	33.700	32.350	31.900	32.800	31.850	31.200	32.500	41.950	41.500	42.400
7	39.000	38.600	39.400	37.200	36.800	37.600	34.250	33.800	34.700	33.200	32.900	33.500	43.000	42.600	43.400
14	40.900	40.800	41.000	41.200	40.700	41.700	41.750	40.100	43.400	38.800	38.500	39.100	43.650	42.700	44.600
28	44.650	44.000	45.300	42.850	41.400	44.300	41.800	41.400	42.200	39.300	39.000	39.600	42.450	41.700	43.200

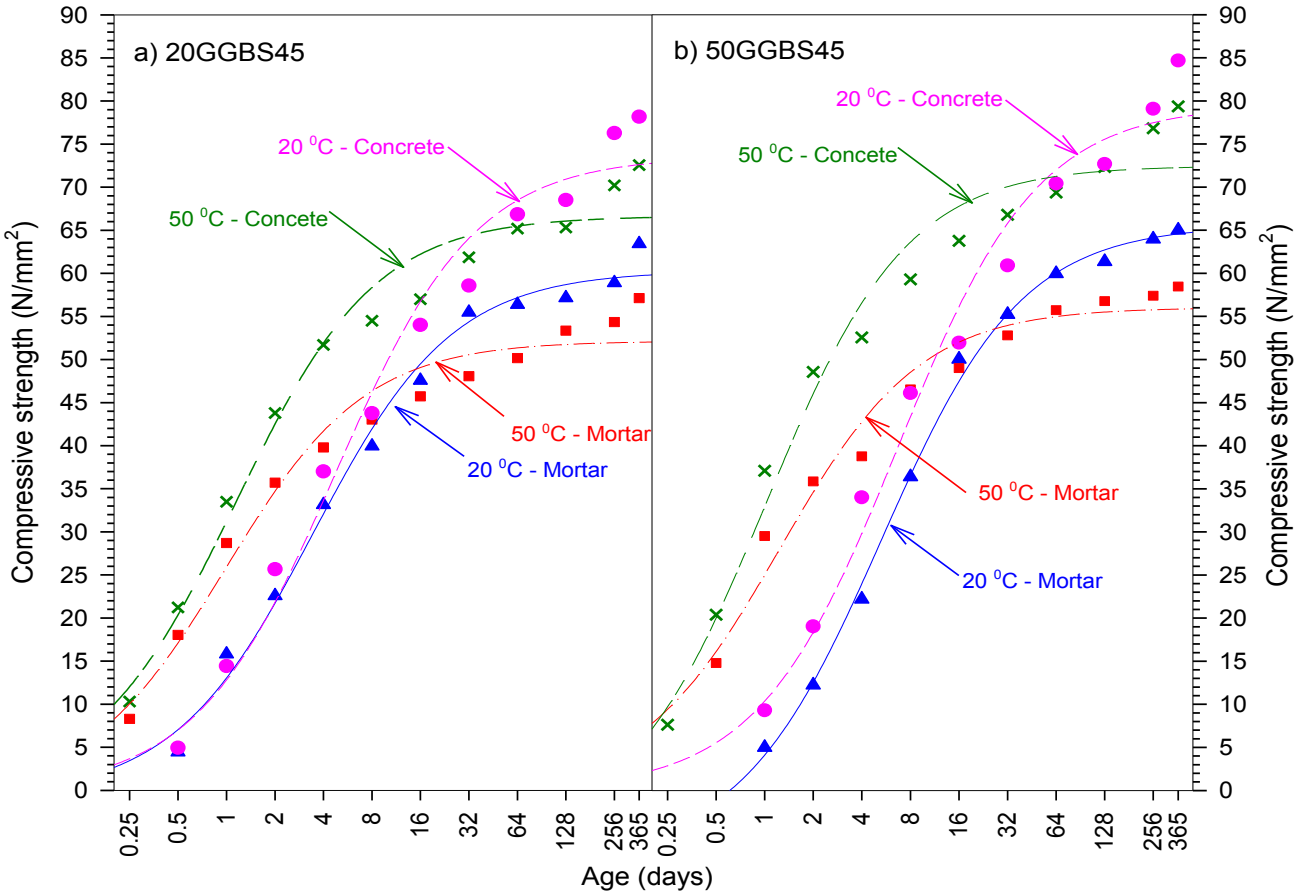

Figure E - 1: Strength developments of mortar and concrete **grade C45** with 20 and 50% of GGBS cured at 20 and 50^{0}C

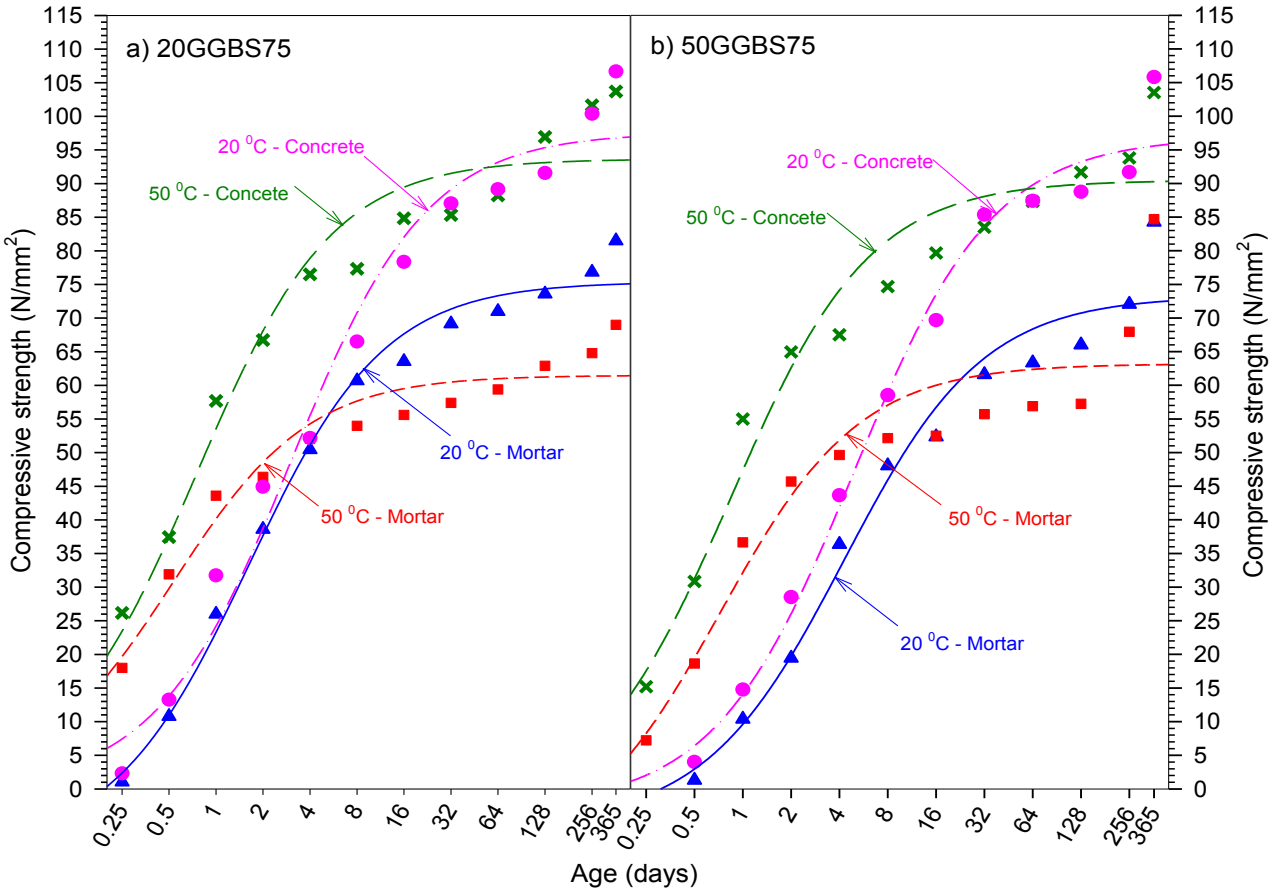

Figure E - 2: Strength developments of mortar and concrete **grade C75** with 20 and 50% of GGBS cured at 20 and 50^{0}C

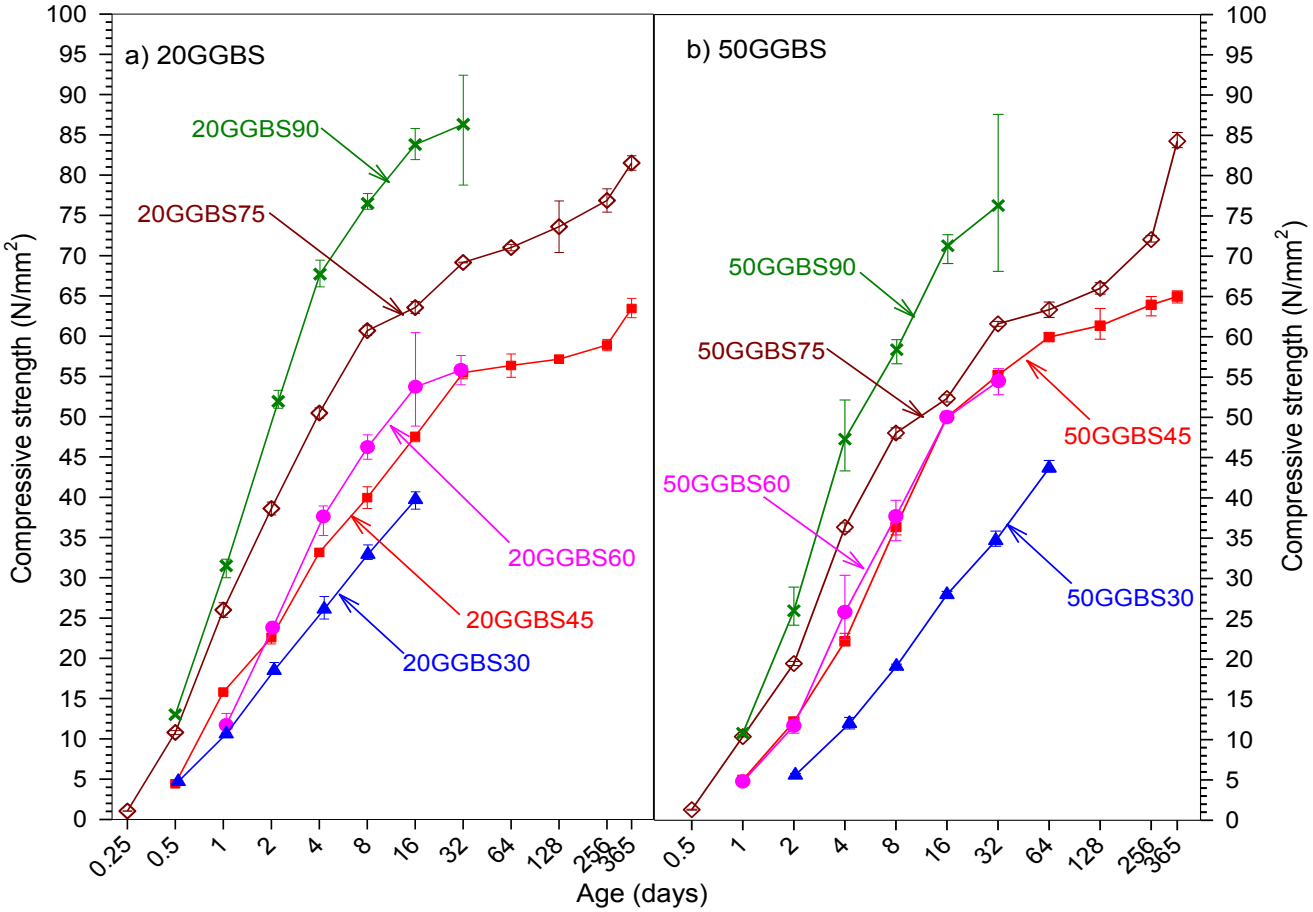

Figure E - 3: Strength developments of mortars with 20 and 50% of GGBS levels cured at 20^0C **(grade C30, C45, C60, C75** and **C90)**

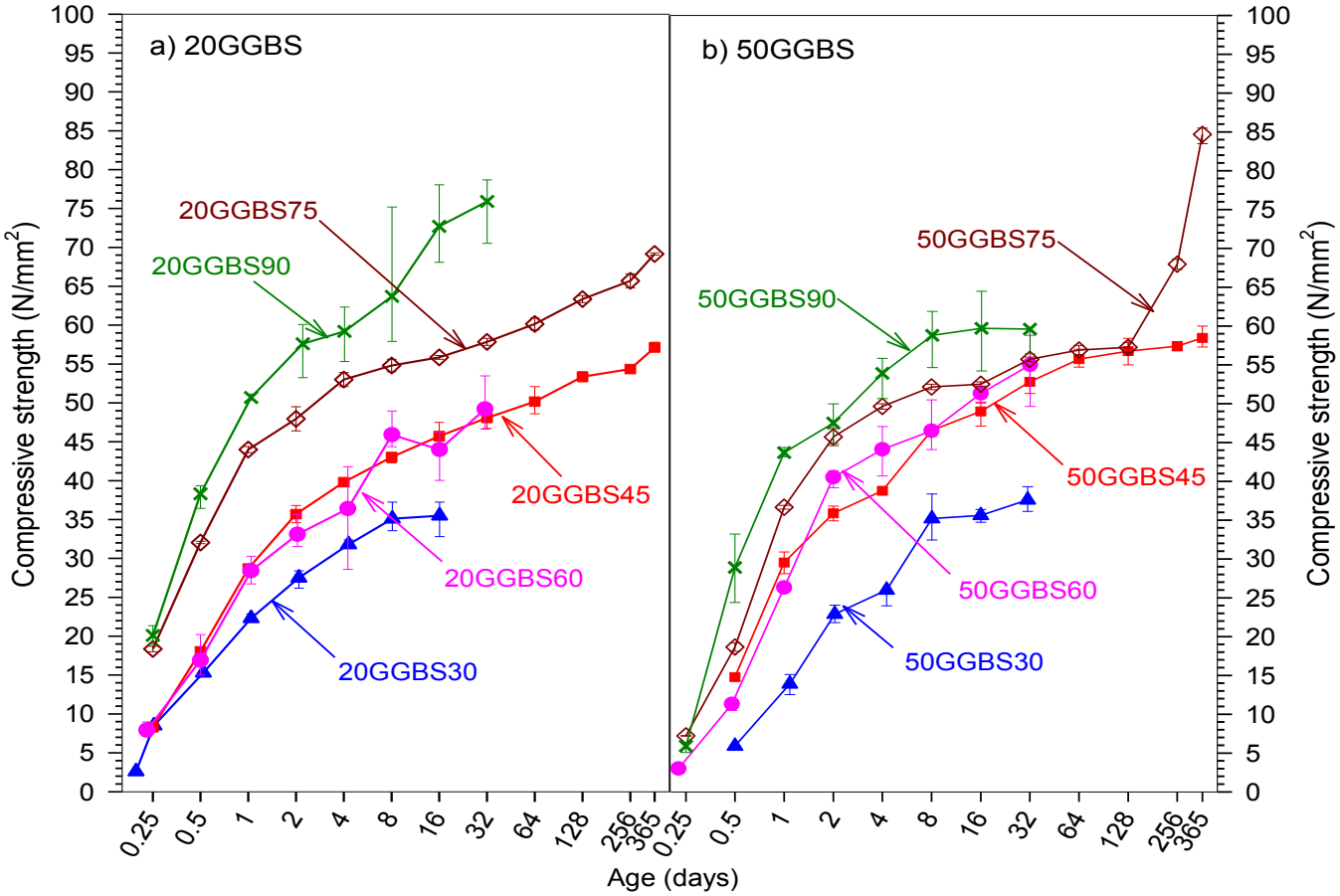

Figure E - 4: Strength developments of mortars with 20 and 50% of GGBS levels cured at 50^0C **(grade C30, C45, C60, C75** and **C90)**

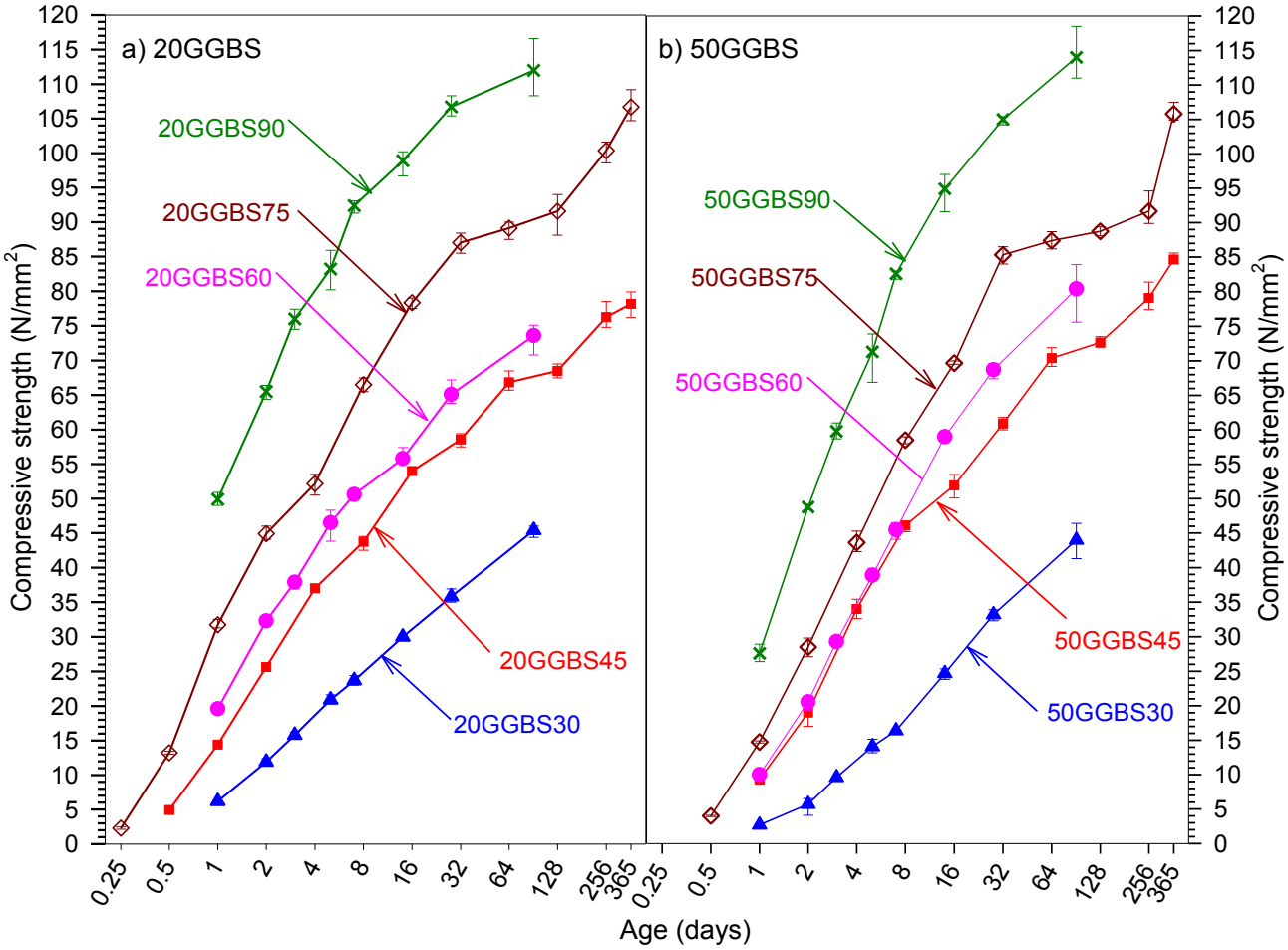

Figure E - 5: Strength developments of concretes with 20 and 50% of GGBS levels cured at 20^0C **(grade C30, C45, C60, C75** and **C90)**

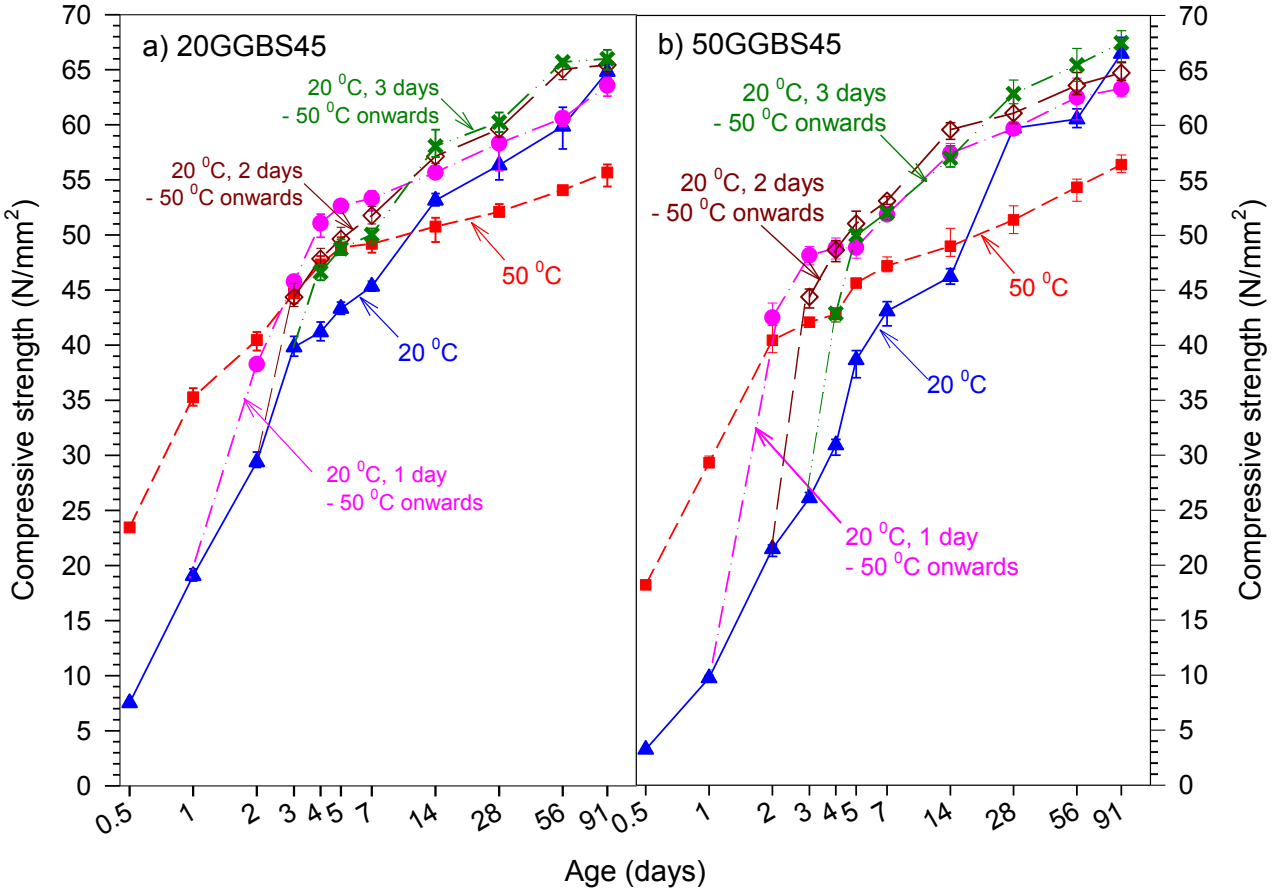

Figure E - 6: Strength development of mortar **grade C45** with 20 and 50% GGBS cured under changing curing temperature

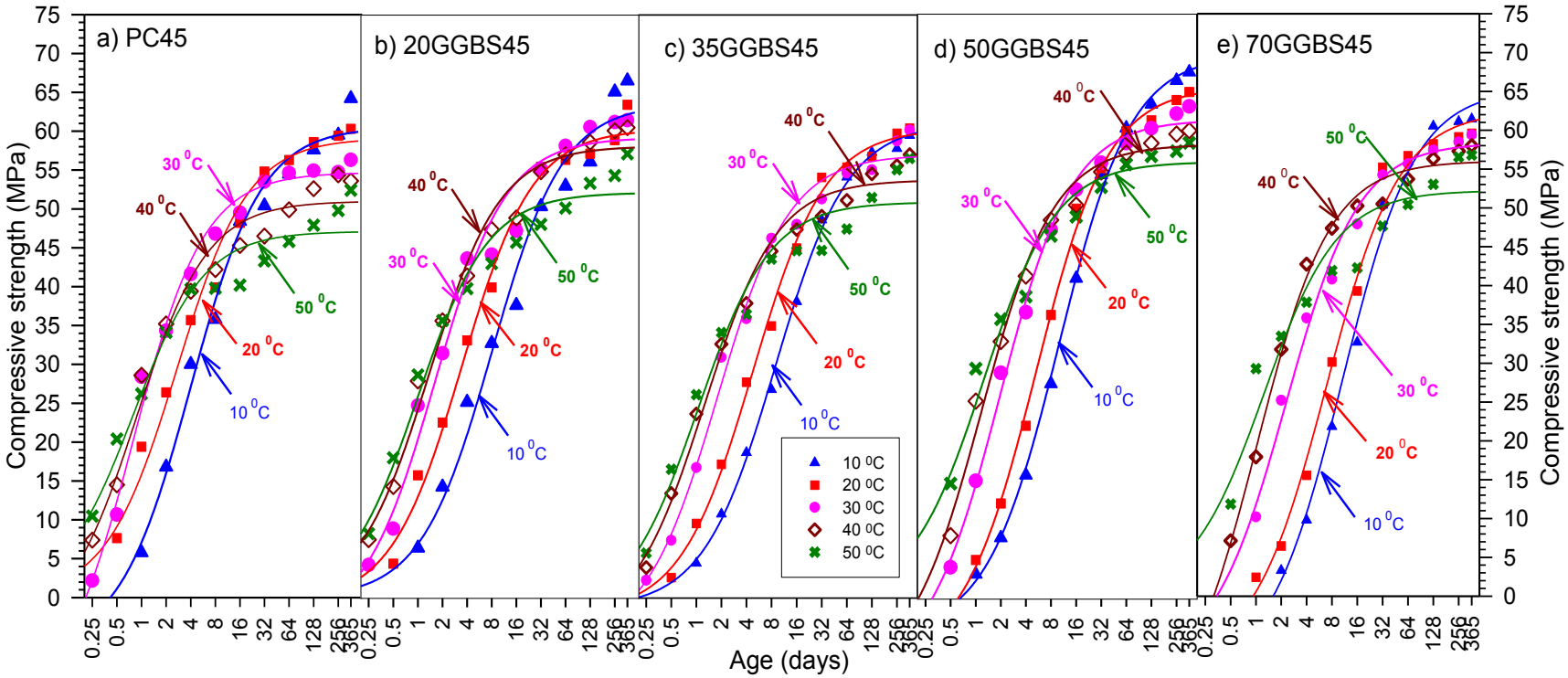

Figure E - 7: Regression analysis based on Carino equation for mortar **grade C45**

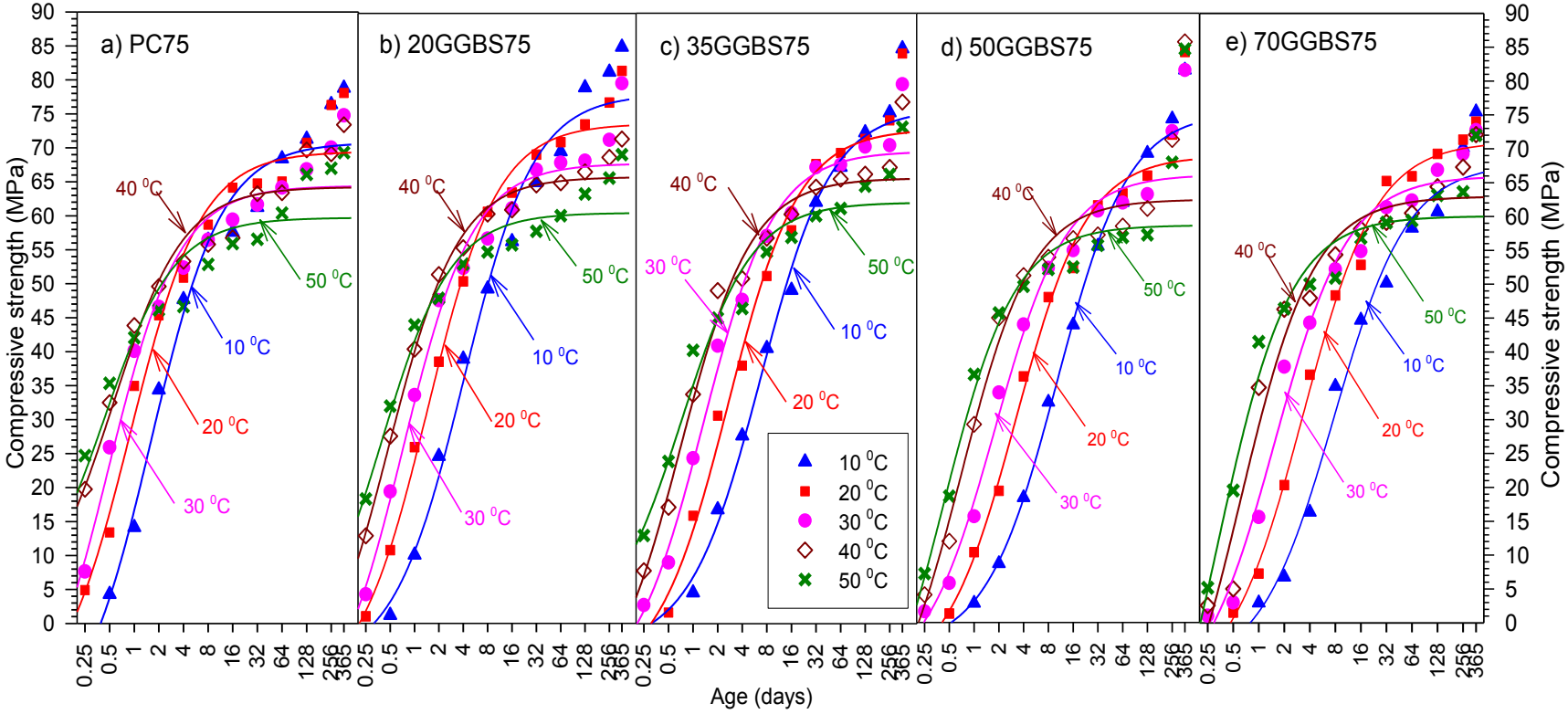

Figure E- 8: Regression analysis based on Carino equation for mortar **grade C75**

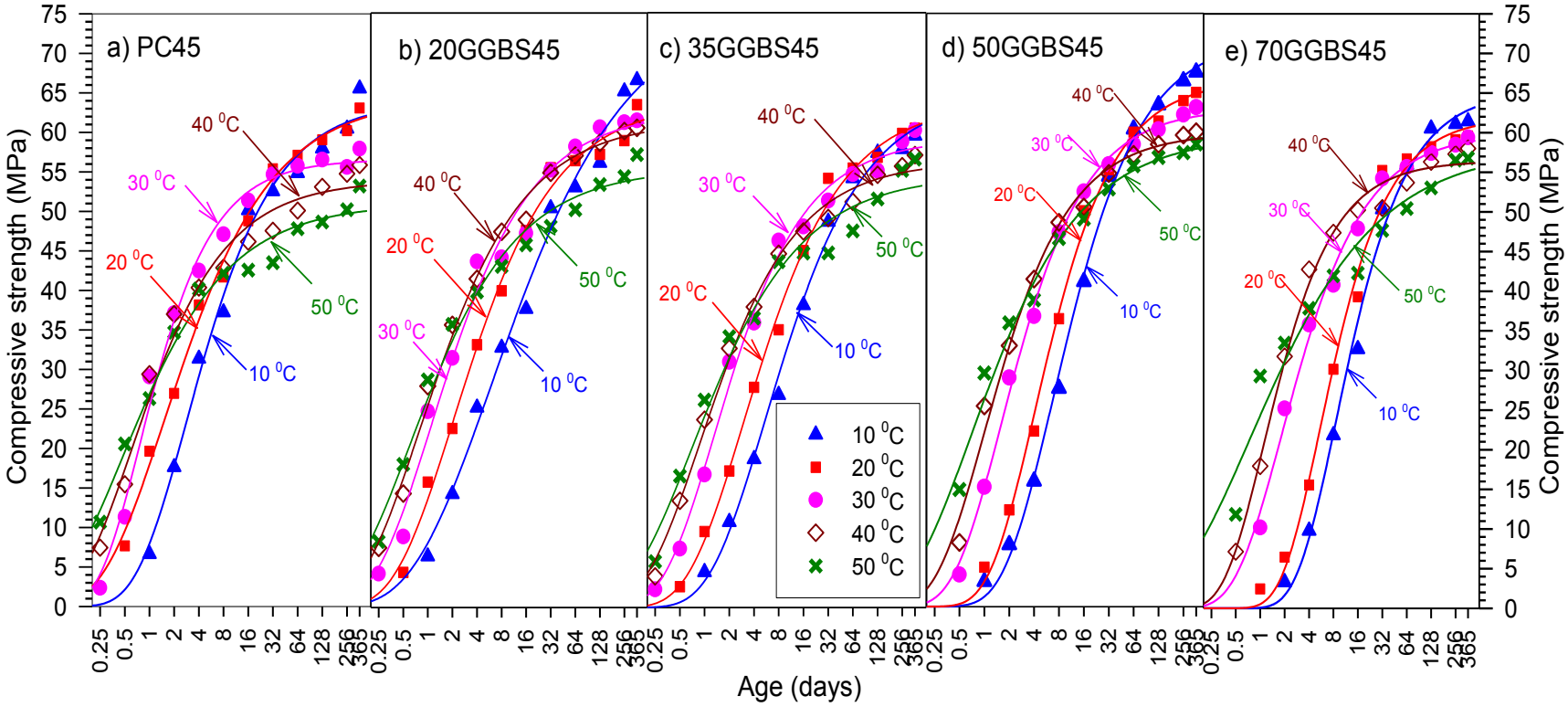

Figure E - 9: Regression analysis based on TPE method for mortar **grade C45**

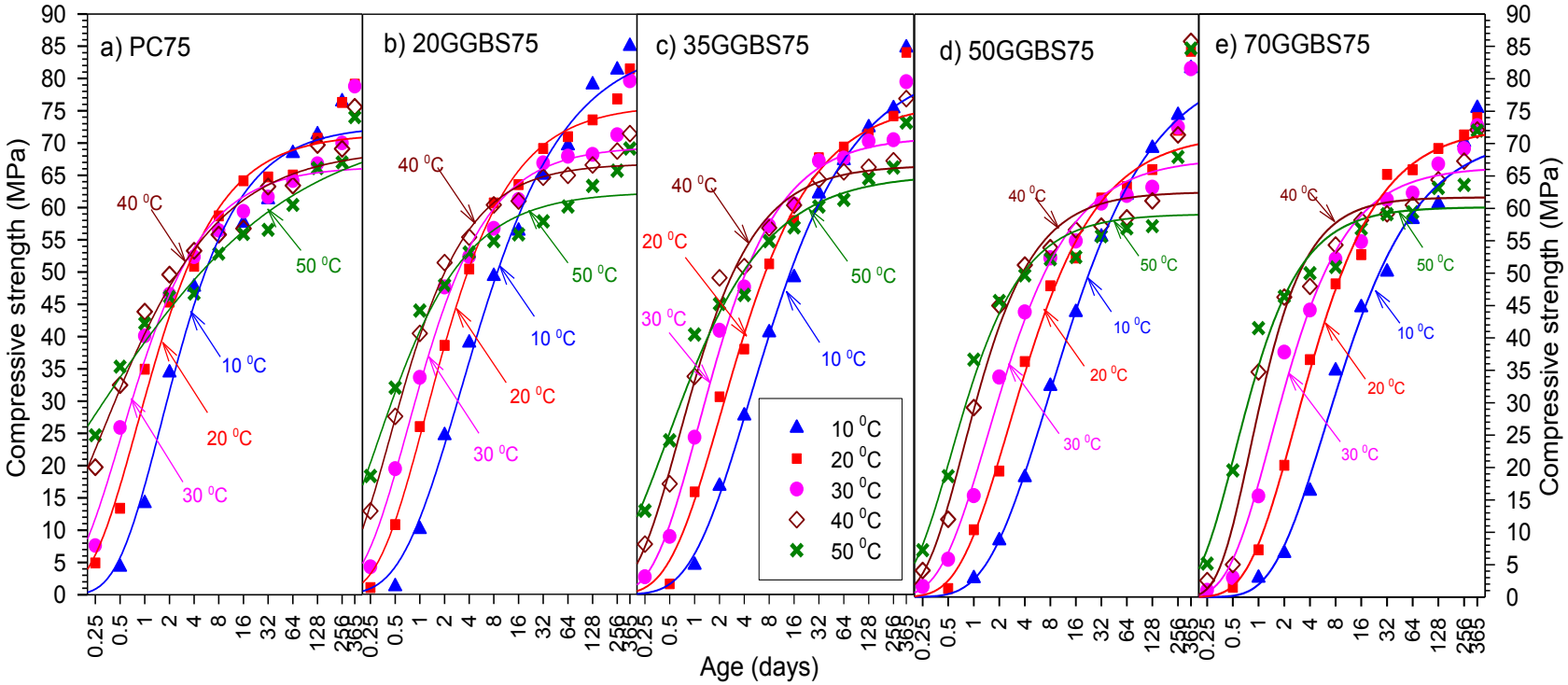

Figure E - 10: Regression analysis based on TPE method for mortar **grade C75**

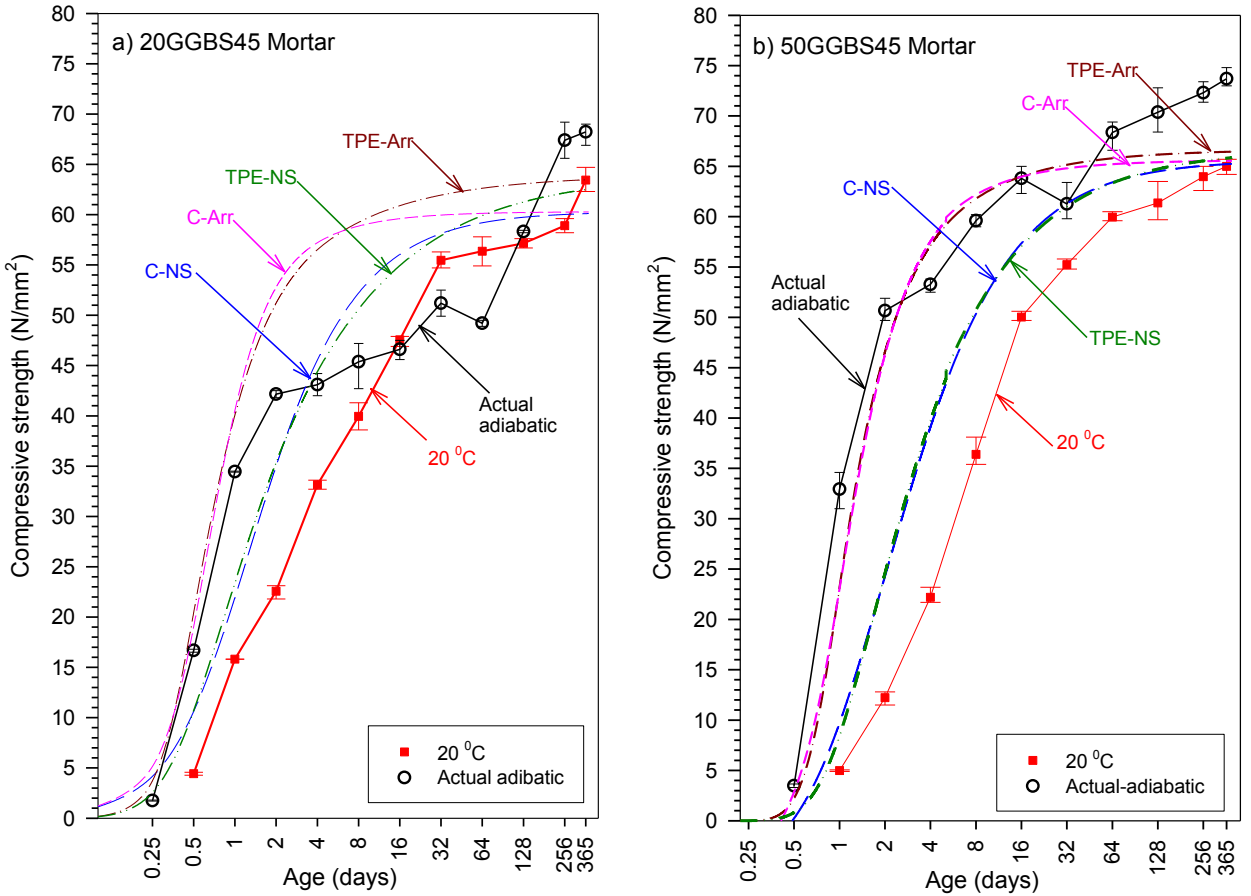

Figure E - 11: Predicted adiabatic strength development based on the Carino and TPE equation using datum temperature of -11^{0}C mortar with 20 and 50% GGBS **grade C45**

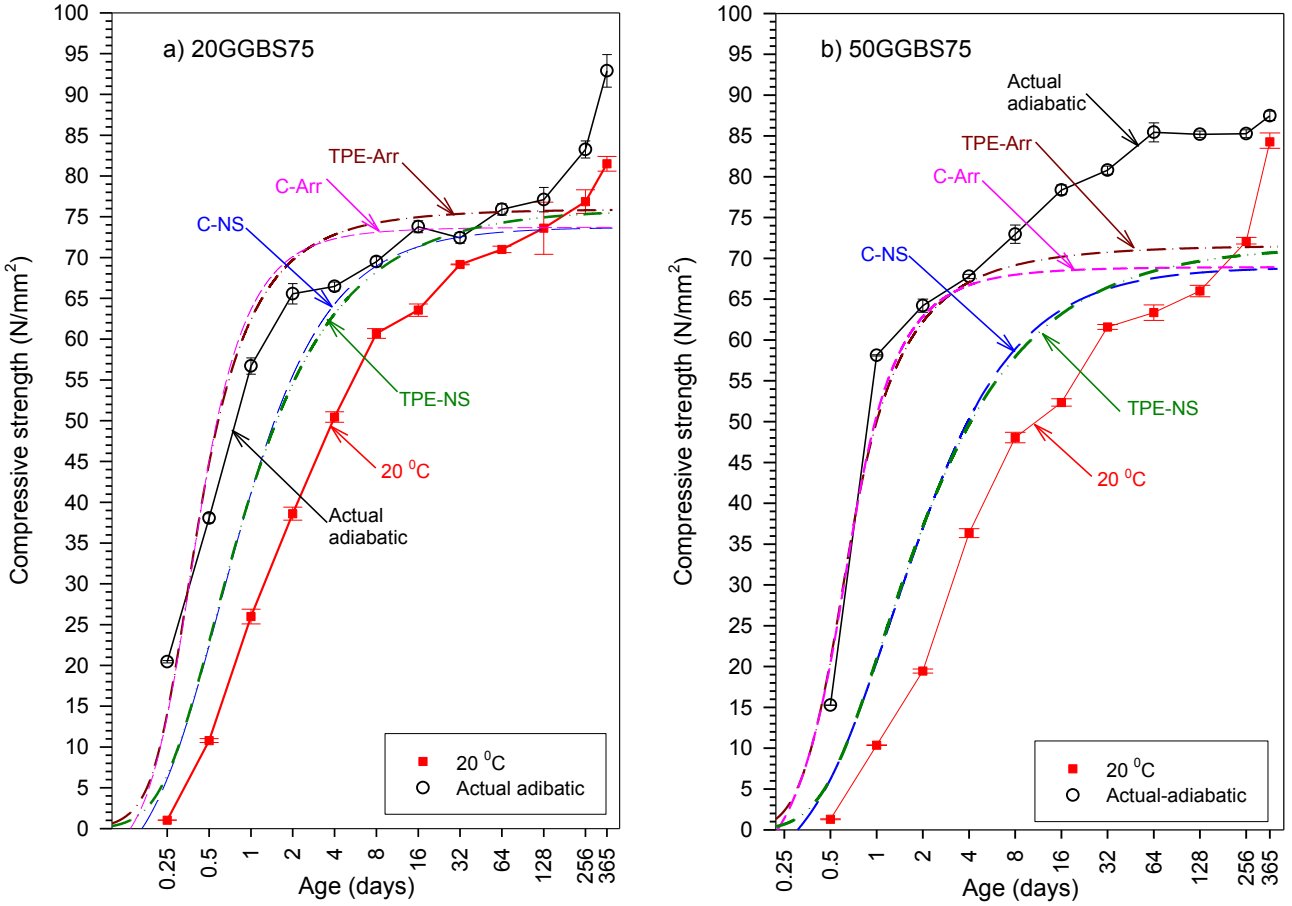

Figure E - 12: Predicted adiabatic strength development based on the Carino and TPE equation using datum temperature of -11^{0}C mortar with 20 and 50% GGBS **grade C75**

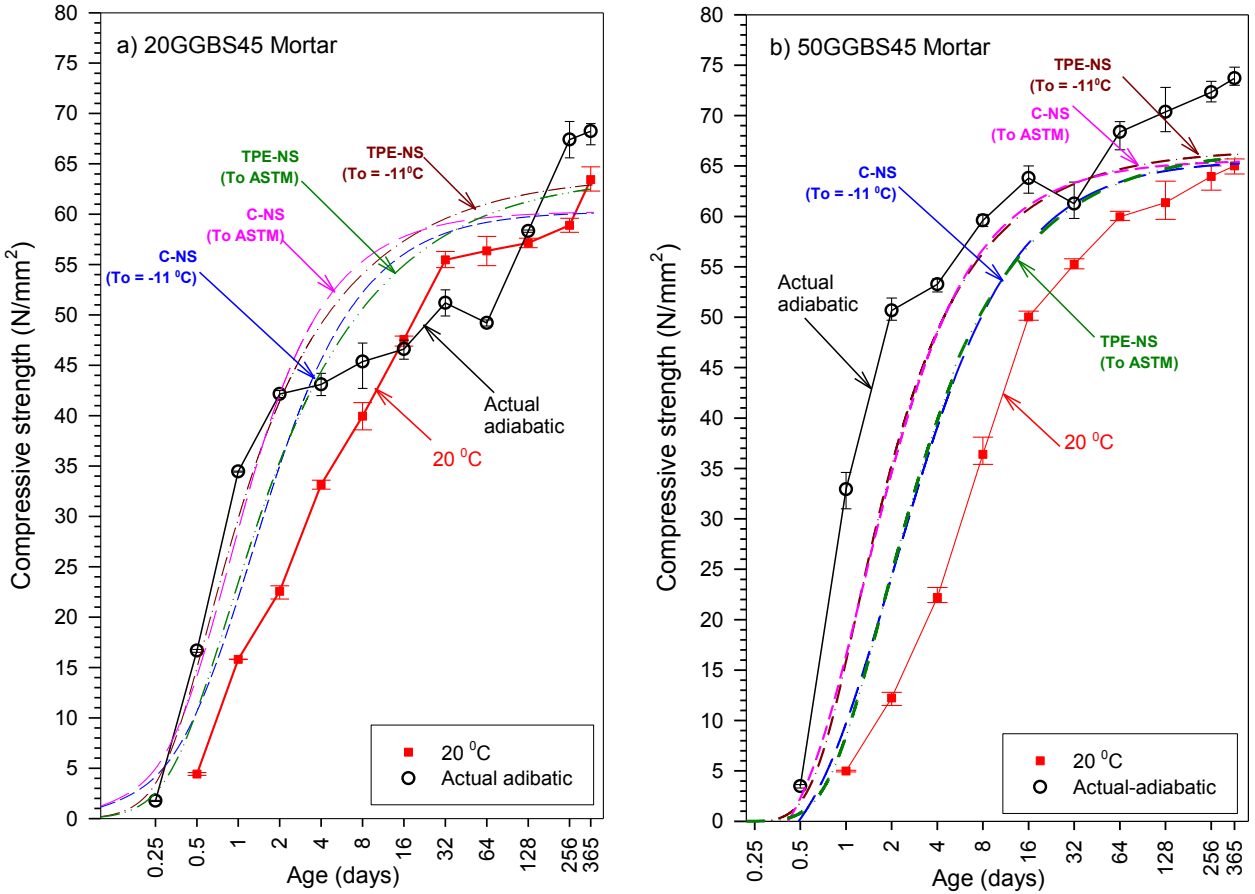

Figure E - 13: Predicted adiabatic strength development using the Carino and TPE equations with a datum temperature based on ASTM C 1074 mortar with 20 and 50% GGBS **grade C45**

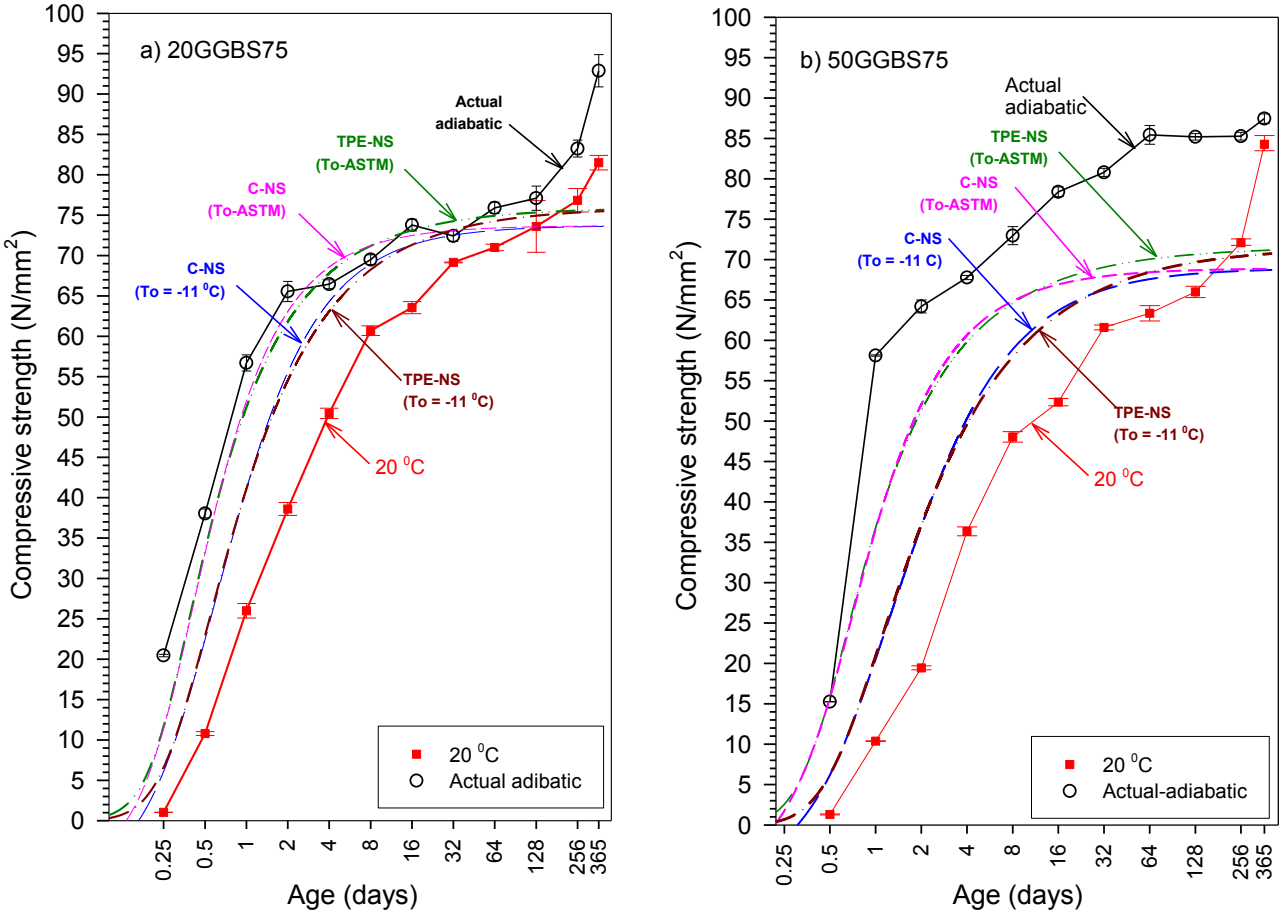

Figure E - 14: Predicted adiabatic strength development using the Carino and TPE equations with a datum temperature based on ASTM C 1074 mortar with 20 and 50% GGBS **grade C75**

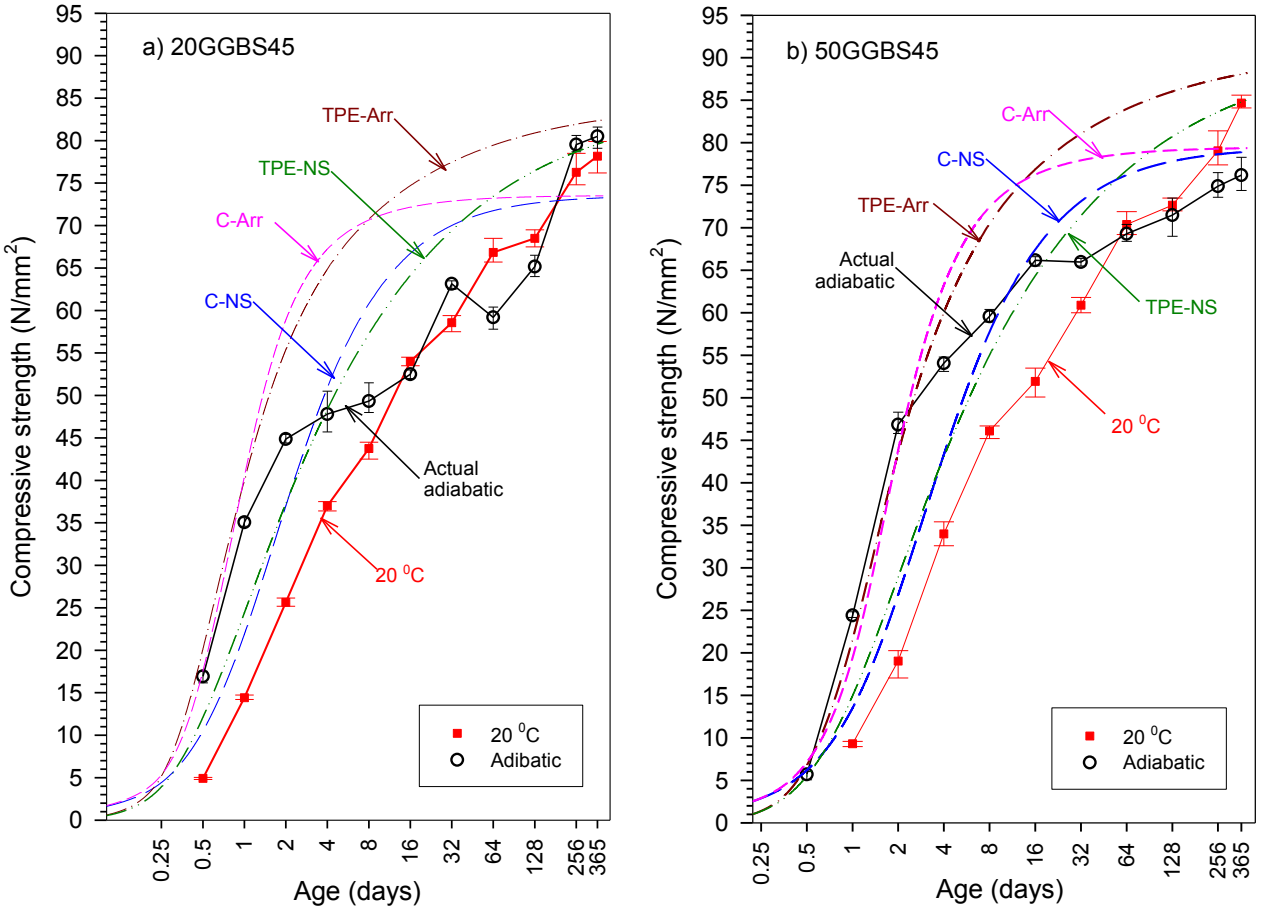

Figure E - 15: Predicted adiabatic strength development based on the Carino and TPE equation using datum temperature of -11^{0}C concrete with 20 and 50% GGBS **grade C45**

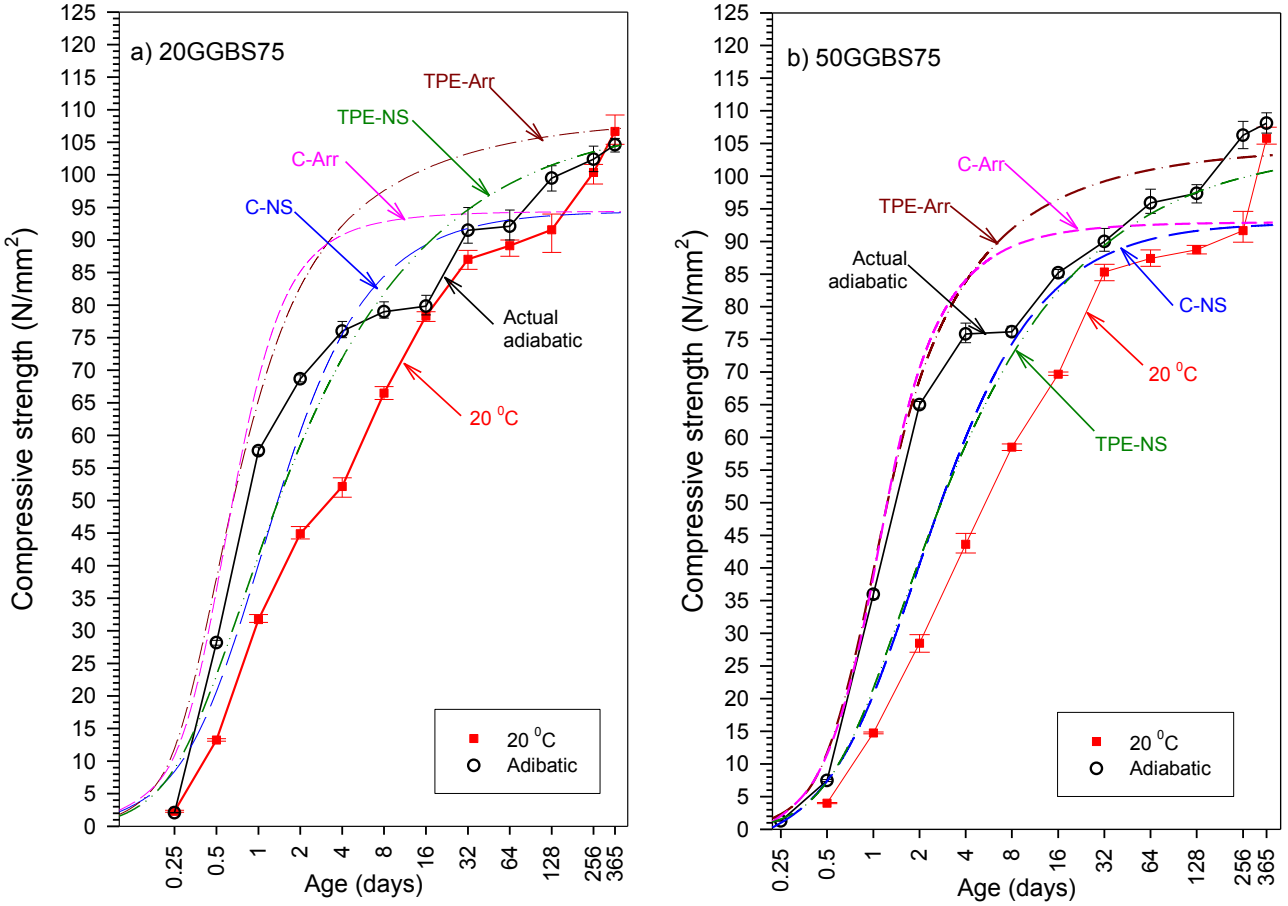

Figure E - 16: Predicted adiabatic strength development based on the Carino and TPE equation using datum temperature of -11^{0}C concrete with 20 and 50% GGBS **grade C75**

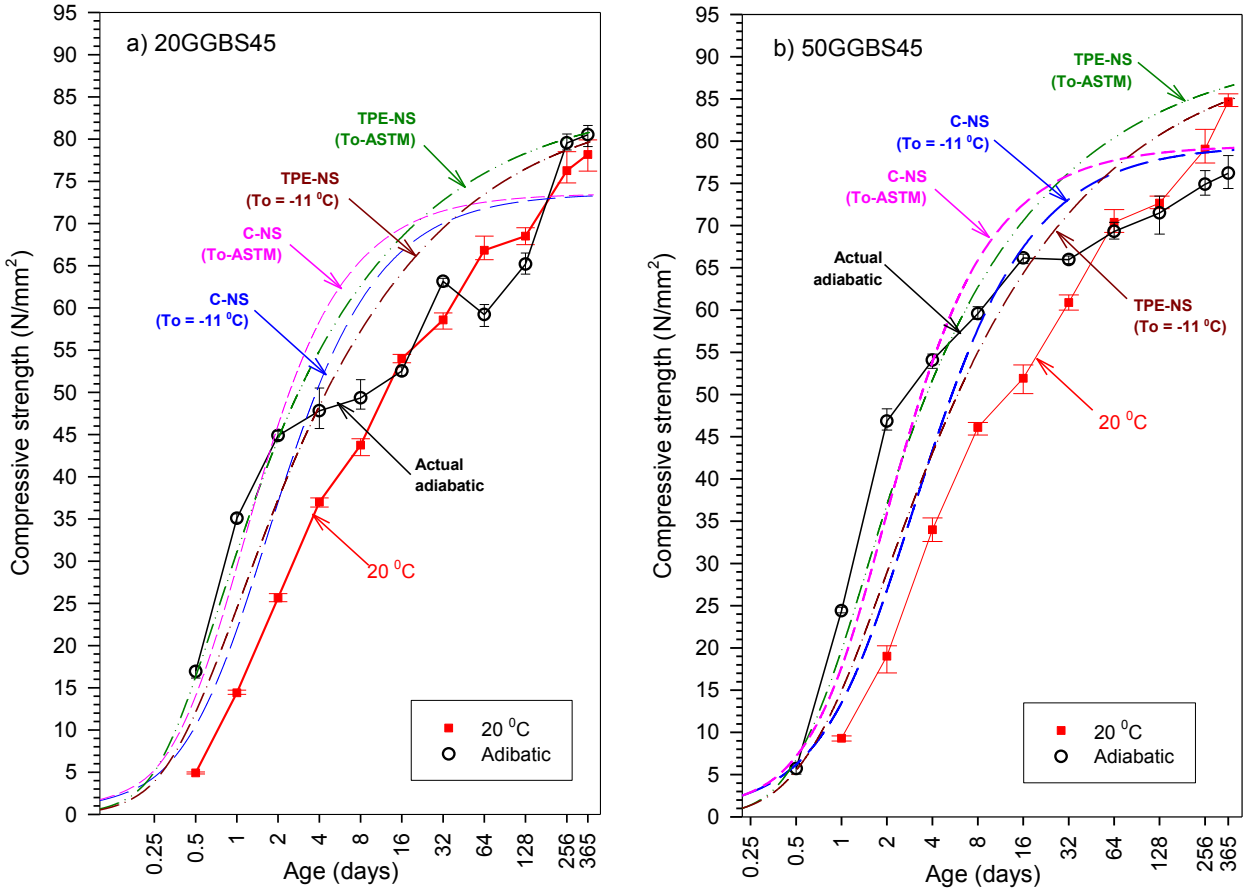

Figure E - 17: Predicted adiabatic strength development using the Carino and TPE equations with a datum temperature based on ASTM C 1074 concrete with 20 and 50% GGBS **grade C45**

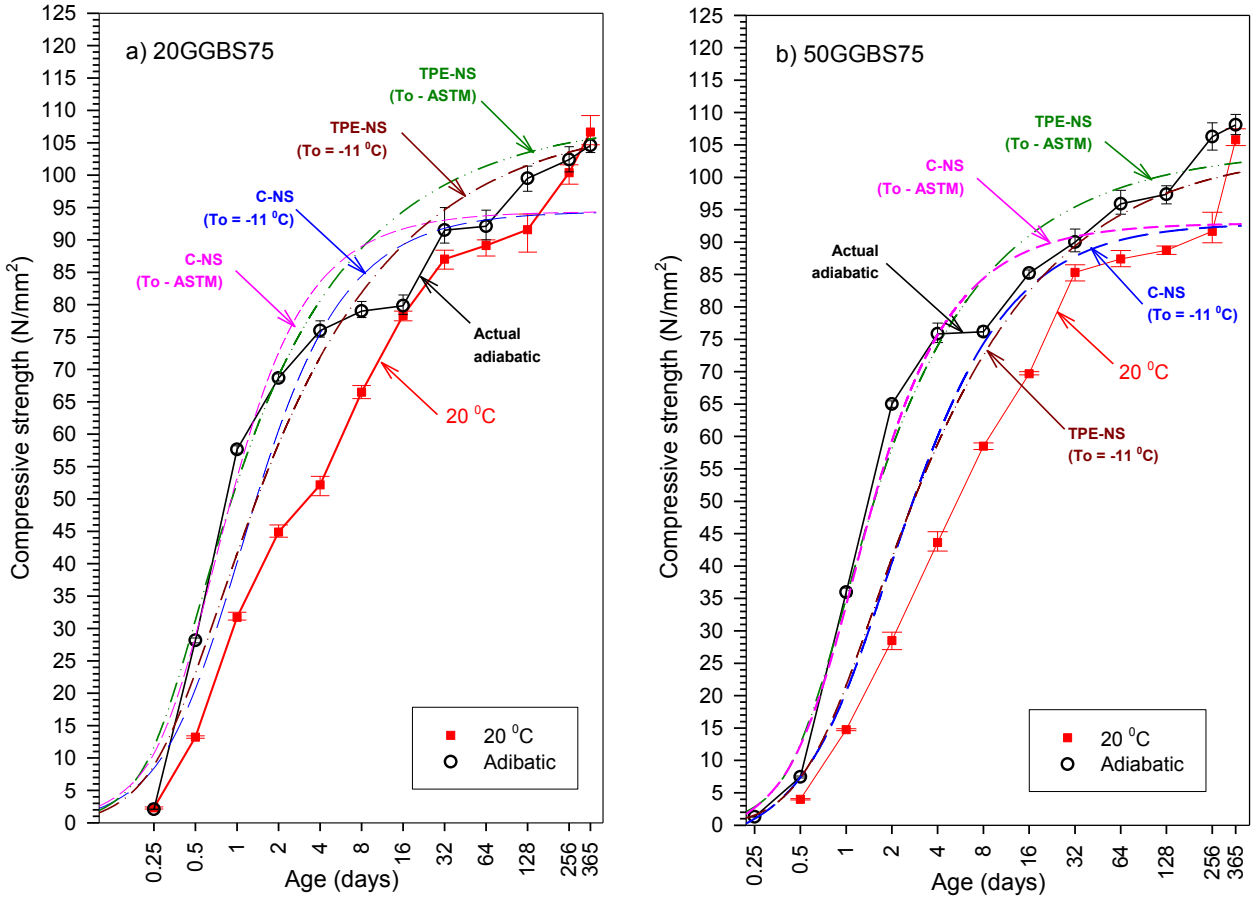

Figure E - 18: Predicted adiabatic strength development using the Carino and TPE equations with a datum temperature based on ASTM C 1074 concrete with 20 and 50% GGBS **grade C75**

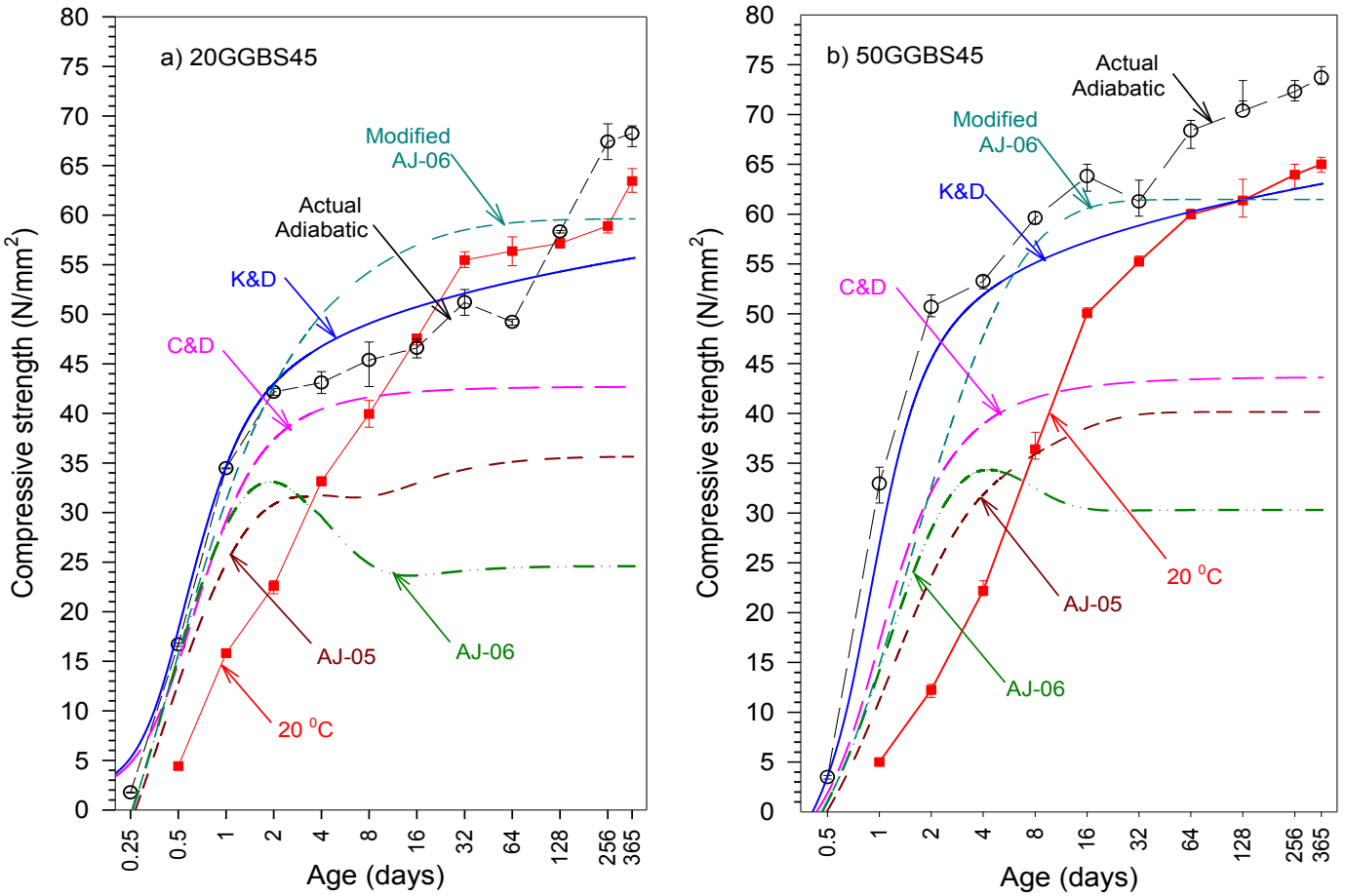

Figure E - 19: Predicted adiabatic strength development of mortar with 20 and 50% GGBS **grade C45** using some recent maturity equations

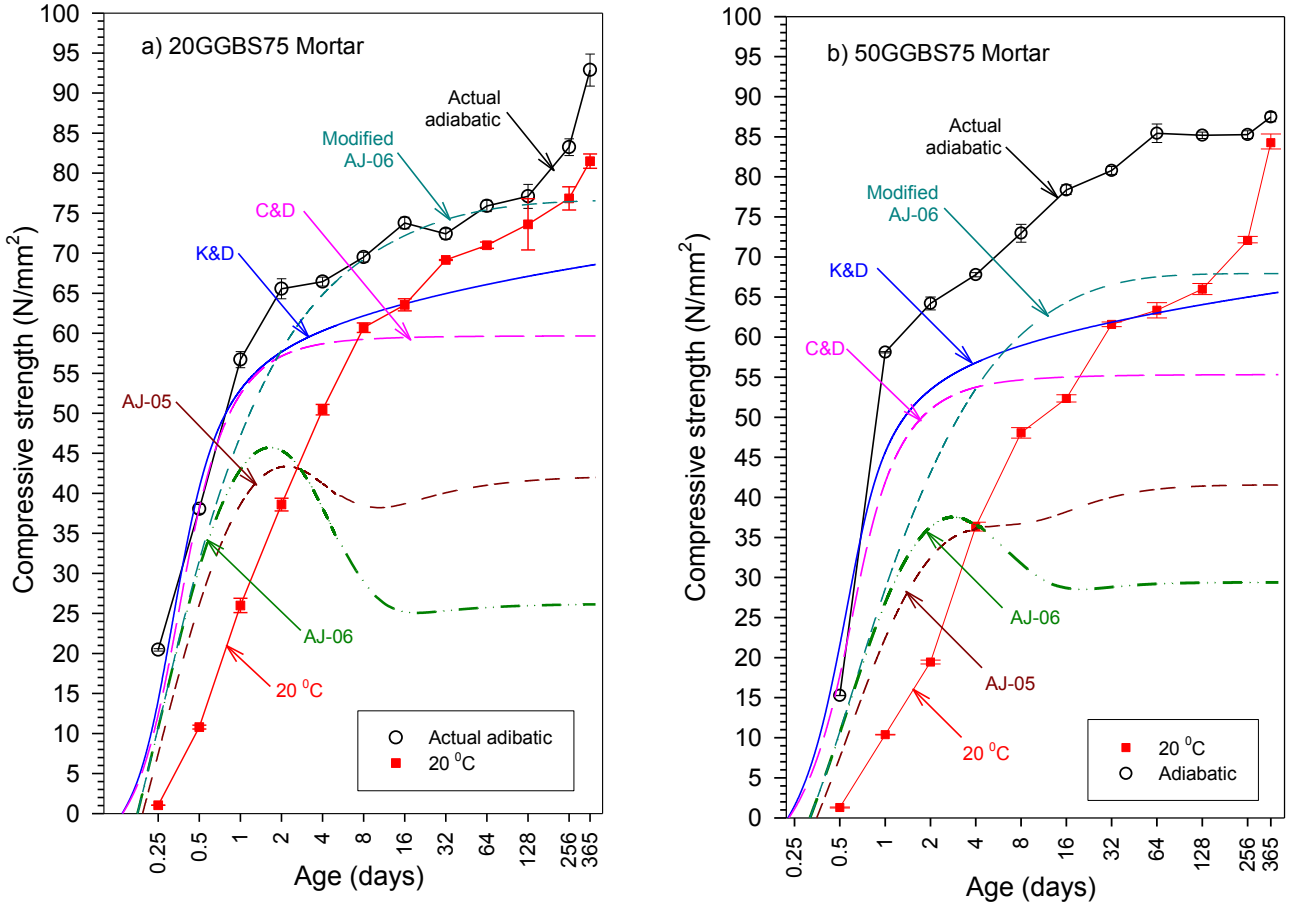

Figure E - 20: Predicted adiabatic strength development of mortar with 20 and 50% GGBS **grade C75** using some recent maturity equations

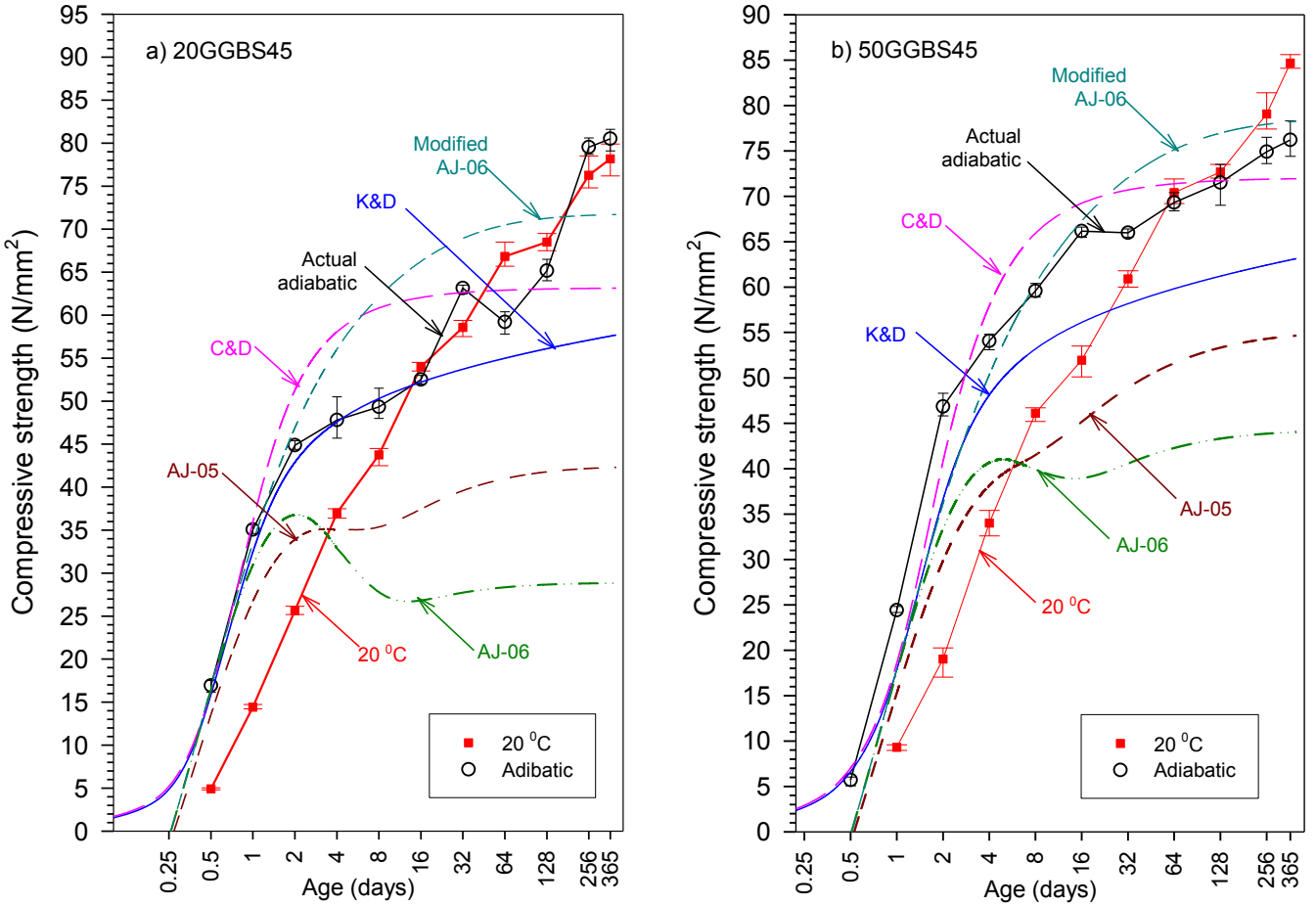

Figure E - 21: Predicted adiabatic strength development of concrete with 20 and 50% GGBS **grade C45** using some recent maturity equations

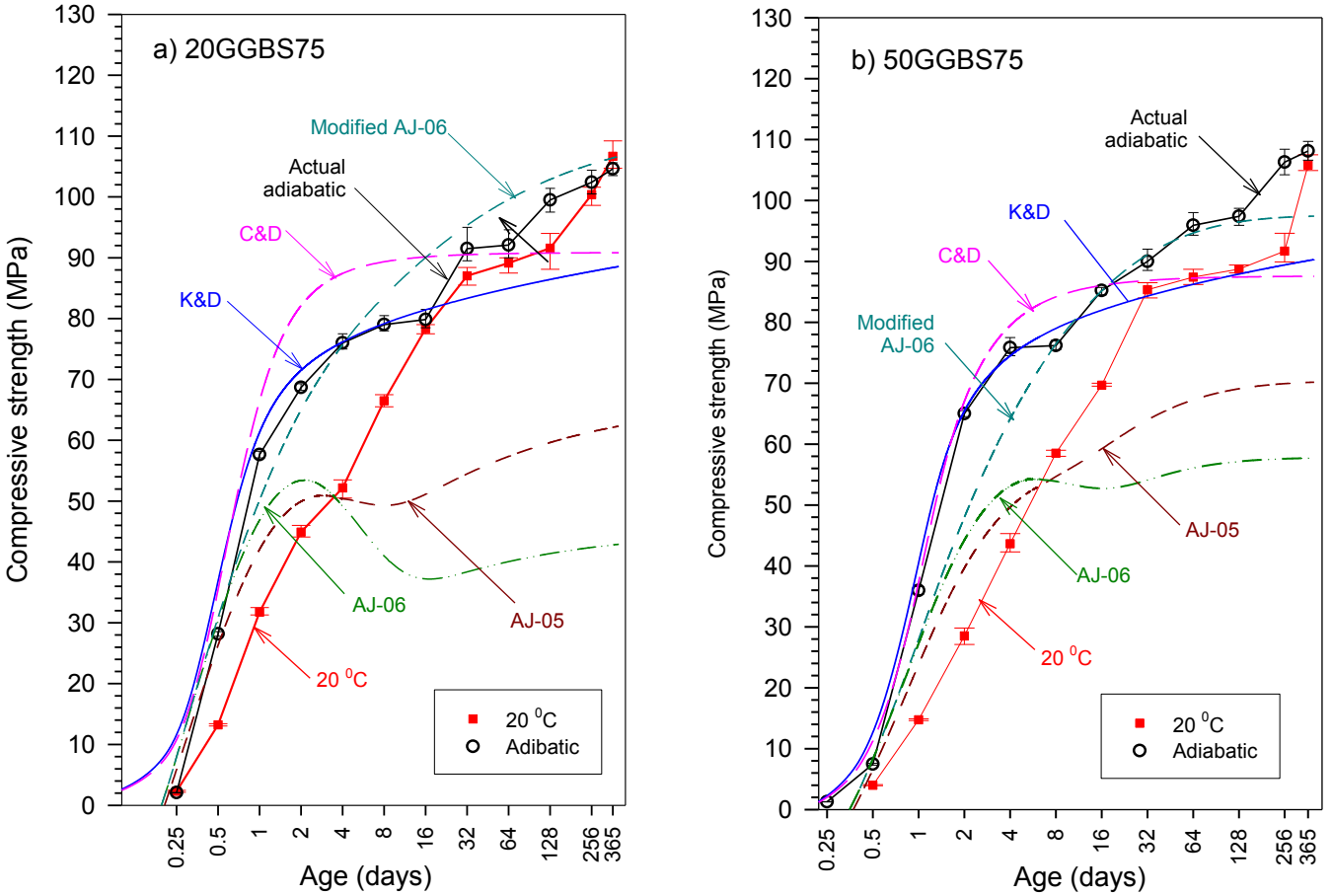

Figure E - 22: Predicted adiabatic strength development of concrete with 20 and 50% GGBS **grade C75** using recent maturity equation

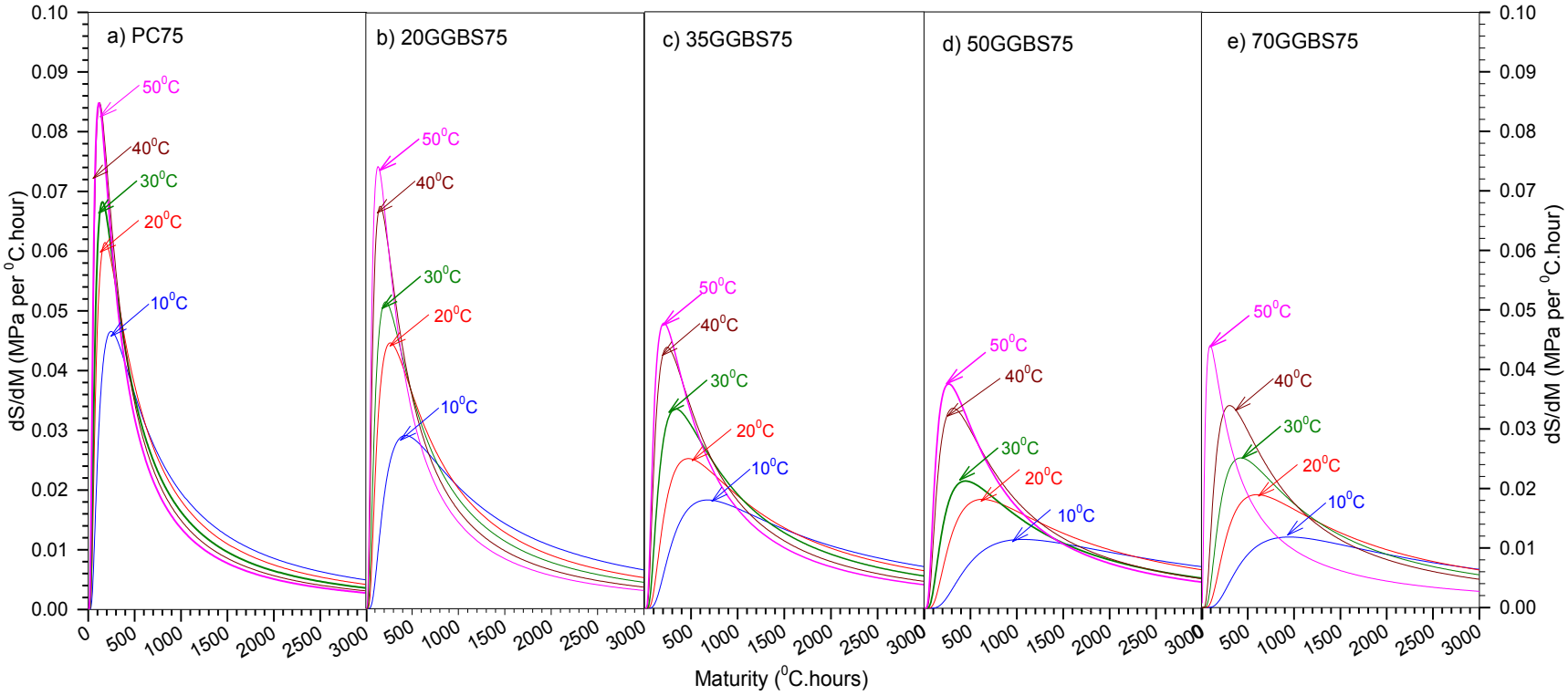

Figure E - 23: Rate of compressive strength gain with respect to maturity (dS/dM) vs. maturity (^{0}C.hours) mortar **grade C75**

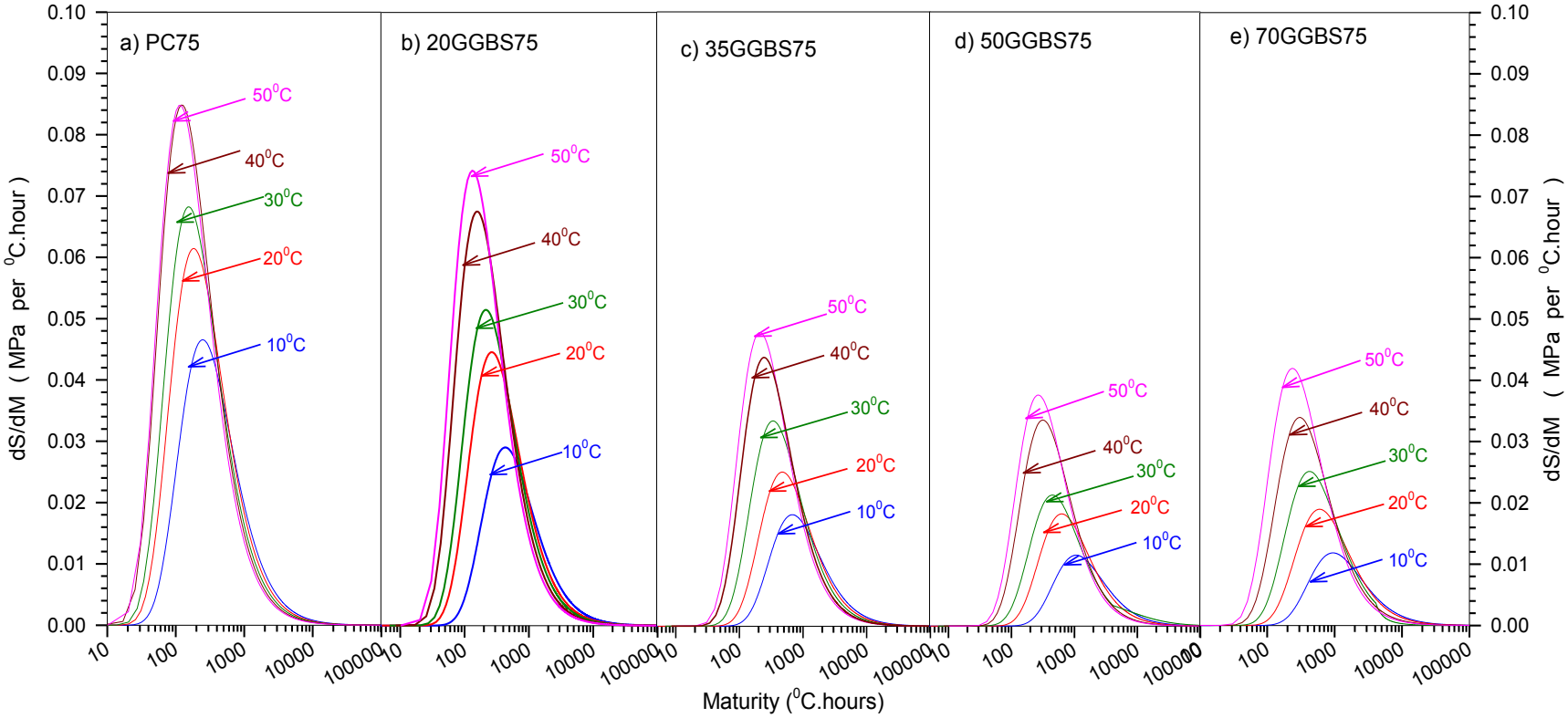

Figure E - 24: Rate of compressive strength gain with respect to maturity (dS/dM) vs. maturity (^{0}C.hours) plotted on a logarithmic axis for mortar **grade C75**

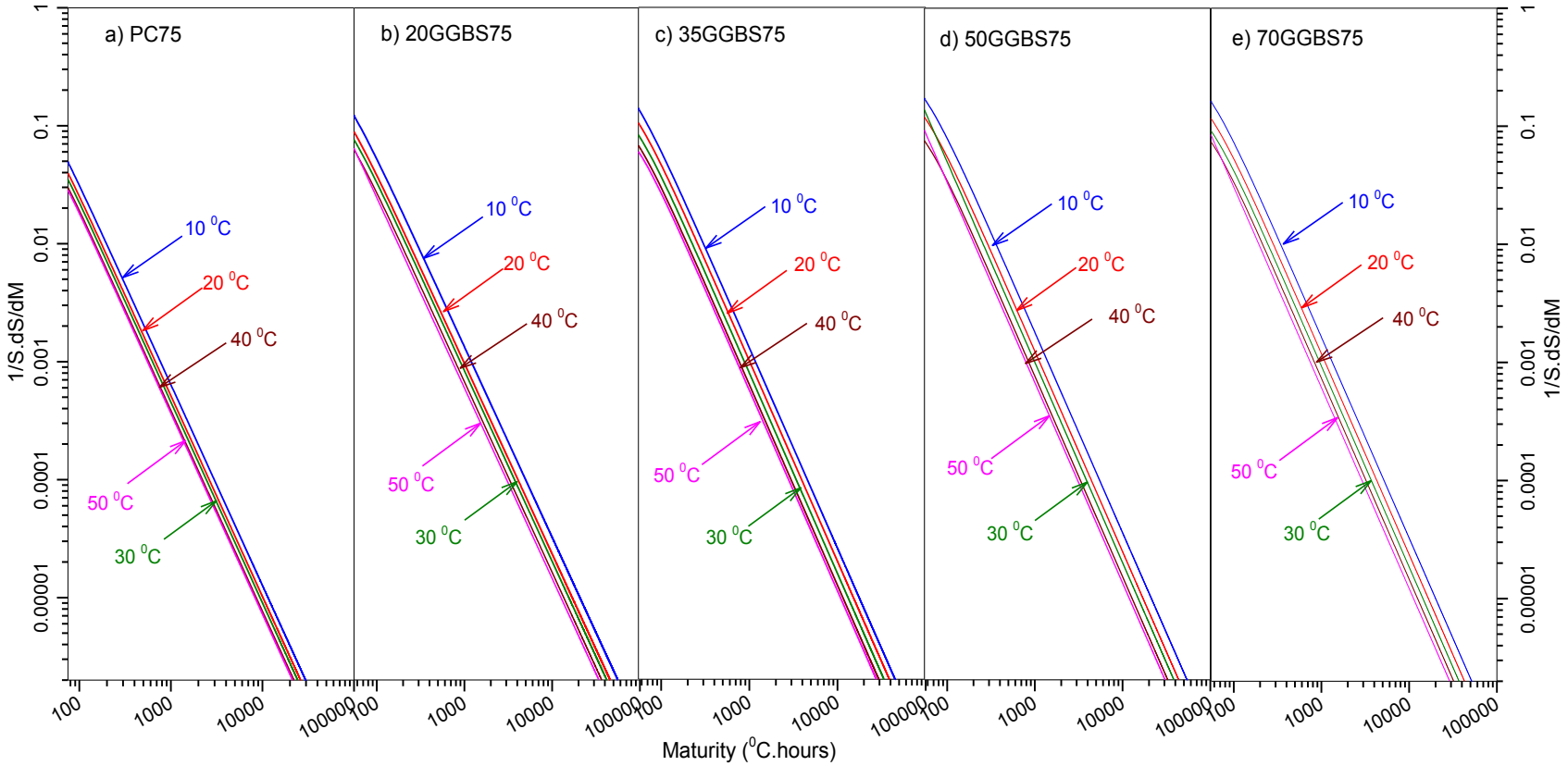

Figure E - 25: Relationship of 1/S.dS/dM with maturity for different curing temperatures mortar **grade C75**

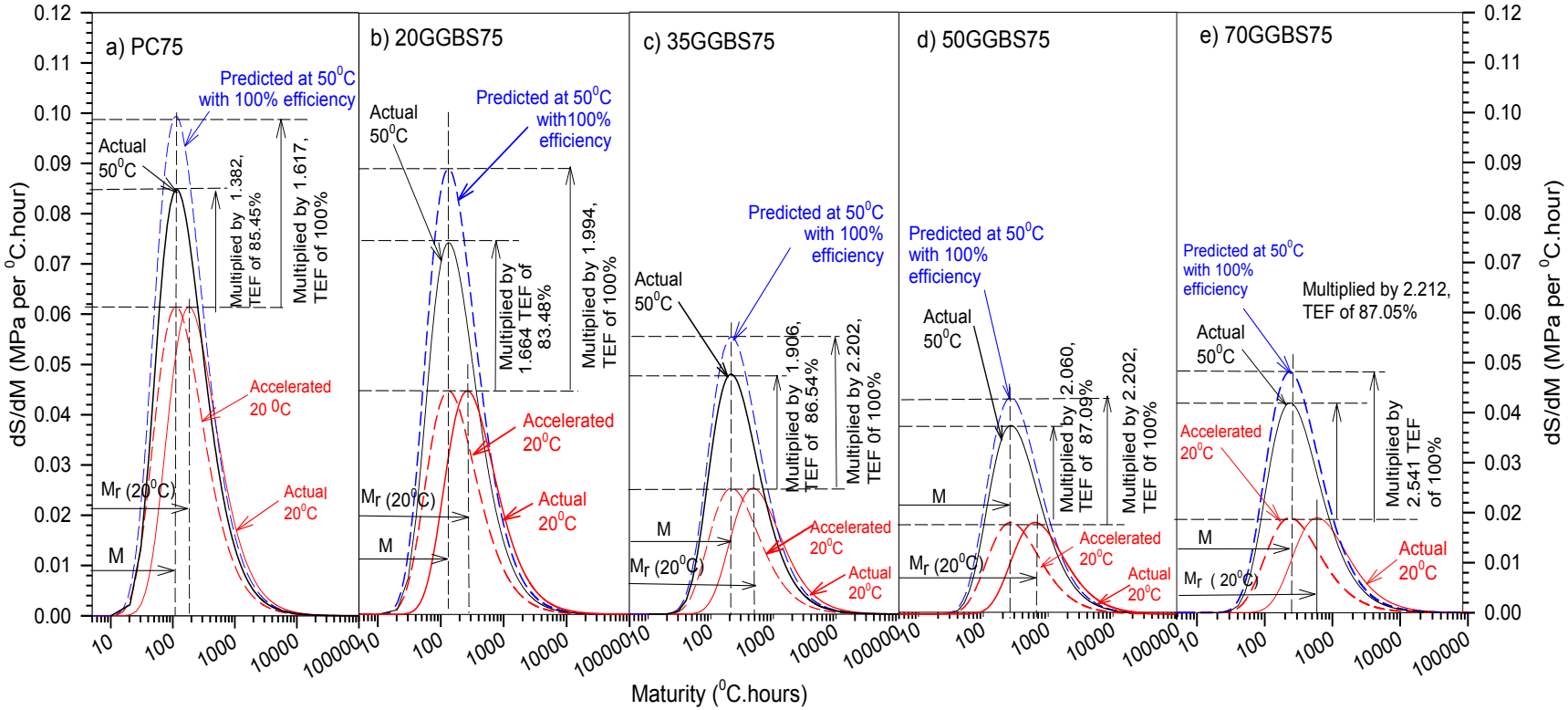

Figure E - 26: "Acceleration (M_r/M)" and "temperature efficiency" factors used to transform the 20^{0}C rate of compressive strength gain (dS/dM) to that 50^{0}C for mortar **grade C75**

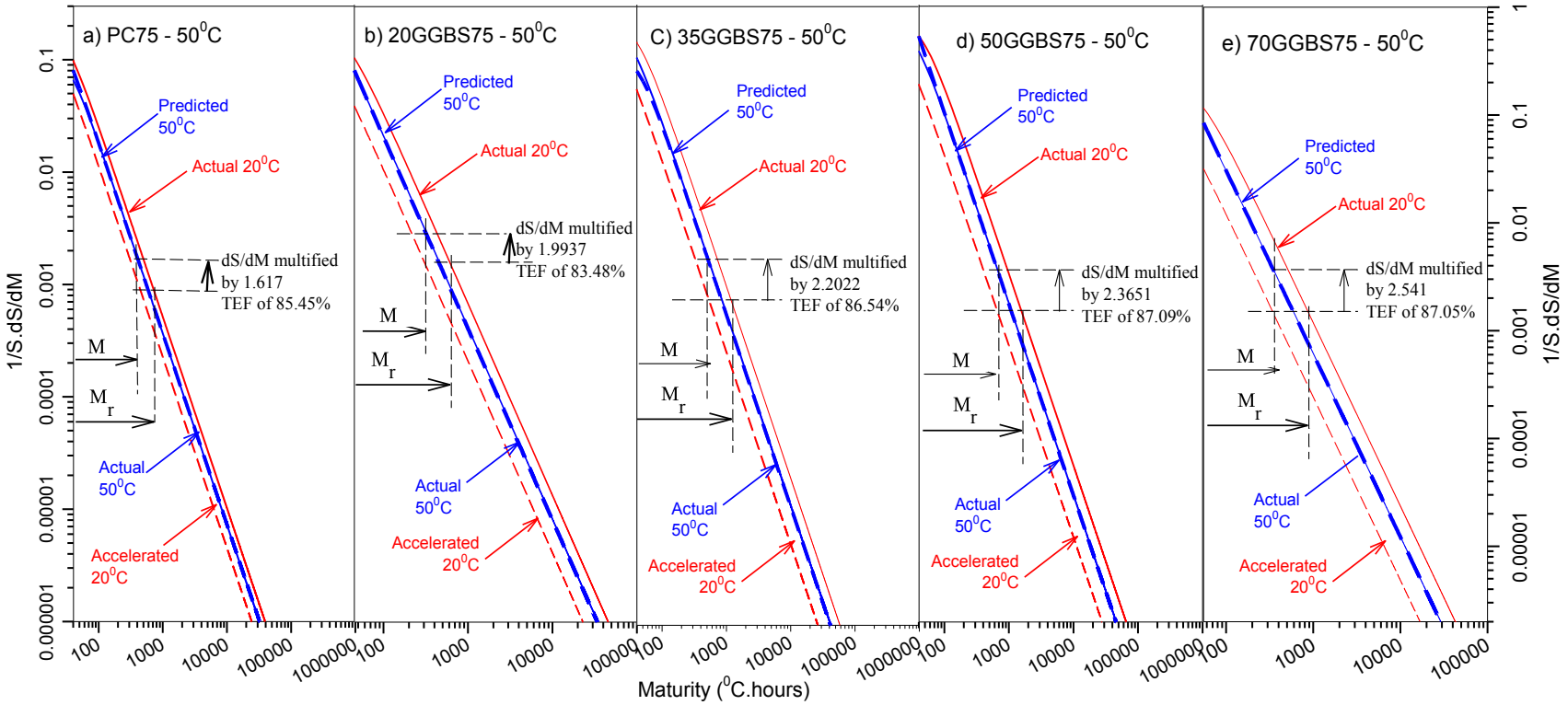

Figure E - 27: "Acceleration (M_r/M)" and "temperature efficiency" factors used to transform the 20^0C relationship between 1/S.dS/dM and maturity to that of specimens cured at 50^0C for mortar **grade C75**

Table E - 1: Regression analysis strength-age based on ASTM method for mortar grade C45

Mortar Mixes	Curing Temp. ^{0}C	Regression Parameters			
		Su (MPa)	k (days^{-1})	t_o (days)	R^2
PC45	10	61.3569	0.2446	0.4203	0.9841
	20	60.1811	0.3803	2.86E-10	0.9852
	30	55.9093	1.0617	0.2101	0.9901
	40	51.7348	1.1457	0.0934	0.9701
	50	48.3342	1.2294	8.03E-12	0.9964
20GGBS45	10	63.5726	0.1236	4.37E-09	0.9747
	20	60.2967	0.2870	0.0388	0.9892
	30	59.2165	0.5842	0.0993	0.9759
	40	58.1126	0.7205	0.0068	0.9833
	50	52.1476	0.9986	0.0117	0.9680
35GGBS45	10	61.0509	0.1096	0.1907	0.9983
	20	60.3481	0.2026	0.1595	0.9963
	30	57.0029	0.5510	0.1698	0.9895
	40	53.7638	0.7409	0.0934	0.9860
	50	50.9174	0.9174	0.0482	0.9558
50GGBS45	10	69.7522	0.0942	0.6368	0.9984
	20	65.6114	0.1700	0.6067	0.9972
	30	61.4243	0.4450	0.2982	0.9950
	40	58.2628	0.7252	0.2035	0.9851
	50	56.0385	0.8061	1.06E-09	0.9661
70GGBS45	10	65.2881	0.0822	1.6044	0.9928
	20	62.4328	0.1286	0.9273	0.9902
	30	58.3687	0.3837	0.3416	0.9891
	40	56.0283	0.7459	0.3143	0.9909
	50	52.2247	0.7992	8.20E-10	0.9158

Table E - 2: Regression analysis strength-age based on ASTM method for mortar grade C75

Mortar Mixes	Curing Temp. ^{0}C	Regression Parameters			
		Su (MPa)	k (days^{-1})	t_o (days)	R^2
PC75	10	70.7861	0.5032	0.3879	0.9786
	20	69.4512	0.9386	1.74E-01	0.9778
	30	64.4064	1.6144	0.1446	0.9755
	40	64.2289	1.8322	0.0000	0.9476
	50	59.7180	2.3707	1.83E-09	0.8789
20GGBS75	10	78.0369	0.2287	3.15E-01	0.9854
	20	73.7092	0.6036	0.2078	0.9955
	30	67.8313	1.1185	0.1717	0.9882
	40	65.8422	1.7325	0.1023	0.9927
	50	60.5601	2.3081	0.0479	0.9656
35GGBS75	10	75.8731	0.1423	0.3042	0.9948
	20	72.9002	0.3349	0.3049	0.9907
	30	69.6362	0.6517	0.2065	0.9942
	40	65.6813	1.1789	0.1476	0.9893
	50	62.0884	1.3384	0.0273	0.9665
50GGBS75	10	75.3480	0.0924	0.5258	0.9976
	20	68.9303	0.2742	0.4073	0.9923
	30	66.1459	0.4907	0.2439	0.9848
	40	62.4803	1.1058	0.2110	0.9693
	50	58.6724	1.6772	1.73E-01	0.9595
70GGBS75	10	67.7805	0.1172	0.7909	0.7909
	20	71.0519	0.2657	0.4626	0.9945
	30	65.9771	0.5442	0.2942	0.9835
	40	62.9684	1.1589	0.2598	0.9635
	50	60.0565	1.9408	2.04E-01	0.9728

Table E - 3: Regression analysis strength-age based on TPE equation for mortar grade C45

Mortar Mixes	Curing Temp. ^{0}C	Regression Parameters			
		Su (MPa)	τ (days)	a	R^2
PC45	10	63.9030	2.8453	0.7040	0.9880
	20	64.3340	1.5302	0.5770	0.9940
	30	56.5500	0.7747	0.8550	0.9910
	40	53.9230	0.6045	0.6630	0.9810
	50	50.9830	0.4640	0.5810	0.9800
20GGBS45	10	76.5910	6.0424	0.4490	0.9900
	20	63.9240	2.0441	0.6060	0.9930
	30	62.6050	1.1088	0.6190	0.9860
	40	61.3410	0.8048	0.5950	0.9940
	50	55.3960	0.5965	0.5760	0.9850
35GGBS45	10	64.7550	5.5441	0.6340	0.9950
	20	63.6170	3.0044	0.6360	0.9960
	30	59.0820	1.3122	0.6940	0.9930
	40	56.2510	0.8756	0.6450	0.9940
	50	54.5220	0.6998	0.5700	0.9740
50GGBS45	10	72.1090	6.8707	0.7250	0.9970
	20	66.6530	4.0508	0.7960	0.9970
	30	63.0210	1.6115	0.7530	0.9970
	40	59.8690	1.0027	0.7400	0.9900
	50	59.5170	0.7067	0.5710	0.9850
70GGBS45	10	65.2130	8.7587	0.8830	0.9930
	20	61.9320	5.5079	0.9150	0.9920
	30	59.9480	1.8602	0.7500	0.9930
	40	56.4360	1.1138	0.8880	0.9920
	50	58.1300	0.7493	0.4760	0.9530

Table E - 4: Regression analysis strength-age based on TPE equation for mortar grade C75

Mortar Mixes	Curing Temp. ^{0}C	Regression Parameters			
		Su (MPa)	τ (days)	a	R^2
PC75	10	72.6343	1.6009	0.8008	0.9815
	20	71.4355	0.8113	0.7595	0.9818
	30	66.3850	0.5129	0.7592	0.9804
	40	69.1281	0.3096	0.5319	0.9728
	50	73.8340	0.2274	0.3071	0.9727
20GGBS75	10	85.5568	3.1342	0.5989	0.9931
	20	75.9206	1.1858	0.7433	0.9971
	30	69.4865	0.7052	0.7828	0.9908
	40	66.8141	0.4378	0.8094	0.9950
	50	62.4230	0.2936	0.6979	0.9754
35GGBS75	10	82.2904	4.6538	0.6141	0.9974
	20	76.4323	2.0800	0.6881	0.9931
	30	70.9527	1.1105	0.7907	0.9961
	40	66.5525	0.6484	0.8270	0.9913
	50	65.1898	0.4635	0.6260	0.9798
50GGBS75	10	82.8441	7.4934	0.6112	0.9994
	20	71.5530	2.5968	0.7320	0.9940
	30	67.7402	1.4582	0.7729	0.9880
	40	62.5542	0.7614	0.9389	0.9715
	50	59.1399	0.5332	0.9093	0.9606
70GGBS75	10	71.3637	6.0552	0.7111	0.9897
	20	72.6303	2.6908	0.7862	0.9957
	30	66.3832	1.3893	0.8711	0.9870
	40	61.7037	0.7944	1.1733	0.9678
	50	60.1943	0.5242	1.0025	0.9702

Table E - 5: Regression analysis strength-maturity based on ASTM method for mortar grade C45

Mortar Mixes	Curing Temp. ^{0}C	Regression Parameters			
		Su (MPa)	k (^{0}C.days)$^{-1}$	M_o (^{0}C.days)	R^2
PC45	10	62.1081	0.0097	2.3305E-08	0.9806
	20	60.1810	0.0123	4.1966E-08	0.9852
	30	55.9093	0.0259	8.6145	0.9901
	40	51.7348	0.0225	4.7642	0.9701
	50	48.3351	0.0202	3.3494E-08	0.9664
20GGBS45	10	63.5726	0.0059	2.2516E-08	0.9747
	20	60.2967	0.0093	1.2037	0.9892
	30	59.2165	0.0142	4.0703	0.9759
	40	58.1413	0.0140	2.0868E-08	0.9833
	50	52.1974	0.0161	2.7212E-08	0.9680
35GGBS45	10	61.0509	0.0052	4.0055	0.9983
	20	60.3481	0.0065	4.9459	0.9963
	30	57.0029	0.0125	6.9626	0.9895
	40	53.7638	0.0145	4.7645	0.9860
	50	50.9174	0.0150	2.9425	0.9558
50GGBS45	10	69.7522	0.0045	13.3718	0.9984
	20	65.6114	0.0055	18.8089	0.9972
	30	61.4243	0.0109	12.2251	0.9950
	40	58.2628	0.0142	10.3807	0.9851
	50	56.0386	0.0132	2.4076E-08	0.9661
70GGBS45	10	65.2881	0.0039	33.6933	0.9928
	20	62.4328	0.0041	28.7459	0.9902
	30	58.3687	0.0094	14.0037	0.9891
	40	56.0283	0.0146	16.0293	0.9909
	50	52.2480	0.0130	2.2876E-08	0.9158

Table E - 6: Regression analysis strength-maturity based on ASTM method for mortar grade C75

Mortar Mixes	Curing Temp. ^{0}C	Regression Parameters			
		Su (MPa)	k (^{0}C.days)$^{-1}$	M_o (^{0}C.days)	R^2
PC75	10	72.6587	0.0216	7.5399	0.9723
	20	71.1294	0.0273	4.8454	0.9701
	30	66.2812	0.0337	4.8593	0.9572
	40	65.6512	0.0333	1.8721E-10	0.9290
	50	61.1726	0.0354	1.45E-07	0.8593
20GGBS75	10	80.3865	0.0097	5.1539	0.9823
	20	75.4003	0.0178	5.9380	0.9894
	30	70.0630	0.0235	6.0562	0.9691
	40	66.8068	0.0315	4.5454	0.9858
	50	62.0533	0.0319	0.5035	0.9438
35GGBS75	10	75.9959	0.0134	4.6231	0.9774
	20	71.6981	0.0188	5.7997	0.9834
	30	71.6981	0.0142	7.6705	0.9834
	40	67.7181	0.0202	6.4267	0.9694
	50	64.2778	0.0182	3.5206E-09	0.9419
50GGBS75	10	78.7527	0.0038	7.2220	0.9916
	20	73.2721	0.0070	9.5351	0.9673
	30	69.6170	0.0099	8.5126	0.9615
	40	66.7209	0.0167	9.1376	0.9018
	50	63.1918	0.0193	7.5063	0.8500
70GGBS75	10	71.1252	0.0047	13.6309	0.9796
	20	71.9983	0.0082	13.8840	0.9937
	30	67.4339	0.0123	11.7181	0.9798
	40	64.5406	0.0209	13.0218	0.9552
	50	61.9959	0.0276	11.7559	0.9468

Table E - 7: Regression analysis strength-maturity based on TPE equation for mortar grade C45

Mortar Mixes	Curing Temp. ^{0}C	Regression Parameters			
		Su (MPa)	τ (^{0}C.days)	a	R^2
PC45	10	63.9034	59.7514	0.7035	0.9880
	20	64.3340	47.4347	0.5773	0.9941
	30	56.5497	31.7627	0.8553	0.9908
	40	53.9228	30.8315	0.6628	0.9806
	50	50.9828	28.3048	0.581	0.9803
20GGBS45	10	76.5908	126.8900	0.4491	0.9902
	20	63.9242	63.3683	0.6058	0.9931
	30	62.6046	45.4621	0.6193	0.9856
	40	61.3406	41.0426	0.5954	0.9939
	50	55.3959	36.3849	0.5758	0.9852
35GGBS45	10	64.7546	116.4268	0.6345	0.9948
	20	63.6173	93.1356	0.6359	0.9961
	30	59.0816	53.7982	0.6939	0.9934
	40	56.2513	44.6551	0.6445	0.9941
	50	54.5225	42.6896	0.5699	0.9738
50GGBS45	10	72.1088	144.2848	0.7248	0.9967
	20	66.6525	125.5735	0.7961	0.9965
	30	63.0207	66.0712	0.7527	0.9971
	40	59.8692	51.1352	0.7399	0.9901
	50	59.5167	43.1078	0.571	0.9849
70GGBS45	10	65.2125	183.9316	0.8828	0.9931
	20	61.9324	170.7454	0.9151	0.9916
	30	59.9476	76.2680	0.7499	0.9928
	40	56.4357	56.8020	0.8878	0.9920
	50	58.1302	45.7073	0.4763	0.9531

Table E - 8: Regression analysis strength- maturity based on TPE equation for mortar grade C75

Mortar Mixes	Curing Temp. ^{0}C	Regression Parameters			
		Su (MPa)	τ (^{0}C.days)	a	R^2
PC75	10	75.7150	35.9979	0.7176	0.9784
	20	74.0441	26.7274	0.6883	0.9778
	30	69.4381	22.4158	0.6576	0.9697
	40	72.3639	16.5661	0.4608	0.9686
	50	77.6179	15.6899	0.2743	0.9750
20GGBS75	10	88.6169	71.1749	0.5634	0.9928
	20	78.3832	38.9549	0.6900	0.9936
	30	73.0553	31.4222	0.6811	0.9775
	40	68.1169	22.8122	0.7594	0.9903
	50	65.0661	18.1475	0.5921	0.9632
35GGBS75	10	81.4990	49.6824	0.6060	0.9853
	20	74.2125	37.1623	0.7072	0.9880
	30	74.2125	49.1502	0.7072	0.9880
	40	69.7581	35.4109	0.7202	0.9754
	50	69.2059	30.9845	0.5267	0.9670
50GGBS75	10	89.1775	184.2650	0.5487	0.9967
	20	80.2795	101.0903	0.5821	0.9767
	30	74.7020	71.8203	0.6125	0.9709
	40	71.4260	47.7504	0.6184	0.9135
	50	70.7055	42.5496	0.5019	0.8727
70GGBS75	10	78.1645	151.5729	0.6059	0.9862
	20	73.9139	85.8906	0.7567	0.9954
	30	68.8616	60.3613	0.7873	0.9839
	40	64.4602	42.5056	0.9797	0.9571
	50	63.3909	34.0068	0.8233	63.3909

Table E - 9: Parameters obtained from transformation the strength rate at 20^0C to 10, 30, 40 and 50^0C for mortar grade C45

Mix	Temp. (^{0}C)	Age conversion factor (β)	Maturity at peak dS/dM	(dS/dM) max	a_C	a_M
20GGBS45	10	0.6774	504.0000	0.0175	0.7538	0.7791
	20	1.0000	392.6667	0.0232	1.0000	1.0000
	30	1.3226	287.0000	0.0315	1.3596	1.3682
	40	1.6452	255.0000	0.0340	1.4680	1.5399
	50	1.9677	223.6667	0.0350	1.5122	1.7556
35GGBS45	10	0.6774	777.0000	0.0122	0.7959	0.7713
	20	1.0000	599.3333	0.0154	1.0000	1.0000
	30	1.3226	348.5000	0.0251	1.6314	1.7198
	40	1.6452	280.5000	0.0288	1.8749	2.1367
	50	1.9677	244.0000	0.0311	2.0214	2.4563
50GGBS45	10	0.6774	1018.5000	0.0108	0.9353	0.8827
	20	1.0000	899.0000	0.0116	1.0000	1.0000
	30	1.3226	451.0000	0.0213	1.8387	1.9933
	40	1.6452	340.0000	0.0264	2.2757	2.6441
	50	1.9677	284.6667	0.0298	2.5696	3.1581
70GGBS45	10	0.6774	1494.5000	7.36E-03	0.9538	0.8989
	20	1.0000	1343.3333	7.72E-03	1.0000	1.0000
	30	1.3226	519.3333	0.0176	2.2763	2.5866
	40	1.6452	382.5000	0.0229	2.9720	3.5120
	50	1.9677	264.3333	0.0287	3.7158	5.0820

Table E - 10: Parameters obtained from transformation the strength rate at 20^0C to 10, 30, 40 and 50^0C for mortar grade C75

Mix	Temp. (^{0}C)	Age conversion factor (β)	Maturity at peak dS/dM	(dS/dM) max	a_C	a_M
PC75	10	0.6774	252.0000	0.0465	0.7576	0.7176
	20	1.0000	180.8333	0.0614	1.0000	1.0000
	30	1.3226	157.1667	0.0682	1.1107	1.1506
	40	1.6452	119.0000	0.0848	1.3809	1.5196
	50	1.9677	111.8333	0.0849	1.3818	1.6170
20GGBS75	10	0.6774	430.5000	0.0291	0.6515	0.6121
	20	1.0000	263.5000	0.0446	1.0000	1.0000
	30	1.3226	211.8333	0.0515	1.1547	1.2439
	40	1.6452	161.5000	0.0675	1.5141	1.6316
	50	1.9677	132.1667	0.0742	1.6643	1.9937
35GGBS75	10	0.6774	682.5000	0.0181	0.7236	0.6889
	20	1.0000	470.1667	0.0251	1.0000	1.0000
	30	1.3226	334.8333	0.0334	1.3322	1.4042
	40	1.6452	246.5000	0.0437	1.7439	1.9074
	50	1.9677	213.5000	0.0478	1.9058	2.2022
50GGBS75	10	0.6774	1060.5000	0.0115	0.6314	0.5895
	20	1.0000	625.1670	0.0183	1.0000	1.0000
	30	1.3226	464.6670	0.0235	1.2875	1.3454
	40	1.6452	314.5000	0.0335	1.8363	1.9878
	50	1.9677	264.3333	0.0376	2.0597	2.3651
70GGBS75	10	0.6774	924.0000	0.0118	0.6240	0.6430
	20	1.0000	594.1667	0.0190	1.0000	1.0000
	30	1.3226	423.6667	0.0251	1.3250	1.4020
	40	1.6452	306.0000	0.0339	1.7900	1.9420
	50	1.9677	233.8333	0.0419	2.2120	2.5410

Table E - 11: Regression analysis strength-age based on ASTM method for concrete grade C45

Concrete Mixes	Curing Temp. ^{0}C	Regression Parameters			
		Su (MPa)	k (days^{-1})	t_o (days)	R^2
PC45	20	63.7659	0.3768	0.0694	0.9799
	50	60.1243	1.2080	3.15E-10	0.9300
20GGBS45	20	73.5627	0.2103	1.63E-09	0.9789
	50	66.6556	0.8781	4.87E-12	0.9740
35GGBS45	20	73.6790	0.1743	0.0287	0.9895
	50	66.1387	0.6511	5.21E-10	0.9633
50GGBS45	20	79.4912	0.1498	1.95E-09	0.9788
	50	72.4709	0.9052	0.0799	0.9706
70GGBS45	20	68.3989	0.1527	0.5310	0.9885
	50	60.9050	0.8931	1.91E-09	0.9045

Table E - 12: Regression analysis strength-age based on ASTM method for concrete grade C75

Concrete Mixes	Curing Temp. ^{0}C	Regression Parameters			
		Su (MPa)	k (days^{-1})	t_o (days)	R^2
PC75	20	91.0106	0.7226	0.1167	0.9853
	50	87.0969	2.3784	6.94E-12	0.9592
20GGBS75	20	94.3979	0.3756	0.0435	0.9835
	50	91.7027	1.4285	6.43E-10	0.9572
35GGBS75	20	97.9760	0.2776	0.0831	0.9875
	50	96.7312	1.1682	2.37E-10	0.9664
50GGBS75	20	92.9457	0.2308	0.2335	0.9968
	50	87.4248	1.3870	0.0858	0.9688
70GGBS75	20	91.2301	0.2234	0.6554	0.9936
	50	81.9783	1.8020	0.1779	0.9638

Table E - 13: Regression analysis strength-age based on TPE Equation for concrete grade C45

Concrete Mixes	Curing Temp. ^{0}C	Regression Parameters			
		Su (MPa)	τ (days)	a	R^2
PC45	20	68.2673	1.6494	0.5888	0.9918
	50	66.6600	0.4915	0.4698	0.9596
20GGBS45	20	84.6214	3.1750	0.4788	0.9946
	50	70.7306	0.6624	0.5773	0.9881
35GGBS45	20	81.3221	3.5688	0.5437	0.9964
	50	73.3568	0.9489	0.4946	0.9869
50GGBS45	20	91.0983	4.4802	0.4981	0.9925
	50	76.5907	0.7327	0.6138	0.9841
70GGBS45	20	72.2369	4.5106	0.6734	0.9928
	50	71.4076	0.6757	0.3898	0.9608

Table E - 14: Regression analysis strength-age based on TPE Equation for concrete grade C75

Concrete Mixes	Curing Temp. ^{0}C	Regression Parameters			
		Su (MPa)	τ (days)	a	R^2
PC75	20	94.6721	0.9123	0.6673	0.9912
	50	92.1156	0.2159	5.37E-01	0.9863
20GGBS75	20	108.6266	1.8655	0.5060	0.9903
	50	103.0939	0.4284	0.4744	0.9746
35GGBS75	20	103.6385	2.1507	0.6137	0.9922
	50	108.2958	0.5438	0.5008	0.9769
50GGBS75	20	104.3644	3.1678	0.5918	0.9891
	50	96.8515	0.5587	0.5642	0.9659
70GGBS75	20	98.1364	3.6243	0.7201	0.9891
	50	86.4475	0.5399	0.7648	0.9554

Table E - 15: Regression analysis strength-maturity based on ASTM method for concrete grade C45

Concrete Mixes	Curing Temp. ^{0}C	Regression Parameters			
		Su (MPa)	k (^{0}C.days)$^{-1}$	M_o (^{0}C.days)	R^2
PC45	20	63.9707	0.0116	2.269E-08	0.9797
	50	60.1243	0.0198	2.99E-08	0.9300
20GGBS45	20	73.5627	0.0068	1.51E-08	0.9789
	50	66.6626	0.0144	2.40E-08	0.9740
35GGBS45	20	73.6790	0.0056	0.8890	0.9895
	50	66.1387	0.0107	1.99E-08	0.9633
50GGBS45	20	79.4912	0.0048	6.96E-08	0.9788
	50	72.4709	0.0148	4.8718	0.9706
70GGBS45	20	68.3989	0.0049	16.4622	0.9885
	50	60.9053	0.0146	1.10E-07	0.9045

Table E - 16: Regression analysis strength-maturity based on ASTM method for concrete grade C75

Concrete Mixes	Curing Temp. ^{0}C	Regression Parameters			
		Su (MPa)	k (^{0}C.days)$^{-1}$	M_o (^{0}C.days)	R^2
PC75	20	91.0106	0.0233	3.6184	0.9853
	50	87.0969	0.0390	2.08E-09	0.9592
20GGBS75	20	97.6009	0.0106	2.36E-08	0.9764
	50	93.6644	0.0218	2.60E-08	0.9440
35GGBS75	20	97.8995	0.0090	2.5924	0.9890
	50	99.0987	0.0177	2.33E-08	0.9515
50GGBS75	20	97.3600	0.0060	2.08E-08	0.9848
	50	90.7972	0.0174	4.23E-08	0.9446
70GGBS75	20	94.3157	0.0064	17.7877	0.9854
	50	84.0050	0.0263	1.01E+01	0.9504

Table E - 17: Regression analysis strength-maturity based on ASTM method for concrete grade C45

Concrete Mixes	Curing Temp. ^{0}C	Regression Parameters			
		Su (MPa)	τ (^{0}C.days)	a	R^2
PC45	20	68.2673	51.1302	0.5888	0.9918
	50	66.6600	29.9844	0.4698	0.9596
20GGBS45	20	84.6214	98.4263	0.4788	0.9946
	50	70.7306	40.4069	0.5773	0.9881
35GGBS45	20	81.3221	110.6336	0.5437	0.9964
	50	73.3568	57.8830	0.4946	0.9869
50GGBS45	20	91.0983	138.8872	0.4981	0.9925
	50	76.5907	44.6969	0.6138	0.9841
70GGBS45	20	72.2369	139.8284	0.6734	0.9928
	50	71.4076	41.2154	0.3898	0.9608

Table E - 18: Regression analysis strength-maturity based on ASTM method for concrete grade C75

Concrete Mixes	Curing Temp. ^{0}C	Regression Parameters			
		Su (MPa)	τ (^{0}C.days)	a	R^2
PC75	20	94.6721	28.2820	0.6673	0.9912
	50	92.1156	13.1692	0.5365	0.9863
20GGBS75	20	108.6267	57.8317	0.5060	0.9903
	50	103.0940	26.1304	0.4744	0.9746
35GGBS75	20	103.6385	66.6707	0.6137	0.9922
	50	108.2959	33.1689	0.5008	0.9769
50GGBS75	20	104.3644	98.2023	0.5918	0.9891
	50	96.8514	34.0795	0.5642	0.9659
70GGBS75	20	98.1364	112.3523	0.7201	0.9891
	50	86.4475	32.9334	0.7648	0.9554

Table E - 19: Regression analysis strength-age relationship based on ASTM method for Lightweight and Self Compacting concretes

Concrete Mixes	Curing Temp. °C	Regression Parameters			
		Su (MPa)	k (1/day)	t_o (day)	R^2
LW-PC Control	20	45.134	1.075	0.220	0.998
	30	46.564	1.485	0.182	0.997
	40	43.666	2.329	0.114	0.992
	50	42.803	1.932	0.062	0.975
LW-PFA	20	36.068	0.363	0.276	0.993
	30	37.200	0.482	0.142	0.990
	40	42.695	0.487	0.030	0.988
	50	40.288	1.037	0.082	0.990
LW-PFA act	20	32.848	0.665	0.194	0.976
	30	37.952	0.681	0.021	0.959
	40	34.728	1.240	0.069	0.987
	50	32.080	1.631	0.000	0.965
LW-GGBS	20	47.935	0.242	0.362	0.995
	30	50.217	0.413	0.225	0.999
	40	48.084	0.734	0.171	0.991
	50	43.295	1.135	0.120	0.996
LW-GGBS act	20	40.087	0.552	0.261	0.997
	30	40.574	0.871	0.198	0.998
	40	39.961	1.007	0.020	0.990
	50	33.356	2.126	0.000	0.916
NWSCC-PC	20	63.379	0.595	0.398	0.996
	30	60.082	0.872	0.198	0.994
	40	57.986	1.000	0.046	0.994
	50	54.887	1.475	0.065	0.979
LWSCC-GGBS	20	52.064	0.783	0.396	1.000
	30	54.408	1.094	0.235	0.999
	40	52.255	1.726	0.197	0.997
	50	51.656	2.450	0.106	0.999
LWSCC-LSP	20	44.512	0.910	0.362	0.995
	30	41.458	1.540	0.191	0.991
	40	39.359	1.828	0.110	0.979
	50	37.519	2.052	0.052	0.984

Table E - 20: Regression analysis strength-age relationship based on TPE method for Lightweight and Self Compacting concretes

Concrete Mixes	Curing Temp. °C	Regression Parameters			
		Su (MPa)	τ (day)	α	R^2
LW-PC Control	20	45.390	0.784	0.917	0.997
	30	46.835	0.590	0.930	0.997
	40	44.277	0.380	0.896	0.990
	50	46.315	0.394	0.646	0.982
LW-PFA	20	37.408	1.942	0.759	0.995
	30	42.332	1.596	0.598	0.993
	40	52.351	1.648	0.491	0.991
	50	41.679	0.648	0.736	0.987
LW-PFA act	20	36.882	1.265	0.640	0.981
	30	48.236	1.427	0.463	0.976
	40	37.769	0.586	0.637	0.991
	50	36.072	0.399	0.536	0.969
LW-GGBS	20	52.550	3.112	0.675	0.995
	30	52.606	1.708	0.735	1.000
	40	49.860	0.998	0.766	1.000
	50	43.248	0.638	0.883	0.997
LW-GGBS act	20	40.402	1.329	0.850	0.998
	30	41.518	0.894	0.826	0.998
	40	42.679	0.639	0.652	0.995
	50	37.553	0.344	0.556	0.967
NWSCC-PC	20	64.499	1.431	0.883	0.995
	30	62.392	0.910	0.789	0.994
	40	62.450	0.669	0.642	0.997
	50	60.417	0.512	0.617	0.987
LWSCC-GGBS	20	57.773	1.361	0.850	0.996
	30	54.870	0.800	0.942	0.997
	40	52.450	0.557	0.998	0.995
	50	51.687	0.355	0.961	0.999
LWSCC-LSP	20	45.439	1.067	0.974	0.995
	30	43.020	0.616	0.897	0.990
	40	42.897	0.495	0.732	0.981
	50	41.740	0.385	0.629	0.990

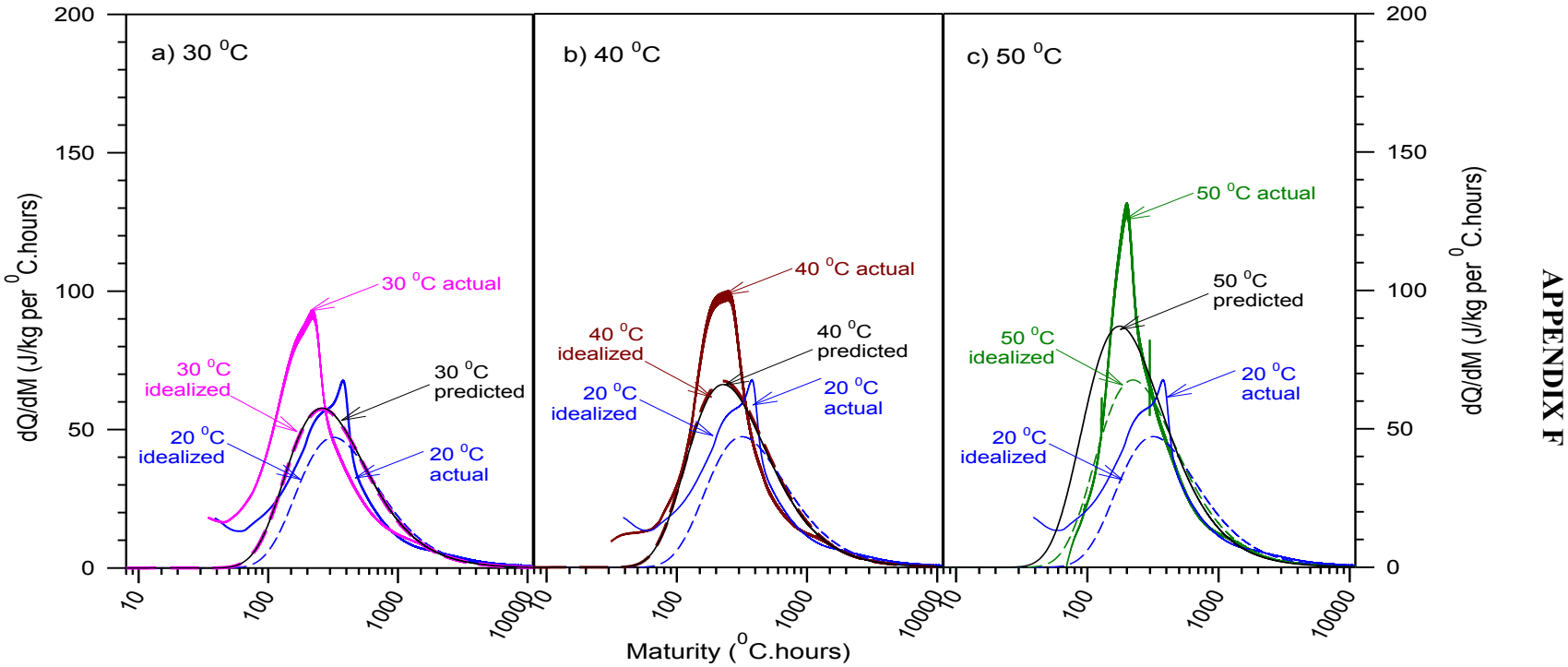

Figure F.1: Transformation of rate of heat output dQ/dM for 30, 40 and 50^{0}C vs. maturity on a logarithmic scale for concrete **20GGBS45**

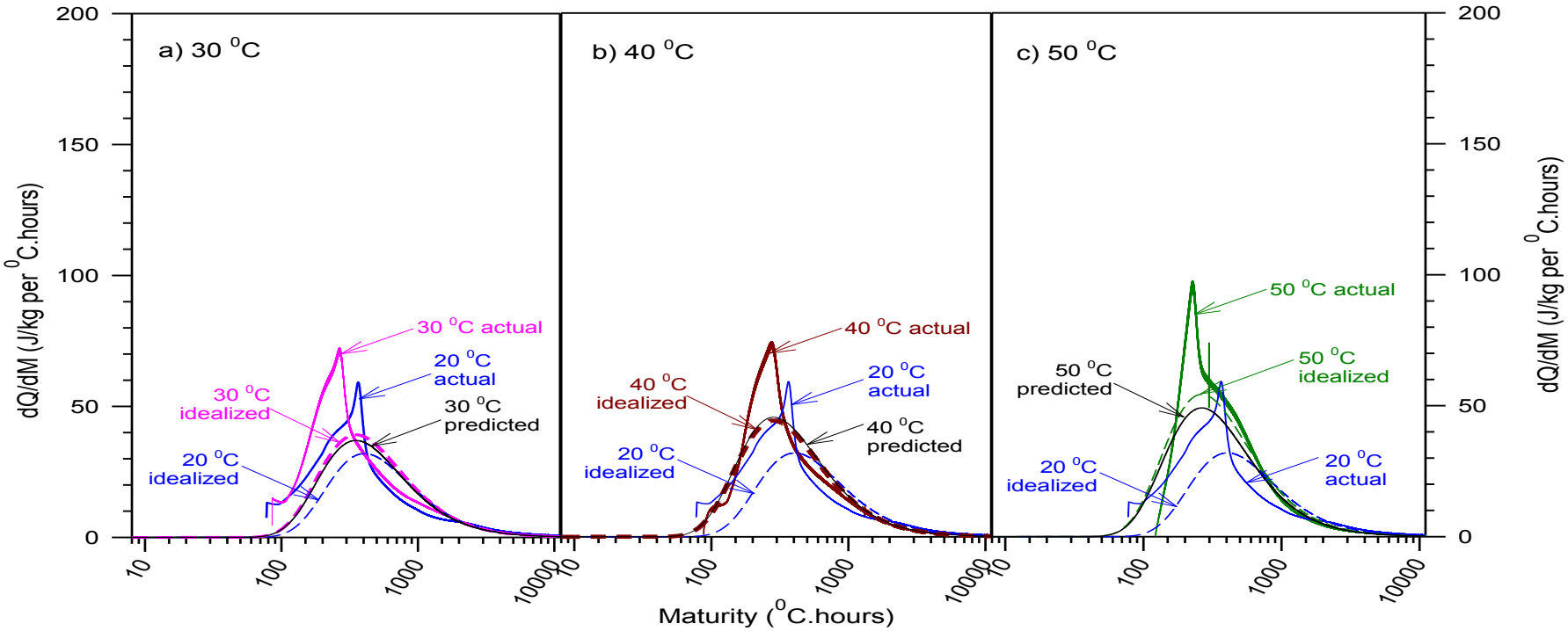

Figure F.2: Transformation of rate of heat output dQ/dM for 30, 40 and 50^{0}C vs. maturity on a logarithmic scale for concrete **50GGBS45**

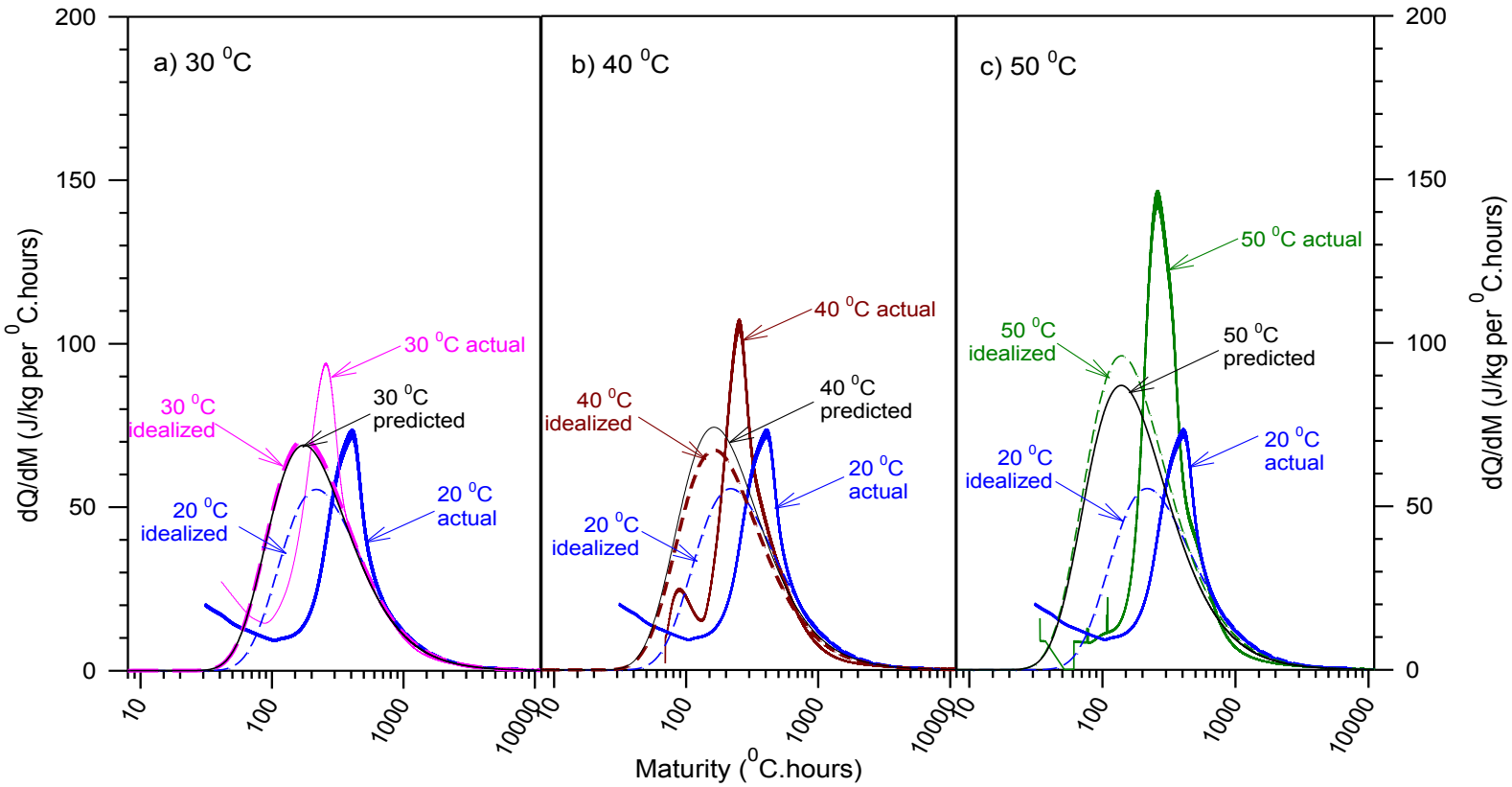

Figure F.3: Transformation of rate of heat output dQ/dM for 30, 40 and 50 C vs. maturity on a logarithmic scale for concrete **PC75**

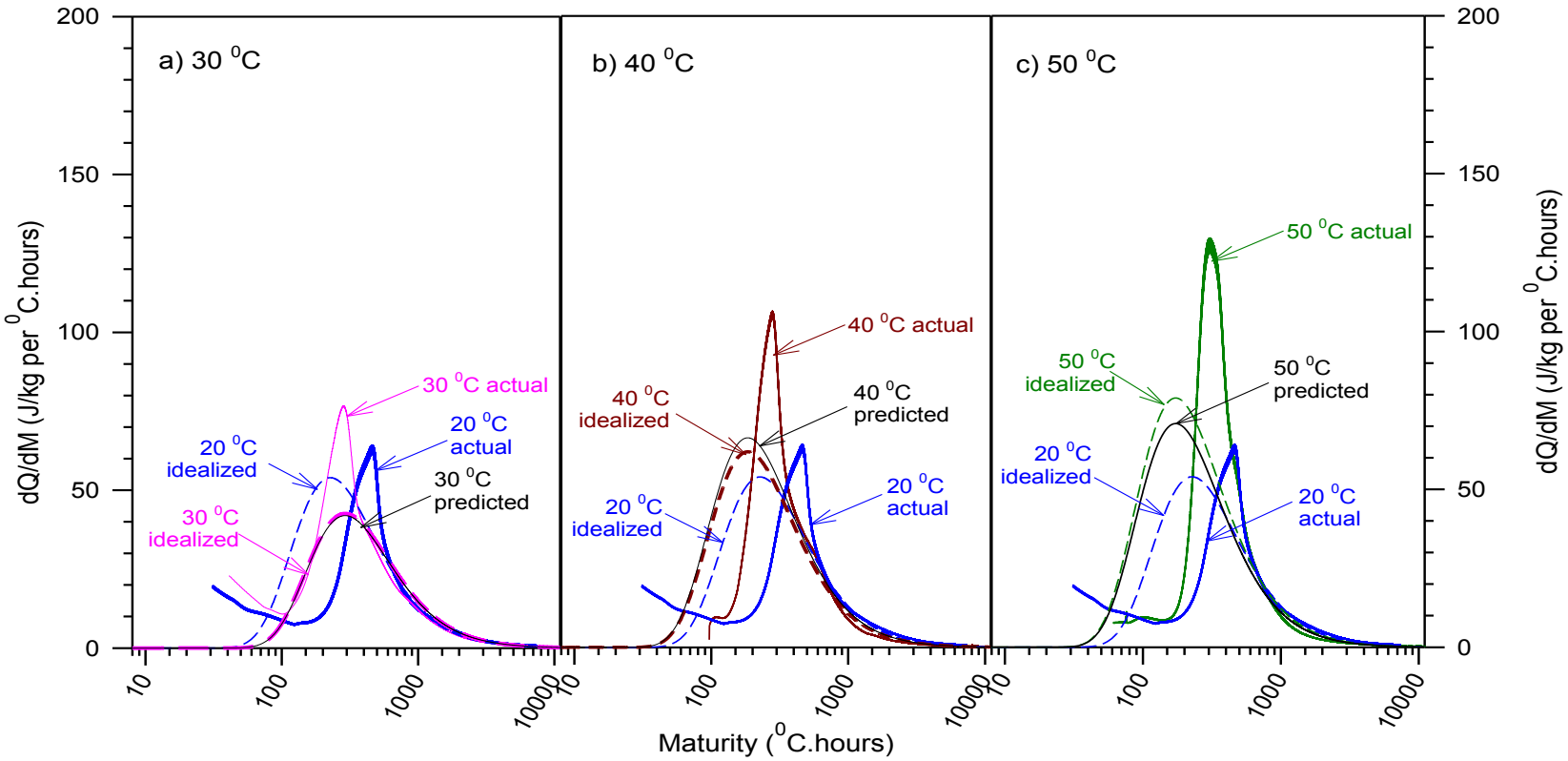

Figure F.4: Transformation of rate of heat output dQ/dM for 30, 40 and 50^{0}C vs. maturity on a logarithmic scale for concrete **20GGBS75**

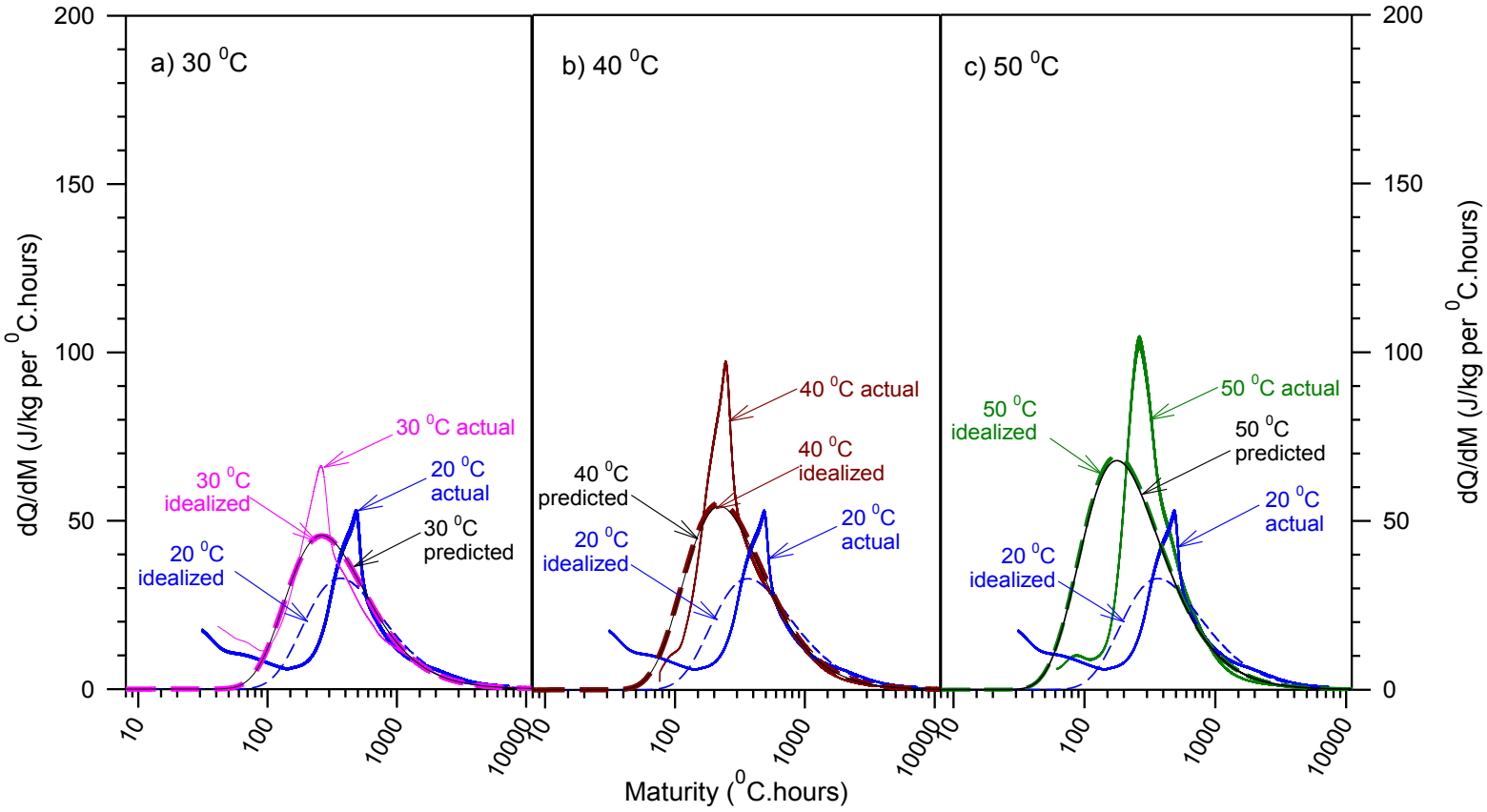

Figure F.5: Transformation of rate of heat output dQ/dM for 30, 40 and 50^{0}C vs. maturity on a logarithmic scale for concrete **35GGBS75**

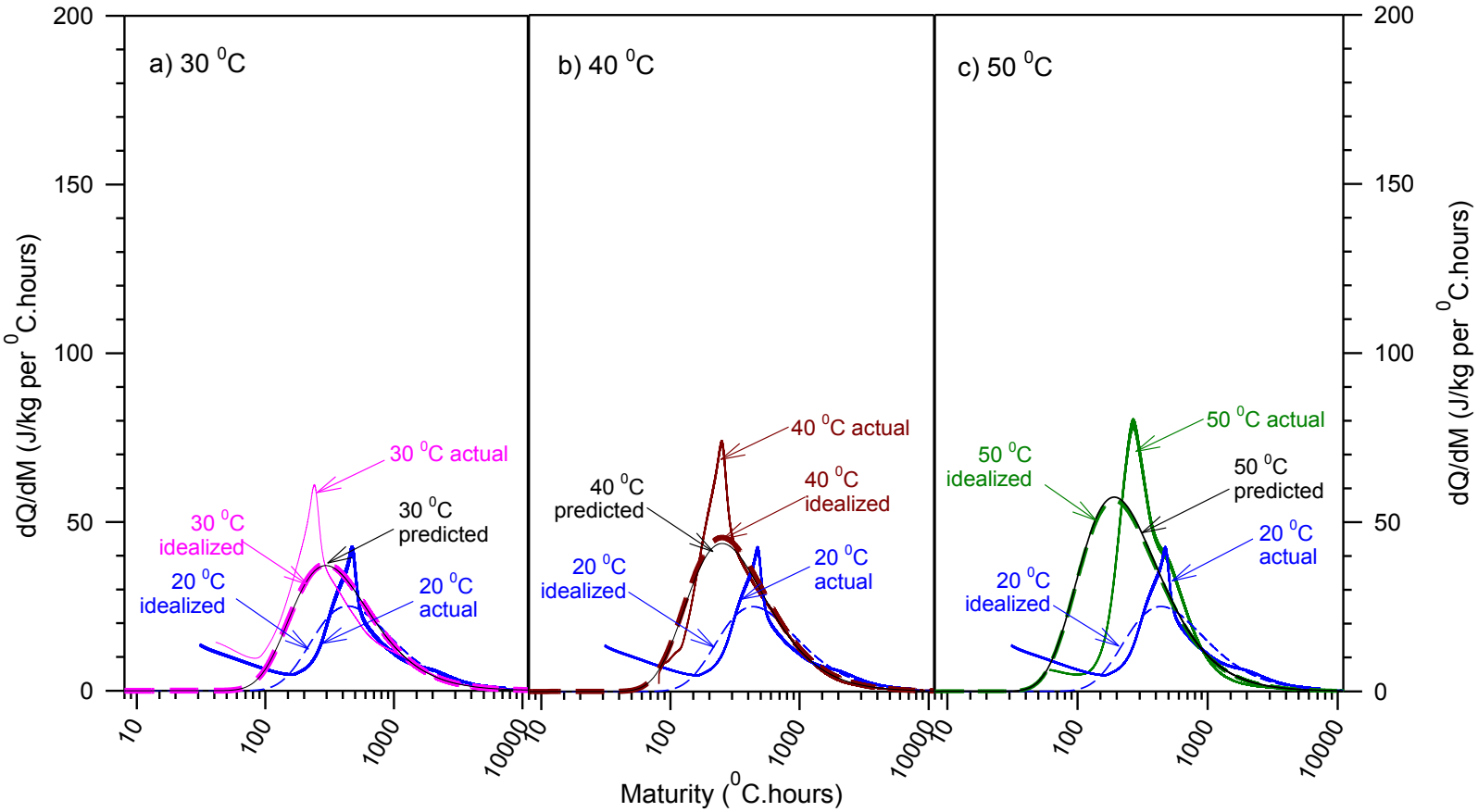

Figure F.6: Transformation of rate of heat output dQ/dM for 30, 40 and 50^{0}C vs. maturity on a logarithmic scale for concrete **50GGBS75**

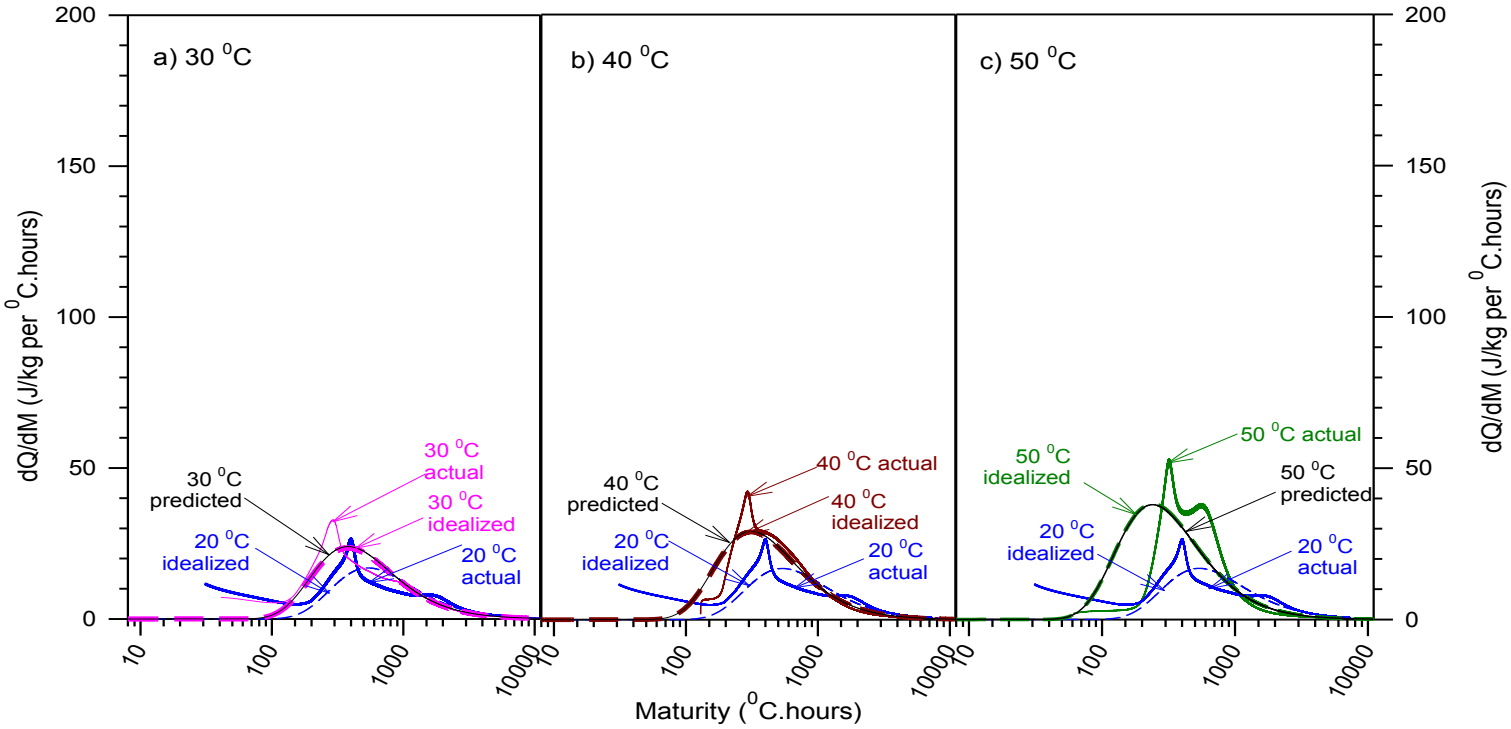

Figure F.7: Transformation of rate of heat output dQ/dM for 30, 40 and 50^{0}C vs. maturity on a logarithmic scale for concrete **70GGBS75**

APPENDIX G – Modelling in COMSOL SOFTWARE PACKAGE

G.1. Geometry and Meshing

The geometry of structural element was created using the program's CAD facilities. After the geometry is completed, COMSOL automatically, non-uniformly meshed the geometry.

G.2. Thermal Properties of Concrete

The heat equation shown in Equation 8.1 could be simplified for heat transfer by conduction as follows[247]:

$$\delta_{ts}\ \rho\ C_p \frac{\partial T}{\partial t} - \nabla(k\nabla T) = Q \qquad \text{Equation G.1}$$

where:

$\boldsymbol{\delta_{ts}}$ = Time scaling coefficient = 1

$\boldsymbol{\rho}$ = Density of concrete, (kg/m^3)

$\boldsymbol{c_p}$ = Heat capacity at constant pressure (specific heat), (J/kg k)

$\boldsymbol{k}$ = Thermal conductivity, (W/m k)

$\boldsymbol{Q}$ = Heat source, (W/m^3)

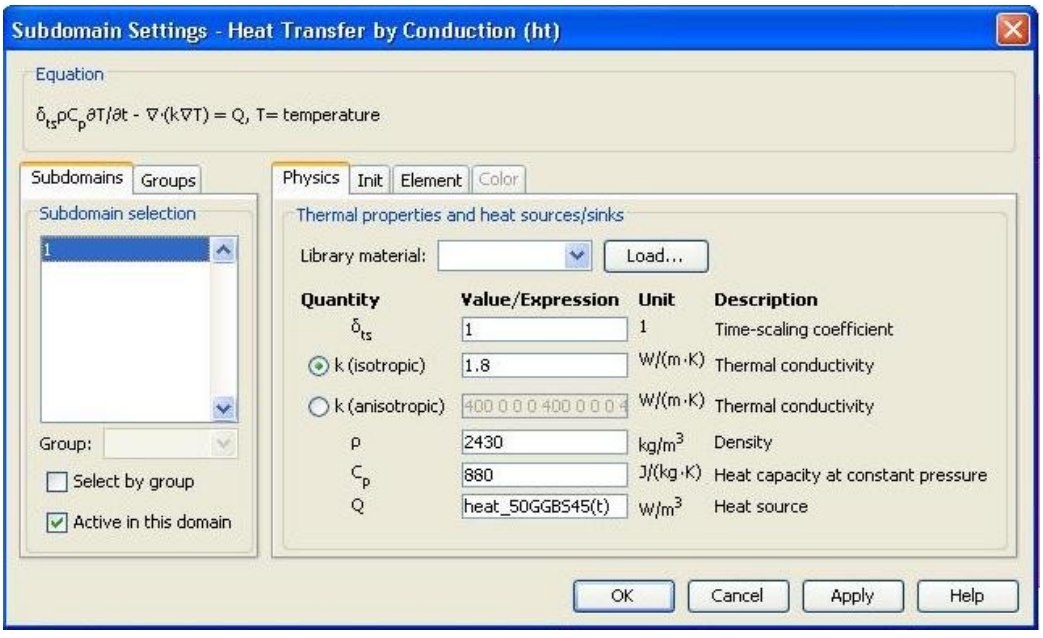

Figure G.1: Subdomain menu

The thermal properties of concrete were loaded in the Sub domain Setting menu shown in Figure G.1 above. The heat source is simply defined as the heat generation within a concrete structure that is released from the reaction between binder and water. The heat source describes heat generation within the domain, which expresses heating and cooling with positive and negative values, respectively, which is expressed in W/m^3. In this study, the heat loaded was experimentally measured, i.e. the adiabatic heat output and the predicted adiabatic heat output, using the heat output obtained from the isothermal calorimeter cured at 20^0C.

The heat source, which is in a Notepad format file is loaded through the Option menu and then choose Function. The file name in the sub domain menu should be the same with that of in Function name menu.

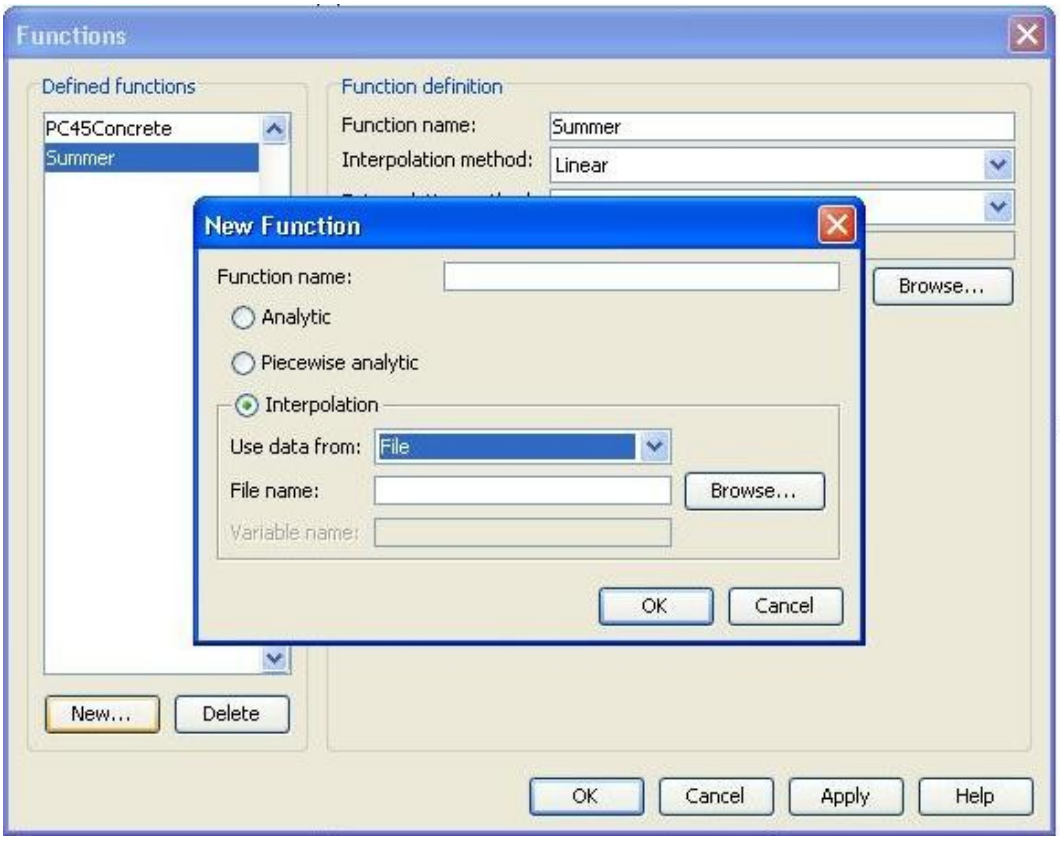

Figure G.2: Loaded the heat source (Q) into COMSOL.

G.3. Boundary Condition

In-situ concrete is usually affected by the surrounding environment, such as: ambient temperature; relative humidity; wind velocity; and solar radiation. Those conditions can affect the heat loss or gain in concrete, depending on the size of structural element. Those conditions are presented in Comsol as presented in Equation 8.1.

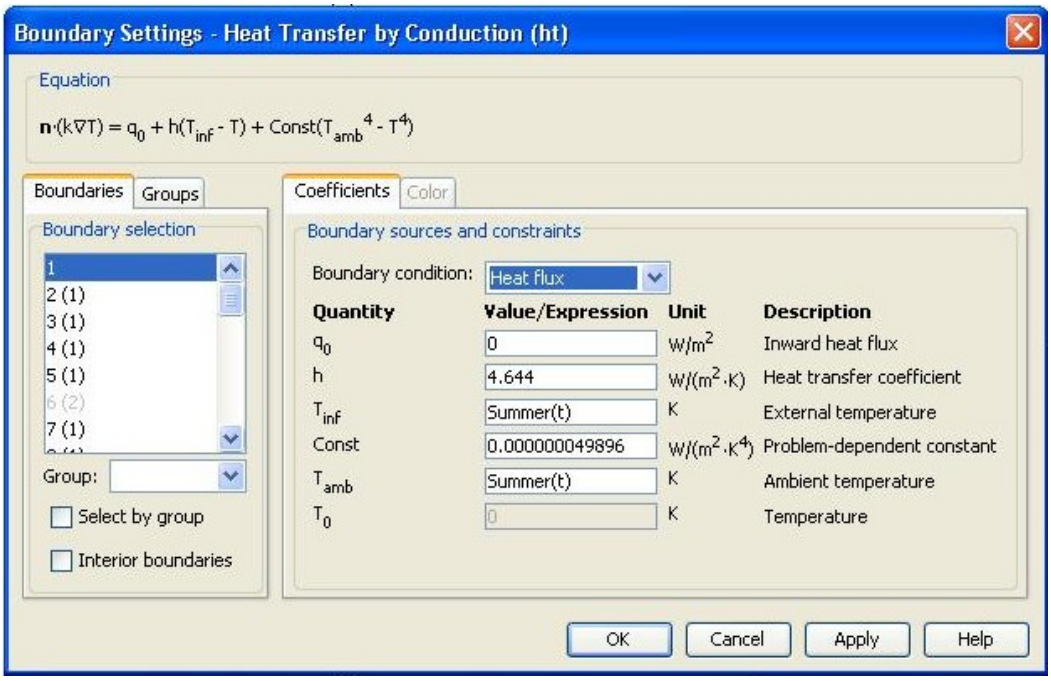

Figure G.3: Boundary settings menu for Heat Flux condition

Figure G.2 shows how the constraints are loaded into boundary setting in Comsol. The external temperature, which is in a Notepad format file, can be loaded from menu option and the choose Function.

When the domain is well insulated such concrete cured under adiabatic conditions, the boundary conditions can be expressed as the following equation[247]:

$$\boldsymbol{n}\,(\,\boldsymbol{k}\,\boldsymbol{\nabla T})\,=\,\mathbf{0} \qquad \text{Equation G.2}$$

For this to be true, the temperature on one side of the boundary must equal the temperature on the other side. Because there is no temperature difference across the boundary, heat cannot transfer across it. The boundary setting menu appears as shown in Figure G.3.

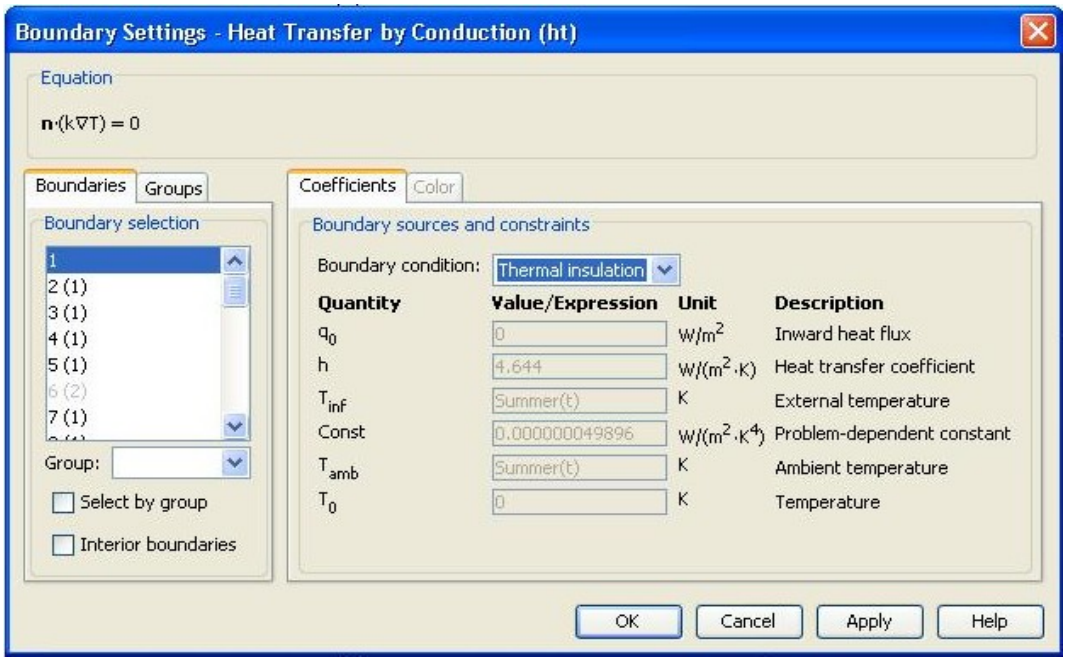

Figure G.4: Boundary settings menu for Heat Flux condition

G.4. Solver parameters

There is no fluid flow in the heat transfer in concrete and its temperatures are dependent on time, so the time dependent solver, with a time step equal to 3600 second was used, as shown in figure G.5.

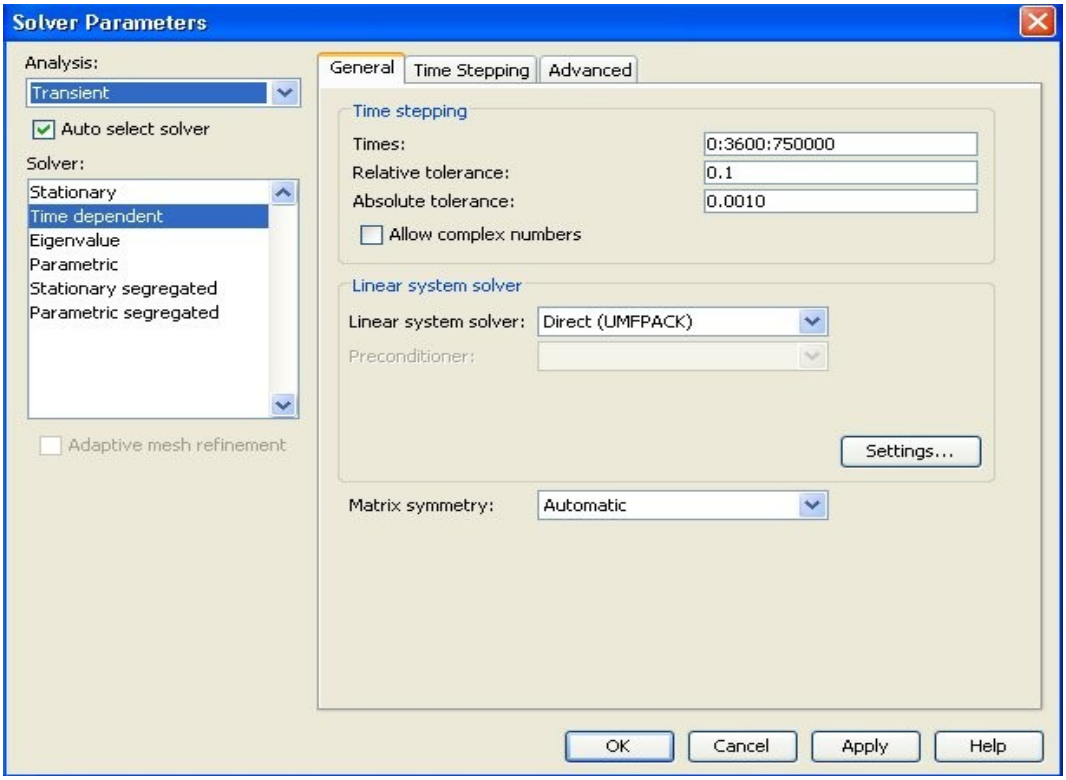

Figure G.5: Solver parameter menu

G.5. Postprocessing Menu

The results obtained from modelling with COMSOL can be seen through postprocessing menu. As shown in Figure G.5.

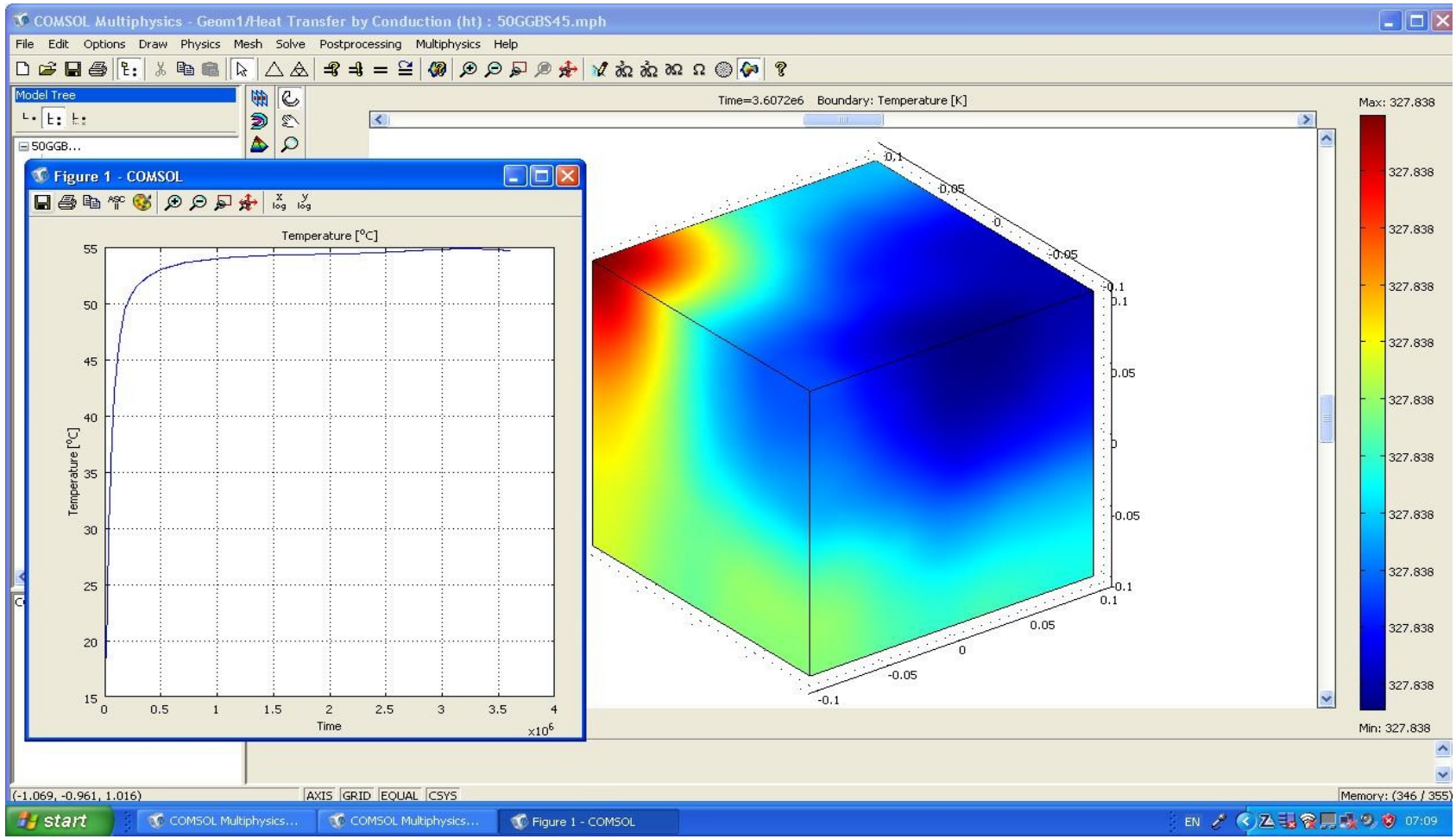

Figure G.6: COMSOL result